The chronology of Waikato pā:

A spatio-temporal investigation of pā in the Middle Waikato Basin

A thesis

submitted in fulfilment of the requirements for the degree

of

Doctor of Philosophy in Earth Sciences

at

The University of Waikato

by

Rowan Tayler McBride

THE UNIVERSITY OF
WAIKATO
Te Whare Wānanga o Waikato

2024

Abstract

This study considers the chronology of pā construction, proliferation, and development through a spatio-temporal investigation of palisade construction activity identified at six pā within the Middle Waikato Basin. The centrality of pā to pre-European Māori society is well evidenced through the archaeological record and traditional history. However, direct chronological evidence concerning their establishment, progression, and spread throughout the country is limited. Beyond a proposed commencement date of pā construction in New Zealand (AD 1500–1550), interpretations of the motivations and variables responsible for their appearance and proliferation largely rely on archaeological interpretations and limited radiocarbon (^{14}C) dating evidence. This state includes the predominant hypothesis proposing pā construction as a reflection of resource-driven conflict and territoriality primarily associated with the development of pre-European Māori horticultural production. While recent research has added nuance to the archaeological discourse on pā, highlighting possible social and cultural influences for their construction and relation to Māori warfare traditions, the challenge of creating meaningful chronologies to test these ideas persists.

This situation primarily results from the imprecision of the ^{14}C data used for chronological development. This lack of precision is largely the product of uniform periods of atmospheric ^{14}C production observed within the Southern Hemisphere during long periods since New Zealand's settlement. However, the effect of this imprecision is compounded by New Zealand's short chronology, resulting in a short window of time to explore the development and evolution of Māori culture before European arrival. Additionally, limitations in the application of ^{14}C dating within New Zealand (i.e., small sample numbers, poor sample taphonomy and provenance, and the limited application of Bayesian chronological modelling) have further restricted meaningful chronological development on the timescale required for dealing with palimpsests within the archaeological record. These three factors have ultimately inhibited explorations of the link between pā and the broader archaeological landscape.

This thesis establishes a comprehensive chronological framework that addresses these constraints. Wiggle-match dating is used to provide an accurate and precise calendar date for the felling of a tree used in the construction of a palisade defence. These specific events are examined using the theory of time perspectivism, focusing on three distinct scales of analysis: Event, Local, and Regional.

The event scale of analysis successfully produced 20 high-precision Felling Dates on posts recovered from Lake Mangakaware 1 (MA1), Lake Mangakaware 2 (MA2), Lake Mangahia (MGA), Taraheke Pā (TAR), Te Uapata Pā (TEU) and Lake Rotokauri (ROT). The local scale analysis utilised these Felling Dates to track the development of the identified palisade defences over time, identifying multiple palisade construction phases, representing construction, repair and redevelopment episodes at MA1, MA2, MGA and TEU. Finally, the regional scale analysis integrated this evidence into a broader chronological framework, identifying shared episodes of palisade construction activity within the Middle Waikato Basin. This analysis highlights three critical periods of socio-political stress and stability between the late fifteenth and early nineteenth centuries, related to hypothesised influential variables from the broader cultural and archaeological landscape that are proposed to be responsible for the emergence, proliferation and development of pā over time.

Acknowledgements

Many people have greatly assisted me in completing this thesis, and I owe a debt of gratitude to all of them for their support throughout this process. First and foremost, I wish to thank my chief supervisor, Professor Alan Hogg. The support and guidance you have offered me throughout my PhD have been far over and beyond what is to be expected, and I am truly grateful. I also wish to thank my co-supervisors, A. Prof. Gretel Boswijk, Prof. David Lowe, A. Prof Fiona Petchey, and A. Prof Waikaremoana Waitoki, and my colleagues in the Rua Mātītī Rua Mātātā Pā Research Project team, Dr Warren Gumbley, Prof. Tom Roa and Prof. Atholl Anderson, who have each contributed their time, energy and enthusiasm throughout this research. To all of you, thank you for your guidance, patience, and expertise. Working and learning alongside you all has been a pleasure. Special mention must go to my fellow PhD candidate, Zac McIvor, who never failed to check in on me and offer his help when required. Thank you for being a good friend, and I wish you all the best for what I am sure will be an illustrious career.

In addition to those directly associated with the Rua Mātītī Rua Mātātā Pā Research Project, I have also relied on the expertise of several individuals who have provided me with specialised technical guidance and advice. First, thank you to Dr Rodd Wallace and Dr Lloyd Donaldson, who took time out of their busy schedules to educate me on the specialist technique of tree species identification via thin-section microscopy. As a rare skill in our discipline that takes time to master, your guidance has provided me with a valuable tool that can be used for years to come. Second, thank you to Professor Sturt Manning (Cornell University) for your advice and detailed discussion on OxCal modelling and the interpretation of wiggle-match dates. Our correspondence was influential in the interpretation of my results and undoubtedly made for a better thesis. Finally, thank you to the Waikato University Radiocarbon Laboratory technical staff for sharing your laboratory with me and assisting me with your expert skills.

I would also like to acknowledge the large support network that has supported me throughout my research: my parents, Wendy and Tim McBride; my partner, Erica Peck; my sister and brother-in-law, Sarah and John Wickman; my home away from home with Tom and Danielle Page-McCowan; and the ArchBOP team, Ken Phillips, Cam McCaffrey and Alex Queenin.

Your unwavering support, encouragement, and understanding during this journey cannot be understated. I'm not sure where I would be without you all, and it is a privilege to call you family and friends.

Thank you to the funding agencies and organisations that have financially supported this research, including the premier NZ Govt fund (administered by the Royal Society's Marsden Fund) and the University of Waikato. Their investment has allowed me to study and fulfil my academic goals.

Finally, I would like to acknowledge the mana whenua of the Waikato, both past and present. Specifically, I would like to thank the kaitiaki I have engaged with from Ngā Iwi Tōpu o Waipā (NITOW), e Haa o te whenua o Kirikiriroa (THaWK), Ngāti Hikairo (Te Awamutu district); Taupiri Marae (Ngāti Kuiaarangi, Ngāti Mahuta, Ngāti Tai and Ngāti Whāwhākia); Horahora Marae (Ngāti Naho); Hauraki iwi (Ngāti Hako). The privilege of being able to conduct archaeological research on these significant places is not taken for granted. Thank you for your blessing and support; this research would not have been possible without it.

Table of Contents

List of Figures

List of Tables.

Chapter 1. Introduction

1.1 Research Overview

The construction of pā (fortified places) in Aotearoa/New Zealand represents a significant shift in pre-European Māori settlement patterns, providing one of the most visible representations of cultural change in the archaeological record. Pā are a site classification within Polynesia that is unique to New Zealand, characterised by the presence of defensive features (terraces, ditches, banks, palisades, etc.) that imply a primary function of the site type. Archaeological excavations have shown that the form of these defences can range in scale and complexity. Additionally, the types of habitation and communal activities (religious, economic and domestic) associated with these sites are similarly diverse (Gorbey, 1970; Green, 1970; Groube, 1970; Bellwood, 1971b, 1971c, 1972b; Law & Green, 1972; Fox, 1976; Bellwood, 1978a; Davidson, 1987; Wilkes, 1995; Barber, 1996; Sutton et al., 2003). Therefore, while defence is considered a primary function of this site classification, pā were also multifunctional spaces constructed in response to motivations that inevitably varied and changed over time (Mihaljevic, 1973; Daugherty, 1979; Davidson, 1984; Marshall, 1987; Phillips, 1995; Barber, 1996).

Previous research indicates pā were first constructed during the Transitional Period (AD 1450–1650) (Schmidt, 1996; Anderson, 2016), a 200-year episode of proposed environmental change and cultural development (see Newnham et al., 1998a; Lorrey, 2008; Mann, 2009; Fowler et al., 2012; Abram, 2014; Anderson, 2014; Goodwin et al., 2014; Roop, 2015; Newnham et al., 2018; Anderson & Petchey, 2020; Brown & Crema, 2021; Bunbury et al., 2022). This initial period of fortification is thought to reflect a response to this changing landscape, as regional-specific climate declines and associated changes in resource availability resulted in population migration into regions exhibiting conditions favourable for horticultural production, leading to this period of cultural change. As a part of this process, pā emerged as populations sought to establish central places within these contested landscapes while also exhibiting a physical representation of community identity (Groube, 1964, 1965, 1970; Mihaljevic, 1973; Fox, 1976; Daugherty, 1979; Allen, 1994; Sutton et al., 2003; Anderson, 2014; Allen, 2016; Anderson, 2016; McCoy & Ladefoged, 2019; Irwin, 2020).

Figure 1.1.1. The distribution of pā (yellow dots) in New Zealand[1].

However, over time, pā continued to be constructed throughout New Zealand, with these sites subject to periodic abandonment, reoccupation and redevelopment in response to a range of theorised variables (Irwin, 1985; Davidson, 1987; Marshall, 1987; Allen, 1994; Barber, 1996;

[1] This figure contains data sourced from the New Zealand Archaeological Association's Site Recording Scheme (Archsite) and the LINZ Data Service, which is licensed for reuse under CC BY 4.0.

Sutton et al., 2003; Marshall, 2004; Allen, 2008a; Irwin, 2013; Allen, 2016; Irwin, 2020). Crucially, over 7,000 pā are recorded nationally (Figure 1.1.1), the majority of which are located in regions of the North Island that supported pre-European horticulture (Best, 1927; Gorbey, 1970; Groube, 1970; Fox, 1976; Irwin, 1982; Davidson, 1984; Irwin, 1985; Davidson, 1987; Allen, 1994, 2008a, 2016). This observation has led to the predominant hypothesis that the continued proliferation of pā across the country was closely associated with the development and spread of horticultural practices, resulting in resource-driven (economic) conflict and increased territoriality and competition over favourable gardening areas. While compelling, it must be acknowledged that this idea is largely based on the spatial correlation of pā within areas with a favourable climate for kūmara production.

Environmental processes, resource availability, and the control of territory undoubtedly spurred conflict. Economic (resource-driven) causes of friction within Māori society are evident in traditional records, including conflict over horticultural land, fishing grounds and eel weirs (pā tuna). However, so too were murder, prestige and status (mana), infringement of tapu (traditional prohibitions), the rebalancing of perceived slights (utu), and existing traditions of warfare (i.e., taua muru, a hostile plundering expedition) (see Ballara, 1976). Therefore, the social and political structures of Māori society were also influential, which, while challenging to identify archaeologically, are central to understanding variation in the frequency and scale of aggression (Clark & Lister, 2022, p. 22). The centrality of these social structures is evident when considering that the control and/or management of resources is not solely related to group survival, and can also be related to the desire to maintain and expand existing economic and social systems (Clark & Lister, 2022, p. 11). Therefore, alternate reasons for conflict and pā construction are often overlooked during this period by focusing purely on resource-driven motives. Importantly, one or a combination of these variables at any one time could result in an episode of pā construction, with the influence of these motivations changing over time. Therefore, explanations of the variables responsible for pā construction must reflect this complexity.

Despite the evident importance of pā within Māori society, it remains difficult to generalise about their proliferation and development over time. While many pā have been recorded throughout the landscape, few have been extensively investigated archaeologically, and even

fewer have an established occupation history evidenced by a comprehensive radiocarbon dataset (< 2%). Thus far, Schmidt's (1996) research is the only attempt to place pā in a national chronological sequence, proposing that pā construction likely began between AD 1500–1550. Beyond the commencement of pā construction in New Zealand, chronologies derived from locally or regionally specific research are yet to be linked into a comprehensive national sequence (Gorbey, 1970; Fox, 1976; Green, 1978; Davidson, 1984, 1987; Sutton, 1993b; Sutton et al., 2003; Irwin & Jones, 2004; Davidson, 2011; Irwin, 2013; McIvor & Ladefoged, 2015; Allen, 2016; McCoy & Ladefoged, 2019; Irwin, 2020).

New Zealand's short chronology has contributed to this lack of meaningful chronological development (see Anderson, 1995; Higham & Hogg, 1997; Newnham et al., 1998b; Higham & Jones, 2004; Lowe & Newnham, 2004; Walter et al., 2017; Bunbury et al., 2022), taking place over a period associated with considerable variation in the concentration of atmospheric radiocarbon (^{14}C) (McCormac et al., 1998b; McCormac et al., 2002; Hogg et al., 2020; Hogg et al., 2022). Specifically, ^{14}C calibration curves developed for the Southern Hemisphere show extended periods of uniform atmospheric ^{14}C levels (plateaux) around AD 1100, 1350, 1550, and 1750, which together span the entire history of New Zealand prior to sustained European settlement. (see Hogg et al., 2013a; Hogg et al., 2020). Consequently, even AMS radiocarbon dates (with small standard errors) derived from archaeological material that coincides with these plateaux can suffer from low precision calendar age ranges, if the precision of the ^{14}C analysis is such that it cannot distinguish between the wiggles in the calibration curve, inhibiting their interpretation to the broader archaeological landscape. The last two calibration plateaux (AD 1550 and 1750) are particularly relevant for this study, as they cover a large portion of the period in which pā were constructed and occupied.

This lack of precision is compounded by further issues associated with the application of radiocarbon dating in New Zealand, including discrete small-scale excavations with limited stratigraphic controls, insufficient ^{14}C sample numbers, poor understanding of sample provenance and taphonomy resulting from historical excavations, a reliance on bulk terrestrial (charcoal) ^{14}C samples for standard radiometric dating with large standard errors (which until recently were due to insufficient data for marine sample calibration and correction, see Petchey & Schmid, 2020), and the limited application of Bayesian chronological modelling. This

scenario has restricted meaningful chronological development, preventing fine-grained examinations of pā and the processes responsible for their emergence, spread, and development.

Overcoming these limitations remains one of the most significant challenges when investigating pā. However, recent applications of accelerator mass spectrometry (AMS) ^{14}C dating (e.g., Anderson & Petchey, 2020; Petchey & Schmid, 2020; Bunbury et al., 2022) and wiggle-match dating (WMD) in New Zealand (see Hogg et al., 2012; Hogg et al., 2017; Hogg et al., 2019b), have shown promise in defining fine-grained chronological frameworks, providing accurate and precise calendar dates for specific events within defined periods, that can potentially be linked to overarching cultural and environmental processes of change. Of relevance is the pilot study conducted for this research (see Hogg et al., 2017), which investigated the potential of WMD to produce accurate calendar ages for Otāhau Pā in the Waikato region. The chronological approach implemented by Hogg et al. (2017) demonstrated that precise calendar dates could be generated for artefacts (posts) from wetland environments that directly relate to single-phase archaeological events (the construction of a palisade), achieved on a generational timescale (< 25 years). The research presented here seeks to build upon the research presented by Hogg et al. (2017), expanding this chronological approach within the Middle Waikato Basin (also known as the Hamilton Basin).

1.2 Thesis Aim

This thesis aims to establish a comprehensive chronology of pā construction, proliferation, and development within the Middle Waikato Basin. Wiggle-match dating generates precise 'Felling Dates' for posts that were installed within palisade defences at six pā. These Felling Dates are interpreted using a multi-scalar research approach, providing direct evidence for when these sites were first fortified, how the palisade defences at each pā developed over time, and how shared episodes of palisade construction activity relate on a regional scale. This multi-scalar research approach allows the identified palisade construction activity to be contextualised with respect to the events, activities and behaviours observed within the archaeological record, facilitating fine-grained interpretations and chronological comparisons between local, regional and national archaeological landscapes.

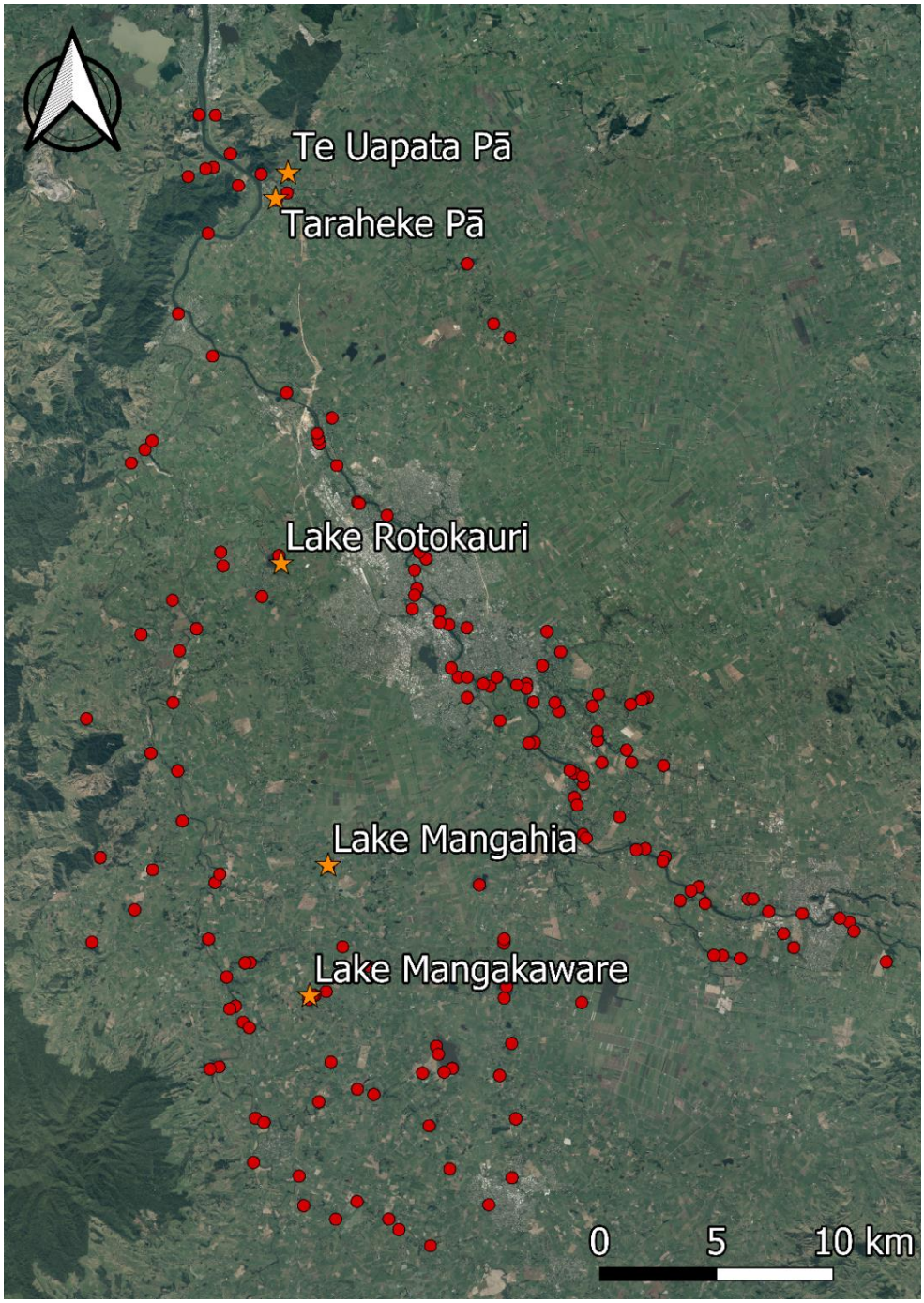

Figure 1.2.1. The distribution of pā (red dots) within the Middle Waikato Basin[2].

The Middle Waikato Basin (see Lowe, 2010) was specifically chosen for this analysis because it has a long history of archaeological research (e.g., Law, 1968; Pick, 1968; Bellwood, 1971b, 1972a; Cassels, 1972a; Law & Green, 1972; Clarke, 1977; Bellwood, 1978a; Singleton, 1988;

[2] This figure contains data from the New Zealand Archaeological Association's Site recording scheme (Archsite) and the LINZ Data Service, which is licenced for reuse under the CC BY 4.0 licence.

Gumbley, 2021), a rich recorded traditional history of the Tainui peoples (Jones & Biggs, 1995; Phillips, 1995; Kelly, 2002), and has over 150 pā sites recorded in the landscape (Figure 1.2.1). Six pā were selected for inclusion in this study: Lake Mangakaware 1 (MA1), Lake Mangakaware 2 (MA2), Lake Mangahia (MGA), Taraheke Pā (TAR), Te Uapata Pā (TEU) and Lake Rotokauri (ROT). Archaeological excavations were conducted at these sites to identify, map, and record palisade defences *in situ* (i.e., in their original position or place), with a selection of posts from each site sampled for analysis. Pā situated in wetland environments (i.e., pā found around lakes, in swamps and on river headlands) were targeted for this research because they exhibit the necessary environmental conditions required to preserve their palisade defences (e.g., Hewitt et al., 2021a). However, the interpretations and conclusions generated from this research are representative of pa in general from within the Middle Waikato Basin, allowing broader regional and national comparisons.

As with any attempt to develop a chronological framework for archaeological processes, careful consideration of time theory is essential. In this research, the theory of time perspectivism is applied (see Bailey, 1981; Wandsnider, 2004; Bailey, 2005, 2007; Altizer, 2008; Bailey, 2008; Sullivan, 2008; Epp, 2010; Rzepecki, 2014), and defined by four key ideas: different phenomena operate at disparate timespans and resolutions; these individual phenomena should be viewed at their own timescale; differential time has a distorting effect on perspectives which an awareness of perspective corrects; and observations of time are inherently subjective (Bailey, 2008, p. 201). In this way, time perspectivism applies multiple scales of explanation to examine the archaeological record (Holdaway & Wandsnider, 2008), allowing the exploration of the distinct environmental and cultural processes embodied in the archaeological record (Hull, 2005). A time perspectivism approach is applied through three scales of analysis: event, local and regional.

1.2.1 Objective One (Event Scale)

The first objective focuses on the scale of an individual event: the felling of a tree used to construct a palisade (Felling Date). WMD provides an accurate and precise calendar date for this event, interpreted as a TPQ (*terminus post quem*) for the installation of a post in a palisade row. A TPQ refers to the earliest possible date for an event or artefact deposited in the

archaeological record. This interpretation assumes that each Felling Date represents the year in which the post was installed (i.e., timber was not stored over multiple years and used in multiple phases of palisade construction). This assumption is based on two considerations: (i) the motivation for building a palisade and (ii) the time, resources and organisation required. Firstly, there must be a specific motivation for the construction of these defences, with this event representing a physical response to some internal and/or external variable(s) (economic/socio-political) affecting these populations within a distinct period. Secondly, constructing these defences is a major task requiring considerable labour, time and planning. Therefore, it is unlikely that substantial amounts of timber were felled at a specific time and stored for an unplanned future use. Based on these considerations, in consultation with available archaeological evidence, the earliest Felling Date determined for each pā is used as proxy evidence for when palisades were first constructed (in association with the available archaeological, radiocarbon and traditional history evidence), possibly representing when the site was first occupied as a pā.

1.2.2 Objective Two (Local Scale)

The second objective focuses on the local scale (individual pā site), aiming to identify the development of the palisade defences through time. This scale of analysis assumes that once palisades were constructed, they would have continued to be maintained and/or changed over time. Therefore, while a Felling Date produced on a single post from a specific alignment can be interpreted as a distinct event, when several posts are sampled and analysed from multiple contexts (different palisade rows and areas of a pā), the resulting assemblage likely represents a cumulative palimpsest of multiple events over time (see Section 3.1). Consequently, WMD on several posts from each site can be used to identify possible phases of palisade construction activity. Possible phasing within these defensive structures includes initial construction periods, repair episodes (individual posts replaced within a singular alignment) and redevelopment activities (constructing additional palisade rows within the same area).

1.2.3 Objective Three (Regional Scale)

The third objective focuses on a regional scale, relating all identified phases of palisade construction activity from individual pā into a regional chronological framework. As an

assemblage of posts recovered from an individual pā can represent multiple events over time, an assemblage of posts recovered from multiple pā within a landscape can also be considered a cumulative palimpsest on a regional scale. Therefore, the regional scale of analysis seeks to identify shared spatio-temporal patterns of palisade construction activity in the Middle Waikato Basin over time, including shared episodes of palisade construction, repair and redevelopment. Shared regional episodes of palisade construction activity are interpreted here as evidence of the overarching controlling variables responsible for the emergence, occupation and development of pā over time.

1.3 Chapter Outline

This thesis is divided into thirteen chapters to achieve the above-mentioned aim and objectives. Chapter 2 begins with a discussion on the chronology of New Zealand, focusing on the Transitional Period and the proposed environmental and cultural processes which led to the emergence of pā. Following this discussion, the history of archaeological investigation into pā is explored, outlining the dominant theoretical approaches, the close association of pā with horticulture and warfare, and previous attempts to establish chronological frameworks for pā, highlighting the challenges and limitations of these approaches.

Chapter 3 explores the importance of time theory and its application in chronological development. The theory of time perspectivism is championed as a practical, theoretical approach for interpreting archaeological data, emphasising the importance of a multi-scalar research strategy when undertaking archaeological analysis. Chapter 3 also provides a general overview of radiocarbon dating, including the basic theory and history of the technique, developments associated with calibration and detection methods (AMS), and the application of Bayesian analysis and the WMD technique.

Chapter 4 provides contextual information about the six pā investigated in this study. This review of each site includes a basic site overview, any previous archaeological research conducted, and the publicly available radiocarbon data. Chapter 5 describes the methods used to conduct this research, focusing on archaeological excavation, recording and sampling,

sample assessment and preparation, tree species identification, tree-ring analysis, ^{14}C ring-block sampling and pretreatment, and WMD parameters.

Chapters 6 to 11 detail the results of investigations and analysis from each pā, focusing on the archaeological excavations, assessments of the post assemblages, tree species identification, tree-ring analysis, and WMD (event scale of analysis). Chapter 12 presents the method and results of the local and regional scale analyses, outlining how Bayesian analysis via OxCal modelling is used to interpret the local development of identified palisade defences and episodes of shared regional palisade construction activity. Finally, Chapter 13 presents a synthesis of the research conducted in this study, including a detailed discussion of the conclusions, limitations, and interpretations made during each analysis stage. This chapter culminates with concluding remarks and future research possibilities.

Chapter 2. Context and Background

2.1 The Transitional Period (AD 1450–1650)

Several different hypotheses concerning New Zealand's settlement date have been put forward since the 1980s (see Davidson, 1985; Kirch, 1986; Sutton, 1987; Anderson, 1991, 1995; Higham & Hogg, 1997; Lowe et al., 1998; Newnham et al., 1998b; Lowe et al., 2002; Hogg et al., 2003; Higham & Jones, 2004; Walter & Jacomb, 2007; Wilmshurst et al., 2008; Walter et al., 2010; Wilmshurst et al., 2011; Walter et al., 2017). However, an archaeological consensus of New Zealand's settlement in the late thirteenth century is now generally accepted, with Bunbury et al. (2022) identifying a quantifiable temporal gap between the initial human settlement of the North and South Islands of New Zealand, beginning in the North Island (AD 1250–1275), with the South Island colonised a decade later (AD 1280–1295). This settlement date constrains the period before sustained European contact in the eighteenth century to around 500 years. Within this time frame, 'traditional' Māori society (as encountered by Europeans) emerged from its ancestral Polynesian roots, adapting to a range of theorised environmental and cultural processes. This period of cultural transformation is defined by Anderson (2016, p. 7) as the Transitional Period (AD 1450–1650), describing it as a "shadowland between highlights of Polynesian colonisation and classic Māori culture". The Transitional Period is characterised by several interconnected variables: regionally specific climate deteriorations, the northward retreat of horticultural practices, fluctuating population dynamics, and changes to the social structures of Māori society. Crucially, this period is also when pā are thought to have emerged in New Zealand (Schmidt, 1996), representing a significant change to Māori settlement patterns and a visible sign of this cultural change.

2.1.1 Climate Fluctuation

While archaeological discourse surrounding the influence of climate fluctuations on pre-European Māori society is not new (see Leach, 1981), recent research has sought to clarify the timing and nature of its effects (see Lorrey, 2008; Mann, 2009; Abram, 2014; Goodwin et al., 2014; Roop, 2015; Anderson, 2016; Bunbury et al., 2022). Generally, three broad climatic regimes characterise the climate patterns of New Zealand: La Niña (Blocking), El Niño (Zonal),

and Trough (see Kidson, 2000). The La Niña regime sees wet conditions affecting the north and east of both main islands, with drier conditions in the west. The El Niño regime brings wet conditions to the south and west of the South Island but drier conditions elsewhere. Finally, the Trough regime affects the entire country and is characterised by wet, cloudier and colder conditions (Anderson, 2016, p. 5).

These three climate regimes have varied over New Zealand's occupation history, influencing national and regional climate conditions. For example, the La Niña regime with high precipitation rates was prevalent in the North Island between AD 1350–1500, coinciding with both "near-normal" temperatures before AD 1450 and cooler temperatures after AD 1450 (Lorrey, 2008; Bunbury et al., 2022). In the South Island, dry and mild La Niña conditions were prevalent from AD 1360–1385, with wet and cold Trough conditions around AD 1385–1435 (Roop, 2015). Additionally, unstable Trough conditions have been shown to coincide with the negative phase of the Southern Annular Mode (SAM) wind circulation patterns (Abram, 2014), which are linked to the Little Ice Age (LIA). The timing of these Trough conditions aligns with the lowest temperatures in the Northern Hemisphere during the LIA (AD 1400–1700) (Mann, 2009). Additionally, Petchey and Schmid (2020) identified an extreme oceanic event between AD 1350–1400, coinciding with the LIA's start. In contrast, the short-lived return of the marine ^{14}C signal to its usual level corresponds to a period of stable weather from AD 1400–1450 in the North Island. This climate pattern is indicative of the LIA, which drastically altered the environmental conditions of New Zealand and brought frequent climate downturns accompanied by southerly fronts (Fowler et al., 2012; Lorrey et al., 2014; Roop, 2015). Consequently, it appears probable that cooler seasonal temperatures (linked to the LIA) in the South Island during this period (AD 1400–1700) considerably impacted the Māori economy and subsistence strategies (e.g., Barber & Higham, 2021; Bunbury et al., 2022).

2.1.2 Limitations on Horticultural Production

A significant effect of this fluctuating climate was the extent to which kūmara could be grown in the southern margins of New Zealand. The commencement date of Māori horticultural activities in New Zealand is still debated (see Section 2.2.2). However, Anderson and Petchey (2020) recently reviewed a wide range of evidence regarding the introduction of kūmara to

New Zealand and its dispersal. They found that terrestrial and marine ^{14}C ages modelled with the South Pacific curve (see Petchey and Schmid, 2020) point to horticultural production being established across the North Island coast by AD 1250–1300 and in the South Island by AD 1290–1390. This introduction coincides with widespread landscape burning in the South Island (see Perry et al., 2014; Newnham et al., 2018), which during this period is thought to reflect the vulnerability of these forests to fire rather than any horticultural intent, except perhaps in the northernmost districts. However, Bunbury et al. (2022, p. 5) propose that this period of forest clearance could reflect horticultural practices in the South Island between AD 1280–1450, highlighting that this process continued for approximately 30 years after moa hunting had diminished (i.e., reflecting a change in subsistence). In the North Island, where forests were more resilient to burning, Newnham et al. (2018) previously described a two-step pattern of forest burning, with an initial phase of forest clearance starting just before the Kaharoa tephra deposit, AD 1314 ± 12 (Hogg et al., 2003; Lowe et al., 1998; Newnham et al., 1998b), followed by more extensive inland deforestation around AD 1400–1450. Bunbury et al. (2022, p. 5) suggest that this second phase of North Island inland deforestation is synchronous with expanding horticulture practices between AD 1390–1450, a brief period of finer weather in the North Island, and the expiration of moa as a primary food resource in the South Island. They conclude that the onset of the LIA in the South Island (AD 1385–1435) and the reduction in moa subsistence (AD 1400–1420) pushed Māori communities to their economic limits, increasing mobility to the economically more stable North Island.

Kūmara will not grow in soil temperatures of less than 15 °C (Anderson, 2022, p. 55). Previous research suggests that kūmara cultivation in the early period (before AD 1450) may have reached as far south as the Kaikoura coast and possibly to Banks Peninsula (Trotter & McCulloch, 1999; Bassett et al., 2004). However, a fall in mean annual temperature of 1.0–1.5 °C at sea level by the sixteenth century is suggested to have shifted the viable cultivation limit 145 km north, with cultivation no longer occurring south of the lower half of the North Island (Burtenshaw et al., 2003; Leach, 2005; Burtenshaw & Harris, 2007; Barber, 2012; Anderson, 2022) or cultivation was at least substantially constrained. This proposed shift results in the marginal limit of agriculture being almost as far north as Hawkes Bay (Anderson, 2016), implying a northward retreat in gardening practices coinciding with the LIA (see also Newnham et al., 1998a; Newnham et al., 2018). Heavy rainfall was also problematic for kūmara production and preservation. Rainfall increased substantially over most of New

Zealand in the coldest years of the LIA (AD 1400–1560). It is quite possible that this increased rainfall led to the frequent rotting of kūmara in the ground and while stored, potentially creating a food production crisis in regions of marginal horticultural production (Anderson, 2022, p. 55).

2.1.3 Population Dynamics

Models of past population dynamics have played a key role in investigations of sociocultural change in much of Polynesia (e.g., Kirch, 1984b; Kirch & Rallu, 2007; Pulestion & Tuljapurkar, 2008). These models generally examine the relationship between food production and population growth (Kirch, 1984b, p. 103) and typically describe a small founding population that undergoes rapid demographic expansion through the exploitation of abundant natural environments and resources (Anderson, 2002). These natural resources supplemented settler populations as they transitioned their subsistence strategies into food-producing economies (see Kennet et al., 2006). Once these settler populations were established, population levels continued to increase via agricultural intensification, investment in landesque capital (e.g., Ladefoged & Graves, 2007), and the spread of agriculture into marginal production zones (see Kirch, 1984b, 2007). Population growth eventually plateaus due to environmental constraints and/or social processes relating to the emergence of socio-political hierarchies (Kirch, 1984b). However, unique regional-scale variations in population growth are evident through proposed links between ecological, demographic, and cultural factors (Kirch, 2007). In particular, population growth patterns are influenced by the regional suitability for Polynesian food production and the increased competition associated with establishing these systems (see Anderson, 2001; Kirch, 2004, 2007; Kirch & Rallu, 2007; Lee & Tuljapurkar, 2008; Thomas, 2008). Because of this relationship, local and regional scale palaeodemographic models are crucial when attempting to develop a detailed understanding of the past.

Brown and Crema (2021) demonstrated the importance of this regional scale, revealing that nationwide demographic models obscure regional variation in New Zealand. They suggest a low population density in the northern horticultural area until AD 1450–1500, followed by a period of growth that culminates in a distinct population plateau. This population growth model is similar to the “logistic” settlement hypothesis (see Kirch, 1984b; Anderson, 2002), which

proposes that populations in the north reached carrying capacity when the landscape became densely populated and the productive and marginal horticultural regions were exhausted. Brown and Crema's (2021) model for the non-horticultural south suggests that the population rapidly grew before sharply declining as faunal resources diminished around AD 1450 (see also Allentoft et al., 2014; Jacomb et al., 2014). Building upon the work of Brown and Crema (2021), Bunbury et al. (2022) utilised a much larger and diverse ^{14}C dataset, proposing a logistic population growth (up to AD 1400) as a general population trend in New Zealand. They also highlight significant differences in North Island and South Island population trends, including a shift in population ~100 years earlier than previously suggested, that corresponds with regional climate trends, deforestation patterns, and changes in subsistence practices.

Closely associated with population dynamic trends is the occurrence of population migration. Migration is a characteristic feature of the Transitional Period and is a dominant theme in the oral traditions of that time (e.g., Jones & Biggs, 1995; Phillips, 1995; Kelly, 2002; Anderson, 2014). For example, deliberate inland Tainui migration inland from Kawhia in the Waikato is proposed to have begun around AD 1520, and by around AD 1550, people had moved further east, north, and south (Anderson, 2014, pp. 114–119). Anderson (2016) hypothesised that a rising population was reaching the point where the redistribution of people was becoming necessary, or a drop in mean annual temperature in the period between AD 1400–1700 (associated with the unstable trough conditions which coincided with the negative phase of the SAM wind circulation patterns discussed above (see Abram, 2014)) affected groups on the horticultural margins, stimulating migration to regions with a warmer and more stable climate (see also Newnham et al., 1998a; Newnham et al., 2018; Brown & Crema, 2021; Bunbury et al., 2022).

Later, Anderson (2022, p. 46) proposed that population migrations in New Zealand were almost inevitably hostile incursions involving warfare, inducing subsequent migration and additional episodes of conflict. Ultimately, migrational conflict resulted in the establishment of residential rights for newly arrived migrants. Following this hypothesis, Anderson (2022, p. 46–53) proposes that population migrations can be used as an index of the frequency of notable warfare (c.f. Thorpe, 2003, p. 146), highlighting three phases of long-term patterns in warfare and migration: (i) Phase I: Colonising migration (AD 1280–1340), (ii) Phase II: Early tribal

migration (AD 1460–1640), and (iii) Phase III: Late tribal migration (AD 1820 onwards). These three phases are evenly spaced across the pre-European era and are proposed to be separated by intervals of less frequent warfare that lasted a century or more. Anderson (2022, p. 53) argues that the peaks of this activity occurred about AD 1300, AD 1500–1600 and AD 1820, approximately 200 years apart. Anderson highlights that these periods are more or less equidistant in time, implying that they could represent a cyclical behaviour of cultural activity.

2.1.4 The Emergence of Pā

The appearance of pā in the Transitional Period is thought to reflect the emerging pressure brought on by these environmental and cultural processes. Schmidt (1996) proposes the national onset of pā construction around AD 1500–1550. Generally, the emergence of pā in the archaeological record is stated to reflect a response to protect horticultural zones and food stores during increasing population density and competition (Groube, 1970; Law & Green, 1972; Green, 1975; Fox, 1976; Davidson, 1985; Irwin, 1985; Davidson, 1987; Allen, 2008a; Anderson, 2014; Allen, 2016; Anderson, 2016). Horticultural constraints consequent to migration from the tropics to temperate New Zealand meant that only one kūmara crop could be produced yearly (Burtenshaw et al., 2003; Leach, 2005; Burtenshaw & Harris, 2007; Barber, 2012; Anderson & Petchey, 2020). Consequently, protecting that single harvest for food and seed tubers and the rich sources of wild plant foods was more critical (Anderson, 2022, p. 43). Anderson (2016, 13) hypothesised that this increased competition influenced the construction and distribution of pā sites, which closely follows the distribution of horticulture. However, the construction and occupation of pā cannot solely be thought of as a function of kūmara storage and protection (see Section 2.2.1), as these sites are also associated with habitation, community identity, religion, and status (Mihaljevic, 1973; Daugherty, 1979; Irwin, 1982; Davidson, 1984; Barber, 1996; Sutton et al., 2003).

2.2 An Archaeological Examination of Pā

Pā have long been the focus of rigorous archaeological debate and discussion (e.g., Best, 1927; Groube, 1964; Pick, 1968; Gorbey, 1970; Green, 1970; Groube, 1970; Law & Green, 1972; Fox, 1976; Irwin, 1982; Davidson, 1984; Irwin, 1985; Davidson, 1987; Marshall, 1987; Sutton, 1993a, 1993b; Allen, 1996; Schmidt, 1996; Allen, 2008b; Hogg et al., 2017). Early

archaeological interpretations of pā were dominated by two theoretical paradigms: (i) culture history studies and (ii) settlement pattern analysis. Both approaches attempt to simplify the archaeological evidence identified at pā by controlling for spatial and chronological variation. The culture history approach attempted to use material culture (i.e., diagnostic artefacts) recovered from defined stratigraphic contexts to establish temporal relationships between sites in different regions. This approach sought to tie pā together in a regional sequence using the presence or absence of specific 'diagnostic' artefacts and complementary ^{14}C dating (see Golson, 1960a; Golson, 1960b; Shawcross, 1964, 1968; Fox, 1976). However, identifying portable artefacts suitable for use as a diagnostic chronological signature proved challenging, with several extensive pā excavations failing to produce the required artefacts (see Parker, 1962; Shawcross, 1963, 1966; Furey, 1996). Furthermore, the resulting evidence from these excavations suggested that pā were not short-term, single-phase sites. Instead, pā often exhibit long and complex occupation histories, which further complicated attempts to classify pā into regional temporal sequences (see Golson, 1961a, 1961b; Ambrose, 1962; Davidson, 1987).

Consequently, pā were treated as diagnostic artefacts, with the form and scale of their defences defining specific pā typologies (Golson, 1959, p. 54; Green, 1967, p. 102). These classifications were based on the presence or absence of features, such as terracing, ditches, and banks (e.g., Groube, 1970; Bellwood, 1972a, 1972b). This solution viewed changes in form as developmental, which could theoretically be tracked chronologically (Golson, 1957; Golson & Green, 1958; Fomison, 1959; Buist, 1964; Groube, 1964, 1970; Fox, 1976). While this solved the lack of traditional diagnostic artefacts, the proposed classifications could not be quantified by ^{14}C evidence due to limitations of ^{14}C sample number, a reliance on bulk charcoal radiometric ^{14}C dates affected by inbuilt age, and the absence of Bayesian chronological modelling. Therefore, the developed typologies could not be seriated chronologically (Jones, 1983; Irwin, 1985; Sutton, 1993b). Furthermore, viewing pā as an artefact makes it easy to lose sight of the social context and physical landscape in which they were situated. In this way, pā are viewed as a singularity, devoid of the human experience and agency associated with the settlement.

In contrast to the culture history approach, settlement pattern analysis uses archaeological materials to reconstruct a landscape settlement system during a specific period, allowing an

examination of the communities that occupied these settlements (see Groube, 1964, 1965; Green, 1967; Gorbey, 1970; Cassels, 1972a, 1972b; Law & Green, 1972; Clarke, 1980; Kirch, 2004; Phillips & Campbell, 2004; Irwin, 2013). This approach generally focuses on two broad influences on observed settlement patterns (Morrison & O'Connor, 2015, p. 2). First is the influence of the environment on where communities undertook activities within the landscape, focusing on the relationship between spatial organisation and variation in land use concerning environmental variability. Second is the influence of the location, size, and arrangement of social groups within the landscape, focusing on the relationship between communities and the development of different forms of human spatial organisation. These two focuses require an examination of both natural (environmental) and social (cultural) environments and how they influence the configuration of the archaeological record (see Fish, 1999). Essentially, the settlement pattern approach integrates the spatial, economic, pedological, and ecological data related to a site (pā) to contextualise it with the surrounding landscape.

The strength of the settlement pattern approach is that all sites and site types are analysed with equal weight. However, the prominence and importance of pā within a landscape are challenging to integrate within these investigations without overshadowing considerations of 'peripheral' sites. Inevitably, the prominence, size and visibility of pā have resulted in these sites occupying a significant focus within settlement pattern analysis in New Zealand (e.g., Groube, 1964a, 1965; Green, 1970; Davidson, 1978; Irwin, 1985; 2013, 2020; Allen, 1994, 1996, 2008a), which, in turn, has created several acknowledged methodological biases, including varying approaches to site and landscape surveys, chronological controls, interpretations of environmental change, and the use of traditional knowledge sets and theoretical approaches (see Phillips & Campbell, 2010, pp. 96–99).

Almost all settlement pattern analyses involve some interpretation, approaching the survey and geospatial mapping of a landscape with some predeterminations about the resulting settlement pattern. However, these interpretations can lead to a lack of standardisation in the recorded data, as no two individuals will interpret the landscape in the same way owing to factors such as experience, method, and the time and date of each survey. Furthermore, considerations of the scale of an archaeological site and how they are contextualised within the landscape (i.e., the grouping or separation of deposits and features within the landscape) are inconsistently

applied. Site classifications are almost always the product of functional, topographic, morphological or chronological considerations and, therefore, can also be applied inconsistently. It must also be remembered that observed settlement patterns are physical representations of complex socio-political and economic processes. Thus, the complexities of these variables can be lost in context when focusing solely on the physical remnants of past occupations. Archaeological sites can also be obscured in the landscape for several reasons, including limited occupation size, post-depositional processes, and timescale. Nevertheless, these 'invisible' sites are important when interpreting settlement patterns because focusing on prominent 'visible' sites distorts our understanding of the archaeological landscape. This effect can be mitigated to a certain extent through intensive site survey and excavation, where all site types (i.e., from small midden sites to large pā) are investigated on an equal scale. However, such an intensive approach is rarely applied (see Davidson 1978, for example).

The 1980s saw a resurgence of pā investigations (Prickett, 1980, 1982; Jones, 1983; Prickett, 1983; Irwin, 1985; Lilburn, 1985; O'Keeffe, 1991), with several large-scale archaeological projects undertaken regionally. The Pouērua Archaeological Project (Marshall, 1987; Sutton, 1993a; Sutton et al., 2003) aimed to combine both settlement pattern analysis and culture history studies. Socio-political factors influencing occupation were a central theme of the project, with the archaeological landscape seen as the product of interactions between the cultural and natural landscape. When the pā at Pouērua were scrutinised, their specific forms, functions, and meanings were contextualised within the broader archaeological landscape. Once an understanding of the local context was gathered, the broader connotations of pā on a national scale were considered. The Pouērua project concluded that pā could not simply be described as an artefact, proposing that pā performed various complex functions and have complicated occupation histories. It is clear from the evidence gathered from Pouērua that people put an immense amount of effort into constructing, maintaining, and remodelling pā, making them the most visible evidence of occupation in the landscape. This observation led Sutton et al. (2003) to suggest that visibility may be their most important function. This interpretation also has consequences concerning aspects of community identity and considerations of status or mana within inter-hapū relationships.

2.2.1 Classification and Function

As discussed above, previous attempts to classify and understand pā were firmly based on form and function analysis. For example, Groube (1964a) defined four functional classes of pā: fortified village, citadel fortification, retreats, and fortress, distinguishing between these classes through the nature of the habitation associated with the pā. Occupation length and population size were critical variables used to distinguish between these typologies. These classifications were widely influential and were adopted by many archaeologists at the time, including by Bellwood (1971c, 1971a) in his interpretations of pā at Lake Mangakaware and Otakanini Pā. Later, Mihaljevic (1973, p. 150) proposed a tri-functional pā classification scheme, defining pā as settlements, fortresses, or temples, stating that any pā could have specialised in one or a combination of these functions. His classifications focused on the site's defensive structures, their ritual nature, and the type of habitation occurring at the pā. Mihaljevic emphasised the role of defences as symbolic boundaries, defining a space of community pride and prestige. Daugherty (1979) also developed a pā classification scheme, with particular emphasis on the style of warfare catered for in the pā's construction, seeking to explain the variation of forms and similarities to fortifications in Polynesia. Daugherty distinguished three functional types: homeland, refuge, and strategic, with the critical difference being the nature of habitation.

These classification schemes all attempt to define pā typologies by their defensive characteristics and the perceived nature of the associated community activities. The nature of these considerations tends to emphasise cultural processes (i.e., demographic change – hāpu formation and division) and economic tensions (i.e., resource protection) within the broader cultural landscape, leading to the construction and occupation of pā. However, Barber (1996, p. 876) notes that the appearance of pā in regions of both high and low population density, including the non-horticultural and sparsely populated far south of New Zealand, is difficult to explain as a factor of demographic pressure or as a direct economic link to horticultural production. However, it should also be noted that the number of pā recorded in the South Island is low (compared to the horticultural north) and could represent different motivations for construction than those built in the north.

Despite these classification schemes differentiating pā through considerations of functions other than defence (i.e., habitation, religious, economic), defence is always considered a primary function of the site type. This situation stems from the observation that apart from the built defences, most archaeological features identified at pā are also found at undefended sites. This situation raises important questions about how these defences are used to differentiate pā from other site types. For example, can archaeological sites located in environments with topographical defences (e.g., a storage pit cluster situated on a high point that is protected on multiple sides by steep ridges) be differentiated from pā with built defences? Both examples provide a defensible location, with the difference being that one is entirely natural while the other is built at the cost of time, workforce, and resources. This example highlights how focusing on the form and function of these defences can lead to defining other functions as secondary. Pā are frequently the most visible representation of community identity within a landscape, often built on an elevated platform, on a grand scale, and at a high cost. This observation was noted by Davidson (1984, p. 185), who remarked: "The significance of pā as focal points of community activity and centres of community pride and prestige is an important point". However, she also pointed out that these considerations should not be overemphasised at the expense of their defensive function (see also Irwin, 2013). Conversely, by overemphasising the defensive function of pā, it could be argued that other critical functions of pā and what they represented to the communities that inhabited them are being neglected or underplayed.

While it is clear that some pā were little more than fortified food stores (e.g., Law & Green, 1972), others were complex sites exhibiting a range of features and functions with complex histories (e.g., Ambrose, 1967; Shawcross, 1968; Bellwood, 1971a; Fox, 1976, pp. 22–23; Davidson, 1984, p. 185; Jones, 1994; Wilkes, 1995; Irwin, 2004a; Furey et al., 2017). Wilkes (1995, p. 255) suggests that the defensive arrangements identified at certain pā are often "massively out of proportion" to the site's size or "any conceivable scale of attack" and that their construction in some cases can be considered for "prestige rather than from dire necessity". However, such notions are difficult to assess because it is hard to determine the frequency or scale of conflict associated with a specific pā at a particular time. This observation also does not account for time depth, with the defences remodelled and adapted over time in response to changing variables in the cultural landscape. Crucially, this variability indicates that these

defences also functioned to bind space and modify behaviour rather than solely operating as a defensive feature.

This concept was explored further in the 1990s, with a specific focus on the phenomenon of monumentality (Kirch, 1990; Graves & Sweeney, 1993; Herdrich & Clark, 1993; Kolb, 1994). Barber (1996, p. 868) describes how monumental architecture has long served as a physical representation of "chiefly dominance and hegemony" in stratified Polynesian societies. However, if socio-political complexity is archaeologically linked to monumentality, large-scale buildings in less complex societies must also be accounted for (Barber, 1996, p. 868). Throughout Polynesia, several societies have built large, highly visible structures advertising their presence in the landscape, thus asserting their ongoing attachment to the land (Bellwood, 1978b; Jennings, 1979; Kirch, 1984a, 1990; Graves & Sweeney, 1993; Kirch & Green, 2001; Kennett & McClure, 2012). These structures all require great communal effort, display occupancy and identity, and exhibit a signal of power. Additionally, pā construction for ideological or religious purposes cannot be ruled out and, in some cases, could potentially represent a change in Māori religious orientation favouring the agricultural deity Rongo (Anderson, 2022, p. 45).

Importing these ideas to New Zealand contexts, Marshall (1987) interprets specific pā at Pouērua as places of mana and communal activity similar to Polynesian marae. Sutton (1990, 1991, 1993b, 1993a) and Sutton, Furey, and Marshall (2003) also emphasise the replication of crucial social structures in the internal organisation of Pouērua Pā, especially as represented by differential elevation. Ultimately, these interpretations suggest that pā may be considered a form of ritual architecture in that they were prominent symbols in the landscape and a physical manifestation of a community's identity and wealth (Sutton et al., 2003, p. 237). However, again, it must be remembered that pā were not static settlements. Therefore, pā, as viewed by archaeologists, represent an amalgamation of past functions and behaviours in association with other key variables such as terrain, economic needs, social relations, the association of broader societal groups (i.e., iwi) and social considerations (i.e., ideology), and time (Davidson, 1984, pp. 185–188; Barber, 1996, p. 876).

Regardless of their primary function, Barber (1996, p. 986) suggests that pā served as permanent foci of community identity within the landscape, creating visible spatial relationships which competing groups could view. In this sense, the defences at these sites ensure the physical and spiritual security, productivity, and permanence of crucial places of settlement, economy, and ceremonial power in the territory of the occupying hapū (Barber, 1996, p. 876). Effectively, sustained pā construction and occupation ensured that mana and productivity increased, as well as the physical security of the place, as descent-group identity was enhanced (Schwimmer, 1978; Phillips, 1995; Allen, 2008a). While the defensive features of a pā are crucial to their interpretation, it is also clear that pā performed a range of functions beyond providing a fortified refuge. Therefore, pā must be considered multifunctional spaces, defined in this research as fortified places, capable of performing various roles for local populations, which inevitably change and vary over time.

2.2.2 Association with Māori Horticulture

The link between pā and the facilitation and protection of economic production is an idea that is continually referred to in archaeological discourse (see Green & Shawcross, 1962; Pick, 1968; Groube, 1970; Bellwood, 1971b; Cassels, 1972a; Law & Green, 1972; Fox, 1976; Irwin, 1982; Davidson, 1985; Irwin, 1985; Davidson, 1987; Allen, 1994, 2008a; McIvor & Ladefoged, 2015; Allen, 2016), including the relationship between the development of horticultural practices and storage pit technology with the construction and proliferation of pā. The spatial correlation between the distribution of pā and the horticultural landscapes throughout New Zealand is convincing. Pā are overwhelmingly concentrated in the horticultural north of the country, situated around environments (i.e., lakes, rivers, and appropriate soil types) that facilitated crop production (particularly kūmara) in New Zealand's temperate climate. These horticultural landscapes are often large in scale, emphasising how these activities were part of a complex, time-consuming, and energy-intensive process, thought to reflect substantial population levels and social organisation. Along with the substantial investment involved and the difficulty of producing these crops in a suboptimal climate (i.e., limited growing season, restricted distribution of viable soils, and the difficulty of clearing land), these activities are often thought to have been associated with increased levels of competition and territoriality, reflected by the construction of pā within these landscapes. Therefore, to contextualise the relationship between pā and resource-driven competition and conflict, it is necessary to

examine the archaeological discourse surrounding Māori horticulture, considering these landscapes within the Middle Waikato Basin with respect to the distribution of pā throughout the study area.

Six tropical plant species are known to have been grown around the country: kūmara (*Ipomoea batatas*), gourd/hue (*Lagenaria siceraria*), yam/uwhi (*Dioscorea alata*), taro (*Colocasia esculenta*), paper mulberry/aute (*Broussonetia papyrifera*), and ti pore (*Cordyline fruticose*) (Bassett et al., 2004). Several of these species are evidenced to have been grown across the North Island and, to a lesser extent, at the top of the South Island (Barber, 2004). However, yam, aute, and ti pore were not grown beyond the extent of the northern North Island (Barber, 2004; Furey, 2006). The earliest considerations of Māori subsistence strategies suggested that at the time of New Zealand's settlement, populations were without horticulture, with early economies primarily focused on hunting and gathering (i.e., the 'Moa-hunter Period') (Best, 1925; Buck, 1950; Duff, 1956). However, Golson (1959) was the first to cast doubt on this hypothesis, highlighting the strong influence of research focused on the South Island, where horticulture was probably limited. Later, Green (1972) rightly questioned why migrating Polynesians would retain material culture links to their ancestral homeland but abandon elements of their subsistence strategy.

The first suggestion of a staged model of horticultural introduction and development was proposed by Yen (1961), who argued for a three-stage model: introduction, experimental and systematic. Groube (1967) proposed that the first two stages of Yen's model could be achieved in as little as two generations or less, and that early horticultural practices underwent adaptation in Northland before the technology was transmitted to increasingly more marginal areas. This idea was expanded on by Green and Shawcross (1962), who proposed six developmental phases, allowing for horticulture to be present within the Settlement Phase of New Zealand, but with this period characterised by potential crop failure (see also Green, 1970). Later, Leach (1979b, 1979a) refined Yen's model, allowing for the regression of horticulture due to climate deterioration. Leach's model proposed five phases: (i) Introduction, (ii) Experimentation, (iii) Regional Consolidation, (iv) Expansion from Secondary Centres, (v) Retrenchment and Revival.

It is now understood that early forms of Māori horticulture probably commenced almost immediately after settlement (Anderson & Petchey, 2020), with evidence of early horticultural sites recorded at the Clarence River mouth in Marlborough, the Wairarapa coast and Whangamatā in Coromandel (Leach & Leach, 1979; Trotter & McCulloch, 1997; Gumbley, 2014a; Gumbley & Laumea, 2019). However, it is also clear that horticultural practices developed over time, resulting in more complex questions surrounding the intensification and systematisation of gardening practices and subsequent economic and socio-political changes to Māori society (see Anderson & Petchey, 2020). These considerations are particularly relevant when considering the development of high-intensity and systemised gardening within the northern interior (see Law, 1968; Higham & Gumbley, 2001; Sutton et al., 2003; Barber, 2004; Bassett et al., 2004; Gumbley et al., 2004; Furey, 2006; Law, 2008; Barber, 2012; Gumbley & Hutchinson, 2013; Gumbley, 2014a; Anderson, 2016; Gumbley & Laumea, 2019; Anderson & Petchey, 2020; Barber & Higham, 2021; Gumbley, 2021). The most extensive pre-European Māori horticultural landscapes are concentrated in the Auckland, Bay of Plenty, Taranaki and Waikato regions (Taylor, 1958; Sullivan, 1972; Barber, 2004; Gumbley et al., 2004; Furey, 2006; Law, 2008; Anderson, 2016; Anderson & Petchey, 2020; Gumbley, 2021).

This spatial distribution is unsurprising, as the tephra- and alluvium-derived soils suitable for intensive horticultural production are situated across these regions, covering roughly 40% of the North Island of New Zealand (see Hewitt et al., 2021b). These soils can broadly be classified into two main groups: (i) Pumice Soils (15% of the North Island) and (ii) Allophanic Soils (12% of the North Island). Pumice Soils are common across the central and eastern North Island and are formed on very young, weakly consolidated pyroclastic deposits that are low in clay content and deficient in major nutrients and trace elements (Hewitt et al., 2021b). Allophanic Soils are identified mainly in central North Island, formed mainly on fine-grained tephra layers in Taranaki, south and west of the Volcanic Plateau, and in parts of the King Country, Waikato and western Bay of Plenty (Hewitt et al., 2021b). Smaller areas of Allophanic Soils can be found on basaltic scoria cones in Auckland and Northland. Allophanic soils have high organic carbon content, good aeration and water retention, low bulk density, and are free draining. All the areas where these soils are identified have extensive evidence of Māori horticulture (Law, 1968; Higham & Gumbley, 2001; Sutton et al., 2003; Barber, 2004; Bassett et al., 2004; Gumbley et al., 2004; Furey, 2006; Law, 2008; Barber, 2012; Gumbley &

Hutchinson, 2013; Gumbley, 2014a; Anderson, 2016; Gumbley & Laumea, 2019; Anderson & Petchey, 2020; Barber & Higham, 2021; Gumbley, 2021).

Since the early 2000s, research on horticultural production has featured prominently in the archaeological literature of New Zealand (Higham & Gumbley, 2001; Barber, 2004; Gumbley et al., 2004; Furey, 2006; Barber, 2010, 2012; Anderson & Petchey, 2020). However, the absence of considered research focusing on crops, yield volumes, and agronomy has previously made it impossible to rigorously assess the impact of changes in production (see summary in Barber, 2004). Recently, Gumbley (2021) conducted a multidisciplinary examination of the Waikato Horticultural Complex (Figure 2.2.1). Gumbley defines pre-European Māori garden sites in the Waikato by three defining features: (i) the presence of borrow pits, (ii) (adjacent) soils that have been heavily modified (including mounding) by the addition of sand and gravel as well as charcoal, and (iii) the presence of small-scale domestic activity components (interpreted to represent seasonal kāinga). These horticultural sites in the Waikato are concentrated along the Waikato River from Arapuni to Taupiri, in areas on the Horotiu Plain, and along the margins of the Waipā River and its tributaries (see Grange et al., 1939; Taylor, 1958; Law, 1968; Clarke, 1977; Gumbley et al., 2004; Gumbley & Hutchinson, 2013; Hewitt et al., 2021a; Gumbley, 2021). Waterways are natural highways for the movement of people and resources, and provide a clear boundary where disputes over territory and resources are likely to occur (Pardoe, 2014). Therefore, it is no surprise that pā within the region are clustered around these areas (Figure 2.2.2), following the main rivers (Waikato and Waipā) and tributaries that cross the landscape. However, the spatio-temporal relationship between these two archaeological features has yet to be explicitly tested within the region.

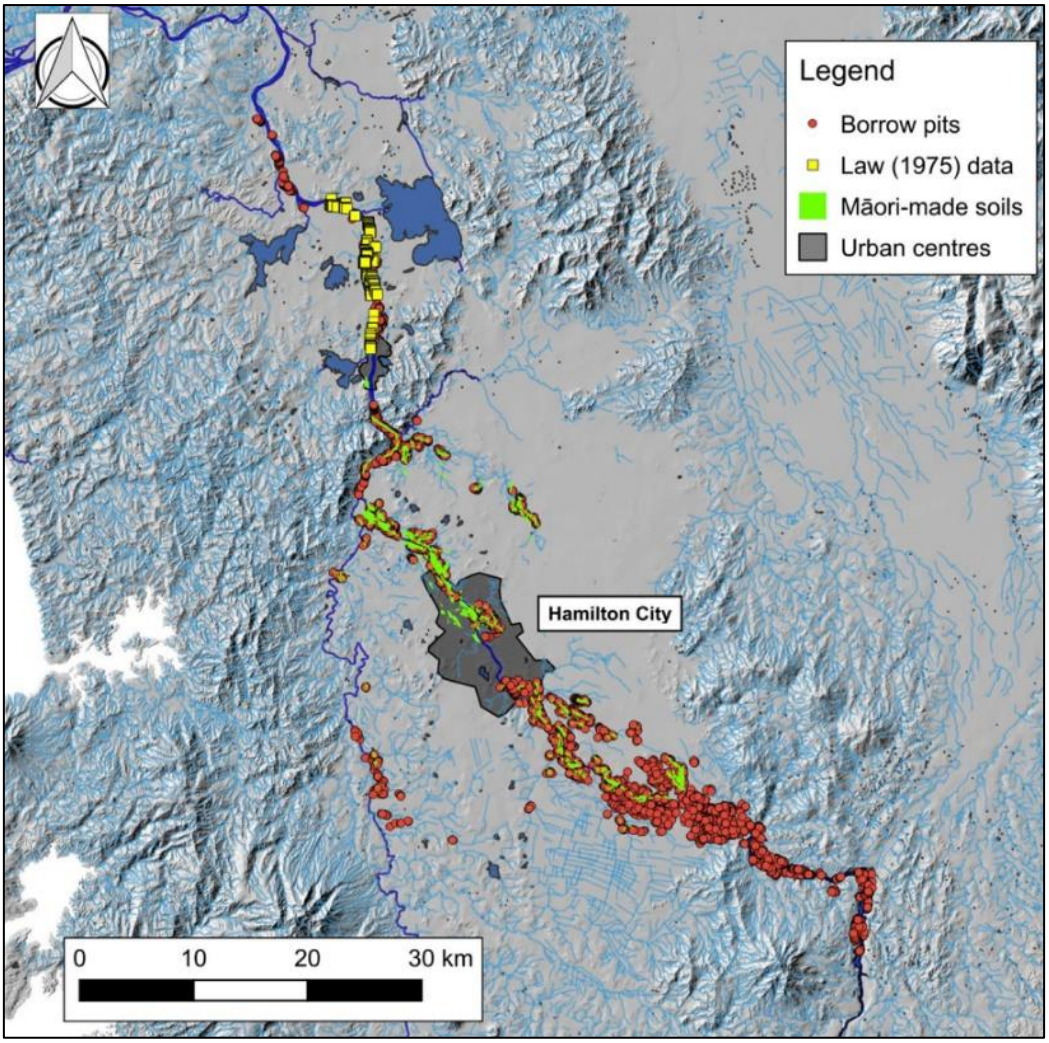

Figure 2.2.1. The spatial extent of the Waikato Horticultural Complex[3].

[3] This figure was originally produced by Gumbley (2021), Figure 5.1, and is included with permission.

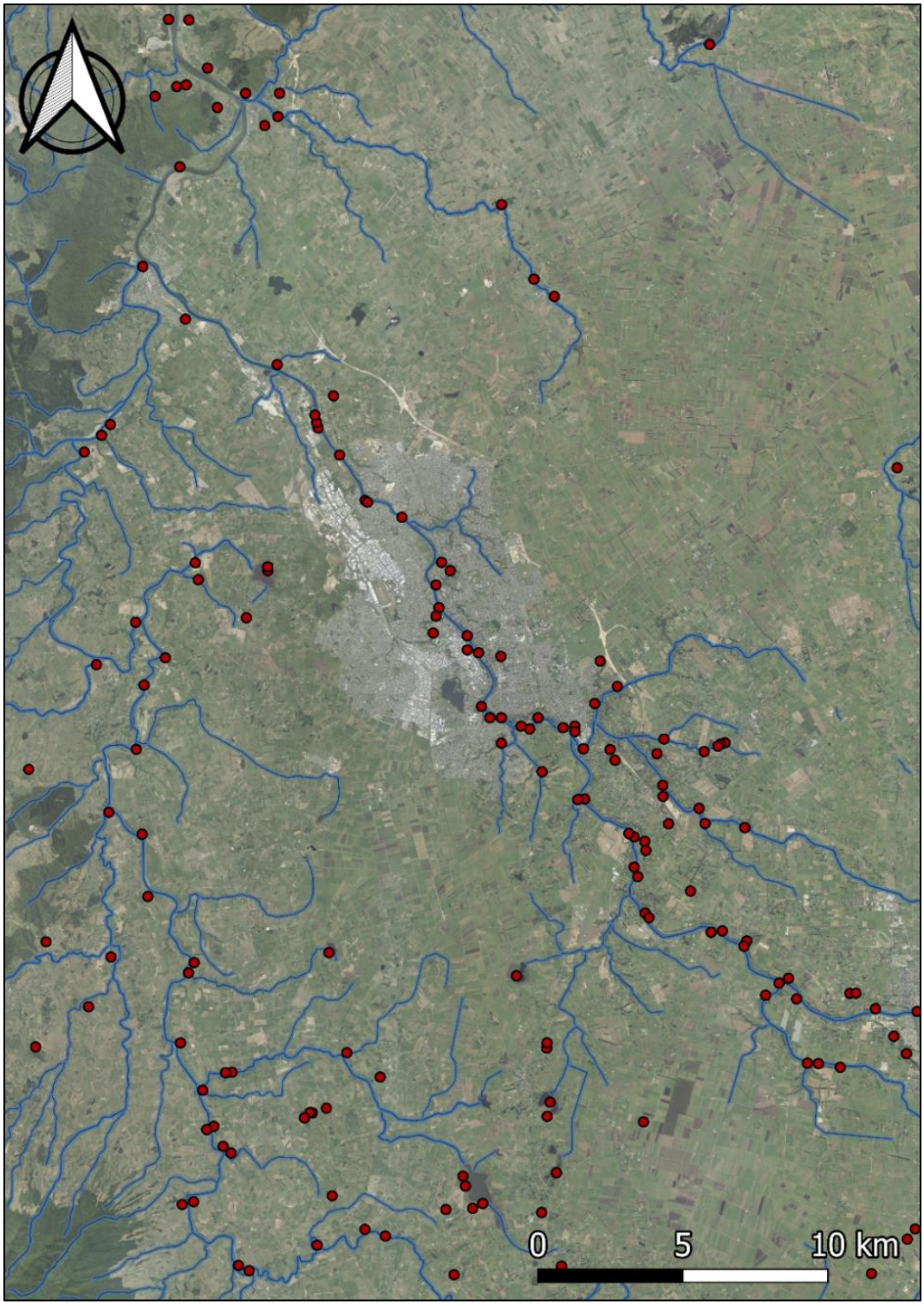

Figure 2.2.2. The spatial relationship between pā (red points) and the Middle Waikato Basin's main rivers and tributaries (blue lines)[4].

[4] This figure contains data from the New Zealand Archaeological Association's Site recording scheme (Archsite) and the LINZ Data Service, which is licenced for reuse under the CC BY 4.0 licence.

Gumbley (2021, pp. 161–168) estimates the establishment of the Waikato Horticultural Complex at some point in the sixteenth century, with continuous replication until the early or middle nineteenth century. Radiocarbon data indicates that the Cambridge and Leamington areas were the early focus of these activities, with sites near the river appearing in the early to middle sixteenth century. Sites more distant from the Waikato River are consistently much younger, with the most remote sites dating to the eighteenth or early nineteenth centuries. By the late sixteenth to early seventeenth centuries, these horticultural practices had spread ~50 km down the Waikato River, at least as far as Taupiri. Given the established spatial relationship between pā and these horticultural zones, if resource-driven competition stemming from the availability of these areas and the resources they provided is the primary variable driving the construction and occupation of pā, it seems probable that the spatio-temporal distribution of pā should follow the spread of the Waikato Horticultural Complex northward from Cambridge/Leamington to Taupiri/Huntly.

2.2.3 Competition, Conflict and Pā

The implicit relationship between horticultural production, storage technology, and pā construction also led to the development of the ecological model of Māori warfare. This model, first proposed by Vayda (1960), was based on an analysis of Māori oral history, ethnography, and ethnohistory. Vayda highlighted the scarcity of appropriate gardening areas in New Zealand and the difficulty of clearing temperate rain forests, creating a scenario favouring endemic resource-driven warfare (Vayda, 1956, 1960, 1976; Davidson, 1984, 1987; Kirch, 2000). This model suggests that warfare, which was central to the rest of Polynesia, became a crucial feature of Māori society, evidenced by the construction and proliferation of pā (see also Vayda, 1960, 1976; McGlone, 1983; Davidson, 1984, 1987; Anderson & McGlone, 1992; McGlone et al., 1994; Kirch, 2000). The difficulty of clearing temperate rainforests is largely overplayed in Vayda's model, as forest clearance was primarily achieved via fire rather than felling (Anderson, 2022, p. 43). Additionally, rather than replanting previously cleared forest areas, Māori preferred to clear virgin areas to expose and exploit the most fertile soils for horticultural production (Ballara, 2003, p. 18). Additionally, Māori traditional history or historical observation does not support incremental territorial expansion through warfare. Conflicts occurred between neighbouring families and hapu, but organised warfare was

conducted primarily against groups at some distance away, usually non-kin (Anderson, 2022, p. 43).

Later, Vayda (1976) refined his views on the relationship between ecology and culture (see also Scaglion, 2008). However, the premise of populations limited by environmental variables, available horticultural zones, and increasing socio-political pressures resulting in cycles of food-driven conflict has continued to dominate archaeological research on warfare in the Pacific (e.g., Younger, 2008; Field & Lape, 2010). However, material evidence of past conflict and warfare is often vague, providing limited insights into the type of observed conflict, the participants and the motivation for warfare and aggression (Clark & Lister, 2022). Ongoing research since the 1990s has complicated the dominant ecological model by making a case for additional factors that appear to have been critical to how Māori society evolved (Irwin, 1985; Sutton, 1990; Allen, 1994; Barber, 1996; Allen, 2008a, 2008b, 2016; McCoy & Ladefoged, 2019).

Allen (1996) investigated the economic bases of Māori chiefdoms in Hawke's Bay, exploring the relationship between the potential for economic control and the size, complexity, and integration of chiefdoms and other social groups. Allen's research presented a political model interpreting the distribution of larger pā in ecologically rich areas as reflecting the consolidation of resources and power by chiefdoms (see also Allen, 2008b, 2008a, 2016). He argued that security in the pre-European cultural landscape became tied to access to productive horticultural soils and other resources, including investments in land clearance and garden productivity. This dependence was the foundation for forming polities, with chiefs gaining political power by providing security to populations through the control of territory and their ability to protect it from other competing groups in the region. Allen argues that pā were the principal focus of this process. In essence, the construction of pā close to horticultural land allowed a chief to produce and protect valuable resources, meaning they could mobilise labour and create regional organisations (Allen, 1996). However, Allen failed to include the distribution of other site types in his analysis, focusing solely on pā as an expression of chiefly power rather than community solidarity (Phillips & Campbell, 2004, p. 98). Additionally, Allen's assumption that pā can be equated to discrete social groups occupying fixed territories is problematic within the context of Māori society during this period (Marshall, 2004, p. 70).

Irwin (2013) also focused on the significant change represented by the appearance and spread of pā in New Zealand (see also Irwin, 1985). In a case study, Irwin highlighted the Pouto Peninsula, located on the northern Kaipara Harbour, where twenty pā of small or medium size are located in the horticultural hinterland, with three large pā located at the borders of Pouto. Irwin (2013, p. 321) suggests that around the middle of the seventeenth century, only a few pā were occupied on the peninsula and that most of the pā recorded in the area were built around AD 1800. This suggestion implies that at some point, the cultural landscape of Poutu passed through a stress threshold, resulting in a wave of pā building in the late eighteenth and early nineteenth centuries. Irwin hypothesised that the settlement system experienced some form of pressure, either internal, such as the decreasing availability of horticultural land, or external, such as competition from neighbouring populations, resulting in the need for defence at a regional level. Irwin emphasised the bilateral kinship of Māori society, resulting in a flexible system of multiple rights to resources and land, highlighting that in both the North and South Islands, settlements were frequently occupied by members of more than one hapū. Thus, rights to resources overlapped on the ground, and mobility was high, resulting in fluid social relations (see also Anderson, 1998; Ballara, 1998; Phillips, 2000). However, regardless of the community's composition, Irwin suggests that these pā were defended collectively, with the scale of defences reflecting the scale of the polity. Therefore, as the density of pā increased, social relations and political leadership would have been impacted as settlements and competition intensified in the north.

However, when Irwin's chronological analysis of the pā located on the Pouto Peninsula is closely scrutinised, it is clear his interpretations are based on limited chronological evidence. Thirteen pā on the Pouto Peninsula have been radiocarbon dated, each represented by a single radiometric ^{14}C date with large standard errors and calibrated age ranges. These ^{14}C dates come from terrestrial (charcoal) and marine (shell) materials and, as previously discussed, suffer from precision issues associated with calibrating ^{14}C ages into calendrical time throughout a period of relatively uniform ^{14}C production. It is also important to note that a single ^{14}C date does not accurately reflect the occupation history of a pā, which requires a far larger dataset with strict stratigraphic and provenance controls to define a construction date. Therefore, while thought-provoking, his interpretations would benefit greatly from further excavations and chronological refinement.

Later, Irwin (2020) investigated the history of pā on Pōnui Island. Pōnui is the easternmost island of the inner Hauraki Gulf and is approximately eight km long and four km wide (see also Irwin, 1985). Despite its size, Pōnui Island supported 23 pā. The study examined the spatio-temporal distribution of pā on the island, comparing the results to those of other regions. Irwin interprets the ^{14}C evidence to suggest that pā were first constructed on the island in the sixteenth century, with episodes of pā construction continuing until the early nineteenth century. Irwin (2020, p. 52) also suggests that the density of pā in the sixteenth century was as great as in the eighteenth century, interpreting that the island's fortification was not incremental over time. From this interpretation, Irwin proposed that each pā was associated with a social group that resided at times in the vicinity, suggesting that the density of sites makes it likely that a number were occupied contemporaneously. Ultimately, Irwin argues that the occupation of Pōnui Island passed through a stress threshold in the early sixteenth century, following which the island was quickly fortified. Irwin (2020, p. 52) also relates the construction of pā to imply group leadership, with the size of the pā used as a proxy for the scale of the communities that built them (see also Buist, 1964). However, he argues that by AD 1800, the presence of pā in the landscape did not represent discrete territories of local groups. Social changes around this time had shifted from single-hapū to multi-hapū communities as operational units (see Anderson, 1998; Ballara, 1998; Phillips, 2000), which, as Sissons (1988) suggested, resulted in a reordering of northern Māori society in the eighteenth century because of such changes in social organisation. The implication of these considerations suggests that on Pōnui, the pā built around AD 1600 could have controlled territories more mutually exclusive than those occupied around AD 1800, implying that there could have been significant changes in land tenure and social organisation (Irwin, 2020).

Unfortunately, as with his study on the pā of Pouto Island, Irwin's conclusions lack sufficient quantifiable data to back them up. The proposed Pōnui pā chronology is based on just 24 radiocarbon dates associated with the construction of defensive banks at 19 of the pā on Pōnui. Again, a limited number of ^{14}C dates were collected from each site, reflecting the period in which each pā was constructed and occupied. However, as shown from previous investigations of pā within the Bay of Islands (e.g., Groube, 1964b, 1965, 1966; Campbell, 2008; McCoy, 2009; Bedford, 2013), these pā are unlikely to be single-phase occupations and were likely occupied, abandoned, re-occupied and remodelled over time. Therefore, a single ^{14}C date representing the fortification date of these sites is not an accurate representation of the

occupation history. Additionally, these radiometric ^{14}C dates were produced from charcoal and shell materials and, again, suffer from CRA and calibration precision issues (see Irwin, 2020, pp. 45–55). Therefore, these ^{14}C dates provide limited quantitative evidence to support Irwin's statements about pā construction and occupation on Pōnui Island.

The Northland Archaeological Project (2007–2013) was a multiyear research project aiming to determine how warfare influenced the development of Māori society (see McCoy, 2009; McCoy & Ladefoged, 2012; McCoy & Carpenter, 2014; McCoy & Robles, 2016). Using the results of this research, McCoy and Ladefoged (2019) considered when, in the past, conflict most resembled the parameters described by Vayda (1960). The research focused on large-scale geospatial patterning in fortification construction in New Zealand, testing the results of this analysis on the construction history of three fortifications on Urupukapuka Island: Whangapau Pā (Q05/86), Ihumata Pā (Q05/87), and an unnamed pā (Q05/84).

Firstly, McCoy and Ladefoged (2019) investigated the significant periods of pā construction across New Zealand via the presence or absence of ^{14}C dates on pā within the same area over time. To achieve this, they divided the country into arbitrary 37.5 km^2 sections. Site continuity was defined by the presence of ^{14}C dates in the same grid in both centuries under examination; abandonment as the presence of ^{14}C dates in the earlier century but absence in the next; and expansion as the absence of ^{14}C dates in the earlier century but presence in the next. Using this metric, McCoy and Ladefoged (2019, p. 7) interpret early fortification construction between AD 1400–1600 as overwhelmingly dominated by a process of expansion. In contrast, between AD 1600–1800, later fortification use showed only slight gains in continuity and an even amount of abandonment and expansion, a pattern consistent with the reshuffling of where fortifications were being constructed and occupied. However, these findings are to be expected, as pā construction before AD 1400–1600 was likely non-existent given current understandings of the commencement of pā construction. Whereas pā abandonment and expansion would only be possible once pā had been established and occupied for a time.

Despite the simplistic nature of this metric, the juxtaposition between these two periods is important because the ecological warfare model proposed by Vayda (1960) suggests that

groups actively choose the conquest of their neighbours over expansion into new areas. Therefore, McCoy and Ladefoged (2019) suggest this model of Māori warfare is a poor fit for the expansion of the earliest fortifications (AD 1400–1600) when populations were increasing in the North Island with new locations marked out by pā. However, they suggest that this warfare model is more suited for the reshuffling that appears to have occurred around AD 1650 when the expansion and abandonment of pā are evenly matched.

It is important to note here that McCoy and Ladefoged (2019) did not attempt to evaluate the ^{14}C data used in this analysis and accepted all the ^{14}C information collated in the New Zealand Radiocarbon Database (see McFadgen et al., 2000). However, most of this historical ^{14}C data has not been adequately assessed concerning sample provenance, sample size (i.e., number of samples) and inbuilt age. Noting this problem, they state that the nature of the underlying radiometric data is such that these classifications should only be indicative of an area rather than having been definitively established for a particular site. Further evaluating this dataset through a process of ^{14}C sample review (in relation to archaeological records associated with each ^{14}C date if available) and a 'chronometric hygiene' regime (e.g., Spriggs, 1989; Anderson, 1991; Spriggs & Anderson, 1993; Schmidt, 1996; Higham & Hogg, 1997) would improve the quality of the dataset and provide a more accurate representation of pā occupation, abandonment and expansion. However, this process would also dramatically reduce the available dataset size, resulting in a lack of data to define specific areas, which reflects the state of comprehensive archaeological investigation of pā in New Zealand.

Following this spatial analysis, McCoy and Ladefoged (2019) tested their hypothesis by focusing on regional-scale geospatial patterning in fortification construction on Urupukapuka Island. A stratigraphic occupation sequence for Whangapau Pā, Ihumata Pā and Q05/84 was established using small-scale excavations, targeting specific terraces and banks at these pā. It should be noted that all three pā are relatively complex in form, exhibiting multiple terraces, banks and ditches. Therefore, these discrete excavation units provide limited stratigraphic controls that are used to define the entire occupation sequence of each pā. Seven terrestrial ^{14}C samples were collected from these excavations, including two from Whangapau Pā (Beta-321108 and -321107), four from Ihumata Pā (Beta-321102, Beta-321103, Beta-321104 and Beta-321105), and one from the un-named pā (Q05/84) (Beta-321106). Utilising

interpretations from these excavations and the resulting ^{14}C dates, McCoy and Ladefoged (2019, p. 11) suggest that in the Bay of Islands, warfare in the era after sustained European contact (AD 1769) is evident in the re-building of pā fortifications, citing the second phase of bank construction at Ihumata Pā (Q05/87), and the remodelling identified at Paeroa Pā (Q05/39) (see also Groube, 1964b, 1965). They state that these activities specifically reflect the adoption of defences to accommodate the introduction of muskets. These conclusions are supported by references to several other studies showing a lack of good evidence for conflict around AD 1500 and an abundance of evidence around AD 1650 (e.g., Phillips, 2000; Sutton et al., 2003; Allen, 2012; McCoy & Carpenter, 2014; McCoy et al., 2014; Allen, 2016). However, the precision of the ^{14}C dates collected from these pā is limited, exhibiting large calibrated age ranges with multimodal distributions owing to their interaction with the calibration plateau in the later eighteenth century (see McCoy & Ladefoged, 2019, p. 7). Therefore, the chronological evidence presented provides limited quantitative evidence to support McCoy and Ladefoged's conclusions.

Despite these challenges, McCoy and Ladefoged (2019) rightly conclude that the onset of endemic warfare requires a more nuanced view of the environment, culture, and historical contingency, pointing to Barber's (1996) research, which highlights a sense of environmental loss after the initial impacts of human occupation, along with climate fluctuations associated with the LIA (Anderson, 2016), raising the perceived need to mitigate the impacts of people on the environment. Additionally, McCoy and Ladefoged (2019, p. 11) suggest that the inherently low spatial density of fortifications at the onset of pā construction may have left ambiguity in many regions about who had the authority to prohibit the use of natural resources through other regulatory means (i.e., tapu and rāhui), and that this ambiguity could have led to even more conflict. As discussed, wars were frequently fought to restore mana following an injury or perceived injustice of some kind (Ballara, 2003, p.26).

It is clear from these investigations that the traditions of Māori warfare were not stagnant over time, and changing environmental and social pressures influenced periods of competition and conflict, fuelling subsequent episodes of pā construction and proliferation (see Allen, 1994, 1996; Irwin, 2013; Allen, 2016; McCoy & Ladefoged, 2019; Irwin, 2020). When importing these models to understand pā construction trends in the Middle Waikato Basin, we would

expect to see an initial wave of pā construction, representing a process of expansion into the region during this period of cultural change. This expansion process would be closely associated with population increases, regional migration and evolving social structures, with the aim of consolidating control of key regional resource zones. Subsequently, applying the work of Gumbley (2021), we would expect to see additional waves of pā construction, redevelopment, and repair associated with the spread of the Waikato Horticultural Complex. These waves would represent increasing economic and socio-political tensions relating to perceived decreases in the availability of prime horticultural land or increasing competition from neighbouring populations.

2.2.4 Considerations of Chronology

The first large-scale review of radiocarbon evidence relating to pā construction was conducted by Schmidt (1996), utilising an initial database of 132 pā, represented by 317 ^{14}C dates. Of the 132 pā included in the database, only 54 had been comprehensively investigated archaeologically. Therefore, less than half of the radiocarbon dates were derived from pā with a complete (more than rudimentary) understanding of their occupation history. Schmidt initially had to restrict this assemblage through considerations of sample provenance and site history, resulting in 221 dates to determine the beginning of pā construction in New Zealand. However, Schmidt also had to remove further ^{14}C dates from the assemblage through a discard protocol based on earlier 'chronometric hygiene' regimes presented by Spriggs (1989), Anderson (1991) and Spriggs and Anderson (1993). This discard protocol resulted in just 60 acceptable dates being retained in the assemblage, representing only 49 pā from across the country. Considering that over 7,000 pā are recorded nationally, this dataset is already a limited representation of pā occupation. Moreover, like many archaeological sites, pā are an accumulation of short-term events over time. Therefore, tracing a chronological sequence through the archaeological features identified at pā is challenging, requiring a considered approach and a sizeable ^{14}C dataset. This challenge is noted by Schmidt (1996, p. 447), who acknowledges that a single ^{14}C date is likely only a reflection of one of several fortification episodes over time.

Despite these limitations, Schmidt proposes the onset of pā construction nationally around AD 1500–1550, with a maximum date range between AD 1400–1800. A spatio-temporal relationship between Groube's (1970) pā classifications could not be established. Similarly, the analysis provided no evidence as to the regional origin of pā. Groube (1970) previously proposed that ring-ditch pā were brought from the northwest coast of the North Island by Ngāti Awa into the Taranaki and Bay of Plenty regions. However, Schmidt pointed out that neither region has sufficient sample numbers to distinguish when pā were first constructed in these regions. Similarly, Schmidt states that even far-removed regions, such as Tauranga and Pouto, show similar periods where fortifications were present, given the broad timescale of the results. This similarity indicates that the precision required to establish the spatio-temporal proliferation of pā across the country is beyond the limits of traditional approaches to chronology building. Therefore, the lack of concrete conclusions stemming from Schmidt's work ultimately derives from a lack of precision. Although important, the results of Schmidt's analysis have generally generated more questions than answers.

Unfortunately, research focusing on the chronology of pā construction since Schmidt's study has been limited, with investigations primarily focusing on refining the chronological sequence of pā from within specific regions (e.g., Sutton et al., 2003; McCoy & Ladefoged, 2019; Irwin, 2020). However, as discussed above, even these more recent studies have resulted in archaeological interpretations of occupation histories that cannot be established or quantified by definitive ^{14}C data. The lack of precision associated with ^{14}C dating within the context of New Zealand's short occupation history is primarily associated with variation in the concentration of atmospheric ^{14}C. This variation, referred to as 'wiggles', causes a divergence between radiocarbon age and calendar years, requiring radiocarbon ages to be corrected using a calibration curve (see Section 3.2.2). However, as exhibited in the current Southern Hemisphere calibration curve (SHCal20), uniform atmospheric ^{14}C levels are observed across several calendar periods around AD 1100, 1350, 1550, and 1750, known as calibration plateaux (Hogg et al., 2020). Due to these uniform periods, even high-precision (AMS) ^{14}C dates derived from archaeological material that coincide with a plateau result in low-precision calendar date ranges. This imprecision results because the ^{14}C age of the sample corresponds to a broad calendar period. The effect of these plateaux can be mitigated via the application of large ^{14}C sample numbers and considered Bayesian chronological modelling. However, the sample numbers required for such an analysis are rarely applied in practice. This lack of precision is

particularly relevant when attempting to establish accurate and precise chronologies for pā, as the last two calibration plateaux (AD 1500 and 1750) cover large portions of time where pā were constructed and occupied.

Inconsistent applications of ^{14}C sampling strategies and analysis further compound this lack of precision. A majority of the ^{14}C dates derived from pā were sampled during relatively old archaeological excavations at these sites (e.g., Irwin, 1985; Bellwood, 1978a; Green, 1978; Marshall, 1987; Irwin & Jones, 2004; McCoy & Ladefoged, 2019), with modern excavations at pā being rare. This situation has created a reliance on these historical ^{14}C datasets that were produced before advancements in radiocarbon procedures and technology (i.e., the application of AMS ^{14}C dating utilising much smaller sample sizes and better sampling procedures). Therefore, these historical ^{14}C datasets are often affected by issues such as in-built age, as the material was not routinely identified to species level or was not produced on short-lived (i.e., twigs) or single element (i.e., seeds) materials (e.g., Bellwood, 1978a). Additionally, ^{14}C samples were often restricted to terrestrial materials (charcoal and wood) owing to insufficient data for the calibration and correction of marine ^{14}C dates, including inaccurate regional offsets using a DeltaR without sufficient variance (see Petchey & Schmid, 2020). A DeltaR (ΔR) is a local 'reservoir offset' applied to the marine curve (Marine20) to account for regional variation for a specific location (Stuiver et al., 1986; Heaton et al., 2020b; Petchey & Schmid, 2020, p. 2). This reliance on bulk terrestrial ^{14}C samples (exhibiting CRAs with large standard errors) also limited the availability of ^{14}C samples, restricting sampling to contexts where the provenance or taphonomic link to a site's construction is limited (e.g., charcoal from hearths, the backfill of storage pits, or shell middens).

Ultimately, these factors have led to a situation where modern chronological research on pā (using ^{14}C dates produced on samples collected from past excavations) relies on insufficient ^{14}C datasets at a site-by-site level, where often just one ^{14}C date is available per site (e.g., Irwin, 2013, 2020). Even when several samples are available, their relationship to the pā's occupation is uncertain. For example, the chronology of Kohika was developed using stratigraphic evidence, tephrochronology, and radiocarbon dating, proposing a short occupation history of less than 70–80 years in the latter half of the seventeenth century. However, when the ^{14}C dataset is closely scrutinised, several issues are apparent. Just eight ^{14}C samples relating to the

occupation of the pā were collected from various structural contexts. However, four of these samples suffer from potential issues of in-built age (NZ6583, NZ6611, NZ6618 and Wk10292), analysed on samples of unidentified species or kānuka posts. Additionally, one sample was collected from marine material (NZ6580) affected by the marine reservoir issues discussed above. This results in just three viable ^{14}C dates for interpretation, sampled from charcoal identified within the backfill of a storage pit and below a floor of clay silt and stones, and charcoal interpreted as secondary vegetation burning outside the palisade defences. Therefore, while well-considered, the proposed short occupation history largely relies on archaeological interpretations of the stratigraphic evidence and OxCal modelling (start and end boundaries), with limited ^{14}C evidence anchoring the chronology.

Furthermore, even when more modern excavations are conducted, such as those conducted at Pouērua Pā (see Marshall, 1987; Sutton et al., 2003), the scale of these excavations is often limited in scope compared to the size and complexity of the pā, relying on archaeological interpretations and assumptions to link discrete excavation areas into a complete occupation history for the site (e.g., Sutton et al., 2003 pp. 189–199). Only 11 ^{14}C dates anchor the chronology of Pouērua Pā, including just a single ^{14}C date representing the entirety of the 'defence' period (sampled from one discrete excavation area: Area III). As discussed above, a single ^{14}C date recovered from a defined archaeological context is a poor representation of a defined period of a pā occupation, especially one such as Pouērua Pā, with evidence of extensive terracing and defences that were likely constructed, repaired and modified over time. Furthermore, all eleven ^{14}C dates have standard error ranges of more than 35 years (± 36–60 years) resulting in broad calendar date ranges (Sutton et al., 2003, pp. 189–199). This results in several statements about the occupation sequence that the ^{14}C evidence cannot quantify and support.

More recently, Hogg et al. (2017) investigated the potential of applying high-precision AMS wiggle-match dating (WMD) to preserved palisade posts from Otāhau Pā. Hogg et al. (2017) recognised that systematic chronological investigations of pā have previously been hampered by the problems of the historical approaches discussed above. WMD was used to address these issues, providing accurate and precise calendar dates for the felling of trees used in the construction of a palisade defence. By focusing efforts on identifying chronological evidence

of a specific event (the construction of a palisade), which plausibly indicates the initial construction of the defences, issues of taphonomy or provenance are removed. Investigations at Otāhau pā identified a series of palisade posts along the northeastern side of the pā, located in the stream approximately 1–2 m from the bank. These *in situ* posts formed both distinct single and double rows of palisades. Seven posts were extracted and sampled for analysis, resulting in three WMDs. The results of this analysis dated the construction of the palisade defences at Otāhau pā to a defined point during the middle 1700s (AD 1768 ± 4 at 95% probability).

The chronological approach implemented by Hogg et al. (2017) demonstrated for the first time that accurate calendar ages for pā can be generated, with minor calendar errors, that directly relate to single-phase archaeological events (i.e., the construction of a palisade). Notably, the results show WMD can produce calendar date ranges within the scale of a single generation (< 25 years), allowing fine-grain archaeological interpretation of the occupational history of the pā and its association with the broader archaeological landscape and traditional history records (e.g., Māori whakapapa, oral traditions etc.). As discussed previously, the Otāhau pā study represents a significant advance in archaeological science in New Zealand, demonstrating the potential for WMD to revolutionise our understanding of the chronology of pā in New Zealand. The improved accuracy and precision resulting from this dating technique have the potential to clarify the history of pā construction and occupation and, thus, provide valuable insights into the environmental and social processes affecting Māori during this period. As discussed in Section 1.2 above, the research presented here seeks to build upon the research presented by Hogg et al. (2017), expanding this chronological approach within the Middle Waikato Basin.

Chapter 3. Time and Chronology

3.1 Theoretical Considerations of Time

Time depth, temporal change and patterns of cultural transformation are quintessential aspects of archaeological investigation. Archaeological deposits provide proxy evidence for conceptualising the past, and therefore, investigations of the archaeological record provide an opportunity to explore beyond the realm of ethnography (Bailey, 2007, p. 198). Cartesian interpretations of time assume that objects have both a position in space and a trajectory through time independent of other objects (Holdaway & Wandsnider, 2008, p. 4). This interpretation illustrates how artefacts can move back and forth between different archaeological contexts through the effects of depositional and taphonomic processes, demonstrating the temporal complexity of the archaeological record and the varied scales at which those processes are visible (Schiffer, 1976, 1987; O'Brian & Lyman, 2000). Therefore, to attain a comprehensive understanding of the past, archaeologists rely on an accurate and precise measurement of time, facilitating more complex and consequential questions of the archaeological record (Rossignol & Wandsnider, 1992; Stahl, 1993; Zvelebil, 1993; Stern, 1994; Ramenofsky & Steffen, 1998; Lock & Molyneaux, 2006; Bailey, 2007; Holdaway & Wandsnider, 2008).

Research focusing on the influence of 'objective time' (time as constructed or measured) in archaeology centres on the spatio-temporal properties of the observed evidence, considering how datasets are interpreted through temporal scale and resolution to constrain or expand specific research questions (See Ebert, 1992; Rossignol & Wandsnider, 1992; Stahl, 1993; Zvelebil, 1993; Stern, 1994; Ramenofsky & Steffen, 1998; Lock & Molyneaux, 2006). Objective time theories focus on the long-term nature of the archaeological record, highlighting the unsuitability of interpretive models drawn from short-term observation and ethnohistory (Hull, 2005, p. 354). These discussions derive from previous explorations of site formation processes (e.g., Schiffer, 1976, 1987) and causation concerning temporal scales and rates of change (e.g., Bailey, 1981, 1983, 1987; McGlade, 1995b, 1995a). Ultimately, theoretical considerations of objective time emphasise the importance of an accurate and precise chronology when attempting to reconstruct the past, allowing specific and detailed questions

to be asked of the gathered dataset (e.g., Stahl, 1993; Ramenofsky & Steffen, 1998; Murray, 1999; Lucas, 2005).

In contrast, considerations of 'subjective time' (time as experienced by individuals) are primarily developed through social anthropological theory, focusing on the temporal awareness of past peoples and how time was conceived and experienced by individuals and cultures. These explorations of subjective time highlight how these concepts may contribute to the behaviours archaeologists seek to understand (See Shanks & Tilley, 1987; Bradley, 1991; Cooper, 1993; Deitler & Herbich, 1993; Zvelebil, 1993; Gosden, 1994; Thomas, 1996). Advocates of such an approach are critical of applying a multi-temporal perspective in archaeology, rejecting the idea that subjective and objective time can be reconciled through varying the scale of analysis (e.g., Shanks & Tilley, 1987). Unfortunately, these critiques have directed attention away from the fundamental premise of objective time as applied in archaeology – that different cultural and environmental processes affecting, created by, or defining individuals and communities operate on disparate timescales, and all scales should be considered when exploring the causality behind cultural change (Bailey, 1981, 1983, 1987, 2008). It is important to reiterate that these processes may operate independently (due to a variety of factors) and may be imperceptible within short timespans (i.e., one generation) unless specifically sought and measured with high precision (Hull, 2005, p. 357). This imperceptibility inherently limits our ability to recognise and deal with the analytical challenges posed by palimpsests (Bailey, 1981; Binford, 1981; Bailey, 1983; Schiffer, 1985; Bailey, 1987).

The archaeological record is a physical representation of the activities and behaviours of individuals and communities interacting with a landscape over time (Anschuetz et al., 2001, p. 160). However, the observed archaeological record is seldom presented as a clear and precise sequence of depositional events (Binford, 1980; Schacht, 1984; Stern, 1994), and time depth results in the accumulation and potential loss of successive interactions, resulting in a palimpsest (see Section 3.1.1). The term palimpsest has a long history of use in archaeology (see Binford, 1981), and generally refers to the accumulation or superimposition of successive activities in the archaeological record, the material traces of which are partially destroyed, modified or re-worked, resulting in the possible erasure of earlier traces (Lucas, 2005, p. 37;

Bailey, 2007, p. 203). Ultimately, palimpsests limit the observability of distinct activities or events by imposing an incomplete record that cannot be readily distinguished in time.

Palimpsests in the archaeological record can be understood in various ways, specified by the nature of the relationship between the processes of deposition and disturbance (see Bailey, 2007). Strict definitions define true palimpsests as the erasure of all traces of earlier activity from the archaeological record except for the most recent. In this situation, the occupation history of an archaeological site essentially starts anew, severing all connections between the past and present. In contrast, cumulative palimpsests occur when successive episodes of deposition, or layers of activity, remain superimposed, resulting in an archaeological record that is reworked and mixed temporally, making it difficult to separate and observe the original constituents. Thus, the primary problem when interpreting palimpsests is that while events in the archaeological record can be observed, identifying how those events are related temporally before being ordered into a deposition sequence is often challenging. Consequentially, archaeologists often use the term 'palimpsest' to define deposits that are difficult to resolve chronologically, whether due to poor temporal resolution or impaired stratigraphic association (e.g., Carr, 1987; Gillespie & Brook, 2006; Henry, 2012; Sharon et al., 2014).

This discussion highlights how interpretations of the archaeological record are limited by the temporal resolution in which they can be visualised. However, as several scholars have pointed out, palimpsests also provide a unique opportunity to focus on the accumulative and transforming properties of the archaeological record through the loss and destruction of evidence (see Bailey, 1981; Binford, 1981; Foley, 1981; Bailey, 1983; Wandsnider, 1996; Lucas, 2010). Therefore, the disentanglement of observed palimpsests provides a means to understand how different aspects of assemblage formation pertain to establishing the temporal scale of an archaeological site (Sullivan, 2008). In this way, controlling the temporal scale at which the past is viewed allows a clearer understanding of how the archaeological record is formed and the changes witnessed through time. In essence, this is the application of time perspectivism.

3.1.1 Time Perspectivism

Bailey (1981, p. 103) first described time perspectivism as "the belief that differing timescales bring different features of behaviour into focus, requiring different explanatory principles". Few archaeologists would deny that the past can be thought about at different scales and that different questions come into focus depending on the analytical lens employed (Harris, 2017, p. 2). Thus, the application of scale in archaeological research has occupied a prominent place in the discourse when seeking to understand and explain change in the archaeological record, whether explicitly or implicitly (e.g., Lock & Molyneaux, 2006; Robb & Pauketat, 2013; Harris, 2017). Two principal ideas underpin this theory. First, changing the observation scale (particularly the timescale) changes what we observe in the archaeological record. Second, structurally the archaeological record is inherently a palimpsest, and the coarse resolution of the material determines what we can or cannot know about the past (see also Ramenofsky & Steffen, 1998). However, rather than being a limitation, the theory of time perspectivism approaches this lack of resolution as an opportunity to focus on scales of phenomena not available to ethnography and the study of present-day processes or events.

Applying the theory of time perspectivism requires reading the archaeological record as a unique historical dataset on which to base multiple scales of explanation (Holdaway & Wandsnider, 2008, p. 2). Each scale of examination explores the interrelationship between natural and cultural timescales and the processes which underpin the formation of the archaeological record (Wandsnider, 2008). When expressed this way, Bailey's (1981) definition highlights how processes operate independently of the observer, with the added implication that how these processes are perceived or observed changes their interpretation (Bailey, 2007 p. 5).

The two principal ideas outlined above embody two distinct aspects of timescale: time depth (long or short) and time span (resolution) (Bailey, 2008, p. 14). These two aspects are inherently linked, as large high-resolution datasets resulting in accurate chronologies permit a focus on shorter time spans. In comparison, smaller datasets of lower resolution are inherently limited to considerations of longer time spans. However, this correlation is not absolute and is primarily defined by the temporal context of the research. Principally, what can be observed in

the archaeological record changes depending on how close in time we are to the phenomena being observed (Bailey, 1981). Closeness in time (short time depth) allows observation of finer detail within a narrow field of view, while remoteness in time (long time depth) results in a loss of local definition but the potential to observe larger patterns (cf. Renfrew, 1981). Bailey (1983 p. 186) expanded on these themes, developing the concept of 'time as representation' rather than time as process, highlighting how different observers incorporate time theory into their research through different 'time structures' (i.e., cognitive, conceptual, psychological, cultural, or cosmological). This conception of time exposes the contrast between "environmentalist" (ecological and environmental) and "internalist" (social and symbolic) approaches to time, relating the former to long-time scales and the latter to short-time scales.

This conception of time is the foundation of critiques suggesting time perspectivism is just another extension of the Annales approach to history (Bintliff, 1991; Harding, 2005). The Annales approach, as championed by Braudel (1972, 1980), is critical of traditional history written as a simple sequence of events. Braudel (1972) defined three specific timescales over which history can be examined: the long, medium and short term. The long term, or longue durée, refers to over-arching (slow-moving) processes such as environment; the medium-term refers to social or structural history, covering concepts such as persistent social or economic organisation forms; and, the short term relates to specific events or actions by individuals (Lucas, 2008, p. 15). Archaeological interest in the Annales approach emerged in the late 1980s and early 1990s, with several publications drawing inspiration from this school of thought (see Hodder, 1987; Bintliff, 1991; Knapp, 1992; Gurevuch, 1995; Last, 1995). However, Bailey (2007 p. 6) argues that the comparison of time perspectivism to the Annales school of thought oversimplifies the varied intellectual genealogies of these different approaches. Within his argument, Bailey (2007, p. 6) highlights the differing sources of empirical inspiration and the range of timespans and scales embraced by these two approaches. Importantly, time perspectivism uses specific research questions to determine the scale of the analysis rather than defining the event by the overarching temporal structure (Bailey, 2007, p. 202). Critically, as also pointed out by Harding (2005 p. 95), the way in which these critics have interpreted Braudel's approach considers each timescale as structural rather than inherent to the activities that form them, placing the composition of history outside the processes that produce it.

The juxtaposition between long-term (environmental or ecological) and short-term (social) processes is also the foundation of critiques from the post-processual wing of theoretical archaeology, suggesting time perspectivism is environmental determinism or ecological functionalism by another name, ignoring social and cognitive variables as short-term 'noise' (Tilley, 1981; Shanks & Tilley, 1987; Thomas, 1996; Robb & Pauketat, 2013). However, Bailey (2007, p. 5) addressed this critique by reiterating that time perspectivism does not remove consideration of social factors from the long term. Instead, the theoretical approach questions the appropriateness of theories and concepts drawn from social anthropology, cultural geographers, historians and sociologists, who approach the historical record from different contexts, scales and types of evidence. This difference is highlighted in Bailey's (1983) earlier work, where he expressed a need to move beyond simple temporal categorisations of environmental and internalist processes, as both might operate on long and short time scales. However, Bailey (1983, p. 182) stipulates that their relative influence and the nature of their interaction with the archaeological record might differ depending on the observation scale, and these differences should be investigated rather than assumed.

The theory of time perspectivism gained momentum in the 2000s, with several theoretical and practical applications of the approach (see Stern et al., 2002; Wandsnider, 2004; Hull, 2005; Holdaway & Wandsnider, 2006; Whittle & Bayliss, 2007; Altizer, 2008; Sullivan, 2008; Wandsnider, 2008). In one such application, Wandsnider (2004) critiqued approaches to the study of Mediterranean surface archaeology, describing a condition of 'multiple paradigm disorder' with two clear competing theoretical approaches: a regional settlement pattern paradigm focused on functional and processual approaches and a multi-temporal paradigm fixated on formational approaches. Wandsnider (2004) suggests that the application of regional settlement pattern studies, focused on a 'flat-time' functional approach, is fundamentally flawed. She submits that this approach does not deal well with the complexity identified in the archaeological record, utilising intensive non-site methods that document taphonomic variation to pursue functional goals that do not satisfactorily assign meaning to the varied archaeological landscape. Instead, Wandsnider argues for an acceptance of the 'formational metaphysic', highlighting time perspectivism, which offers an understanding of agency, causation, and temporality that is inherently linked to the archaeological record and the human and natural processes operating at various temporal scales. Wandsnider (2004, pp. 55–56) advocates for archaeologists to take a multi-scalar approach, examining changes within the long-term

structures of the archaeological record by focusing on the accumulated characteristics of the material assemblage.

This multi-scalar research strategy approaches archaeological assemblages by narrowing or widening the observation scale. Bailey (2007) refers to this process as the 'microscopic' or the 'macroscopic' tendencies. The 'microscopic tendency' shrinks the focus of the research question, working down through successively smaller scales of analysis to the levels of individual actions, beliefs, and social interactions. Conversely, the 'macroscopic tendency' broadens the scope of analysis, placing phenomena in a widening perspective of large-scale comparison. Changing the scale of analysis in this way makes the data more amenable to interrogation by applying differing research questions. The principal argument underpinning the time perspective approach is that regardless of the scale applied, whether microscopic or macroscopic, archaeologists will still be confronted with palimpsests of varying degrees. Therefore, no one type of scale is the best, and the analysis approach should be tailored to the temporal resolution of the dataset and the applied research questions.

Hull (2005) demonstrated how disparate concepts of time can be reconciled through a perception-based approach to time perspectivism, broadening the scale of analysis from the minimum (microscopic) scale of the average human lifespan. Hull investigated how processes affecting culture operate at different timescales using hunter-gatherer remains from Yosemite Valley in California. This case study demonstrated how archaeologists can explore past change rates to determine perceptions of these processes (or lack thereof), utilising multiple analytical scales to identify the variables that define cultures through cause and effect. This approach uses considerations of succession, duration, simultaneity, and pace of events to reconcile objective and subjective time and examine the overarching process responsible for cultural change. Critically, the relationship between the long and short temporal views enhances the interpretation of both scales. Hull (2005, p. 374) notes that while Bailey (1983) did not initially explore potential methodological approaches for multi-temporal analysis on shorter time scales, his consideration of past behaviour as a product of different processes indicates the applicability of a narrow focus. Hull champions the time perspectivism approach and its ability to reveal distinct, overlapping trends that likely relate to various phenomena and their influence on disparate temporal scales, and concludes that if archaeological analysis ignores a multi-

scalar approach, it can be at risk of simply observing (i.e., succession) rather than explaining (i.e., process) these phenomena.

At the same time, Lucas (2005, pp. 43–49) criticised time perspectivism through his distinctions between 'chronological' time (objective time) and 'real' time (narrative time). Lucas reiterates how a chronological framework of numerical time inherently emphasises time as a succession of unilinear events. Lucas argues that such frameworks ultimately lead to explanations with a similar structure, tracking progressive evolutionary stages of development from primitive to advanced, enlightened by the position of the modern observer. Lucas describes these approaches as a totalising grand narrative that legitimises the power of those who promote it. In contrast, Lucas (2005, pp. 49–60) suggests narrative time emphasises time as duration and flow rather than as a sequence, which corresponds more closely to time as experienced by the individual, which can result in many different temporalities and narratives (see also Lucas 2008, 2010, 2012). When reflecting on the two competing ideologies of time as applied to archaeology (objective and subjective), Bailey (2008) states that theoretical considerations of time are just a source of inspiration, one point of view, and that view should not become an obsession in disregarding others. Archaeology provides the opportunity to observe human history through a wide range of scales, and archaeologists risk missing overarching controlling processes by ignoring possible larger-scale processes on the grounds of determinism.

Following these critiques, Bailey (2007, p. 201) clarified his definition of time perspectivism by redefining four crucial ideas: different phenomena operate on independent timespans and resolutions; these phenomena should be viewed at their own timescale; differential time has a distorting effect on perspectives, which an awareness of perspective corrects; and observations of time are subjective. Bailey (2007, p. 35) argues that the contrast between real-time and 'narrative time' is vastly over-simplified and confuses reference to a structured chronology with chronology as a form of temporal interpretation. The premise of this argument is that using a chronological framework does not inherently mean archaeologists are predestined to construct linear or progressive types of explanations which minimise subjective experiences of time. More recent efforts to break down this dichotomy have recognised that different 'kinds' of time can be found in all societies and that when exploring these concepts, archaeologists

must still consolidate observations of the archaeological record to scientific chronological frameworks (Gardner, 2001; Harding, 2005; Lucas, 2008; Herzfeld, 2009). Such work has drawn on similar debates in anthropology to produce accounts of temporal experience, which are multi-scale and pluralist (Gardner, 2012, p. 147).

Three more recent case studies have since been published utilising Bailey's theoretical approach: (i) Epp (2010) applied time perspectivism in their study of three Mennonite cemeteries in York County, Nebraska. This case study provides an example of short-term scale change, using headstone inscriptions and decorative motifs, highlighting the Mennonite's transition from Standard German to English. (ii) Gardner (2012) studied a Romano-British farmstead in the Cotswolds, considering palimpsests and aggregates to examine overarching patterns within the archaeological record, demonstrating the community's "varied tempos and temporalities of action" across time. Gardner's approach included considering sporadic and continuous change events in the archaeological record due to outside economic and structural shifts. (iii) Rzepecki (2014) analysed two Polish megalithic tombs, Sarnowo 1 and Świerczynek, re-evaluating these sites as multi-phased cumulative palimpsests. Gardner found that while both tombs exhibited defined style variations, they also showed evidence of sustained funerary meaning over the long term.

New Zealand's short chronology provides a unique setting from which to examine palimpsests through a time perspectivism approach, as it exhibits a limited time depth for palimpsests to form when compared to archaeological landscapes worldwide. However, the palimpsests encountered within New Zealand's archaeological record are still distinct, and are inherently created within very narrow periods (i.e., one generation). These palimpsests challenge archaeologists, as the temporal resolution required to disentangle the sequence of observed activities and events calls for a precision that has historically been beyond the capacity of previously applied approaches. As discussed previously, fine-grained chronological development in New Zealand has been hampered by several persistent issues, resulting in a temporal resolution too imprecise to provide meaningful interpretations of the archaeological record. This imprecision has particularly affected attempts to seriate pā or track their proliferation over time at local and regional scales. However, with the appropriate application of modern high-precision ^{14}C techniques and sampling strategies, refined chronological

frameworks can be established that permit the observation of activities that occur within this narrow window of time.

As outlined in Section 1.2, the research presented here aims to investigate the construction, development and proliferation of pā in the Middle Waikato Basin using a time perspectivism approach. This approach is applied through three objectives focusing on different scales of analysis: Event, Local and Regional. Ultimately, this multi-scalar approach identifies events, actions and behaviours within a defined timespan, allowing the lived experience of the people and communities occupying this pā to be linked to influential processes resulting from the broader environmental and cultural landscape. These processes are observed as the scale of analysis broadens, focusing on a longer timescale, highlighting how the influence of these processes shifts and evolves, which is captured in the archaeological record.

3.2 Radiocarbon (^{14}C) Dating

One of the primary goals of archaeologists since the nineteenth century has been the control of chronology, specifically the ability to define sites, features and events within a defined chronological framework (Lucas, 2015). Before the advent and development of 'objective' chronologies (based on absolute measurements of time), the past was described by Renfrew (1973) as "chaotic", with chronologies primarily based on the relative ordering of events through stratigraphy, typologies and seriations between sites (see Piggott, 1954; Childe, 1957; Thomas & Ehrich, 1969; Renfrew, 1973). However, the invention of radiocarbon dating by Willard Libby and his colleagues (Arnold & Libby, 1949, 1950; Libby, 1951) provided a method for developing independent (numerical) chronologies for disparate archaeological sites and events in time. The ^{14}C dating method enabled archaeologists to examine deposits and associated events independent of typology, with chronological frameworks anchored using measurements of ^{14}C, resulting in a range of new research hypotheses and paradigms that restructured our understanding of prehistoric archaeology around the world (e.g., Renfrew, 1973; Manning & Weninger, 1992; Needham et al., 1997; Manning et al., 2001; Sharon et al., 2007; Kuzmin, 2009; Bronk Ramsey et al., 2010b; Higham et al., 2014; Manning et al., 2020; Hafner et al., 2021).

The application of radiocarbon dating is now routine globally, with the advancement of modern ^{14}C techniques described as some of the most significant advances in archaeological science (see Manning, 2014 for review). In the years since its development, significant technical and methodological refinements have continued to shape our understanding of the past, including improvements to the instruments used to detect and measure radiocarbon, ongoing efforts to improve the calibration datasets that convert ^{14}C age to calendrical time, and the development of statistical methods of analysis (Renfrew, 1973; Litherland, 1980; Allen, 1987; Dennell, 1987; Harris et al., 1987; Buck et al., 1991; Taylor, 1995; Goslar & Madry, 1998; Bronk Ramsey, 2001; McCormac et al., 2002; Buck & Blackwell, 2004; Buck & Millard, 2004; Bronk Ramsey et al., 2006; Bronk Ramsey, 2008; Bayliss, 2009; Bronk Ramsey et al., 2010a; Steinhof, 2016; Kruschke & Liddell, 2018; Hogg et al., 2019a; Hajdas et al., 2021; Reimer, 2022). As Clark (1970, p. 38) stated, "^{14}C dating is the reason the study of world prehistory is possible, with the discipline contributing the first worldwide chronometric timescale that transcends local, regional and continental boundaries".

3.2.1 Basic Theory

The ^{14}C dating method is based upon three empirical observations: the production of natural ^{14}C in the atmosphere, its dispersal into the biosphere through photosynthesis, and the exponential decay of ^{14}C in a sample after it is removed from the carbon cycle (see Bronk Ramsey, 2008, for a complete review). Natural ^{14}C is a radioactive isotope of carbon continuously generated in the upper atmosphere through neutron bombardment, resulting from the interaction of ^{14}N with cosmic ray-induced neutrons (Pandow et al., 1960). ^{14}C atoms rapidly oxidise in the air and enter the global carbon cycle as $^{14}CO_2$ (Aitken, 1990). The production rate of ^{14}C is relatively steady (though not constant) and is influenced by the influx of cosmic rays, solar activity and the strength of Earth's magnetic field (O'Brien, 1979; Vogel et al., 1986; Vogt et al., 1990; Masarik & Reedy, 1995; Masarik & Beer, 1999; Channell et al., 2000; Laj et al., 2000; Beer et al., 2012). While the global ^{14}C production rate has been estimated by modelled reactions (O'Brien, 1979; Masarik & Reedy, 1995) and by calculating from current concentrations (Suess, 1965; Damon et al., 1978), attempts to directly measure the production rate of ^{14}C have produced varied results (see Bronk Ramsey et al., 2007). On the timescales generally considered in archaeology, ^{14}C production is assumed to be fairly

constant. However, short-term production events resulting from individual events can have significant implications (Damon et al., 1995).

Short-term ^{14}C production fluctuations from individual events (i.e., production variations, e.g., supernovae or ameliorating variations, e.g., from changes in solar output, geomagnetic field strength, or from the global carbon cycle) are known to have generated short-term wiggles in the radiocarbon calibration curve (Bronk Ramsey, 2008, p. 251). Several of these events have been observed and measured (see Voelker et al., 2000; Wagner et al., 2000; Laj et al., 2002; Hughen et al., 2004b; Miyake et al., 2012; Miyake et al., 2013). Of relevance are "Miyaki events", which are characterised by sudden, single-year leaps in the concentration of ^{14}C in trees, as well as beryllium-10 and chlorine-36 in ice sheets (Miyake et al., 2012; Miyake et al., 2013; Jull et al., 2014). The source of these phenomena is still debated. However, supernovas (Miyake et al., 2012) or solar effects (Usoskin et al., 2013) are considered the likely cause. The observation of these events demonstrates the potential for short-term variability of atmospheric radiocarbon and the subsequent implications for calibrating calendar age. Therefore, the necessary conclusion from the production process is that while it is assumed to be constant, it can also fluctuate on various timescales (Bronk Ramsey, 2008, p. 251).

Radiocarbon is distributed through the Earth's atmospheric, terrestrial, and marine carbon reservoirs by the global carbon cycle. Around 90% of all ^{14}C resides in the world's oceans, which can be further divided into three zones: surface, intermediate, and deep ocean zones. The marine reservoir contains a variety of carbon-containing inorganics and organics, including various classes of carbonates and bicarbonates, dissolved organic carbon (DOC) compounds, and marine organisms (Taylor & Bar-Yosef, 2014a, p. 32). Carbon is incorporated into the main atmospheric and aquatic carbon reservoirs via photosynthesis (Taylor & Bar-Yosef, 2014b). In simple plant organisms (e.g. algae), the proportion of radiocarbon provides a snapshot of the reservoir in which the organism lived. In the case of longer-lived plants (e.g., trees), this ^{14}C signature is captured within the cell's cellulose. As those cells die, their carbon exchange ceases, providing a record (i.e., tree ring) of the ambient radiocarbon isotope ratio over a more prolonged period (Bronk Ramsey, 2008, p. 253). Animals ingest ^{14}C via the food chain while releasing a portion of ^{14}C through respiration and excretion. Ultimately, when an

organism dies, its carbon exchange with the biosphere (including the atmosphere) ceases, and radiocarbon decay causes the level to decrease with time (Bronk Ramsey, 2008, p. 253).

Radiocarbon decay occurs through beta decay (Bronk Ramsey, 2008, p. 254), emitting a beta-minus (β–) or negatively charged beta particle (electron) from its nucleus to form ^{14}N and an electron antineutrino. Like all radioactive decay, this is a random process which can occur at any time from formation. For ^{14}C dating applications, the fundamental constant that permits age calculation based on a measurement of a residual ^{14}C concentration in a sample is the decay constant or half-life of ^{14}C (the time taken for 50% of nuclei to decay). This half-life is often quoted as two different values. The first is 5568 ± 30 years, established by Engelkemeir et al. (1949). The second is the Cambridge-half life of 5730 ± 40 years, which is considered a better overall estimate (Godwin, 1962). It should also be noted that the Decay Data Evaluation Project has more recently established the half-life at 5700 ± 30 (Bé et al., 2004). However, the critical aspect of radiocarbon decay is that once ^{14}C has been locked into an organism from the environment, and the organism dies, the proportion of radiocarbon will drop exponentially at a rate that is entirely independent of any chemical or physical conditions, and this drop can be measured accurately resulting in a radiocarbon date (Bronk Ramsey, 2008, p. 254).

3.2.2 Calibration

Soon after the method was developed, it became clear that radiocarbon measurements and calendar years are not directly correlated due to variations in past atmospheric ^{14}C levels (Suess, 1955; de Vries, 1958, 1959). Recognition of the need to calibrate conventional radiocarbon ages into calendar time is cited as the second revolution in radiocarbon dating (Renfrew, 1973). Atmospheric ^{14}C levels are affected by a variety of complex factors which cannot be modelled mechanistically. As discussed above, these include solar cycles and storms, geomagnetic variations in the Earth, unpredictable up-welling of old carbon from substantial reservoirs (oceans), and human activity such as atomic bomb testing and release of old carbon in fossil fuels (O'Brien, 1979; Vogel et al., 1986; Vogt et al., 1990; Stuiver et al., 1991; Masarik & Reedy, 1995; Masarik & Beer, 1999; Channell et al., 2000; Laj et al., 2000; Beer et al., 2012; Skinner et al., 2019; Hua et al., 2020; Heaton et al., 2021).

Therefore, converting radiocarbon ages (^{14}C ages) into calendar time requires measured ^{14}C concentrations from the dated material to accurately reflect atmospheric ^{14}C levels during the period of growth (Hogg et al., 2019a, p. 1265). Without this correction, radiocarbon ages cannot be directly compared to historical dates or ages measured by other methods (e.g., dendrochronology). Therefore, the calibration curve lies at the foundation of ^{14}C dating and its application. For the periods where it is possible, the main backbone of calibration is dendrochronologically dated tree rings (Reimer et al., 2020; Van der Plicht et al., 2020). Dendrochronologically dated tree ring sequences offer unsurpassed accuracy and resolution for atmospheric ^{14}C levels when developed from a reliable tree-ring chronology and if the pretreated dated fraction accurately reflects atmospheric ^{14}C concentrations during the time of growth (McCormac et al., 1998a). This situation has resulted in a long history of calibration datasets developed using these records, which have evolved in response to innovations and updated data (see Reimer, 2022, for a complete review).

3.2.2.1 The Evolution of Calibration Datasets

Hessel de Vries (1958, 1959) was the first to convincingly demonstrate that atmospheric radiocarbon concentration varied by up to 1% over the last 400 years, which was previously hypothesised by Suess (1955). Throughout the 1960s, variations in the ^{14}C time scale were documented via ^{14}C determinations on dendrochronologically dated wood, including tree ring chronologies obtained from giant California sequoia (*Sequoia gigantea*), European oaks (*Quercus spp*.) and bristlecone pine (*Pinus longaeva*) (Ralph & Struckenrath, 1960; Willis et al., 1960; Stuiver, 1961, 1965; Suess, 1965; Stuiver & Suess, 1966). This research identified that the ^{14}C data exhibited two types of cyclicity: a major trend of long-term 'sine wave' characteristics (Suess effect) and medium to short-term fluctuations of various durations (de Vries effects).

Pivotal to this early work was research conducted by Hans Suess, who developed a hand-drawn calibration curve using a method called 'cosmic schwung' (Suess, 1967, 1970). The development of the bristlecone pine chronology was particularly influential (Ferguson et al., 1966), as it extended radiocarbon calibration from 4100 BC to AD 1500 (Suess, 1967). Building on the bristlecone pine chronology, the calibration curve was extended from 5400 BC

to the present by Suess (1970). However, at the time, Suess's calibration curve was not overwhelmingly accepted, with several critiques of the curve's construction method and structure (see Burleigh et al., 1972; Adams, 1973; Switsur, 1973; Damon et al., 1974; Ralph et al., 1974). These critiques culminated in a review by Renfrew and Clark (1974), who examined all previously developed curves and calibration methods and found all to be statistically unsatisfactory (see also Wendland & Donley, 1971; Clark, 1975). It was not until the development of high-precision gas and liquid scintillation spectrometers that the structure of the calibration curve was further refined (Pearson et al., 1977; Tans & Mook, 1978; de Jong et al., 1979; Pearson, 1979; Stuiver et al., 1979; Stuiver & Quay, 1980), confirming the existence of the Suess-type wiggles.

The 1980s saw a dramatic increase in the number of available calibration datasets and curves, including the first officially recommended bi-decadal curves (Pearson & Stuiver, 1986; Stuiver & Pearson, 1986). These curves were primarily based on measurements of Irish oak tree ring chronologies (Pilcher et al., 1984) and trees from the western U.S. (Stuiver & Becker, 1986). These developments resulted in the atm20 calibration curve for terrestrial samples implemented using the computer program CALIB (Stuiver & Reimer, 1986). Oeschger et al. (1975) also developed a 'global' marine calibration curve using an ocean-atmosphere box model with the atmospheric curve as input age (Stuiver et al., 1986).

The 1980s concluded with a review conducted by Aitchison et al. (1989), who investigated the 1986 calibration datasets, methods and programs. This review resulted in the further development and application of Bayesian calibration models, initially developed by Buck et al. (1991) and later refined using probabilistic methods for calibration (Stuiver & Reimer, 1993; van Der Plicht, 1993; Bronk Ramsey, 1994), along with a new statistical framework for dealing with multiple ^{14}C dates (Buck et al., 1991; Buck et al., 1992; Buck et al., 1994; Christen, 1994; Christen & Litton, 1995; Buck et al., 1996). When these computational methods were first developed, even relatively small models used considerable computing power, spurring the development of purpose-built calibration statistical packages such as OxCal, BCal, Calib, DateLab, Bpeat, and Bacon (Stuiver & Reimer, 1993; Bronk Ramsey, 1994; Buck et al., 1999; Bronk Ramsey, 2001; Jones & Nicholls, 2002; Blaauw et al., 2018).

Following further improvements to the calibration datasets in the late 1990s, including the 1993 and 1996 updates (see Bard et al., 1998; Burr et al., 1998; Goslar & Madry, 1998; Hughen et al., 1998; McCormac et al., 1998a; McCormac et al., 1998b; Spurk et al., 1998; Stuiver et al., 1998a; Stuiver et al., 1998b), the first meeting of the IntCal Working Group (IWG) in 2002 determined a criteria for data included within the planned IntCal04 calibration curve (Reimer, 2004). Additionally, a random walk model was chosen as the new statistical method for calibration, accounting for the uncertainty of the sample's calendar and ^{14}C ages to calculate the curve (Buck & Blackwell, 2004). A preliminary Southern Hemisphere atmosphere calibration curve was also established, SHCal02 (McCormac et al., 2002), which was extended to 11,000 cal BP using the IntCal04 curve tree-ring data and a modelled Southern Hemisphere offset (see also McCormac et al., 2004). Since this first meeting, the IWG has provided updated ^{14}C calibration curves at semi-regular intervals. Continuing updates are required as new datasets are made available and as our understanding of the natural fluctuations in ^{14}C in the atmosphere and oceans improves, with curves (or particular datasets) becoming obsolete over time (see Hughen et al., 2004a; Reimer, 2004; Reimer et al., 2009; Hogg et al., 2013a; Reimer et al., 2013; Hogg et al., 2020; Reimer et al., 2020). The latest calibration curve iterations are IntCal20 (Reimer et al., 2020), Marine20 (Heaton et al., 2020b), and SHCal20 (Hogg et al., 2020).

3.2.2.2 Southern Hemisphere Calibration

Currently, SHCal20 (Hogg et al., 2020) is the only atmospheric ^{14}C reservoir recognised for dating pre-AD 1950 terrestrial material in the Southern Hemisphere. The need for separate hemispheric calibration curves derives from an observed offset in atmospheric ^{14}C concentrations between the Northern (NH) and Southern Hemispheres (SH). This offset was recognised via observations of depleted ^{14}C levels in measurements of SH tree rings, which exhibited older values compared to the NH's contemporaneous tree rings (Lerman et al., 1970; Vogel et al., 1986). Continued research has shown that the north/south (N/S) ^{14}C offset varies over time, creating structural differences between the calibration curves for each hemisphere (McCormac et al., 1998a; McCormac et al., 1998b; Hogg et al., 2002; McCormac et al., 2002). The most recent estimate of the mean N/S offset is calculated to be 36 ± 27 ^{14}C yrs (Hogg et al., 2020). The N/S offset is proposed to result from a higher sea-air $^{14}CO_2$ flux from the more immense SH oceans (Rodgers et al., 2011; Goosse et al., 2024).

The first SH calibration curve (SHCal02) was published by McCormac et al. (2002), composed of dendrochronologically dated tree rings from New Zealand, Tasmania, Chile, and South Africa for the second millennium AD. At that time, a correction value of 41 ± 14 yrs for IntCal98 was used for the period outside this range (Stuiver et al., 1998a). For the 2004 update (SHCal04) by McCormac et al. (2004), the SHCal02 datasets were extended to 11,000 cal BP through a random effects model (Buck & Blackwell, 2004) that accounted for the slow variations of the interhemispheric offset over time. However, the possibility of large-scale carbon reservoir changes that may have altered the interhemispheric offset before the Holocene limited the calibration of samples older than 11,000 cal BP (Hogg et al., 2013).

The 2013 update (SHCal13) also utilised the datasets incorporated into SHCal04 from 0–1000 cal BP, with the addition of ANSTO Huon data from 325–175 cal BP (Hogg et al., 2013a). SHCal13 was also extended with the inclusion of Waikato kauri, Huon and modified CAMS Huon datasets (Zimmerman et al., 2010; Hogg et al., 2013a; Hogg et al., 2013b). Additionally, SHCal13 was constructed using a Markov chain Monte Carlo (MCMC) implementation of the random walk model (Blackwell & Buck, 2008; Heaton et al., 2009; Niu et al., 2013). The random walk model incorporates an approximate Bayesian method that considers additional aspects of the component data, such as the potential uncertainty in the calendar ages of older determinations, and that many tree-ring observations related to multiple years of metabolisation (Buck & Blackwell, 2004). Ultimately, this approach enabled the unique structures in the calibration datasets to be included in the curve, such as floating sequences of tree rings and more complex covariances in the calendar age estimates provided by wiggle-matching or paleoclimate tie-pointing (Heaton et al., 2020a, p. 882). However, the random walk method did have several limitations. Firstly, the method was slow to run, requiring many highly dependent parameters. Secondly, assessing whether the MCMC had reached its equilibrium distribution was challenging. These inherent aspects of the random walk method restricted the ability to explore the impact of specific modelling assumptions or individual data on the final curve (Heaton et al., 2020a).

In 2020, both hemispheric calibration curves were redesigned from the random walk construction method used in previous versions to an approach based on Bayesian splines with errors-in-variables (Heaton et al., 2020a; Hogg et al., 2020; Reimer et al., 2020). The Bayesian

spline construction method creates a calibration curve based upon a trade-off between the quality of the curve's fit to the calibration datasets and its roughness/wiggliness (Reimer, 2022, p. 532). This penalty on roughness limits "over-fitting" and the potential introduction of false variability. An additive error term was also included, dealing with any potential additional variability in observed tree-ring ^{14}C measurements and explicitly recognising rapid atmospheric ^{14}C change events (e.g., Miyake et al., 2012; Miyake et al., 2013). Therefore, the main difference in applying SHCal20 to previous versions of the SH calibration curve is the increase in the level of detail within the structure of the curve and the introduction of prediction intervals which recognise potential additional sources of variation in observed ^{14}C determinations beyond that occurring in laboratory measurement (Heaton et al., 2020a, p. 859).

3.2.3 Accelerator Mass Spectrometry (AMS)

The measurement of radiocarbon is inherently restricted by its low abundance, placing a statistical limit on the precision of any radiocarbon date. This problem is highlighted by Bronk Ramsay (2008, p. 258), who states that for a measurement with an overall precision of 25 years (0.3%), you need to have at least 10^5 atoms present, implying 2 μg C for a modern sample, or about 10 μg C for a sample that is 12,000 years (12 ka) old. Thus, the technique's measurement stage aims to accurately measure the isotope ratio with high precision (Bronk Ramsey, 2008, p. 258). Over the past 50 years, there has been a steady improvement in ^{14}C dating measurement methods, particularly regarding precision and cost efficiency. Until the late 1970s, the sole technique for evaluating the ^{14}C concentration ratio in a sample was by measuring its radioactivity: the emission rate of beta particles per gram of total carbon. Initially, this was achieved using modified Geiger counters and gas proportional counters, and later, liquid scintillation spectrometers were developed (e.g., Pearson et al., 1977; Tans & Mook, 1978; de Jong et al., 1979; Pearson, 1979; Stuiver et al., 1979; Stuiver & Quay, 1980).

However, one of the most significant developments is the introduction of accelerator mass spectrometry (AMS) for directly detecting radiocarbon (Bronk Ramsey, 2008, p. 258). AMS combines mass spectrometry with an accelerator to measure isotopic ratios (Litherland, 1980; Allen, 1987; Synal & Wacker, 2010). In a ^{14}C sample, negative beta decay, monitored over several weeks or months, will occur in only a tiny fraction of the ^{14}C atoms present. Decay

counting systems infer the concentration of ^{14}C in an organic sample by measuring the rate of ^{14}C beta decay exhibited by that sample and comparing it against a contemporary standard. However, an AMS system directly measures the isotope ratios of ^{14}C relative to ^{13}C and ^{12}C, comparing that value with the $^{14}C/^{12}C$ ratio exhibited by a contemporary standard.

The development of AMS has been heralded as revolutionary for archaeological applications because it provided the ability to date tiny samples (Taylor, 1995), opening a range of new research questions which previously were beyond the reach owing to available datable material being too small or precious (see Damon et al., 1989). Consequently, AMS technology has permitted the measurement of very specific target organics containing trace amounts of carbon (i.e., individual seeds, pollen species, specific molecular weight fractions, single amino acids, or a specific protein isolated from samples of bone or teeth). Ultimately, this technique has resulted in an increased efficiency compared to traditional decay counting methods, with this increase in efficiency resulting in smaller sample sizes (in the order of a milligram of carbon) (Bronk Ramsey, 2008, p. 258). As described by Harris et al. (1987), the development of AMS has fundamentally transformed our understanding of early plant domestication, the spread of anatomically modern humans, and the population of the New World. AMS radiocarbon dates now dominate most archaeological and paleoenvironmental chronologies (see Bayliss, 2009; Hajas, 2009; Kuzmin, 2009), as almost every site produces numerous datable samples (and, where possible, single-entity samples) (Ashmore, 1999). Therefore, rather than simply dating a single sample, it is now standard practice for archaeologists to combine large numbers of radiocarbon dates to create chronological models designed to test specific hypotheses (Bayliss, 2009).

3.2.4 Bayesian Analysis

Another influential development in ^{14}C dating has been the rise of Bayesian analysis (Christen & Litton, 1995; Goslar & Madry, 1998; Buck & Millard, 2004; Bayliss, 2009; Bronk Ramsey, 2009a). Bayesian statistical analysis is a widely used tool for investigating chronology because it allows relevant archaeological information to be incorporated into the analysis logically, coherently, and explicitly, offering a comprehensive chronological framework (Christen & Litton, 1995). The Bayesian approach combines calibrated radiocarbon dates with known 'prior'

information (Bayliss, 2015, p. 680), resulting in a chronological framework with functional, analytical tools, allowing ^{14}C dates to be integrated with archaeological information to develop an informed fine-grained chronology, integrating places, people and things (e.g., Bayliss et al., 2007; Whittle et al., 2011). Therefore, the application of Bayesian analysis results in dating probabilities that not only relate to the ^{14}C data in the model but also to intervals or events within the archaeological sequence. This includes the modelled time between dated contexts, or the span represented by a set of dates. Bayes' theorem was first developed in the eighteenth century. In probability theory and statistics, the theorem, named after Thomas Bayes, describes the probability of an event based on prior knowledge of conditions that might be related to the event. The mathematical basis for Bayes' theorem can be expressed as:

$$p\,(\mathrm{t}\,|\,\mathrm{y}) \propto p\,(\mathrm{y}\,|\,\mathrm{t})\,p\,(\mathrm{t})$$

As described by Bronk Ramsey (2009a, p. 338), 't' is the set of parameters and 'y' is the observations or measurements made. The prior, 'p(t),' is the known information we have about the parameters (mostly events). The likelihood, p(y|t), is the measurement given a set of parameters. The posterior probability, p(t|y), is the probability of a particular parameter set given the measurements and the prior. In a Bayesian analysis, we must express the information we have about the chronology in these terms (Figure 3.2.1).

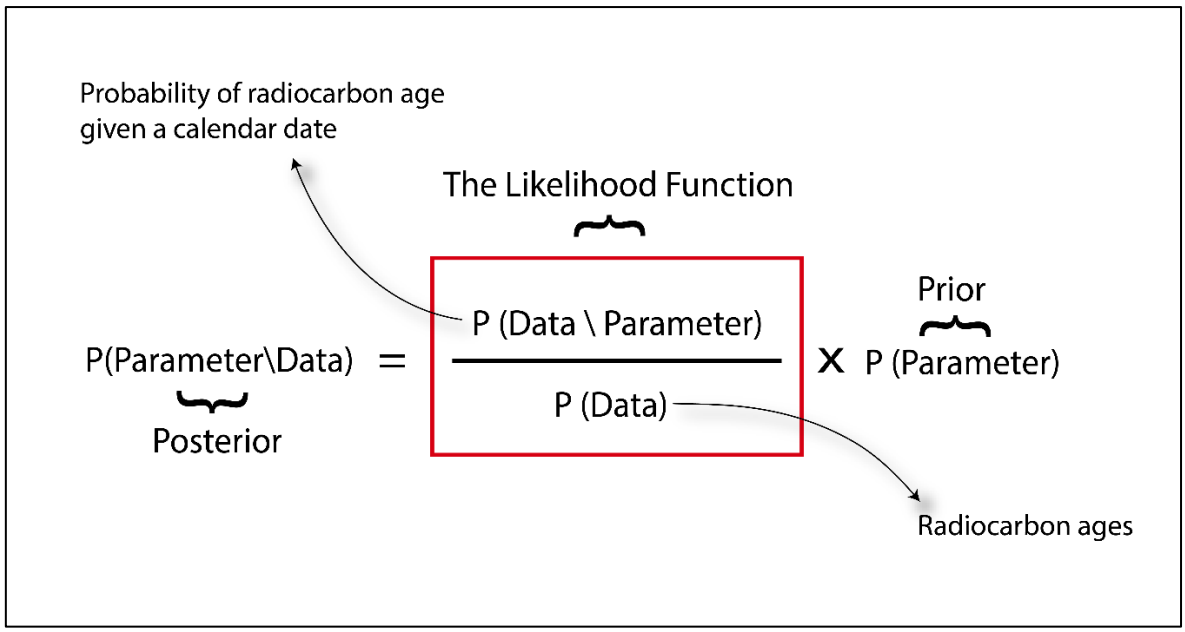

Figure 3.2.1. Chronological application of Bayes Theorem.

When applying this theorem in chronological applications, numerical calibrated radiocarbon ages (likelihoods) can be combined with independent information about the chronology (priors) to calculate an improved chronological model (the posterior) (Hajdas et al., 2021, p. 15). Therefore, Bayesian analysis creates a suitable posterior that reflects evidence from the archaeological record and the temporal relationship between dated events. These statistical methods have been incorporated into purpose-built statistical packages such as OxCal, BCal, CALIB, DateLab, and Bacon (Buck et al., 1991; Stuiver & Reimer, 1993; Bronk Ramsey, 1994; Buck et al., 1999; Bronk Ramsey, 2001; Nicholls & Jones, 2001; Jones & Nicholls, 2002; Blaauw et al., 2018).

The reason Bayesian analysis has been so widely adopted in radiocarbon dating can be summarised in three points. First, combining radiocarbon dates with prior information can dramatically improve precision, making it possible to explore research questions within short time spans (Cleal et al., 1995; Bayliss et al., 2007; Meadows et al., 2007; Whittle & Bayliss, 2007; Bronk Ramsey et al., 2010b). Second, Bayesian analysis allows uncertainties within the model to be quantified, resulting in the ability to make robust comparisons between the chronology of regions or cultures (see Needham et al., 1997; Manning et al., 2006; Sharon et al., 2007; Higham et al., 2014). Third, strategies for dealing with outliers can be incorporated

into the analysis, specifically testing that the radiocarbon measurement data agrees with the included prior information (e.g., Higham et al., 2010).

3.2.5 Wiggle-Match Dating (WMD)

The calibration of a single ^{14}C date from the notional '^{14}C age' to an accurate 'calendar age' almost always results in a considerable loss of precision, resulting from the nonlinear nature of calibration curves. Therefore, no single-valued, differentiable, inverse function can be used as a straightforward calibration (Bronk Ramsey et al., 2001, p. 381). Yet, if several different points on this curve are sampled, where the calendar age relationship is well characterised, the ^{14}C data can be fitted to the shape of the calibration curve. For example, if multiple ^{14}C samples of tree rings are taken from a timber post, where the age difference between the rings is known (by ring counting), and the terminal tree ring is included in the final sample, the corresponding ^{14}C results can be formed into a floating curve that can be compared with the applied calibration curve to give a precise calendar date for when the tree was cut down (Christen & Litton, 1995, p. 719). This technique is known as wiggle-match dating (WMD) (Christen & Litton, 1995; Bronk Ramsey et al., 2001, p. 381; Galimberti et al., 2004). Matching the ^{14}C data to the wiggles in the calibration curve significantly improves the calibration's precision and reduces the influence of minor offsets (Bronk Ramsey et al., 2001).

Within the Bayesian framework (OxCal D_Sequence model), a WMD is essentially a normal sequence model with a very strong prior, where the only parameter of interest is the final modelled date (Felling Date). However, this technique is not only restricted to tree ring applications and can be applied in cases where the relationships are described only in terms of sequences, phases and other similar constraints (see Manning & Weninger, 1992; Weninger, 1997; Lange, 1998; Blaauw et al., 2003; Mellstrom et al., 2013). This approach has been shown to produce very precise calibrated results under certain conditions, with fewer than ten measurements spaced at decadal intervals or better, giving 95% probability ranges of only a few decades (Bronk Ramsey et al., 2001, p. 264; Hogg et al., 2003; Hamilton et al., 2007; Nakamura et al., 2007; Hogg et al., 2012; Meadows & Zunde, 2014; Hogg et al., 2017). This dating technique uses the inherent wiggly nature of the calibration curve to its advantage

because well-characterised and rapid changes in radiocarbon concentration in the atmosphere can be identified and accounted for in the dating model.

The WMD method was initially tested by Galimberti et al. (2004), who utilised simulations to examine the influence of several variables on the technique (e.g. sequence length, sampling frequency, and measurement precision), determining the optimum sample number and ^{14}C date precision required to generate accurate calendar ages for archaeological material with high precision. Since this study, WMD has been applied in archaeological contexts around the world (see Manning & Weninger, 1992; Weninger, 1995; Manning et al., 2001; Hogg et al., 2003; Hamilton et al., 2007; Quarta et al., 2010; Hogg et al., 2012; Meadows & Zunde, 2014; Bayliss et al., 2017; Hogg et al., 2017), and was first applied in New Zealand to produce calendar age dates of two important volcanic eruptions (which generated tephras): the Kaharoa eruption using a carbonised log (Hogg et al., 2003) and the Taupo eruption using a tree felled by the blast generated by the emplacement of the climactic pyroclastic flow deposit (non-welded ignimbrite) at the Buried Forest at Pureora (Sparks et al., 1995; Hogg et al., 2012; Hogg et al., 2019b; Lowe & Pittari, 2021).

However, there are limitations to the technique. Specifically, the ability of an atmospheric calibration curve to provide accurate calendar age information for radiocarbon dates derived from samples from a specific locality is influenced by four factors (Hogg et al., 2019, p. 1267):

1. Differences in atmospheric ^{14}C levels within each of the two reservoirs (intra-hemispheric homogeneity), which may vary with time;
2. The difference in timing of growing seasons (see Manning et al., 2020);
3. The accuracy, precision, and reproducibility of component data sets; and
4. The suitability of the statistical approach that combines the component ^{14}C data sets into the calibration curve and the linked approach used to calibrate a new determination against it.

Therefore, the precision of a WMD date relies on the accuracy, precision and reproducibility of the applied calibration curve. As discussed above, the SH calibration curve (SHCal20) over the last 1000 years comprises a range of tree-ring datasets, resulting from measurements from various laboratories, comprising some one-year, two-year, three-year, five-year and ten-year tree-ring blocks (Hogg et al., 2020). The lack of continuous one-year data means that short-term variations in the atmospheric concentration of ^{14}C are possibly not well represented within the calibration curve for some periods, thus affecting the accuracy and precision of the produced WMD (Bronk Ramsey, 2008, p. 264; Hogg et al., 2022).

These factors were highlighted by a study conducted by Bayliss et al. (2017) in the Northern Hemisphere, which tested whether WMD could produce accurate calendar ages for a series of short tree-ring sequences (~30 annual rings) within the Medieval Period. This analysis showed that less than half (47.7%) of the short WMDs resulted in accurate calendar ages (compared to the dendrochronological dates of the same sample material). Several possible reasons for such low success rates were suggested, including high levels of annual ^{14}C variation not captured by the decadal or bi-decadal data used in the applied calibration curve (IntCal13) and additional sources of variation present in the data, such as geographical offsets, seasonal offsets, or laboratory biases (see Bronk Ramsey et al., 2010a; Hogg et al., 2013b; Bayliss et al., 2017; Hogg et al., 2017; Hogg et al., 2019a).

Laboratory offsets are commonly reported and can result from issues with dendrochronological reliability, the efficiency of pretreatment processes to remove modern or background contamination, and the applied measurement method (Hogg et al., 2017). For example, Hogg et al. (2013b) examined the possibility of inter-laboratory offsets using twelve contiguous decadal kauri samples analysed by five different radiocarbon dating laboratories. This analysis reported initial inter-laboratory offsets from weighted mean values of up to 41 ^{14}C years. Hogg et al. (2013b) determined that these results were likely caused by inconsistencies in the pretreatment regimes and measurement processes used by each laboratory. With these results in mind, in the pilot study conducted before the research presented here, Hogg et al. (2017) also checked for possible laboratory analytic offsets in SHCal13 by measuring duplicate 5-ring blocks of kauri (sample SPC002) for the relevant time interval, AD 1650–1829. Generally, the ^{14}C data from the known dendro-age kauri closely followed the shape of the SHCal13

calibration curve. However, the kauri data were slightly older, with a mean offset to SHCal13 of 12.7 ± 1.1 ^{14}C years, suggesting a possible laboratory analytic offset to SHCal13 may exist.

To investigate this result further, Hogg et al. (2019a) examined the accuracy, precision, and reproducibility of the component ^{14}C datasets within SHCal13 and investigated the statistical model used to create the SHCal13 calibration curve. In this study, Hogg et al. (2019a) constructed a new version of the SHCal13 calibration curve (SHCal13-NEW) using the Bayesian spline construction method, including the same five datasets included in SHCal13 for the post-Little Ice Age (LIA) interval AD 1500–1950. The structure of SHCal13-NEW predominantly followed the same shape as SHCal13. However, in some periods (e.g., AD 1760–1800 and 1900–1920), it appeared to show higher inter-annual variation, as indicated by more highly attenuated peaks and troughs. The affected periods heavily depend upon the Quaternary Isotope Lab (QL) datasets, which may create a younger bias to other parts of the calibration curve unless compensated for in the modelling. Crucially, in regions where QL data overlap with other data, QL was consistently younger, suggesting such a bias may exist.

Despite the improvements made in SHCal20 (compared to previous versions), the possibility of laboratory biases affecting specific datasets and periods within the SHCal20 calibration curve persists. Therefore, in parallel to this research, Prof Alan Hogg and colleagues have continued to test the accuracy and improve the resolution of the Southern Hemisphere calibration curve. So far, three time periods have been investigated (AD 1450–1649, AD 1650–1829 and AD 1830–1855), with interim results suggesting specific datasets within SHCal20 may be biased towards younger ages (Hogg, 2023 personal communication). However, the results of these investigations are not yet published, and more work is required to confirm them. Despite these limitations, when applied in the appropriate situation with accurate calibration data, WMD has the potential to develop accurate calendar ages for specific events in time at a far higher precision than other ^{14}C dating methods.

Chapter 4. Site Information

4.1 Site Selection and Review

Several factors were considered when selecting which pā to include in this study. First, a geographic spread of sites across the region was prioritised, ensuring pā in the region's north, centre, and south were represented. This criterion aimed to ensure that the regional spatial-temporal relationships were captured within the sampled post-assemblage. Second, wetland sites exhibiting the environmental conditions suitable for wooden artefact preservation were targeted — sites with anaerobic and chemically reduced waterlogged conditions (Wallace, 1985). Generally, pā within this region have not been investigated since they were first recorded or excavated in the late 1960s and early 1970s, and the environmental conditions surrounding these pā have varied over time (i.e., water table rise or fall). Focusing on pā that have retained their wetland environment, providing the best possible conditions for wood preservation, aimed to ensure an adequate sample number for analysis. Finally, pā with a history of previous archaeological investigation were targeted, prioritising those with recorded evidence of preserved *in situ* palisade defences. As the excavations conducted in this study primarily focus on identifying and sampling identified palisade posts, any previous archaeological interpretations provide valuable contextual information when developing an accurate picture of the site's occupation history.

The selection process began with a detailed review of pā within the Middle Waikato Basin. Various literature sources were covered, including site record forms from the NZ Archaeological Association's Site Recording Scheme (Archsite) (see Appendix A), previously published archaeological reports, and unpublished excavation notes, surveys and plans. Additionally, site visits were conducted to all the pā considered in this study, with walkover surveys used to assess the likelihood of identifying preserved palisade defences. Following this review, six pā were selected for investigation (Figure 4.1.1). The selection includes two pā from Taupiri in the north: Taraheke Pā (TAR) and Te Uapata Pā (TEU); three from the southern Waipa area: Lake Mangakaware 1 (MA1), Lake Mangakaware 2 (MA2), and Lake Mangahia

(MGA); and one from the outskirts of the Hamilton City area: Lake Rotokauri (ROT). The information collated from each of these pā is summarised below.

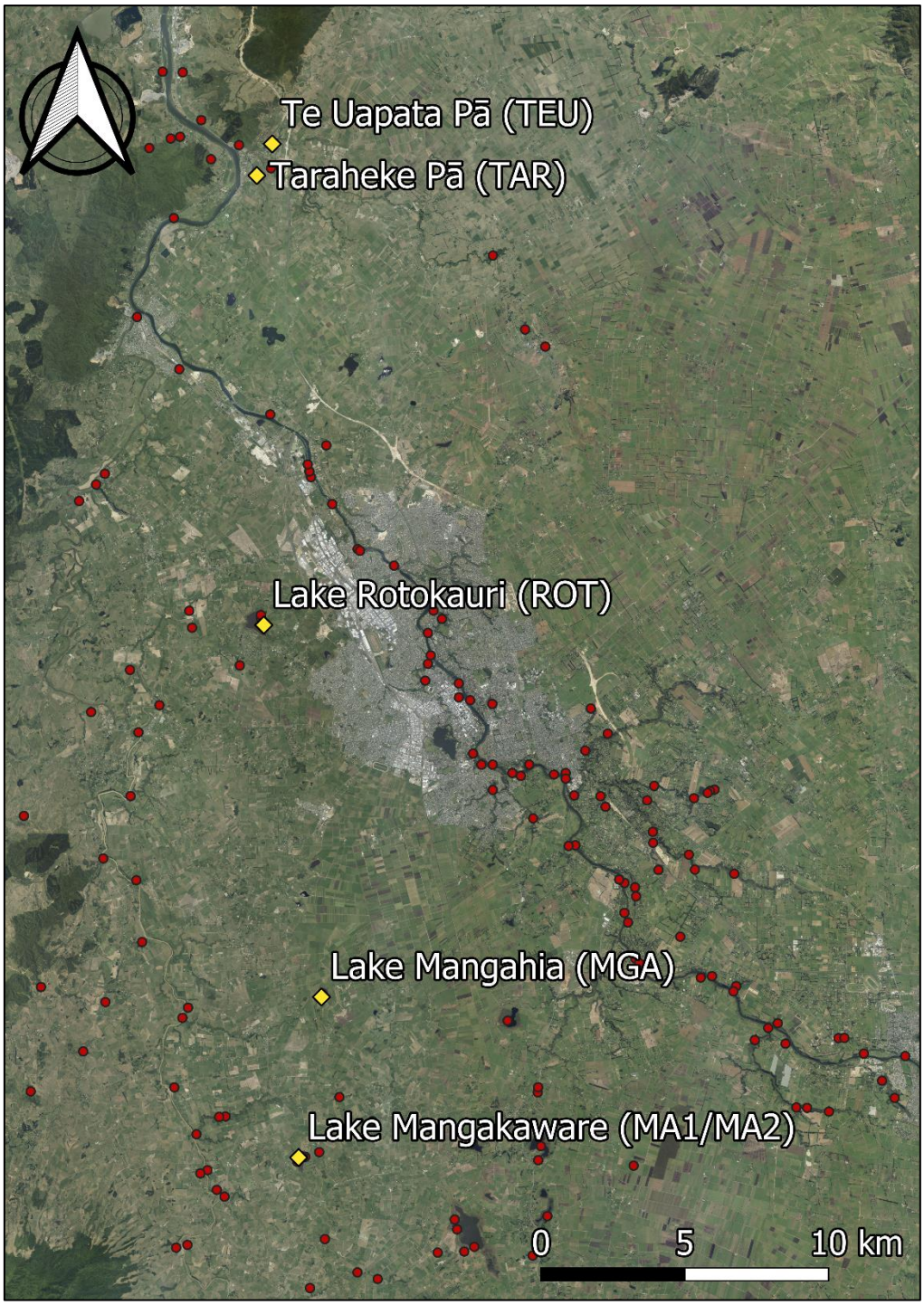

Figure 4.1.1. Distribution of the subject pā (yellow diamonds) and recorded pā (red dots) within the Middle Waikato Basin[5].

[5] This figure includes data sourced from the LINZ Data Service, licensed for reuse under the CC BY 4.0.

4.1.1 Lake Mangakaware

Lake Mangakaware is located 13 km northwest of Te Awamutu, just south of Ngāhinapōuri, and is one of several small peaty lakes in Waipā district. The lake is situated at an elevation of 38 m above sea level (asl), covering an area of 12.9 ha, is up to ~4.8 m deep, and is classed as an old (~20 ka) blocked-valley riverine lake in origin (Lowe & Green, 2024). Two pā are recorded around the lake (see Appendix A.1 and A.2), referred to previously as MA1 (S15/16) and MA2 (S15/18) (see Bellwood, 1969b, 1971a; Peters, 1971; Bellwood, 1972b, 1978a). A third pā is also recorded east of MA1, referred to as MA3 (S15/361). While previously recorded as a stand-alone pā (see Appendix A.3), current archaeological investigations suggest this small mound is likely an extension of MA1, functioning as an annexe for cooking and processing activities (Figure 4.1.2). The outlet stream of Lake Mangakaware once connected the lake to the Waipā River, providing a valuable transport route throughout the region and to the coast. Access to the coast is also possible via the land-based Pirongia mountain crossing (Bellwood, 1978a, p. 11). The pā recorded around Lake Mangakaware are in an ideal defensive position, surrounded by a rich supply of native fauna and flora resources, and close to pockets of sandy soils ideal for constructing living surfaces and horticultural activities (see Cassels, 1972a).

Figure 4.1.2. Location of MA1 (S15/16), MA2 (S15/18) and MA3 (S15/361) at Lake Mangakaware.

The Waikato Museum Archaeological Society undertook excavations at Lake Mangakaware between August 1968 and December 1970. These excavations focused on MA1 and MA2, with several studies published on the results (see Pick, 1968; Bellwood, 1969b, 1971a, 1971b; Peters, 1971; Bellwood, 1972b, 1978a). The findings from these investigations are summarised below. In addition to this published information, three site visits were conducted at Lake Mangakaware in June, July, and November of 2019. Walkover surveys of each pā observed that the surface of all three sites was covered in vegetation and undergrowth, obscuring the visibility of the natural topography. Clear evidence of pugging and stock trampling was observed at MA2, as the pā is still routinely grazed by stock, whereas MA1 and MA3 are in an area retired from grazing. Despite these conditions, the surveys identified several visible palisade rows at MA1 and MA2. Given the previous archaeological excavations conducted at Lake Mangakaware and the identification of preserved palisade defences, these pā were considered prime candidates for investigation.

4.1.1.1 Lake Mangakaware 1 (MA1)

The Waikato Museum Archaeological Society conducted excavations at MA1 in 1969. The subsurface excavations encompassed four trenches (Northern x 2, Western and Southern) and five excavation squares (A1, A2, B1, B2 and B3) (Figure 4.1.3). These excavation areas identified evidence of multiple imported sediment layers (constructed living surfaces), the remnants of several structures and house floors, and several defensive rows of palisades (Peters, 1971, p. 128). Several lakebed dive zones were also investigated, recovering a sizeable wooden artefact assemblage.

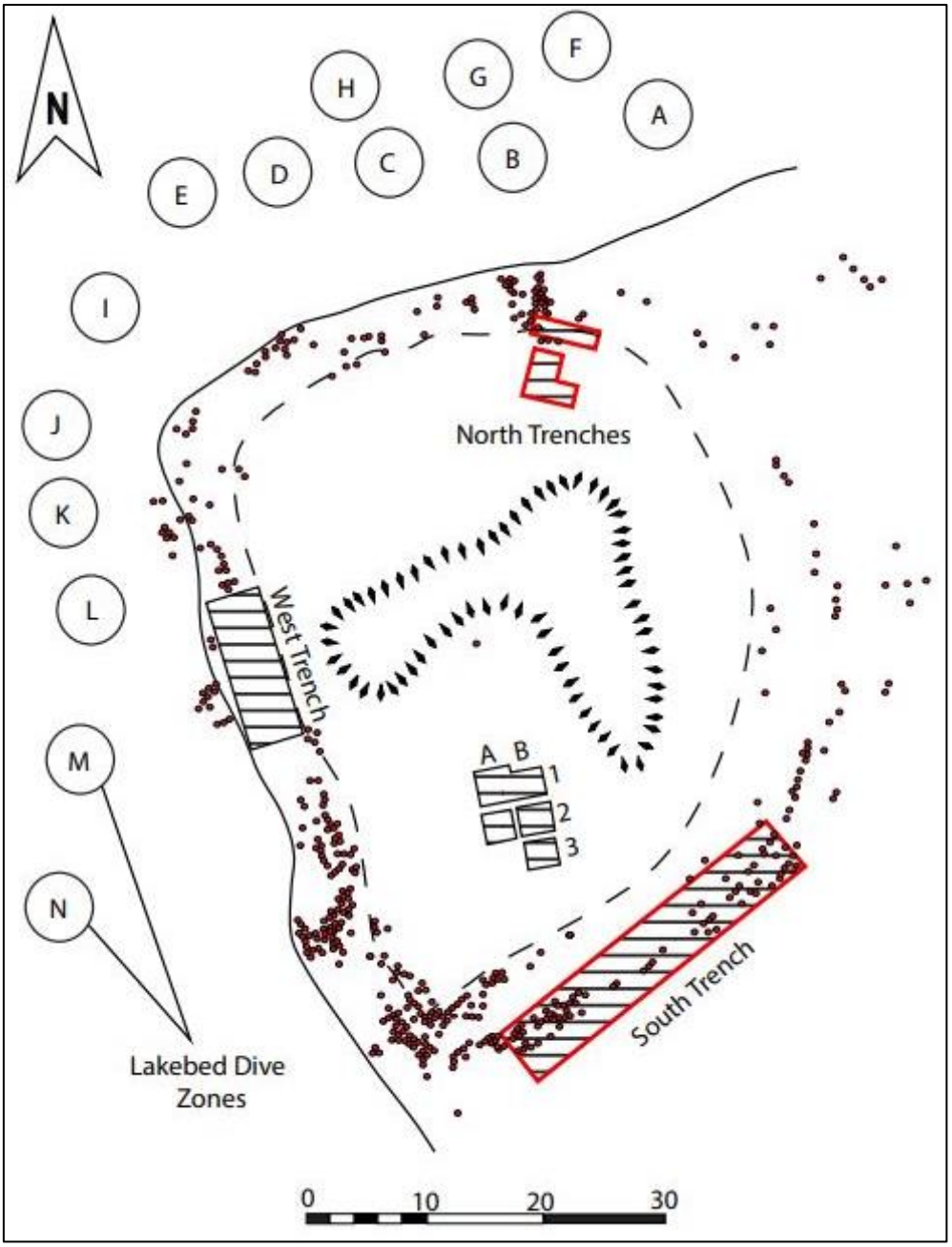

Figure 4.1.3. Digitised site plan of the 1969 excavations at MA1[6,7].

Excavation in the Northern trenches identified two distinct 'pathways' leading from the lake edge, through the palisade defences, to the centre of the pā. These 'pathways' are described as linear depressions and give the appearance of constant foot traffic (Peters, 1971, p. 131). A

[6] This plan drawing was digitised from the original site plan drawings with permission from Prof Peter Bellwood.
[7] Note. The locations of the Northern and Southern trenches are highlighted, as their positions are relevant to current excavations.

prominent oven feature containing freshwater mussel periostracum (*Echyridella menziesii*) was identified underneath one of these pathways, suggesting this area was previously used for cooking and processing activities. Excavation of the western trench exposed a continuous build-up of packed 'clay' floors (imported sediment), stratified with old, strongly weathered (clayey) ash and black peaty soil. These sediment layers abutted a line of vertical stakes and horizontally laid timber, hypothesised to be part of a retaining wall or a structure built at the toe of the raised mound (Peters, 1971, p. 130). Several large cobbles (presumably sourced from Mount Pirongia) were identified along the lake edge. Peters (1971, p.130) proposed that these cobbles protected the pā against rising water levels. Four palisade rows were also identified in this area, with a smaller fifth row of stakes positioned on the toe of the raised mound. Of these posts, four large rectangular posts (cross-section shape) identified on the southwestern side of the Western trench were suggested to represent an independent structure, potentially a storehouse (Peters, 1971, p. 130). Excavation in the Southern trench revealed evidence of up to six rows of palisades, with over 60 posts identified in this area (Figure 4.1.4). The level of fortification identified in the southern trench is striking, situated on the landward side of the pā and greeting individuals or groups approaching from the south. The extensive palisading present in this area could be interpreted as intentional, providing a visual representation of the defensive strength of the pā.

The central excavation squares (Al, A2, Bl, B2, and B3) uncovered evidence of three house floors with associated postholes, plank slots, and remnants of semi-decomposed posts. The house floor outlines were orientated in a southwest-northeast direction, with the floors in B2 and A2 superimposed on each other. The house floors comprised a 'yellow sandy clay' interspersed with black soil mixed with charcoal concentrations, stones, and shells (Peters, 1971, p. 134). These inclusions are proposed to result from intensive living activities, representing cooking and heating hearths. Whether these deposits were redistributed throughout the site for rebuilding purposes could not be determined at the time. Finally, Peters (1971) suggested that further house floors likely existed in this area; however, the limited scope of the 1969 excavation prevented them from investigating this further.

Figure 4.1.4. 1969 excavation photograph of the southern trench at MA1 (Bellwood, 1969a).

In summary, Bellwood (1978a, p. 11) describes MA1 as a heavily defended and stratified pā. Six hundred and fifty palisade posts were recorded, with one post on the northern side of the pā described as still standing three metres tall (Bellwood, 1978a, p. 13). Additionally, up to six rows of palisades were identified on the southern side of the pā, with the inner rows consisting of large posts, while the outer rows were composed of 'lesser' timbers. In addition to the palisade defences, excavations recorded imported soil deposits up to two metres deep, with foundational timbers identified in the wettest areas of the pā (Bellwood, 1978a, p. 13). Structures identified at MA1 include several phases of house floor construction, possible raised storehouses and canoe landing stages. From these results, Bellwood interprets a long occupation history for MA1, with multiple superimposed living surfaces, cooking features, and activity areas. The 1969 excavation areas are still identifiable on the ground surface, and oven stones, cobbles, and charcoal-enriched soils are still readily identifiable on the northern side of the pā.

4.1.1.2 Lake Mangakaware 2 (MA2)

The Waikato Museum Archaeological Society also conducted excavations at MA2 in 1968 (Pick, 1968) (Figure 4.1.5). Investigations focused on areas where clay/sand lensing was present, and it was estimated that as much as 20% of the pā was excavated (Bellwood, 1978a, p. 14). Bellwood (1978a, p. 16) considered the palisade defences of MA2 as far less complex than MA1, with a total of 110 posts recorded. The palisade rows identified on the southern side of the pā are described as a "heavy inner row and a lighter outer row, separated by eight metres of open space". During the excavations, six posts were extracted using hydraulic equipment (Pick, 1968, p. 31). These posts were said to be embedded three metres in the ground and were hypothesised to be at least four metres tall above the ground surface during the site's occupation.

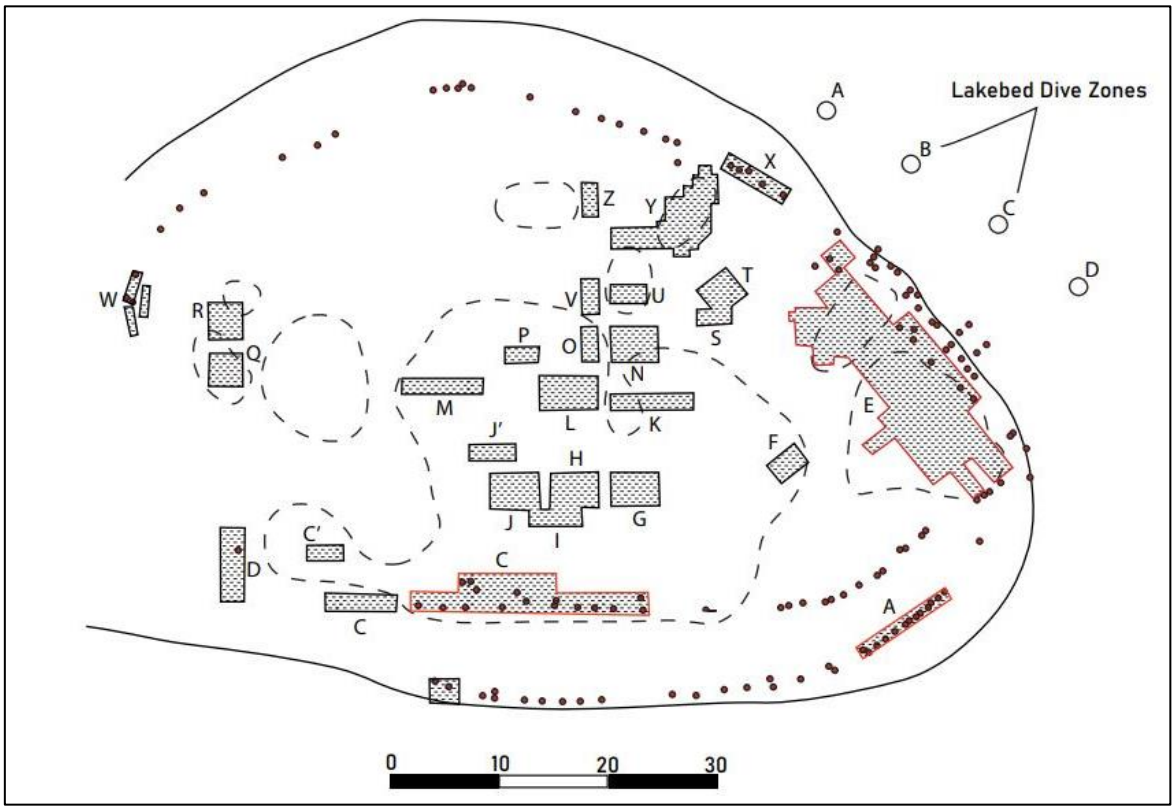

Figure 4.1.5. Digitised plan drawing of the 1969 excavations at MA2[8,9].

[8] Note. Locations of excavation areas A, C and E are highlighted in red, as their positions are relevant to current excavations

[9] This plan drawing was digitised from the original plan drawings with permission from Prof Peter Bellwood.

Bellwood (1978a, p. 16) used the characteristics of the extracted posts to develop a classification scheme describing variation in their form and construction. The classification scheme includes three typologies (Table 4.1.1). Bellwood (1978a, p. 18) suggests that Type A posts were only used to construct the inner landward side palisade rows, while Type B and C posts were used for general palisades and house structures. Additionally, Pick (1968, p. 2) notes that several posts featured tapered ends that were 'fire hardened', hypothesised to help drive the posts down into the soft peaty soil.

Table 4.1.1. Bellwood's (1978a, p. 16) palisade classification scheme.

Classification	Description
Type A	Large split or unsplit tree trunks with shaped lower ends facilitate the driving of posts into the ground.
Type B	Adze dressed timbers of square or rectangular cross-sections with tapered bases.
Type C	Undressed timbers with tapered bases.

The central area of MA2 is recorded as being built up with multiple sand lenses, interpreted as the 'marae' of the pā. This area (represented by Trenches F–P and S–V) covered approximately 750 m^2. Apart from evidence of possible raised storehouses and cooking features around its edges, this area was free of formal structures. The perceived distribution of archaeological features suggests that this area was the focus of outdoor activities at the site (Bellwood, 1972b, p. 28). The structures recorded at MA2 are grouped in a semicircle around the lake edge, located inside the palisade defences. The floors of these structures are constructed using imported sediment and/or sand, which were built up over time as they were maintained and re-laid as needed. Several floors contained successive (superimposed) sand layers and living debris of up to 80 cm (Bellwood, 1972b, p. 29).

Trench C was positioned on the southern side of the pā, identifying what Bellwood (1978a, p. 17) describes as a 'ngutu' entrance. Within this entranceway, eleven artefacts were identified, including five fragments of war clubs (ōnewa), two bird spear fragments, two adzes, eight fragments of human femur (smashed, burnt and covered in red ochre) and a large chunk of red ochre next to the bones (Bellwood, 1978a, p. 19). In addition to these artefacts, a small

breastbone pendant was found outside the palisade defence. Bellwood (1978a, p. 19) concluded that these artefacts represent the remains of a 'battle' within the entranceway.

Trench E was positioned on the eastern edge of the pā and provides detailed evidence of the stratigraphic layering, structural complexity, and site economy for MA2 (Bellwood, 1978a, pp. 25–31). Fourteen primary sand lenses, varying in size and shape, were identified in this area. Some form overlapping series, whereas others are not superimposed at all. Therefore, it was not easy to ascertain how many structures were used at once. The occupation history of MA2 is extensively commented on by Bellwood (1978a, p. 31), interpreted as evidence of four phases of occupation in Trench E. Year-round occupation of the site was hypothesised, highlighting three houses built with solid walls and hearths (presumably for heating). The 'bedding' from House 1 in Trench E appears to have been laid in autumn, supported by the observation of enclosed kahikatea seeds. Belwood (1978a, pp. 70–71) obtained six ^{14}C dates to anchor the chronology of MA2 (Table 4.1.2), providing evidence supporting an occupation history between AD 1450–1750. However, Bellwood (1978a, p. 71) notes that this occupation sequence seems long, given the lack of stratigraphic depth.

Table 4.1.2. Radiocarbon samples from the 1968 excavations at MA2 (see Bellwood, 1978a)[10].

Lab ID	Material	Provenance	CRA	$\delta^{13}C$ (‰)
NZ1120	Charcoal (unidentified)	Hearth: Trench A	2760 ± 78	-25.7
NZ1121	Wood (tree fern)	Floor of central shelter: Trench E	428 ± 84	-25.0
NZ1125	Wood (tree fern)	Post from house 1: Trench E	286 ± 83	-25.0
NZ1677	Charcoal (unidentified)	Post of shelter: Tench T	1191 ± 60	-23.3
NZ1678	Wood (tree fern)	Post from house 1: Trench E	221 ± 46	-30.3
NZ1679	Wood (unidentified)	Occupation level below House 2	382 ± 57	-23.4

When critically evaluating the ^{14}C samples recovered from MA2, it is clear there are some substantial issues within the assemblage. Foremost is the issue of in-built age. Both unidentified charcoal samples (NZ1120 and NZ1677) are too old to represent the occupation of MA2. Bellwood (1978a, p. 70) previously interpreted these samples as evidence for the use of old 'dried out' swamp timber. The remaining ^{14}C samples are from wooden material, described by

[10] Data is sourced from Petchey et al. (2022).

Bellwood (1978a, p. 71) as ‘presumably made from freshly cut young timber’. However, the basis of this statement is not reported. Three of these samples are described as ‘tree fern.’ There are two main groups of tree ferns in New Zealand: Cyathea and Dicksonia, the most common of which are *Cyathea dealbata* (silver fern), *C. medullaris* (mamaku), *C. smithii* (katote), and *Dicksonia squarrosa* (wheki) (see Dawson & Lucas, 2016). Tree ferns do not form trunks in the same way that conifers or flowering trees do (see Dawson & Lucas, 2016, pp. 52–53), which add a new layer of wood each year from a layer of cells (cambium) between the wood and bark. Tree ferns do not have a cambium layer. Instead, their trunk comprises an outer region (the cortex), including bundles of xylem and phloem that transport water and nutrients. Surrounding these bundles are more rigid tissues (sclerenchyma) that support the trunk. Therefore, unlike conifers, the outer region of the tree fern’s trunk does not represent the newest (youngest) region of cellular growth. Instead, the trunk represents the combined age of the tree fern, which inherently makes it susceptible to in-built age and an unsuitable species for radiocarbon dating.

While all four of these samples come from relevant archaeological contexts (when ignoring their sample type), they also suffer from the precision issues previously discussed in Section 2.2.4. This is especially relevant given Bellwood’s interpretation of phasing from the structural layout of Trench E, which cannot be established by the available ^{14}C data, even with modern applications of OxCal Bayesian modelling (see Appendix C.1). In conclusion, the 1968 excavations at MA2 were extensive, with a large proportion of the site excavated. Of relevance to the current study are the defences identified in Trench C and the occupation areas and palisade defences in Trench E. These two areas of the pā are well preserved to the present day and present the opportunity to link current-day excavations with the historical 1968 excavations.

4.1.2 Lake Mangahia (MGA)

Lake Mangahia is located approximately 3 km northeast of Ngāhinapōuri. The lake is classed as an old (~20 ka) blocked-valley riverine-phytogenic lake (a true ‘peat lake’), covering 8.4 ha at 39 m asl with a maximum depth of 1.8 m (Lowe & Green, 2024). The pā (S15/14) was first recorded by Doug Pick in November 1964, who described it as an artificially raised mound on the lake’s southern shore (Figure 4.1.6). A unique feature of the pā is the distinct causeway

(raised pathway), extending from the raised mound to the dry land to the south. As this causeway is visible in the 1943 aerial photographs, it appears to be related to the pre-European occupation of the site. However, it is also clear that the causeway has been widened to accommodate vehicle access. This pā is relatively isolated from other recorded archaeological sites in the surrounding area. However, three sites are recorded within a 4 km radius of Lake Mangahia, including a previously unrecorded soil quarry on the hill slope approximately 250 m to the south of the pā, a cluster of borrow pits (S15/733) on the southern side of the Mangahia Stream (which drains the lake), and a pā 3.5 km to the south (S15/90).

Figure 4.1.6. Location of the pā at Lake Mangahia[11].

The site record form provides limited information about the pā (see Appendix A.4), describing it as covering an area of approximately 1000 m^2, with the mound sitting about 2 m above the 1978 water level (Figure 4.1.7). In the late 1960s (dates not specified), Waikato Museum Archaeological Society members recorded palisades along the lake edge and landward sides of

[11] This figure includes data sourced from the LINZ Data Service and is licensed for reuse under the CC BY 4.0.

the pā, with the defences described as very heavy fortifications. Twenty palisade posts were said to be standing to a height of 3 m, with many more decayed to water level but preserved below the ground surface. Midden deposits of shell, ash, charcoal and oven stones were also observed at depths of 30–60 cm. Later (date not specified), Duffy Roach and Mr Lovell excavated three posts, described as 6–12 ft long, showing similar shape and taper characteristics to those described by Bellwood (1978a, p. 16) from Lake Mangakaware.

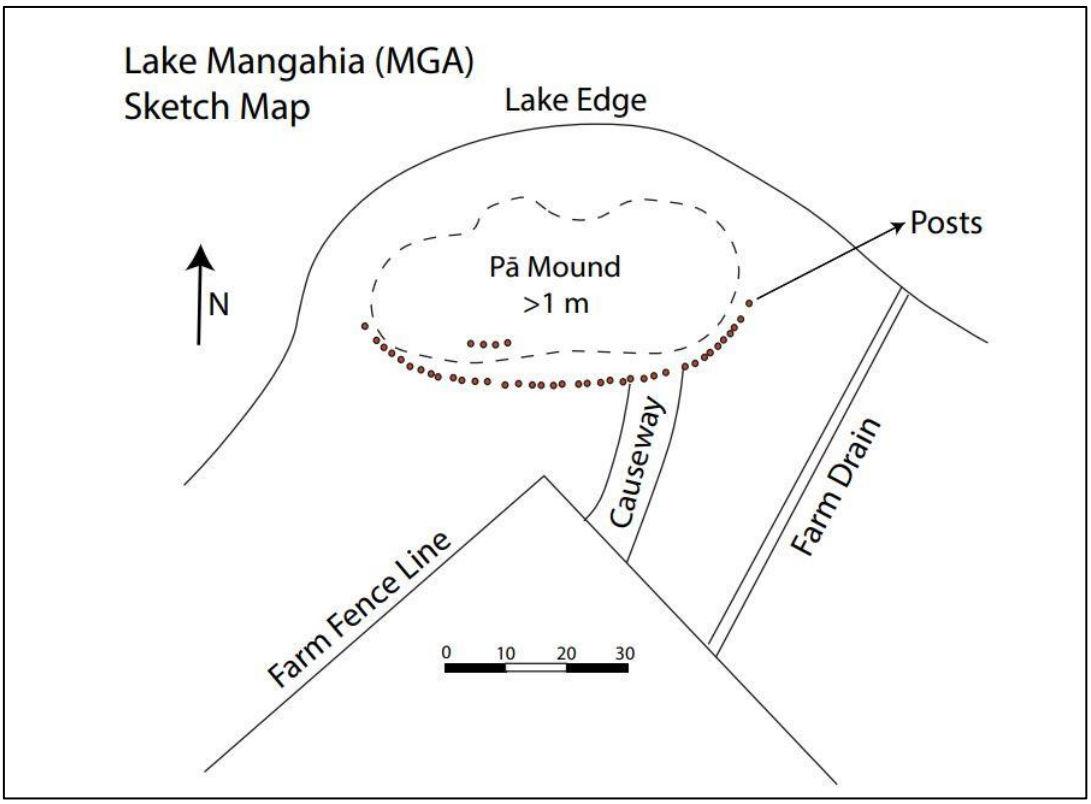

Figure 4.1.7. Digitised sketch drawing of the pā at Lake Mangahia[12].

A site visit to MGA was conducted on the 13th of July 2020. The pā was observed to be well-preserved, covered in long grass with occasional shrubby vegetation (mostly mānuka). A walkover survey identified a central platform with multiple peripheral terraces. Forty-two posts were identified, primarily located on the northern (lakeside) and southern (landside) borders of the pā. Several identified posts stood approximately 1 m tall (Figure 4.1.8), and one sizeable

[12] This sketch map was drawing by Mr Owen Wilkes and was source from the site record form (see Appendix A.4).

spilt post had a rectangular cross-section over 50 cm wide (Figure 4.1.9). The palisade defences identified at Lake Mangahia are exceptionally well preserved compared to the other pā investigated in this study. Because of these characteristics, the pā at Lake Mangahia was considered a prime excavation candidate.

Figure 4.1.8. Zac McIvor (left) and Rowan McBride (right) inspect a row of palisades at Lake Mangahia[13].

[13] This photograph was taken by Alan Hogg and is used with permission.

Figure 4.1.9. A large split palisade post standing >1 m tall and > 0.5 m wide at Lake Mangahia[14].

4.1.3 Taraheke Pā (TAR)

Taraheke Pā (S14/22) is one of six prominent pā located in Taupiri, close to the intersection of the Mangawara Stream and Waikato River (Figure 4.1.10). Taupiri was a significant region within the cultural landscape of the Waikato, with the number of pā in the area standing as a testament to its importance. The populations inhabiting this region likely controlled the movement of people and resources up and down the river. Additionally, the natural resources in the Taupiri area are plentiful, including high-quality horticultural soils and native flora and fauna within the river, streams and wetlands. Large areas of horticultural soils are recorded in the area, recognised by the distinctive borrow pits and anthropic soils that were converted into gardens by Māori (Gainsford & Gumbley, 2020; Gumbley, 2021). No previous archaeological excavation has been conducted at Taraheke Pā (see Appendix A.5). However, Sian Keith Archaeology has undertaken mitigation investigations of kūmara storage pits on the western bank of the Mangawara stream, approximately 70 m from the pā (S14/489) (Keith, 2019).

[14] This photograph was taken by Alan Hogg and is used with permission.

Figure 4.1.10. The six prominent pā located around the Taupiri river junction[15].

Taraheke Pā is located 800 m up the Whangamaire tributary, which flows into the Mangawara stream close to the junction with the Waikato River. The pā is situated on a headland that projects into the stream, with large banks up to 4 m above the waterway. The pā covers an area of 5000 m^2, defined by a large defensive ditch protecting the pā from land-based assault (Figure 4.1.11). A distinct linear ditch that bisects the length of the pā is visible on the ground and in lidar-derived imagery, extending across the defensive ditch to a point approximately 30 m south. Lidar imagery also shows a less well-defined transverse ditch approximately 30 m north of the main defensive ditch. This transverse ditch appears to be the remains of some form of internal division of the pā, perhaps representing an early phase of its defences.

[15] This figure includes data sourced from the LINZ Data Service and is licensed for reuse under the CC BY 4.0

Figure 4.1.11. Defensive ditches and linear ditch at Taraheke Pā[16].

Two site visits were conducted to Taraheke Pā in January and February 2020. The walkover survey identified a swampy margin surrounding the base of the headland, exhibiting the environmental conditions required to preserve wooden archaeological material (Figure 4.1.12). While no palisades were immediately visible in this environment, it was determined that they would likely be located within this wetland margin if they were retained *in situ*. Several test pits were dug within this environment to test this hypothesis, assess the soil profile, and identify potential excavation areas. Test pitting determined that the soil profile of this environment comprised two distinct silt layers. The upper silt layer (~20–40 cm) is formed from material eroding down the side of the headland (slope wash) and was devoid of cultural deposits. The lower silt layer (~40 cm thick) was water-logged and rich with organic material (natural and cultural), including wood, charcoal and freshwater mussel periostracum (*E. menziesii*). Finally, underlying this organic material was a layer of pale grey alluvial sand (Hinuera Formation: see Lowe and Green, 2024), which probably constitutes the original streambed. This soil profile

[16] This figure includes data sourced from the LINZ Data Service and is licensed for reuse under the CC BY 4.0.

suggests that if palisade defences were retained in this environment, the posts would most likely be encountered within the lower organic silt layer and its interface with the natural sandy deposit below. Given these observations and the environmental conditions surrounding the pā, it was determined that exploratory excavations within this zone could possibly identify palisade remains. Therefore, Taraheke Pā was selected for inclusion in this study.

Figure 4.1.12. The swampy margin around Taraheke Pā.

4.1.4 Te Uapata Pā (TEU)

Te Uapata Pā (S14/20) is another of the six prominent pā concentrated around the junction of the Mangawara Stream and the Waikato River in Taupiri (Figure 4.1.10). Whilst most of the pā in Taupiri are located beside the main waterways, Te Uapata Pā is situated on the edge of a lagoon close to the mouth of the Whangamaire Stream. The pā sits on a promontory that divides the major and minor channels, rising 2 m above the level of the adjacent streams. Te Uapata Pā was first recorded in February 1977 by S. Edson of the Waikato Art Museum. The original site record form contains minimal information about the pā, including the location of the site and a brief description (see Appendix A.6). In January 1996, Owen Wilkes updated the site record following a site visit. The pā is described as small by Wilkes as covering less than 2500 m^2, defined by a large defensive ditch and the stream edge. A second transverse ditch stretches across the headland's tip, enclosing the highest area of the pā (Figure 4.1.13).

Figure 4.1.13. A site plan of Te Uapata Pā[17].

Traditional Māori history associates Te Uapata Pā with the well-documented ancestor Mahuta, who established the pā following his migration inland from Kawhia (Jones & Biggs, 1995; Phillips, 1995). This association suggests that Te Uapata is an early pā connected with the Tainui migration inland. Mahuta's grandsons, Wharetipeti and Tapaue, are said to have occupied Te Uapata for a time until they left to try and claim the better gardening land available on the western bank of the Waikato River, opposite Mount Taupiri at Kaitotehe. Jones and Biggs (1995) describe the soils around Te Uapata as swampy, which may have led to Wharetipeti and Tapaue's desire for good (non-peaty) soils to grow their horticultural crops. Using a ruse, where they offered to assist Te Iranui and his people with planting kūmara, Wharetipeti and Tapuae overpowered Te Iranui and captured his tribes' lands on the west bank of the Waikato River. Wharetipeti and Tapaue then remained at Kaitotehe, which became their stronghold (Jones & Biggs, 1995, pp. 280–286; Phillips, 1995, p. 114; Kelly, 2002). Ultimately,

[17] This figure includes data sourced from the LINZ Data Service and is licensed for reuse under the CC BY 4.0.

both brothers were killed by Te Ruinga (Rangihoto's son) and his friend Maoa as a result of their deeds, with Jones and Biggs (1995, p. 280) dating these events to around AD 1700.

Archaeological investigations at Te Uapata Pā were undertaken by Gainsford and Gumbley (2020) in 2019, recording archaeological deposits directly affected by the installation of cultural symbolism at the site. Investigations near the headland's tip identified twenty-three archaeological features and evidence of an introduced sediment deposit. Archaeological features included three fireplaces (F1–3), one linear feature containing charcoal and 'rakeout' (F4) and a series of 18 postholes (F5–23). Bulk samples were taken from four features during the investigation (F1–4), with substantial amounts of freshwater mussel periostracum (*E. menziesii*) identified in the fill of F2. Ground-penetrating radar was used to survey the pā, identifying several potential storage pits adjacent to the surface depressions east of the platform. The results of the ground-penetrating radar survey also identified another possible defensive ditch, approximately 15 m southeast of the main defensive ditch. Eight charcoal ^{14}C samples were acquired from the bulk samples recovered from F1–4 (paired samples from each feature), comprising short-lived material (twigs) of manuka (*Leptospermum scoparium*) and akeake (*Dodonaea viscosa*) (Table 4.1.3).

Table 4.1.3. ^{14}C samples collected from TEU by Gainsford and Gumbley (2020).

Lab ID	CRA	Provenance	Sample type
Wk46316	189 ± 16	Fireplace (F1)	Mānuka (*Leptospermum scoparium*)
Wk46880	203 ± 18	Fireplace (F1)	Mānuka (*Leptospermum scoparium*)
Wk46315	200 ± 16	Fireplace (F2)	Mānuka (*Leptospermum scoparium*)
Wk46881*	433 ± 18	Fireplace (F2)	Mānuka (*Leptospermum scoparium*)
Wk46314	153 ± 17	Fireplace (F3)	Mānuka (*Leptospermum scoparium*)
Wk46882	224 ± 17	Fireplace (F3)	Mānuka (*Leptospermum scoparium*)
Wk46313	224 ± 16	Linear feature (F4)	Akeake (*Dodonaea viscosa*)
Wk46883	265 ± 17	Linear feature (F4)	Akeake (*Dodonaea viscosa*)

Note. Wk46881 is an outlier, possibly due to in-built age and 'old' wood use.

These ^{14}C dates were recalibrated using OxCal v4.4, implemented using SHCal20 atmospheric calibration data, with the internal consistency of the model tested using the General t-type outlier model (General, T(5), U(0,4), t) (see Appendix C.2). The results of this analysis were generally consistent, producing date ranges between AD 1650–1850 (95% HPD) (see also Gainsford & Gumbley, 2020, pp. 36–37). Two outliers were detected during the analysis:

Wk46314 and Wk46881. As the ^{14}C samples were collected as pairs from each feature, these results could reflect a problem with the analyses or in-built age. Unfortunately, the calendar position of the remaining ^{14}C dates coincides with the calibration plateau in the late eighteenth century, affecting the precision of the results. This lack of precision limits their use in the current study and provides only a broad indication of the site's occupation history.

Lastly, a site visit was conducted to Te Uapata Pā in February 2020. The initial walkover survey focused on the swampy margins at the base of the promontory, where the headland interacts with the lagoon and the adjacent streams. This environment was deemed the most likely to retain evidence of palisade defences. However, dense head-high vegetation significantly affects visibility in these areas. Despite this lack of visibility, several posts were identified along the toe of the eastern bank of the pā, recorded with a Leica RTK GPS unit so they could be located at a later excavation date (Figure 4.1.14). In addition to the preserved palisade row identified on the eastern bank of the pā, significant effort was made to locate posts on the western banks of the pā. However, these efforts were unsuccessful, likely due to the fluctuating water table of the western stream, with water levels significantly lower than those found on the eastern banks. Given the traditional history recorded for the pā and preserved palisade defences, Te Uapata was considered a prime candidate for inclusion in the current study.

Figure 4.1.14. Zac McIvor recording the location of a palisade post at Te Uapata Pā.

4.1.5 Lake Rotokauri (ROT)

Lake Rotokauri is located approximately 7 km to the northwest of Hamilton City. The lake is classified as an old (~20 ka) blocked-valley riverine lake that lies at 46 m asl and covers an area of approximately 42 ha, with a maximum depth of 4 m (Lowe and Green, 2024). Lake Rotokauri drains into the Waipā River via the Ohote Stream, providing a useful transport route through the region and out to the coast. The pā (S14/5) is close to a swampy peninsula on the northeastern corner of Lake Rotokauri (Figure 4.1.15). Similar to the pā at Lake Mangakaware and Lake Mangahia, the pā at Lake Rotokauri is situated in an ideal defensive position, surrounded by a rich supply of native fauna and flora resources, and close to pockets of tephric and sandy soils ideal for constructing living surfaces and horticulture.

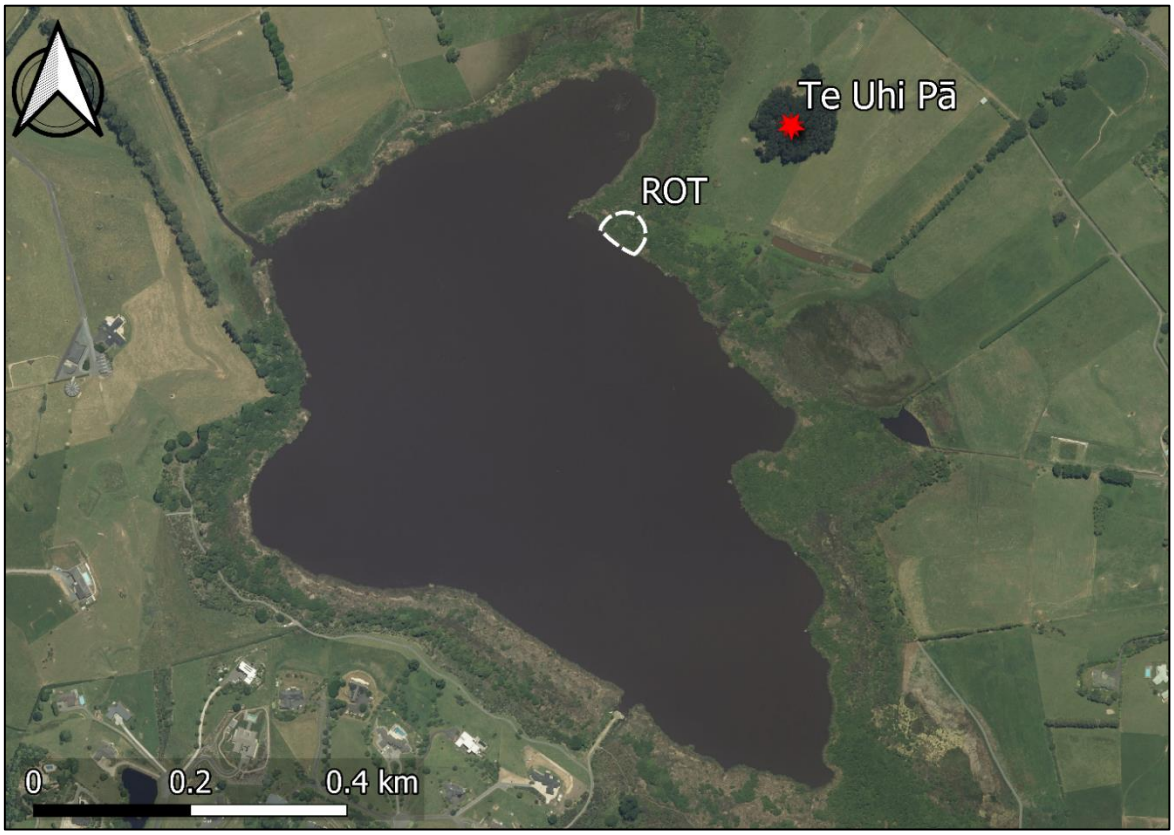

Figure 4.1.15. Location of the pā (ROT) on the shore of Lake Rotokauri[18].

[18] This figure includes data sourced from the LINZ Data Service and is licensed for reuse under the CC BY 4.0.

A large hilltop pā, Te Uhi (S14/486), is recorded less than 250 m from the pā on the shore of Lake Rotokauri. Information contained within the site record form suggests Te Uhi Pā is associated with Ngāti Ngārape and Ngāti Hourua (Appendix A.7), and that the pā was occupied up until the early 1800s when Ngāti Ngārape left to join their relatives at Takapaunui, Raglan. Additionally, three further pā are recorded 2–3 km to the west and south (S14/8, S14/50 and S14/69). Despite traditional history recording the occupation of Te Uhi Pā, limited information is available about the pā on the lake's edge. Notes in the site record form by Owen Wilkes suggest that the Waikato Museum Archaeological Society conducted archaeological excavations at the site between 1973–74. Some limited records of these excavations are held at the Waikato Museum, including field notes and plan drawings from two field seasons (Figure 4.1.16). Doug Pick (1968) wrote a brief paper about these excavations, indicating that a site survey and some limited sub-surface testing were undertaken. However, a complete account of these excavations has never been published.

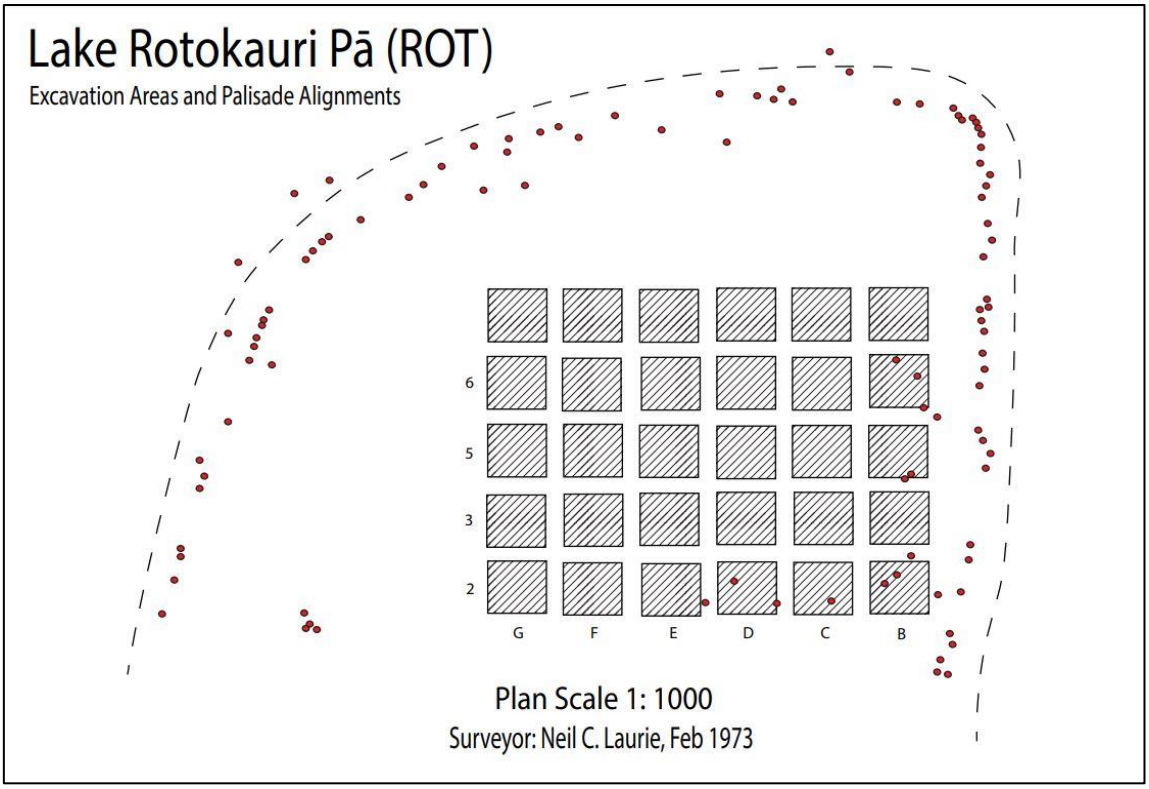

Figure 4.1.16. Site plan of excavations undertaken by the Waikato Museum Archaeological Society at Lake Rotokauri[19].

[19] This is a digitised copy of the original (unpublished) site plan sourced from the Waikato Museum.

The unpublished field notes from these excavations describe the pā as approximately 1/6th of an acre (~675 m^2), covered in charcoal-bearing soil deposits, and surrounded by roughly 80 posts and 80 stakes. The raised mound was approximately 4 ft (~1.2 m) above the water level. Many artefacts and samples were recovered during these excavations (housed in the stores of the Waikato Museum), including stone adzes, pounders, obsidian, pumice, and wooden implements. Although no ^{14}C dates were obtained from these excavations, the artefacts suggest an occupation in the pre-European period. The site record form contains an additional note from Doug Pick regarding the site and its history (see Appendix A.7):

"When I first saw the site, it was covered with blackberry and willow. There was an outer row of palisade butts across the neck and some on the lakeside. Many stakes stood in the water, out about 10 to 20 yards, suggesting an eel weir or canoe harbour. The most important features were the totara stakes and posts that stood at all angles within the perimeter. Few were upright, but most were at angles suggesting braces or stays. Their layout had no apparent order; most were 3' to 5' (90–150 cm) above the soggy ground and all of totara. The whole arrangement suggested to me a platform pā. In 1996, I took Janet Davidson to see the site, but some vandals (had] cut down every palisade. There were two small canoes; Lyn Peart removed one, and the other was partly buried by persons unknown".

Based on this information, a site visit was conducted to the pā in November 2021. Unfortunately, this area of the lake was densely covered in thick vegetation, completely obscuring the location and topography of the site. Despite this, the pā mound was located. However, a large proportion of the site was submerged by the lake, indicating that the water level was considerably higher than in the past. Despite reports that every post was cut down, the site visit identified four *in situ* posts on the northeastern boundary of the pā. Two posts stood approximately 1 m tall, while the last was only preserved just above the ground surface. Although the pā at Lake Rotokauri was not immediately considered an ideal candidate for investigation (due to the complicated history described above), the central location of the pā within the subject area and the observation of *in situ* palisade posts proved sufficient for inclusion in the project.

Chapter 5. Methods

5.1 Archaeological Excavation

The primary aim of the excavations conducted in this study was to identify, record and sample the extent of the surviving palisade defences at each of the six pā investigated. For this reason, excavations were targeted to specific locations of interest around each pā and did not explicitly seek to identify archaeological deposits relating to the site's occupation. All excavation areas were excavated by hand, except at Taraheke Pā, where a small digger was employed to remove the substantial overburden of post-depositional slope wash (see Section 9.1). Multi-context recording was used to document the information gathered from these excavations, with unique identifiers generated for all excavation areas (EA#), palisade posts (P#), artefacts (A#) and archaeological contexts such as sediment layers (C#). All archaeological deposits were recorded *in situ* using a Leica RTK GPS and photography. Finally, spatial analysis was undertaken using QGIS Geographic Information System Spatial Analysis Software v3.20.2.

5.1.1 Post Extraction and Sampling

Once the extent of the surviving palisade defences had been determined at a site, the posts in each identified palisade row were assessed to determine their suitability for extraction (removal from the ground) and sampling (for analytical purposes). This assessment was conducted via the observation of three specific post characteristics, scrutinised via small squares excavated around the base of each likely post (Figure 5.1.1 (A)):

1. The terminal tree ring (last annual growth period) had to be retained on the post, as evidenced by bark retention on the outer surface or observation of the waney surface (outer surface of a tree under the bark). Retention of the terminal tree ring is essential for the applied dating method, as it directly relates to the year the tree was felled, providing a TPQ for when the post was installed in a palisade row.
2. Ideally, a sampled post exhibited a diameter of >9 cm. This size requirement ensured a sufficient calendar spread of ^{14}C dates across the calibration curve during WMD (ideally >40 tree rings).

3. Selected posts had to be well preserved and in good condition, excluding posts displaying evidence of substantial decay, burning, scarring or buttressing. This requirement aimed to ensure that most of the posts sampled for analysis would survive and progress through the applied analytical stages.

Ultimately, this criterion aimed to ensure robust sampling procedures for analysis. However, where sufficient posts with these characteristics were limited at a site, this criterion was expanded to include posts with minor limiting characteristics (i.e., smaller diameter posts or posts exhibiting partial charring or damage that did not affect the entire growth sequence). Expanding the sampling criteria in this way prioritised a sufficient assemblage size over considerations of an individual post's characteristics, intending to ensure posts from all identified contexts (rows and areas) were represented, even when specific samples were dropped from the assemblage during the various stages of analysis.

Post extraction was achieved using a galvanised metal tripod with a block and tackle pulley mechanism. A soft nylon strap was wrapped around each exposed post (placed as far down the post as possible) before being gently levered out of the ground (Figure 5.1.1 (B)). This extraction method was applied in most cases. However, several of the largest (diameter and length) posts identified at MA1 were deemed too large to be extracted safely (see Section 6.1.1), as the force required to extract these posts exceeded the safety limits of the block and tackle. In these cases, the post was raised to an appropriate height (with the distal end remaining in the ground), and a sample section was cut from the base of the post. Once extracted, posts were cleaned with water before being recorded and photographed.

(A) *(B)*

Figure 5.1.1. (A) An example of a small square excavated around a palisade post. (B) Alan Hogg (left), Rowan McBride (centre), and Warren Gumbley (right) after extracting a post at MA2[20].

5.1.2 Recorded Information

Several characteristics of each extracted post were recorded, including maximum length, maximum diameter, height above ground surface, depth below ground surface, cross-sectional shape, taper type, and general comments. All size dimensions were recorded to the nearest cm (Figure 5.1.2). The maximum length was measured from the distal to proximal ends of the post. Maximum diameter was recorded using a diameter tape (specifically designed to record the diameter of trees), with the diameter recorded from the thickest part of the extracted post. Height above ground surface was measured *in situ* from the ground surface to the proximal end. Depth below ground surface was measured from the point at which the post entered the ground to the distal end. The cross-sectional shape was recorded as oval, round, square, rectangular,

[20] This photograph was taken by Zac McIvor and is used with permission.

or irregular. General comments noted all other characteristics such as preservation quality, scaring, charring, buttressing, removed branches, and overall shape (i.e., straight or 'kinked').

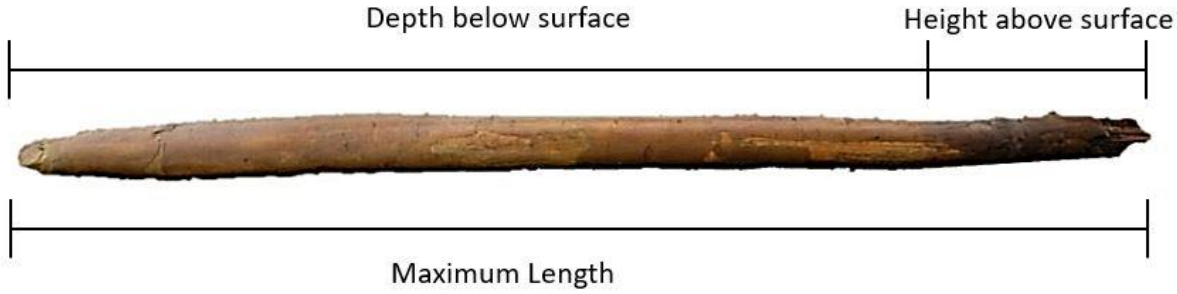

Figure 5.1.2. Size dimensions recorded for each palisade post.

Table 5.1.1. Applied taper classification scheme.

Taper Type	Description
Long	A taper that is adze-dressed on one or more sides, with the adzed surface extending more than 30 cm.
Short	A taper that is adze-dressed on two or more sides and is short in length (<30 cm in length). In most cases, this taper type appears to have been formed as the tree was felled.
Bulbed	A taper that is adze-dressed on all sides, exhibiting a distinctive bulbed end. This taper type appears to be an effort to make the post more challenging to pull out of the ground. Notably, this taper type is only found on large-diameter posts.
Notched	A taper that is adze-dressed on all sides with a square or rectangular cross-section and a distinctive notch cut into the side. Again, this taper appears to be an effort to make the post more challenging to pull out of the ground, and it is only found on large-diameter posts.
Irregular	Any taper which does not conform to the above categories. Generally, the irregular taper classification consists of crude examples that could result from the tree snapping as it was felled.

Specific consideration was given to the tapers of the extracted posts. As previously discussed, Bellwood (1978a, pp. 16–18) defined three post typologies following excavations at MA1 in the 1960s. Following the sampling strategy outlined above, all extracted posts could be classified as either Type A or C (as adze-dressed timbers were specifically not selected). However, after the extraction of several posts, it was clear that Bellwood's typologies did not adequately capture the variety of tapered ends encountered. Therefore, a new taper classification system was developed to record the specific form variations encountered (Table 5.1.1 and Figure 5.1.3).

(A)

(B)

(C)

(D)

(E)

Figure 5.1.3. Examples of each of the five taper types identified during excavation: (A) long taper, (B) Short taper, (C) Bulb taper, (D) Notched taper and (E) Irregular Taper.

5.1.3 Post Sectioning

Once a post was selected for sampling, a 25 cm section was cut just above the taper (or at the lowest point of the exposed posts that were not fully extracted). Each annual tree ring grows upwards and outwards from the base of the tree. Cutting the section as close to the taper as

possible (largest diameter point) maximised the number of tree rings captured within each section (from pith to the terminal tree ring). These sections were labelled and submerged in water before being removed from the site and stored at the University of Waikato. After sampling, following the conditions of the archaeological authority, the remaining post pieces were placed back in their original position, which was recorded for future reference.

5.2 Section Sampling

Two samples were cut per post section: one for species identification and one for tree-ring analysis. A simple wooden vice held each section, while a fine-bladed hand saw cut a 2.5 cm thick cross-section (Figure 5.2.1). Once cut, the samples were labelled and stored in water until analysis.

Figure 5.2.1. Example of a post sample cut, sanded and bleached for tree-ring analysis.

5.3 Species Identification

Species identification via thin-section microscopy was undertaken at the University of Waikato. Thin-section microscopy is routinely performed for tree species identification (Hather, 2000) and remains the only low-cost and reliable way to identify wooden archaeological material from wetland environments (Gregory & Jensen, 2006). The cellular structure of wood can be divided into the axial and radial systems (Meylan & Butterfield, 1978). The axial system is dominant in cell number and type, with the vascular cells within the axial system transporting water along the length of the tree's axis. The radial system comprises rays that transport water across the radius. Species identification is achieved by observing specific anatomical characteristics that vary between species, genera, and families (Hather, 2000, p. 4). These characteristics are viewed as thin sections of woody tissue. Therefore, the three-dimensional tissue is observed on a two-dimensional plane. Three two-dimensional visual planes are used for diagnostic purposes: (i) Transverse Section (TS), (ii) Radial Section (RLS), and (iii) Tangential Longitudinal Section (TLS) (Figure 5.3.1). Each visual plane views the axial and radial systems from a different perspective. By examining the same cellular features from different perspectives, the TS, RLS and TLS visual planes can build up a three-dimensional picture of the wood's anatomy, and the species of the wood sample can be determined.

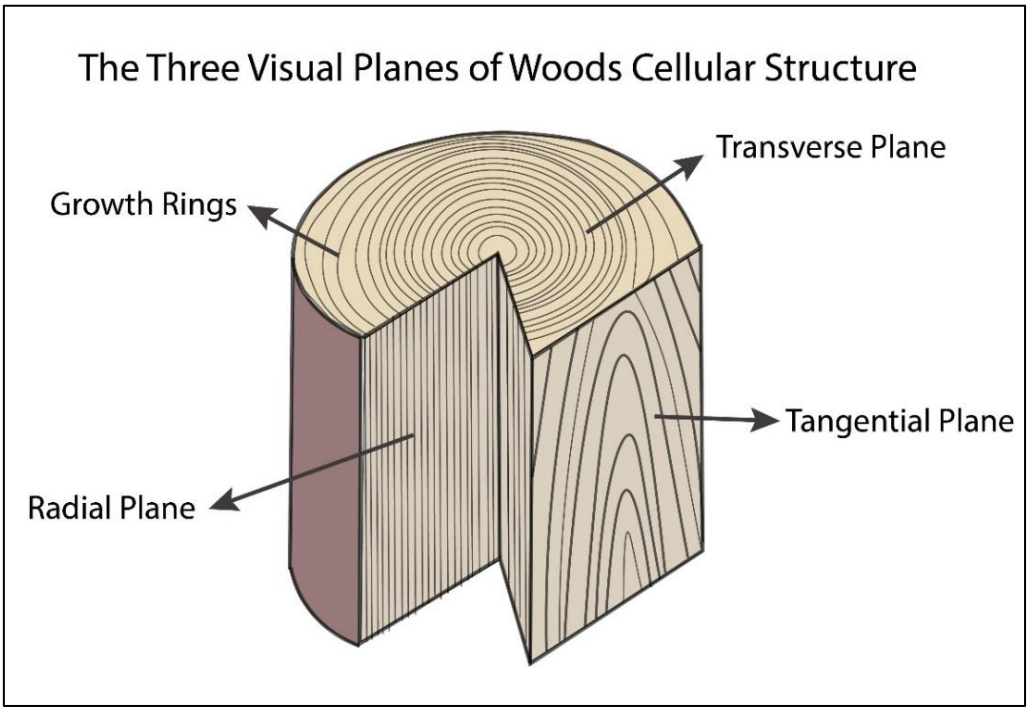

Figure 5.3.1. Diagram of the visual planes used for species identification.

Dr Rodd Wallace (University of Auckland) and Dr Lloyd Donaldson (Scion Research facility) taught thin-section microscopy to the author. The Scion Research facility contains a complete reference collection of New Zealand tree species for species identification. A selection of this reference collection (see Figure 5.3.2 for examples) was used in comparison with the reference information collated by Meylan and Butterfield (1978) and Patel (1967a, 1967b, 1968, 1973, 1987). Three thin sections, one for each anatomical plane (TS, RLS, and TLS), were prepared for each post sample (using a single-edge razor blade). The thin sections were mounted on a microscope slide using a 50/50 solution of water and glycerol and covered by a coverslip. A binocular microscope at magnifications of x10–100 was used to compare the cellular structure of each sample to the reference collections mentioned above. Samples that could not be identified to species level were classified in broader terms, such as hardwood (angiosperms) or softwood (gymnosperms).

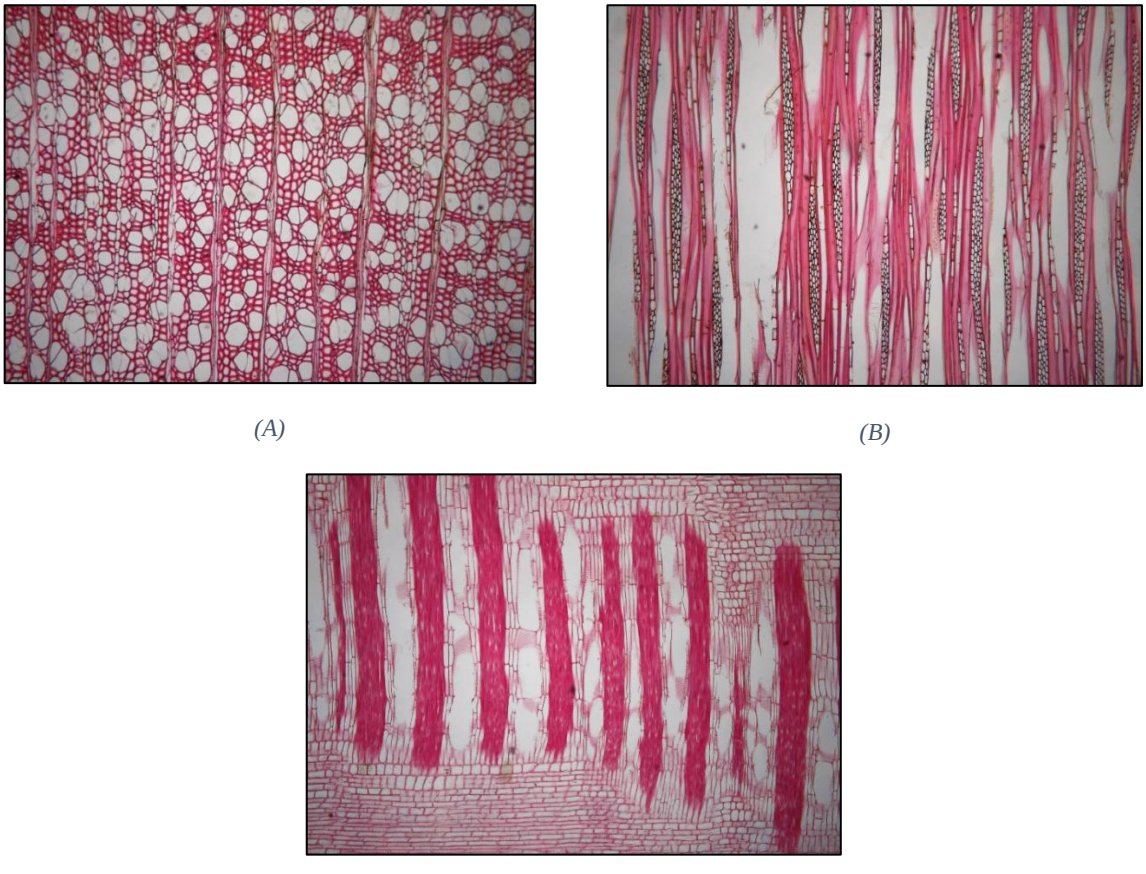

(A) *(B)* *(C)*

Figure 5.3.2. Examples of the three anatomical planes of pukatea (L. novae-zelandiae): (A) Transverse Section, (B) Tangential Longitudinal Section and (C) Radial Section. Note. These cross-sections are stained for display purposes.

Table 5.3.1. A composite list of tree species with recorded use by pre-European Māori.

Common Name	Scientific Name	Subdivision
Tawa	*Beilschmiedia tawa*	Angiosperm
Karaka	*Corynocarpus laevigatus*	Angiosperm
Kanuka	*Kunzea ericoides*	Angiosperm
Pukatea	*Laurelia novaezelandiae*	Angiosperm
Manuka	*Leptospermum scoparium*	Angiosperm
Mahoe	*Melicytus ramiflorus*	Angiosperm
Rata/Pohutukawa	*Metrosideros spp.*	Angiosperm
Maire	*Nestegis cunninghamii*	Angiosperm
Turepo	*Sterblus heterophyllus*	Angiosperm
Puriri	*Vitex lucens*	Angiosperm
Towai	*Weinmannia silvicola*	Angiosperm
Titoki	*Alectryon excelsus*	Angiosperm
Kawaka	*Libocedrus plumosa*	Angiosperm
Mapou	*Myrsine australis*	Angiosperm
Pigeonwood	*Hedycarya arborea*	Angiosperm
Akeake	*Dodonaea viscosa*	Angiosperm
Ramarama	*Lophomyrtus bullata*	Angiosperm
Rewarewa	*Knightia excelsa*	Angiosperm
Kowhai	*Sophora microphylla*	Angiosperm
Rangiora	*Brachyglottis repanda*	Angiosperm
Kamahi	*Weinmannia racemosa*	Angiosperm
Putaputaweta	*Carpodetus serratus*	Angiosperm
Pāte	*Schefflera digitata*	Angiosperm
Hutu	*Ascarina lucida*	Angiosperm
Tarairi	*Beilschmiedia tarairi*	Angiosperm
Horoeka	*Pseudopanax crassifolius*	Angiosperm
Ironwood	*Nestegis apetala*	Angiosperm
Kapuka	*Griselinia littoralis*	Angiosperm
Lacebark	*Hoheria populnea*	Angiosperm
Mahoe	*Melicytus ramiflorus*	Angiosperm
Kauri	*Agathis australis*	Gymnosperm
Kahikatea	*Dacrycarpus dacrydioides*	Gymnosperm
Rimu	*Dacrydium cupressinum*	Gymnosperm
Totara	*Podocarpus totara*	Gymnosperm
Matai	*Prumnopitys taxifolia*	Gymnosperm
Miro	*Prumnopitys ferruginea*	Gymnosperm
Tanekaha	*Phyllocladus trichomanoides*	Gymnosperm
Monoao	*Halocarpus kirkii*	Gymnosperm
Hall's Totara	*Podocarpus laetus*	Gymnosperm
Silver pine	*Manoao colensoi*	Gymnosperm

Note. (Data sourced from Wallace, 1985, 1989; Wallace & Irwin, 2004a, 2004b; Johns et al., 2014; Boswijk et al., 2016; Hogg et al., 2017; Irwin et al., 2017; Boswijk & Johns, 2018; Boswijk et al., 2019; Boswijk et al., 2021).

Table 5.3.2. A general description of tree species identified at the six investigated pā.

Species	Description
Titoki	a small tree species that grows up to 10 m tall with a trunk diameter of 50 cm or more. This species is typically found in coastal forests, growing along the more exposed margins. Titoki is also commonly found in fertile alluvial river flats or sandy plains at low elevations (Dawson & Lucas, 2016 p. 100).
Rewarewa	A large tree species that grows up to 30 m tall with a trunk diameter of up to 1 m or more. This species is widespread in New Zealand, preferring coastal and lowland forest environments. This species favours well-drained, fertile, alluvial soils along riverbanks and associated terraces (Dawson and Lucas 2016, p. 226).
Pukatea	A large tree species that grows up to 35 m tall with a trunk diameter of up to 2 m. This species is commonly found from Northland to Marlborough and Westland and prefers wet, swampy environments. Pukatea exhibit a distinctive plank buttressing and an extensive root system to cope with these less stable (wet) soils (Dawson and Lucas 2016, p. 234).
Kahikatea	A large tree species that grows up to 60 m tall with a trunk diameter of up to 1.5 m. This species is common in the lowland forests of New Zealand and was formerly dominant on frequently flooded and/or poorly drained alluvial soils. Kahikatea is recorded as forming dense groves when grown in well-aerated wet soils (Dawson & Lucas, 2016 p. 19).
Tawa	A large tree species that grows up to 30 m or more, with a trunk diameter of up to 1.5 m. This species is among the most common lowland forest trees of the North Island and northern South Island. Tawa grows as a canopy or understorey tree in mixed conifer–broadleaf forest and is often found growing with podocarps such as rimu (*D. cupressinum*) (Dawson & Lucas, 2016, p. 112).
Pigeonwood	a small tree species that grows up to 12 m tall. This species is found throughout the lowland forests of the North and South Island. This species' common name comes from its fleshy fruit, a favourite of the kererū (*Hemiphaga novaeseelandiae*). This species is very shade tolerant, preferring moist situations and damp gullies (Dawson & Lucas, 2016 p. 210).
Tanekaha	A large tree species that grows up to 25 m or more, with a trunk diameter of up to 1 m. This species prefers inhabiting forests on shallow, dry soils, and ridges. Tanekaha are commonly found in lowland forests from Te Puke to the Ruahine range in Northland and from northern Marlborough to the top of the South Island. Mature tanekaha can be as old as 300–500 years (Dawson & Lucas, 2016 p. 38).
Miro	A large tree species that grows up to 25 m tall and 1 m or more in diameter. Miro likes to grow on soils similar to rimu and with the same accompanying trees (*D. cupressinum*). The largest miro trees occur on deep pumice soils in the central North Island (Dawson & Lucas, 2016 p. 46).
Matai	A large tree species that grows up to 25 m tall and 1.25 m or more in diameter. Matai are prominent on fertile, well-drained soils where rainfall is relatively low (the east of both islands). The largest matai trees are often found on the deep pumice soils of the Central North Island and well-drained lowland alluviums (Dawson & Lucas, 2016 p. 48).
Rimu	one of the most abundant and widespread conifers in New Zealand and can be found throughout the country wherever rainfall is well distributed. Rimu can grow up to 35 m tall, with a trunk up to 2 m in diameter (Dawson & Lucas, 2016 p. 20).

New Zealand's native flora is composed of 18 gymnosperms (conifers) and over 525 angiosperms (flowering plants) (Meylan & Butterfield, 1978, p. 8). Māori used a variety of these species to create structures, household goods, tools, waka, weapons, and carvings (Wallace, 1989; Wallace & Irwin, 2004b, 2004a; Boswijk et al., 2016; Boswijk et al., 2021). Examples of these wooden objects have been recovered from several wetland sites (Table 5.3.1 and Table 5.3.2), including Kohika Pā (Irwin, 2004b), Otāhau Pā (Hogg et al., 2017), and several pā in the Hauraki Plains (Phillips, 2000).

5.4 Preparation for Tree-ring Analysis

Preparing a sample for tree-ring analysis involved a two-step process: (i) sanding the transverse plane (see Section 5.3) of the sample to a high polish and (ii) bleaching the sample to improve the visibility of the tree-ring growth sequence. A ¼ sheet orbital hand sander was used to sand the transverse plane, progressing from coarse to finer grit sandpaper (100, 150, 220, 400, 600, 800, and 1200 grit). Following sanding, bleaching was undertaken at either the University of Waikato's Radiocarbon Dating Laboratory or the University of Auckland's Chemistry Laboratory. Bleaching was conducted in large plastic containers within a ventilation hood using a solution of 900 ml of water, 6 ml of undiluted hydrochloric acid (HCl), and 15 g sodium chlorite ($NaClO_2$). Each sample was soaked in this solution for 20-min, with this process repeated a minimum of three times until the sample was bleached entirely (Figure 5.4.1). Once bleached, the sample was stored in water overnight to remove the excess bleaching solution.

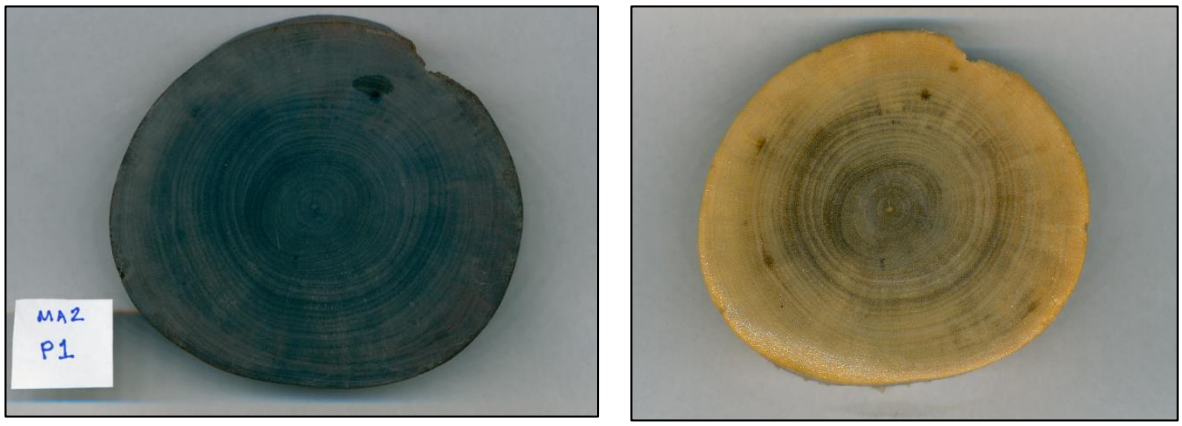

(A) *(B)*

Figure 5.4.1. Comparison of an unbleached (A) and bleached sample (B) before soaking overnight.

5.5 Condition Assessment

A condition assessment was also conducted before tree-ring analysis, recording the various characteristics of each sample. While all the sampled posts were scrutinised in the field, until a sample from each post section was prepared for tree-ring analysis, potential limiting factors could not be accurately assessed. The characteristics reviewed during this assessment include preservation quality, the presence of charring, scaring, dark staining (limiting tree-ring visibility), and any tree-ring growth anomalies that could limit ring count accuracy. This assessment was undertaken using a low-powered light microscope, also noting the shape of the cross-section, the location of the pith (central or off-centre), and the shape of the growth pattern (concentric or non-concentric). During this assessment, each sample was also scanned (Figure 5.5.1), preserving the unaltered tree-ring growth sequence in case it was damaged during analysis (i.e., letting the sample dry out and causing it to crack). These scans (black and white/colour) were also used during the analysis, as changes in the image's contrast and composition could be used to observe specific areas of the tree-ring growth sequence that were hard to visualise under the microscope. Following this assessment, samples with limiting characteristics were dropped from the analysis. In most cases, these characteristics meant the samples would not produce viable ^{14}C samples (ring-block samples) that would survive pretreatment.

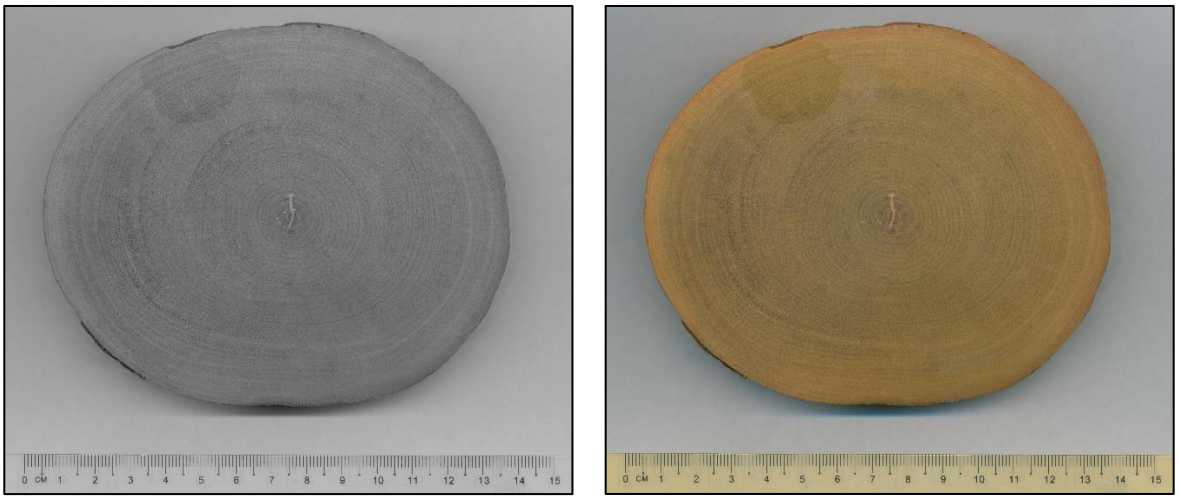

(A) *(B)*

Figure 5.5.1. Example of sample scans in black/white (A) and colour (B).

5.6 Tree-Ring Analysis

Tree-ring analysis was undertaken in the specialist dendrochronology lab at the University of Auckland under the supervision of A/Prof. Gretel Boswijk. Tree-ring analysis was a three-step process: (i) tree-ring count and measurement analysis, (ii) ring count reconciliation, and (iii) ring-block sampling.

5.6.1 Ring Count and Measurement

Ring count and measurement were undertaken on three separate radii per sample. These radii were selected to capture the complete tree-ring growth sequence and highlight observed tree-ring anomalies, such as locally absent rings (rings missing from a portion of the circumference), false rings (false tree-ring boundaries), tree-ring suppression (narrow annual growth periods), lobate growth (widening of the annual growth periods) and abnormal late/early wood colouring (see Kaennel & Schweingruber, 1995 for definitions). The challenges of conducting tree-ring analysis on New Zealand tree species in dendrochronological settings are well-documented (Dunwiddie, 1979; Bellingham, 1982; Boswijk & Johns, 2018; Boswijk et al., 2019; Boswijk et al., 2021), highlighting the limiting growth characteristics and ring anomalies that are common in many tree species. By measuring three radii per sample, each radius' ring count and measurements can be compared (both statistically and visually), with any inconsistencies resolved into a reconciled tree-ring sequence. The three selected radii were marked on the transverse plane of each sample using a ruler and sharp compass point, creating a thin line visible on the surface. These lines are referred to as 'tracks' and are labelled A, B, and C for each sample. Each track allowed the radius to be followed under the microscope, ensuring the accuracy of the ring count. Tree-ring widths were measured to an accuracy of 0.01 mm using a LINTAB measuring table (travelling stage) and the measurement function in TSAP-Win Scientific V4.69i (Rinn, 2002–2015). This process was completed at least three times for each radius to ensure accuracy.

5.6.2 Ring Count Reconciliation

Ring count reconciliation was achieved via visual matching, comparing each radii's ring count and measurement as plotted graphs using TSAP-Win Scientific V4.69i (Rinn 2002–2015).

Similarities and differences between the ring patterns of each track were observed, noting contemporaneity or differences caused by ring abnormalities. When a growth abnormality was identified, the ring count position was noted in the graph (i.e., a locally absent ring), allowing for periods of inconsistent growth to be checked between radii, accurately reconciling the final ring count for each sample. If the three measured radii of a sample could not be adequately reconciled into a final ring count, owing to the severity of the growth anomalies identified, the sample was dropped from the analysis. Following reconciliation, the sharp point of a maths compass was used to pinprick decadal marks along the tree-ring growth sequence, providing a visual reference of the reconciled ring count. These pinpricks were used as a visual guide during ring-block sampling.

5.6.3 Ring-block Sampling

A ring-block sample is a ^{14}C sample containing several sequential tree rings, treated as an average of the radiocarbon content across all included rings. Generally, five tree rings were included in each ring-block sample, with a minimum of five ring-block samples collected per post sample, increasing to seven ring-block samples if the post contained more than 80 tree rings. Ring-block sampling was undertaken under a low-power microscope using a scalpel blade. Generally, ring-block samples were collected from the innermost five tree rings (the oldest/first five tree rings), the outermost five tree rings (the youngest/last five tree rings), and, where possible, at regular intervals throughout the tree-ring growth sequence. The resulting ring-block samples were placed in a labelled and sterilised plastic vial (20–40 mg of wooden material required for AMS ^{14}C dating) to await chemical pretreatment. Samples submitted to the Waikato Radiocarbon Laboratory were assigned a unique Wk laboratory number, identifying each specific ring-block sample throughout the pretreatment phases and dating protocols.

Two limitations were encountered during ring-block sampling, resulting from tree-ring anomalies identified across the growth sequence of specific samples. First, tree-ring anomalies limited the periods of growth available for ^{14}C sampling. Specifically, tree-ring suppression can make it difficult to sample sufficient material (wood) for ^{14}C dating purposes, primarily when it occurs in the innermost tree rings with the smallest circumference. If an area of tree-

ring growth was deemed insufficient for sampling, the next five appropriately sized tree rings were selected. In extreme cases, this limited the number of ring-block samples collected from a post sample. Second, tree-ring growth anomalies created a challenge when trying to sample five sequential tree rings accurately. On multiple occasions, a tree-ring boundary was unintentionally crossed or not crossed during ring-block sampling, resulting in the ring-block sample containing more or fewer than five tree rings. Often, this situation was only identified during additional checks after the sample had been ^{14}C dated.

5.6.4 Dendrochronology

Dendrochronology was attempted on one post sample (MGAP313) recovered from the pā at Lake Mangahia (MGA). This particular post was identified as the species tanekaha (*P. trichomanoides*). Tree-ring width measurements were compared with master tanekaha chronologies constructed by Palmer (1982, 1989). Two methods of cross-matching were employed: visual matching and statistical testing. Visual matching is similar to the tree-ring analysis process outlined above, utilising the measured tree-ring sequences plotted as graphs in TSAP-Win Scientific V4.69i (Rinn 2002–2015). The reconciled tree-ring growth pattern is superimposed over the master chronology to identify similarities and determine a probable cross-match. While subjective, visual matching is used by dendrochronologists worldwide and has been proven to produce results similar to those of statistical analysis methods (Hillam & Tylers, 1995).

Statistical methods of cross-matching identify areas of ‘overlap’ between the master chronology and the measured tree-ring growth sequence. Generally, statistical methods of cross-matching utilise specialist computer programs. For example, CROS (Baillie & Pilcher, 1973) calculates a product-moment correlation coefficient ‘r’ for each ‘position of overlap’ between the two datasets. A ‘Student’s t’ value is then calculated from r to introduce a measure of significance concerning the overlap length. This t value measures the probability that the observed value of r has arisen by chance. For example, when cross-matching a growth sequence of English oak with 100 rings or more (*Quercus robur*), a t value of 3.5 provides a 0.1% significance level for ring patterns with 100+ rings. That is, a value of 3.5 should happen by chance about once in every 1000 mismatches (Baillie, 1982, p. 84). However, not every t value

of 3.5 represents an accurate cross-match, and t values can often range in value. Therefore, it is common for dendrochronologists to use visual matching to verify the statistical results. Unfortunately, attempts at cross-matching were unsuccessful. While unsuccessful, this application shows promise for future research, where samples of kauri (*A. australis*) or tanekaha (*P. trichomanoides*) from suitable archaeological contexts are identified.

5.7 Pretreatment Protocols

5.7.1 Physical Pretreatment of 5-ring Block Samples

Physical pretreatment involved inspecting the ring-block samples under a low-powered light microscope (>10x magnification), ensuring that no foreign particulates or contaminants were introduced into the sample. If potential contaminants were identified, they were removed using a scalpel or tweezer. Following visual inspection, the ring-block samples were cut or crushed into fine shavings (<0.5 mm), increasing the surface area for chemical pretreatment. The resulting material (20–40 mg required for AMS dating) was transferred into a test tube pre-baked at 500°C (for sterilisation).

5.7.2 Chemical Pretreatment

The resulting ^{14}C samples were chemically pretreated to α-cellulose following the specific pretreatment protocols utilised by the Waikato Radiocarbon Dating Laboratory. Chemical pretreatment involved a four-step procedure: (i) solvent extraction with acetone, (ii) acid-base-acid (ABA) treatment, (iii) isolation of holocellulose via acidified $NaClO_2$, and (iv) a final base-acid extraction. All chemical pretreatment protocols were completed in 13 mm test tubes with vented closures, with the aid of a test tube rack, a heat block set at 70°C, and a pipette for accurate chemical measurements. A summary of these chemical pretreatment protocols is provided below (see Waikato Radiocarbon Dating Laboratory, 2017, p. 2).

Solvent extraction proceeded with successive acetone treatments (6 mL) on a heat block for 30-min (replicated at least three times, with new acetone added each time). After acetone extraction, the ^{14}C samples were washed with ultrapure water (minimum of three times)

separated by 5-min on a heat block. ABA pretreatment proceeded with applying 6 mL of 1N HCl for 30-min on a heat block. Following HCl treatment, three successive 30-min treatments with 6 mL of 1N NaOH were applied. Once the supernatant liquid remained transparent, ABA pretreatment ended with a final 30-min 1N HCl wash.

Holocellulose was isolated by applying equal volumes of 2.5 mL 1N HCl and 2.5 mL 1M $NaClO_2$ on a heat block. The ^{14}C samples were bleached with three successive treatments until the samples were completely white and without colour. Following bleaching, the samples were washed with ultrapure water on a heat block for 5-min until the samples registered a neutral pH (a minimum of three times). For α-cellulose extraction, the bleached holocellulose was treated with 6 mL of 5N NaOH for 1 hour at room temperature. Following α-cellulose extraction, the sample was treated with 1N HCl at 70 °C for 30 min to remove any absorbed atmospheric CO_2, followed by a minimum of five 5-min treatments with ultrapure water on a heat block. The test tubes (including the ^{14}C samples) were then placed in a beaker without vented closures and dried overnight in an oven at 70°C overnight. The following morning, the samples were visually inspected under a binocular microscope to check for any foreign material which may have entered the test tubes overnight. After visual inspection, the samples were covered with a tinfoil cap and placed in a test-tube rack ready for graphitisation.

5.7.3 Graphitisation

The resulting α-cellulose ^{14}C samples were converted to CO_2 by the University of Waikato AMS technical staff via a process known as graphitisation (see Waikato Radiocarbon Dating Laboratory, 2017, p. 4). Graphitisation was undertaken in dedicated glass vacuum lines connected by Ultra-Torr® Swagelok® Cajons, maintained under vacuum by Pfeiffer HiCube 80 turbo drag pumps. Cellulose samples were converted to CO_2 by oxidation at 800°C overnight in the presence of pre-baked CuO wire (JT Baker) and silver wire. CO_2 was then converted to graphite on one of three CO_2/graphitisation lines, each with eight hydrogen reduction units (reactors) that routinely graphitise 0.5–0.2 mg C targets following the method outlined in Santos et al. (2004). The cooled graphite was pressed to 350 psi using a NEC cathode press and stored in a wet cabinet with a NaOH reservoir to reduce CO_2 concentration before being packaged and sent to the Keck AMS Radiocarbon Dating Laboratory at the

University of California at Irvine for analysis. Samples were stored for no more than four weeks before being analysed.

5.8 AMS Radiocarbon Dating

Pressed graphite targets were analysed at the Keck Radiocarbon Dating Laboratory (KCCAMS) at the University of California Irvine on a NEC 0.5 MV 1.5SDH-1 AMS system coupled with an in-house modified ion source (Beverly et al., 2010). Data analysis was undertaken at the Keck facility as per Santos et al. (2007) (see Waikato Radiocarbon Dating Laboratory, 2017, p. 4).

5.8.1 Continuity Standards

$^{14}C/^{12}C$ measurements supplied by the KCCAMS laboratory routinely have uncertainties approximating ± 15 years at Modern. The Waikato Radiocarbon Dating Laboratory's internal reproducibility is assessed by analysing appropriate in-house continuity standards included within each sample batch (wheel) (see Waikato Radiocarbon Dating Laboratory, 2017, pp. 5–6). Three specific continuity standards were included in each sample wheel for this study: Kiri Wood (Wk-20690), an ancient kauri background blank standard (MIS7 Manukau kauri, Renton Road) (Marra et al., 2006; Hogg et al., 2007), and a dendrochronologically dated (AD 1666) kauri wood standard. The AD 1666 standard (collected from dendrochronologically dated building timber) was provided by Gretel Boswijk. These continuity standards were chosen to match the ^{14}C samples and their expected ^{14}C age, providing an essential check of the accuracy and reproducibility of the pretreatment, CO_2 generation and graphitisation processes. These three standards were subjected to the same physical and chemical pretreatment protocols outlined above. Long-term trends in the results of these standards allow for an analysis of the accuracy and precision of the resulting ^{14}C measurements. For a particular continuity standard, the ratio between the Gaussian (population) standard deviation derived from the last ten wheels and the individual wheel continuity standard deviations allows the calculation of additional laboratory uncertainties for a specific wheel. For this research, this ratio was used to increase the uncertainty for each ^{14}C result (based on measurements of the Kiri Wood standard). This decision was made to account for any possible internal variability and to ensure that the resulting WMDs were not over-defined on the applied calibration curve (SHCal20).

5.8.2 D_Sequence Model Parameters (WMD)

Within a Bayesian framework, a WMD (OxCal D_Sequence model) can be considered a Sequence with a very strong prior, where the Felling Date (see discussion below) constitutes the only parameter of interest (see Section 3.2.5). WMD was conducted using the Bayesian approach described by Bronk Ramsey et al. (2001), implemented using the D_Sequence option in the calibration software OxCal v4.4 (Bronk Ramsey, 2009a). Each D_Sequence was calibrated using the Southern Hemisphere atmospheric calibration data (SHCal20) (Hogg et al., 2020), with a resolution of 1, and the MCMC algorithm set to 3000k Iterations. A range of commands (Chronological Query Language (CQL2)) offered by OxCal 4.4 were utilised in the construction of each D_Sequence model (Table 5.8.1).

Table 5.8.1. OxCal commands applied in the D_Sequence models (Bronk Ramsey, 1994).

Command	Function
Plot	plot grouping
Curve	define the radiocarbon calibration curve to be used for R_Date and R_Combine
Outlier Model	Defines the model for outliers with a probability assigned to them
Sequence	Used to define elements or groups that are in a particular order
D_Sequence	A sequence model where the exact gaps between elements are known: for example, a tree ring sequence
R_Date	Calculates the likelihood distribution for the calibrated date as a function of radiocarbon concentration
Outlier	Used to define the outlier probability for the analysis of an Outlier Model.
Gap	defines the gap between two events
Date	A type conversion function that returns a date or PDF for a date from an expression
Before	A group function that returns a PDF for being before all of the grouped elements
Colour	allows the user to define the colour used for a distribution or a curve in plots

Each D_Sequence model included multiple sequential AMS ^{14}C determinations (R_Date), separated by known calendar interval spacings (Gap). As the last R_Date in the D_Sequence model represents the ^{14}C concentration of multiple tree rings, a final Gap is included at the end of the Sequence, defined by half the number of tree rings in the last ring-block sample. Following this last Gap, a Date command is included that produces a modelled posterior probability distribution that reflects the year of the terminal tree ring (referred to as the Felling Date). The Felling Date for each post is reported as a median calibrated age (cal. AD) ± one standard deviation, along with the highest posterior density (HPD) date ranges (at 68% and 95% probability).

5.8.3 Identification of Outliers

Several critical assumptions are involved when using Bayesian statistical methods to analyse groups of ^{14}C dates. Two such assumptions are that all ^{14}C measurements included in the model are correct in their context and that the atmospheric calibration data properly represents the original ^{14}C concentration of the sample. However, outliers are commonly reported following analysis. Therefore, a statistical method is required to identify, down-weight or reject potential outliers. There are two primary ways to deal with outliers. The first is to identify all outliers and manually eliminate them from the analysis (see Bronk Ramsey, 1995). The second method assumes we cannot be sure whether any measurement is an outlier. Therefore, the results must be weighted according to how likely they are to be correct in a model using an averaging approach (see Christen, 1994; Bronk Ramsey, 1995, 2009b). OxCal offers two different statistical approaches to identify measurement data that do not agree with a model: (i) agreement index and (ii) outlier analysis (Bronk Ramsey, 2009a).

The agreement index approach uses the overlap between the likelihood and marginal posterior distributions to indicate a potential outlier within the model, with all measurements given equal weight unless a sample has been rejected. While this approach is not a formal statistical method with a well-defined cut-off, it has the advantage that the model itself is unaffected (Bronk Ramsey, 2009a, p. 356). There are four forms of the agreement index calculated by OxCal v 4.4: individual agreement indices (A), combination agreement indices (A_{comb}), model agreement index (A_{model}), and Overall agreement index ($A_{overall}$). The individual agreement index is a product of the individual agreement indices and helps identify which samples do not agree with the model parameters. The rejection of a sample should be considered if the individual agreement index falls below 60%. However, it is essential to remember that approximately 1 in 20 samples is likely to fall below this level, and rejection should also be based on other criteria. The combination agreement indices test whether the posterior distributions can be combined. The acceptance threshold for A_{comb} is $1/\sqrt{(2n)}$ and depends on the number of items ('n'). This acceptance threshold is referred to as the A_{comb} (An) threshold in text. The model agreement index is used to see if the model as a whole is not likely given the data. The acceptance threshold for A_{model} is also >60%. The thresholds for these indices are chosen so that they are close to the 5% confidence level of the X^2 (Chi-squared) test for simple combinations (Christen & Litton, 1995, p. 428).

However, when outlier analysis is applied, outliers are progressively down-weighted, so the results are essentially an average between a model in which the measurement is accepted and one in which it is rejected (Bronk Ramsey et al., 2009b, p. 1024). The outlier analysis approach requires an applied outlier model, specifying how the model should be revised (concerning any identified outliers) in the context of all other information available. A prior outlier probability is specified within this model, representing how likely any individual measurement will be an outlier. OxCal v4.4 offers a variety of outlier models for a diverse set of situations. The Outlier_Model command defines which outlier model is applied, and the Outlier command specifies the prior outlier probability and to which specific R_Date or other likelihood information it is applied to in the model. The outlier model is defined by five parameters (Table 5.8.2).

Table 5.8.2. OxCal outlier parameters (Bronk Ramsey, 1995, 2001, 2009b).

Model parameters	Description
Name	the name of the specific outlier model applied.
Distribution	defines how the outliers are to be distributed. For example, N(0,2) is a simple normal distribution.
Scale	defines the scaling of the outliers, expressed in powers of 10. The scale can be a single number (i.e., 0 for no scaling or 2 for a scale of 100 yr), or it can act as a distribution, allowing the analysis to determine the appropriate scale (i.e., a scale of U(0,4) can be defined anywhere between 1–10,000 yr).
Type	defines the kind of outlier you have. One of three outlier types can be chosen: 't' for outliers in the time variable, 'r' for those in the ^{14}C isotope ratio, and 's' for those that scale with the uncertainty in the ^{14}C concentration.
Prior	defines the prior probability that the sample is an outlier. A typical value for this would be 0.05 for a 1 in 20 chance that the measurement needs to be shifted somehow.

For this research, the internal consistency of the D_Sequence models was tested using the SSimple s-type outlier model ("SSimple", N(0,2), 0, s) with a prior outlier probability of 0.05 (5%). The SSimple s-type model draws the shifts from a normal distribution, with a mean of zero and a standard deviation of two. The shifts are then multiplied by the uncertainty in the date and applied to the ^{14}C measurement. If the uncertainties in all the measurements are 50, the possible shifts are drawn from a normal distribution with a mean of zero and a standard deviation of 10 (Bronk Ramsey, 2009b, p. 1026). This method was the primary outlier

identification strategy used, and all presented results reflect the application of this outlier model unless otherwise specified.

However, to further test the consistency and accuracy of some results, the D_Sequence models were recalibrated using agreement index analysis and an RScaled r-type outlier model ("RScaled", T(5), U(0,4), r). The Rscaled outlier model is applied when there is an unidentified reason why the ^{14}C dates and the calibration curve data are not the same within a defined calendar period (Bronk Ramsey, 2009b, p. 1027). This RScaled r-type model also draws from a long-tailed distribution (T(5)) and finds the scale anywhere between 10^0 and 10^4 years (U(0,4)). However, the r-type indicates that the offsets are not related to the uncertainty in the measurement. These outlier detection methods were used to compare to the original (SSimple outlier model) results.

5.8.4 Threshold for Success

The D_Sequence models applied in this study produced results which ranged in accuracy and precision, reflecting possible sources of error and limitations. These errors and limitations include impacts resulting from tree-ring analysis (ring count error), the non-monotonic form of the ^{14}C calibration curve (SHCal20), and the accuracy and precision of the component data sets (Hogg et al., 2019a). Therefore, the results of each D_Sequence model were scrutinised before determining their success. This process involved several steps, including reviewing the results of the continuity standards included within each sample wheel, assessing the agreement and posterior outlier values of each R_Date, recalibrating each D_Sequence model using different outlier detection methods, comparing the likelihood and posterior distributions of each ^{14}C date within the D_Sequence, and evaluating the structure (shape) of the WMD in relation to the atmospheric ^{14}C data provided by SHCal20. This process highlighted potential inaccuracies within the results of some of the D_Sequence models, primarily presenting as minor outliers or ^{14}C offsets from the calibration curve. Two suspected causes of these offsets are proposed: (i) errors in the reconciled ring count (offsets in calendar years) and (ii) possible inconsistencies with the calibration data (offsets in ^{14}C age) associated with calibration plateaus in SHCal20. When calendar year offsets were identified (caused by errors in the reconciled ring count that could not be ratified), the WMD was rejected and removed from the analysis. When ^{14}C age

offsets were identified, the results of each D_Sequence model were interpreted through the available data to determine their accuracy and precision. The process for determining the success of each D_Sequence is fully described in Chapters 6–11, with a further discussion of the process presented in Section 13.1.5.

Chapter 6. Lake Mangakaware 1 (MA1)

6.1 Archaeological Excavations at MA1 (S15/16)

Excavations at MA1 were conducted over two short field seasons, focusing on two specific areas highlighted by desktop research and site visits as the most likely to retain evidence of palisading. Area A was excavated in May 2020, focusing on the northern lake edge of the pā. Area B was excavated in February 2021, focusing on the southern side of the pā (Figure 6.1.1). Excavations aimed to determine the extent of the surviving palisades in each area, with the objective of sampling posts from each defensive row for WMD purposes.

Figure 6.1.1. Location of excavation focus at MA1[21].

[21] This figure includes data sourced from the LINZ Data Service and is licensed for reuse under the CC BY 4.0.

6.1.1 Excavation in Area A (MA1)

Investigations in Area A focused on an area of approximately 24 x 10 m (Figure 6.1.2). Once this area was cleared of overlying vegetation, several *in situ* palisade rows and stone cobbles were visible. Additionally, imported sediment deposits (with charcoal inclusions) eroding from the toe of the pā mound were identified. Given the prominent visibility of the palisade defences and the proximity of the water table, large-scale exploratory excavation areas were deemed unnecessary, and efforts focused on the visible posts within the cleared area.

Figure 6.1.2. Area A cleared of vegetation and woody debris.

Eighty-four *in situ* posts were recorded in Area A, comprising at least six palisade rows, ranging from the lake edge to the toe of the raised pā mound. These palisade rows were constructed using paired large-diameter posts interspersed with smaller-diameter posts (Figure 6.1.3). Interestingly, the twelve stone cobbles displayed a distinct spatial relationship to the middle palisade rows in Area A. Peters (1971, p. 130) previously suggested these cobbles could have been used to protect the pā from rising water levels. However, this close spatial relationship, in association with the robusticity of the palisade defences, suggests a fighting

stage was constructed in this area, with the cobbles positioned on the fighting stage for use in the pā's defence. Additionally, a distinct gap in the palisade defences was identified at the eastern end of Area A. This gap is associated with a linear depression in the raised mound that runs towards the centre of the pā. This linear depression aligns with the location of a possible 'pathway' identified by Peters (1971, p. 131).

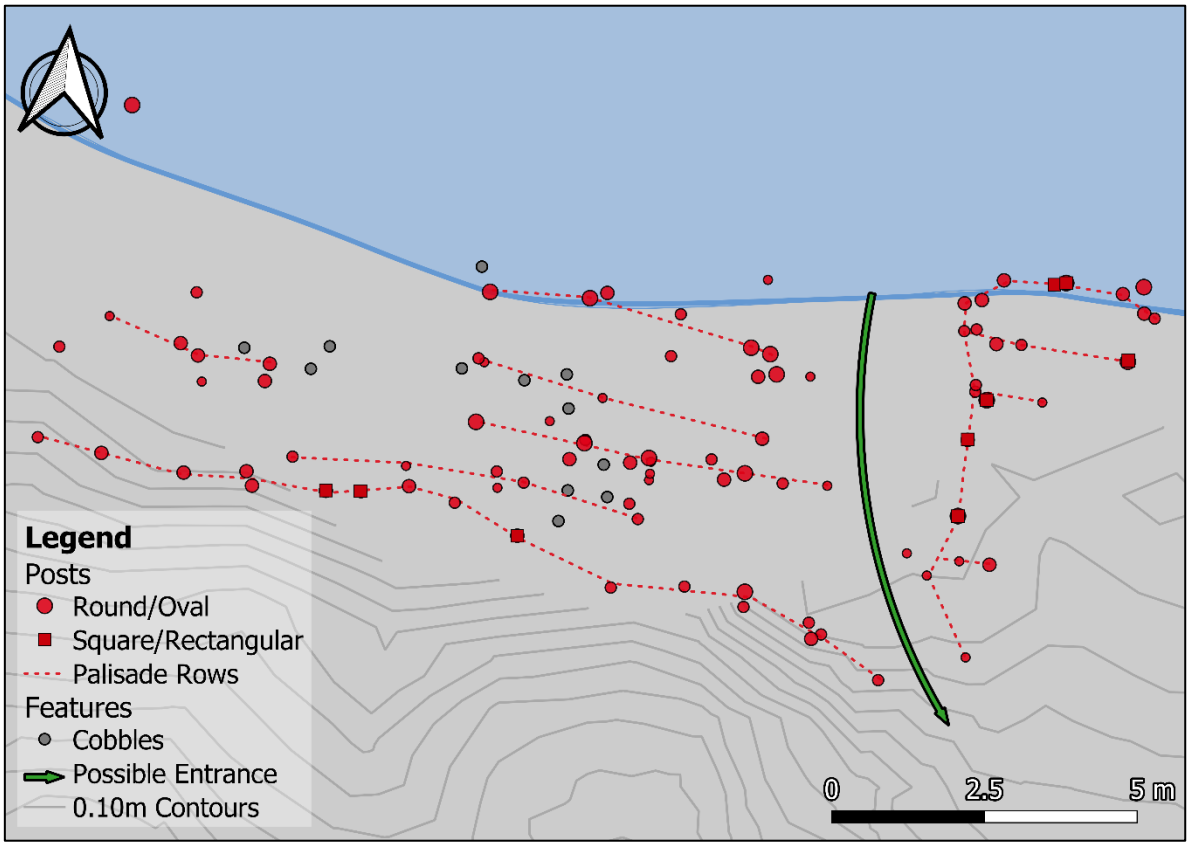

Figure 6.1.3. Plan drawing showing the palisade rows and probable entranceway identified in Area A

Several small excavation units (EA8–28) were positioned around a selection of the most prominent posts to determine their suitability for extraction and sampling (Figure 6.1.5). Observation of these posts established that a large proportion suffered from varying degrees of decay, predominantly affecting the posts close to or on the raised pā mound (furthest from the water table). While poor preservation limited the number of posts suitable for sampling, 12 of the most prominent posts passed the selection criteria for extraction (Figure 6.1.6). However, as discussed in Section 6.1.1, the force required to extract these posts placed the block and tackle under considerable pressure. Therefore, in the interests of safety, the decision was made

to alter the extraction method, sampling each post while the distal end remained in the ground. As a result, only one post was fully extracted (MA1P48 – maximum length of 5.1 m), with the remaining posts only raised to a safe height before sampling (Figure 6.1.4).

Figure 6.1.4. MA1P42 partially extracted from the ground.

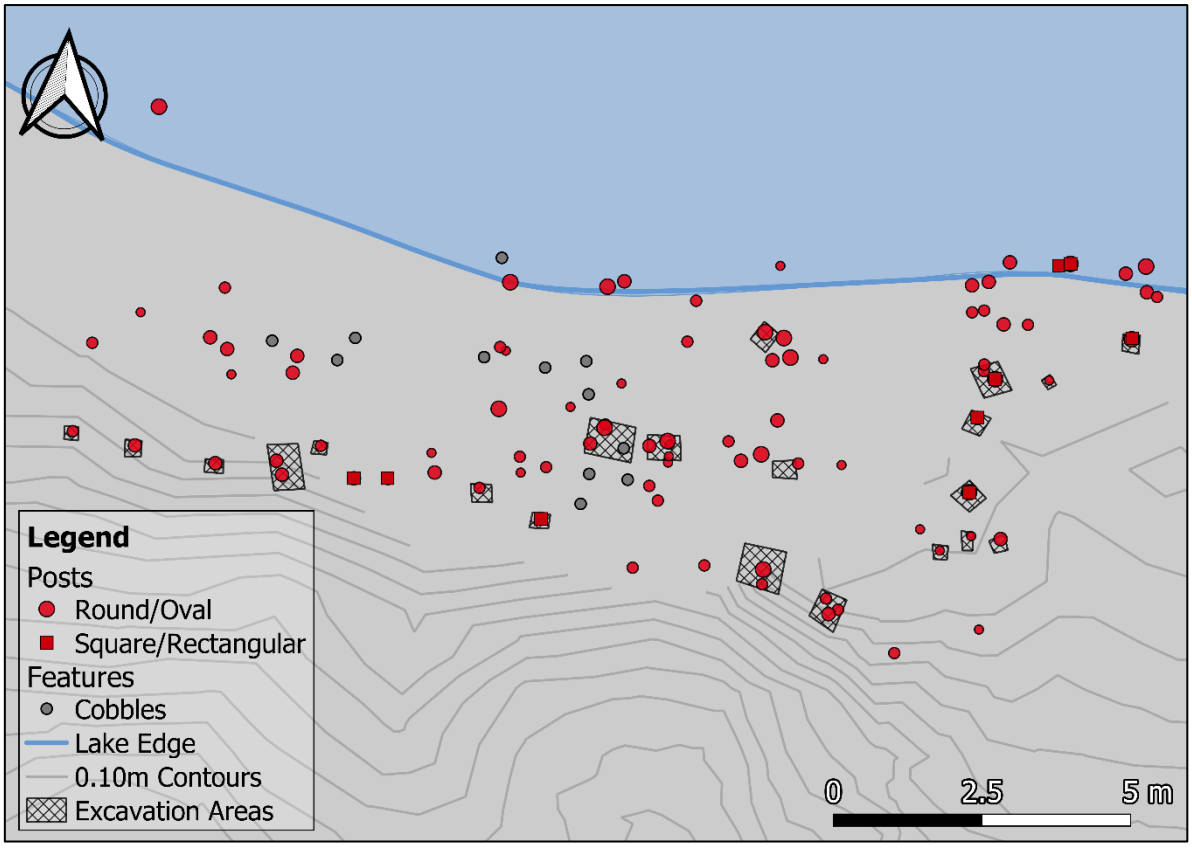

Figure 6.1.5. Plan drawing showing the position of excavation areas in Area A at MA1.

Seven of the 12 extracted posts were deemed unsuitable for sampling (Table 6.1.1), including three posts that broke during extraction (due to poor preservation and the force required to raise the posts), two posts that did not retain evidence of the terminal growth ring (adzed cross sections identified below the ground surface), one post exhibiting burning/charring on the outer surface of its distal end (removing the evidence of the terminal growth ring), and one post identified on-site as the species rewarewa (*K. excelsa*). Unfortunately, rewarewa is unsuitable for WMD because instead of disernable tree rings, the cellular structure comprises broad uniseriate and multiseriate rays. The remaining five posts extracted from Area A were all sampled for analysis (25 cm section), including three from the lake's edge (MA1P42, MA1P50 and MA1P57) and two from the robust middle palisade rows further up the bank (MA1P53 and MA1P48). Unfortunately, no posts from the innermost palisade row (cut into the toe of the mound) passed the sampling criteria owing to their poor state of preservation.

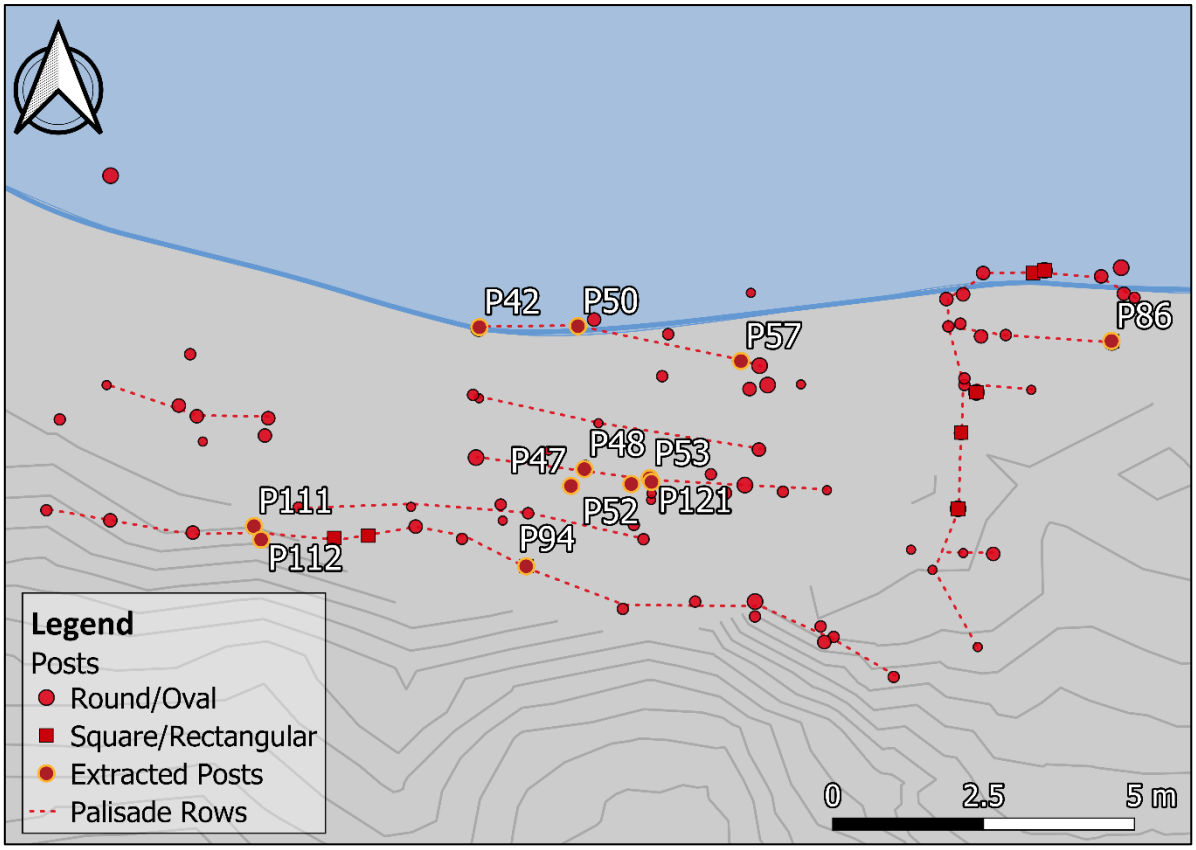

Figure 6.1.6. Plan drawing showing the position of extracted posts in Area A at MA1.

Table 6.1.1. Recorded information for posts extracted from Area A at MA1.

Post ID	Cross Section	Diameter (cm)	Condition	Sampled
MA1P42	Round	18.5	Suitable for sampling (partially charred)	Yes
MA1P47	Round	10.9	Poor preservation (broke during extraction)	No
MA1P48	Round	20.5	Suitable for sampling	Yes
MA1P50	Round	16.4	Suitable for sampling	Yes
MA1P52	Round	14.0	Poor preservation (broke during extraction)	No
MA1P53	Round	19.2	Suitable for sampling	Yes
MA1P57	Round	19.0	Suitable for sampling	Yes
MA1P86	Rectangle	17.8	Adzed (entire circumference)	No
MA1P94	Oval	11.9	Charred (entire circumference)	No
MA1P111	Square	11.5	Adzed (entire circumference)	No
MA1P112*	Round	12.9	Identified as rewarewa	No
MA1P121	Round	13.0	Poor preservation (broke during extraction)	No

*Note. * indicates the post dropped from the assemblage.*

6.1.2 Excavation in Area B (MA1)

Investigations in Area B focused on an area of 10 x 10 m (Figure 6.1.7). Once the area was cleared of overlying vegetation, several *in situ* posts were identified, primarily in a single row determined to be the outermost surviving palisade row. Peters (1971, p. 130) previously reported that >60 posts were identified in this area, visible at no more than 30 cm deep (Figure 6.1.8). Therefore, exploratory excavation areas were strategically positioned to identify surviving palisades below the ground surface (EA44–48) (Figure 6.1.9). The posts identified within these excavation areas represent the extent of the surviving palisade rows present in Area B.

Figure 6.1.7. Zac McIvor (left) and Warren Gumbley (right) inspect the cleared surface of Area B[22].

[22] This photograph is looking northeast towards the pā mound.

Figure 6.1.8. A historical excavation photograph of the western end of the Southern trench at MA1 (Bellwood, 1969a).

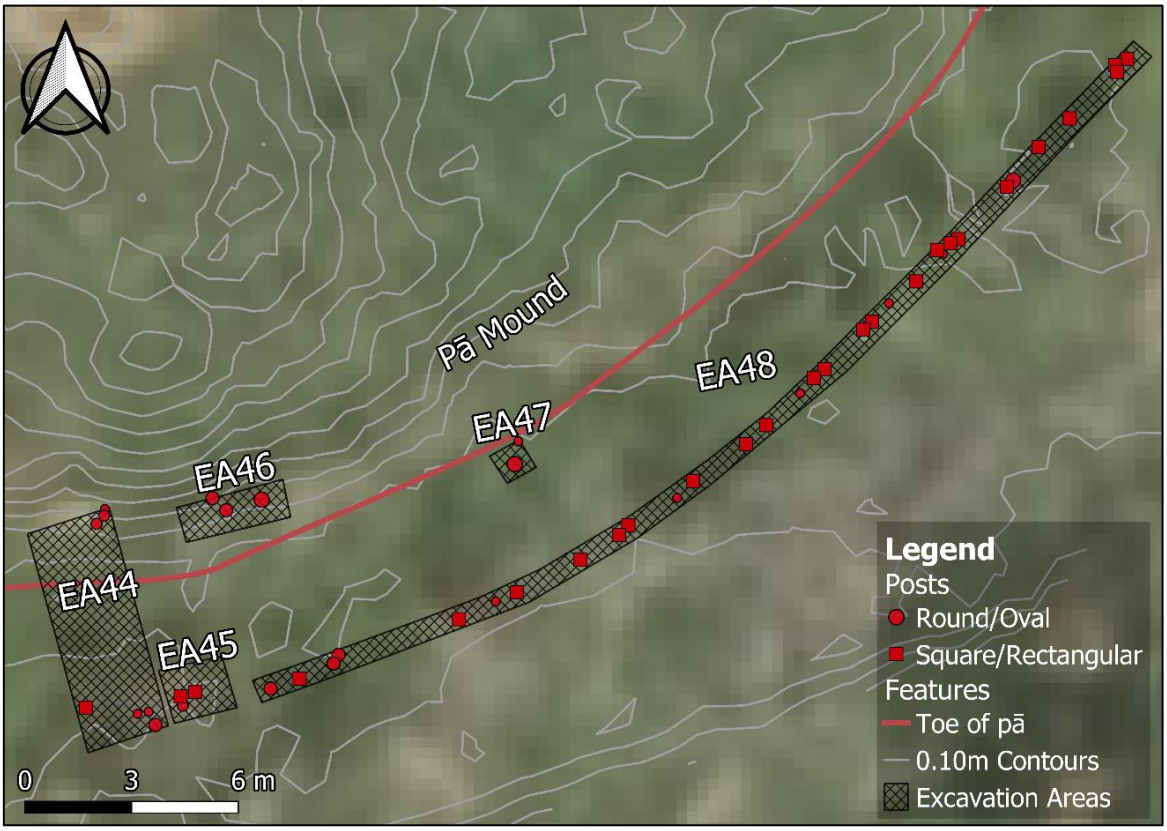

Figure 6.1.9. Position of the excavation areas in Area B at MA1.

EA44 covered an area of 6 x 2.5 m, excavated along the western edge of Area B, with the aim of determining the number of palisade rows between the toe of the pā mound and the outermost palisade row (Figure 6.1.10). Seven posts were identified in this excavation area, three at the northern toe of the raised pā mound and four in the southern outermost palisade row. Interestingly, no posts were identified within the middle of the excavation area, with approximately 5 m separating the surviving innermost and outermost palisade rows. Fifteen postholes were identified at the southern end of EA44 (Figure 6.1.11), grouped into three alignments and interspersed with smaller stakeholes. These postholes indicate that further posts in this alignment were either removed (by the Waikato Museum Archaeological Society or fossickers) or have decayed since the previous excavations.

Figure 6.1.10. Zac McIvor excavates EA44 in Area B at MA1[23].

[23] This photograph looks northwest towards the southwestern corner of MA1 and shows the positions of EA44 and EA45.

Figure 6.1.11. Post-excavation photograph of the southern end of EA44 at MA1.

The section profile of EA44 comprised two distinct cultural layers typifying the stratigraphy of Area B (Figure 6.1.12). The uppermost cultural layer (L1) consists of black organic silt with charcoal and fire-cracked rock (FCR) inclusions. At approximately 35–50 cm deep, the soil composition changes slightly, becoming more compact, organic and flaky (L2). At the base of L2, approximately 60–70 cm deep, is a layer of freshwater mussel periostracum (*E. menziesii*) across the entire excavation area. This mussel periostracum layer is presumed to be of cultural origin. Imported soil inclusions (C10) were identified within the top 70 cm of the profile, consisting of a yellowish-brown silty clay (10YR 4/4). This imported material typifies the raised pā mound, and while its source location is unknown, it is similar to the deposits forming the local hills (which include the strongly weathered, clay-rich Hamilton Ash beds and older volcanogenic deposits: Lowe, 2010, 2023).

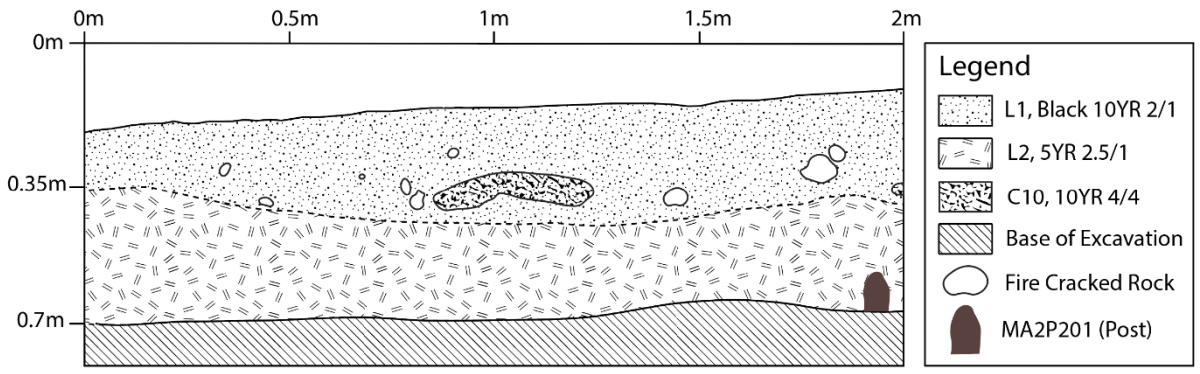

Figure 6.1.12. Section drawing of the northern baulk of EA44 at MA1.

Excavation in EA44 indicated that most of the surviving posts were limited to the outermost identified palisade row. Two additional excavation areas (EA45 and EA48) were positioned along this alignment to determine the extent of the surviving posts in this row. EA45 was a small excavation square directly adjacent to EA44, revealing three posts and six postholes, aligning with the posts and postholes identified in EA44 (Figure 6.1.13). EA48 was a long trench (30 x 0.5 m) excavated the length of the outermost palisade row to a depth of 20 cm. Thirty-one posts were recorded in EA48, spaced unevenly along the length of the trench (Figure 6.1.14). Interestingly, most of the posts identified in this outer row were split and/or adzed, resulting in a square or rectangular cross-section (Figure 6.1.15). This observation indicates that a different construction method was employed on the posts within this row. Unfortunately, this construction method makes these posts unsuitable for WMD. Therefore, the dating methodology employed by this study cannot investigate if this represents a distinct phase of palisade construction employing adzed posts. However, round posts within this row that retained the terminal growth ring were sampled for analysis. The posts located at the southern end of EA44 and EA45, with the addition of the posts found in EA48, represent the entire surviving outermost palisade defences.

Figure 6.1.13. EA45 (front) and the southern end of EA44 (rear) at MA1.

Figure 6.1.14. The eastern end of EA48 at MA1.

Figure 6.1.15. A pre-excavation photograph of MA1P175.

Figure 6.1.16. Warren Gumbley excavating the northern end of EA44 at MA1.

EA46 covered an area of 3 x 1 m, running east-west along the toe of the pā mound (Figure 6.1.16 and Figure 6.1.17). Excavation in EA46 identified two more posts and a large posthole. These two posts and the three posts identified at the northern end of EA44 represent the extent of the surviving palisade row located on top of (cut into) the toe of the raised pā mound. A large root/branch was also identified at the western end of EA46, extending into the northern baulk. Peters (1971, p. 130) previously reported horizontal timbers at this depth, hypothesising they were positioned under imported sediment deposits to provide a stable foundation for the pā mound.

Figure 6.1.17. A post-excavation photograph of EA46 at MA1.

EA47 was the final area excavated, positioned around a single post visible above the ground surface, 6 m east of EA46 (Figure 6.1.18). This post was positioned at the base of the raised pā mound, outside (south) of the innermost palisade alignment identified in EA44 and EA46. Excavations in EA47 extended 0.5 m deep, identifying one further post below the ground surface. These two posts represent the extent of the surviving palisade row at the base of the pā mound.

Figure 6.1.18. A post-excavation photograph of EA47 at MA1.

In summary, forty-six palisade posts were identified within five excavation areas in Area B. These posts were identified within a minimum of three distinct palisade rows. However, as shown in Section 4.1.1.1, these three rows do not represent the full extent of the palisade rows previously identified at MA1. Ten of these posts were selected for extraction (Figure 6.1.19 and Table 6.1.2), with five deemed unsuitable for sampling, including two poorly preserved posts, two with adzed cross-sections, and one with charring present on its outer surface (resulting in a loss of the terminal growth ring). The remaining five posts were all sampled for further analysis (25 cm section), including three from the outer palisade row and two from rows

close to the pā mound. Three distinct taper types were recorded: two long, three short, and two bulb-shaped tapers (Figure 6.1.20, Figure 6.1.21 and Figure 6.1.22).

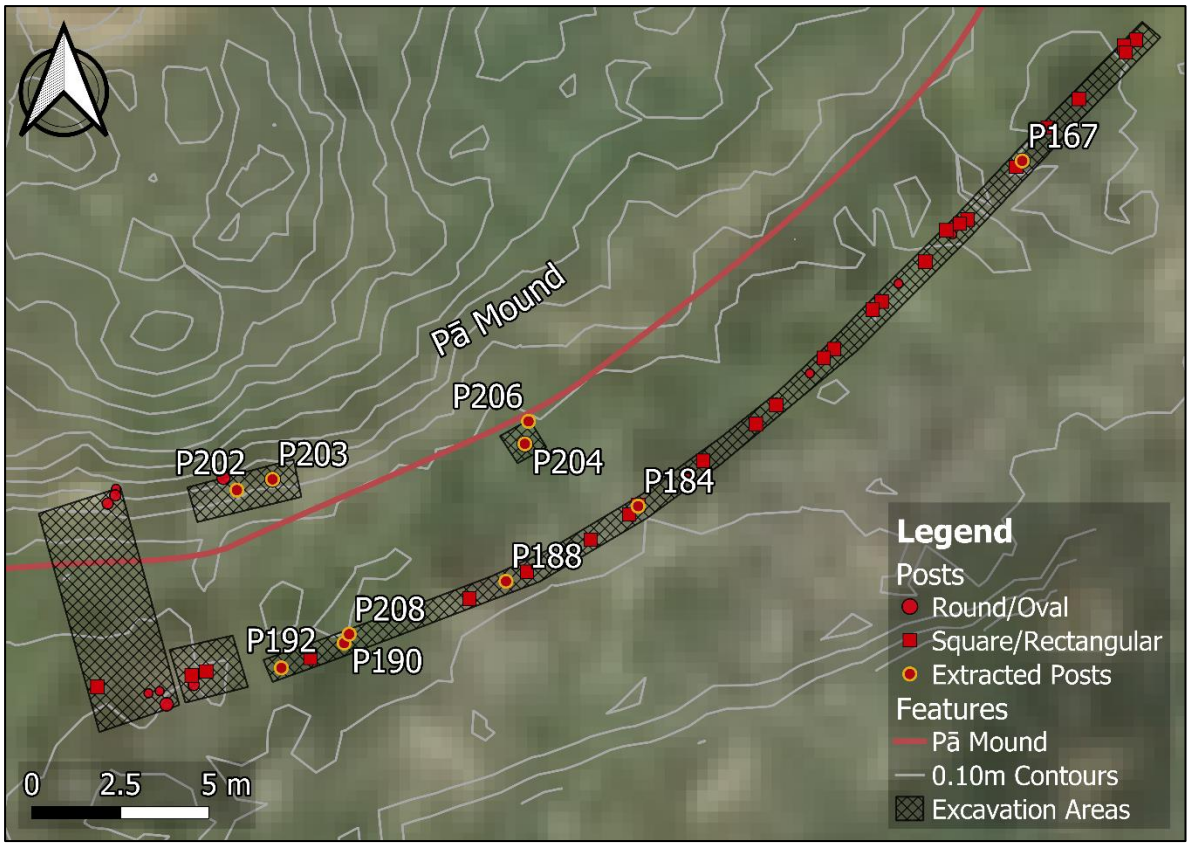

Figure 6.1.19. Plan drawing showing the location of extracted posts in Area B at MA1.

Table 6.1.2. Recorded information for extracted posts from Area B at MA1.

Post ID	Cross Section Shape	Max Length (cm)	Diameter (cm)	Taper Shape	Condition	Sampled
MA1P167	Round	-	15.0	-	Adzed distal end	No
MA1P184	Round	-	-	-	Charring identified	No
MA1P188	Round	163	12.1	Long	Adzed distal end	No
MA1P190	Round	178	13.4	Long	Suitable for sampling	Yes
MA1P192	Round	132	11.1	Short	Suitable for sampling	Yes
MA1P202	Oval	49	12.8	Short	Poor preservation	No
MA1P203	Oval	142	19.8	Short	Suitable for sampling	Yes
MA1P204	Round	144	15.3	Bulb	Suitable for sampling	Yes
MA1P206	Round	-	-	-	Poor preservation	No
MA1P208	Oval	121	14.4	Bulb	Suitable for sampling	Yes

Figure 6.1.20. Post-extraction photograph of MA1P208.

Figure 6.1.21. Post-extraction photograph of MA1P203.

Figure 6.1.22. Post-extraction photograph of MA1P190.

6.2 Species Identification

Thin-section microscopy of the post assemblage (10 posts) sampled from MA1 identified four tree species: pukatea (*L. novae-zelandiae*), kahikatea (*D. dacrydioides*), titoki (*A. excelsus*) and rewarewa *(K. excelsa*) (Table 6.2.1). All four species are commonly found in the lowland forests of the North and South Islands and are typical of the swampy or peaty environments surrounding the rivers and lakes of the Middle Waikato Basin (see Table 5.3.2). Sample MA1P50 was excluded from further analysis following species identification because rewarewa is unsuitable for tree-ring analysis.

Table 6.2.1. Tree Species identified in the post assemblage from MA1.

Post ID	Common Name	Scientific Name
MA1P42	pukatea	*Laurelia novae-zelandiae*
MA1P48	pukatea	*Laurelia novae-zelandiae*
MA1P50*	rewarewa	*Knightia excelsa*
MA1P53	pukatea	*Laurelia novae-zelandiae*
MA1P57	pukatea	*Laurelia novae-zelandiae*
MA1P190	pukatea	*Laurelia novae-zelandiae*
MA1P192	pukatea	*Laurelia novae-zelandiae*
MA1P203	kahikatea	*Dacrycarpus dacrydioides*
MA1P204	kahikatea	*Dacrycarpus dacrydioides*
MA1P208	titoki	*Alectryon excelsus*

*Note. * indicates the post dropped from tree-ring analysis due to unsuitable species.*

6.3 Sample Condition Assessment

All nine prepared post samples were inspected under a low-powered light microscope to assess their condition and suitability for tree-ring analysis, ring-block sampling, and AMS radiocarbon dating (see Section 5.5 and Table 6.3.1). Following this assessment, two samples (MA1P42 and MA1P203) were of poor quality and excluded from further analysis. The characteristics of the remaining seven samples are discussed in Section 6.4 below.

Table 6.3.1. MA1 sample condition assessment.

Post ID	Poor preservation	Charring present	Scaring present	Dark staining	Growth anomalies	Passed
MA1P42*	☐	☑	☐	☑	☑	No
MA1P48	☐	☐	☐	☐	☑	Yes
MA1P53	☐	☐	☑	☑	☑	Yes
MA1P57	☐	☐	☑	☑	☑	Yes
MA1P190	☐	☐	☐	☐	☑	Yes
MA1P192	☐	☐	☐	☐	☑	Yes
MA1P203*	☑	☐	☐	☑	☑	No
MA1P204	☐	☐	☑	☑	☑	Yes
MA1P208	☐	☐	☐	☑	☑	Yes

*Note. * indicates samples excluded from tree-ring analysis due to unsuitable characteristics.*

6.4 Tree-ring Analysis Results

The reconciled ring count information for each post sample in the MA1 assemblage is summarised in Table 6.4.1 (see Section 5.6 for method). The reconciled ring counts presented below represent the most accurate information attainable for these samples, with any persistent inconsistencies discussed further in Section 6.5.

Table 6.4.1. A summary of the reconciled ring count information for the posts sampled from MA1.

Post ID	Species ID	Reconciled ring count	Diameter (cm)
MA1P48*	Pukatea (*L. novae-zelandiae)*	225*	20.5
MA1P53	Pukatea (*L. novae-zelandiae)*	152	19.2
MA1P57	Pukatea (*L. novae-zelandiae)*	106	19.0
MA1P190	Pukatea (*L. novae-zelandiae)*	54	13.4
MA1P192	Pukatea (*L. novae-zelandiae)*	23	11.1
MA1P204	Kahikatea (*D. dacrydioides*)	99	15.3
MA1P208	Titoki (*A. excelsus*)	73	14.4

*Note. * Indicates ring count information for MA1P48 is a minimum estimation.*

6.4.1 MA1P48 (pukatea, *L. novae-zelandiae*)

MA1P48 was characterised by a round cross-sectional shape, central pith location, and a non-concentric tree-ring growth pattern. Several tree-ring growth anomalies were identified, including areas of tree-ring suppression, false rings, and locally absent rings (Figure 6.4.1). Abnormal late-wood patterning also affected tree-ring visibility across the growth sequence. This patterning occurs due to poor growth conditions, resulting in the typical colour of the earlywood (light in colour) and latewood (dark in colour) reversing. Finally, the terminal growth ring was missing from a portion of the sample's circumference, owing to damage on the post's outer surface. These growth characteristics resulted in differences of up to 70 rings between the three radii analysed (Table 6.4.2). Despite multiple attempts, these radii could not be reconciled into an accurate final ring count, and the sample was rejected from further analysis.

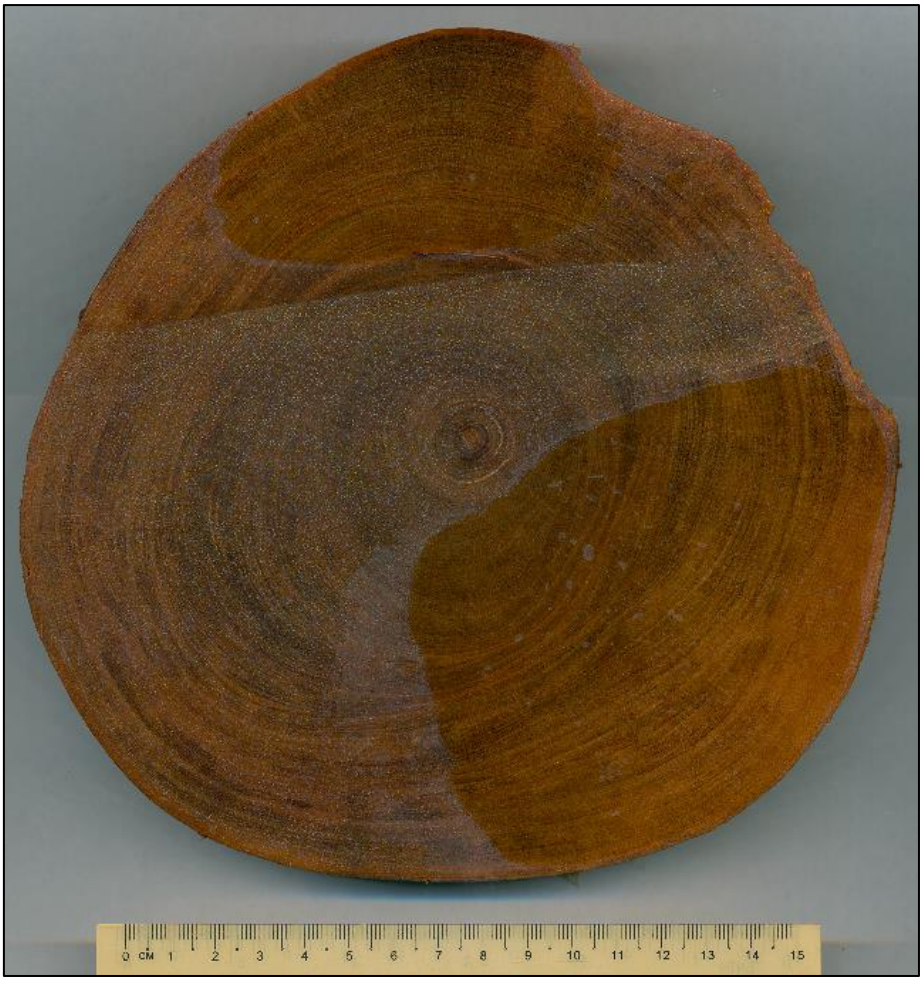

Figure 6.4.1. Digital scan of MA1P48.

Table 6.4.2. Ring count information for MA1P48.

Ring Counts	Track A	Track B	Track C	Reconciled
MA1P48	225	200	155	225

Note. Ring count numbers are given as minimum estimations.

6.4.2 MA1P53 (pukatea, *L. novae-zelandiae*)

MA1P53 was characterised by an oval cross-section, central pith location, and concentric tree-ring growth pattern. Additionally, the terminal growth ring was missing from a portion of the sample's circumference, owing to damage to the outer surface (Figure 6.4.2). Tree-ring growth anomalies also affected the growth sequence, including multiple episodes of tree-ring suppression and locally absent rings that were particularly prevalent between rings 30 and 60. Locally absent rings mainly affected the ring count of Track A, as reflected in the ring count

discrepancies presented in Table 6.4.3. Despite these challenges, the reconciliation of these three measured radii resulted in a final ring count of 152. Based on this reconciled ring count, eight ring-block samples were collected at semi-regular intervals throughout the tree-ring growth sequence (Table 6.4.4). Larger ring gaps were necessary between specific samples due to episodes of tree-ring suppression. Additionally, three ring-block samples contained more or fewer than five tree rings, owing to sampling errors during periods of narrow annual growth. These inconsistencies were identified following ring count information checks undertaken after the initial WMD results were calibrated.

Figure 6.4.2. Digital scan of MA1P53.

Table 6.4.3. Ring count information for MA1P53.

Ring counts	Track A	Track B	Track C	Reconciled
MA1P53	127	151	152	152

Table 6.4.4. Ring-block sampling information for MA1P53.

Wk Number	Sample Code	First ring	Middle ring	Last ring	# of rings in block	Ring gap to next Sample
52101	1_MA1P53 (1–5)	1	3	5	5	9
52858	2_MA1P53 (10–14)	10	12	14	5	23.5
52357*	3_MA1P53 (33–38)	33	35.5	38	6	36.5
52102	4_MA1P53 (70–74)	70	72	74	5	19.5
52859*	5_MA1P53 (90–93)	90	91.5	93	4	17
52358*	6_MA1P53 (106–111)	106	108.5	111	6	26.5
52860	7_MA1P53 (133–137)	133	135	137	5	15
52103	8_MA1P53 (148–152)	148	150	152	5	2.5

*Note. * Indicates three ring-block samples that do not contain five tree rings: 3_MA1P53 (33–38), 5_MA1P53 (90–93) and 6_MA1P53 (106–111).*

6.4.3 MA1P57 (pukatea, *L. novae-zelandiae*)

MA1P57 presented a round cross-sectional shape, relatively central pith location, and concentric tree-ring growth pattern. Additionally, scaring caused by insect damage was identified, affecting a portion of the oldest (innermost) tree rings (Figure 6.4.3). Episodes of tree-ring suppression and locally absent rings were also observed, particularly affecting the second half (outermost half) of the tree-ring growth sequence. Reconciliation of the three measured radii resulted in a final ring count of 106 (Table 6.4.5). Five ring-block samples were collected semi-regularly across the tree-ring growth ring sequence (Table 6.4.6). Ideally, the sampling resolution for MA1P57 should have increased from five to seven ring-block samples. However, owing to the previously mentioned episodes of tree-ring suppression, the ring-block samples had to be strategically positioned to ensure sampling accuracy. Despite this caution, two ring-block samples contained more or fewer than five tree rings, resulting from sampling errors associated with narrow annual growth periods within the sampling locations.

Figure 6.4.3. Digital scan of MA1P57.

Table 6.4.5. Ring count information for MA1P57.

Ring Counts	Track A	Track B	Track C	Reconciled
MA1P57	97	89	75	106

Table 6.4.6. Ring-block sampling information for MA1P57.

Wk Number	Sample Code	First ring	Middle ring	Last ring	# of rings in block	Ring gap to next sample
52104	9_MA1P57 (1–5)	1	3	5	5	14
52355	10_MA1P57 (15–19)	15	17	19	5	31.5
52105*	11_MA1P57 (47–50)	47	48.5	50	4	21.5
52356	12_MA1P57 (68–72)	68	70	72	5	26.5
52106*	13_MA1P57 (93–100)	93	96.5	100	8	9.5

*Note. * Indicates three ring-block samples that do not contain five tree rings: 11_MA1P57 (47–50) and 13_MA1P57 (93–100).*

6.4.4 MA1P190 (pukatea, *L. novae-zelandiae*)

MA1P190 presented a round cross-sectional shape, off-centre pith location, and non-concentric tree-ring growth pattern (Figure 6.4.4). Episodes of tree-ring suppression and locally absent rings were present across the growth sequence, primarily related to the non-concentric growth pattern. A large scar radiating from the pith to the terminal tree ring was also observed. Tree-ring count and measurement analysis identified only minor differences between the three measured radii (Table 6.4.7), resulting in a reconciled final tree-ring count of 54. Based on this reconciled ring count, five ring-block samples were collected at semi-regular across the tree-ring growth sequence (Table 6.4.8). One ring-block sample contained fewer than five tree rings, resulting from sampling errors associated with narrow annual growth periods.

Figure 6.4.4. Digital scan of MA1P190.

Table 6.4.7. Ring count information for MA1P190.

Ring Counts	Track A	Track B	Track C	Reconciled
MA1P190	54	54	47	54

Table 6.4.8. Ring-block sampling information for MA1P190.

Wk number	Sample code	First ring	Middle ring	Last ring	# of rings in block	Ring gap to next sample
52737	14_MA1P190 (1–5)	1	3	5	5	10
52738	15_MA1P190 (11–15)	11	13	15	5	15
52739	16_MA1P190 (26–30)	26	28	30	5	15
52740	17_MA1P190 (41–45)	41	43	45	5	9.5
52741*	18_MA1P190 (51–54)	51	52.5	54	4	2

*Note. *Indicates ring-block sample that does not contain five tree-rings: 18_MA1P190 (51–54).*

6.4.5 MA1P192 (pukatea, *L. novae-zelandiae*)

An irregular cross-sectional shape, central pith location, and non-concentric tree-ring growth pattern characterised MA1P192 (Figure 6.4.5). Episodes of tree-ring suppression were particularly prevalent late in the growth sequence (outermost tree-rings). Additionally, the tree-ring boundaries across the growth sequence were poorly defined, further limiting the clarity of the growth sequence. Reconciliation of these three ring counts resulted in a final ring count of 23 (Table 6.4.9). Owing to this short tree-ring growth sequence, only four ring-block samples could be collected (Table 6.4.10). No sampling errors were identified across any ring-block samples; all four contained five tree rings.

Figure 6.4.5. Digital scan of MA1P192.

Table 6.4.9. Ring count information for MA1P192.

Ring Counts	Track A	Track B	Track C	Reconciled
MA1P192	22	23	22	23

Table 6.4.10. Ring-block sampling information for MA1P192.

Wk number	Sample code	First ring	Middle ring	Last ring	# of rings in block	Ring gap to next sample
52742	19_MA1P192 (1–5)	1	3	5	5	5
52743	20_MA1P192 (6–10)	6	8	10	5	5
52744	21_MA1P192 (11–15)	11	13	15	5	8
52745	22_MA1P192 (19–23)	19	21	23	5	2.5

6.4.6 MA1P204 (kahikatea, *D. dacrydioides*)

MA1P204 presented a round cross-sectional shape, central pith location, and non-concentric tree-ring growth pattern. Additionally, this sample was affected by a large area of scarring impacting the tree-ring growth ring sequence (Figure 6.4.6). Multiple episodes of tree-ring

suppression and locally absent rings were also identified, primarily related to the scarring and non-concentric growth patterns. Tree-ring count and measurement analysis identified minor differences between the three tracks measured, with locally absent rings accounting for the differences. Reconciliation of these three radii resulted in a final ring count of 99 (Table 6.4.11), with five ring-block samples collected at semi-regular intervals across the growth sequence (Table 6.4.12). Ideally, the sampling resolution for MA1P204 would have increased from five to seven ring-block samples. However, owing to the scaring and tree-ring suppression, the ring-block samples had to be strategically positioned to ensure sampling accuracy. Despite this caution, one ring-block sample contained fewer than five tree rings, resulting from sampling errors within a narrow annual growth period.

Figure 6.4.6. Digital scan of MA1P204.

Table 6.4.11. Ring count information for MA1P204.

Ring Counts	Track A	Track B	Track C	Reconciled
MA1P204	95	98	99	99

Table 6.4.12. Ring-block sampling information for MA1P204.

Wk Number	Sample Code	First ring	Middle ring	Last ring	# of rings in block	Ring gap to next sample
52746	23_MA1P204 (30–34)	30	32	34	5	10
52747	24_MA1P204 (40–44)	40	42	44	5	31
52748	25_MA1P204 (71–75)	71	73	75	5	15
52749	26_MA1P204 (86–90)	86	88	90	5	9.5
52750*	27_MA1P204 (96–99)	96	97.5	99	4	2

*Note. * Indicates that the sample only contains four tree rings.*

6.4.7 MA1P208 (titoki, *A. excelsus*)

The final sample from MA1, MA1P208, presented an irregular cross-sectional shape and an off-centre pith location, creating a non-concentric tree-ring growth pattern (Figure 6.4.7). The tree-ring count and measurement analysis identified minor differences between the three measured radii (Table 6.4.13), accounted for by areas of tree-ring suppression and locally absent rings. Reconciliation of the three measured tracks resulted in a final count of 73, with five ring-block samples collected at semi-regular intervals across the tree-ring growth sequence (Table 6.4.14). No sampling errors were identified across any ring-block samples; all five contained five tree rings.

Figure 6.4.7. Digital scan of MA1P208.

Table 6.4.13. Ring count information for MA1P208.

Ring Counts	Track A	Track B	Track C	Reconciled
MA1P208	73	72	66	73

Table 6.4.14. Ring-block sampling information for MA1P208.

Wk Number	Sample Code	First ring	Middle ring	Last ring	# of rings in block	Ring gap to next sample
52751	28_MA1P208 (1–5)	1	3	5	5	16
52752	29_MA1P208 (17–21)	17	19	21	5	19
52753	30_MA1P208 (36–40)	36	38	40	5	15
52754	31_MA1P208 (51–55)	51	53	55	5	18
52755	32_MA1P208 (69–73)	69	71	73	5	2.5

6.5 Wiggle-Match Dating Results (Event Scale)

This section presents the results of WMD on the post-assemblage (six posts) sampled from MA1. The WMD results presented below represent the event scale of analysis, with each Felling Date interpreted as a TPQ for the construction of a post used in palisade defence. The WMD method (OxCal D_Sequence model) is fully described in Section 5.8.2, and the full array of OxCal codes relating to each post analysed can be viewed in Appendix D.1. Finally, the interpretation of each WMD is discussed in detail below.

6.5.1 MA1P53

The D_Sequence model for MA1P53 comprises eight AMS ^{14}C dates, separated by known calendar intervals, spread across the 152-year tree-ring growth sequence (Table 6.5.1). The Felling Date of MA1P53 has a median calibrated age of AD 1754 ± 3, with a modelled date range between AD 1749–1761 (95% HPD). The D_Sequence model does not pass the A_{comb} (An) threshold (A_{comb} > An), and two of the eight ^{14}C dates were flagged as outliers during the analysis, one minor: 2_MA1P53 (10–14) and one major: 6_MA1P53 (106–111). These outlier results are reflected on the curve plot (Figure 6.5.1), as both ^{14}C dates are offset from SHCal20. To investigate these offsets further, the D_Sequence model calibrated using the RScaled outlier model was reviewed (see Appendix D.1.1), with the results of this analysis showing sample 2_MA1P53 (10–14) was not flagged as an outlier. When considering this result, it is essential to remember that SHCal20 is a modelled probability band describing a combined ^{14}C calibration dataset (of varying resolution) within a defined calendar period. Therefore, minor offsets (and outliers) observed between a ^{14}C result and the calibration curve that can be identified and down-weighted by the applied outlier models are anticipated. However, the posterior outlier value for sample 6_MA1P53 (106–111) is of more concern, as the ^{14}C age is completely implausible within the defined calendar period (Figure 6.5.2). Therefore, possible causes of these results must be considered.

Table 6.5.1. D_Sequence (SSimple) result for MA1P53.

Wk Number	Sample Code	^{14}C Age (BP)	Outlier analysis (posterior/prior)	Convergence
52101	1_MA1P53 (1–5)	413 ± 22	3/5	99
52858	2_MA1P53 (10–14)	440 ± 20	12/5	99
52357	3_MA1P53 (33–38)	334 ± 21	3/5	99
52102	4_MA1P53 (70–74)	195 ± 21	4/5	99
52859	5_MA1P53 (90–93)	172 ± 21	2/5	99
52358	6_MA1P53 (106–111)	253 ± 21	99/5	99
52860	7_MA1P53 (133–137)	236 ± 21	4/5	99
52103	8_MA1P53 (148–152)	277 ± 21	2/5	99

Felling Date Results

Median cal. Age (AD)	HPD 68%	HPD 95%	A_{comb} (An)
1754 ± 3	AD 1751–1757	AD 1749–1761	2 (25)

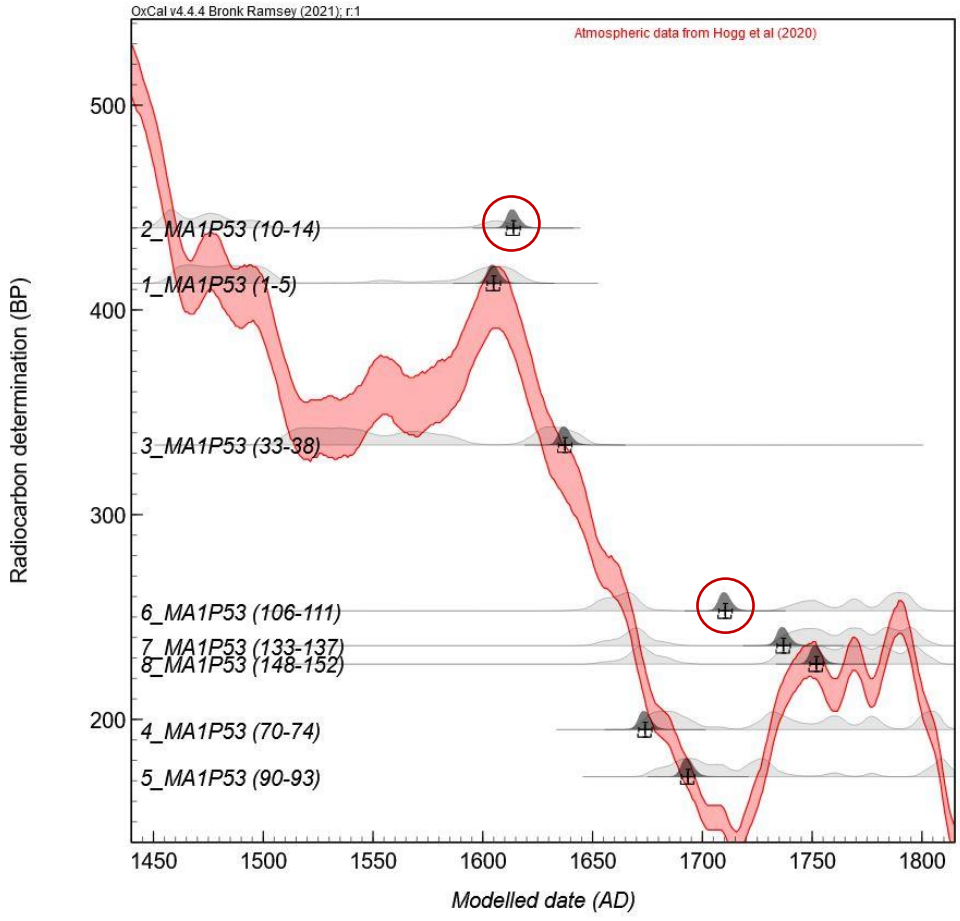

Figure 6.5.1. OxCal generated curve plot of the D_Sequence model for MA1P53[24].

[24] Red circles highlight the two outliers detected during the analysis.

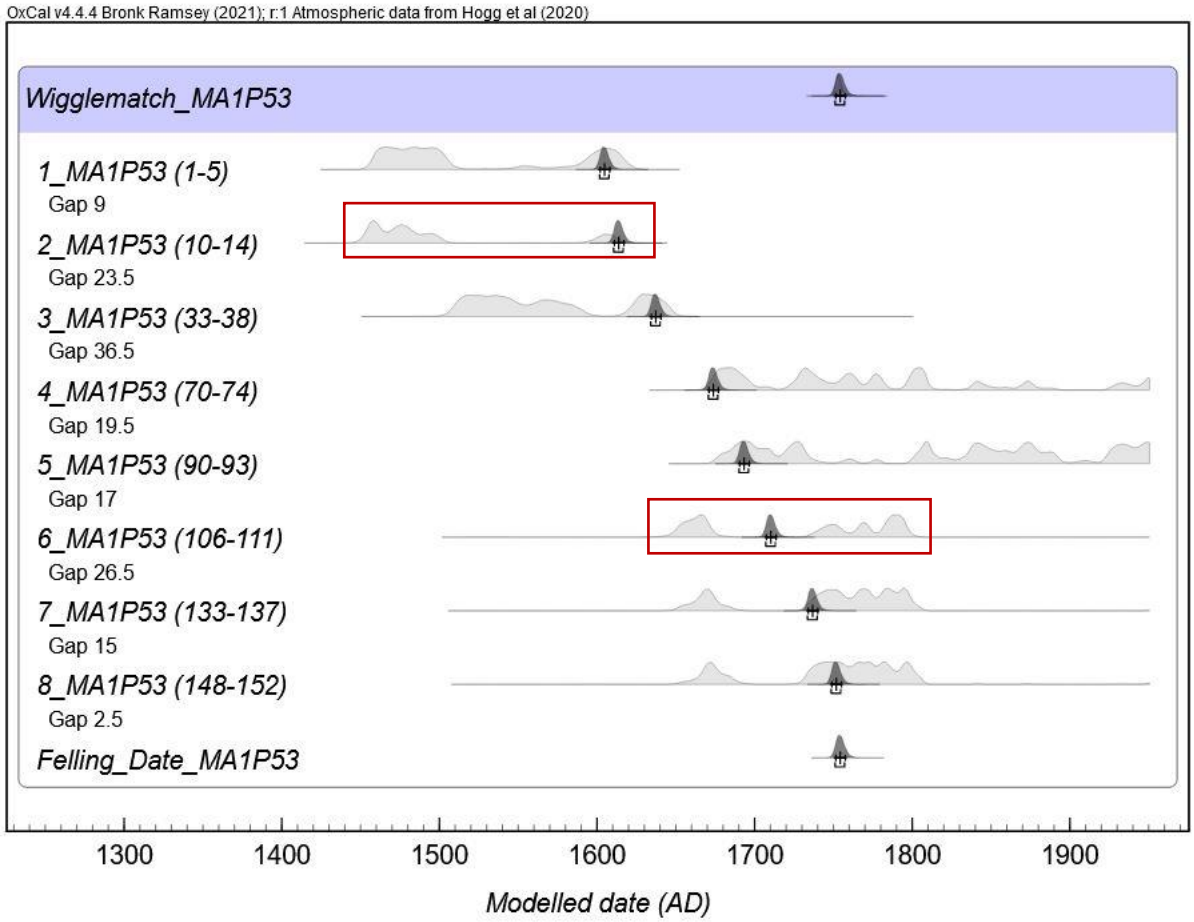

Figure 6.5.2. OxCal generated multiplot of the D_Sequence model for MA1P53[25].

As discussed, tree-ring analysis of MA1P53 identified a prominent episode of tree-ring suppression between rings 30–60. Possible errors within the reconciled ring count associated with this period of growth would affect the calendar spacings between the ^{14}C dates within the D_Sequence. However, the remaining ^{14}C dates within the WMD are not flagged as outliers and generally reflect the shape of SHCal20. Furthermore, additional ring count checks could not identify inconsistencies within the reconciled ring count for MA1P53. These results and observations indicate that the ^{14}C offset of sample 6_MA1P53 (106–111) is unrelated to potential ring count errors. In this case, the appropriate action would be to resample new material for sample 6_MA1P53 (106–111) to determine other possible causes of this result (e.g., a laboratory error during pretreatment or measurement). However, as this is not possible in the current analysis, the D_Sequence model for MA1P53 was recalibrated with sample

[25] Red boxes highlight the two outliers detected during the analysis.

6_MA1P53 (106–111) removed from the model (see Appendix D.1.2). This analysis produced an identical Felling Date to the original model, identified no outliers, had universal high convergence (> 95%), and passed the A_{comb} (An) threshold: 78 (27). Consequently, the WMD for MA1P53 is considered accurate and is included in the local and regional scales of analysis.

6.5.2 MA1P57

The D_Sequence model for MA1P57 comprises five AMS ^{14}C dates, separated by known calendar intervals, spread across the 106-year tree-ring growth sequence (Table 6.5.2). The Felling Date of MA1P57 has a median calibrated age of AD 1719 ± 7, with a modelled date range between AD 1707–1745 (95% HPD). However, the model's results indicate a problem. The D_Sequence model does not pass the A_{comb} (An) threshold, and the analysis flagged two minor outliers: 10_MA1P57 (15–19) and 13_MA1P57 (93–100). Additionally, when reviewing the curve plot of the analysis, the WMD is shown to poorly reflect the shape of SHCal20 (Figure 6.5.3), with three of the five ^{14}C dates offset from the curve. The ^{14}C offset for sample 13_MA1P57 (93–100) is of particular concern, as it is the last sample in the D_Sequence model and defines the calendar spacing to the modelled Felling Date.

As discussed above, tree-ring analysis of MA1P57 identified several episodes of tree-ring suppression across the tree-ring growth sequence, resulting in locally absent rings and narrow annual growth periods. These episodes were particularly prevalent during the second half of the growth sequence. Possible errors in the reconciled ring count associated with these periods of growth would impact the calendar spacing between the ^{14}C dates. Notably, the ^{14}C age order reversal identified between the last two samples in the WMD suggests that these samples should be positioned across the calibration plateau in the eighteenth century. This observation is reinforced by comparing the likelihood and posterior distributions (Figure 6.5.4), supporting a calendar position within this period. Therefore, errors in the reconciled ring count are determined to be the most likely cause of the poor result, and the WMD for MA1P57 is deemed inaccurate and excluded from the local and regional scale analyses.

Table 6.5.2. Sequence (SSimple) result for MA1P57.

Wk Number	Sample Code	^{14}C Age (BP)	Outlier analysis (posterior/prior)	Convergence
52104	9_MA1P57 (1–5)	398 ± 22	5/5	99
52355	10_MA1P57 (15–19)	274 ± 21	6/5	99
52105	11_MA1P57 (47–50)	254 ± 21	5/5	99
52356	12_MA1P57 (68–72)	229 ± 21	5/5	99
52106	13_MA1P57 (93–100)	254 ± 22	6/5	99

Felling Date Results

Median cal. Age (AD)	HPD 68%	HPD 95%	A_{comb} (An)
1719 ± 7	AD 1715–1723	AD 1707–1745	4 (32)

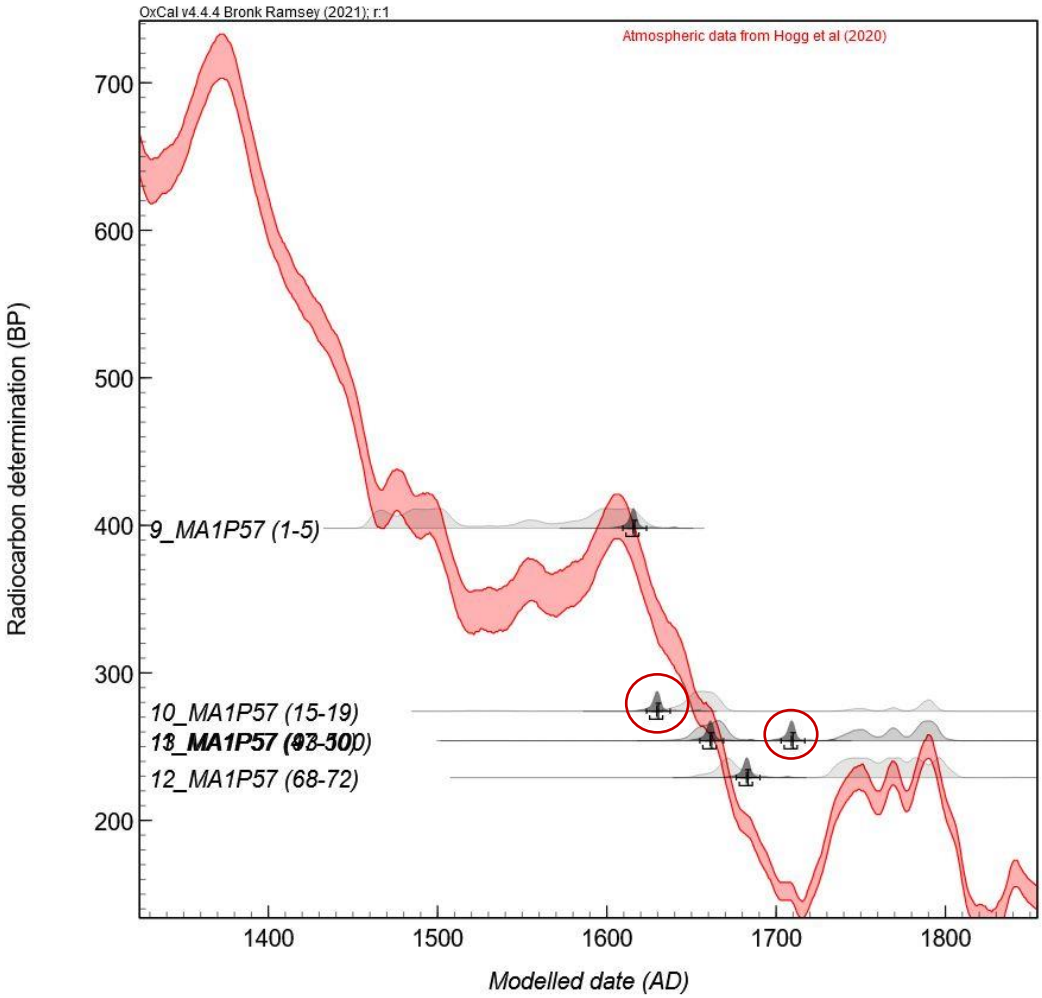

Figure 6.5.3. OxCal generated curve plot of the D_Sequence model for MA1P53[26].

[26] Red circles highlight the two outliers (potential calendar age offsets) detected during the analysis. See Section 13.1.5 for discussion.

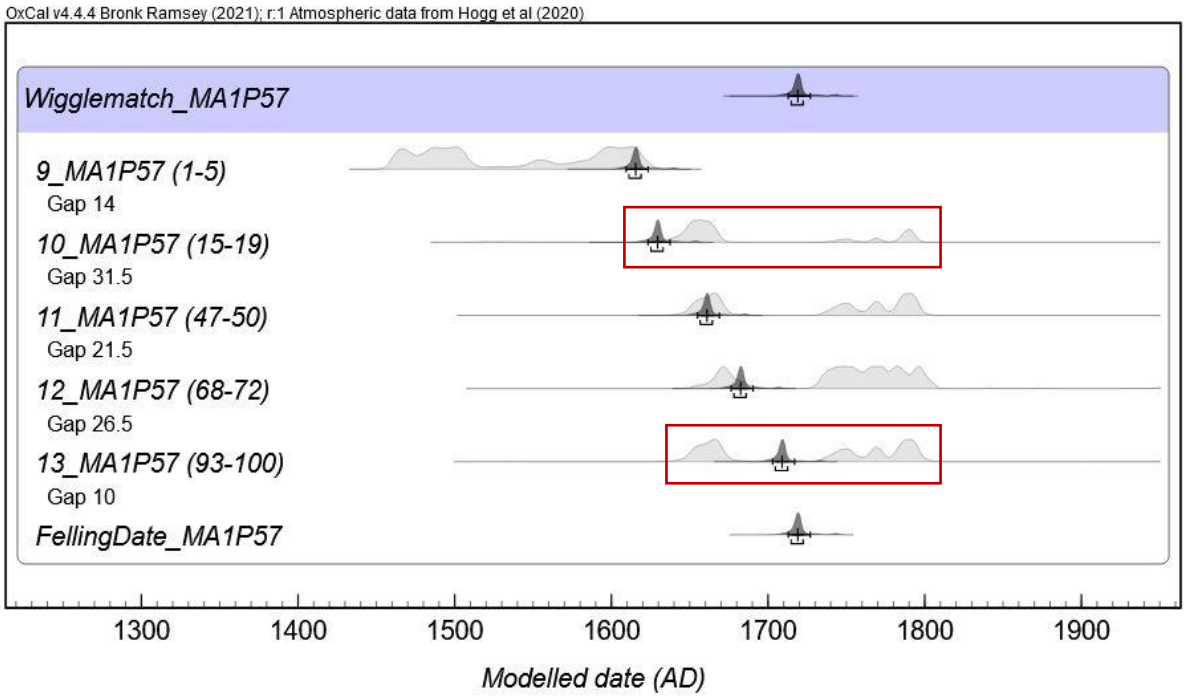

Figure 6.5.4. OxCal generated multiplot of the D_Sequence model for MA1P57[27].

6.5.3 MA1P190

The D_Sequence model for MA1P190 comprises five AMS ^{14}C dates, separated by known calendar intervals, spread across the 54-year tree-ring growth sequence (Table 6.5.3). The Felling Date of MA1P190 has a median calibrated age of AD 1803 ± 5, with a modelled date range between AD 1796–1811 (95% HPD). No outliers were identified during the analysis, and convergence values remained universally high (99%), indicating that the model is robust. When reviewing the curve plot of the analysis, the WMD generally reflects the shape of SHCal20 (Figure 6.5.5), and the posterior and likelihood distributions correlate well (Figure 6.5.6). Additionally, the ^{14}C age order reversals observed within the D_Sequence model suggest that the calendar position of the WMD in the late eighteenth century is correct. When the D_Sequence model was calibrated using alternative outlier detection methods (RScaled outlier model and agreement index analysis, see Appendix D.1.4), the results were consistent with the original model. Therefore, the WMD for MA1P190 is interpreted as accurate and is included in the local and regional scale analyses.

[27] Red boxes highlight the two outliers (potential calendar age offsets) detected during the analysis. See Section 13.1.5 for discussion.

Table 6.5.3. Sequence (SSimple) result for MA1P190.

Wk Number	Sample Code	^{14}C Age (BP)	Outlier analysis (posterior/prior)	Convergence
52737	14_MA1P190 (1–5)	245 ± 22	5/5	99
52738	15_MA1P190 (11–15)	233 ± 22	5/5	99
52739	16_MA1P190 (26–30)	223 ± 22	5/5	99
52740	17_MA1P190 (41–45)	264 ± 22	5/5	99
52741	18_MA1P190 (51–54)	190 ± 22	5/5	99

Felling Date Results

Median cal. Age (AD)	HPD 68%	HPD 95%	A_{comb} (An)
1803 ± 5	AD 1800–1807	AD 1796–1811	125 (32)

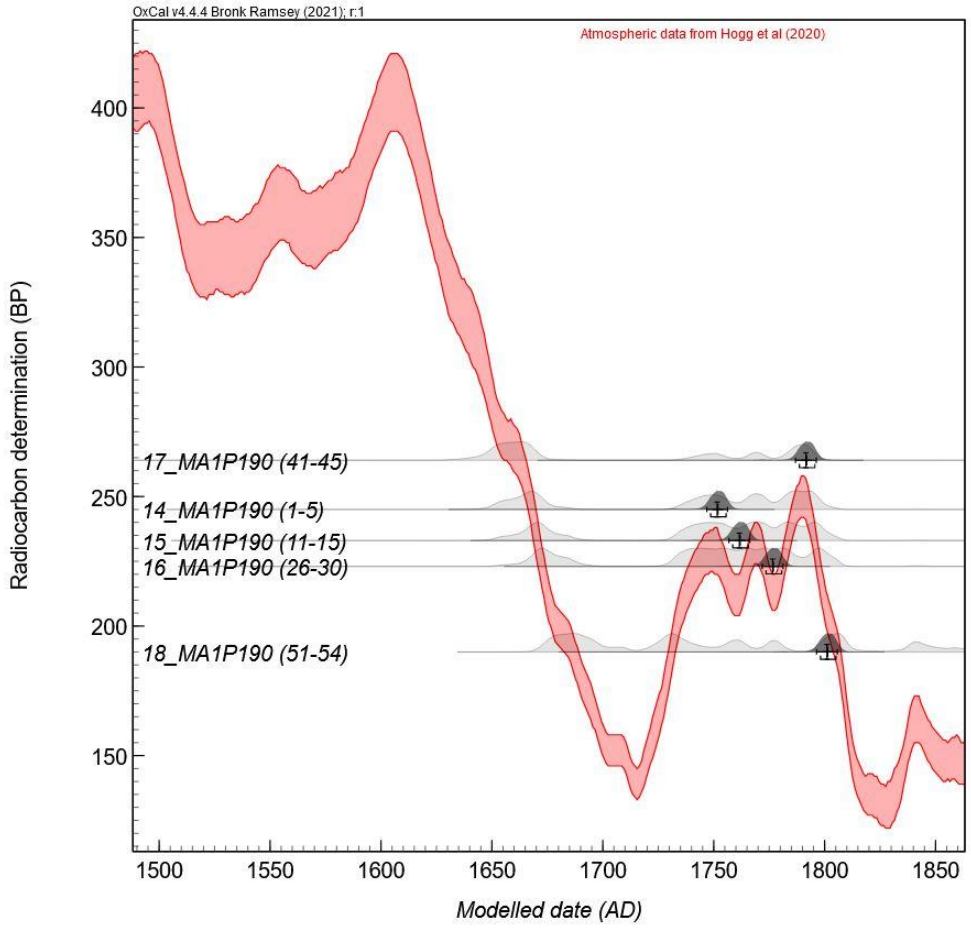

Figure 6.5.5. OxCal generated curve plot of the D_Sequence model for MA1P190.

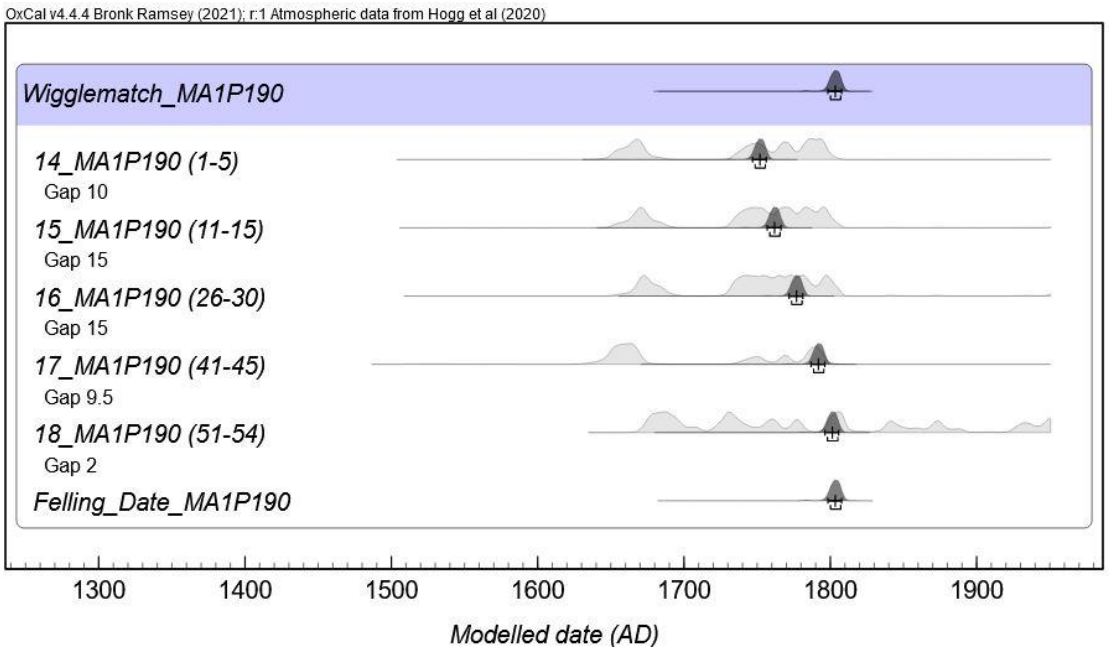

Figure 6.5.6. OxCal generated multiplot graph of the D_Sequence model for MA1P190.

6.5.4 MA1P192

The D_Sequence model for MA1P192 comprises four AMS ^{14}C dates, separated by known calendar intervals, spread across the 23-year tree-ring growth sequence (Table 6.5.4). Unfortunately, the short tree-ring growth sequence of MA1P192 results in a limited calendar spread across SHCal20. The Felling Date of MA1P192 has a median calibrated age of AD 1714 ± 54, with a modelled date range between AD 1693–1865 (HPD 95%). The analysis detected no outliers and convergence values remained universally high (99%). However, the Felling Date's lack of precision limits its information potential. For this reason, the D_Sequence model was constrained using the OxCal 'Before' function (see Section 5.8.2). The Before function acts as a TAQ (*terminus ante quem*), representing a date before the tree was felled. The battle of Ōrākau Pā was chosen as the constraint, which is an important historical event associated with the end of the Waikato land wars, with a known historical date of AD 1864 (see Hitiri te & Mair, 1888; Bader, 2013; O'Malley, 2013; Gumbley, 2014b; O'Malley, 2016). Additionally, when reviewing the curve plot of the WMD, the last ^{14}C date within the D_Sequence model is offset from SHCal20 (Figure 6.5.7). While not flagged as an outlier, this result is of concern as sample 22_MA1P57 (19–23) defines the calendar position of the modelled Felling Date.

Table 6.5.4. Sequence (SSimple) result for MA1P192.

Wk Number	Sample Code	^{14}C Age (BP)	Outlier analysis (posterior/prior)	Convergence
52742	19_MA1P192 (1–5)	201 ± 22	5/5	99
52743	20_MA1P192 (6–10)	159 ± 21	5/5	99
52744	21_MA1P192 (11–15)	151 ± 23	5/5	99
52745	22_MA1P192 (19–23)	203 ± 27	5/5	99

Felling Date Results

Median cal. Age (AD)	HPD 68%	HPD 95%	A_{comb} (An)
1714 ± 54	AD 1697–1863	AD 1693–1865	57 (35)

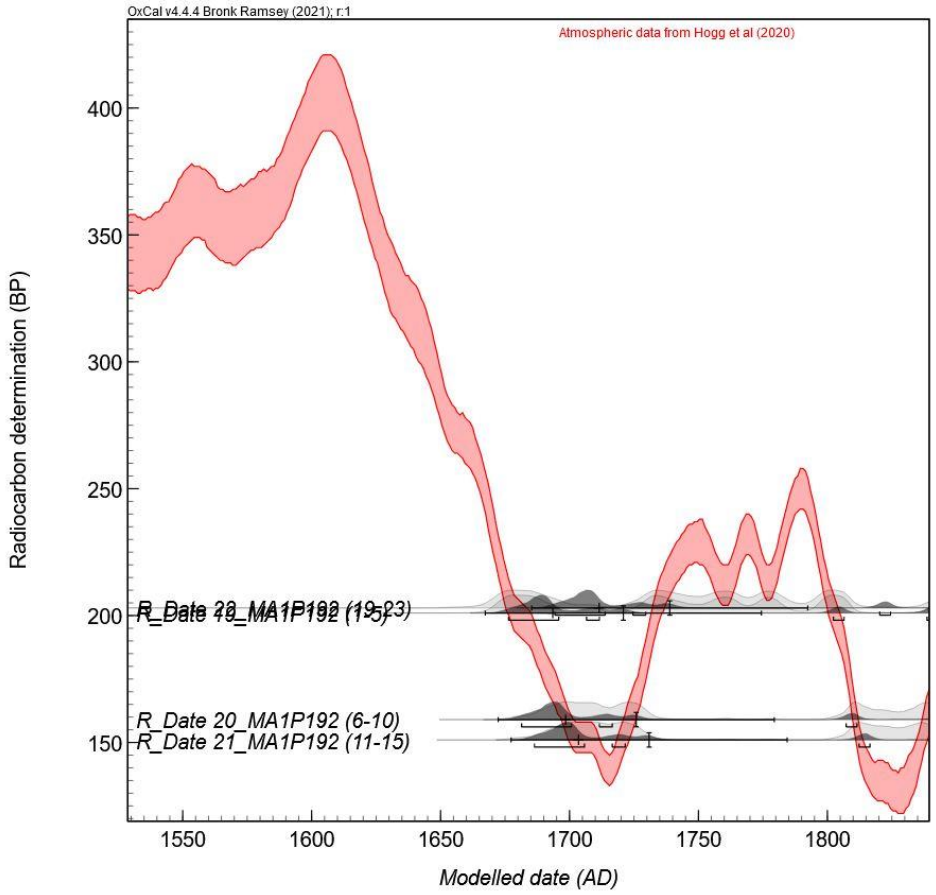

Figure 6.5.7. OxCal generated curve plot of the D_Sequence model for MA1P192.

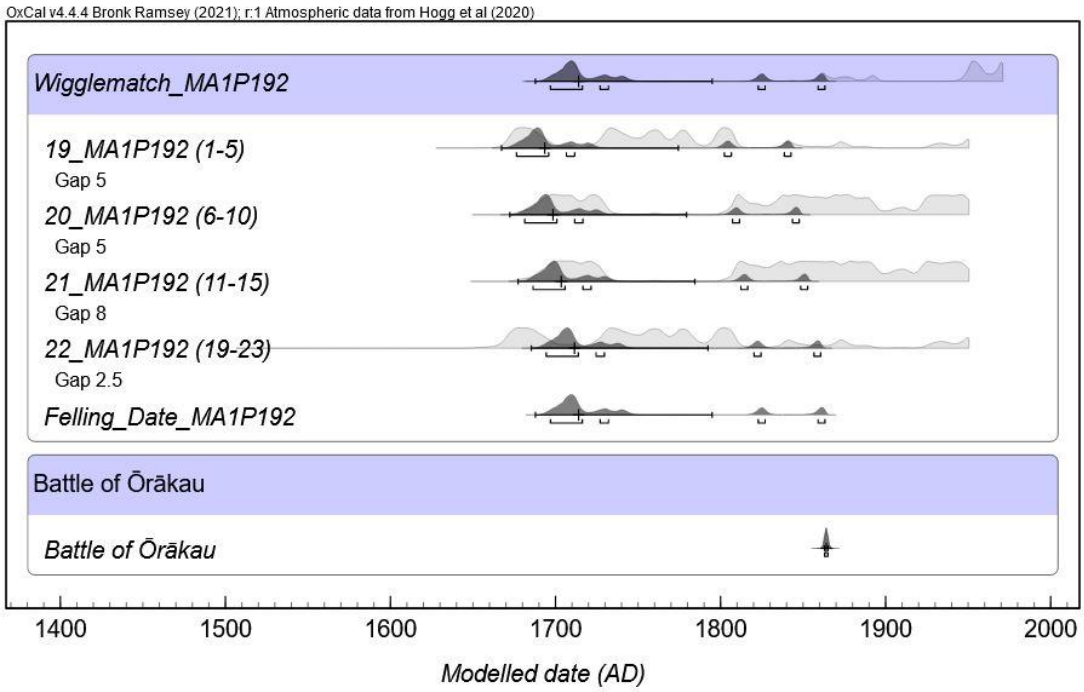

Figure 6.5.8. OxCal generated multiplot graph of the D_Sequence model for MA1P192.

Tree-ring analysis of MA1P192 identified episodes of tree-ring suppression late in the growth sequence, resulting in narrow periods of annual growth and poorly defined tree-ring boundaries, limiting the clarity of the growth sequence. Possible errors in the reconciled ring count associated with these periods of growth would impact the calendar spacing between the ^{14}C dates. When comparing the likelihood and posterior distributions of sample 22_MA1P192 (19–23), an estimated calendar position later in the 1700s (AD 1730–1740) would produce a far better result for the WMD. Therefore, the errors within the reconciled ring count are determined as the most probable cause of the poor result. While the Felling Date range produced for MA1P192 likely encompasses when the tree was cut down for use in a palisade at MA1 (AD 1692–1864), the imprecision of the WMD limits its use in a fine-grained chronological framework. Therefore, the WMD was excluded from the local and regional scale analyses.

6.5.5 MA1P204

The D_Sequence model for MA1P204 comprises five AMS ^{14}C dates, separated by known calendar intervals, spread across the 99-year tree-ring growth sequence (Table 6.5.5). The Felling Date of MA1P204 has a median calibrated age of AD 1711 ± 8, with a modelled date range between AD 1701–1724 (95% HPD). No outliers were detected during the analysis, and

convergence values remained universally high (99%). When reviewing the curve plot of the analysis, the WMD generally reflects the shape of SHCal20 (Figure 6.5.9), and the posterior and likelihood distributions correlate well (Figure 6.5.10). Additionally, given the ^{14}C ages reported for the samples within the D_Sequence model, the calendar position of the WMD over the late seventeenth and early eighteenth centuries is the only plausible calendar position the WMD would match SHCal20. Finally, the results were consistent with the original model when the D_Sequence model was calibrated using alternative outlier detection methods (see Appendix D.1.6). Therefore, the WMD for MA1P204 is interpreted as accurate and is included in the local and regional scale analyses.

Table 6.5.5. Sequence (SSimple) result for MA1P204.

Wk Number	Sample Code	^{14}C Age (BP)	Outlier analysis (posterior/prior)	Convergence
52746	23_MA1P204 (30–34)	293 ± 21	5/5	99
52747	24_MA1P204 (40–44)	260 ± 21	5/5	99
52748	25_MA1P204 (71–75)	210 ± 24	5/5	99
52749	26_MA1P204 (86–90)	173 ± 23	5/5	99
52750	27_MA1P204 (96–99)	162 ± 21	5/5	99
Felling Date Results				
Median cal. Age (AD)	HPD 68%		HPD 95%	A_{comb} (An)
1711 ± 8	AD 1706–1718		AD 1701–1724	135 (32)

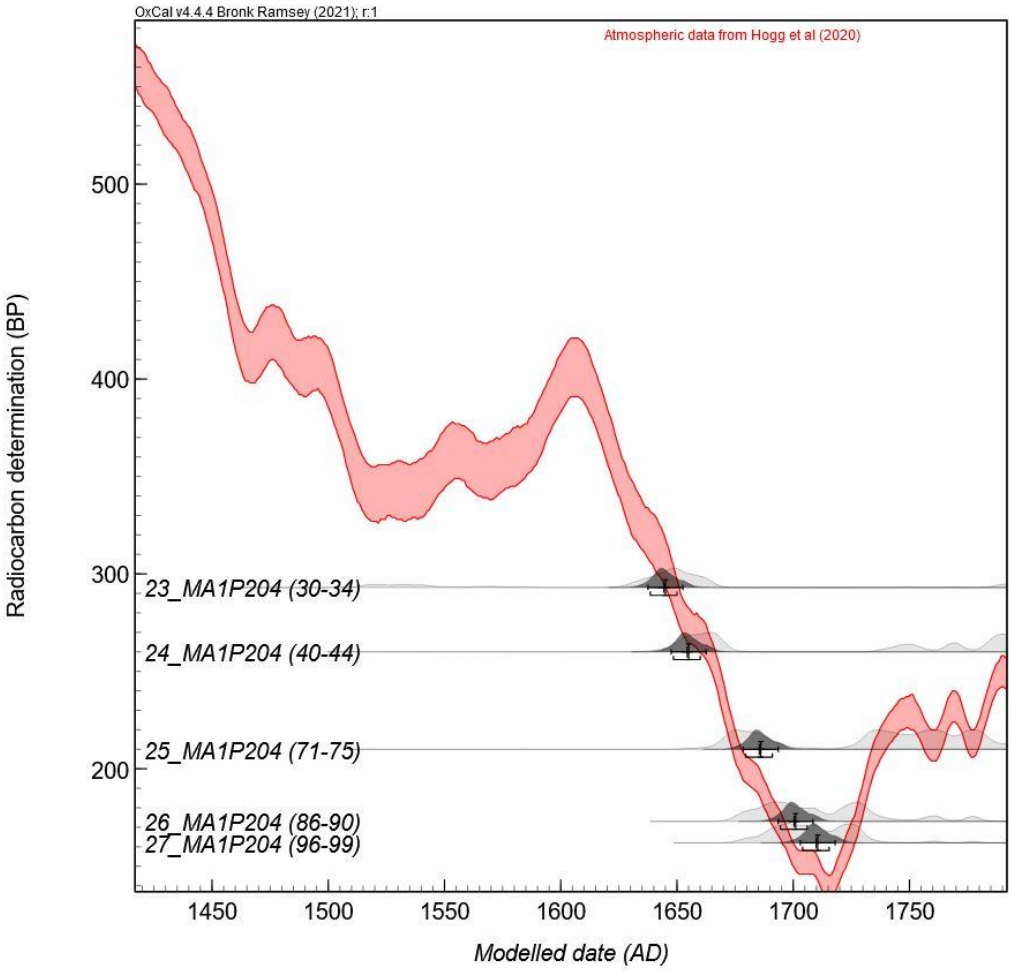

Figure 6.5.9. OxCal generated curve plot of the D_Sequence model for MA1P204.

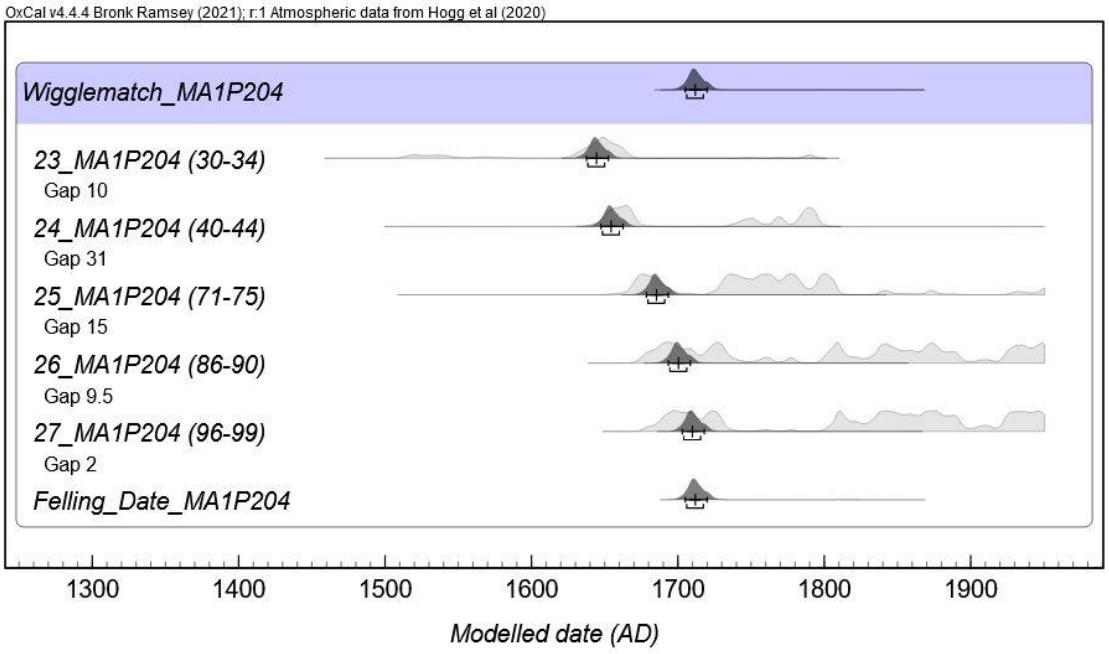

Figure 6.5.10. OxCal generated multiplot graph of the D_Sequence model for MA1P204.

6.5.6 MA1P208

The D_Sequence model for MA1P208 comprises five AMS ^{14}C dates, separated by known calendar intervals, spread across the 73-year tree-ring growth sequence (Table 6.5.6). The Felling Date of MA1P208 has a median calibrated age of AD 1817 ± 18, with a modelled date range between AD 1803–1831 (95% HPD). The analysis detected no outliers and convergence values remained universally high (99%). When reviewing the curve plot of the analysis, the WMD generally reflects the shape of SHCal20 (Figure 6.5.11), with the ^{14}C age order reversals observed between the second and third samples in the D_Sequence model suggesting the calendar placement over the calibration plateau within the late eighteenth century is correct. However, the first sample within the D_Sequence, 28_MA1P208 (1–5), is offset from the calibration curve. When reviewing the posterior and likelihood distributions for the last four samples within the WMD, it is clear that they correlate well with their respective calendar positions (Figure 6.5.12), indicating that errors in the reconciled ring count are unlikely to be the cause of the offset. This observation is confirmed by the results of the tree-ring analysis, which identified minimal inconsistencies. As the WMD is positioned over a calibration plateau, it is plausible that ^{14}C age discrepancies exist between SHCal20 and this specific ^{14}C date. When the D_Sequence model was calibrated using the RScaled outlier model (see Appendix D.1.7), the analysis results improved slightly, and sample 28_MA1P208 (1–5) is still not flagged as an outlier. This result, in association with the universally high convergence values generated by OxCal (99%), indicates that the overall model is robust. Therefore, the original WMD is interpreted as accurate and is included in the local and regional scale analyses.

Table 6.5.6. Sequence (SSimple) result for MA1P208.

Wk Number	Sample Code	^{14}C Age (BP)	Outlier analysis (posterior/prior)	Convergence
52751	28_MA1P208 (1–5)	259 ± 21	5/5	99
52752	29_MA1P208 (17–21)	216 ± 26	5/5	99
52753	30_MA1P208 (36–40)	230 ± 21	5/5	99
52754	31_MA1P208 (51–55)	210 ± 24	5/5	99
52755	32_MA1P208 (69–73)	169 ± 22	5/5	99
Felling Date Results				
Median cal. Age (AD)	HPD 68%	HPD 95%	A_{comb} (An)	
1817 ± 18	AD 1813–1824	AD 1803–1831	75 (32)	

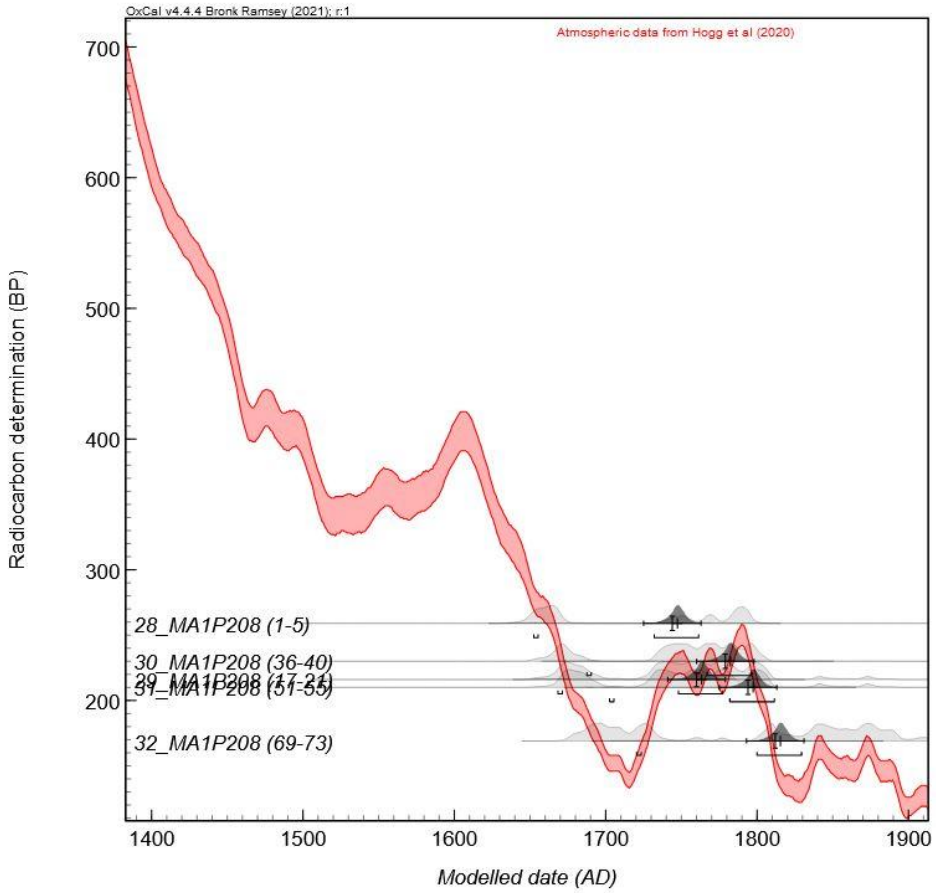

Figure 6.5.11. OxCal generated curve plot of the D_Sequence model for MA1P208.

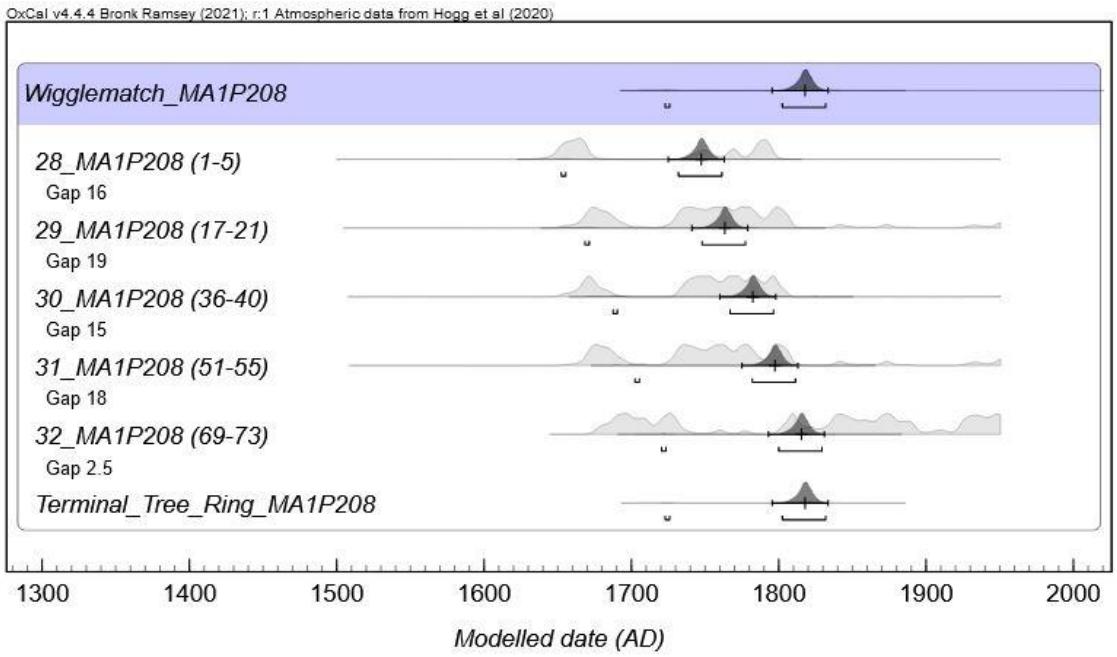

Figure 6.5.12. OxCal generated multiplot graph of the D_Sequence model for MA1P208.

6.5.7 Summary

Table 6.5.7 summarises the WMD results for the post-assemblage (six posts) sampled from MA1. The results indicate multiple potential palisade construction events at MA1, suggesting that the site was first occupied as a defended place in the early 1700s. Furthermore, possible palisade repair or redevelopment activity in the middle 1700s and early 1800s is identified. These events indicate that multiple phases of palisade construction occurred over the occupation span at MA1, which will be investigated further in the local scale analysis. As discussed above, the Felling Dates for MA1P57 and MA1P192 are interpreted as inaccurate due to suspected ring count errors and poor precision. Therefore, they are removed from consideration for further analysis. As a result, only the remaining four WMDs are included in the local and regional analyses presented in Chapter 12.

Table 6.5.7. Summary of WMD results from MA1.

Post ID	Felling Date Results			Local/Regional Analyses
	Median cal. Age	68% HPD	95% HPD	
MA1P53	1754 ± 3	AD 1751–1757	AD 1749–1761	Included
MA1P57*	1719 ± 7	AD 1715–1723	AD 1707–1745	Excluded (Inaccurate)
MA1P190	1803 ± 5	AD 1800–1807	AD 1796–1811	Included
MA1P192*	1714 ± 54	AD 1697–1863	AD 1693–1865	Excluded (Imprecise)
MA1P204	1711 ± 8	AD 1706–1718	AD 1701–1724	Included
MA1P208	1817 ± 18	AD 1813–1824	AD 1803–1831	Included

*Note. *Indicates WMD that are interpreted as inaccurate or imprecise.*

Chapter 7. Lake Mangakaware 2 (MA2)

7.1 Archaeological Excavations at MA2 (S15/18)

Excavations at MA2 were conducted over two short field seasons, focusing on two specific areas highlighted by desktop research and site visits as the most likely to retain evidence of palisading. Area A was excavated in May 2020, focusing on the palisade defences identified on the southeastern lake edge. Area B was excavated in August 2020, concentrating on an area where the palisade defences identified in Area A turned inland (Figure 7.1.1). Excavations aimed to determine the extent of the preserved palisade defences in each area, with the objective of sampling posts from each defensive row for WMD purposes.

Figure 7.1.1. Areas of investigation at MA2.

7.1.1 Excavation in Area A (MA2)

Investigations in Area A focused on an area of approximately 25 x 5 m along the eastern lake edge of MA2, close to an area previously excavated by Doug Pick (1968) (Area E) (Figure 7.1.2). Once the overlying vegetation was cleared to the north and south of the modern jetty (Figure 7.1.3 and Figure 7.1.4), a minimum of two rows of palisades were identified along the lake edge. Three *in situ* posts were also readily visible in the lake (Figure 7.1.5). In total, 28 posts were recorded within this area. Given the visibility of the palisade defences, large-scale exploratory excavation areas were deemed unnecessary, and efforts focused on the visible posts within the cleared area (EA1–7).

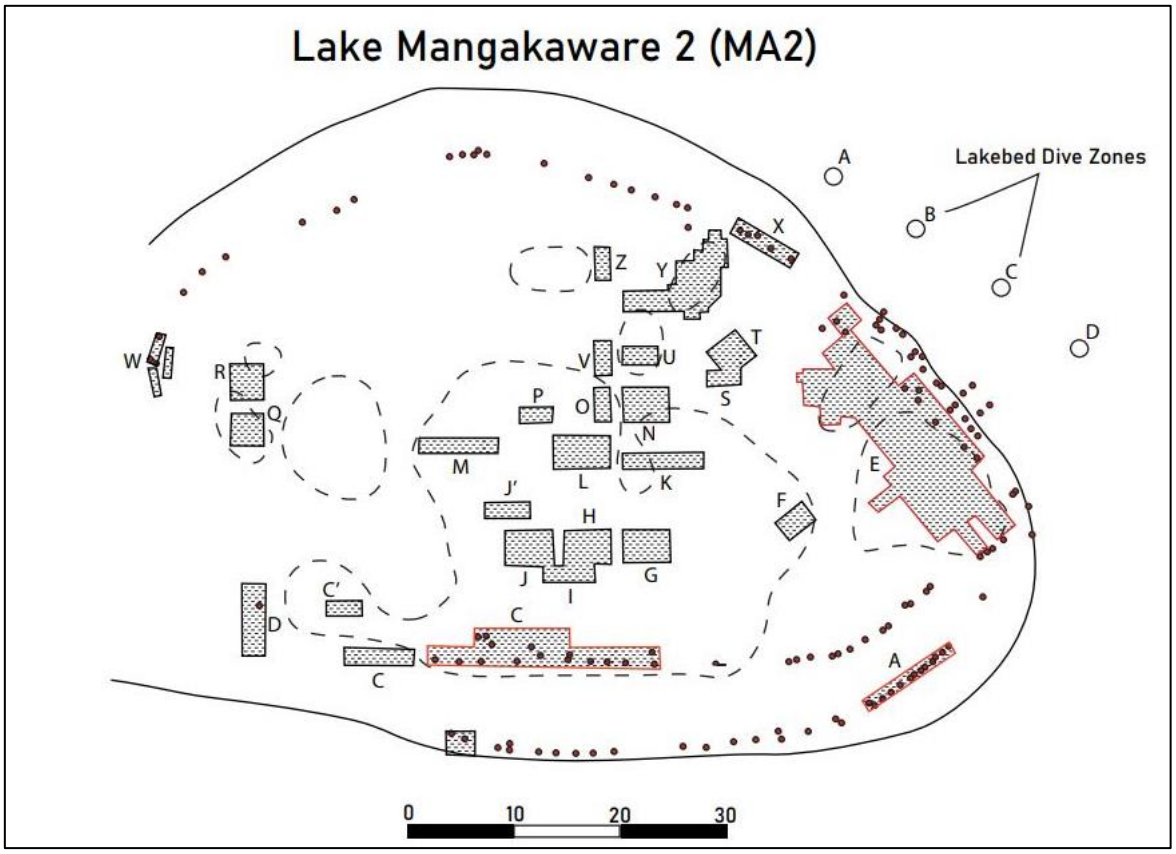

Figure 7.1.2. Digitised plan drawing from the 1969 excavations at MA2[28, 29].

[28] This map has been recreated from the original plan drawing with permission from Peter Bellwood (1978a).
[29] Trenches A, C and E are highlighted (red) as they are referred to in text.

Figure 7.1.3. Rowan McBride recording the locations of palisade posts along the lake edge of MA2[30].

Figure 7.1.4. The northern end of Area A cleared of vegetation.

[30] This photograph was taken by Zac McIvor and is used with permission.

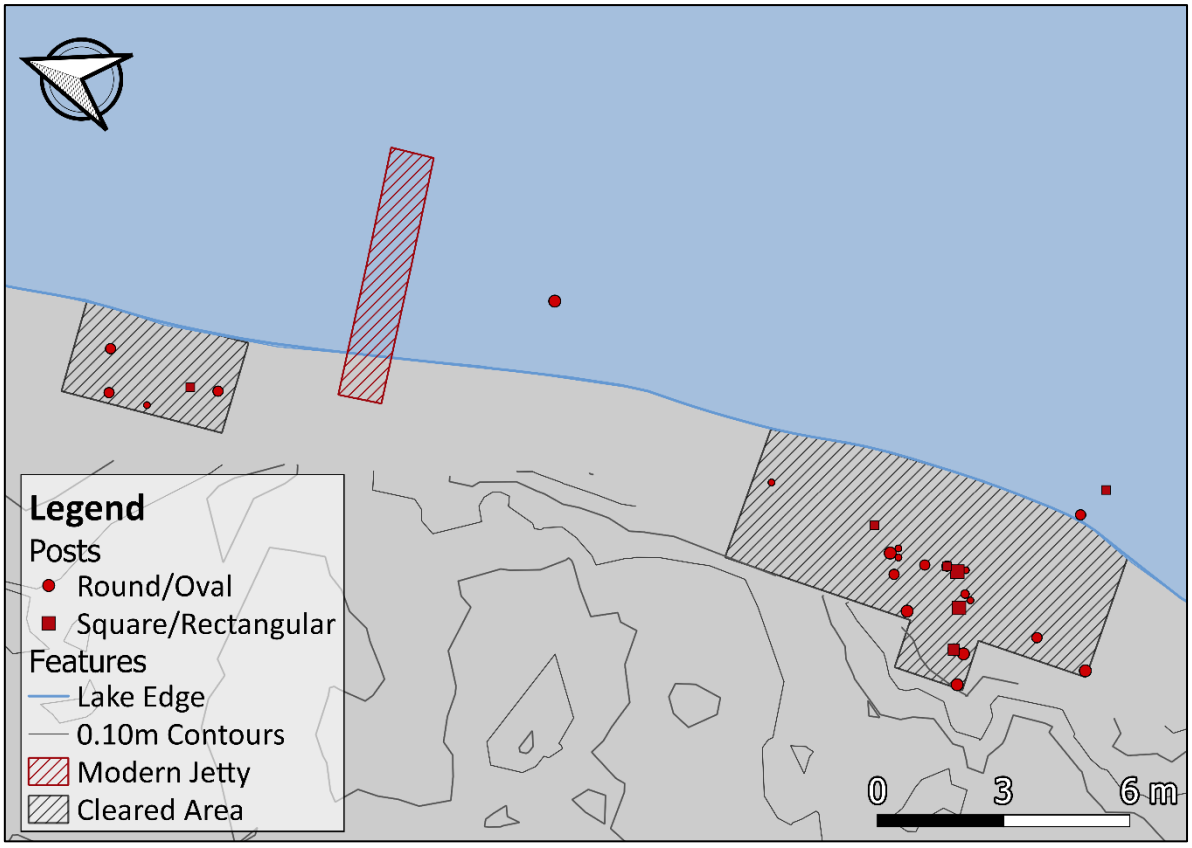

Figure 7.1.5. A plan drawing of Area A at MA2.

EA1 encompassed an area of 3 x 3 m, positioned at the southern end of the identified palisade alignments. This excavation area covered a distinct 'corner' in the palisade defences, where the inner palisade rows turned inland (west) away from the lake edge (Figure 7.1.6). Twelve posts were recorded in EA1, encountered at a depth of <10 cm. Intercutting tree roots from the nearby willow tree limited visibility within EA1, pushing several palisades over through post-depositional processes (Figure 7.1.7). Fire-cracked rock (FCR) concentrations were observed in moderation across the entire excavation unit, along with occasional charcoal inclusions and wood chips (debitage from adze dressing). The remaining six excavation areas (EA2–7) were small squares positioned around posts to assess their suitability for extraction and sampling (Figure 7.1.8).

Figure 7.1.6. A mid-excavation photograph of EA1 (looking south).

Figure 7.1.7. A mid-excavation photograph of EA1 (looking west).

Figure 7.1.8. A partially extracted post (MA2P3) at MA2.

Nine posts were extracted in Area A (Figure 7.1.9), with the recorded data presented in Table 7.1.1. Two posts (MA2P5 and MA2P9) broke during extraction due to their poor condition, and two more (MA2P4 and MA2P13) were adzed dressed, making them unsuitable for sampling. The five remaining posts were sampled for analysis: MA2P1, MA2P2, MA2P7, MA2P14 and MA2P15. On average, these posts were embedded >2.5 m in the ground (2.66 m), with an average length of 2.74 m and an average diameter of 12.9 cm (e.g., Figure 7.1.11 and Figure 7.1.12). Two distinct taper types were recorded: four long and one short taper.

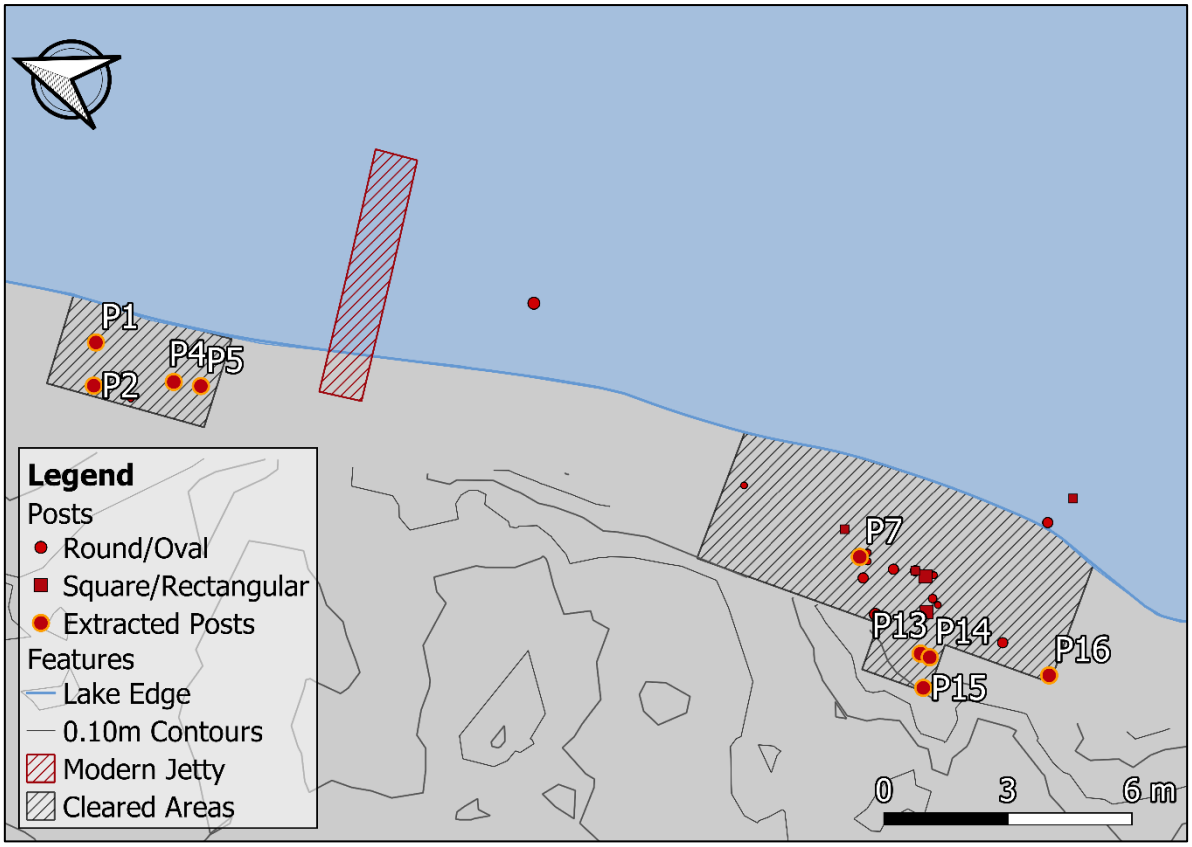

Figure 7.1.9. Plan drawing showing the locations of extracted posts at MA2.

Table 7.1.1. Recorded information for posts extracted from Area A at MA2.

Post ID	Cross Section Shape	Max Length (cm)	Diameter (cm)	Taper Shape	Condition	Sampled
MA2P1	Round	320	11.2	Long	Suitable for sampling	Yes
MA2P2	Round	210	11.3	Long	Suitable for sampling	Yes
MA2P4*	Square	-	-	-	Adzed	No
MA2P5*	Round	-	10.2	-	Severely degraded	No
MA2P7	Round	263	13.0	Long	Suitable for sampling	Yes
MA2P13*	Square	-	15.0	-	Adzed	No
MA2P14	Oval/Irregular	280	16.0	Short	Suitable for sampling	Yes
MA2P15	Oval	300	14.5	Long	Suitable for sampling	Yes
MA2P16*	Round	-	11.9	-	Severely degraded	No

*Note. * indicates posts that were extracted but were not suitable for sampling.*

Figure 7.1.10. Photograph of Alan Hogg (left), Rowan McBride (centre) and Warren Gumbley (right) standing next to a post extracted from Area A at MA2[31].

[31] This photograph was taken by Zac McIvor and is used with permission.

Figure 7.1.11. Post-extraction photograph of MA2P7.

Figure 7.1.12. Post-extraction photograph of MA2P2.

7.1.2 Excavation in Area B (MA2)

Investigations in Area B covered approximately 15 m x 10 m (Figure 7.1.13 and Figure 7.1.14). This area is approximately in the location of Trench A (see Bellwood, 1978a), excavated by Doug Pick (1968) and the Waikato Museum Archaeological Society in the late 1960s. Two distinct palisade rows were previously recorded in this area (see Section 4.1.1.2). Given this information, two exploratory trenches were initially excavated to establish the location of these palisade rows (EA37 and EA40). Once located, a further six excavation areas were positioned along the length of the *in situ* palisade rows (EA38–44).

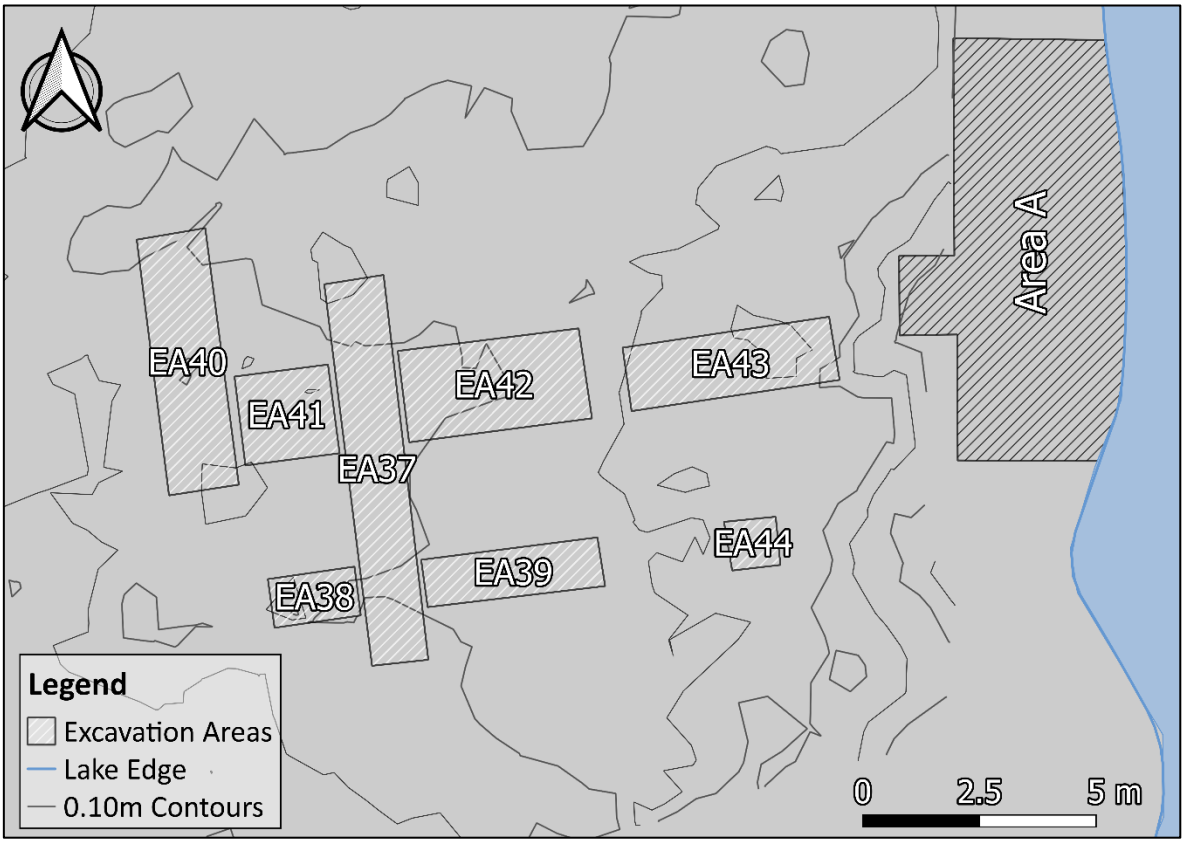

Figure 7.1.13. Plan drawing of the excavation areas in Area B at MA2.

Figure 7.1.14. Excavation areas in Area B at MA2 (looking southeast).

EA37 covered an area of 12 x 1 m (Figure 7.1.15), initially excavated to a depth of 15 cm. Charcoal deposits and mussel periostracum (*E. menziesii*) were present in moderation across the length of EA37, along with coarse charcoal deposits associated with a clay lens observable in the western baulk. The deposits of mussel periostracum and charcoal (located at the base of EA37: 15 cm deep) became gradually less dense from north to south (from the pā mound towards the outer palisade defences) and were observed *in situ* outside the outer palisade row. This observation suggests that this cultural layer predates the palisade defences, indicating that the site was occupied before the defences were constructed. FCR concentrations were isolated to the northern end of the excavation area, located next to a depression (possible oven feature) and several artefacts. The depression in the northwestern corner of EA37 was lined with a silty clay-like sediment (similar to the sediment lens found in EA44) and was full of FCR. The artefacts identified adjacent to the depression include a pumice bowl, a complete patu, an obsidian core and small concentrations of red ochre (Figure 7.1.16).

Figure 7.1.15. Mid-excavation photograph of EA37 (looking southwest)

Figure 7.1.16. Mid-excavation photograph of the northern end of EA37.

One post was recorded at the southern end of EA37 (MA2P147). This post was used to determine the location of the outer palisade alignment (furthest away from the pā mound), with EA38 and EA39 excavated along the length of the alignment (Figure 7.1.17). Once excavated, EA37–39 were connected, and the excavation area was extended below the water table. Two small electric pumps removed the water from the excavation areas, exposing the palisade row and the soil profile (Figure 7.1.18). Eight posts were identified in EA37–39, representing the extent of surviving posts identified in the outer palisade row.

Figure 7.1.17. Warren Gumbley (left), Alan Hogg (centre) and Zac McIvor (right) examine the palisade row identified within EA37–39.

Similarly, the inner palisade row was identified using three excavation areas that were later extended and joined (EA41–43). The inner palisade row comprised six posts, including one in EA41 that was separated by a gap of approximately 9 m from the remaining five in EA43. EA42 was devoid of posts. However, a pumice/sand lens was recorded within this excavation area (Figure 7.1.19).

Figure 7.1.18. Rowan McBride (left), Warren Gumbley (centre) and Alan Hogg (right) use water pumps to excavate below the water table.

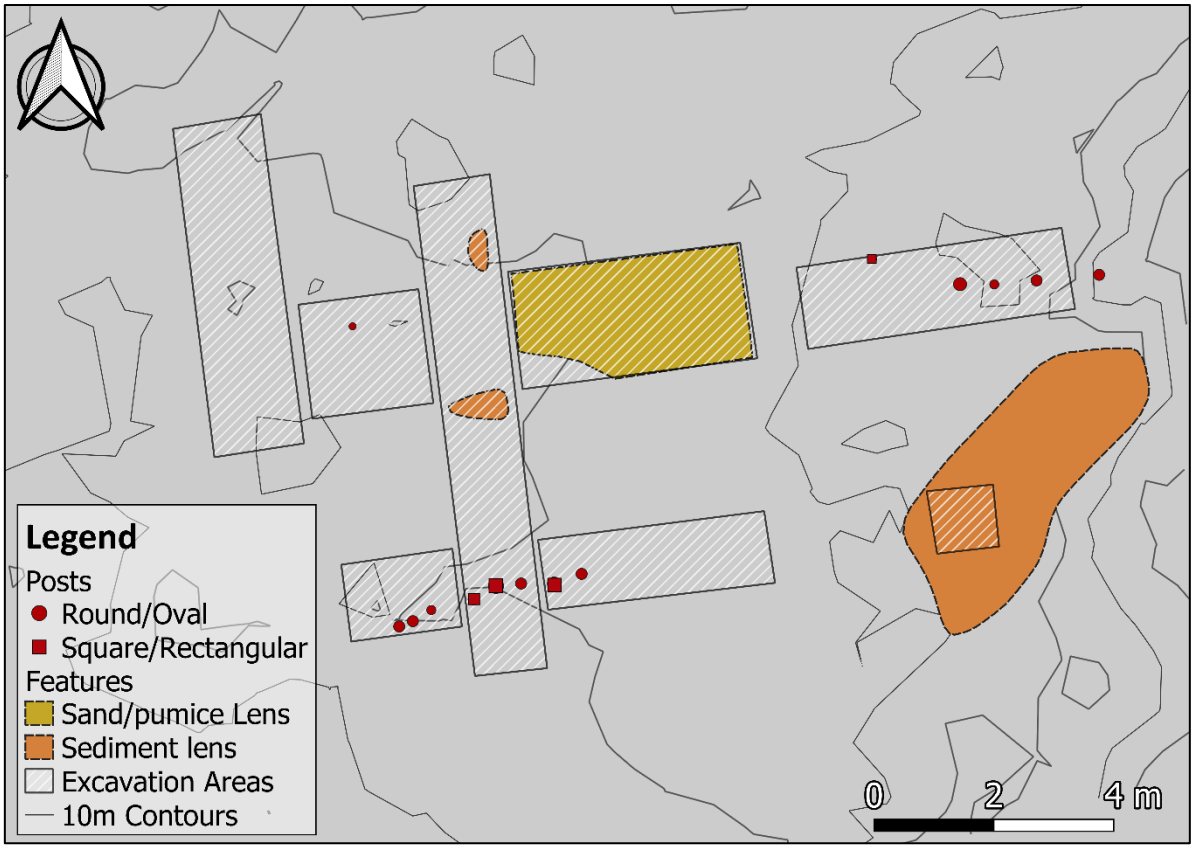

Figure 7.1.19. Plan drawing of Area B at MA2.

The section profile of EA42 comprises three distinct layers that typify the stratigraphy of MA2 (Figure 7.1.20). Layer 1 (L1) consists of a dark black organic soil matrix and root zone. Directly below L1 is a lens of fine pumice sand/gravel, closely associated with moderate concentrations of mussel periostracum (*E. menziesii*). This pumice sand/gravel lens was most prominent in the eastern end of EA42, where the lens dips below the water table. The butt of an adze was located on the surface of this lens, as well as moderate concentrations of FCR. The pumice sand/gravel lens appears stratigraphically below the clay-like sediment lenses identified in EA37 and EA44. Below this pumice lens, the soil matrix changes composition to reddish-black sediment (2.5YR 5/1) in Layer 2 (L2). The observation that the lens dips below the water table suggests that the water level during the occupation was significantly lower than in modern times.

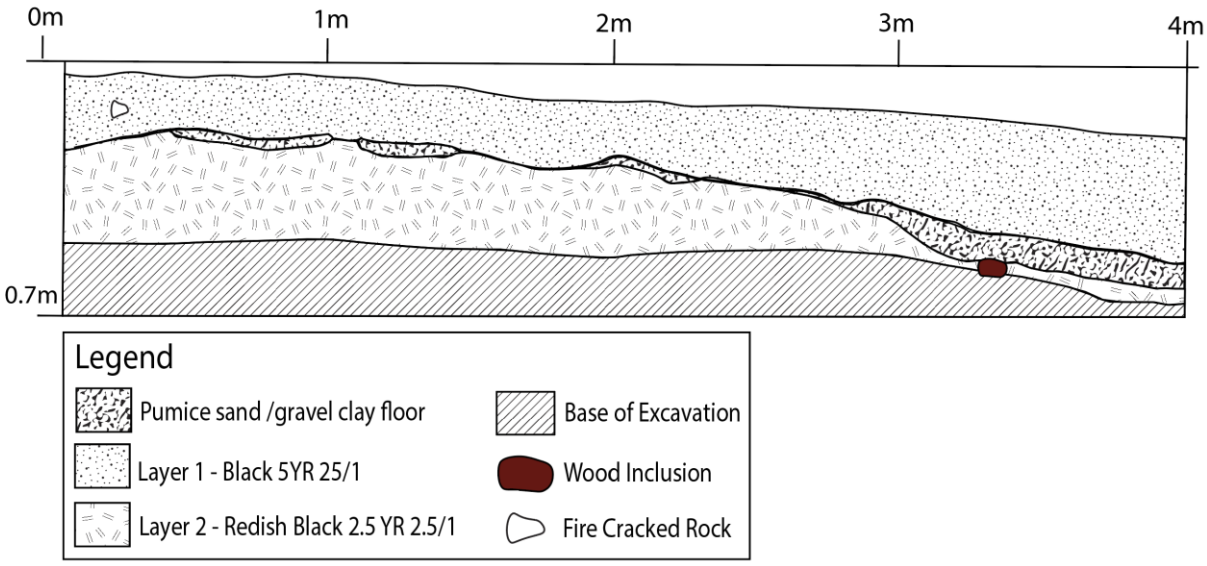

Figure 7.1.20. Section drawing of the northern baulk in EA42.

Finally, EA44 was the last and smallest excavation area investigated, initially excavated to ascertain if the surviving outer palisade row extended east towards the lake edge. EA44 was excavated to a depth of 20 cm, with excavations identifying a distinct lens of silty clay-like sediment up to 12 cm thick. The clay-like lens covered the full extent of EA44, and a soil auger was used to ascertain the lens size, covering an area of approximately 3 m x 2m (Figure 7.1.19). This clay lens is comparable to the two clay lenses identified in EA37.

Ten posts were extracted from Area B (Figure 7.1.21 and Table 7.1.2). In contrast to the findings of Pick (1968), charring was only identified on the distal end of one post (MA2P147). Interestingly, this post exhibited burning along its entire length, including the distal tapered end. This observation indicates either the intentional burning of the post or the reuse of a previously burnt post. Also of note is the unique shape of MA2P154 (Figure 7.1.24), which exhibits a unique curved shape, starkly contrasting to the long and straight shape typifying the other posts extracted from Area B (Figure 7.1.25). Finally, two taper types were recorded, including five long and five short tapers (Figure 7.1.22 and Figure 7.1.23).

Figure 7.1.21. Location of posts extracted from Area B at MA2.

Table 7.1.2. Recorded information for the posts extracted from Area B at MA2.

Post ID	Cross section	Max length (cm)	Diameter (cm)	Taper shape	Condition	Sampled
MA2P147*	Rectangle	190	17.5	Long	Adzed (completely)	No
MA2P149	Oval	213	12.6	Long	Suitable for sampling	Yes
MA2P152	Round	152	16.0	Short	Suitable for sampling	Yes
MA2P153	Round	252	10.0	Short	Suitable for sampling	Yes
MA2P154	Round	227	12.2	Short	Suitable for sampling	Yes
MA2P155	Round	89	11.3	Short	Suitable for sampling	Yes
MA2P156	Oval	121	10.5	Long	Suitable for sampling	Yes
MA2P157	Round	108	11.9	Long	Suitable for sampling	Yes
MA2P158*	Oval	124	12.8	Long	Severely degraded	No
MA2P161	Round	203	12.2	Short	Suitable for sampling	Yes

*Note. *Indicates posts that were extracted but not sampled.*

Figure 7.1.22. Post-extraction photograph showing the long taper of MA2P149.

Figure 7.1.23. Post-extraction photograph showing the short taper of MA2P153.

Figure 7.1.24. Post-extraction photograph of MA2P154.

Figure 7.1.25. Post-extraction photograph of MA2P153.

7.2 Species Identification

Thin-section microscopy of the post assemblage (13 posts) sampled from MA2 identified five tree species: pukatea (*L. novae-zelandiae*), kahikatea (*D. dacrydioides*), titoki (*A. excelsus*), tawa (*B. tawa*) and pigeonwood (*H. arborea*) (Table 7.2.1). All five species can be found in the lowland forests of the North and South Islands and are typically species found in swampy environments surrounding the rivers and lakes of the Middle Waikato Basin. All five species meet the requirements for tree-ring analysis (see Table 5.3.2).

Table 7.2.1. Tree species identified in the post assemblage from MA2.

Post ID	Common Name	Scientific Name
MA2P1	tawa	*Beilschmiedia tawa*
MA2P2	titoki	*Alectryon excelsus*
MA2P7	pukatea	*Laurelia novae-zelandiae*
MA2P14	pukatea	*Laurelia novae-zelandiae*
MA2P15	pukatea	*Laurelia novae-zelandiae*
MA2P149	kahikatea	*Dacrycarpus dacrydioides*
MA2P152	pukatea	*Laurelia novae-zelandiae*
MA2P153	pukatea	*Laurelia novae-zelandiae*
MA2P154	pukatea	*Laurelia novae-zelandiae*
MA2P155	tawa	*Beilschmiedia tawa*
MA2P156	titoki	*Alectryon excelsus*
MA2P157	pigeonwood	*Hedycarya arborea*
MA2P161	pukatea	*Laurelia novae-zelandiae*

7.3 Condition Assessment

All prepared post samples were inspected under a low-powered light microscope to assess their condition and suitability for tree-ring analysis, ring-block sampling, and AMS radiocarbon dating (see Section 5.5 and Table 7.3.1). Following this assessment, six samples were determined to be of poor quality and were excluded from further analysis: MA2P1, MA2P2, MA2P7, MA2P155, MA2P156 and MA2P157. The characteristics of the remaining seven samples are discussed in Section 7.4 below.

Table 7.3.1. MA2 sample condition assessment

Post ID	Poor preservation	Charring present	Scaring present	Dark staining	Growth anomalies	Passed
MA2P1*	☑	☐	☐	☑	☑	No
MA2P2*	☑	☐	☐	☑	☑	No
MA2P7*	☑	☐	☐	☑	☑	No
MA2P14	☐	☐	☐	☐	☑	Yes
MA2P15	☐	☐	☐	☑	☑	Yes
MA2P149	☐	☐	☐	☐	☑	Yes
MA2P152	☐	☐	☐	☐	☑	Yes
MA2P153	☐	☐	☐	☐	☑	Yes
MA2P154	☐	☐	☐	☑	☑	Yes
MA2P155*	☑	☐	☑	☐	☑	No
MA2P156*	☑	☐	☐	☐	☑	No
MA2P157*	☑	☐	☐	☐	☑	No
MA2P161	☐	☐	☐	☐	☑	Yes

*Note. * indicates samples excluded from tree-ring analysis due to unsuitable characteristics.*

7.4 Tree-ring Analysis Results (MA2)

The reconciled ring count information for each post sample in the MA2 assemblage is summarised in Table 7.4.1 (see Section 5.6 for method). The reconciled ring counts represent the most accurate information attainable for these samples, with any persistent inconsistencies discussed further in Section 7.5.

Table 7.4.1. A summary of the reconciled ring count information for the posts sampled from MA2.

Post ID	Species ID	Reconciled ring count	Diameter (cm)
MA2P14	Pukatea (*L. novae-zelandiae)*	81	16
MA2P15	Pukatea (*L. novae-zelandiae)*	61	14.5
MA2P149	Pukatea (*L. novae-zelandiae)*	51	12.6
MA2P152	Tawa (*B. tawa)*	73	16
MA2P153	Pukatea (*L. novae-zelandiae)*	52	10
MA2P154	Pigeonwood (*H. arborea)*	63	12.2
MA2P161	Pukatea (*L. novae-zelandiae)*	84	12.2

7.4.1 MA2P14 (pukatea, *L. novae-zelandiae*)

MA2P14 presented an irregular cross-section, relatively central pith location, and non-concentric tree-ring growth pattern. Several tree-ring growth anomalies were identified throughout the growth sequence, including areas of tree-ring suppression, false rings, and locally absent rings (Figure 7.4.1). Tree-ring suppression was most prevalent in the outer half of the growth sequence, with the outermost (youngest) tree rings being particularly narrow. Additionally, a small portion of the sample's circumference did not retain evidence of the terminal tree ring due to damage. Minor differences in the ring counts were identified between the three measured radii (Table 7.4.2), with the reconciliation of these three radii resulting in a final ring count of 81. Five ring-block samples were collected at semi-regular intervals throughout the tree-ring growth sequence (Table 7.4.3). However, larger ring gaps were necessary between specific samples due to narrow annual growth periods. Finally, no sampling errors were identified across any ring-block samples, and all five contained five tree rings.

Figure 7.4.1. Digital scan of MA2P14.

Table 7.4.2. Ring count information for MA2P14.

Ring counts	Track A	Track B	Track C	Reconciled
MA2P14	80	81	81	81

Table 7.4.3. Ring-block sampling information for MA2P14.

Wk number	Sample code	First ring	Middle ring	Last ring	# of rings in block	Ring gap to next sample
52098	33_MA2P14 (1–5)	1	3	5	5	16
52359	34_MA2P14 (17–21)	17	19	21	5	24
52099	35_MA2P14 (41–45)	41	43	45	5	29
52360	36_MA2P14 (70–74)	70	72	74	5	7
52100	37_MA2P14 (77–81)	77	79	81	5	2.5

7.4.2 MA2P15 (pukatea, *L. novae-zelandiae*)

MA2P15 presented an oval cross-sectional shape, relatively central pith location and non-concentric ring pattern (Figure 7.4.2). A large scar was also present close to the central pith region, resulting in tree-ring suppression and locally absent rings early in the tree-ring growth sequence. Only minor ring count differences were identified between the three measured radii, resulting in a reconciled final ring count of 61 (Table 7.4.4). Five ring-block samples were collected regularly throughout the tree-ring growth sequence (Table 7.4.5). No sampling errors were identified across any ring-block samples; all five contained five tree rings.

Figure 7.4.2. Digital scan of MA2P15.

Table 7.4.4. Ring count information for MA2P15.

Ring counts	Track A	Track B	Track C	Reconciled
MA2P15	61	54	58	61

Table 7.4.5. Ring-block sampling information for MA2P15.

Wk number	Sample code	First ring	Middle ring	Last ring	# of rings in block	Ring gap to next sample
52107	38_MA2P15 (1–5)	1	3	5	5	11
52361	39_MA2P15 (12–16)	12	14	16	5	15
52108	40_MA2P15 (27–31)	27	29	31	5	19
52362	41_MA2P15 (46–50)	46	48	50	5	11
52109	42_MA2P15 (57–61)	57	59	61	5	2.5

7.4.3 MA2P149 (pukatea, *L. novae-zelandiae*)

MA2P149 presented a round cross-section, central pith location, and concentric tree-ring growth sequence (Figure 7.4.3). Minor tree-ring suppression, false rings and dark staining were observed early in the tree-ring growth sequence, and poorly defined tree-ring boundaries affected the second half of the growth sequence (rings 25–51). Minor differences in the ring counts of the three measured radii were observed, with Track C having four locally absent rings (Table 7.4.6). Reconciliation of these three ring counts resulted in a final ring count of 51, with five ring-block samples collected regularly throughout the tree-ring growth sequence (Table 7.4.7). Sampling errors associated with the poorly defined tree-ring boundaries resulted in two ring-block samples that contained fewer than five tree rings.

Figure 7.4.3. Digital scan of MA2P149.

Table 7.4.6. Ring count information for MA2P149.

Ring counts	Track A	Track B	Track C	Reconciled
MA2P149	51	51	47	51

Table 7.4.7. Ring-block sampling information for MA2P149.

Wk number	Sample code	First ring	Middle ring	Last ring	# of rings in block	Ring gap to next sample
52229	43_MA2P149 (1–5)	1	3	5	5	11.5
52230*	44_MA2P149 (13–16)	13	14.5	16	4	13.5
52231*	45_MA2P149 (27–29)	27	28	29	3	11
52232	46_MA2P149 (37–41)	37	39	41	5	10
52233	47_MA2P149 (47–51)	47	49	51	5	2.5

*Note. *Sampling errors resulted in 44_MA2P149 (13–16) and 45_MA2P149 (27–29) not containing five rings.*

7.4.4 MA2P152 (tawa, *D. dacrydioides*)

MA2P152 presented a round cross-section, central pith location, and concentric tree-ring growth pattern (Figure 7.4.4). The tree-ring growth sequence was affected by several growth anomalies, including multiple areas of tree-ring suppression, locally absent rings, and poor tree-ring clarity. Despite these characteristics, tree-ring count and measurement analysis identified only minor differences between the three measured radii (Table 7.4.8). Reconciliation of these three radii resulted in a reconciled ring count of 73, with five ring-block samples collected at semi-regular intervals throughout the tree-ring growth sequence. (Table 7.4.9). No sampling errors were identified across any ring-block samples; all five contained five tree rings.

Figure 7.4.4. Digital scan of MA2P152.

Table 7.4.8. Ring count information for MA2P152.

Ring counts	Track A	Track B	Track C	Reconciled
MA2P152	70	71	72	73

Table 7.4.9. Ring-block sampling information for MA2P152.

Wk number	Sample code	First ring	Middle ring	Last ring	# of rings in block	Ring gap to next sample
52239	53_MA2P152 (1–5)	1	3	5	5	11
52240	54_MA2P152 (12–16)	12	14	16	5	14
52241	55_MA2P152 (26–30)	26	28	30	5	21
52242	56_MA2P152 (47–51)	47	49	51	5	22
52243	57_MA2P152 (69–73)	69	71	73	5	2.5

7.4.5 MA2P153 (pukatea, *L. novae-zelandiae*)

MA2P153 presented a round cross-sectional shape, off-centre pith location and concentric tree-ring growth pattern (Figure 7.4.5). A minor episode of tree-ring suppression and dark staining affected the tree-ring growth sequence. Tree-ring count and measurement analysis identified only minor differences between the three measured radii (Table 7.4.10), resulting in a reconciled final ring count of 52. Five ring-block samples were collected at regular intervals throughout the tree-ring growth sequence (Table 7.4.11). No sampling errors were identified across any ring-block samples; all five contained five tree rings.

Figure 7.4.5. Digital scan of MA2P153

Table 7.4.10. Ring count information for MA2P153

Ring counts	Track A	Track B	Track C	Reconciled
MA2P153	52	51	50	52

Table 7.4.11. Ring-block sampling information for MA2P153.

Wk number	Sample code	First ring	Middle ring	Last ring	# of rings in block	Ring gap to next sample
52244	59_MA2P153 (1–5)	1	3	5	5	14
52245	60_MA2P153 (15–19)	15	17	19	5	10
52246	61_MA2P153 (25–29)	25	27	29	5	11
52247	62_MA2P153 (36–40)	36	38	40	5	12
52248	63_MA2P153 (48–52)	48	50	52	5	2.5

7.4.6 MA2P154 (pigeonwood, *H. arborea*)

MA2P154 presented a round cross-sectional shape, off-centre pith location, and concentric tree-ring growth pattern (Figure 7.4.6). Minor areas of tree-ring suppression were present early and late in the tree-ring growth sequence, resulting in poor tree-ring clarity. These

characteristics made it difficult to determine the tree-ring boundaries in certain areas, particularly in the outer part of the tree-ring growth sequence. Additionally, dark staining was present across a large proportion of the growth sequence, further affecting the tree-ring clarity. Despite these issues, tree-ring count and measurement analysis identified only minor differences between the measured radii (Table 7.4.12). Reconciliation of the three radii resulted in a final ring count of 63, with five ring-block samples collected at regular intervals throughout the tree-ring growth sequence (Table 7.4.13). No sampling errors were identified across any ring-block samples; all five contained five tree rings.

Figure 7.4.6. Digital scan of MA2P154.

Table 7.4.12. Ring count information for MA2P154.

Ring counts	Track A	Track B	Track C	Reconciled
MA2P154	62	61	53	63

Table 7.4.13. Ring-block sampling information for MA2P154

Wk number	Sample code	First ring	Middle ring	Last ring	# of rings in block	Ring gap to next sample
52234	48_MA2P154 (1–5)	1	3	5	5	14
52235	49_MA2P154 (15–19)	15	17	19	5	14
52236	50_MA2P154 (29–33)	29	31	33	5	15
52237	51_MA2P154 (44–48)	44	46	48	5	15
52238	52_MA2P154 (59–63)	59	61	63	5	2.5

7.4.7 MA2P161 (pukatea, *L. novae-zelandiae*)

MA2P161 presented a round cross-sectional shape, a central pith location, and a concentric tree-ring growth pattern (Figure 7.4.7). Episodes of tree-ring suppression, locally absent rings and narrow tree rings were present throughout the growth sequence. Additionally, dark staining was present across a large proportion of the growth sequence, limiting tree-ring clarity in some areas. A small scar was also recorded, affecting a limited portion of the tree-ring growth sequence. Tree ring count and measurement analysis identified only minor differences between the measured tracks (Table 7.4.14), resulting in a reconciled final ring count of 84. Five ring-block samples were collected at regular intervals throughout the tree-ring growth sequence (Table 7.4.15). No sampling errors were identified across any ring-block samples; all five contained five tree rings.

Figure 7.4.7. Digital scan of MA2P161.

Table 7.4.14. Ring count information for MA2P161.

Ring counts	Track A	Track B	Track C	Reconciled
MA2P161	83	81	80	84

Table 7.4.15. Ring-block sampling information for MA2P161.

Wk number	Sample code	First ring	Middle ring	Last ring	# of rings in block	Ring gap to next sample
52249	64_MA2P161 (1–5)	1	3	5	5	19
52250	65_MA2P161 (20–24)	20	22	24	5	19
52251	66_MA2P161 (39–43)	39	41	43	5	19
52252	67_MA2P161 (58–62)	58	60	62	5	22
52253	68_MA2P161 (80–84)	80	82	84	5	2.5

7.5 Wiggle-Match Dating Results

This section presents the WMD results for the post-assemblage (seven posts) sampled from MA2 (see Section 5.8.2 for method), and the full array of OxCal codes relating to each post analysed can be viewed in Appendix D.2. The interpretation of each WMD is discussed in detail below.

7.5.1 MA2P14

The D_Sequence model for MA2P14 comprises five AMS ^{14}C dates, separated by known calendar intervals, spread across the 81-year tree-ring growth sequence (Table 7.5.1). The Felling Date for MA2P14 has a median calibrated age of AD 1779 ± 10, with a modelled date range between AD 1766–1806 (95% HPD). While no outliers were detected during the analysis, the D_Sequence does not pass the A_{comb} (An) threshold, and several of the ^{14}C dates within the WMD are offset from SHCal20 (Figure 7.5.1). These offsets are reflected in the comparison between the posterior and likelihood distributions (Figure 7.5.2). Therefore, possible causes of these results must be considered.

Table 7.5.1. D_Sequence (SSimple) result for MA2P14.

Wk number	Sample code	^{14}C Age (BP)	Outlier analysis (Posterior/Prior)	Convergence
52098	33_MA2P14 (1–5)	202 ± 21	5/5	100
52359	34_MA2P14 (17–21)	161 ±21	5/5	100
52099	35_MA2P14 (41–45)	240 ± 21	5/5	100
52360	36_MA2P14 (70–74)	269 ± 21	5/5	100
52100	37_MA2P14 (77–81)	217 ± 21	5/5	100
Felling Date Results				
Median cal. Age (AD)	HPD 68%	HPD 95%	A_{comb} (An)	
1779 ± 10	AD 1770–1787	AD 1766–1806	31.5 (31.6)	

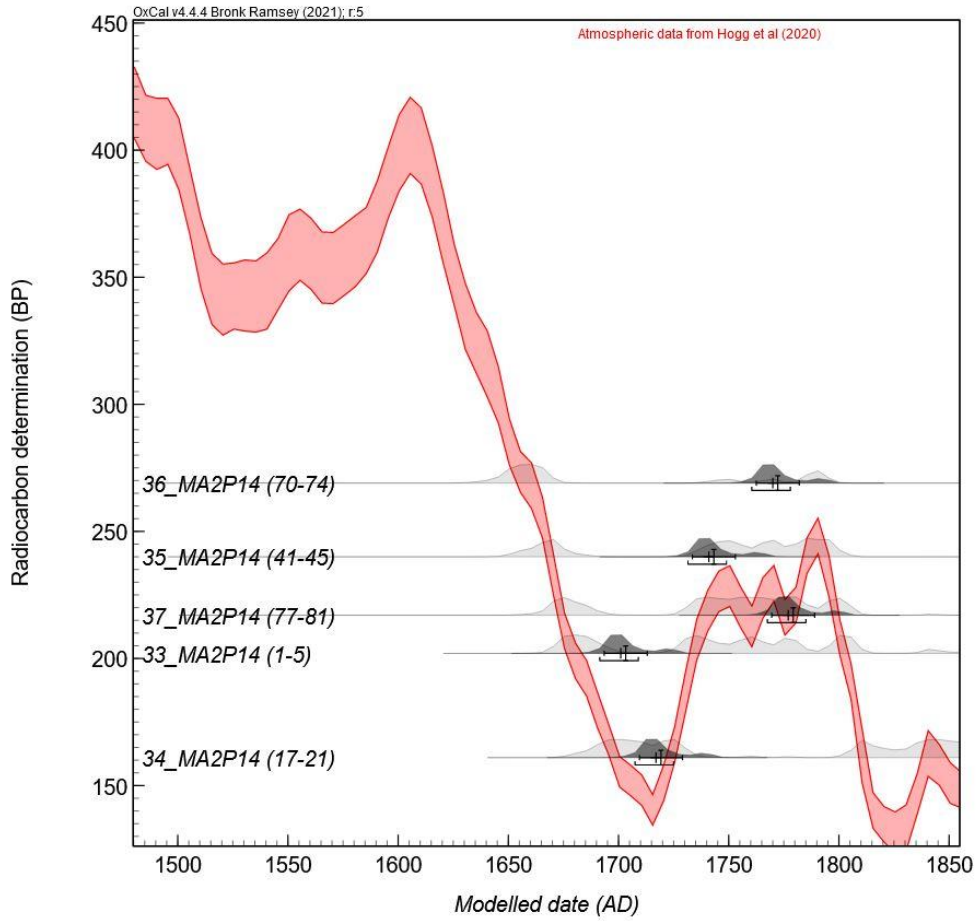

Figure 7.5.1. OxCal generated curve plot of the D_Sequence model for MA2P14.

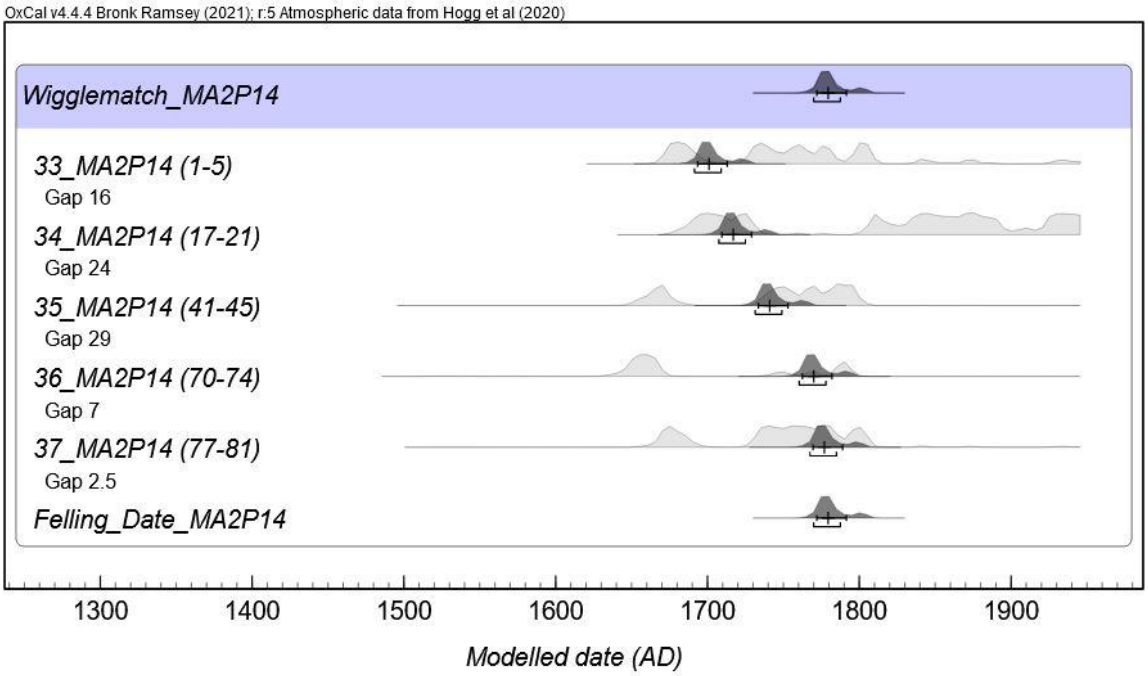

Figure 7.5.2. OxCal generated multiplot of the D_Sequence model for MA2P14.

Tree-ring analysis of MA2P14 identified episodes of tree-ring suppression throughout the tree-ring growth sequence. These episodes were most prevalent in the second half of the growth sequence, with the outermost (youngest) tree rings being particularly narrow. Possible errors in the reconciled ring count associated with these periods of growth would impact the calendar spacing between the ^{14}C dates. Given the ^{14}C age order reversals observed between the final three ^{14}C dates within the D_Sequence, the WMD must be positioned over the calibration plateau in the late eighteenth century. However, it is apparent that the final two samples within the D_Sequence model would more accurately reflect the shape of SHCal20 at the end of the calibration plateau. Additionally, the first two samples within the D_Sequence would produce a better fit on the negative slope of SHCal20 in the late seventeenth and early eighteenth centuries. Given these characteristics and the tree-ring analysis evidence, errors within the reconciled ring are suspected within the D_Sequence model. Therefore, the WMD for MA2P14 is deemed inaccurate and is excluded from the local and regional scale analyses.

7.5.2 MA2P15

The D_Sequence model for MA2P15 comprises five AMS ^{14}C dates, separated by known calendar intervals, spread across the 61-year tree-ring growth sequence (Table 7.5.2). The Felling Date for MA2P15 has a median calibrated age of AD 1805 ± 5, with a modelled date range between AD 1796–1811 (95% HPD). No outliers were identified during the analysis, and convergence values remained universally high (100%). When reviewing the curve plot of the analysis, the WMD generally reflects the shape of SHCal20 (Figure 7.5.3). Additionally, the ^{14}C age order reversals observed within the D_Sequence series indicate that a calendar placement over the calibration plateau in the late eighteenth century is correct. However, the ^{14}C date for sample 39_MA2P15 (12–16) is offset from SHCal20. As sample 39_MA2P15 (12–16) is not flagged as an outlier, is positioned over the calibration plateau, and the remaining four samples within the series accurately reflect the shape of SHCal20 (Figure 7.5.4), this offset is not considered a concern. This interpretation is supported by the results of the RScaled D_Sequence model for MA2P15, as they were consistent with the original D_Sequence results, with no outliers detected and universally good convergence and agreement, indicating that the model is robust (see Appendix D.2.2). Therefore, the original WMD is interpreted as accurate and is included in the local and regional scale analyses.

Table 7.5.2. D_Sequence (SSimple) result for MA2P15.

Wk number	Sample code	^{14}C Age (BP)	Outlier analysis (posterior/prior)	Convergence
52107	38_MA2P15 (1–5)	231 ± 22	5/5	99
52361	39_MA2P15 (12–16)	177 ± 22	5/5	99
52108	40_MA2P15 (27–31)	211 ± 21	5/5	99
52362	41_MA2P15 (46–50)	255 ± 21	5/5	99
52109	42_MA2P15 (57–61)	212 ± 21	5/5	99

Felling Date Results

Median cal. Age (AD)	HPD 68%	HPD 95%	A_{comb} (An)
1805 ± 5	AD 1802–1809	AD 1796 – 1811	87.7 (31.6)

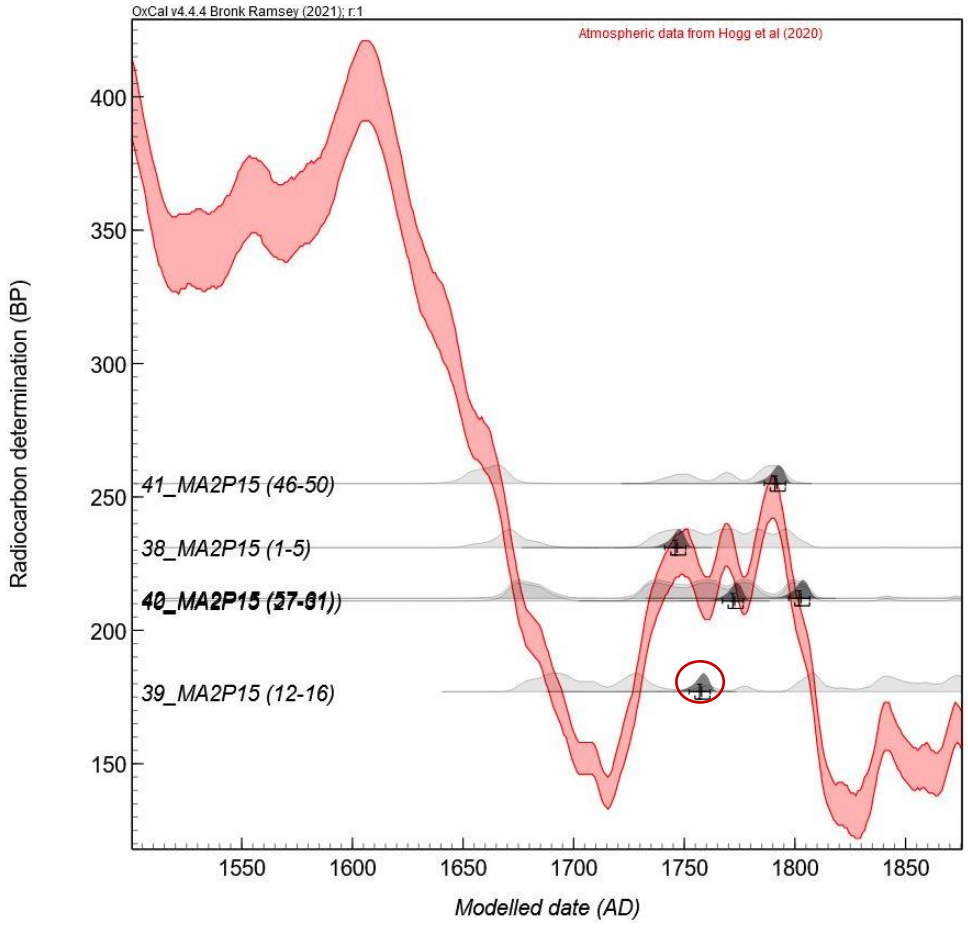

Figure 7.5.3. OxCal generated curve plot of the WMD for MA2P15[32].

[32] Red circle highlights a potential ^{14}C age offset of sample 39_MA2P15 (12–16). See Section 13.1.5 for discussion.

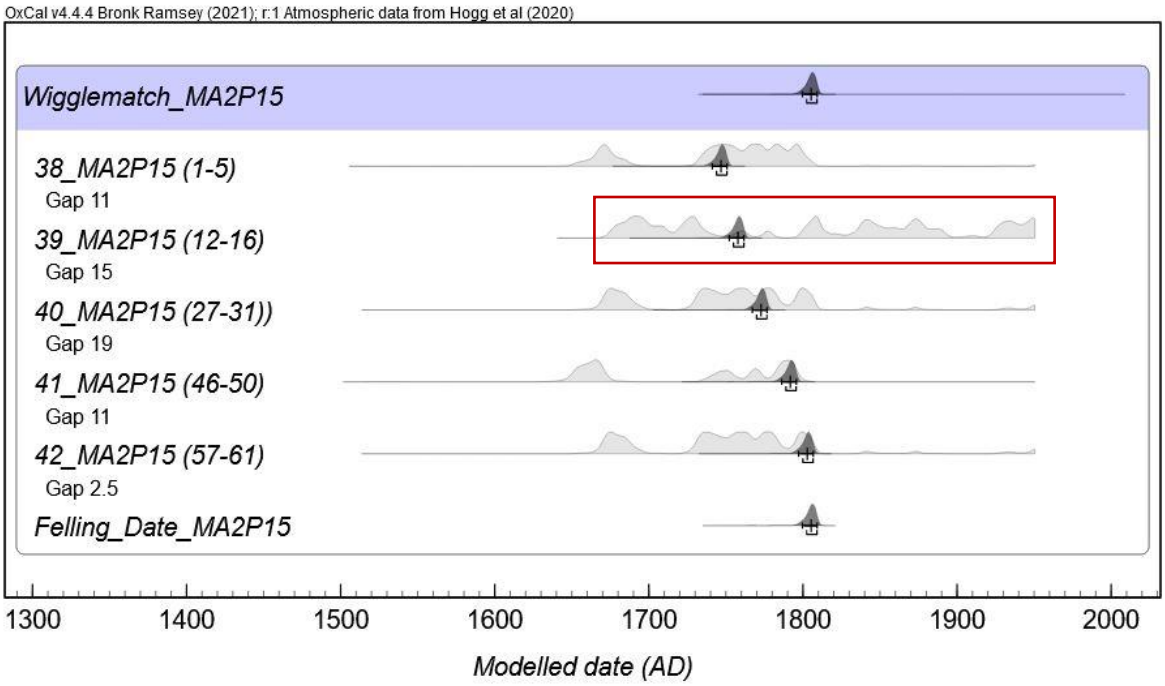

Figure 7.5.4. OxCal generated multiplot of the D_Sequence model for MA2P15[33].

7.5.3 MA2P149

The D_Sequence model for MA2P149 comprises five AMS ^{14}C dates, separated by known calendar intervals, spread across the 51-year tree-ring growth sequence (Table 7.5.3). The Felling Date of MA2P149 has a median calibrated age of AD 1802 ± 20, with a modelled date range between AD 1678–1810 (95% HPD). Outlier analysis identified and down-weighted one minor outlier: 46_MA2P149 (37–41), reflected in the comparison between the posterior and likelihood distributions (Figure 7.5.6). Additionally, the model did not pass the A_{comb} (An) threshold. When reviewing the curve plot of the analysis (Figure 7.5.5), the first four ^{14}C dates within the WMD are all offset from SHCal20. However, the ^{14}C age order reversals observed within the D_Sequence model indicate that a calendar placement over the calibration plateau in the late eighteenth century is correct, and the reduced precision of the Felling Date means the modelled date range likely encompasses when the parent tree was cut down. To explore this result further, the D_Sequence model calibrated using the RScaled outlier model (see Appendix D.2.3) was reviewed, with the analysis producing results consistent with the original Felling Date. Therefore, while the original (SSimple) Felling Date is considered accurate, the

[33] Red circle highlights a potential ^{14}C age offset of sample 39_MA2P15 (12–16). See Section 13.1.5 for discussion.

WMDs poor correlation with SHCal20 (multiple offset ^{14}C dates within the series) in association with the imprecision of the calendar date range limits its suitability for fine-grained chronological development. As the WMD for MA2P149 is the only post analysed from the outer palisade row, and cannot be compared to other Felling dates produced from this context, it is excluded from the local and regional scale analyses.

Table 7.5.3. D_Sequence (SSimple) result for MA2P149.

Wk number	Sample code	^{14}C Age (BP)	Outlier analysis (posterior/prior)	Convergence
52229	43_MA2P149 (1–5)	261 ± 21	5/5	99
52230	44_MA2P149 (13–16)	246 ± 21	5/5	99
52231	45_MA2P149 (27–29)	267 ± 21	6/5	99
52232	46_MA2P149 (37–41)	301 ± 22	5/5	99
52233	47_MA2P149 (47–51)	226 ± 21	5/5	99
Felling Date Results				
Median cal. Age (AD)	HPD 68%		HPD 95%	A_{comb} (An)
1802 ± 20	AD 1799–1806		AD 1678–1810	12.3 (31.6)

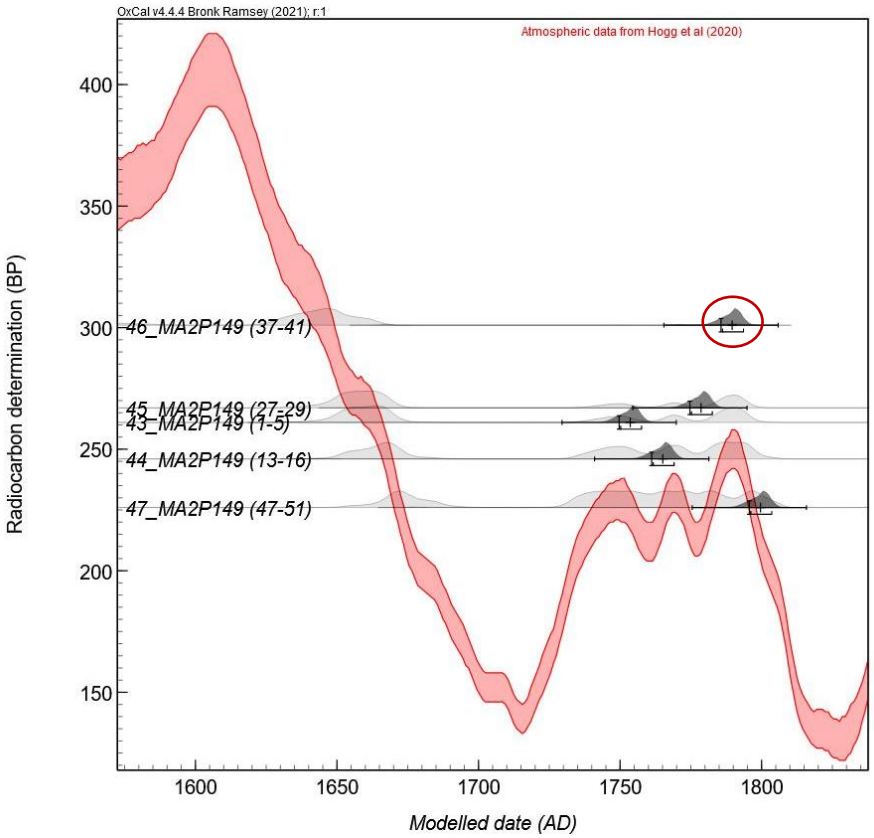

Figure 7.5.5. OxCal generated curve plot of the D_Sequence model for MA2P149[34].

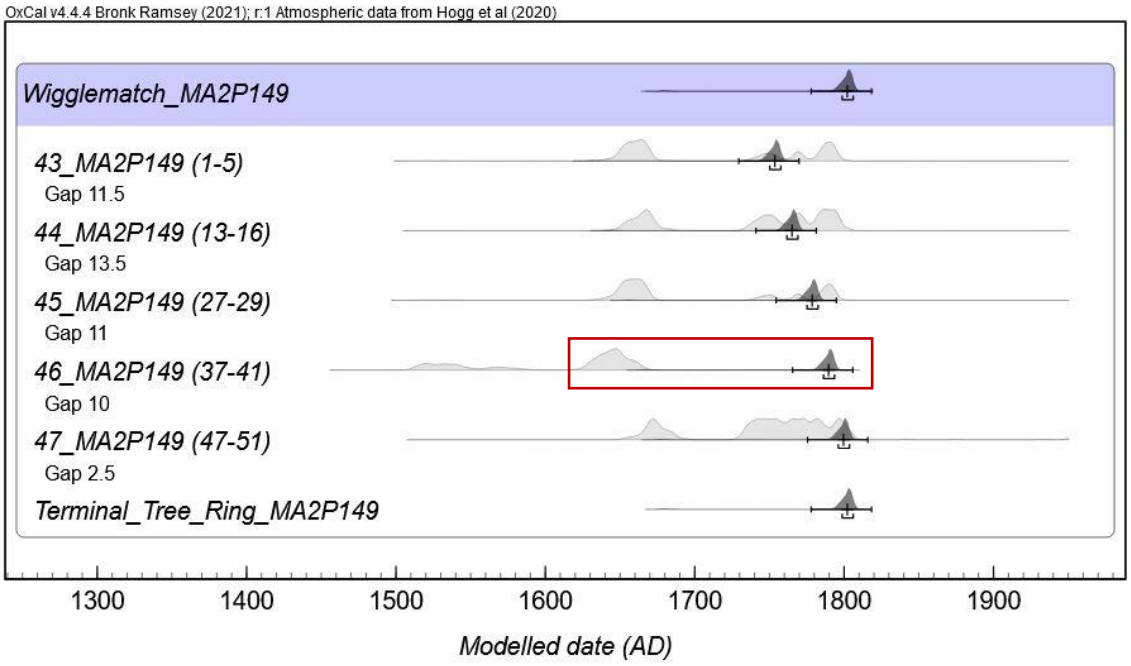

Figure 7.5.6. OxCal generated multiplot graph of the D_Sequence model for MA2P149[35].

[34] Red circle highlights the outlier detected during the analysis.
[35] Red box highlights the outlier detected during the analysis.

7.5.4 MA2P152

The D_Sequence model for MA2P152 comprises five AMS ^{14}C dates, separated by known calendar intervals, spread across the 73-year tree-ring growth sequence (Table 7.5.4). The Felling Date for MA2P152 has a median calibrated age of AD 1807 ± 5, with a modelled date range between AD 1796–1814 (95% HPD). Outlier analysis identified and down-weighted two minor outliers: 55_MA2P152 (26–30) and 57_MA2P152 (69–73). However, the model passed the A_{comb} (An) threshold. The WMD largely reflects the shape of SHCal20 (Figure 7.5.7). However, sample 55_MA2P152 (26–30) is offset over the calibration plateau, reflected in the comparison between the posterior and likelihood distributions (Figure 7.5.8). As no major outliers were identified, and the WMD is located over the calibration plateau, the offset of sample 55_MA2P152 (26–30) is considered unproblematic. The D_Sequence model calibrated using the RScaled outlier model (see Appendix D.2.4) confirms this interpretation, as the results were consistent with the original D_Sequence model. While sample 55_MA2P152 (26–30) is still flagged as a minor outlier, the posterior outlier probability for the terminal sample 57_MA2P152 (69–73) is improved to an acceptable level (5%). Therefore, the original WMD is interpreted as accurate and is included in the local and regional scale analyses.

Table 7.5.4. D_Sequence (SSimple) result for MA2P152.

Wk number	Sample code	^{14}C Age (BP)	Outlier analysis (posterior/prior)	Convergence
52239	53_MA2P152 (1–5)	221 ± 22	5/5	99
52240	54_MA2P152 (12–16)	234 ± 22	5/5	99
52241	55_MA2P152 (26–30)	273 ± 23	6/5	99
52242	56_MA2P152 (47–51)	250 ± 21	5/5	99
52243	57_MA2P152 (69–73)	222 ± 22	6/5	99
Felling Date Results				
Median cal. Age (AD)	HPD 68%		HPD 95%	A_{comb} (An)
1807 ± 5	AD 1800–1813		AD 1796–1814	38.7 (31.6)

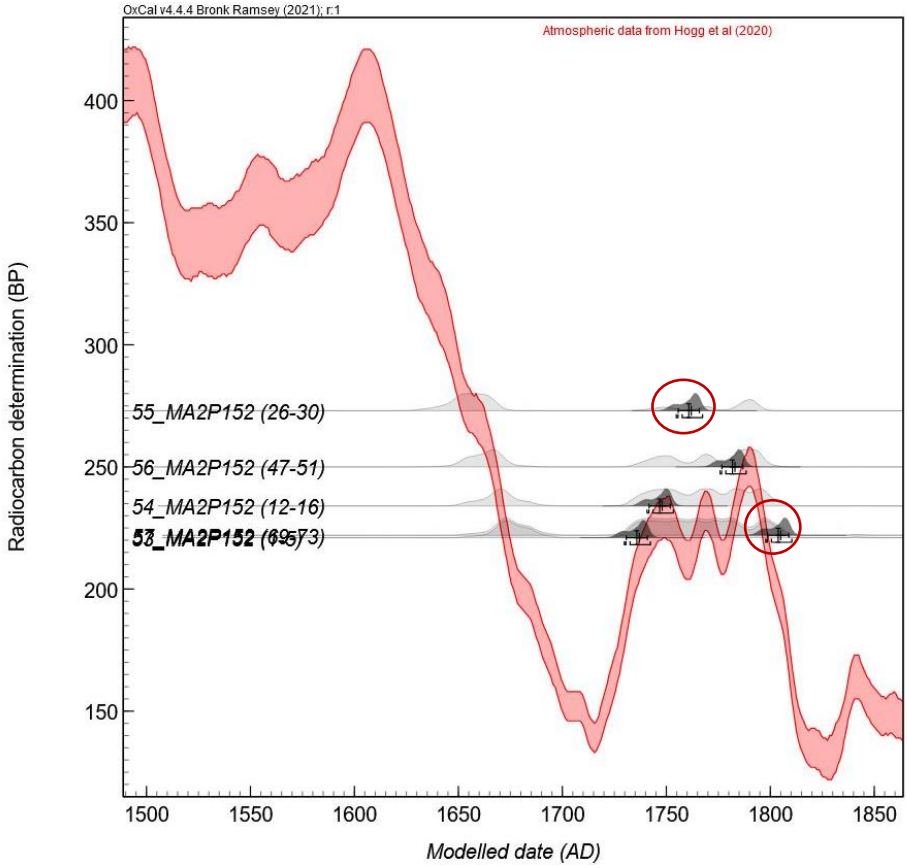

Figure 7.5.7. OxCal generated curve plot of the D_Sequence model for MA2P152[36].

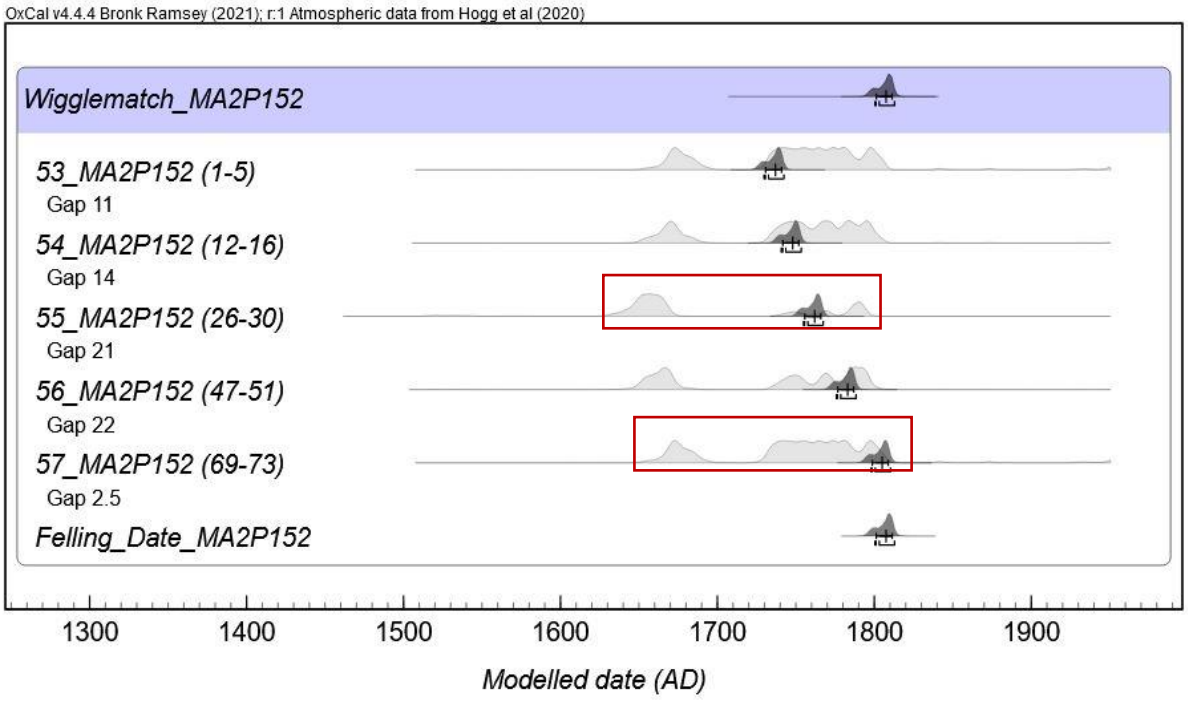

Figure 7.5.8 OxCal generated multiplot of the D_Sequence model for MA2P152[37].

[36] Red circles highlight the two outliers detected during the analysis.
[37] Red boxes highlight the two outliers detected during the analysis.

7.5.5 MA2P153

The D_Sequence model for MA2P153 comprises five AMS ^{14}C dates, separated by known calendar intervals, spread across the 52-year tree-ring growth sequence (Table 7.5.5). The Felling Date of MA2P153 has a median calibrated age of AD 1804 ± 20, with a modelled date range between AD 1686–1813 (95% HPD). One minor outlier was detected and down-weighted during the analysis: 61_MA2P153 (25–29). However, the D_Sequence model passes the A_{comb} (An) threshold. When reviewing the curve plot of the analysis (Figure 7.5.9), the first four ^{14}C dates in the WMD are offset from SHCal20. However, the WMD is situated over the calibration plateau in the late eighteenth century, and the ^{14}C age order reversals observed within the D_Sequence model suggest this calendar placement is correct. Notably, the terminal sample, 63_MA2P153 (48–52), is not offset and shows a good correlation between the posterior and likelihood distributions (Figure 7.5.10). Furthermore, when the D_Sequence was calibrated using the RScaled outlier model (see Appendix D.2.5), it produced results consistent with the original Felling Date, with no outliers detected. This result, in association with the observation that the Fell Date for MA2P153 correlates with the WMD results of other posts from within the same palisade row (MA2P15, MA2P152, MA2P154), indicates that the WMD is accurate. Therefore, the original WMD is included in the local and regional scale analyses.

Table 7.5.5. D_Sequence (SSimple) result for MA2P153.

Wk number	Sample code	^{14}C Age (BP)	Outlier analysis (posterior/prior)	Convergence
52244	59_MA2P153 (1–5)	241 ± 24	5/5	99
52245	60_MA2P153 (15–19)	259 ± 22	5/5	99
52246	61_MA2P153 (25–29)	261 ± 21	6/5	99
52247	62_MA2P153 (36–40)	273 ± 22	5/5	99
52248	63_MA2P153 (48–52)	206 ± 22	5/5	99
Felling Date Results				
Median cal. Age (AD)	HPD 68%		HPD 95%	A_{comb} (An)
1804 ± 20	AD 1801–1809		AD 1686–1813	50.5 (31.6)

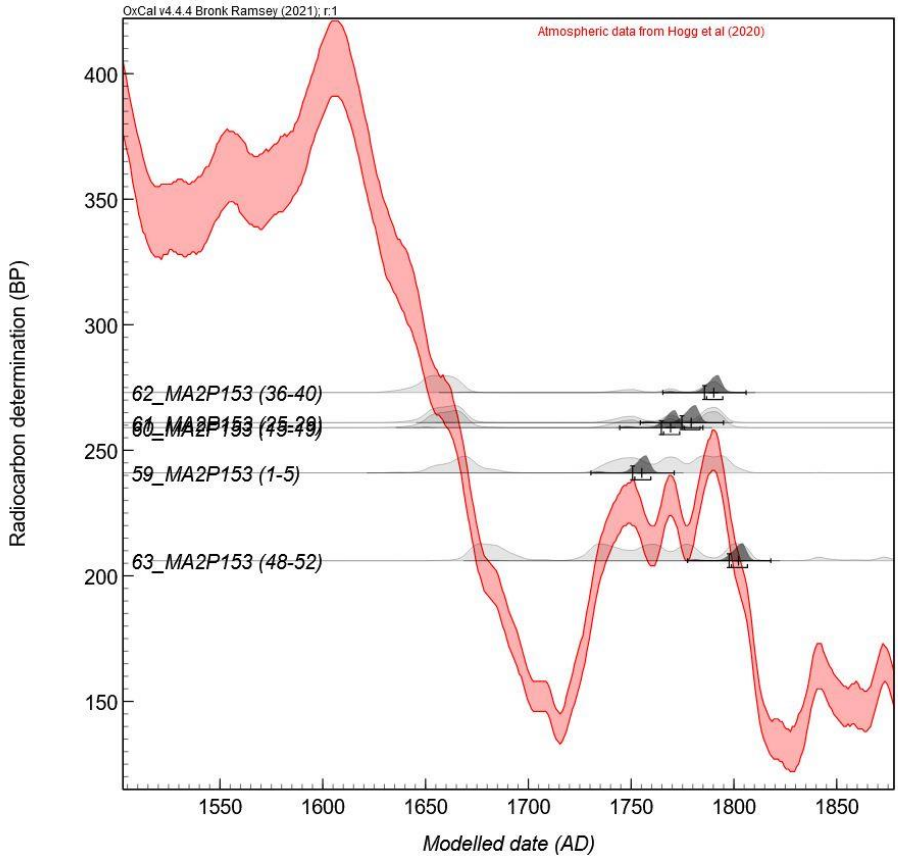

Figure 7.5.9. OxCal generated curve plot of the D_Sequence model for MA2P153.

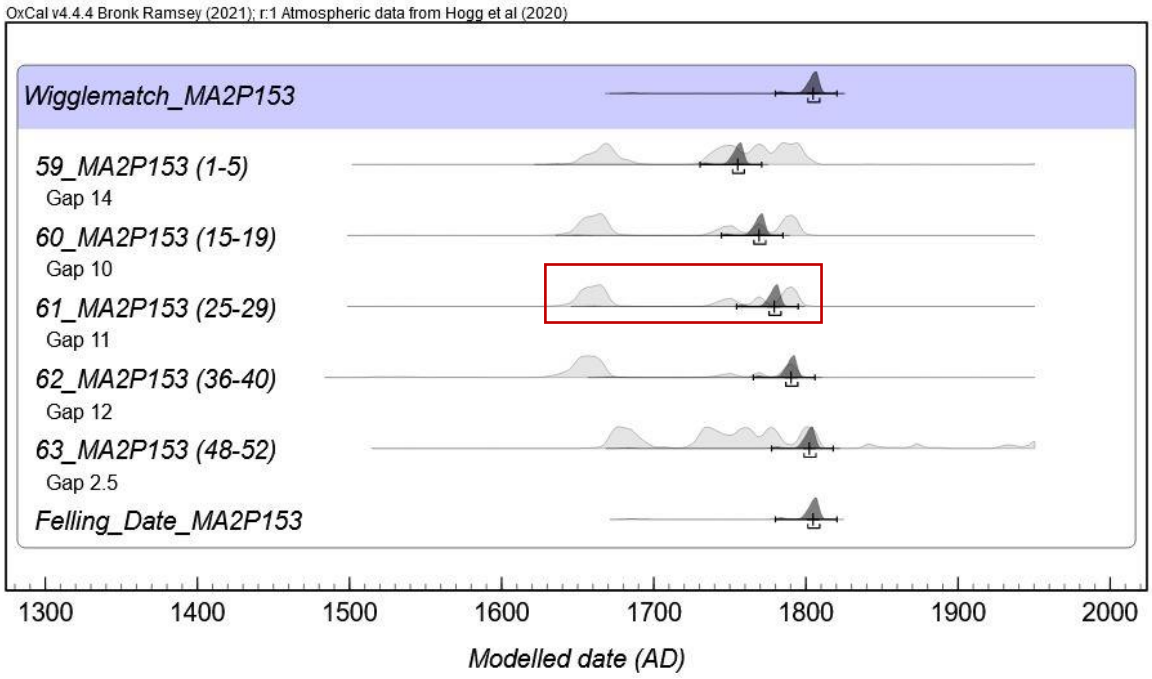

Figure 7.5.10. OxCal generated Multiplot of the D_Sequence model for MA2P153[38].

[38] Red box highlights the outlier detected during the analysis.

7.5.6 MA2P154

The D_Sequence model for MA2P154 comprises five AMS ^{14}C dates, separated by known calendar intervals, spread across the 63-year tree-ring growth sequence (Table 7.5.6). The Felling Date of MA2P154 has a median calibrated age of AD 1805 ± 3, with a modelled date range between AD 1799–1812 (95% HPD). No outliers were identified during the analysis, the model passed the A_{comb} (An) threshold, and convergence values remained universally high (99%). While the WMD generally reflects the shape of SHCal20, samples 48_MA2P154 (1–5) and 51_MA2P154 (44–48) are offset from SHCal20 (Figure 7.5.11). This result is reflected in the comparison between the posterior and likelihood distributions (Figure 7.5.12). However, the ^{14}C age order reversals observed between the ^{14}C dates within the D_Sequence indicate that the calendar position of the WMD over the late eighteenth century is correct. When the D_Sequence model was calibrated using the RScaled outlier model (see Appendix D.2.6), no outliers were identified, and the analysis produced a Felling Date consistent with the original WMD. Considering these results, the WMD for MA2P152 is interpreted as accurate and is included in the local and regional scale analyses.

Table 7.5.6. D_Sequence (SSimple) result for MA2P154.

Wk number	Sample code	^{14}C Age (BP)	Outlier analysis (posterior/prior)	Convergence
52234	48_MA2P154 (1–5)	264 ± 21	5/5	99
52235	49_MA2P154 (15–19)	230 ± 21	5/5	99
52236	50_MA2P154 (29–33)	234 ± 22	5/5	99
52237	51_MA2P154 (44–48)	267 ± 22	5/5	99
52238	52_MA2P154 (59–63)	219 ± 22	5/5	99

Felling Date Results			
Median cal. Age (AD)	HPD 68%	HPD 95%	A_{comb} (An)
1805 ± 3	AD 1802–1809	AD 1799–1812	63.7 (31.6)

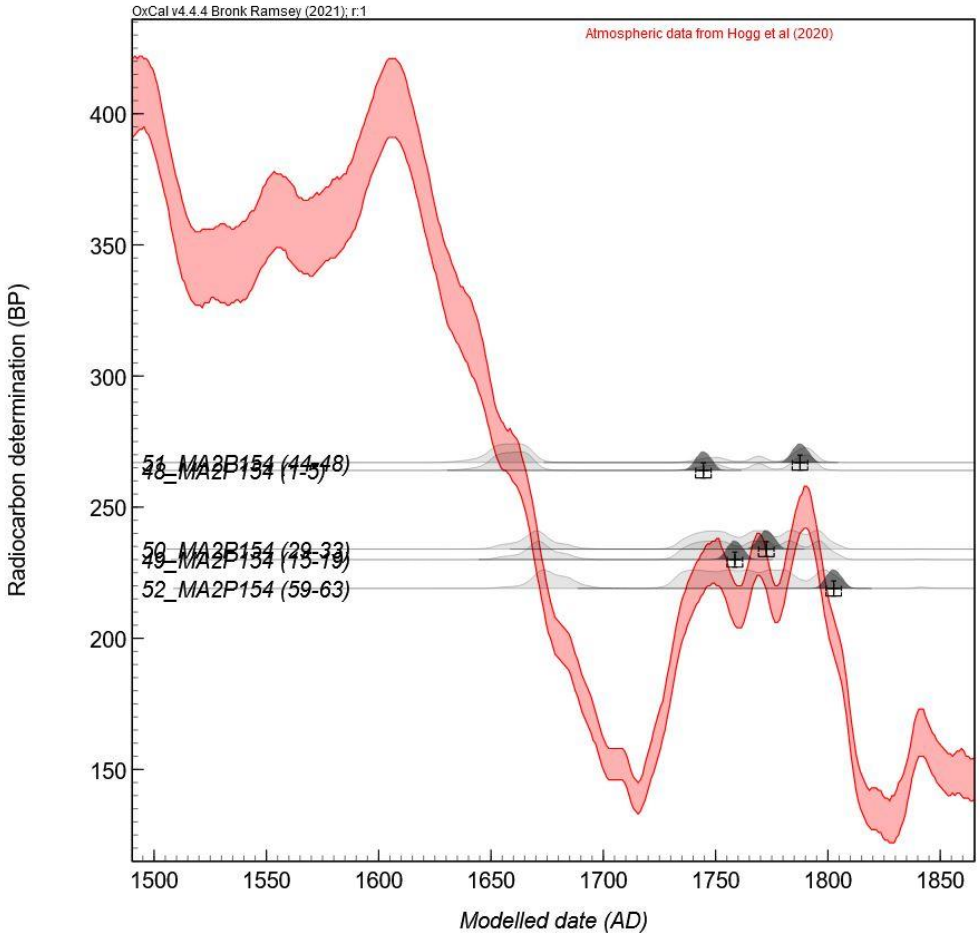

Figure 7.5.11. OxCal generated curve plot of the D_Sequence model for MA2P154.

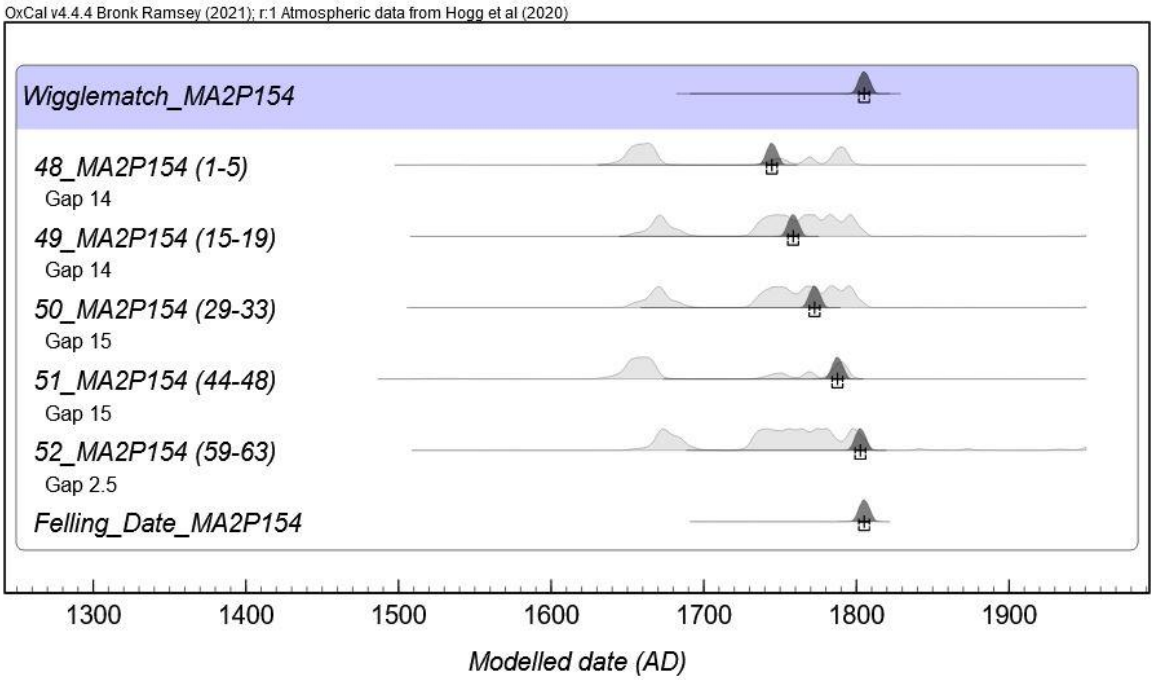

Figure 7.5.12. OxCal generated multiplot of the D_Sequence model for MA2P154.

7.5.7 MA2P161

The D_Sequence model for MA2P161 comprises five AMS ^{14}C dates, separated by known calendar intervals, spread across the 84-year tree-ring growth sequence (Table 7.5.7). The Felling Date of MA2P161 has a median calibrated age of AD 1736 ± 4, with a modelled date range between AD 1729–1746 (95% HPD). No outliers were identified during the analysis, the model passed the A_{comb} (An) threshold, and the convergence values remained universally high (99%). Additionally, the WMD generally matches the shape of SHCal20 (Figure 7.5.13), which is reflected in the comparison between the posterior and likelihood distributions (Figure 7.5.14). Providing further evidence that the WMD for MA2P161 is accurate, when the D_Sequence was calibrated using agreement index analysis (see Appendix D.2.7), the results of this analysis were consistent with the original WMD, reporting universally good agreement values (> 60). Therefore, the WMD for MA2P161 is interpreted as accurate and is included in the local and regional scale analyses.

Table 7.5.7. D_Sequence (SSimple) result for MA2P161.

Wk number	Sample code	^{14}C Age (BP)	Outlier analysis (posterior/prior)	Convergence
52249	64_MA2P161 (1–5)	307 ± 23	5/5	99
52250	65_MA2P161 (20–24)	213 ± 21	5/5	99
52251	66_MA2P161 (39–43)	198 ± 22	5/5	99
52252	67_MA2P161 (58–62)	158 ± 22	5/5	99
52253	68_MA2P161 (80–84)	225 ± 22	5/5	99

Felling Date Results			
Median cal. Age (AD)	HPD 68%	HPD 95%	A_{comb} (An)
1736 ± 4	AD 1732–1741	AD 1729–1746	83.9 (31.6)

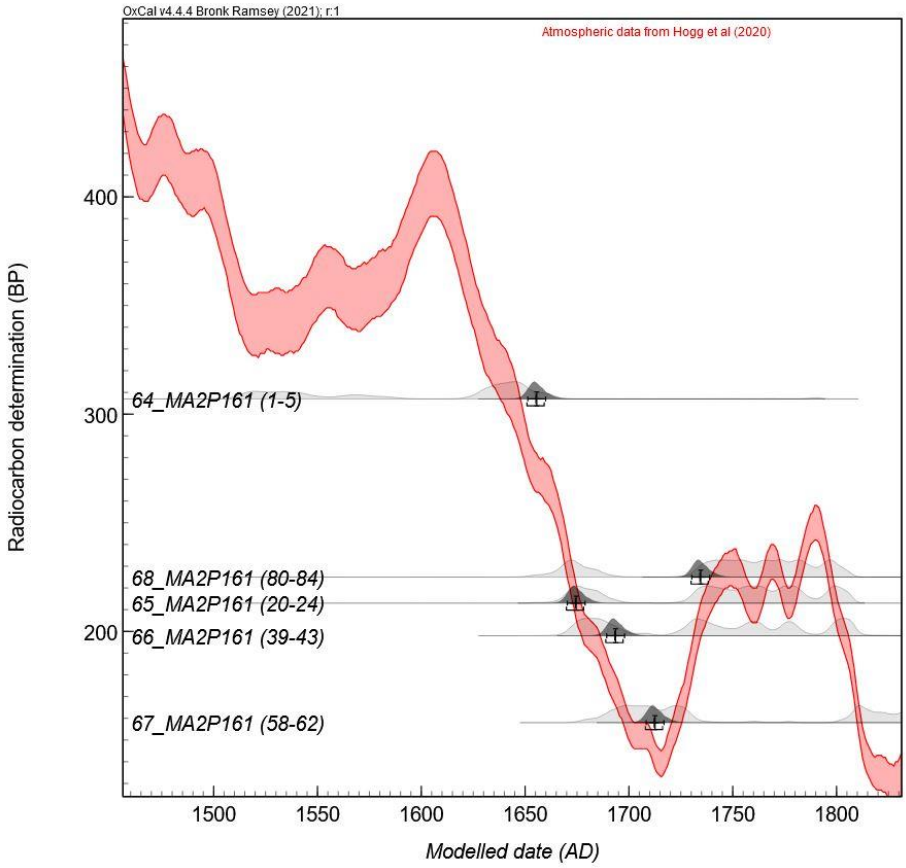

Figure 7.5.13. OxCal generated curve plot of the D_Sequence model for MA2P161.

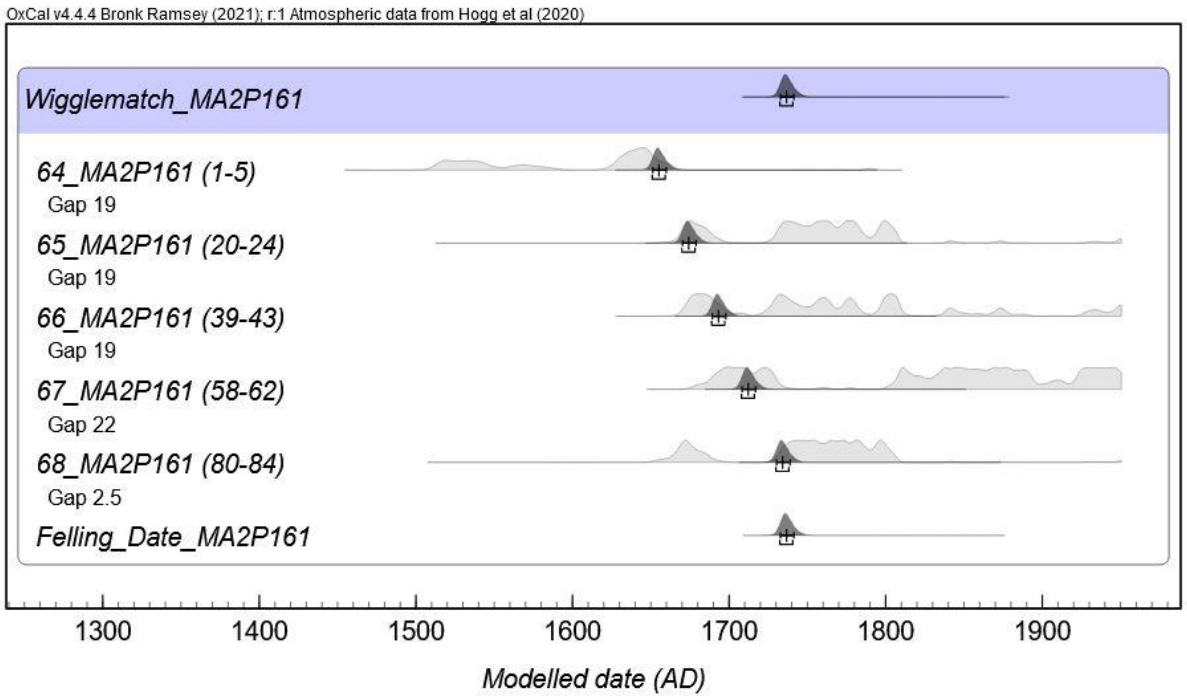

Figure 7.5.14. OxCal generated multiplot of the D_Sequence model for MA2P161.

7.5.8 Summary

Table 7.5.8 summarises the WMD results for the post-assemblage (7 posts) sampled from MA2. The results indicate that the site was first occupied as a defended place from the middle 1700s. Furthermore, the Felling Date results indicate a possible second palisade construction event in the early 1800s. Unfortunately, the only WMD produced on a post from the outer palisade row (MA2P149) was excluded from local and regional analyses due to imprecision. However, while it cannot be definitively proven, the WMD for MA2P149 strongly suggests the outer palisade row was either constructed (representing a redevelopment of the defences) or repaired during the early 1800s. Additionally, the WMD for MA2P14 is interpreted as inaccurate owing to possible ring count errors. The remaining five WMDs are interpreted as accurate and are included in the local and regional analyses (Section 12.1.3). While ^{14}C offsets were prevalent across the D_Sequence model results, the consistency of the calendar position of these offsets (across the calibration plateau in the late eighteenth century) indicates a common underlying cause. This offset pattern will be discussed further in Section 13.1.5.2.

Table 7.5.8. Summary of the WMD results for MA2.

Post ID	Felling Date Results			Local/Regional Analyses
	Median cal. Age	68% HPD	95% HPD	
MA2P14*	1779 ± 10	AD 1770–1787	AD 1766–1806	Excluded (inaccurate)
MA2P15	1805 ± 5	AD 1802–1809	AD 1796 – 1811	Included
MA2P149*	1802 ± 20	AD 1799–1806	AD 1678–1810	Excluded (imprecise)
MA2P152	1807 ± 5	AD 1800–1813	AD 1796–1814	Included
MA2P153	1804 ± 20	AD 1801–1809	AD 1686–1813	Included
MA2P154	1805 ± 3	AD 1802–1809	AD 1799–1812	Included
MA2P161	1736 ± 4	AD 1732–1741	AD 1729–1746	Included

*Note. *Indicates Felling Dates which are interpreted as inaccurate or imprecise.*

Chapter 8. Lake Mangahia (MGA)

8.1 Archaeological Excavations at MGA (S15/14)

Investigations at Lake Mangahia were conducted over one field season in May 2021. Several *in situ* posts were visible around the raised pā mound during previous site visits. Therefore, before beginning subsurface excavation, another walk-over survey of the pā was conducted to record all the visible posts. Eighty-four posts were recorded during this survey, representing at least four defensive rows in some areas (Figure 8.1.1).

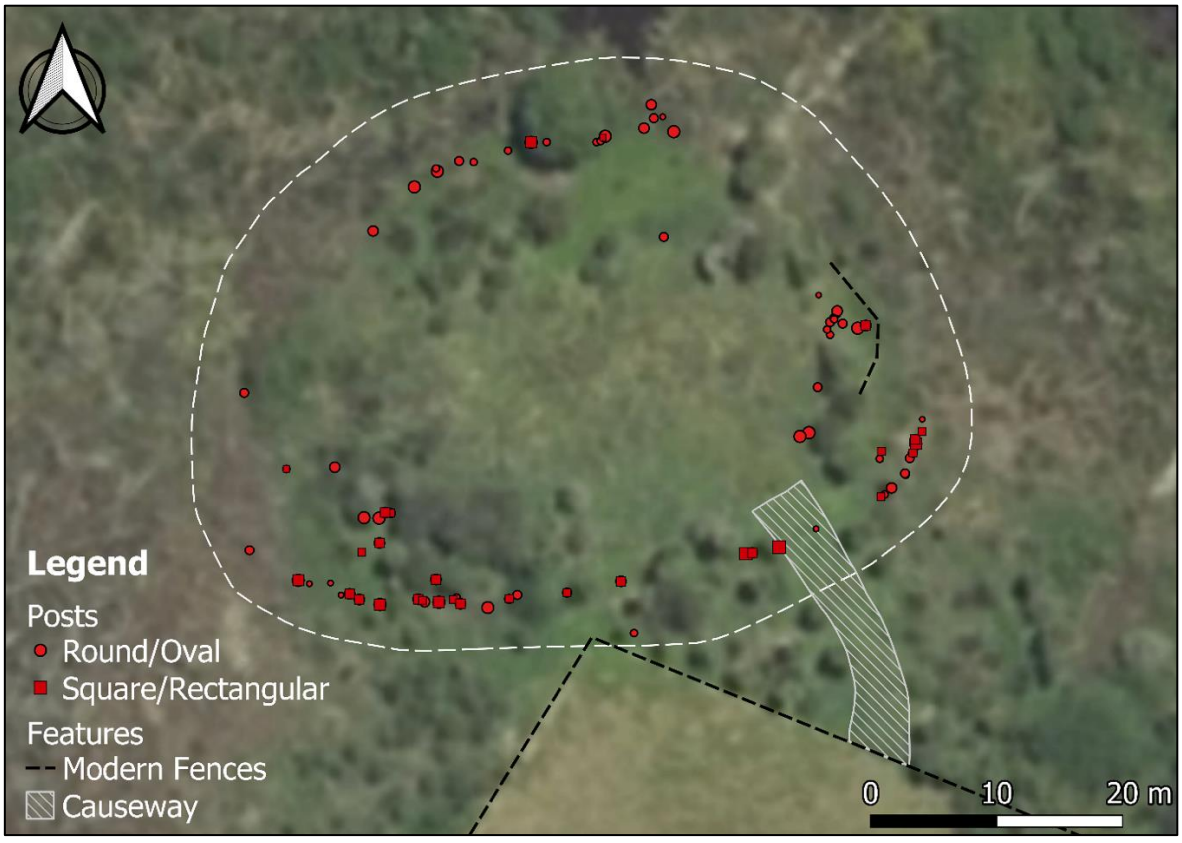

Figure 8.1.1. A site plan of MGA showing the location of the identified palisades.

Interestingly, a large proportion (36%) of the recorded posts exhibited an adzed cross-section (square or rectangular) compared to the other pā included within this study. These split or squared posts were primarily identified in the outermost palisade row on the southern side of the pā, indicating that a specific construction method was used when constructing or repairing

this row. Unfortunately, this construction method removes the terminal tree ring, preventing this hypothesis from being tested. Additionally, posts extending across the raised causeway were identified. Therefore, while the causeway has been modified (widened) to facilitate vehicle access to the lake, it also appears to be a feature of the original occupation of the site.

Figure 8.1.2. Warren Gumbley excavating around a palisade post in EA50 at MGA.

Given the visibility of the surviving palisade defences, excavation areas were limited to four specific locations of interest, excavated around prominent posts close to the toe of the pā mound (EA49–52). These excavation areas allowed these posts to be assessed before extraction and provided stratigraphic information about the imported sediment layers used to construct the mound (Figure 8.1.2 and Figure 8.1.3).

Figure 8.1.3. Alan Hogg (left) and Zac McIvor (right) excavating around palisade posts at MGA.

Figure 8.1.4. EA49 and EA50 positioned around MGAP312 (left) and MGAP311 (right).

EA49 covered an area of 1 m^2, excavated directly around MGAP311, a prominent post identified in the innermost palisade row on the southwestern corner of the pā (Figure 8.1.4). EA49 was excavated to a depth of 70 cm, revealing a complex stratigraphy comprising six distinct sediment layers (Figure 8.1.5). Cultural inclusions were limited to Layer L6a, consisting of black organic silt with moderate charcoal inclusions. The section profile of EA49 suggests multiple layers of imported yellow/brown sandy loam were used to construct the living surfaces of the pā (Figure 8.1.7). This material is similar to that found in the surrounding hills, which are the likely source location. EA51, also covering an area of 1 m^2, was excavated directly around MGAP275, another large post on the eastern side of the pā. The stratigraphy observed in EA51 is like that exhibited in EA49, with up to 10 distinct clay/sandy loam sediment layers (Figure 8.1.6). Pieces of wood were also identified at the base of EA49, possibly acting as foundations for the pā mound.

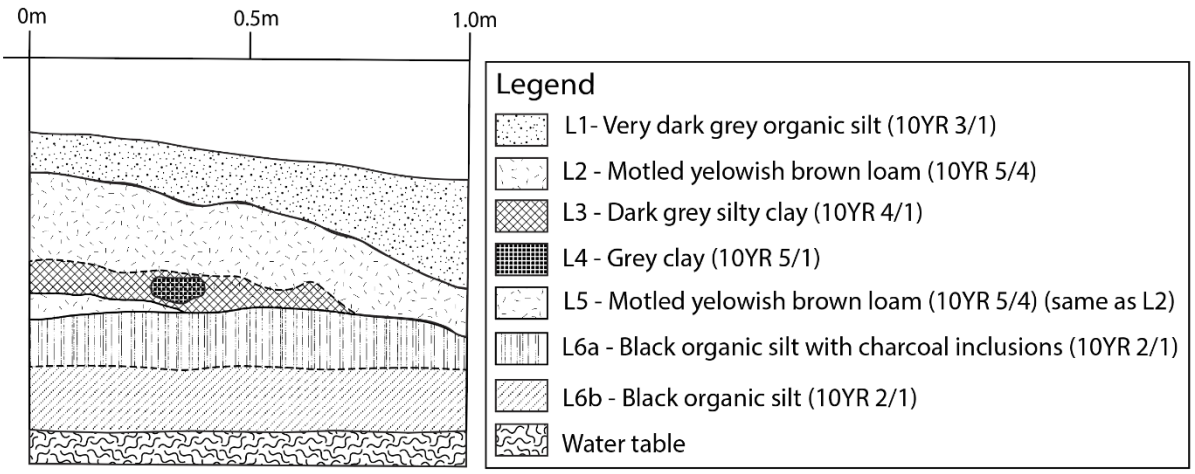

Figure 8.1.5. Section drawing of the southeastern baulk of EA49 at MGA.

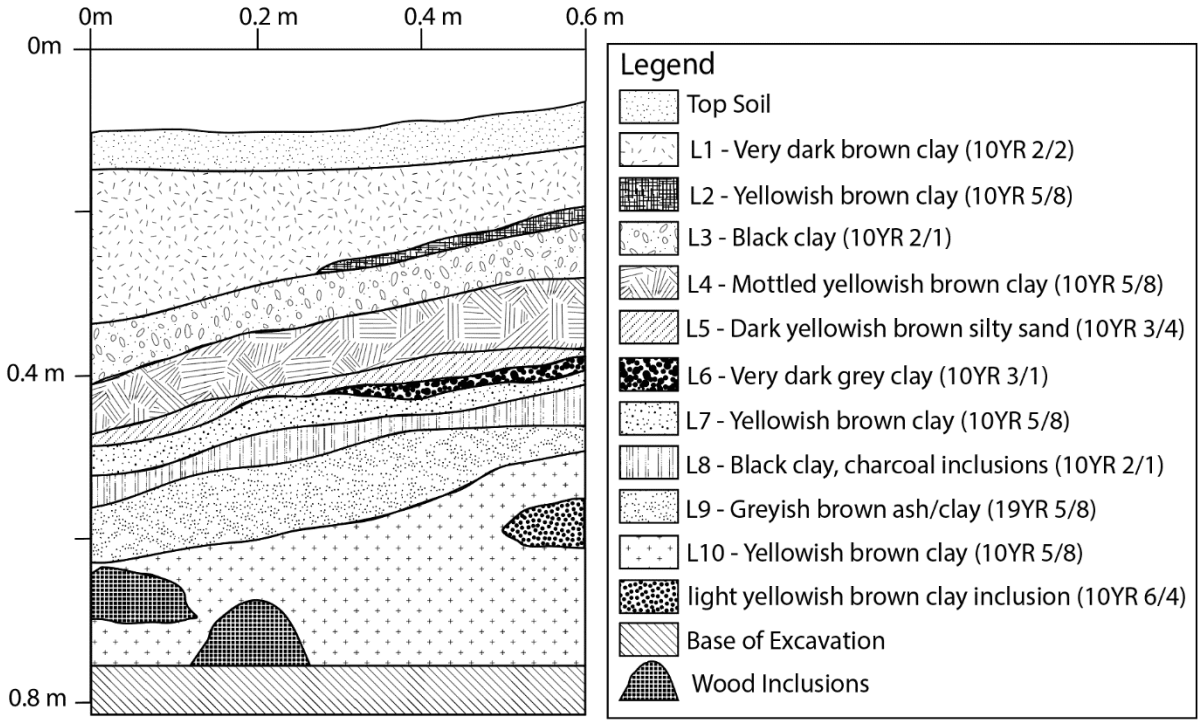

Figure 8.1.6. Section drawing of the southwestern baulk of EA51 at MGA.

Figure 8.1.7. A photograph of the southwestern baulk of EA51.

8.1.1 Extraction, Recording and Sampling

Twelve of the 84 posts were selected for extraction, representing all of the identified surviving palisade rows (Table 8.1.1 and Figure 8.1.8). Four of the extracted posts were noticeably decayed. However, the preservation quality of the posts was significantly better than that of previous sites investigated. Only one post exhibited charring on its outer surface, including the distal tapered end. As previously mentioned, this could represent the intentional burning of the tapered end (fire hardening) or the possible reuse of a previously burnt post. Four distinct taper types were recorded: 8 short, one long, one notched and one irregular taper (Figure 8.1.9, Figure 8.1.10 and Figure 8.1.11). When these tapers were closely scrutinised, four posts from the northern side of the pā (MGAP263, MGAP269, MGAP281 and MGAP316) were observed to exhibit a distinct adze scar pattern with a notable flaw on the blade of the adze that was used (Figure 8.1.12). This observation suggests that all four posts were constructed using the same adze and likely represent a single phase of palisade construction. Finally, seven posts were sampled for analysis.

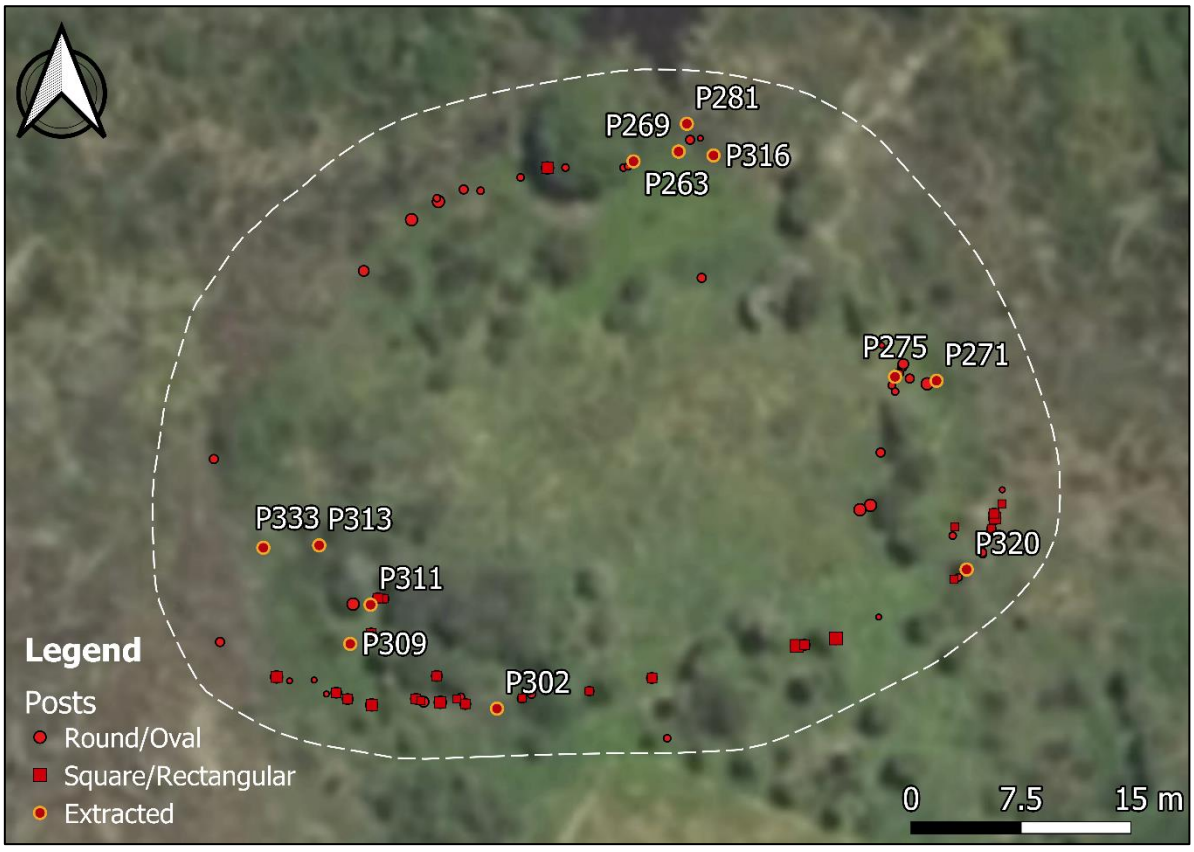

Figure 8.1.8. Location of the extracted posts from Lake Mangahia.

Table 8.1.1. Recorded information for posts extracted at Lake Mangahia (MGA).

Post ID	Cross section	Max length (cm)	Diameter (cm)	Taper shape	Condition	Sampled
MGAP263	Oval	220.6	21.6	Notched	Suitable for sampling	Yes
MGAP269	Oval	149.0	12.8	Short	Suitable for sampling	Yes
MGAP271*	Rectangle	-	13.5	Irregular	Poor preservation	No
MGAP275*	Round	270.4	10.5	Short	Poor preservation	No
MGAP281	Round	263.0	13.8	Short	Suitable for sampling	Yes
MGAP302*	Round	278.0	16.0	Short	Poor preservation	No
MGAP309*	Rectangle	-	-	Short	Suitable for sampling	No
MGAP311	Round	-	29.5	-	Suitable for sampling	Yes
MGAP313	Round	254.0	11.6	Short	Charring identified	Yes
MGAP316	Oval	175.0	15.0	Short	Suitable for sampling	Yes
MGAP320	Round	158.0	14.0	Short	Suitable for sampling	Yes
MGAP333*	Rectangle	-	7.0	Long	Poor preservation	No

*Note. *Indicates extracted posts that were not sampled.*

Figure 8.1.9. Post-extraction photograph of the irregular tapered end of MGAP271.

Figure 8.1.10. Post-extraction photograph of the short tapered end of MGAP316.

Figure 8.1.11. Post-extraction photograph of the notched tapered end of MGAP263.

Figure 8.1.12. Distinctive adze patterning on MGAP316.

8.2 Species Identification

Thin-section microscopy of the post assemblage (7 posts) sampled from the pā at Lake Mangahia identified three tree species: pukatea (*L.novae-zelandiae*), kahikatea (*D. dacrydioides*), tanekaha (*P. trichomanoides*) (Table 8.2.1). All three species are large trees generally found in the lowland forests of the North and South islands and are typical species found in swampy environments surrounding the rivers and lakes of the Middle Waikato Basin (Table 5.3.2).

Table 8.2.1. Tree species in the post assemblage from MGA.

Post ID	Common name	Scientific name
MGAP263	pukatea	*Laurelia novae-zelandiae*
MGAP269	pukatea	*Laurelia novae-zelandiae*
MGAP281	pukatea	*Laurelia novae-zelandiae*
MGAP311	kahikatea	*Dacrycarpus dacrydioides*
MGAP313	tanekaha	*Phyllocladus trichomanoides*
MGAP316	pukatea	*Laurelia novae-zelandiae*
MGAP320	pukatea	*Laurelia novae-zelandiae*

8.3 Condition Assessment

All seven prepared post samples were inspected under a low-powered light microscope to assess their condition and suitability for tree-ring analysis, ring-block sampling, and AMS radiocarbon dating (see Section 5.5 and Table 8.3.1). Following this assessment, all seven samples passed the condition assessment and proceeded to tree-ring analysis.

Table 8.3.1. MGA sample condition assessment.

Post ID	Poor preservation	Charring present	Scaring present	Dark staining	Growth anomalies	Passed
MGAP263	☐	☐	☐	☐	☑	Yes
MGAP269	☐	☐	☐	☑	☑	Yes
MGAP281	☐	☐	☑	☐	☑	Yes
MGAP311	☐	☐	☐	☐	☑	Yes
MGAP313	☐	☑	☐	☐	☑	Yes
MGAP316	☐	☐	☐	☐	☑	Yes
MGAP320	☐	☐	☐	☐	☑	Yes

8.4 Tree Ring Analysis Results

The reconciled ring count information for each post sample in the MGA assemblage is summarised in Table 8.4.1 (see Section 5.6 for method). The ring counts presented below represent the most accurate information attainable for these samples, with any persistent inconsistencies discussed further in Section 8.5.

Table 8.4.1. A summary of the reconciled ring count information for the posts sampled from MGA.

Post ID	Species ID	Reconciled ring count	Diameter (cm)
MGAP263*	Pukatea (*L. novae-zelandiae)*	137	21.6
MGAP269*	Pukatea (*L. novae-zelandiae)*	122	12.8
MGAP281	Pukatea (*L. novae-zelandiae)*	75	13.8
MGAP311	Kahikatea (*D. dacrydioides*)	253	29.5
MGAP313	Tanekaha (*P. trichomanoides*)	109	11.6
MGAP316	Pukatea (*L. novae-zelandiae)*	181	15.0
MGAP320	Pukatea (*L. novae-zelandiae)*	60	14.0

*Note. * Indicates samples with estimated maximum ring counts owing to severe tree-ring growth anomalies.*

8.4.1 MGAP263 (pukatea, *L. novae-zelandiae*)

MGAP263 presented an oval cross-section, non-concentric tree-ring growth pattern, and off-centre pith location. Multiple episodes of tree-ring suppression were identified across the tree-ring growth sequence, resulting in locally absent rings and very narrow annual growth periods (Figure 8.4.1). These characteristics culminated in a challenging growth sequence to count and measure accurately, with discrepancies identified between all three measured tracks (Table 8.4.2). After multiple attempts, the tree-ring growth sequence could not be reconciled into a final ring count, and the sample was rejected from ring-block sampling.

Figure 8.4.1. Digital scan of MGAP263

Table 8.4.2. Ring count information for MGAP263.

Ring counts	Track A	Track B	Track C	Reconciled
MGAP263*	132	137	112	-

Note. Tree-ring counts provided for MGAP263 are estimates only.

8.4.2 MGAP269 (pukatea, *L. novae-zelandiae*)

MGAP269 presented a round cross-section, central pith location, and relatively concentric tree-ring growth pattern. Episodes of tree-ring suppression were identified across the tree-ring growth sequence, primarily associated with an area of scaring. Unfortunately, this resulted in narrow annual growth periods and poorly defined tree-ring boundaries, with evidence of false rings throughout the growth sequence (Figure 8.4.2). Despite multiple attempts, the three measured radii could not be reconciled into a final ring count with the precision required for WMD, and the sample was rejected from ring-block sampling (Table 8.4.3).

Figure 8.4.2. Digital scan of MGAP269

Table 8.4.3. Ring count information for MGAP269.

Ring counts	Track A	Track B	Track C	Reconciled
MGAP269	120	116	122	-

Note. Tree-ring counts provided for MGAP269 are estimates only.

8.4.3 MGAP281 (pukatea, *L. novae-zelandiae*)

MGAP281 presented a relatively round cross-section, central pith location, and concentric tree-ring growth pattern. Minor episodes of tree-ring suppression were identified, primarily associated with the outermost (youngest) tree rings. Two scars were also present, stretching from the pith (centre) to the terminal tree ring, although the effect of this scaring was limited (Figure 8.4.3). Tree ring count and measurement analysis identified track C as being affected by locally absent rings, resulting in a difference of nine rings compared to track A (Table 8.4.4). Reconciliation of the three measured radii resulted in a final ring count of 75, with five ring-block samples collected at regular intervals across the tree ring growth sequence (Table 8.4.5). No sampling errors were identified across the ring-block samples; all five contained five tree rings.

Figure 8.4.3. Digital scan of MGAP281[39].

[39] A black-and-white scan is displayed rather than colour to better contrast the tree-ring growth sequence.

Table 8.4.4. Ring count information for MGAP281.

Ring counts	Track A	Track B	Track C	Reconciled
MGAP281	75	74	66	75

Table 8.4.5. Ring-block sampling information for MGAP281.

Wk number	Sample code	First ring	Middle ring	Last ring	# of rings in block	Ring gap to next sample
53341	114_MGAP281 (8–12)	8	10	12	5	16
53342	115_MGAP281 (24–28)	24	26	28	5	17
53343	116_MGAP281 (41–45)	41	43	45	5	19
53344	117_MGAP281 (60–64)	60	62	64	5	11
53345	118_MGAP281 (71–75)	71	73	75	5	2.5

8.4.4 MGAP311 (tanekaha, *P. trichomanoides*)

MGAP311 presented a relatively oval cross-section, a central pith location and a non-concentric ring pattern. The tree-ring sequence was affected by multiple episodes of tree-ring suppression, resulting in narrow annual growth periods and multiple locally absent rings (Figure 8.4.4). Track A was particularly affected by locally absent rings. However, Tracks B and C were consistent (Table 8.4.6). Reconciliation of these three measured radii resulted in a final ring count of 253, with seven ring-block samples collected at semi-regular intervals throughout the tree ring growth sequence (Table 8.4.7). Ideally, the ring-block sampling density would have been increased to more than seven samples. However, the tree-ring growth anomalies limited suitable sampling locations, and sampling accuracy was prioritised over collecting additional ring-block samples. No sampling errors were identified across any ring-block samples; all seven contained five tree rings.

Figure 8.4.4. Digital scan of MGAP311.

Table 8.4.6. Ring count information for MGAP311.

Ring counts	Track A	Track B	Track C	Reconciled
MGAP311	228	253	252	253

Table 8.4.7. Ring-block sampling information for MGAP311.

Wk number	Sample code	First ring	Middle ring	Last ring	# of rings in block	Ring gap to next sample
53351	124_MGAP311 (1–5)	1	3	5	5	45
53352	125_MGAP311 (46–50)	46	48	50	5	45
53353	126_MGAP311 (91–95)	91	93	95	5	35
53354	127_MGAP311 (126–130)	126	128	130	5	45
53355	128_MGAP311 (171–175)	171	173	175	5	45
53356	129_MGAP311 (216–220)	216	218	220	5	33
53357	130_MGAP311 (249–253)	249	251	253	5	2.5

8.4.5 MGAP313 (kahikatea, *D. dacrydioides*)

MGAP313 was unique in the assemblage, exhibiting prominent dark staining throughout the tree-ring growth sequence, a concentric ring pattern with areas of tree-ring suppression, locally absent rings and minor scaring (Figure 8.4.5). MGAP313 is also partially charred on its outer surface, resulting in a loss of the terminal tree ring around a portion of the sample's circumference. However, bark was observed on the outer surface of the post in areas unaffected by the charring, and the waney surface was identified in these areas, confirming that the terminal tree ring was present. The three measured radii were strategically positioned in locations which retained evidence of the terminal tree. As indicated by the ring count results in Table 8.4.8, all three measured radii were affected by locally absent rings.

Figure 8.4.5. Digital scan of MGAP313[40].

Reconciliation of these three measured radii resulted in a final ring count of 109 (23 rings more than the highest individual ring count). These ring count discrepancies were the result of locally

[40] Note. This sample was scanned after a significant time out of water, resulting in the cracks present around the outer surface.

absent rings situated between all three tracks. Five ring-block samples collected regularly across the tree-ring growth sequence (Table 8.4.9), with no sampling errors were identified across any ring-block samples. ll five contained five tree rings.

Table 8.4.8. Ring count information for MGAP313.

Ring counts	Track A	Track B	Track C	Reconciled
MGAP313	83	86	80	109

Table 8.4.9. Ring-block sampling information for MGAP313.

Wk number	Sample code	First ring	Middle ring	Last ring	# of rings in block	Ring gap to next sample
53329	102_MGAP313 (31–35)	31	33	35	5	19
53330	103_MGAP313 (50–54)	50	52	54	5	18
53331	104_MGAP313 (68–72)	68	70	72	5	19
53332	105_MGAP313 (87–91)	87	89	91	5	18
53333	106_MGAP313 (105–109)	105	107	109	5	2.5

8.4.6 MGAP316 (pukatea, *L. novae-zelandiae*)

MGAP316 presented an oval cross-section, central pith location, and non-concentric tree-ring growth pattern. This sample was affected by multiple episodes of tree-ring suppression, locally absent rings and occasional false rings (Figure 8.4.6). These episodes were prevalent throughout the tree-ring growth sequence and were not isolated to one growth period. As indicated by the ring count results in Table 8.4.10, locally absent rings significantly affected all three measured radii. Tree ring count and measurement analyses resulted in a reconciled final tree-ring count of 181, with seven ring-block samples collected at semi-regular intervals across the growth sequence (Table 8.4.11). Larger ring gaps were necessary between specific samples owing to the abovementioned issues. Despite the measures taken, sampling errors resulted in four ring-block samples containing more or fewer than five tree rings. It is important to note that the parent tree of this sample was very slow growing compared to its age, with a diameter of only 15 cm accounting for all 181 tree rings. This growth rate created challenges during ring-block sampling, as ideal sampling locations were limited, and the narrow width of each tree ring made it difficult to not cross the ring boundaries with the scalpel.

Figure 8.4.6. Digital scan of MGAP316.

Table 8.4.10. Ring count information for MGAP316.

Ring counts	Track A	Track B	Track C	Reconciled
MGAP316	129	154	126	181

Table 8.4.11. Ring-block sampling information for MGAP316.

Wk number	Sample code	First ring	Middle ring	Last ring	# of rings in block	Ring gap to next sample
53334	107_MGAP316 (1–6)	1	3.5	6	6	28
53335	108_MGAP316 (30–33)	30	31.5	33	4	49.5
53336	109_MGAP316 (79–83)	79	81	83	5	16.5
53337	110_MGAP316 (96–99)	96	97.5	99	4	39.5
53338	111_MGAP316 (135–139)	135	137	139	5	23
53339	112_MGAP316 (158–162)	158	160	162	5	17
53340	113_MGAP316 (173–181)	173	177	181	9	4.5

8.4.7 MGAP320 (pukatea, *L. novae-zelandiae*)

MGAP320 presented an oval cross-section, central pith location and concentric tree-ring growth pattern (Figure 8.4.7). This sample was comparatively free from tree-ring growth anomalies, with only minor episodes of tree-ring suppression identified. These growth

characteristics are reflected in the ring count results, which report only minor differences of up to five rings between all three measured tracks (Table 8.4.12). Reconciliation of these measured radii resulted in a final ring count of 60, with seven ring-block samples collected at semi-regular intervals across the tree ring growth sequence (Table 8.4.13). No sampling errors were identified across any ring-block samples; all seven contained five tree rings.

Figure 8.4.7. Digital scan of MGAP320.

Table 8.4.12. Ring count information for MGAP320.

Ring counts	Track A	Track B	Track C	Reconciled
MGAP320	60	56	55	60

Table 8.4.13. Ring-block sampling information for MGAP320.

Wk number	Sample code	First ring	Middle ring	Last ring	# of rings in block	Ring gap to next sample
53346	119_MGAP320 (7–11)	7	9	11	5	11
53347	120_MGAP320 (18–22)	18	20	22	5	10
53348	121_MGAP320 (28–32)	28	30	32	5	14
53349	122_MGAP320 (42–46)	42	44	46	5	14
53350	123_MGAP320 (56–60)	56	58	60	5	2.5

8.5 Wiggle-Match Dating Results

This section presents the WMD results for the post-assemblage (five posts) sampled from MGA (see Section 5.8.2 for method). The full array of OxCal codes relating to each post analysed can be viewed in Appendix D.3. The interpretation of each WMD is discussed in detail below.

8.5.1 MGAP281

The D_Sequence model for MGAP281 comprises five AMS ^{14}C dates, separated by known calendar intervals, spread across the 75-year tree-ring growth sequence (Table 8.5.1). The Felling Date of MGAP281 has a median calibrated age of AD 1788 ± 4, with a modelled date range between AD 1782–1797 (95% HPD). The analysis detected no outliers, the model passed the A_{comb} (An) threshold, and the convergence values generated by OxCal remained universally high (99%). Additionally, the WMD matches the shape of SHCal20 well (Figure 8.5.1), which is reflected in the comparison between the posterior and likelihood distributions (Figure 8.5.2). The first two ^{14}C dates within the D_Sequence series are slightly offset from the calibration curve. However, as tree-ring analysis of MGAP281 reported only minor episodes of ring suppression (primarily associated with the outermost (youngest) tree rings), and no outliers were detected during the analysis, these offsets are not a concern. When the D_Sequence model was calibrated using alternative outlier detection methods (see Appendix D.3.1), the results were consistent with the original Felling Date, reporting no outliers and universal good agreement (>60). Therefore, the WMD for MGAP281 is interpreted as accurate and is included in the local and regional scale analyses.

Table 8.5.1. D_Sequence (SSimple) result for MGAP281.

Wk number	Sample code	^{14}C Age (BP)	Outlier analysis (posterior/prior)	Convergence
53341	114_MGAP281 (8–12)	134 ± 21	5/5	99
53342	115_MGAP281 (24–28)	247 ± 20	5/5	99
53343	116_MGAP281 (41–45)	229 ± 24	5/5	99
53344	117_MGAP281 (60–64)	217 ± 23	5/5	99
53345	118_MGAP281 (71–75)	246 ± 21	5/5	99
Felling Date Results				
Median cal. Age (AD)	HPD 95%		HPD 95%	A_{comb} (An)
1788 ± 4	AD 1785–1793		AD 1782–1797	85.8 (31.6)

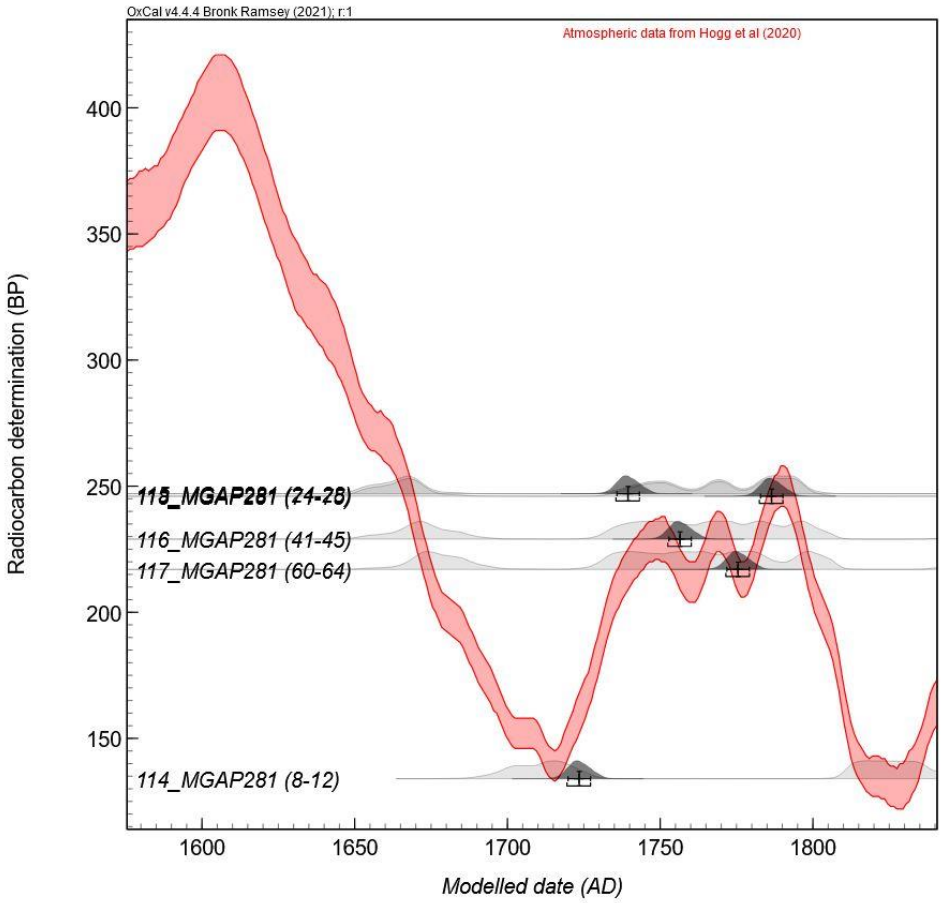

Figure 8.5.1. OxCal generated curve plot of the D_Sequence model for MGAP281.

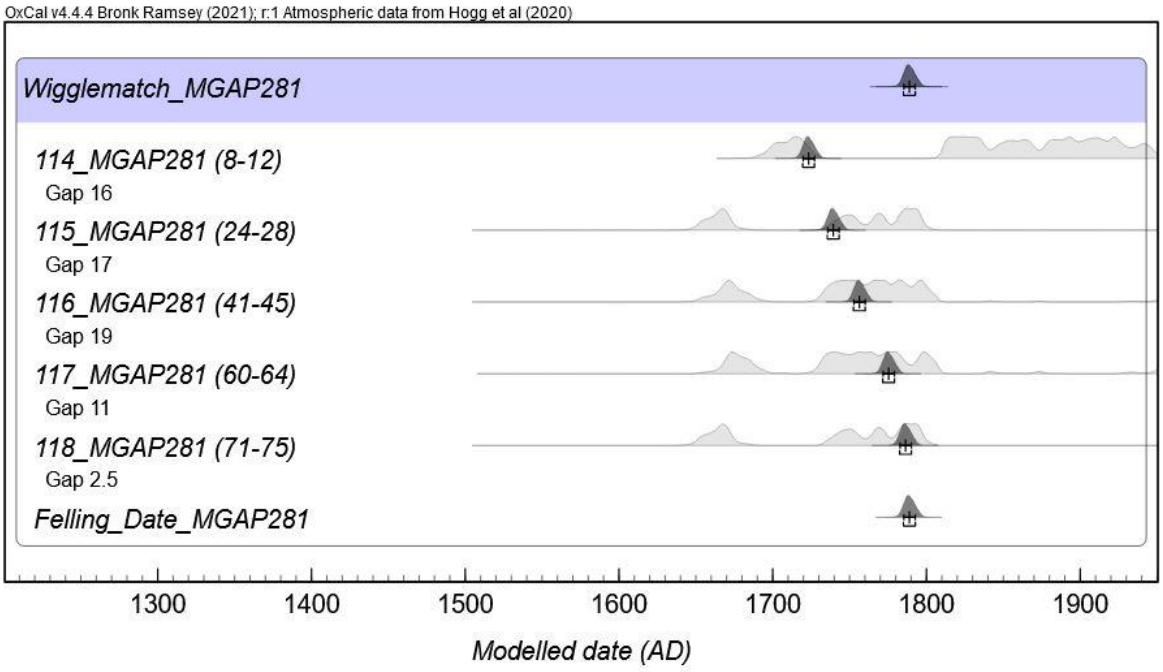

Figure 8.5.2. OxCal generated multiplot of the D_Sequence model for MGAP281.

8.5.2 MGAP311

The D_Sequence model for MGAP311 comprises seven AMS ^{14}C dates, separated by known calendar intervals, spread across the 253-year tree-ring growth sequence (Table 8.5.2). The Felling Date of MGAP311 has a median calibrated age of AD 1776 ± 5, with a modelled date range between AD 1767–1788 (95% HPD). No outliers were identified during the analysis, the model passed the A_{comb} (An) threshold, and convergence values remained universally high (99%). Additionally, the WMD reflects the shape of SHCal20 well (Figure 8.5.3). While the ^{14}C date for sample 125_MGAP311 (46–50) is offset from SHCal20, it is located over the calibration plateau in the late sixteenth century and was not flagged as an outlier by the analysis (Figure 8.5.4). When the D_Sequence model was calibrated using the RScaled outlier model, sample 125_MGAP311 (46–50) was identified and down-weighted as a minor outlier (see Appendix D.3.2). However, the Felling Date result was consistent with the original model while slightly improving the model's agreement. Therefore, the WMD is interpreted as accurate and is included in the local and regional scale of analyses.

Table 8.5.2. D_Sequence (SSimple) result for MGAP311.

Wk number	Sample code	^{14}C Age (BP)	Outlier analysis (posterior/prior)	Convergence
53351	124_MGAP311 (1–5)	358 ± 21	5/5	99
53352	125_MGAP311 (46–50)	424 ± 21	5/5	99
53353	126_MGAP311 (91–95)	393 ± 21	5/5	99
53354	127_MGAP311 (126–130)	292 ± 21	5/5	99
53355	128_MGAP311 (171–175)	163 ± 20	5/5	99
53356	129_MGAP311 (216–220)	226 ± 21	5/5	99
53357	130_MGAP311 (249–253)	226 ± 21	5/5	99

Felling Date Results

Median cal. Age (AD)	HPD 68%	HPD 95%	A_{comb} (An)
1776 ± 5	AD 1772–1782	AD 1767–1788	58.5 (26.7)

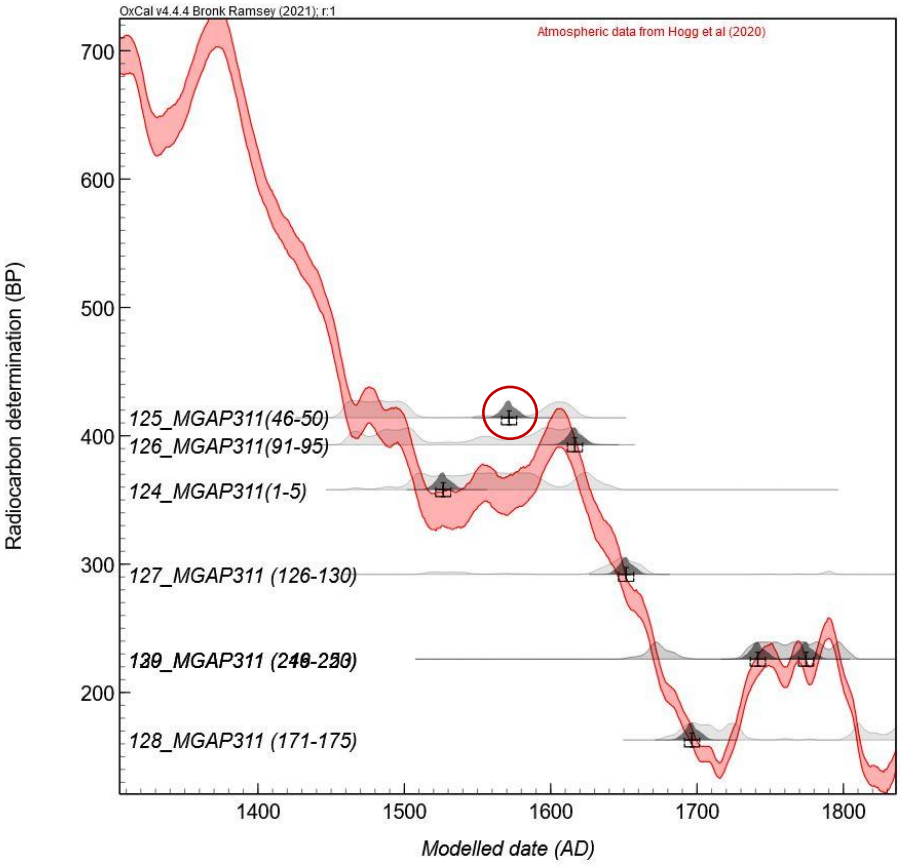

Figure 8.5.3. OxCal generated curve plot of the D_Sequence model for MGAP311[41].

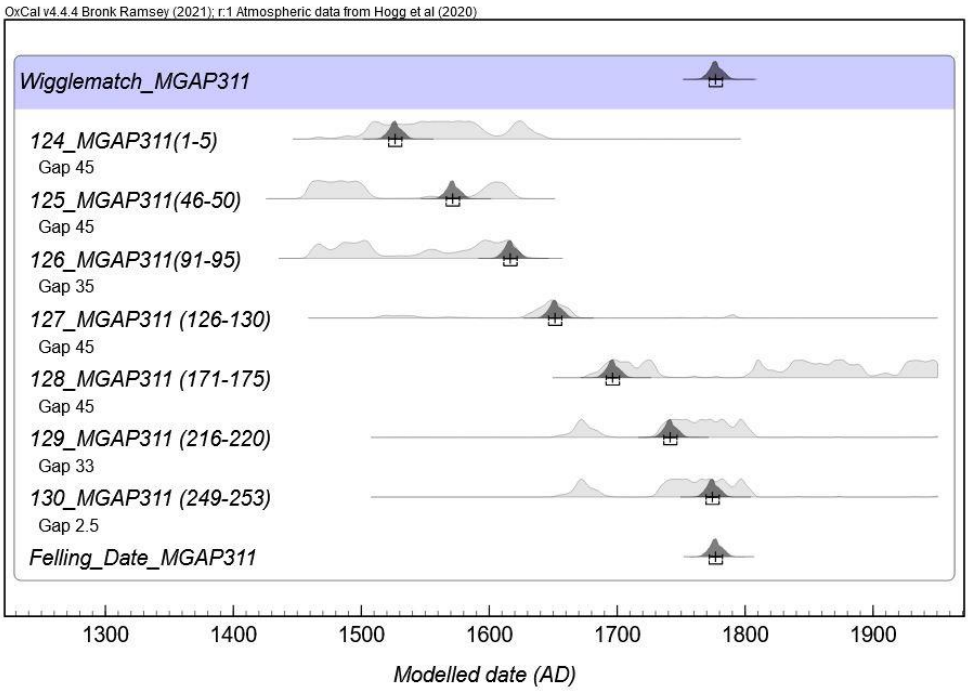

Figure 8.5.4. OxCal generated Multiplot graph of the D_Sequence model for MGAP311.

[41] Red circle highlights a potential ^{14}C age offset. This offset type is discussed further in Section 13.1.5.

8.5.3 MGAP313

The D_Sequence model for MGAP313 comprises five AMS ^{14}C dates, separated by known calendar intervals, spread across the 109-year tree-ring growth sequence (Table 8.5.3). The Felling Date of MGAP313 has a median calibrated age of AD 1551 ± 13, with a modelled date range between AD 1530–1576 (95% HPD). No outliers were detected during the analysis, the model passed the A_{comb} (An) threshold, and convergence values remained universally high. The WMD is positioned over the calibration plateau in the late fifteenth and early sixteenth centuries (Figure 8.5.5), which slightly affects the result's precision. However, the posterior and likelihood distributions are unaffected (Figure 8.5.6). When the D_Sequence model was calibrated using alternative outlier detection methods (see Appendix D.3.3), the results were consistent with the original result, reporting no outliers and universal good agreement (>60). Therefore, the WMD is interpreted as accurate and is included in the local and regional scale of analyses.

Table 8.5.3. D_Sequence (SSimple) result for MGAP313.

Wk number	Sample code	^{14}C Age (BP)	Outlier analysis (posterior/prior)	Convergence
53329	102_MGAP313 (31–35)	412 ± 20	5/5	100
53330	103_MGAP313 (50–54)	410 ± 24	5/5	100
53331	104_MGAP313 (68–72)	375 ± 20	5/5	100
53332	105_MGAP313 (87–91)	372 ± 19	5/5	100
53333	106_MGAP313 (105–109)	384 ± 20	5/5	100
Felling Date Results				
Median cal. Age (AD)	HPD 68%		HPD 95%	A_{comb} (An)
1551 ± 13	AD 1542–1561		AD 1530–1576	81.7 (31.6)

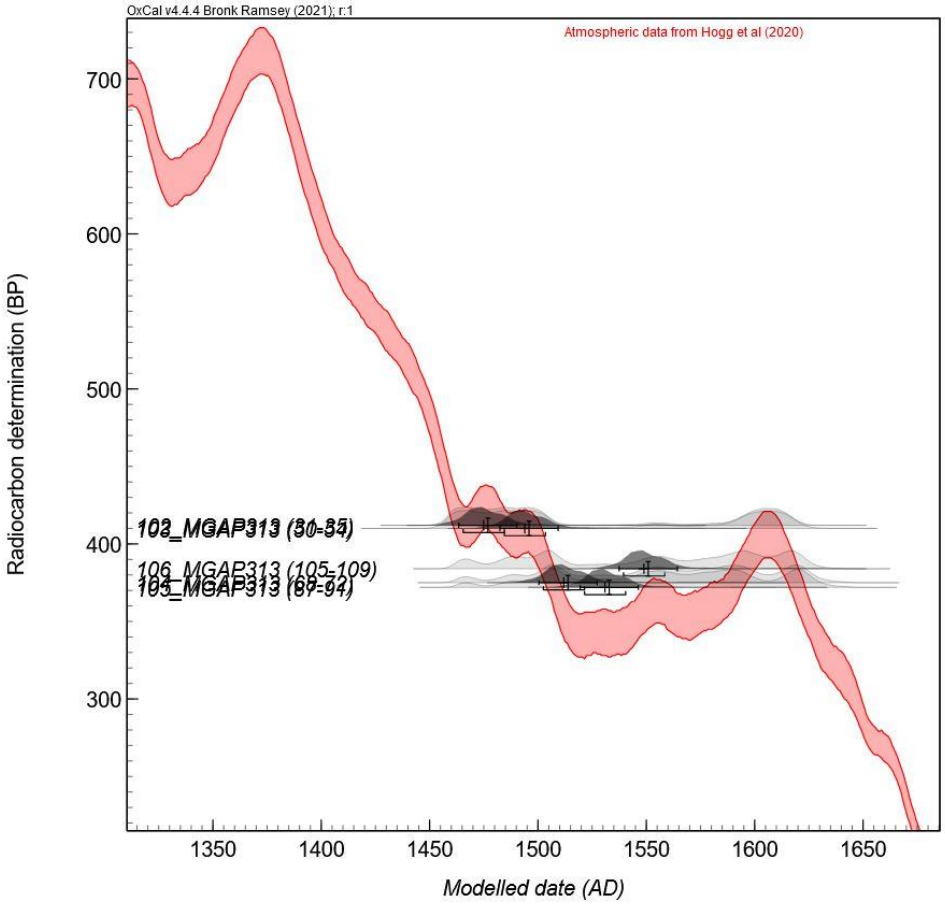

Figure 8.5.5. OxCal generated curve plot of the D_Sequence model for MGAP313.

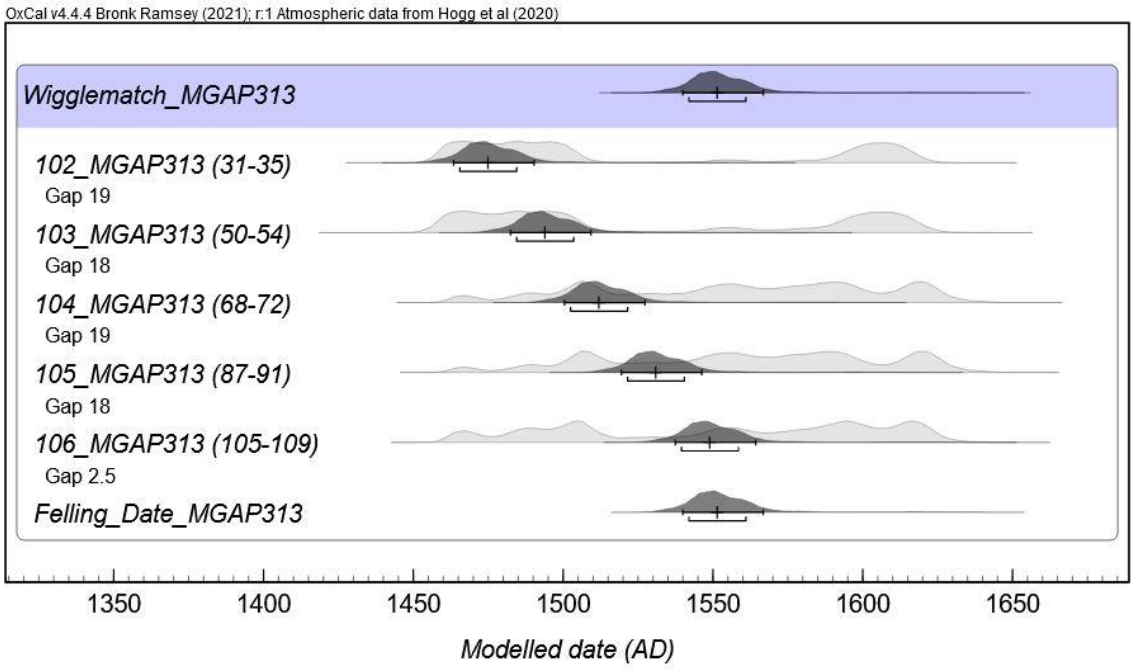

Figure 8.5.6. OxCal generated multiplot of the D_Sequence model for MGAP313.

8.5.4 MGAP316

The D_Sequence model for MGAP316 comprises seven AMS ^{14}C dates, separated by known calendar intervals, spread across the 181-year tree-ring growth sequence (Table 8.5.4). The Felling Date of MGAP316 has a median calibrated age of AD 1777 ± 4, with a modelled date range between AD 1770–1788 (HPD 95%). The model does not pass the A_{comb} (An) threshold, and two minor outliers were detected and down-weighted during the analysis: samples 108_MGAP316 (30–33) and 112_MGAP316 (158–162). When reviewing the curve plot of the WMD (Figure 8.5.7), three of the seven ^{14}C dates within the D_Sequence series are offset from SHCal20, reflected in comparisons between the posterior and likelihood distributions (Figure 8.5.8). However, the ^{14}C age order reversals observed within the D_Sequence model suggest that the calendar position of the final three ^{14}C dates over the calibration plateau in the late eighteenth century is correct. Tree-ring analysis of MGAP316 reported multiple episodes of tree-ring suppression, locally absent rings and occasional false rings. As these episodes were not isolated to one period of growth, it was not immediately clear if these growth anomalies were responsible for this poor result.

Table 8.5.4. Original D_Sequence (SSimple) result for MGAP316.

Wk number	Sample code	^{14}C Age (BP)	Outlier analysis (posterior/prior)	Convergence
53334	107_MGAP316 (1–6)	410 ± 21	5/5	99
53335	108_MGAP316 (30–33)	420 ± 20	7/5	99
53336	109_MGAP316 (79–83)	177 ± 21	5/5	99
53337	110_MGAP316 (96–99)	172 ± 21	5/5	99
53338	111_MGAP316 (135–139)	225 ± 20	5/5	99
53339	112_MGAP316 (158–162)	266 ± 20	6/5	99
53340	113_MGAP316 (173–181)	195 ± 20	5/5	99

Felling Date Results

Median cal. Age (AD)	HPD 68%	HPD 95%	A_{comb} (An)
1777 ± 4	AD 1774–1782	AD 1770–1788	8.8 (26.7)

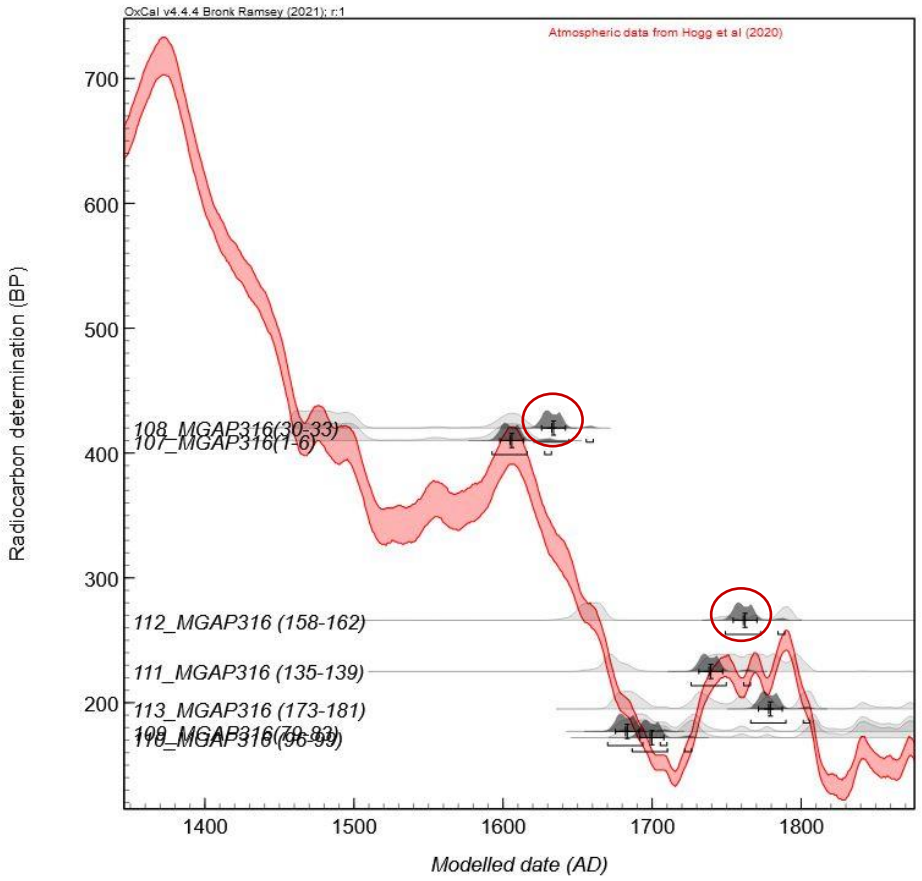

Figure 8.5.7. OxCal generated curve plot of the Original D_Sequence model for MGAP316.

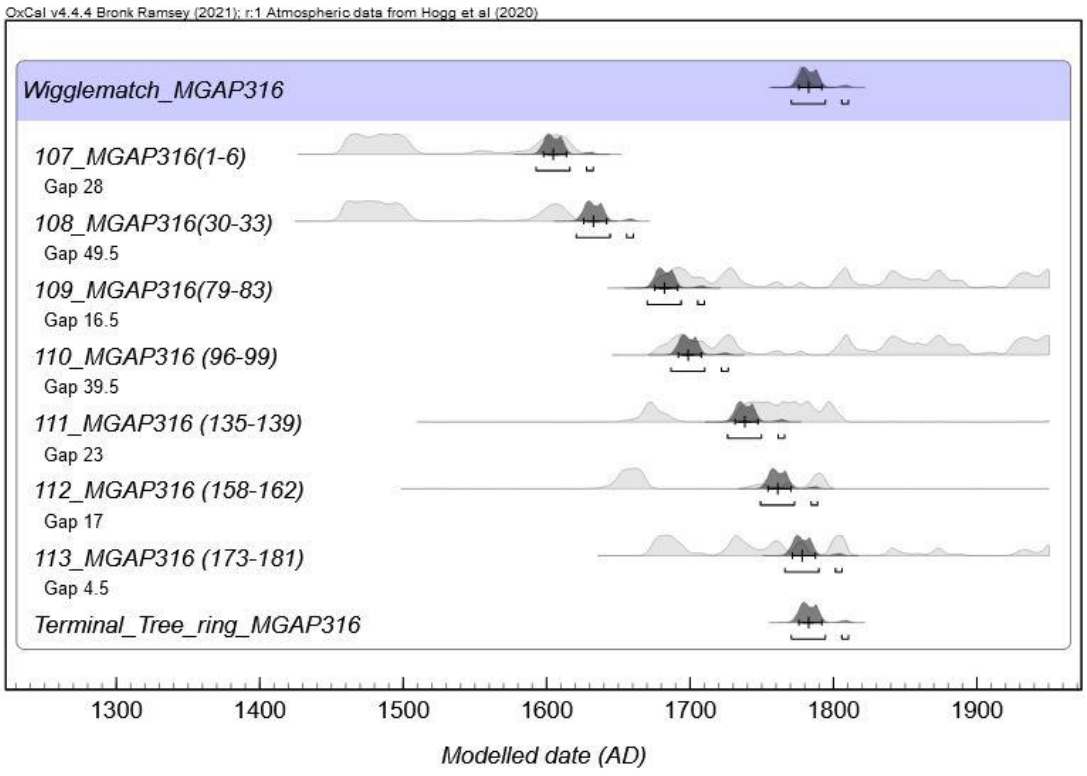

Figure 8.5.8. OxCal generated multiplot of the Original D_Sequence model for MGAP316.

The D_Sequence model calibrated using the RScaled outlier model was reviewed to investigate this WMD further. This second D_Sequence model resulted in a Felling Date with a median calibrated age of AD 1782 ± 8 and a modelled date range between AD 1770–1811 (HPD 95%). The Rscaled outlier model identified and down-weighted one major outlier: sample 108_MGAP316 (30–33). However, samples 112_MGAP316 (158–162) and 113_MGAP316 (173–181) were not flagged as outliers by the RScaled outlier analysis. Given the results of the RScaled outlier model, the original D_Sequence (with the SSimple outlier model applied) was recalibrated with sample 108_MGAP316 (30–33) removed from the D_Sequence series. This updated Felling Date had a median calibrated age of AD 1786 ± 8, with a bimodal modelled date range between AD 1775–1811 (HPD 95%). However, the results strongly suggest a Felling Date between AD 1780–1791 (68% HPD). The new D_Sequence model passed the A_{comb} (An) threshold, detected no outliers, and had universally high convergence (99%). Consequently, the updated WMD for MGAP316 (with sample 108_MGAP316 (30–33) removed from the D_Sequence) is interpreted as accurate and is included in the local and regional scale analyses.

Table 8.5.5. Updated D_Sequence (SSimple) results for MGAP316.

Wk number	Sample code	^{14}C Age (BP)	Outlier analysis (posterior/prior)	Convergence
53334	107_MGAP316 (1–6)	410 ± 21	5/5	99
53336	109_MGAP316 (79–83)	177 ± 21	5/5	99
53337	110_MGAP316 (96–99)	172 ± 21	5/5	99
53338	111_MGAP316 (135–139)	225 ± 20	5/5	99
53339	112_MGAP316 (158–162)	266 ± 20	5/5	99
53340	113_MGAP316 (173–181)	195 ± 20	5/5	99

Felling Date Results

Median cal. Age (AD)	HPD 68%	HPD 95%	A_{comb} (An)
1786 ± 8	AD 1780–1791	AD 1775–1811 (88.8%) AD 1804–1811 (7%)	61.6 (28.9)

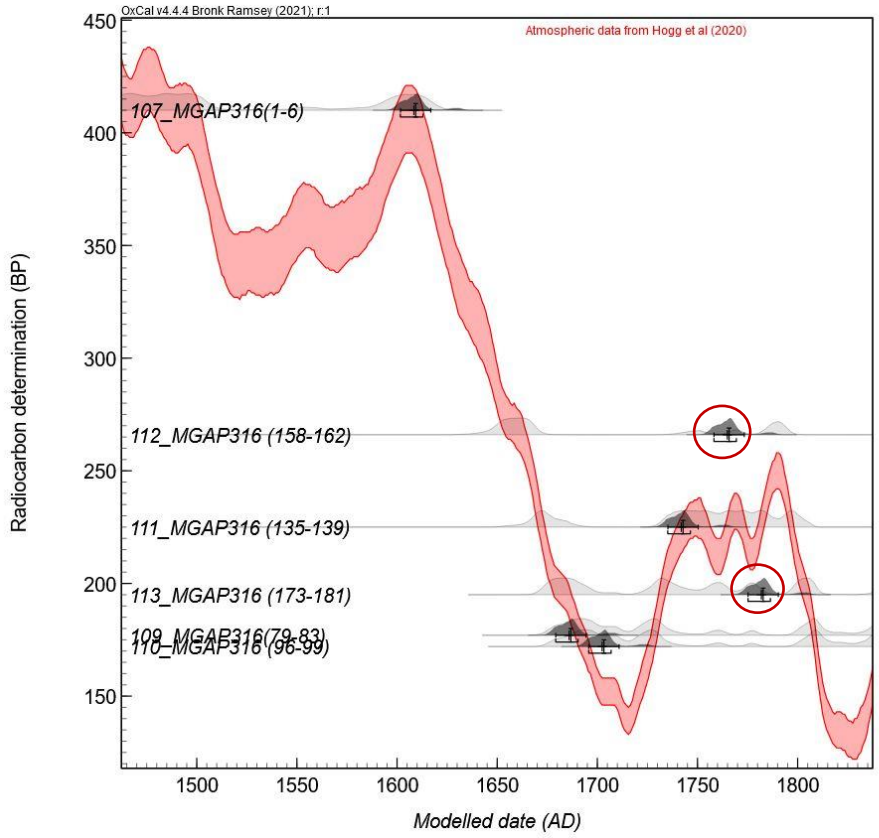

Figure 8.5.9. OxCal generated curve plot for the updated D_Sequence model for MGAP316[42].

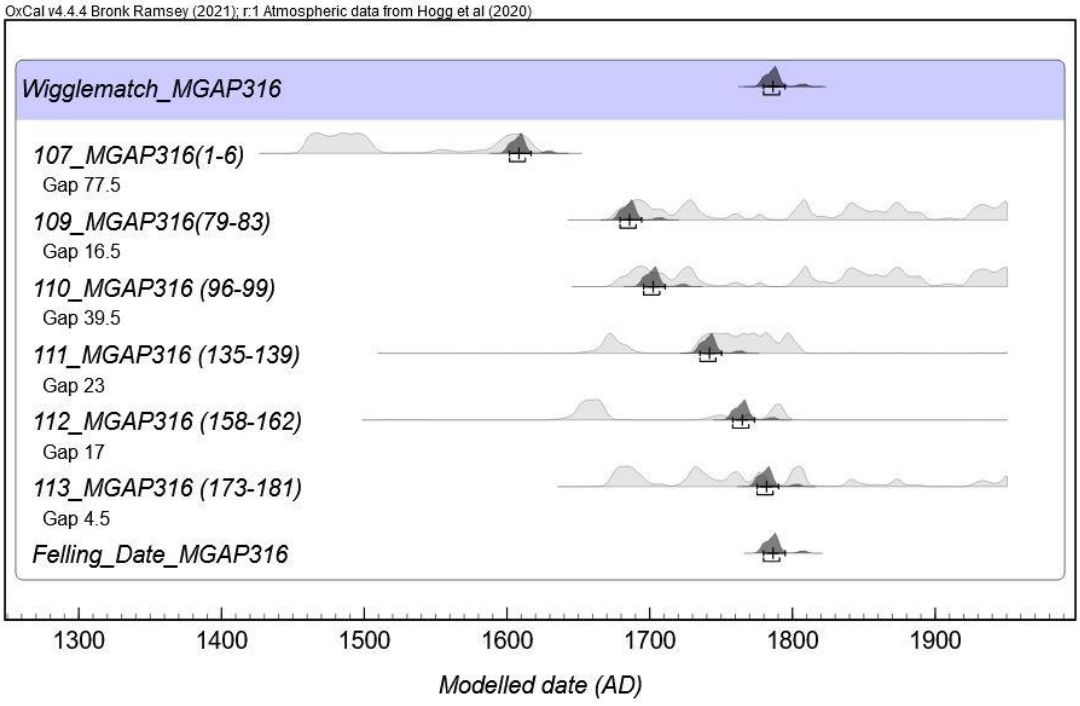

Figure 8.5.10. OxCal generated Multiplot graph of the updated D_Sequence model for MGAP316.

[42] Red circles highlight potential ^{14}C age offsets. This offset type is discussed further in Section 13.1.5.

8.5.5 MGAP320

The D_Sequence model for MGAP320 comprises five AMS ^{14}C dates, separated by known calendar intervals, spread across the 60-year tree-ring growth sequence (Table 8.5.6). The Felling Date of MGAP320 reports a median calibrated age of AD 1803 ± 12, with a bimodal modelled date range between AD 1776–1815. No outliers were detected during the analysis, the model passed the A_{comb} (An) threshold, and convergence values remained universally high. The WMD for MGAP320 is entirely situated over the calibration plateau in the late eighteenth century (Figure 8.5.11). Consequently, the precision of the Felling Date is affected, producing a bimodal result. However, the results strongly suggest a Felling Date between AD 1781–1812 (68% HPD), which is also supported by comparisons of the posterior and likelihood distributions for each of the five ^{14}C dates in the D_Sequence series (Figure 8.5.12). When the D_Sequence model was calibrated using agreement index analysis (see Appendix D.3.5), the results were consistent with the original WMD, reporting universal good agreement. Therefore, the WMD is interpreted as accurate and is included in the local and regional scale of analyses.

Table 8.5.6. D_Sequence (SSimple) result for MGAP320.

Wk number	Sample code	^{14}C Age (BP)	Outlier analysis (posterior/prior)	Convergence
53346	119_MGAP320 (7–11)	200 ± 21	5/5	99
53347	120_MGAP320 (18–22)	201 ± 22	5/5	99
53348	121_MGAP320 (28–32)	228 ± 21	5/5	99
53349	122_MGAP320 (42–46)	249 ± 22	5/5	99
53350	123_MGAP320 (56–60)	193 ± 22	5/5	99

Felling Date Results

Median cal. Age (AD)	HPD 68%	HPD 95%	A_{comb} (An)
1803 ± 12	AD 1781–1784 (9%) AD 1800–1812 (59%)	AD 1776–1788 (25%) AD 1797–1815 (70%)	130.6 (31.6)

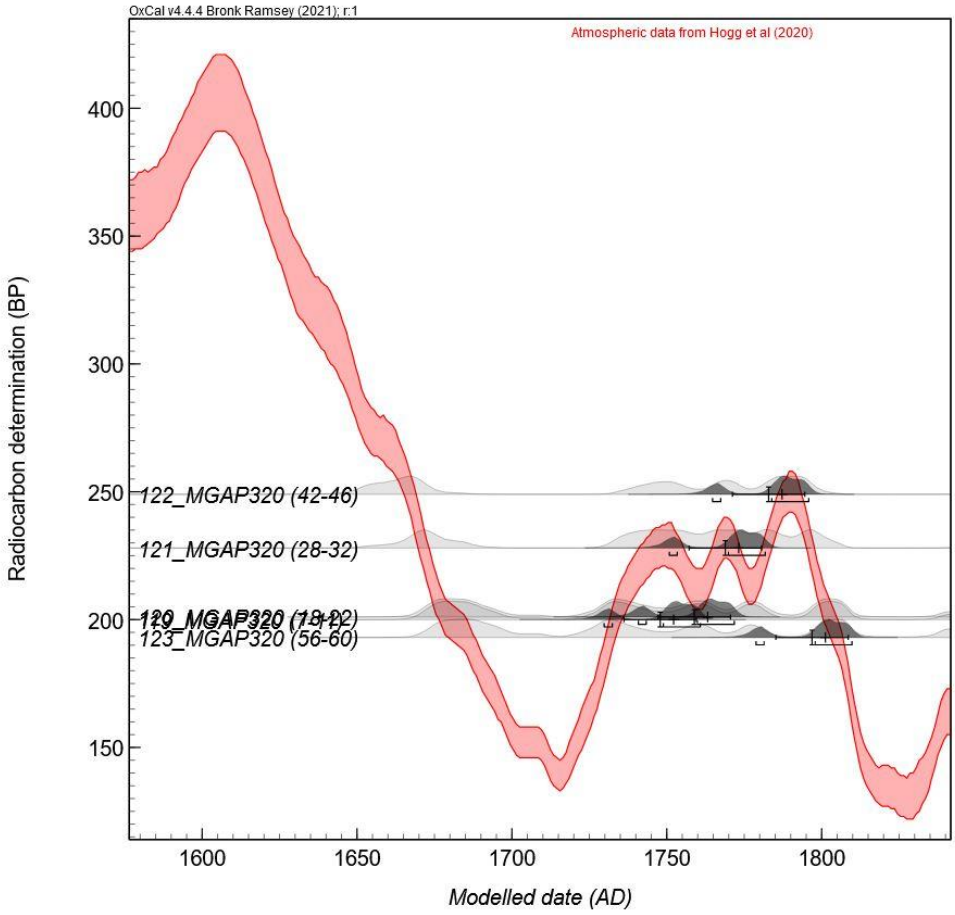

Figure 8.5.11. OxCal generated curve plot of the D_Sequence model for MGAP320.

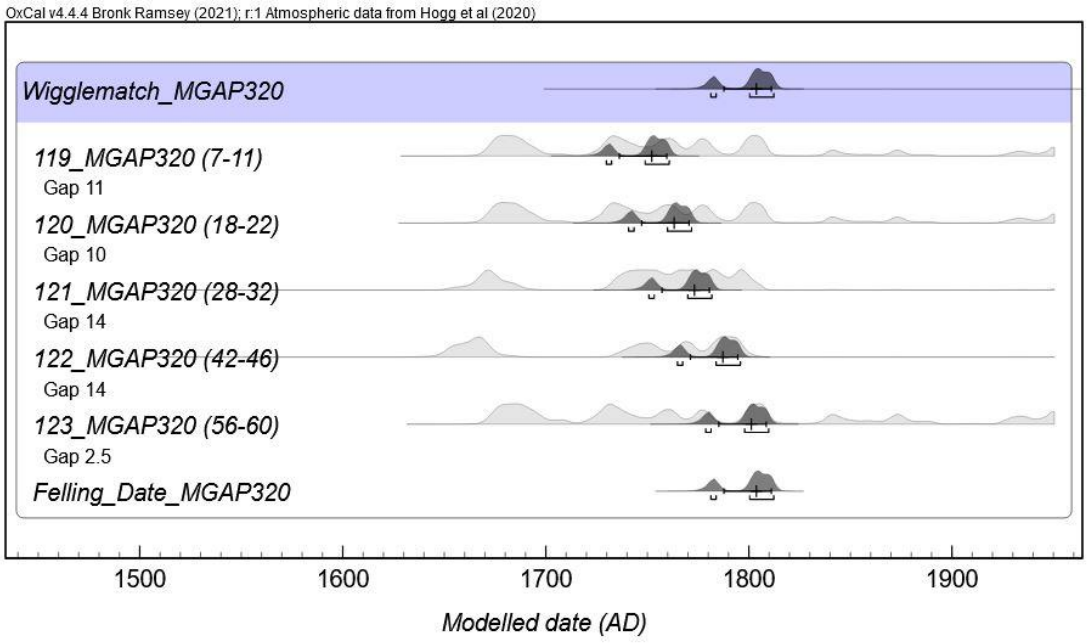

Figure 8.5.12. OxCal generated multiplot of the D_Sequence model for MGAP320.

8.5.6 Summary

Table 8.5.7 summarises the WMD results for the post-assemblage (five posts) sampled from MGA. The results indicate that the site was first occupied as a defended place from the middle 1500s, with evidence of additional palisade construction events in the middle to late 1700s and early 1800s. Encouragingly, the WMDs for MGAP281 and MGAP316 report similar Felling Date results. As discussed in Section 8.1.1, observation of the tapered ends of these two posts suggests they were constructed using the same adze. Therefore, it seems probable that the parent trees of these posts were cut down during the same palisade construction phase. This evidence indicates that the updated WMD for MGAP316 has produced an accurate Felling Date. This hypothesis will be tested during the local scale analysis presented in Section12.1.4.

Table 8.5.7. Summary of WMD results for MGA.

Post ID	Felling Date Results			Local/Regional Analyses
	Median cal. Age (AD)	68% HPD	95% HPD	
MGAP281	1788 ± 4	AD 1785–1793	AD 1782–1797	Included
MGAP311	1776 ± 5	AD 1772–1782	AD 1767–1788	Included
MGAP313	1551 ± 13	AD 1542–1561	AD 1530–1576	Included
MGAP316	1786 ± 8	AD 1780–1791	AD 1775–1811	Included
MGAP320	1803 ± 12	AD 1781–1812	AD 1776–1815	Included

Chapter 9. Taraheke Pā (TAR)

9.1 Archaeological Excavations at TAR (S14/22)

Excavations at Taraheke Pā were conducted over one field season in June 2020. As discussed in Section 4.1.3, no visible palisade defences were identified during the initial site visit. However, test pitting within the swampy margins surrounding the headland identified a distinct cultural sediment layer (L2) under approximately 20 cm of organic silt post-depositional slope wash (L1) (Figure 9.1.1). This cultural layer, containing charcoal inclusions and freshwater mussel periostracum (*E. menziesii*), exhibited the environmental conditions required to preserve organic artefacts (posts). Therefore, a series of exploratory excavation areas were positioned around the perimeter of the pā (EA30–36), extending from the base of the headland into surrounding the swampy margin. Each excavation area initially covered an area of 3 x 1.5 m, with the areas extended as required (Figure 9.1.2). The overlying organic silt (L1) was removed as a single unit by a digger, operated by Greg Gedson (archaeologist) and monitored by Dr Warren Gumbley and the author (Figure 9.1.3), with hand excavation commencing at the interface between L1 and L2.

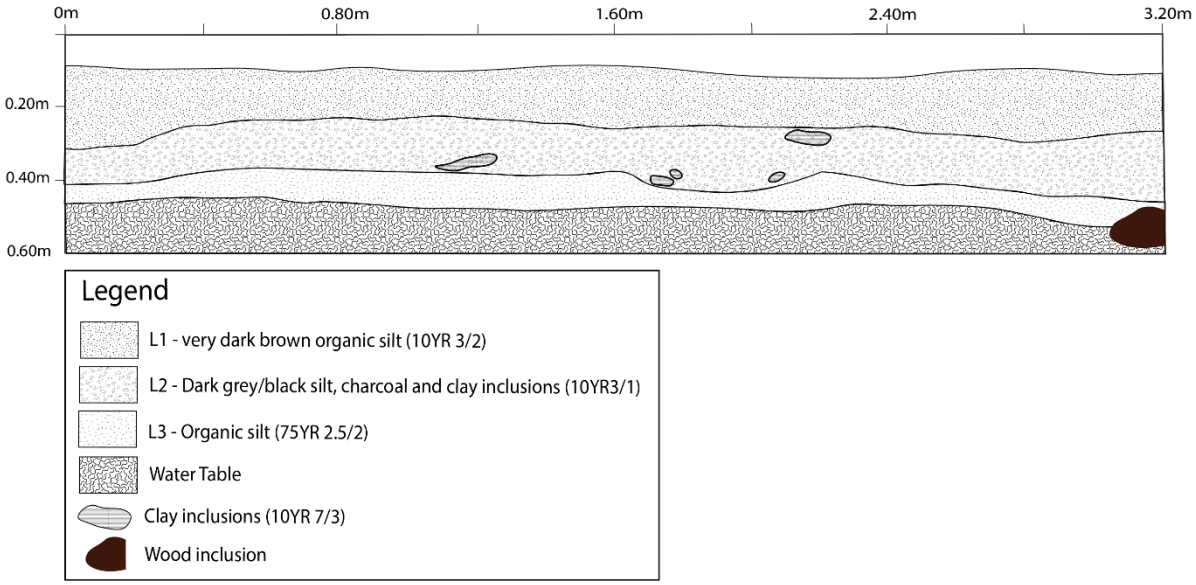

Figure 9.1.1. Section drawing of the southern baulk in EA29.

Figure 9.1.2. Site plan of Taraheke pā showing the location of EA30–35[43].

Figure 9.1.3. Greg Gedson (operator), Warren Gumbley (centre), Zac McIvor (right) and Alan Hogg (right) monitor the removal of L1 from EA31 at TAR

[43] This figure includes data sourced from the LINZ Data Service and is licensed for reuse under the CC BY 4.0.

Unfortunately, most of these excavation areas were devoid of cultural deposits, and no evidence of a traditional palisade row (surrounding the headland pā) was identified. However, six *in situ* posts were recorded close to the headland's tip in EA32 (Figure 9.1.4 and Figure 9.1.5). EA32 covered an 8 x 3 m area, excavated to a depth of 30 cm. All six posts recorded in this area were identified within the interface between L1 and L2. While this post-alignment does not represent a traditional palisade defence, it forms a barrier extending into the adjacent stream (Figure 9.1.6), interpreted as a structure (e.g., eel weir (pa tuna) or waka landing) or a defensive barrier protecting access to the stream or pā (Figure 9.1.7). While not a traditional palisade defence, it was determined that WMD these posts would still provide valuable information regarding the occupation of the pā, and the Felling Dates produced for these posts are still interpreted as a TPQ for a construction event.

Figure 9.1.4. Post alignment identified in EA32 (looking north from the base of the headland)

Figure 9.1.5. A photograph of TARP131 in situ.

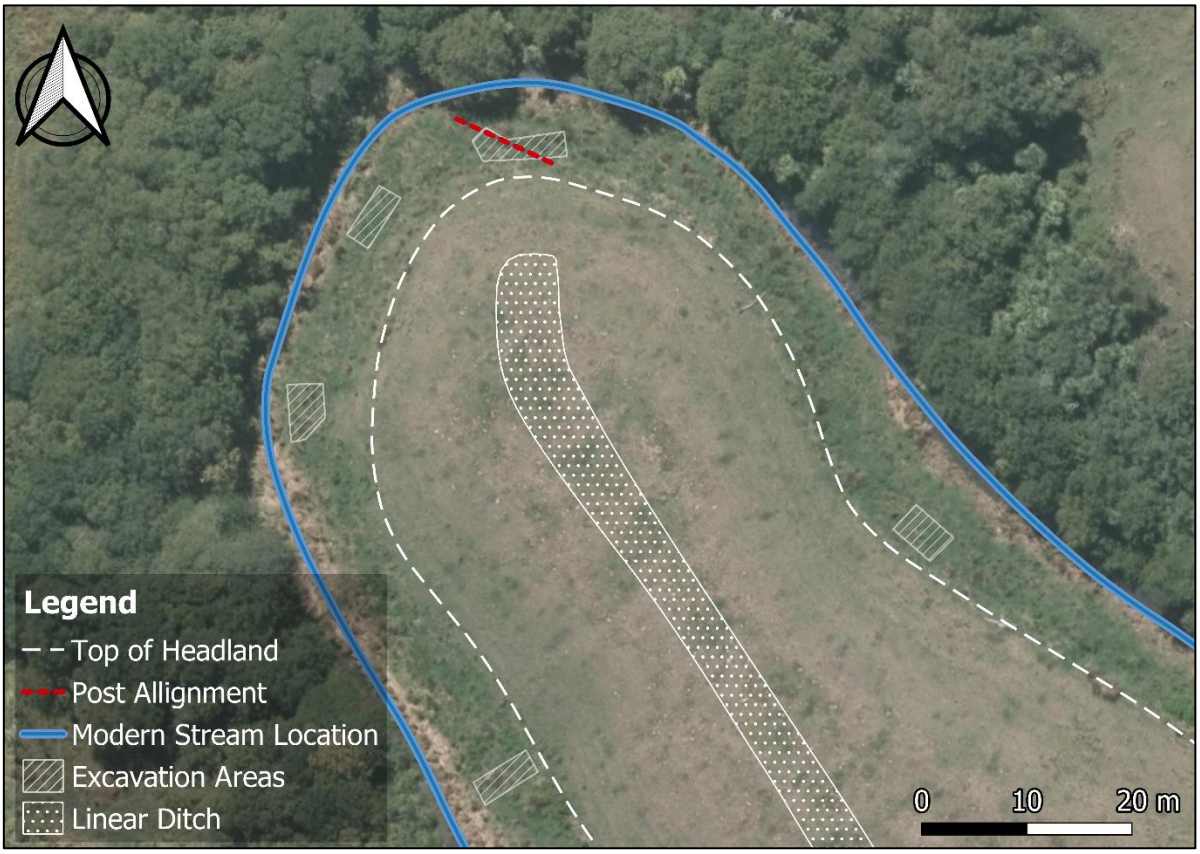

Figure 9.1.6. A site plan showing the orientation of the post-alignment in EA32.

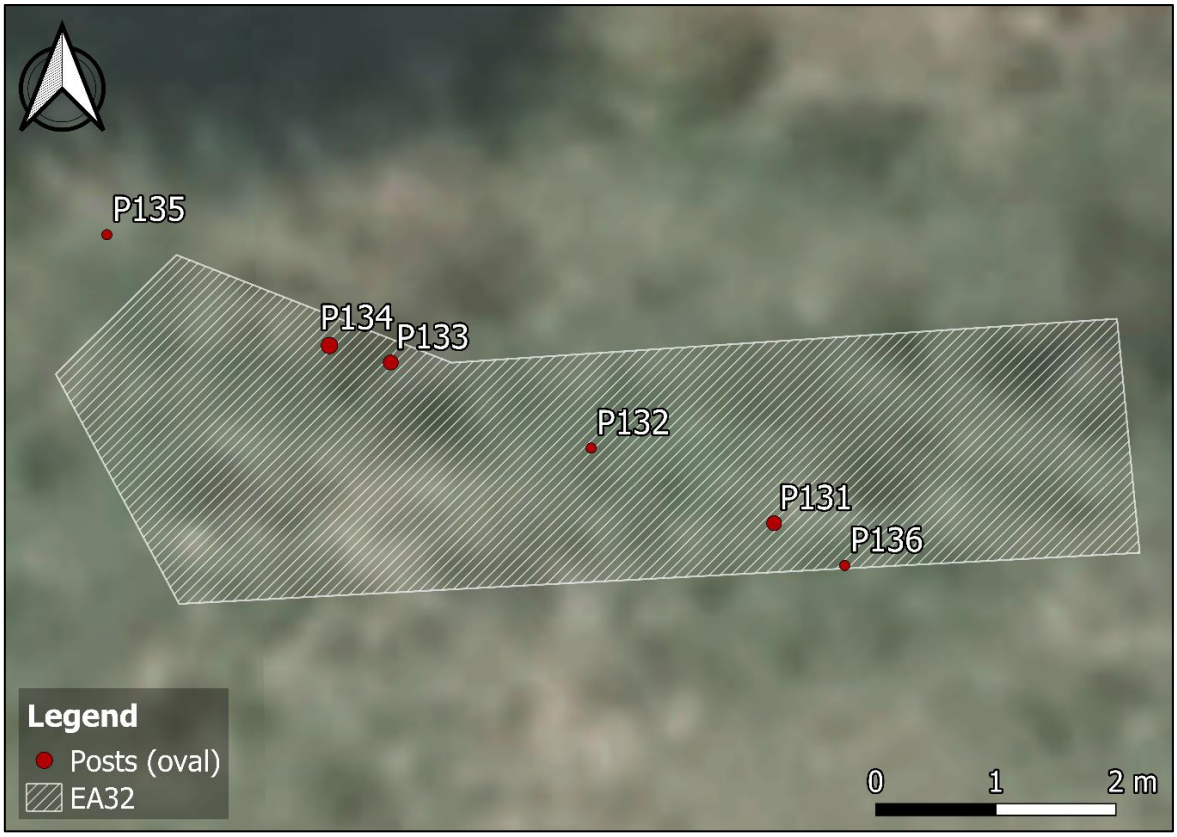

Figure 9.1.7. A plan drawing of EA32.

9.1.1 Extraction, Recording and Sampling

Given the limited number of posts identified, all six were selected for extraction (Table 9.1.1). All were observed to be poorly preserved, with the distal end of three posts lost due to substantial decay (Figure 9.1.8). Partial charring was also identified on the outer surface of TARP133. Three taper types were recorded from the posts that retained their distal ends: one long (Figure 9.1.9), one short and one irregular (Figure 9.1.10). Despite the condition of these posts, evidence of bark retention suggested Felling Dates could still be produced if the samples could pass the condition assessment and survive sample preparation, tree-ring analysis and ^{14}C pretreatment. Therefore, the four best-preserved posts were sampled.

Table 9.1.1. Extracted posts from EA32 at Taraheke pā.

Post ID	Cross section	Max length (cm)	Diameter (cm)	Taper shape	Condition	Sampled
TARP131	Oval	81	16.7	Short	Suitable for sampling	Yes
TARP132	Round	151	11.4	Long	Suitable for sampling	Yes
TARP133	Round	86	17.6	N.A	Suitable for sampling	Yes
TARP134	Oval	110	20.0	Irregular	Suitable for sampling	Yes
TARP135*	Oval	-	15.8	-	Poor Preservation	No
TARP136*	Oval	-	-	-	Poor Preservation	No

*Note. * indicates posts that were extracted but not sampled.*

Figure 9.1.8. A post-extraction photograph of TARP135

Figure 9.1.9. A post-extraction photograph of TARP132.

Figure 9.1.10. A post-extraction photograph of TARP134.

9.2 Species Identification

Thin-section microscopy of the post assemblage (four posts) sampled from Taraheke Pā identified two tree species: miro (*P. ferruginea*) and matai (*P. taxifolia*) (Table 9.2.1). Both species are typical of the forests throughout the North and South islands, and were typically found on the drier substrates of the hills surrounding the rivers and lakes of the Middle Waikato Basin (Table 5.3.2).

Table 9.2.1. Tree species identified in the post assemblage from TAR.

Post ID	Common Name	Scientific Name
TARP131	miro	*Prumnopitys ferruginea*
TARP132	miro	*Prumnopitys ferruginea*
TARP133	matai	*Prumnopitys taxifolia*
TARP134	matai	*Prumnopitys taxifolia*

9.3 Condition Assessment

All four prepared post samples were inspected under a low-powered light microscope to assess their condition and suitability for tree-ring analysis, ring-block sampling, and AMS radiocarbon dating (see Section 5.5 and Table 9.3.1). Following this assessment, two samples were determined to be of poor quality and excluded from further analysis: TARP133 and TARP134. The characteristics of the remaining two samples are discussed in Section 9.4 below.

Table 9.3.1. TAR subsample condition assessment.

Post ID	Poor preservation	Charring present	Scaring present	Dark staining	Growth anomalies	Passed
TARP131	☐	☐	☑	☑	☑	Yes
TARP132	☐	☐	☐	☑	☑	Yes
TARP133*	☑	☑	☑	☑	☑	No
TARP134*	☑	☐	☐	☐	☑	No

*Note. * indicates samples excluded from tree-ring analysis due to unsuitable characteristics.*

9.4 Tree Ring Analysis Results (TAR)

The reconciled ring count information for each post sample in the TAR assemblage is summarised in Table 9.4.1 (see Section 5.6 for method). The reconciled ring counts presented below represent the most accurate information attainable for these samples, with any persistent inconsistencies discussed further in Section 9.5.

Table 9.4.1. A summary of the reconciled ring count information for the posts sampled from TAR

Post ID	Species ID	Reconciled ring count	Diameter (cm)
TARP131	Miro (*P. ferruginea)*	165	16.7
TARP132	Miro (*P. ferruginea)*	73	11.4

9.4.1 TARP131 (miro, *P. ferruginea*)

A damaged oval cross-section, central pith location and concentric ring pattern characterised TARP131. Episodes of tree-ring suppression, locally absent rings and dark staining were prevalent throughout the growth sequence, impacting tree-ring clarity within these areas (Figure 9.4.1). Tree ring count and measurement analysis identified several locally absent tree rings, particularly affecting the ring count for Tracks B and C (Table 9.4.2). However, the three measured radii could be reconciled, resulting in a final ring count of 165. Eight ring-block samples were collected at semi-regular intervals throughout the tree-ring growth sequence (Table 9.4.3). Larger ring gaps were necessary between specific samples owing to narrow annual growth periods, and ideal sampling locations were limited. These growth characteristics resulted in four ring-block samples containing more or fewer than five tree rings.

Figure 9.4.1. Digital scan of TARP131.

Table 9.4.2. Ring count information for TARP131.

Ring Counts	Track A	Track B	Track C	Reconciled
TARP131	165	140	127	165

Table 9.4.3. Ring-block sampling information for TARP131.

Wk number	Sample code	First ring	Middle ring	Last ring	# of rings in block	Ring gap to next sample
52368	74_TARP131 (1–5)	1	3	5	5	16
52862	75_TARP131 (17–21)	17	19	21	5	24
52369	76_TARP131 (41–45)	41	43	45	5	18.5
52863	77_TARP131 (59–64)	59	61.5	64	6	23.5
52370	78_TARP131 (83–87)	83	85	87	5	35.5
52371	79_TARP131 (119–122)	119	120.5	122	4	25
52864	80_TARP131 (143–148)	143	145.5	148	6	18.5
52372	81_TARP131 (163–165)	163	164	165	3	1.5

9.4.2 TARP132 (miro, *P. ferruginea*)

A round cross-section, central pith location and concentric tree-ring growth pattern characterised TARP132. A large scar was also present, affecting a portion of the tree-ring growth sequence. Consequentially, tree-ring suppression and locally absent rings were prevalent, particularly late in the growth sequence. Dark staining was also present late in the growth sequence (youngest tree rings), affecting tree-ring clarity in this area (Figure 9.4.2). Tree-ring analysis identified minor ring count differences between the three measured radii, resulting from locally absent rings in specific periods (Table 9.4.4). Reconciliation of these three tracks resulted in a final ring count of 73, with four ring-block samples collected at regular intervals throughout the tree-ring growth sequence (Table 9.4.5). Unfortunately, ideal sampling locations were limited, and only four ring-block samples could be collected due to the substantial periods of tree-ring suppression. No sampling errors were identified across any of the ring-block samples, and all four ring-block samples contained five tree rings.

Figure 9.4.2. Digital scan of TARP132.

Table 9.4.4. Ring count information for TARP132.

Ring Counts	Track A	Track B	Track C	Reconciled
TARP132	73	66	64	73

Table 9.4.5. Ring-block sampling information for TARP132.

Wk number	Sample code	First ring	Middle ring	Last ring	# of rings in block	Ring gap to next sample
52363	69_TARP132 (1–5)	1	3	5	5	14
52364	70_TARP132 (15–19)	15	17	19	5	16
52365	71_TARP132 (31–35)	31	33	35	5	38
52367	73_TARP132 (69–73)	69	71	73	5	2.5

9.5 Wiggle-Match Dating Results

This section presents the WMD results for the post-assemblage (two posts) sampled from TAR (see Section 5.8.2 for method). The full array of OxCal codes relating to each post analysed can be viewed in Appendix D.4. The interpretation of each WMD is discussed in detail below.

9.5.1 TARP131

The D_Sequence model for TARP131 comprises eight AMS ^{14}C dates, separated by known calendar intervals, spread across the 165-year tree-ring growth sequence (Table 9.5.1). The Felling Date for TARP131 has a median calibrated age of AD 1556 ± 4, with a modelled date range between AD 1549–1564 (HPD 95%). No outliers were detected during the analysis. However, the model only just passes the A_{comb} (An) threshold. Generally, the WMD reflects the shape of SHCal20 (Figure 9.5.1). However, the last two ^{14}C dates within the D_Sequence series are offset from SHCal20, with a calendar position over the calibration plateau in the late sixteenth century. Initially, these offsets appear to be of concern, primarily because the last ^{14}C date defines the calendar position of the modelled Felling Date. Tree-ring analysis of TARP131 identified multiple episodes of tree-ring suppression and locally absent rings throughout the growth sequence. However, the last two ring-block samples were collected across the final 43 tree rings (after sample 79_TARP131 (119–122), rings 143–148 and 163–165), which, compared to other periods of growth were not overly narrow or poorly defined. When considering how many potential 'missing' tree rings would be required to shift the calendar placement of these two ^{14}C dates to match the shape of SHCal20 (to a calendar position in the

early 1600s), it is apparent that a substantial number of tree rings would have to be added to the reconciled ring count (Figure 9.5.2).

Table 9.5.1. D_Sequence (SSimple) result for TARP131.

Wk number	Sample code	^{14}C Age (BP)	Outlier analysis (Posterior/Prior)	Convergence
52368	74_TARP131 (1–5)	625 ± 23	5/5	99
52862	75_TARP131 (17–21)	617 ± 25	5/5	99
52369	76_TARP131 (41–45)	551 ± 23	5/5	99
52863	77_TARP131 (59–64)	459 ± 22	5/5	99
52370	78_TARP131 (83–87)	439 ± 21	5/5	99
52371	79_TARP131 (119–122)	356 ± 22	5/5	99
52864	80_TARP131 (143–148)	412 ± 21	5/5	99
52372	81_TARP131 (163–165)	318 ± 22	5/5	99

Felling Date Results

Median cal. Age (AD)	HPD 68%	HPD 95%	A_{comb} (An)
1556 ± 4	AD 1552–1560	AD 1549–1564	25.3 (25)

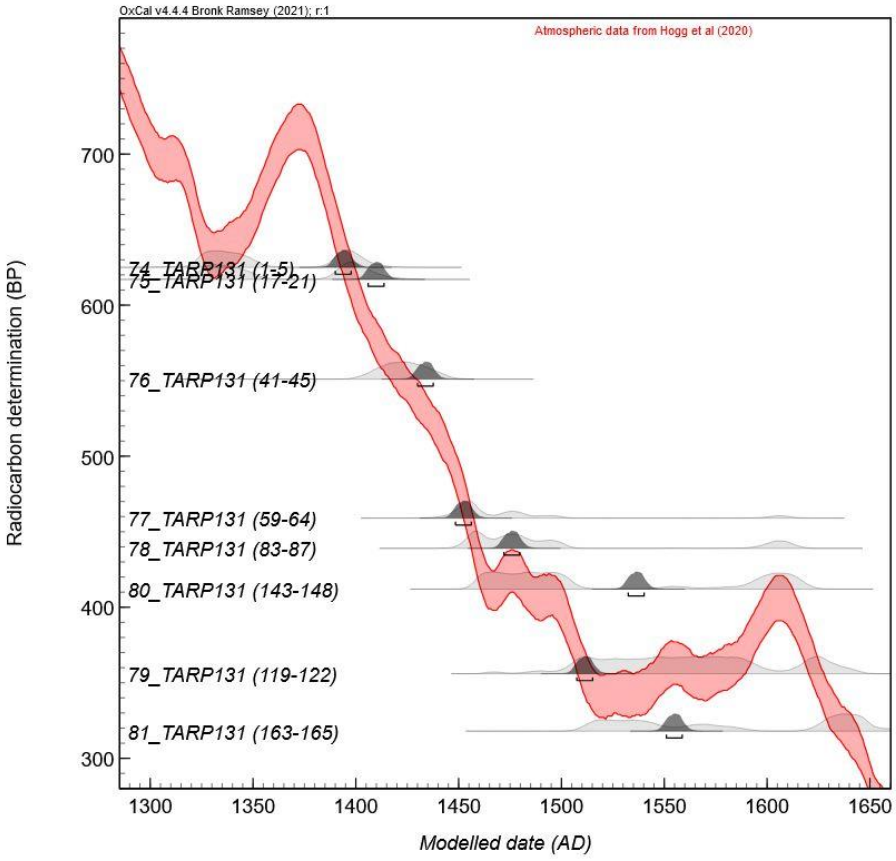

Figure 9.5.1. OxCal generated curve plot of the D_Sequence model for TARP131.

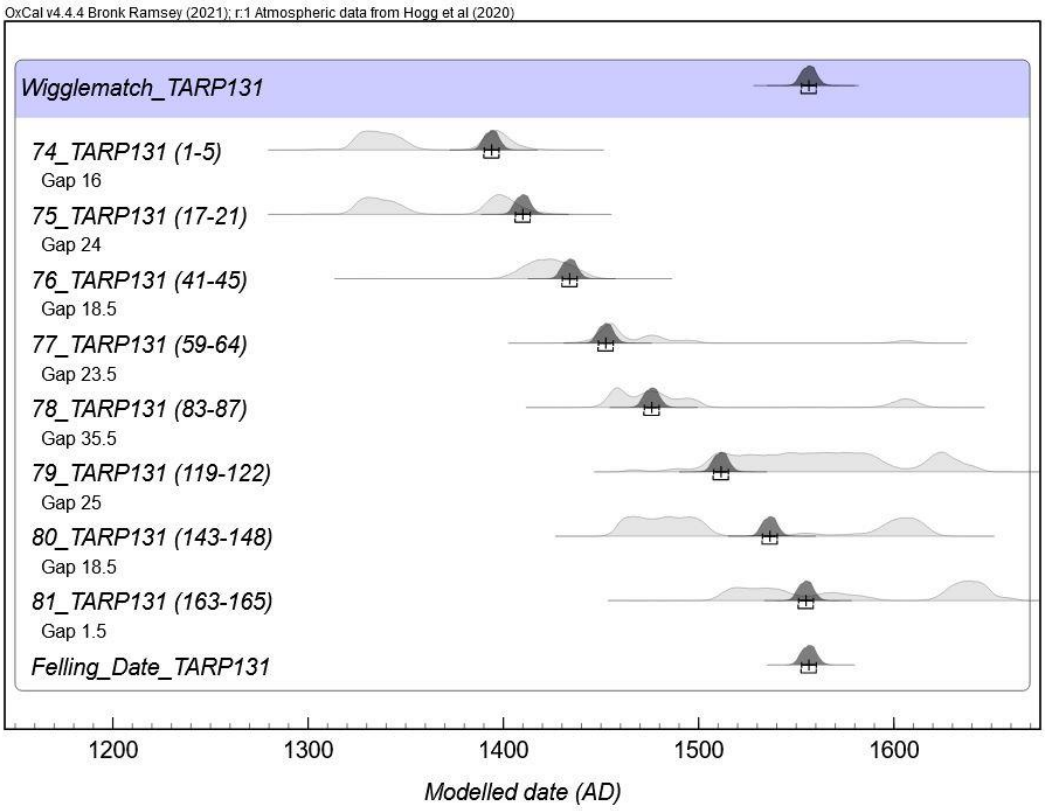

Figure 9.5.2. OxCal generated multiplot of the D_Sequence model for TARP131.

As the first six ^{14}C dates within the D_Sequence series all match the shape of SHCal20 well, all of the (potential) 'missing' tree rings would have to be accounted for across the last 43 rings. Additional ring count checks could not identify inconsistencies within the reconciled ring count data. When the D_Sequence model for TARP131 was calibrated using the RScaled outlier model, the resulting Felling Date produced results consistent with the original model. Therefore, as neither of these two offset ^{14}C dates were identified as outliers during the original analysis, and as they are positioned across the sixteenth century calibration plateau, the original Felling Date is determined accurate. Therefore, the WMD for TARP131 is included in the local and regional scale analyses.

9.5.2 TARP132

The D_Sequence model for TARP132 comprises four AMS ^{14}C dates, separated by known calendar intervals, spread across the 73-year tree-ring growth sequence (Table 9.5.2). The Felling Date of TARP132 reports a median calibrated age of AD 1514 ± 9, with a modelled date range between AD 1502–1535 (HPD 95%). No outliers were detected during the analysis,

the model passed the A_{comb} (An) threshold, and the convergence values generated by the OxCal model remained uniformly high (100%). Additionally, the WMD reflects the shape of SHCa20 (Figure 9.5.3), with no substantial offsets identified, which is reflected in the comparison of the posterior and likelihood distributions (Figure 9.5.4). Finally, when the D_Sequence model was calibrated using alternative outlier detection methods (see Appendix D.4.2), the resulting Felling Dates were consistent with the original model, with no outliers detected and universally good agreement (>60). Therefore, the WMD for TARP132 is interpreted as accurate and is included in the local and regional scale analyses.

Table 9.5.2. D_Sequence (SSimple) result for TARP132.

Wk number	Sample code	^{14}C Age (BP)	Outlier analysis (Posterior/Prior)	Convergence
52363	69_TARP132 (1–5)	468 ± 21	5/5	100
52364	70_TARP132 (15–19)	475 ± 26	5/5	100
52365	71_TARP132 (31–35)	410 ± 21	5/5	100
52367	73_TARP132 (69–73)	375 ± 21	5/5	100
Felling Date Results				
Median cal. age (AD)	HPD 68%		HPD 95%	A_{comb} (An)
1514 ± 9	AD 1506–1528		AD 1502–1535	88.6 (35.4)

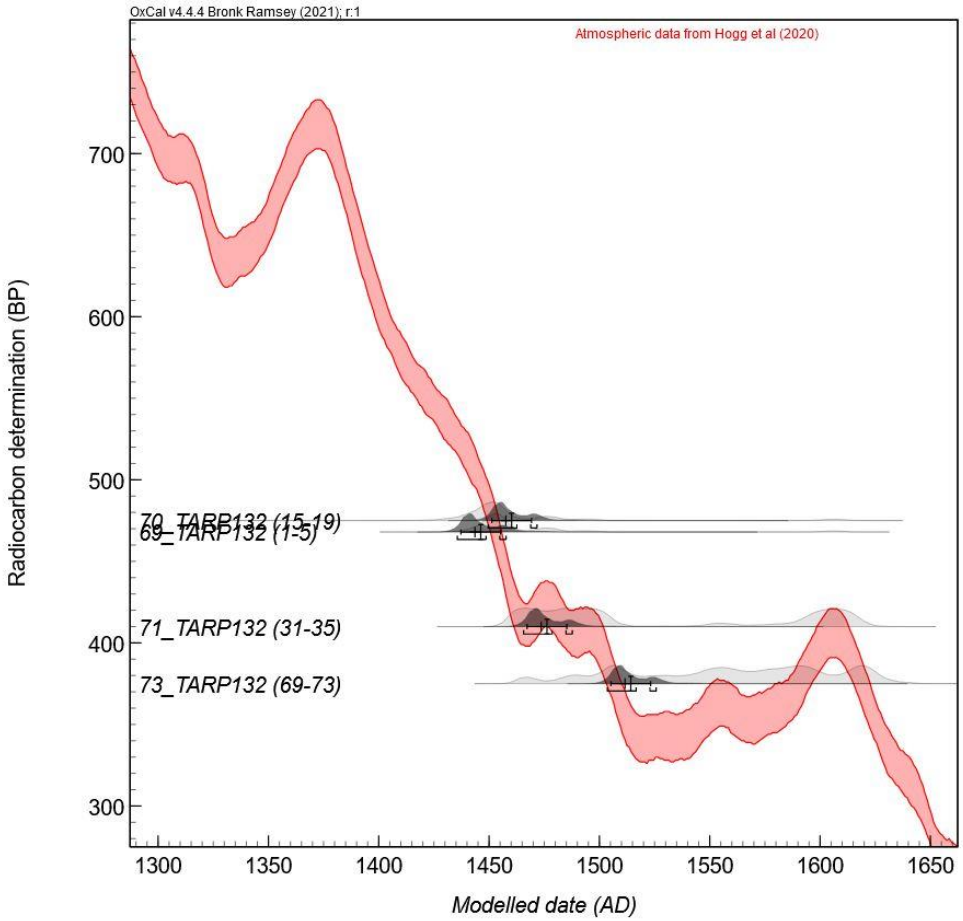

Figure 9.5.3. OxCal generated curve plot of the D_Sequence model for TARP132.

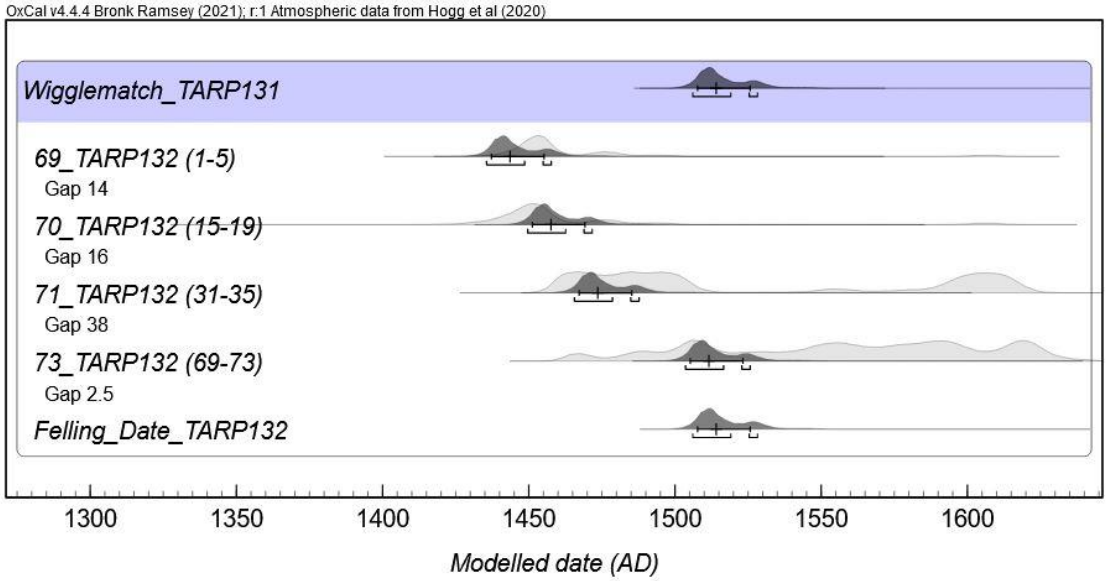

Figure 9.5.4. OxCal generated multiplot of the D_Sequence model for TARP132.

9.5.3 Summary

Table 9.5.3 summarises the WMD results for the post-assemblage (two posts) sampled from TAR. As these Felling Dates do not represent palisade construction events, they can only be interpreted as construction events relating to the structure extending into the adjacent stream. However, it is plausible that this activity still represents the site's occupation as a pā. As discussed above, both Felling Dates are interpreted as accurate. First, the WMD of TARP131 indicates that this structure was first constructed during the early 1500s. Second, the WMD of TARP132 indicates that this structure was repaired during the middle 1500s. This hypothesis will be tested during the local scale analysis in Section 12.1.5.

Table 9.5.3. Summary of wiggle-match dating results from TAR.

Post ID	Convergence	Felling Date (HPD)		Median cal. age (AD)
		68% Probability	95% Probability	
TARP131	99.4	AD 1552–1560	AD 1549–1564	1556 ± 4
TARP132	99.6	AD 1506–1528	AD 1510–1557	1514 ± 9

Chapter 10. Te Uapata Pā (TEU)

10.1 Archaeological Excavations at TEU (S14/20)

Excavations at Te Uapata Pā were conducted over one field season in March 2021. Investigations primarily focused on the eastern stream bank at the base of the headland, where a preserved palisade row was previously identified during an initial site visit. Once the dense vegetation cover was removed from this area, the full extent of the *in situ* palisade row was visible (Figure 10.1.1). Additional efforts were made to identify palisade posts along the western stream bank, including four exploratory excavation areas (EA54–57) positioned at regular intervals along the length of the headland. Each excavation area covered an area of 3 x 2 m, excavated to a depth of 30 cm (Figure 10.1.2). However, no archaeological material was encountered in any of these areas, and it was determined that while palisade defences were likely once present along the western side of the pā, they have probably succumbed to decay due to the fluctuating water levels of the adjacent stream.

Figure 10.1.1. Zac McIvor (right) and Alan Hogg (left) clear vegetation on the eastern side of Te Uapata Pā.

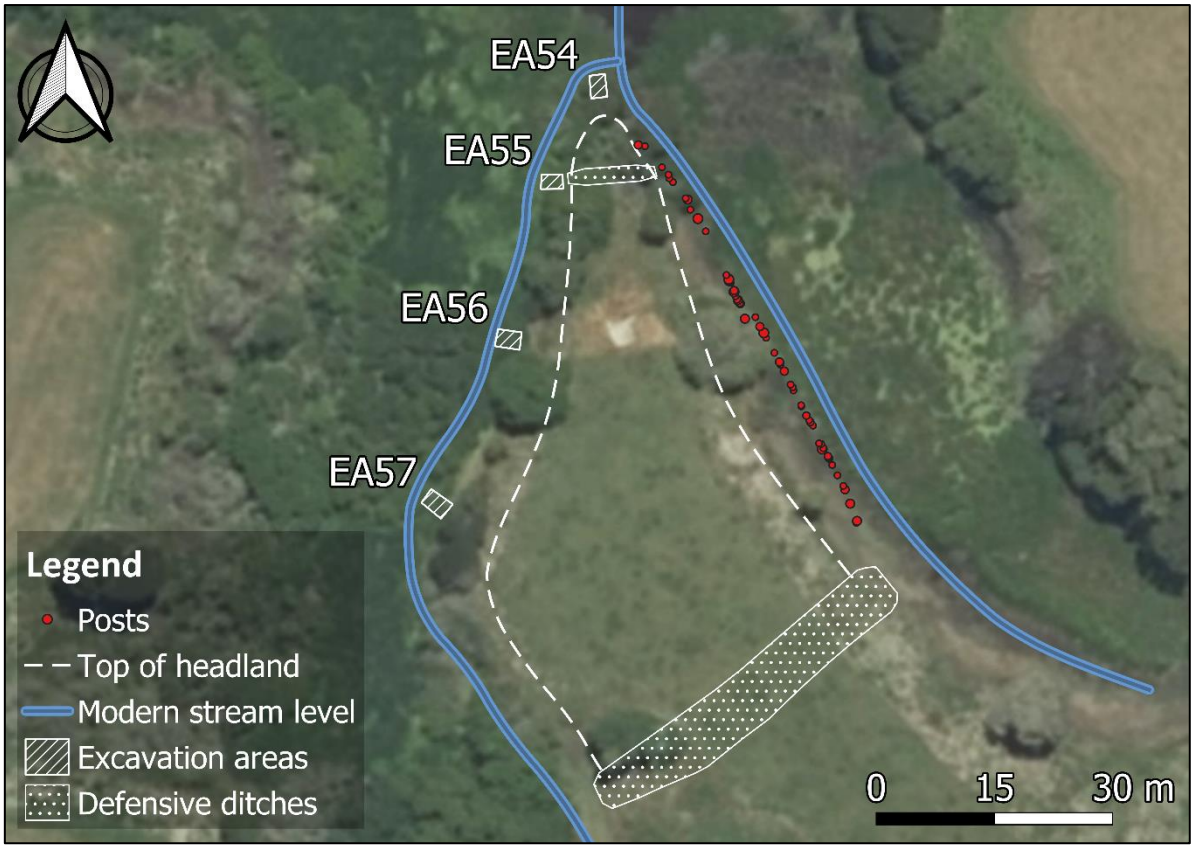

Figure 10.1.2. A site plan of Te Uapata Pā[44].

10.1.1 Extraction, Recording and Sampling

Fifty-three posts were identified within the palisade alignment along the eastern toe of the pā, ranging from the southern defensive ditch towards the northern tip of the headland (Figure 10.1.3). The posts form a single palisade row, which overlaps halfway up the side of the pā. This overlapped section of the palisade row is interpreted as a small entrance to the pā, facilitating access from the adjacent stream. This entranceway splits the palisade alignment into a northern and southern section, with both sections targeted for sampling to determine if they represent different construction events.

[44] This figure contains data sourced from the LINZ Data Service, licenced for reuse under the CC BY 4.0.

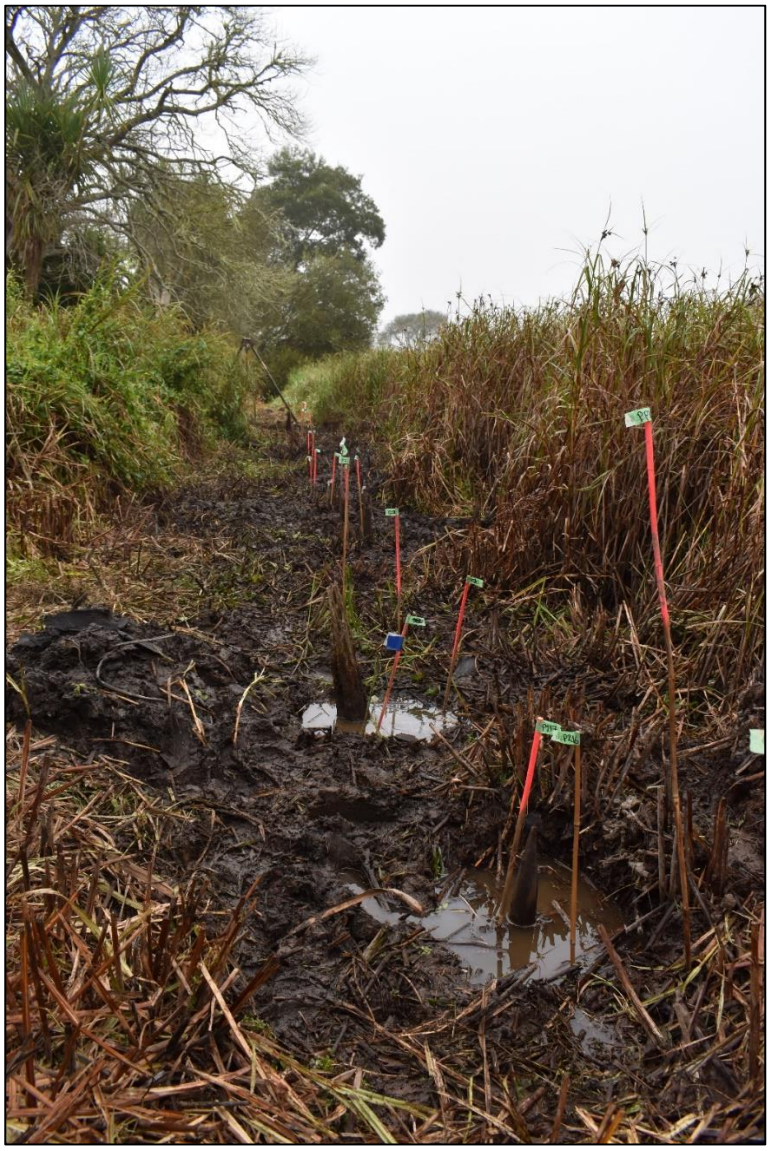

Figure 10.1.3. Looking north along the palisade alignment located on the eastern side of TEU.

Eight posts were selected for extraction (Figure 10.1.4 and Figure 10.1.5), with their recorded data summarised in Table 10.1.1. Interestingly, all 53 posts recorded at Te Uapata exhibited a round or oval cross-section, with no split or adze-dressed posts identified. Additionally, no posts were observed to be charred on their outer surface, including the tapered ends of extracted posts. Finally, two taper types were recorded: six long (Figure 10.1.6) and two short (Figure 10.1.7). One extracted post stood out compared to the rest of the assemblage (TEUP237), exhibiting an irregular shape with a distinct kink along its length (Figure 10.1.8). This observation was the only post identified at Te Uapata with this characteristic. However, posts of similar form were identified at MA2 (see Section 7.1). Finally, seven posts were sampled for analysis.

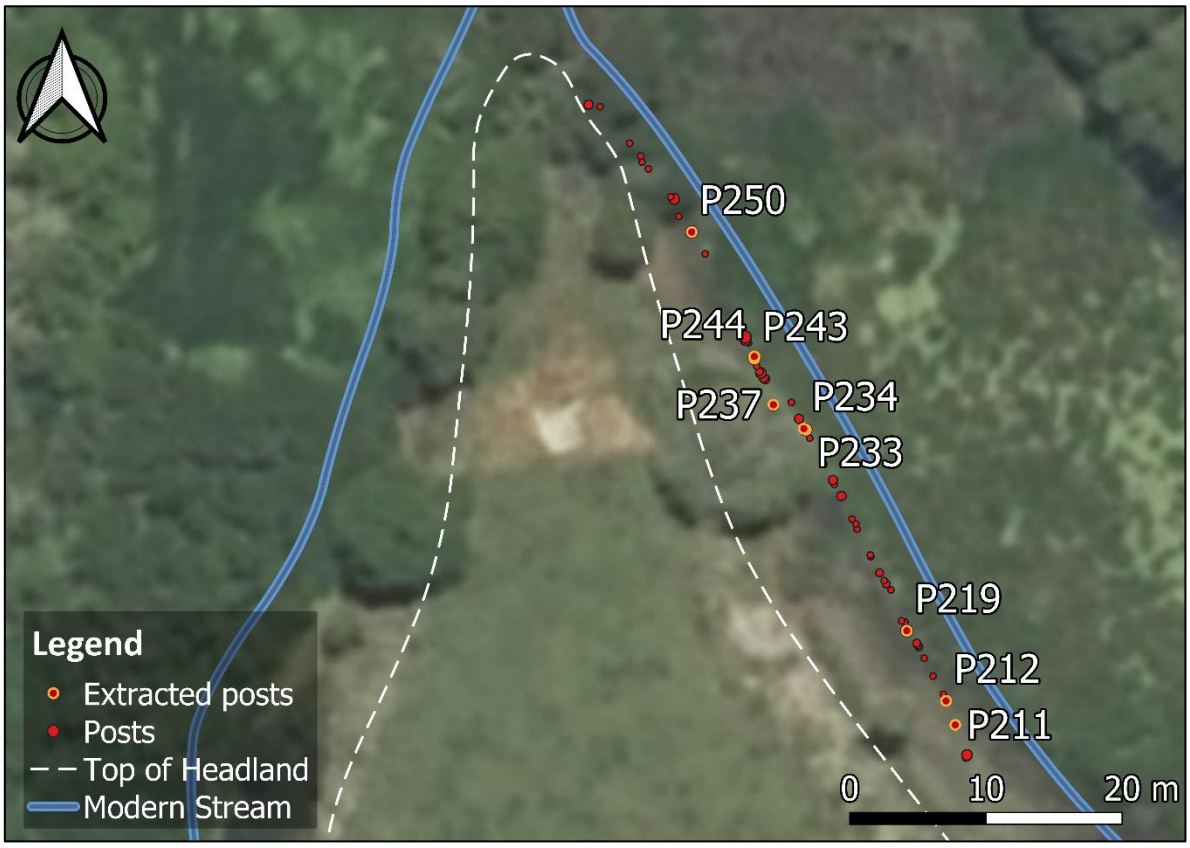

Figure 10.1.4. Location of the extracted posts at Te Uapata Pā[45].

Table 10.1.1. Recorded information for extracted posts from TEU.

Post ID	Cross section	Max length (cm)	Diameter (cm)	Taper shape	Condition	Sampled
TEUP211	Round	121	11.3	Long	Suitable for sampling	Yes
TEUP212*	Round	125	9.8	Long	Poor preservation	No
TEUP219	Round	222	14.3	Long	Suitable for sampling	Yes
TEUP233	Round	248	15.0	Long	Suitable for sampling	Yes
TEUP234	Round	249	15.1	Long	Suitable for sampling	Yes
TEUP237	Round	170	12.1	Long	Suitable for sampling	Yes
TEUP243	Oval	124	13.5	Short	Suitable for sampling	Yes
TEUP244	Round	191	9.5	Short	Suitable for sampling	Yes
TEUP250*	Round	189	15.8	Long	Species: rewarewa	No

*Note. *indicates posts dropped from tree-ring analysis due to unsuitable characteristics.*

[45] This figure contains data sourced from the LINZ Data Service, licenced for reuse under the CC BY 4.0.

Figure 10.1.5. Warren Gumbely (left) and Alan Hogg (right) extract a post at Te Uapata Pā.

Figure 10.1.6. post-extraction photograph of the distal end of TEUP243.

Figure 10.1.7. post-extraction photograph of the distal end of TEUP234.

Figure 10.1.8. Post-extraction photograph of TEUP237.

10.2 Species Identification

Thin-section microscopy of the post assemblage (7 posts) sampled from Te Uapata Pā identified four unique tree species: matai (*P. taxifolia*), miro (*P. ferruginea*), pukatea (*L. novae-zelandiae*) and rimu (*D. cupressinum*) (Table 10.2.1). All four species are large trees generally

found in the lowland forests of the North and South Islands and are typical species found in swampy environments and drier substrates of the hills surrounding the rivers and lakes of the Middle Waikato Basin (Table 5.3.2). Two samples could not be identified at the species level (TEUP241 and TEUP243). However, both were identified as softwood and are likely conifers. Both samples suffered from cellular collapse, resulting from the decay, limiting the visibility of the unique cellular structures associated with each species. Given these samples' poor condition, they were dropped from analysis.

Table 10.2.1. Tree species identified in the post assemblage from TEU.

Post ID	Common name	Scientific name
TEUP219	matai	*Prumnopitys taxifolia*
TEUP233	miro	*Prumnopitys ferruginea*
TEUP234	miro	*Prumnopitys ferruginea*
TEUP237	pukatea	*Laurelia novae-zelandiae*
TEUP241*	gymnosperm (conifer)	-
TEUP243*	gymnosperm (conifer)	-
TEUP244	rimu	*Dacrydium cupressinum*

*Note. *indicates samples that could not be identified to species levels.*

10.3 Condition Assessment

All five prepared post samples were inspected under a low-powered light microscope to assess their condition and suitability for tree-ring analysis, ring-block sampling, and AMS radiocarbon dating (see Section 5.5 and Table 10.3.1). Following this assessment, two samples were determined to be of poor quality and were excluded from further analysis: TEUP233 and TEUP237.

Table 10.3.1. TEU sample condition assessment.

Post ID	Poor preservation	Charring present	Scaring present	Dark staining	Growth anomalies	Passed
TEUP219	☐	☐	☐	☑	☑	Yes
TEUP233*	☑	☐	☐	☑	☑	No
TEUP234	☐	☐	☐	☑	☑	Yes
TEUP237*	☑	☐	☐	☐	☑	No
TEUP244	☐	☐	☐	☑	☑	Yes

*Note. * Indicates samples excluded from tree ring analysis due to unsuitable characteristics.*

10.4 Tree Ring Analysis Results

The reconciled ring count information for each post sample in the TEU assemblage is summarised in Table 10.4.1 (see Section 5.6 for method). The ring counts presented below represent the most accurate information attainable for these samples, with any persistent inconsistencies discussed further in Section 10.5.

Table 10.4.1. A summary of the reconciled ring count information for the posts sampled from TEU.

Post ID	Species ID	Reconciled Ring count	Diameter (cm)
TEUP219	Matai (*P. taxifolia*)	166	14.3
TEUP234	Miro (*P. ferruginea*)	171	13.5
TEUP244	Rimu (*D. cupressinum*)	65	9.5

10.4.1 TEUP219 (matai, *P. taxifolia*)

TEUP219 presented a round cross-sectional shape, off-centre pith location and concentric ring pattern. Dark staining and a small scar affected the early (innermost) period of growth, resulting in tree-ring suppression and locally absent rings (Figure 10.4.1). Additionally, the youngest (outermost) 20 tree rings were particularly slow-growing (narrow), with poorly defined ring boundaries. Consequently, the ring count of Track C was affected by locally absent rings, with considerable ring count differences when compared to Track A and B (Table 10.4.2). Tree ring count and measurement analyses resulted in a reconciled ring count of 166, with seven ring-block samples collected at semi-regular intervals across the tree ring growth sequence (Table 10.4.3). Considering the narrow growth characteristics of the outermost 20 tree rings, it was determined that attempting to sample the last five tree rings would likely result in sampling errors. Therefore, instead of sampling the last five tree rings, the five largest tree rings within this youngest growth period were targeted (rings 148–152), with the remaining tree rings (to the terminal growth ring) added to the final gap in the D_Sequence model. As a result, no sampling errors were identified across any of the ring-block samples, and all 7 contained five tree rings.

Figure 10.4.1. Digital scan of TEUP219.

Table 10.4.2.Ring count information for TEUP219

Ring Counts	Track A	Track B	Track C	Reconciled
TEUP219	166	166	143	166

Table 10.4.3. Ring-block sampling information for TEUP219.

Wk number	Sample code	First ring	Middle ring	Last ring	# of rings in block	Ring gap to next sample
52870	87_TEUP219 (6–10)	6	8	10	5	19
52871	88_TEUP219 (25–29)	25	27	29	5	45
52872	89_TEUP219 (70–74)	70	72	74	5	34
52873	90_TEUP219 (104–108)	104	106	108	5	13
52874	91_TEUP219 (117–121)	117	119	121	5	13
52875	92_TEUP219 (130–134)	130	132	134	5	18
52876	93_TEUP219 (148–152)	148	150	152	5	16.5

Note. Sample 93_TEUP219 (148–152) does not contain the outermost five tree rings.

10.4.2 TEUP234 (miro, *P. ferruginea*)

TEUP234 presented a round cross-sectional shape, off-centre pith location, and concentric tree-ring growth pattern. Abnormal late and early wood colouring and dark staining were present across the growth sequence, along with areas of tree-ring suppression and locally absent rings that were prominent within the innermost (oldest) rings in the growth sequence (Figure 10.4.2). These characteristics resulted in a challenging tree-ring growth sequence to count and measure accurately, with locally absent rings affecting the ring count of Track C (Table 10.4.4). Reconciliation of the three measured radii resulted in a final ring count of 171, with eight ring-block samples collected across the growth sequence (Table 10.4.5). The last 13 tree rings were very narrow, making it difficult to sample the last five tree rings accurately. Therefore, rings 156–160 were sampled, with the remaining tree rings (to the terminal tree ring) added to the final gap in the D_Sequence model. Consequentially, no sampling errors were identified across any ring-block samples; all eight contained five tree rings.

Figure 10.4.2. Digital scan of TEUP234.

Table 10.4.4. Tree ring count information for TEUP234.

Ring Counts	Track A	Track B	Track C	Reconciled
TEUP234	170	171	139	171

Table 10.4.5. Ring-block sampling information for TEUP234.

Wk number	Sample code	First ring	Middle ring	Last ring	# of rings in block	Ring gap to next sample
52877	94_TEUP234 (6–10)	6	8	10	5	15
52878	95_TEUP234 (21–25)	21	23	25	5	79
52879	96_TEUP234 (100–104)	100	102	104	5	15
52880	97_TEUP234 (115–119)	115	117	119	5	16
52881	98_TEUP234 (131–135)	131	133	135	5	9
52882	99_TEUP234 (140–144)	140	142	144	5	10
52883	100_TEUP234 (150–154)	150	152	154	5	6
52884	101_TEUP234 (156–160)	156	158	160	5	13.5

Note. Sample 101_TEUP234 (156–160) does not contain the outermost five tree rings.

10.4.3 TEUP244 (rimu, *D. cupressinum*)

TEUP244 presented a round cross-sectional shape, central pith location and concentric tree ring growth pattern. Dark staining was present across the growth sequence, particularly affecting the innermost (oldest) tree rings and impacting the tree ring clarity in this period of growth. The outermost (youngest) tree rings also exhibited faint tree-ring boundaries, further limiting the tree-ring clarity of the growth sequence (Figure 10.4.3). These characteristics made tree-ring analysis challenging. However, reconciliation of the three measured radii was achieved, resulting in a final ring count of 65 (Table 10.4.6). Five ring-block samples were sampled at regular intervals across the growth sequence (Table 10.4.7). No sampling errors were identified across any ring-block samples; all five samples contained five tree rings.

Figure 10.4.3. Digital scan of TEUP244.

Table 10.4.6. Ring count information for TEUP244.

Ring Counts	Track A	Track B	Track C	Reconciled
TEUP244	65	64	64	65

Table 10.4.7. Ring-block sampling information for TEUP244.

Wk number	Sample code	First ring	Middle ring	Last ring	# of rings in block	Ring gap to next sample
52865	82_TEUP244 (1–15)	1	3	5	5	20
52866	83_TEUP244 (21–25)	21	23	25	5	15
52867	84_TEUP244 (36–40)	36	38	40	5	13
52868	85_TEUP244 (49–53)	49	51	53	5	12
52869	86_TEUP244 (61–65)	61	63	65	5	2.5

10.5 Wiggle-Match Dating Results

This section presents the WMD results for the post-assemblage (three posts) sampled from TEU (see Section 5.8.2 for method). The full array of OxCal codes relating to each post

analysed can be viewed in Appendix D.5. The interpretation of each WMD is discussed in detail below.

10.5.1 TEUP219

The D_Sequence model for TEUP219 comprises seven AMS ^{14}C dates, separated by known calendar intervals, spread across the posts 166 tree-ring growth sequence (Table 10.5.1). The Felling Date of TEUP219 has a median calibrated age of AD 1773 ± 5, with a modelled date range between AD 1767–1783 (HPD 95%). Two minor outliers were detected and downweighed during the analysis: samples 88_TEUP219 (25–29) and 91_TEUP219 (117–121), and the model did not pass the A_{comb} (An) threshold. When reviewing the curve plot of the analysis, the WMD generally reflects the shape of SHCal20 (Figure 10.5.1). However, several samples are offset from SHCal20, reflected in comparisons between the posterior and likelihood distributions (Figure 10.5.2). While only minor outliers were identified during the analysis, these offsets suggest the possibility of errors in the reconciled ring count affecting the calendar spacing of the ^{14}C dates in the D_Sequence series. Any possible ring count errors could affect the accuracy and precision of the Felling Date for TEUP219, and therefore, this possibility was further investigated.

Table 10.5.1. Original D_Sequence (SSimple) result for TEUP219.

Wk number	Sample code	^{14}C Age (BP)	Outlier Analysis (Posterior/Prior)	Convergence
52870	87_TEUP219 (6–10)	413 ± 21	5/5	100
52871	88_TEUP219 (25–29)	408 ± 21	6/5	100
52872	89_TEUP219 (70–74)	198 ± 23	5/5	100
52873	90_TEUP219 (104–108)	185 ± 21	5/5	100
52874	91_TEUP219 (117–121)	216 ± 21	6/5	100
52875	92_TEUP219 (130–134)	236 ± 21	5/5	100
52876	93_TEUP219 (148–152)	211 ± 22	5/5	100

Felling Date Results

Median cal. Age (AD)	HPD 68%	HPD 95%	A_{comb} (An)
1773 ± 5	AD 1778–1781	AD 1767–1783	9.2 (26.7)

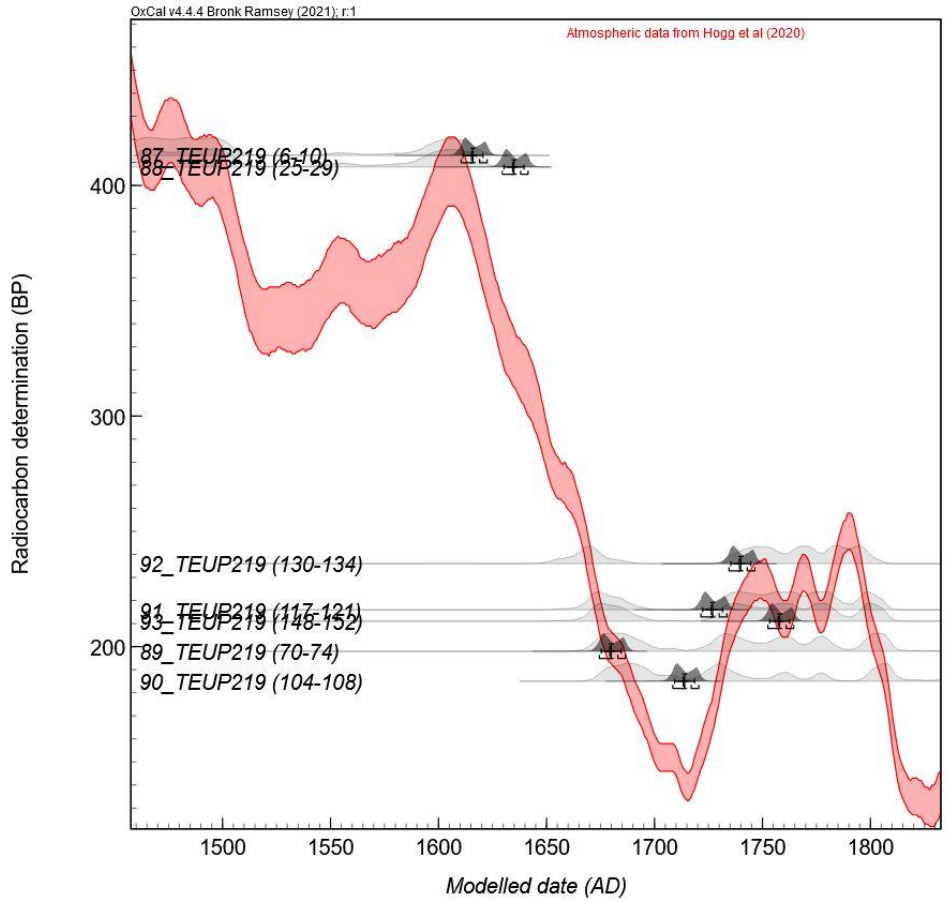

Figure 10.5.1. OxCal generated curve plot of original D_Sequence model for TEUP219.

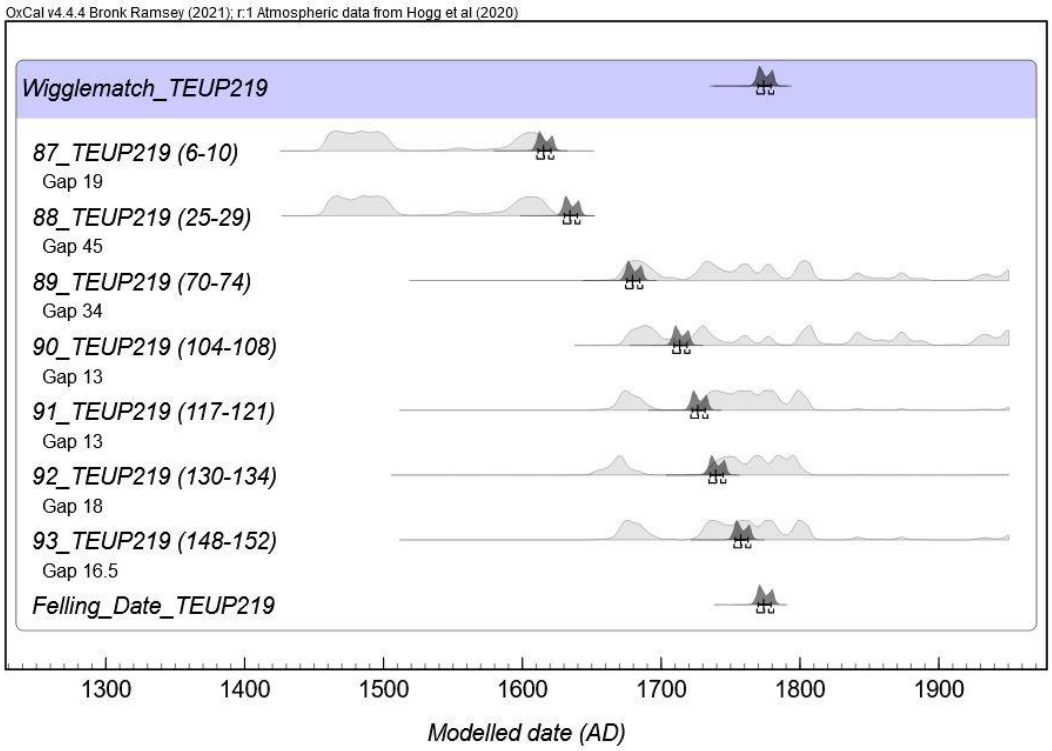

Figure 10.5.2. OxCal generated multiplot of the original D_Sequence model for TEUP219.

As discussed, tree-ring analysis of TEUP219 was challenging, reporting tree-ring suppression and locally absent rings early in the growth sequence (resulting from scarring). Narrow and poorly defined tree-ring boundaries were observed throughout the last 20 rings. However, the effect of these growth anomalies was accounted for during ring-block sampling. When examining the structure of the WMD, additional tree rings between the ^{14}C dates for samples 88_TEUP219 (25–29) and 89_TEUP219 (70–74) could be causing the identified offsets. While errors in the reconciled ring count associated with this early (innermost) portion of growth could not be categorically established, this possibly was investigated further using additional OxCal modelling (see Appendix D.5.2). As samples 87_TEUP219 (6–10) and 88_TEUP219 (25–29) are the first two ^{14}C dates in the D_Sequence series, and the model contains a total of seven ^{14}C dates, these first two ^{14}C dates can be removed from the WMD without affecting the interpretation of the Felling Date. Therefore, the D_Sequence model was recalibrated using only the last five ^{14}C dates. The results of this D_Sequence model report a Felling Date with a median calibrated age of AD 1788 ± 15 and a modelled date range between AD 1776–1827 (95% HPD) (Table 10.5.2). No outliers were identified during the analysis, the model passed the A_{comb} (An) threshold, and convergence remained universally high (99%). Furthermore, the last four ^{14}C dates within the D_Sequence have an improved relationship with SHCal20, as they are no longer offset from the curve (Figure 10.5.3 and Figure 10.5.4).

Table 10.5.2. Updated D_Sequence (SSimple) result for TEUP219.

Wk Number	Sample Code	^{14}C Age (BP)	Outlier Analysis (Posterior/Prior)	Convergence
52872	89_TEUP219 (70–74)	198 ± 23	5/5	99
52873	90_TEUP219 (104–108)	185 ± 21	5/5	99
52874	91_TEUP219 (117–121)	216 ± 21	5/5	99
52875	92_TEUP219 (130–134)	236 ± 21	5/5	99
52876	93_TEUP219 (148–152)	211 ± 22	5/5	99

Felling Date Results

Median cal. Age (AD)	HPD 68%	HPD 95%	A_{comb} (An)
1788 ± 15	AD 1780–1793 (59.4%) AD 1820–1823 (8.9%)	AD 1776–1800 (73.8%) AD 1815–1826 (21.7%)	118 (31.6)

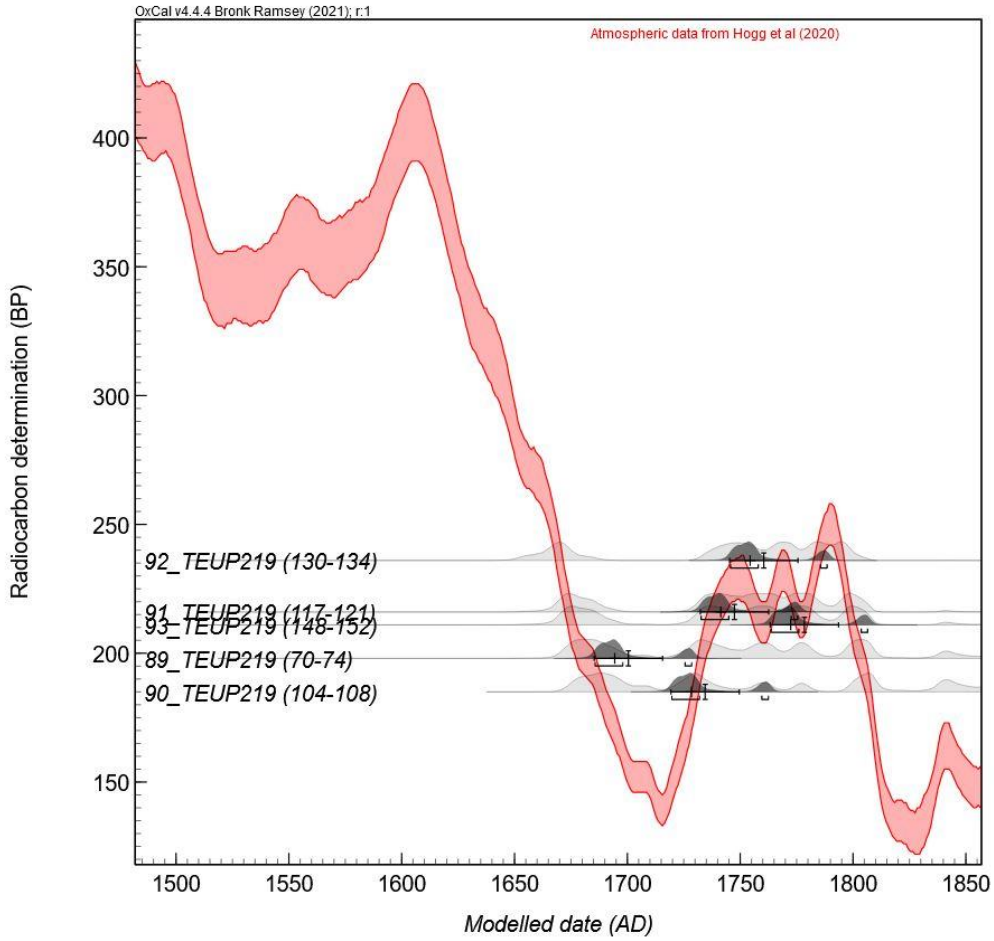

Figure 10.5.3. OxCal generated curve plot of the updated D_Sequence model for TEUP219

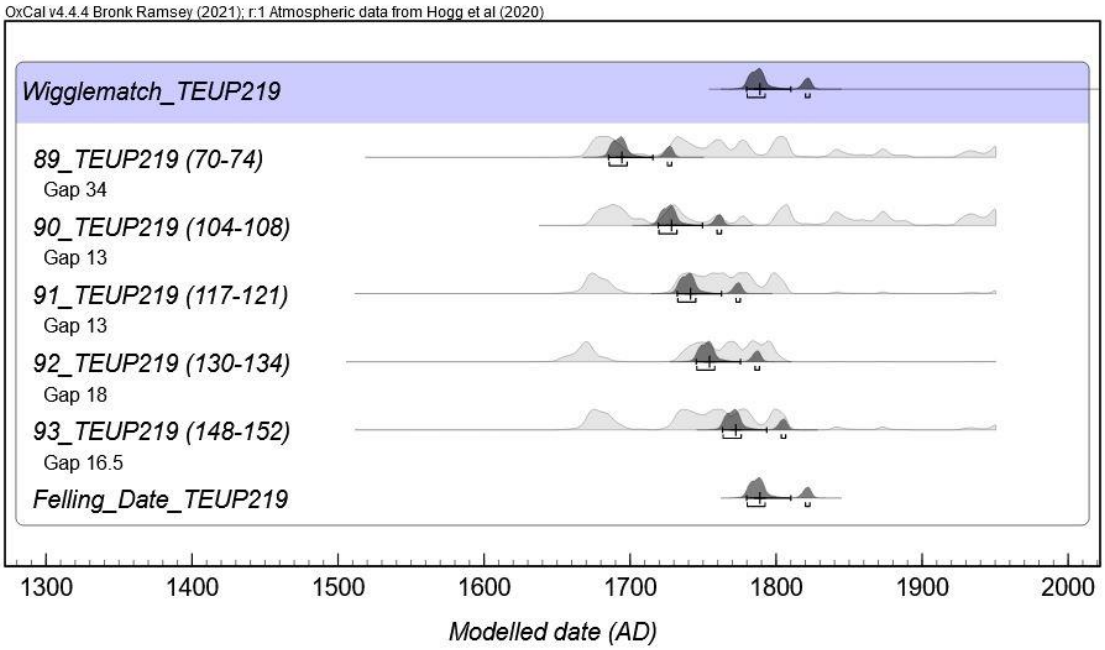

Figure 10.5.4. OxCal generated multiplot of the updated D_Sequence model for TEUP219.

This updated D_Sequence model performs better than the original model (Figure 10.5.4). However, the new Felling Date's precision is decreased owing to its relationship with the calibration plateau in the late eighteenth century, resulting in a bimodal distribution. Despite the decreased precision, the updated D_Sequence produces an older Felling Date compared to the original model, with the results strongly indicating a Felling Date between AD 1780–1793 (68% HPD) (Figure 10.5.4). Therefore, while the model's precision is decreased, this updated D_Sequence model is considered more accurate, as it negates the effects of possible ring count errors from the WMD. Consequently, this updated WMD is included in the local and regional scale analyses (Chapter 12).

10.5.2 TEUP234

The D_Sequence model for TEUP234 comprises eight AMS ^{14}C dates, separated by known calendar intervals, spread across the 171 tree-ring growth sequence (Table 10.5.3). The Felling Date reports a median calibrated age of AD 1778 ± 7, with a modelled date range between AD 1767–1792. Five minor outliers were detected and down-weighted during the analysis: samples 95 TEUP234 (21–25), 96_TEUP234 (100–104), 97_TEUP234 (115–119), 98_TEUP234 (131–135) and 100_TEUP234 (150–154). While all minor, the number of identified outliers suggests a potential problem with the model. The curve plot of the WMD shows that six of the eight ^{14}C dates within the D_Sequence series are offset from SHCal20 (Figure 10.5.5), and all of them show a poor correlation between the posterior and likelihood distributions (Figure 10.5.6). These results indicate that potential ring count errors are affecting the calendar spacing between the ^{14}C dates in the D_Sequence series. Additionally, the ^{14}C age order reversals observed between the last five ^{14}C dates suggest this portion of the WMD should have a calendar position over the calibration plateau in the late eighteenth century. As discussed, tree-ring analysis of TEUP234 identified several limiting growth characteristics, including abnormal late and early wood colouring, episodes of tree-ring suppression, and locally absent rings. Tree-ring suppression was particularly prevalent early (innermost tree rings) in the tree-ring growth sequence. When examining the structure of the WMD, additional 'missing' tree rings between samples 95_TEUP234 (21–25) and 96_TEUP234 (100–104) could be causing the identified offsets and minor outlier results. While errors in the reconciled ring count could not be categorically established, this possibly was investigated further using additional OxCal modelling.

Table 10.5.3. Original D_Sequence (SSimple) result for TEUP234.

Wk number	Sample code	^{14}C Age (BP)	Outlier analysis (Posterior/Prior)	Convergence
52877	94_TEUP234 (6–10)	405 ± 21	5/5	99
52878	95_TEUP234 (21–25)	402 ± 22	6/5	99
52879	96_TEUP234 (100–104)	217 ± 20	6/5	99
52880	97_TEUP234 (115–119)	213 ± 21	6/5	99
52881	98_TEUP234 (131–135)	259 ± 21	6/5	99
52882	99_TEUP234 (140–144)	244 ± 20	5/5	99
52883	100_TEUP234 (150–154)	288 ± 20	6/5	99
52884	101_TEUP234 (156–160)	226 ± 22	5/5	99

Felling Date Results

Median cal. Age (AD)	HPD 68%	HPD 95%	A_{comb} (An)
1778 ± 7	AD 1772–1780 (41.1%) AD 1786–1791 (27.2%)	AD 1767–1792	1.4 (25)

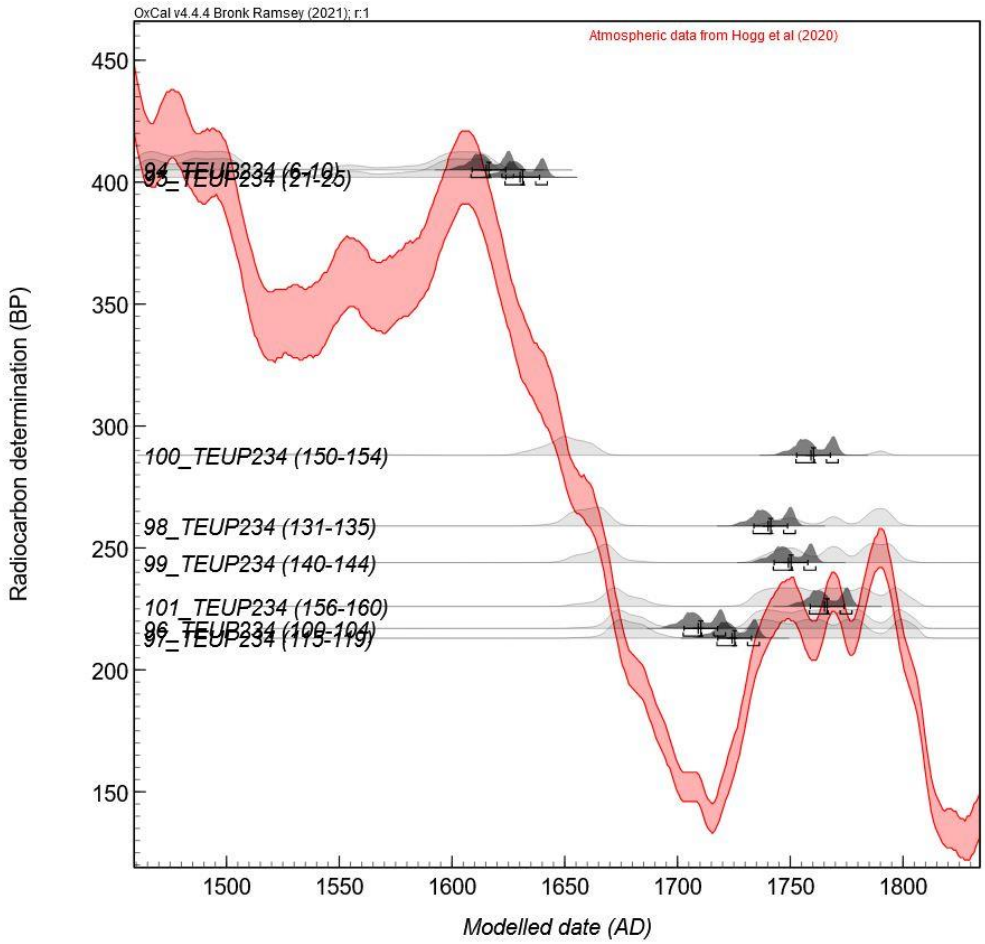

Figure 10.5.5. OxCal generated curve plot of the original D_Sequence model for TEUP234.

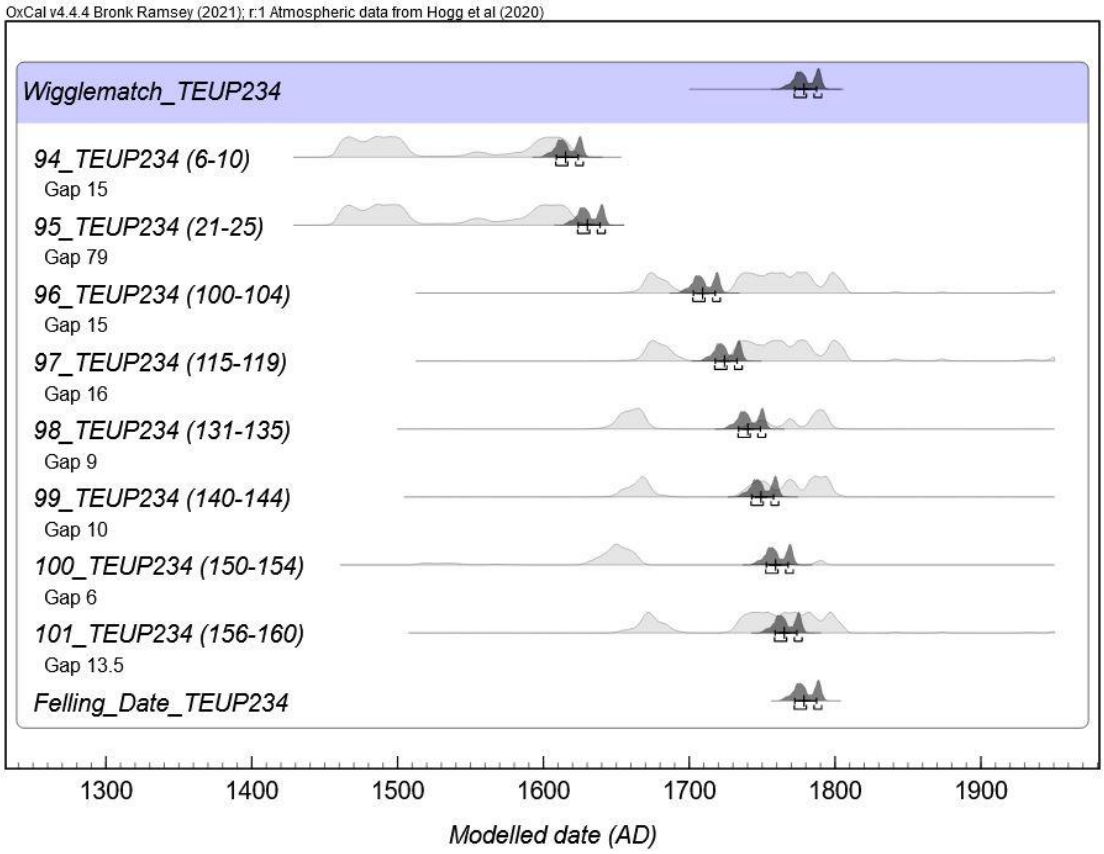

Figure 10.5.6. OxCal generated multiplot of the original D_Sequence model for TEUP234.

Because samples 94_TEUP234 (6–10) and 95_TEUP234 (21–25) are the first two ^{14}C dates in the D_Sequence series, they can be removed from the model without affecting the interpretation of the Felling Date. When this new D_Sequence model is calibrated against SHCal20, the results report a new Felling Date with a median calibrated age of AD 1809 ± 3 and a modelled date range between AD 1804–1815 (95% HPD) (Table 10.5.4). This Felling Date is noticeably older than the results of the previous model, with the ^{14}C dates showing an improved relationship with SHCal20 and between their posterior and likelihood distributions (Figure 10.5.7 and Figure 10.5.8). Importantly, no outliers were detected during this new analysis, the model passed the A_{comb} (An) threshold, and convergence values generated by OxCal remained universally high (99%). While the ^{14}C dates of samples 98_TEUP234 (131–135), 99_TEUP234 (140–144), and 99_TEUP234 (140–144) remain offset from SHCal20, the ^{14}C age order reversals observed between these ^{14}C dates suggest they are in the correct calendar position.

Table 10.5.4. Updated D_Sequence (SSimple) result for TEUP234.

Wk Number	Sample Code	^{14}C Age (BP)	Outlier Analysis (Posterior/Prior)	Convergence
52879	96_TEUP234 (100–104)	217 ± 20	5/5	99
52880	97_TEUP234 (115–119)	213 ± 21	5/5	99
52881	98_TEUP234 (131–135)	259 ± 21	5/5	99
52882	99_TEUP234 (140–144)	244 ± 20	5/5	99
52883	100_TEUP234 (150–154)	288 ± 20	5/5	99
52884	101_TEUP234 (156–160)	226 ± 22	5/5	99

Felling Date Results

Median cal. Age (AD)	HPD 68%	HPD 95%	A_{comb} (An)
1809 ± 3	AD 1808–1812	AD 1804–1815	57.2 (28.9)

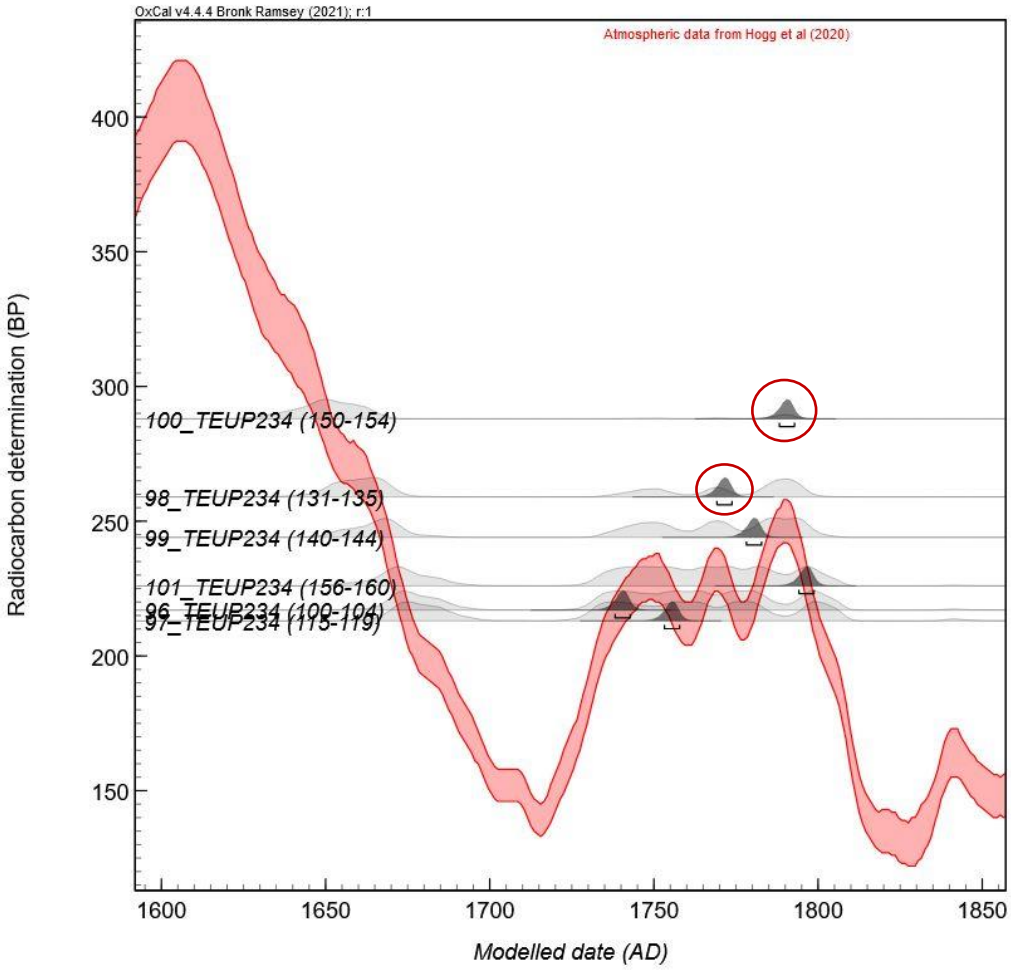

Figure 10.5.7. OxCal generated curve plot of the updated D_Sequence model for TEUP234[46].

[46] Red circles highlight potential ^{14}C age offsets. This offset type is discussed further in Section 13.1.5.

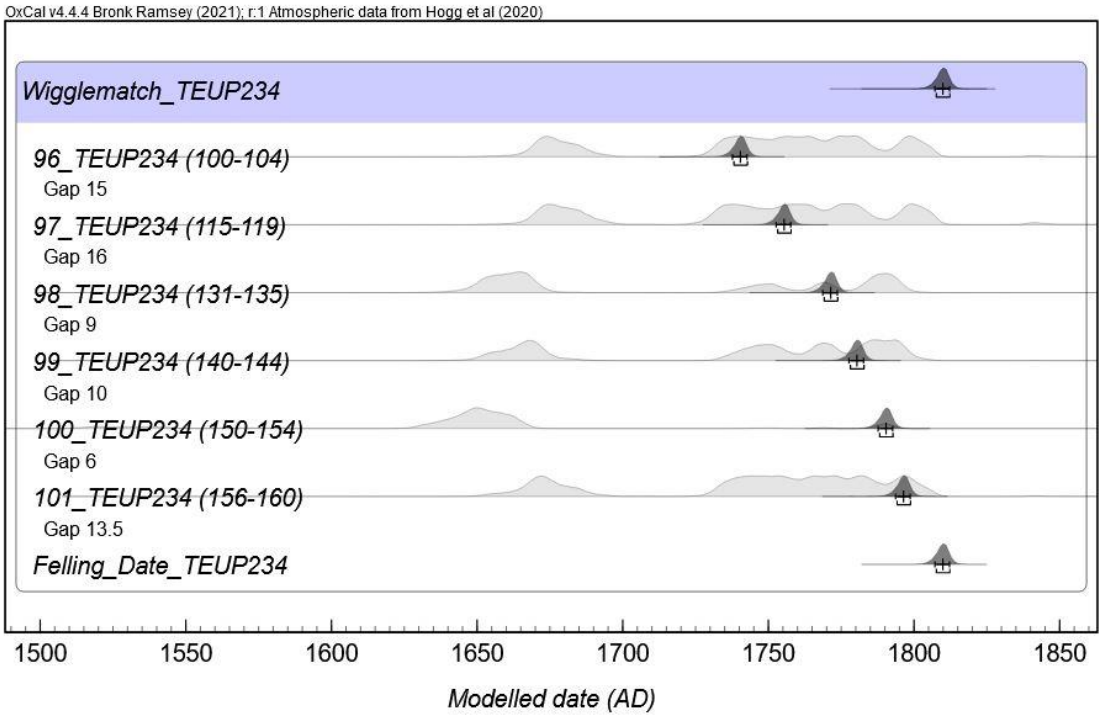

Figure 10.5.8. Oxcal generated multiplot for the updated D_Sequence model for TEUP234.

To test the accuracy of this new Felling Date (with the first two samples removed from the series), the updated D_Sequence model was calibrated using the 'RScaled' outlier model (see Appendix D.5.2), producing results consistent with the SSimple analysis with no outliers identified. The consistency of these two Felling Dates signifies that the updated WMD for TEUP234 is accurate. Therefore, this updated D_Sequence model is considered more accurate than the original model, as it negates the effects of possible ring count errors from the WMD. Consequently, this updated WMD is included in the local and regional scale analyses (Chapter 12).

10.5.3 TEUP244

The D_Sequence model for TEUP244 comprises five AMS ^{14}C dates, separated by known calendar intervals, spread across the 65 tree-ring growth sequence (Table 10.5.5). The Felling Date of TEUP244 reports a median calibrated age of AD 1814 ± 4, with a modelled date range between AD 1805–1822 (95% HPD). No outliers were detected during analysis, the model passed the A_{comb} (An) threshold, and the convergence values generated by the OxCal model remained uniformly high (99%). While situated over the calibration plateau present in the late eighteenth century (Figure 10.5.9), the WMD matches the shape of SHCal20, which is reflected

in the comparison of the posterior and likelihood distributions for each of the five ^{14}C dates in the D_Sequence series (Figure 10.5.10). Furthermore, when the D_Sequence model was recalibrated using agreement index analysis (see Appendix D.5.5), the results were consistent with the original WMD, reporting universal good agreement. Therefore, the WMD is interpreted as accurate and is included in the local and regional scale analyses.

Table 10.5.5. D_Sequence (SSimple) result for TEUP244.

Wk number	Sample code	^{14}C Age (BP)	Outlier analysis (Posterior/Prior)	Convergence
52865	82_TEUP244 (1–5)	214 ± 21	5/5	98
52866	83_TEUP244 (21–25)	207 ± 21	5/5	98
52867	84_TEUP244 (36–40)	267 ± 21	5/5	98
52868	85_TEUP244 (49–53)	233 ± 21	5/5	98
52869	86_TEUP244 (61–65)	165 ± 22	5/5	98

Felling Date Results

Median cal. Age (AD)	HPD 68%	HPD 95%	A_{comb} (An)
1814 ± 4	AD 1811–1818	AD 1805–1822	87.1 (31.6)

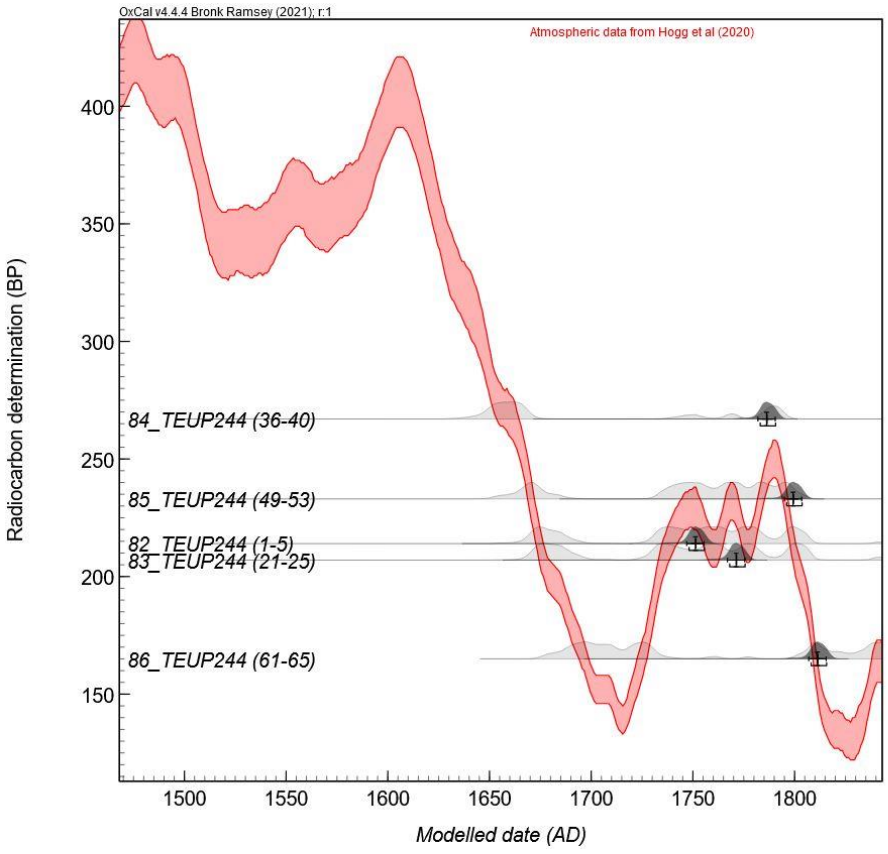

Figure 10.5.9. OxCal generated curve plot of the D_Sequence model for TEUP244.

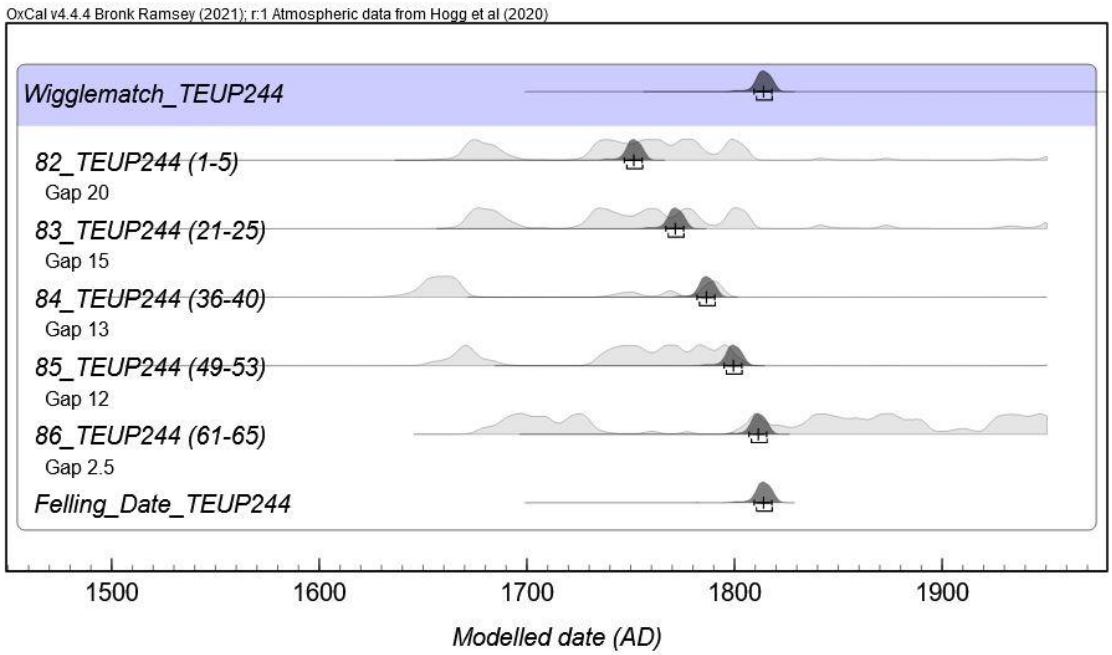

Figure 10.5.10. OxCal generated multiplot of the D_Sequence model for TEUP244.

10.5.4 Summary

Table 10.5.6 summarises the WMD results for the post-assemblage (three posts) sampled from TEU. The results of this analysis indicate that the site was occupied as a defended place during the late 1700s, with a potential second construction event identified in the early 1800s. This hypothesis will be tested during the local scale analysis presented in Section 12.1.6. Although the WMD for TEUP219 and TEUP234 initially presented some challenges, removing the first two samples from the D_Sequence models resulted in accurate Felling Dates. Therefore, all three WMDs are included in the local and regional scale analyses presented in Chapter 12.

Table 10.5.6. Summary of WMD results for TEU.

Post ID	Felling Date Results			Local/Regional Analyses
	Median cal. Age	68% HPD	95% HPD	
TEUP219	1788 ± 15	AD 1780–1793 (59.4%) AD 1820–1823 (8.9%)	AD 1776–1800 (73.8%) AD 1815–1826 (21.7%)	Included
TEUP234	1809 ± 3	AD 1808–1812	AD 1804–1815	Included
TEUP244	1814 ± 4	AD 1811–1818	AD 1805–1822	Included

Chapter 11. Lake Rotokauri (ROT)

11.1 Archaeological Excavations at ROT (S14/5)

As presented in Section 4.1.5, the pā at Lake Rotokauri has a complicated modern site history. Unpublished field notes from excavations undertaken by the Waikato Museum Archaeological Society in 1973–74 suggest that the pā was originally surrounded by roughly 80 posts. However, additional notes in the site record by Doug Pick indicate that by 1996, the pā had been vandalised, with all the posts cut down. Despite this report, the site visit conducted in November 2021 identified four *in situ* posts. Therefore, it was hoped that further evidence of palisade defences would be identified during more thorough investigations. Investigations at Lake Rotokauri were conducted over one field season in December 2021. These investigations began with a second comprehensive walkover survey of the site, including the portion submerged by the lake. However, these efforts were hindered by the dense vegetation overlying the pā (Figure 11.1.1), and no further evidence of palisade defences was identified.

Figure 11.1.1. Alan Hogg standing at the end of a site access corridor, cut through the dense vegetation at ROT.

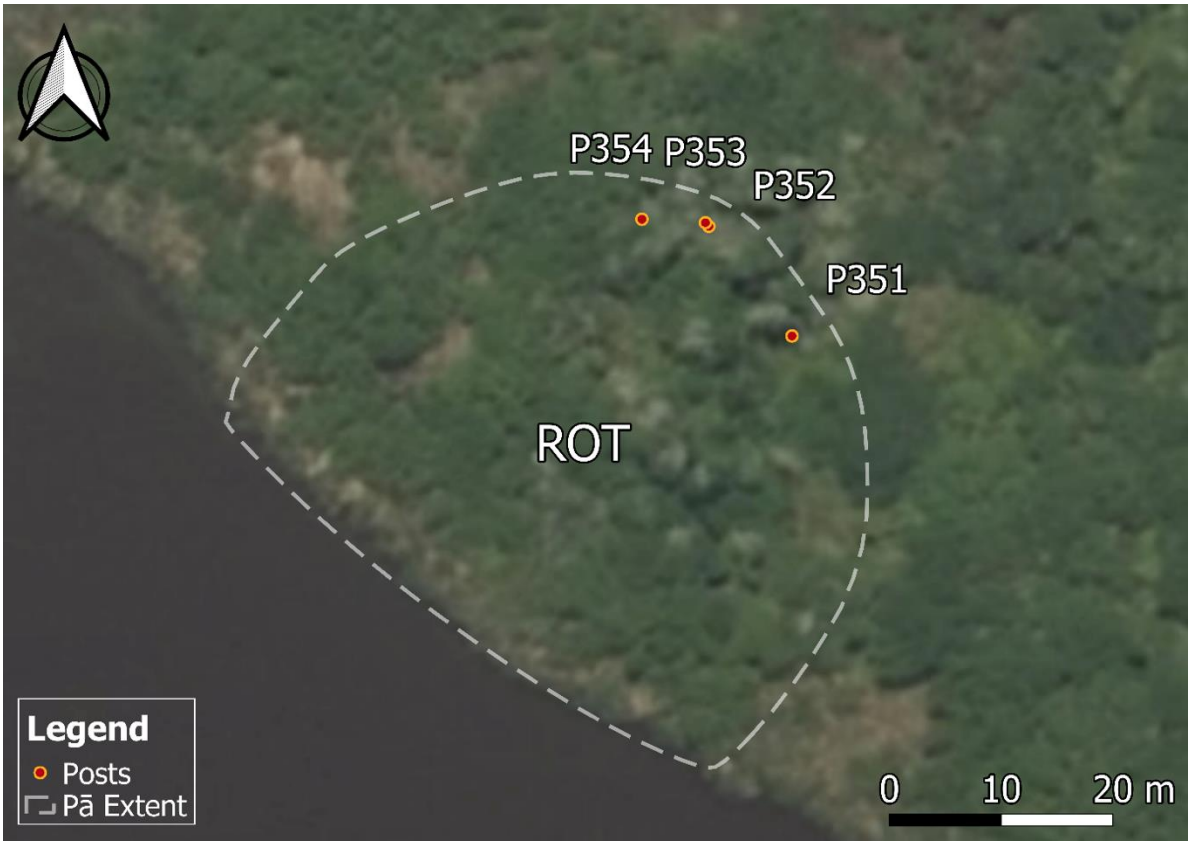

Figure 11.1.2. Location of posts identified at ROT.

Therefore, investigations solely focused on the four posts recorded on the northeastern boundary of the pā (Figure 11.1.2). Three of these posts (ROTP352–354) were visible at a height of >1 m (Figure 11.1.4 and Figure 11.1.5), while the fourth (ROTP351) was only just visible at ground level. Because the focus of these investigations was limited, excavation was confined to three small areas positioned directly around the identified posts to assess their suitability for extraction and sampling. EA53 was the largest of these areas, covering 1 x 0.7 m, excavated until the water table was encountered at a depth of 20 cm. Imported sediment deposits and dense charcoal inclusions were observed in EA53, situated just below the topsoil layer at a depth of 10 cm (Figure 11.1.3). This limited stratigraphy typifies the pā mound, as described previously by the unpublished field notes (see Section 4.1.5).

Figure 11.1.3. Imported sediment and charcoal inclusions identified in EA53.

Figure 11.1.4. Pre-excavation photograph of ROTP352 and ROTP353.

Figure 11.1.5. Pre-excavation photograph of ROTP354.

11.1.1 Extraction, Recording and Sampling

All four posts were extracted (Figure 11.1.6), with their recorded information summarised in Table 11.1.1. Unfortunately, the preservation quality of all four posts was limited, with only ROTP353 considered suitable for sampling (Figure 11.1.7). While largely intact, the centre of ROTP352 was entirely eroded, with only a portion of the youngest tree rings retained. ROTP352 was also bowed along its length, exhibiting a unique post shape not previously identified at any other pā investigated (Figure 11.1.8). Furthermore, only the distal tapered end of ROTP351 was retained, exhibiting a bulbed taper (Figure 11.1.9). Charring was identified on two posts (ROT352 and ROTP354), including their tapered ends, indicating they were burnt before installation (potential reuse or fire hardening). Only ROTP353 exhibited the characteristics required for sampling. However as there was no guarantee that this sole sample would progress through each analysis stage, it was decided to collect an additional sample from ROTP354 (Figure 11.1.10). ROTP354 was the next best-preserved post, and despite the charring observed in the field, it was hoped that a portion of the terminal tree ring was retained (to be investigated during the condition assessment). If not, the sample could still be analysed to produce a TAQ (*terminus ante quem*) for the construction date of this palisade defence,

providing some insurance that the analysis of these samples would provide some chronological information.

Table 11.1.1. Recorded information for the posts extracted from ROT.

Post ID	Cross section	Max length (cm)	Diameter (cm)	Taper shape	Condition	Sampled
ROT351*	Rectangle	72	15.4	Bulb	Adze dressed	No
ROT352*	Round	303	17.5	Irregular	Poor preservation	No
ROT353	Round	297	17.2	Irregular	Suitable for sampling	Yes
ROT354	Round	362	12.3	Irregular	Charring present	Yes

*Note. *indicates posts that were extracted but not sampled.*

Figure 11.1.6. Warren Gumbley (left) and Alan Hogg (right) extract a post at Lake Rotokauri.

Figure 11.1.7. Post-extraction photograph of ROTP353.

Figure 11.1.8 Post-extraction photograph of ROTP352.

Figure 11.1.9. Post-extraction photograph of ROTP351.

Figure 11.1.10. Post-extraction photograph of ROTP354

11.2 Species Identification

Thin-section microscopy of the post assemblage (two posts) sampled from the pā at Lake Rotokauri (ROT) identified two tree species: kahikatea (*D. dacrydioides*) and rimu (*D. cupressinum*) (Table 11.2.1). Both these species are large trees generally found in the lowland forests of the North and South Islands (Table 5.3.2). They are typical of the wetland environments and hills surrounding the rivers and lakes of the Middle Waikato Basin.

Table 11.2.1. Tree species identified at ROT.

Post ID	Common name	Scientific name
ROT353	kahikatea	*Dacrycarpus dacrydioides*
ROT354	rimu	*Dacrydium cupressinum*

11.3 Condition Assessment

Both samples were inspected under a low-powered light microscope to assess their condition and suitability for tree-ring analysis, ring-block sampling, and AMS radiocarbon dating (see Section 5.5 and Table 11.3.1). Critically, the condition assessment of ROTP354 confirmed that the sample did not retain evidence of the terminal tree ring, thereby failing the condition assessment. However, due to the limited number of samples available for analysis, a decision was made to analyse this post, producing a Felling Date that can be interpreted as a TAQ. This decision meant that while the Felling Date does not provide direct evidence of a post construction event, it could provide some chronological evidence relating to the date after which palisade construction was undertaken at the pā at Lake Rotokauri. Therefore, both samples were included in tree-ring analysis.

Table 11.3.1. ROT sample condition assessment.

Post ID	Poor preservation	Charring present	Scaring present	Dark staining	Growth anomalies	Passed
ROT353	☐	☐	☐	☐	☑	Yes
ROT354*	☑	☑	☐	☑	☑	No

*Note. * Indicates that post ROTP354 does not retain evidence of the terminal tree ring.*

11.4 Tree Ring Analysis Results

The reconciled ring count information for each post sample in the ROT assemblage is summarised in Table 11.4.1 (see Section 5.6 for method). The ring counts presented below represent the most accurate information attainable for these samples, with any persistent inconsistencies discussed further in Section 11.5. Unfortunately, the digital scans of both samples were lost during the preparation of this study and cannot be displayed.

Table 11.4.1. A summary of the reconciled ring count information for the posts sampled from ROT.

Post ID	Species ID	Reconciled ring count	Diameter (cm)
ROTP353	Kahikatea (*D. dacrydioides*)	72	17.2
ROTP354*	Rimu (*D. cupressinum*)	70	12.3

*Note. *Indicates that the tree ring count information provided for ROTP354 is not a maximum ring count, as the terminal tree ring is absent.*

11.4.1 ROTP353 (kahikatea, *D. dacrydioides*)

ROTP353 presented a round cross-section, concentric growth pattern and off-centre pith location. Minor episodes of tree-ring suppression and locally absent rings were present across the tree-ring growth sequence. However, the effect of these growth anomalies was limited, providing a clear and visible growth sequence. The three measured radii were positioned to ensure the complete tree-ring growth sequence was captured, and there were minimal ring count differences between the three tracks measured (Table 11.4.2). Reconciliation of these ring counts resulted in a final ring count of 72, with five ring-block samples collected at regular intervals across the growth sequence (Table 11.4.3). No sampling errors were identified across any ring-block samples; all five contained five tree rings.

Table 11.4.2. Ring count information for ROTP353.

Ring counts	Track A	Track B	Track C	Reconciled
ROTP353	71	71	69	72

Table 11.4.3. Ring block sampling information for ROTP353.

Wk number	Sample code	First ring	Middle ring	Last ring	# of rings in block	Ring gap to next sample
54121	131_ROTP353 (20–24)	20	22	24	5	11
54122	132_ROTP353 (31–35)	31	33	35	5	12
54123	133_ROTP353 (43–47)	43	45	47	5	13
54124	134_ROTP353 (56–60)	56	58	60	5	12
54125	135_ROTP353 (68–72)	68	70	72	5	2.5

11.4.2 ROTP354 (rimu, *D. cupressinum)*

A round cross-sectional shape, non-concentric growth pattern and off-centre pith location characterised ROTP354. Multiple episodes of tree-ring suppression affected the tree-ring growth sequence, resulting in locally absent rings and narrow annual growth periods across the growth sequence. These episodes were particularly prevalent in the second half of the growth sequence, creating a challenge when attempting to capture the entire growth sequence using the three measured radii (Table 11.4.4). Reconciliation of these three radii resulted in a final ring count of 70 (not including the terminal tree ring), with five ring-block samples collected at semi-regular intervals across the growth sequence (Table 11.4.5). No sampling errors were identified across any ring-block samples; all five samples contained five tree rings.

Table 11.4.4. Ring count information for ROTP354.

Ring counts	Track A	Track B	Track C	Reconciled
ROTP354	70	69	57	70*

*Note. * Indicates reconciled ring count does not include the terminal tree ring.*

Table 11.4.5. Ring block sampling information for ROTP354.

Wk number	Sample code	First ring	Middle ring	Last ring	# of rings in block	Ring gap to next sample
54126	136_ROTP354 (5–9)	5	7	9	5	14
54127	137_ROTP354 (19–23)	19	21	23	5	19
54128	138_ROTP354 (38–42)	38	40	42	5	10
54129	139_ROTP354 (48–52)	48	50	52	5	18
54130	140_ROTP354 (66–70)	66	68	70	5	2.5*

*Note. *Indicates that the final ring gap for sample 140_ROTP354 (66–70) only represents the gap to the outermost tree ring identified, not the terminal tree ring.*

11.5 Wiggle-Match Dating Results

This section presents the WMD results for the post-assemblage (two posts) sampled from ROT (see Section 5.8.2 for method). The full array of OxCal codes relating to each post analysed can be viewed in Appendix D.6. The interpretation of each WMD is discussed in detail below.

11.5.1 ROTP353

The D_Sequence model for ROTP353 comprises five AMS ^{14}C dates, separated by known calendar intervals, spread across the 72-year tree-ring growth sequence (Table 11.5.1). The Felling Date of ROTP353 has a median calibrated age of AD 1514 ± 15, with a modelled date range between AD 1499–1536 (95% HPD). No outliers were detected during analysis, the model passed the A_{comb} (An) threshold, and the convergence values generated by the OxCal model remained universally high (99%). The curve plot of the analysis shows that the WMD reflects the shape of SHCal20 (Figure 11.5.1), evidenced by the strong relationship between the posterior and likelihood distributions of each ^{14}C date within the series (Figure 11.5.2). Furthermore, when the D_Sequence model was calibrated using alternative outlier detection methods (Appendix D.6.1), the Felling Date results were consistent with the original model, reporting universal good agreement (> 60). Therefore, the WMD for ROTP353 is considered accurate and is included in the local and regional scale analyses presented in Chapter 12.

Table 11.5.1. D_Sequence (SSimple) result for ROTP353.

Wk number	Sample code	^{14}C Age (BP)	Outlier analysis (posterior/prior)	Convergence
54121	131_ROTP353 (20–24)	427 ± 26	5/5	99
54122	132_ROTP353 (31–35)	429 ± 24	5/5	99
54123	133_ROTP353 (43–47)	405 ± 25	5/5	99
54124	134_ROTP353 (56–60)	372 ± 24	5/5	99
54125	135_ROTP353 (68–72)	396 ± 26	5/5	99
Felling Date Results				
Median Cal. Age (AD)	HPD 68%	HPD 95%	A_{comb} (An)	
1514 ± 15	AD 1504–1524	AD 1499–1536	100.7 (31.6)	

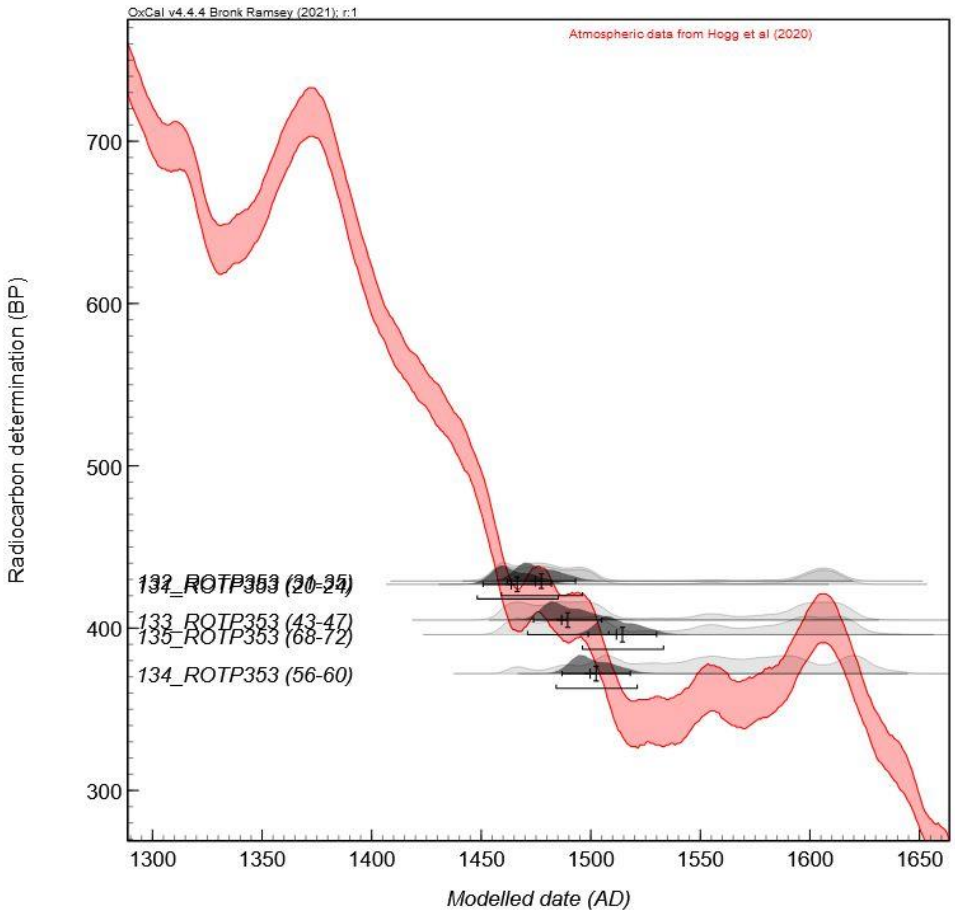

Figure 11.5.1. OxCal generated curve plot of the D_Sequence model for ROTP353.

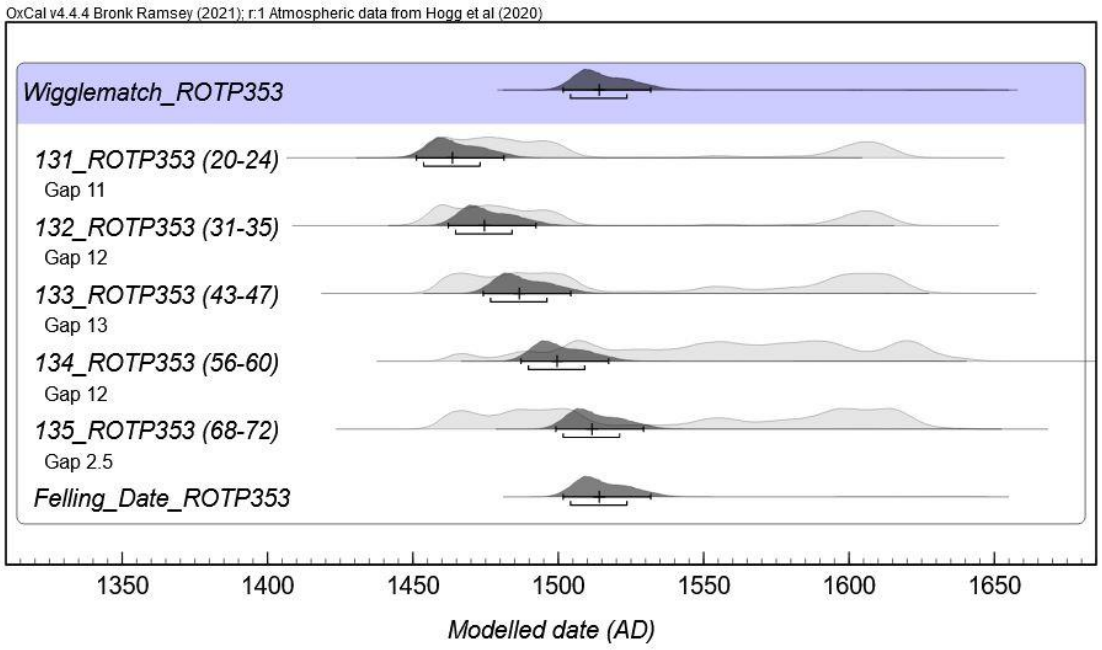

Figure 11.5.2. OxCal generated multiplot of the D_Sequence model for ROTP353.

11.5.2 ROTP354

The D_Sequence model for ROTP354 comprises five AMS ^{14}C dates, separated by known calendar intervals, spread across the 70-year tree-ring growth sequence (Table 11.5.2). The Felling Date of ROTP354 reports a median calibrated age of AD 1214 ± 7, with a modelled date range between AD 1198–1228 (95% HPD). No outliers were detected during the analysis, the model passed the A_{comb} (An) threshold, and the convergence values generated by the OxCal model remained universally high (99%). While accurate and precise, the usefulness of this Felling Date is limited, providing evidence that the parent tree of this sample was felled at some point after AD 1198–1228. Considering the WMD result, this Felling Date is at least 300 years too old given our current understanding of New Zealand's settlement date and the proposed beginning of pā construction (see Schmidt, 1996; Bunbury et al., 2022). A calendar age >300 years older than expected suggests the post may have been constructed using "old" wood (felled naturally and preserved under anaerobic conditions), in addition to the loss of tree rings resulting from the observed charring. For this reason, the WMD for ROTP354 is removed from consideration for future analyses.

Table 11.5.2. D_Sequence (SSimple) result for ROTP354.

Wk number	Sample code	^{14}C Age (BP)	Outlier analysis (posterior/prior)	Convergence
54126	136_ROTP354 (5–9)	962 ± 24	3/5	99
54127	137_ROTP354 (19–23)	914 ± 24	3/5	99
54128	138_ROTP354 (38–42)	916 ± 24	2/5	99
54129	139_ROTP354 (48–52)	927 ± 24	3/5	99
54130	140_ROTP354 (66–70)	894 ± 25	2/5	99
Felling Date Results				
Median Cal. Age (AD)		HPD 68%	HPD 95%	A_{comb} (An)
1214 ± 7		AD 1208–1221	AD 1198–1228	129.9 (31.6)

11.5.3 Summary

Table 11.5.3 summarises the WMD results for the post-assemblage (two posts) sampled from the pā at Lake Rotokauri. The results support that the pā was occupied as a defended place

from the early 1500s. Unfortunately, the limited number of posts suitable for analysis means this is the only evidence of a post construction event at this pā. As a result, local scale analysis will not be conducted on the post assemblage from ROT. However, the WMD for ROTP353 will be included in the regional scale analysis presented in Section 13.1.7.

Table 11.5.3. Summary of WMD results from ROT.

Post ID	Felling Date Results			Local/Regional Analyses
	Median cal. Age	68% HPD	95% HPD	
ROTP353	1514 ± 15	AD 1504–1524	AD 1499–1536	Included
ROTP354	1214 ± 7	AD 1208–1221	AD 1198–1228	Excluded

Chapter 12. Local & Regional Analyses

12.1 Local Scale Analysis

The second objective of this study focuses on the local scale, examining how the palisade defences at a pā developed over time. Evidence of phasing is identified and related to three key stages of construction activity: (i) the earliest evidence of palisade construction at a site, providing proxy evidence for when the site was potentially first fortified, (ii) evidence of repair to an existing palisade row (i.e., a post being installed in an existing palisade row), and (iii) evidence of palisade defence redevelopment (i.e., the addition of a new palisade row). The event scale of analysis produced a Felling Date for each post successfully analysed from a specific pā, interpreted as a TPQ for the installation of that post in a specific palisade row. As anticipated, this produced Felling Dates in contrasting calendar periods, suggesting the existence of multiple palisade construction events at that pā over time. Therefore, a chronological framework was developed for each site, providing further evidence of the spatio-temporal relationships between each of the posts analysed during the event scale of analysis. These frameworks were developed using the Bayesian Sequence model option in OxCal v 4.4, implemented using Southern Hemisphere atmospheric calibration data (SHCal20), with individual outliers identified and down-weighted by the SSimple s-type outlier model (see Section 5.8.3).

12.1.1 Sequence Model Structure and Interpretation (OxCal)

The structure of each local scale Sequence model is unique to each pā (see Appendix E). However, in all cases, specialised OxCal commands (CQL2) are used to develop and test each model, providing evidence to support the interpretation of palisade construction phasing identified at each site (Table 12.1.1). These OxCal commands are capitalised in text for reference. Each Sequence model consists of multiple ‘Phases” arranged sequentially, bound by a start and end ‘Boundary’. Each Phase includes the D_Sequence models (WMD) with Felling Dates that correspond to that particular construction period. A 'Date' command is also included within each Phase, defined by the start and end boundary of each Phase, providing a posterior distribution with a modelled date range that integrates all of the available Felling Dates within each Phase. To avoid confusion, the results of these Date commands are referred to as

‘Modelled Dates’ (MDate), while the D_Sequence model results (WMDs) are referred to as ‘Felling Dates’. These Modelled Dates are used in ‘Difference’ commands that are included in each Sequence model, providing evidence that each Phase represents a distinct period of palisade construction activity. The Difference command calculates the statistical ‘difference’ between two parameters as a BP Age range. ‘Difference’ between two parameters is determined when the resulting BP Age range does not cross zero (e.g., -430 to -80 BP or 27 to 54 BP). The Modelled Dates are used as the parameters for each Difference query for two reasons: (i) because they integrate all of the available Felling Dates within each Phase, and (ii) because their broader date ranges (defined by the start and end Boundary of each Phase) negate the possibility that specific Felling Dates are overly defined (precise) in their calendar position due to (minor) unidentified errors in the D_Sequence model prior information (see Section 13.1.5.1), or inconsistencies associated with their calibration against SHCal20 (see Section 13.1.5.2). Additionally, an ‘Interval’ command separates each Phase (positioned between the two Boundary commands that separate each Phase) to model the time (in years) between each Phase of palisade construction activity. Finally, a ‘Span’ query is included in each Sequence model, providing a modelled calendar year span for the site's occupation based on the identified palisade construction activity (i.e., 90–120 years). As each site was possibly occupied before and/or after the identified palisade construction events, the span query estimates when the site was occupied as a pā (with evidence of fortification). The results of each local scale analysis are presented below, with their interpretation discussed further in Section 13.1.6.

Table 12.1.1. OxCal commands used during Sequence model analysis (Bronk Ramsey, 1994, 2009a).

CQL2 Command	Function
Curve	Defines the radiocarbon calibration curve to be used
Outlier_Model	Defines the outlier model
Sequence	Defines an order for events and groups of events
Boundary	Defines a uniformly distributed group (i.e., Start and End)
Phase	Defines an unordered group of events/parameters
D_Sequence	A sequence where the exact gaps between elements are known (i.e., tree rings)
R_Date	Calculates the likelihood distribution for the calibrated date as a function of radiocarbon concentration
Outlier	Defines the outlier probability for an outlier model
Gap	Defines the gap between events
Interval	A query that finds the interval between events or groups of events in a Sequence
Difference	Calculates the difference between two parameters
Date	A type conversion function that returns a date or PDF for a date from an expression
Span	Group function or query which gives the span of events

12.1.2 Lake Mangakaware 1 (MA1)

Event scale analysis (WMD) conducted on the post assemblage from MA1 yielded four successful Felling Dates, representing three distinct palisade contexts at MA1 (rows and structures). These Felling Dates were incorporated into an OxCal Sequence model (see Appendix E.1) consisting of four sequential Phases (Phase I–IV), supported by the results of Interval, Difference, and Span commands (Table 12.1.2, Table 12.1.3, and Figure 12.1.1). The analysis detected no outliers, all of the WMDs passed the A_{comb} > (An) threshold, and convergence values (C) remained universally high (> 95%).

Table 12.1.2. MA1 local scale Sequence model results.

MA1	Felling Date and MDate Results					
	Parameter	Median Cal. Age	68% HPD	95% HPD	C	A_{comb} (An)
Phase I	**MA1P204**	**AD 1712 ± 6**	**AD 1707–1719**	**AD 1702–1725**	**99**	**135 (32)**
	MDate	AD 1713 ± 14	AD 1705–1724	AD 1687–1740	99	-
Interval 1	-	-	1–28 (yrs)	1–41 (yrs)	100	-
Phase II	**MA1P53**	**AD 1754 ± 3**	**AD 1752–1758**	**AD 1749–1761**	**100**	**78 (27)**
	MDate	AD 1755 ± 11	AD 1746–1765	AD 1731–1782	100	-
Interval 2	-	-	11–43 (yrs)	1–48 (yrs)	100	-
Phase III	**MA1P190**	**AD 1802 ± 5**	**AD 1799–1807**	**AD 1794–1811**	**100**	**125 (32)**
	MDate	AD 1801 ± 9	AD 1795–1809	AD 1778–1814	99	
Interval 3	-	-	1–10 (yrs)	1–19 (yrs)	100	-
Phase IV	**MA1P208**	**AD 1818 ± 5**	**AD 1814–1823**	**AD 1807–1828**	**100**	**75 (32)**
	MDate	AD 1819 ± 10	AD 1812–1825	AD 1805–1841	99	
Span	-	-	101–133 (yrs)	90–174 (yrs)	96	-

Note. Felling Dates produced from posts sampled from MA1 are presented in bold. Interval and Span results are presented in years (yrs).

Table 12.1.3. Results of the difference queries included in the local scale Sequence model for MA1.

MDate Queried	Difference range (BP)	Different (yes/no)
Phase I – Phase II	-57 to -25 (68%) -81 to -10 (95%)	Yes
Phase II – Phase III	-68 to -36 (68%) -89 to -16 (95%)	Yes
Phase III – Phase IV	-28 to -7 (68%) -48 to -2 (95%)	Yes

Note. The BP age range in all three cases does not cross zero, indicating a difference.

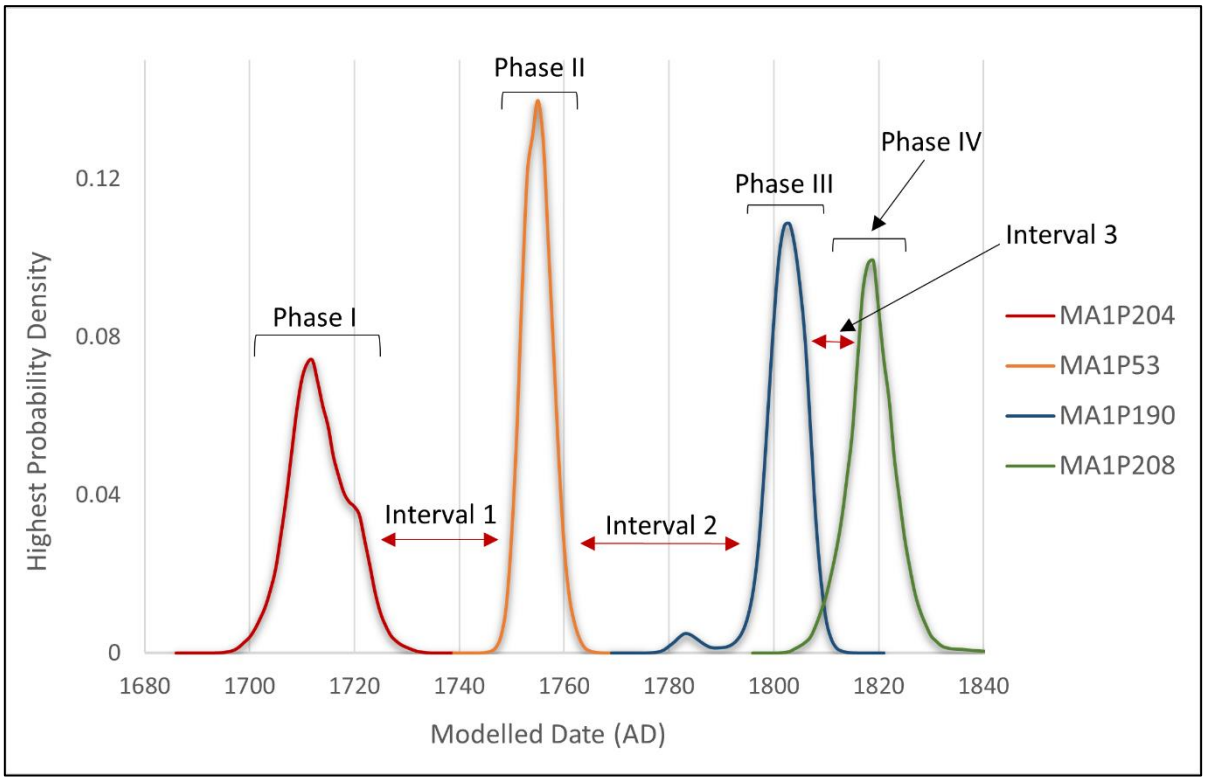

Figure 12.1.1. Felling Dates and phasing identified at MA1[47].

[47] Note. The line graph of each Felling Date is created using the modelled posterior distribution statistics. However, the bars and arrows used to label each Phase and Interval position are descriptive only, and do not represent exact statistical information. This is true for all similar figures presented below.

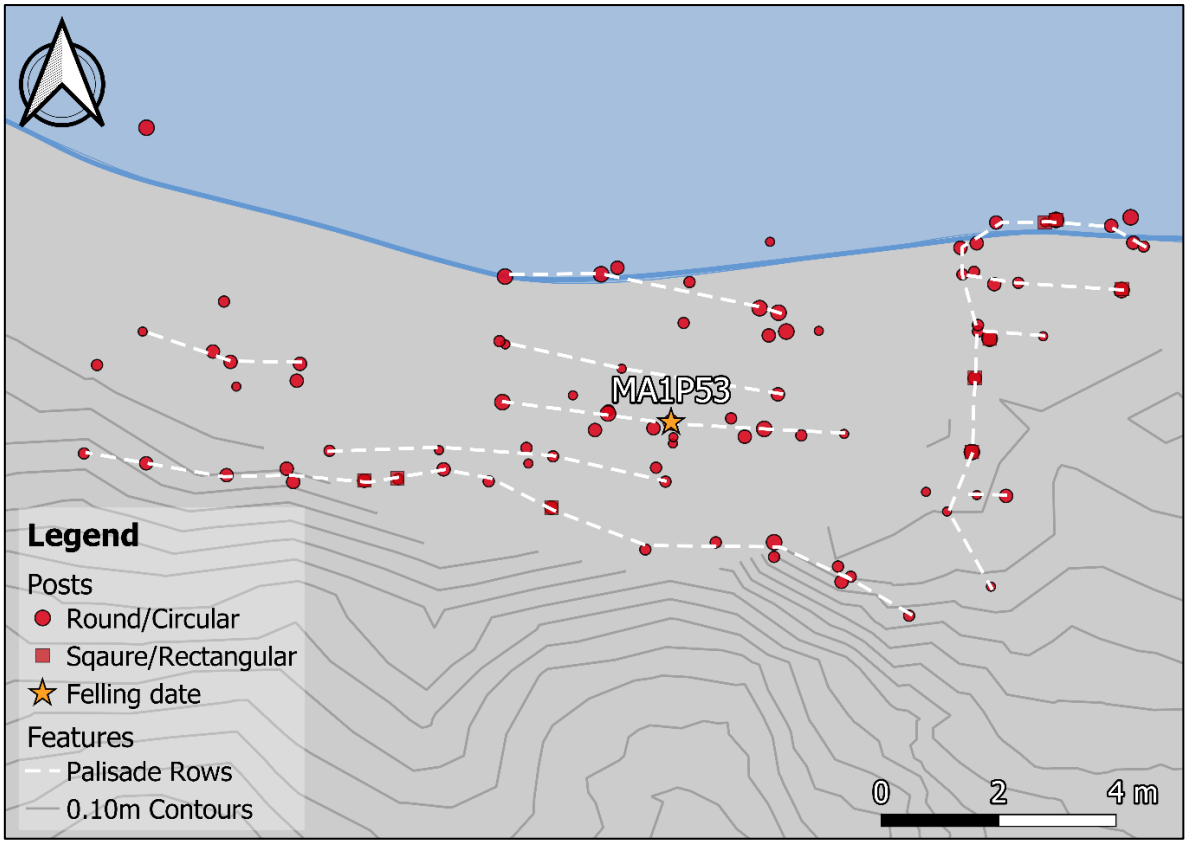

Figure 12.1.2. Site plan of MA1 showing the location of posts that produced successful Felling Dates in Area A.

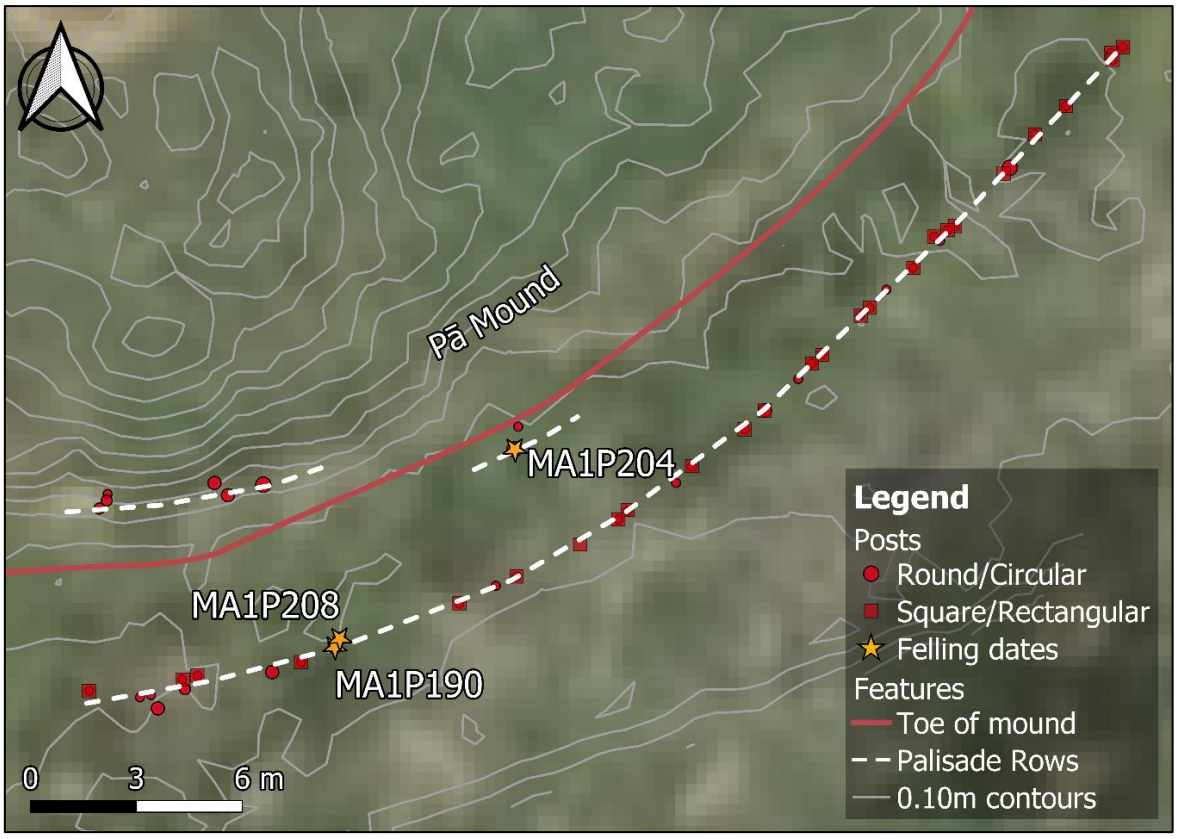

Figure 12.1.3. Site plan of MA1 showing the location of posts that produced successful Felling Dates in Area B.

12.1.2.1 Phase I

The earliest evidence of palisade construction at MA1 is identified in Area B (Phase I) (Table 12.1.2), supported by the Felling Date of MA1P204 (AD 1702–1725, 95% HPD). MA1P204 was located at the base of the raised pā mound (Figure 12.1.3), representing a palisade row abutting the imported sediment layers that comprise the raised mound. The Modelled Date for Phase I provides a date range of AD 1687–1740 (95% HPD), which, in addition to the Felling Date for MA1P204 (Figure 12.1.1), strongly indicates this phase of palisade construction occurred in the early 1700s (Table 12.1.2). As the Felling Date for MA1P204 provides the earliest direct evidence of palisade construction at MA1, Phase I is interpreted as the likely date at which the site was first fortified.

12.1.2.2 Interval 1

The Interval between Phases I and II at MA1 is modelled at 1–41 years (95% HPD) (Table 12.1.2). The Difference command querying the MDate for Phases I and II confirms that both Phases represent statistically different periods (Table 12.1.3).

12.1.2.3 Phase II

The second palisade construction phase at MA1 (Phase II) is supported by the Felling Date of MA1P53 (AD 1749–1761, 95% HPD). MA1P53 was positioned within one of several palisade rows on the northern lake side of the pā (Area A), halfway between the modern lake edge and the raised pā mound (Figure 12.1.2). As outlined in Section 6.1.1, the palisade rows in this area were constructed using paired large-diameter posts, interpreted as evidence of a fighting stage (MA1P53 was paired with MA1P121). The Modelled Date for Phase II provides a date range of AD 1731–1782 (95% HPD), which, in addition to the Felling Date for MA1P53 (Figure 12.1.1), strongly indicates this phase of palisade construction occurred in the middle 1700s (Table 12.1.2). Therefore, the Felling Date for MA1P53 is interpreted as the likely construction date of this fighting stage, classified as a palisade redevelopment activity.

12.1.2.4 Interval 2

The interval between Phases II and III at MA1 is modelled as 1–48 years (95% HPD) (Table 12.1.2). The Difference command querying the MDate for Phases II and III confirms that both Phases represent statistically different periods (Table 12.1.3).

12.1.2.5 Phase III

The third palisade construction phase at MA1 (Phase III) is supported by the Felling Date for MA1P190 (AD 1794–1811, 95% HPD). MA1P190 was located in the outermost palisade row identified in Area B (Figure 12.1.3). The Modelled Date for Phase III provides a date range of AD 1778–1814 (95%), which, in addition to the Felling Date for MA1P190 (Figure 12.1.1), strongly indicates this phase of palisade construction occurred in the late 1700s to early 1800s (Table 12.1.2). As the Felling Date for MA1P190 provides the earliest direct evidence of palisade construction in this row, it is suggested that Phase III represents a palisade redevelopment activity at MA1, with the addition of the outermost palisade row to the pā's defences.

12.1.2.6 Interval 3

The interval between Phases III and IV at MA1 is modelled as 1–19 years (95% HPD) (Table 12.1.2). The Difference command querying the MDate for Phases III and IV confirms that both Phases represent statistically different periods (Table 12.1.3). Interestingly, this period is shorter than the intervals between the two previous phases of palisade construction (Intervals 1 and 2), indicating that a different variable may be responsible for the short length of this period.

12.1.2.7 Phase IV

The final palisade construction phase identified at MA1 (Phase IV) is supported by the Felling Date for MA1P208 (AD 1807–1828, 95% HPD). MA1P208 was also positioned in the outermost palisade row identified in Area B (same row as MA1P190). The Felling Date for MA1P208 was initially interpreted as an event occurring in Phase III. However, the results of additional Bayesian modelling supported that the Felling Date of MA1P208 represents an

independent construction phase compared to the Felling Date of MA1P190. The Modelled Date for Phase IV provides a date range of AD 1805–1841 (95% HPD), which, in addition to the Felling Date for MA1P208 (Figure 12.1.1), strongly indicates this phase of palisade construction occurred in the early 1800s (Table 12.1.2). As the Difference and Interval queries confirm that the Felling Dates for MA1P190 and MA1P208 represent two distinct construction phases, and the felling date for MA1P208 represents direct evidence of sequential construction activity within this outermost palisade row, Phase IV is interpreted here as a palisade repair activity.

12.1.2.8 Occupation Span

The Span query (encompassing all four identified Phases) supports that MA1 was occupied as a defended place for 90–174 years (95% HPD). As discussed in Section 4.1.1.1, Bellwood (1978a, p. 11) describes MA1 as a heavily defended and stratified pā, with up to six rows of palisades identified on the southern side of the pā. Furthermore, these earlier excavations recorded imported soil deposits up to two metres deep (Bellwood, 1978a, p. 13), with several superimposed living surfaces, cooking features, and activity areas identified. Given the extensive archaeological evidence identified at MA1 (implying a long occupation history), and the WMD and Bayesian sequence analysis results presented here, an occupation span of over 100 years is considered a reasonable representation of how long the site was occupied as a pā.

12.1.3 Lake Mangakaware 2 (MA2)

Event scale analysis (WMD) conducted on the post assemblage from MA2 yielded five successful Felling Dates (Section 7.5). All the analysed posts originate from a single palisade row, identified as the innermost (closest to the raised pā mound) of two rows located close to the southeastern boundary of the pā (Figure 12.1.5). Unfortunately, due to sampling restrictions and limitations encountered during tree-ring analysis and WMD, none of the posts sampled from the outer palisade row (second row) produced an accurate Felling Date. The five successful Felling Dates (D_Sequence models) from MA2 were incorporated into an OxCal Sequence model (see Appendix E.2) consisting of two sequential phases (Phase I and II), supported by the results of Interval, Difference, and Span commands (Table 12.1.4). Across all five D_Sequence models, only two minor outliers were detected and down-weighted during the analysis: 55_MA2P152 (26–30) and 61_MA2P153 (25–29), with posterior outlier values

of 6% (Prior: 5%). Both minor outliers were discussed in detail in Section 7.5 and are the result of minor ^{14}C age offsets over the calibration plateau in the eighteenth century. Again, all the D_Sequence models included pass the A_{comb} > (An) threshold and exhibit universally high (> 95%) convergence.

Table 12.1.4. MA2 local scale Sequence model results

MA2	Felling Date and MDate Results					
	Parameter	Median Cal. Age	68% HPD	95% HPD	C	A_{comb} (An)
Phase I	**MA2P161**	**AD 1737 ± 4**	**AD 1733–1741**	**AD 1730–1747**	**100**	**84 (32)**
	MDate	AD 1739 ± 31	AD 1725–1756	AD 1689–1790	99	-
Interval 1	-	-	30–68 (yrs)	4–70 (yrs)	100	-
Phase II	**MA2P15**	**AD 1805 ± 2**	**AD 1804–1808**	**AD 1800–1810**	**100**	**88 (32)**
	MA2P152	**AD 1806 ± 3**	**AD 1803–1810**	**AD 1799–1812**	**100**	**39 (32)**
	MA2P153	**AD 1805 ± 3**	**AD 1804–1808**	**AD 1800–1810**	**100**	**51 (32)**
	MA2P154	**AD 1805 ± 2**	**AD 1803–1808**	**AD 1800–1810**	**100**	**64 (32)**
	MDate	AD 1805 ± 5	AD 1802–1809	AD 1795–1815	100	-
Span	-	-	66–96 (yrs)	58–168 (yrs)	97	-

Note. Felling Dates produced from posts sampled from MA2 are presented in bold. Interval and Span results are presented in calendar years (yrs).

Table 12.1.5. Results of the difference query included in the local scale Sequence model for MA2.

MDate Queried	Difference range (BP)	Different (yes/no)
Phase I – Phase II	-81 to -49 (68%) -117 to -15 (95%)	Yes

Note. The BP age range does not cross zero, indicating a difference.

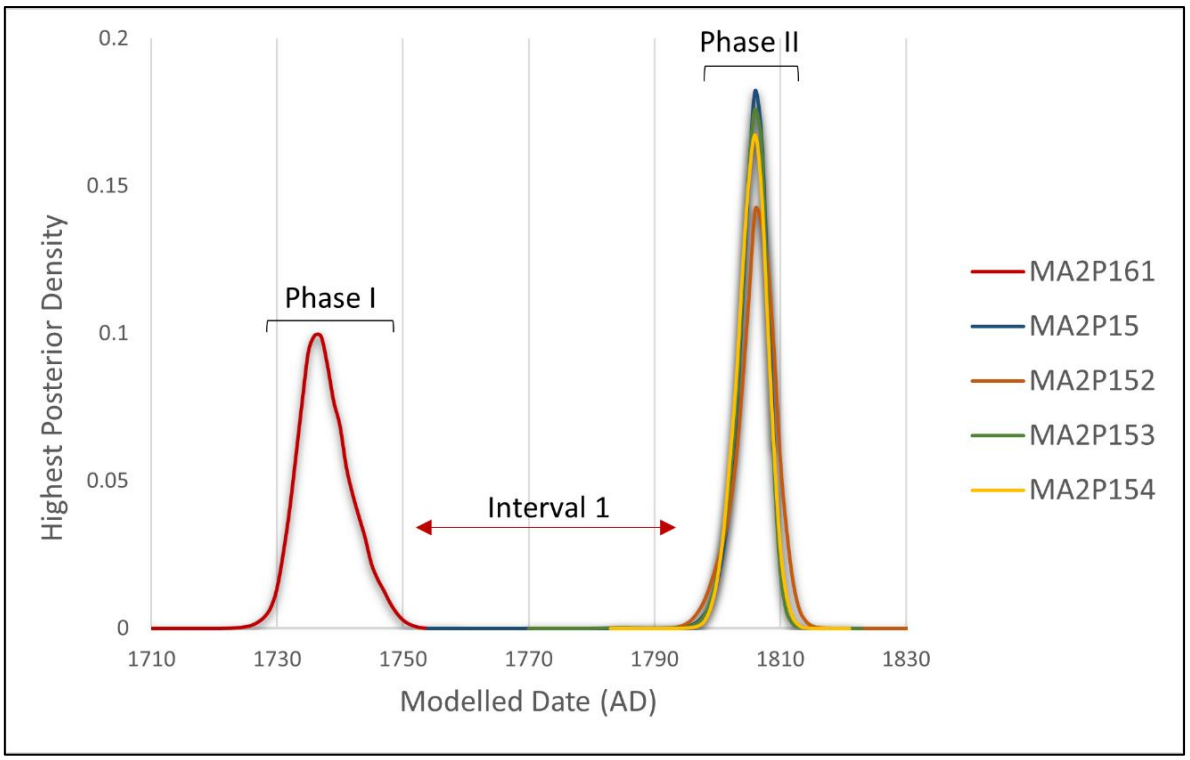

Figure 12.1.4. Felling Dates and phasing identified at MA2.

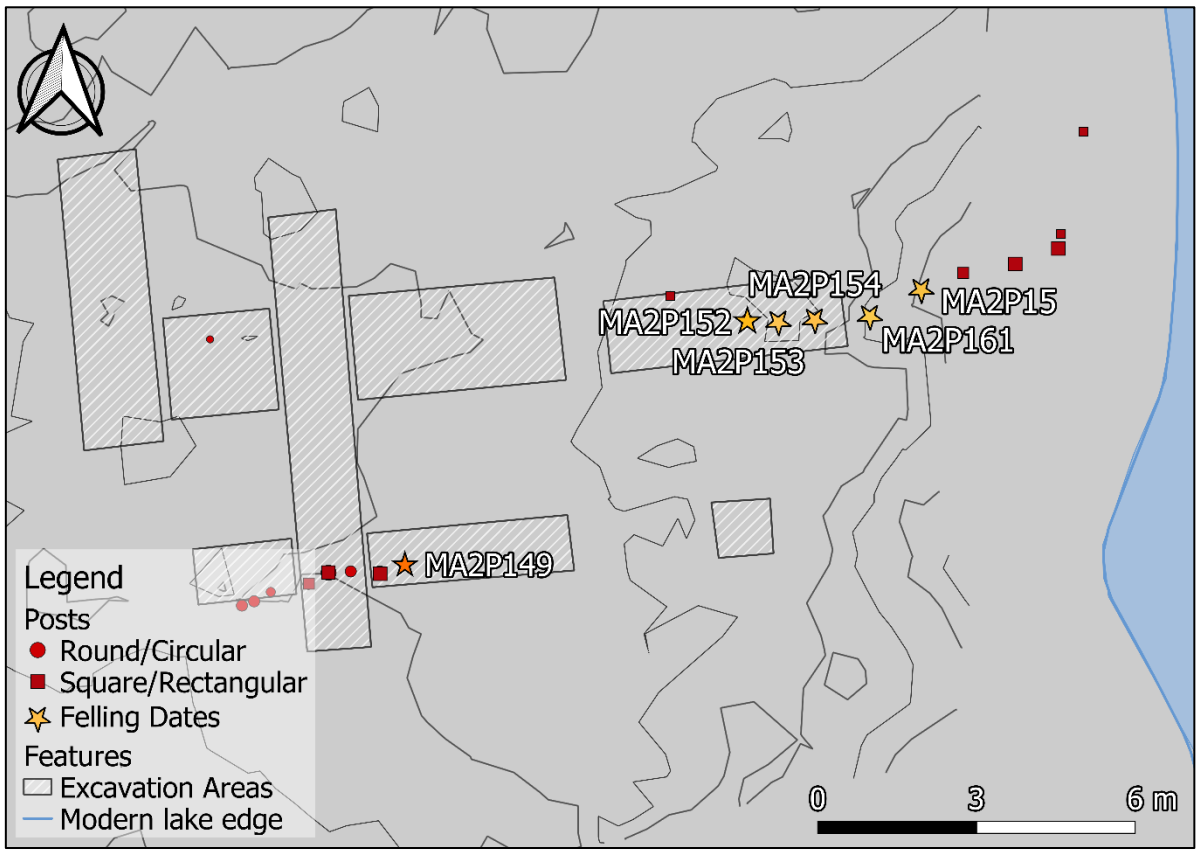

Figure 12.1.5. Site plan of MA2 showing the location of posts that produced successful Felling Dates.

12.1.3.1 Phase I

The earliest evidence of palisade construction at MA2 (Phase I) is provided by the Felling Date of MA2P161 (AD 1730–1747, 95% HPD). The Modelled Date for Phase I reports a date range of AD 1689–1790 (95% HPD), which, in addition to the Felling Date for MA2P161 (Figure 12.1.4), strongly indicates that this phase of palisade construction occurred in the early to middle 1700s (Table 12.1.4). As the Felling Date for MA2P161 provides the earliest direct evidence of palisade construction at MA2, Phase I is interpreted as the likely date at which the site was first fortified.

12.1.3.2 Interval 1

The Interval between Phases I and II at MA2 is modelled as 4–70 years (95% HPD) (Table 12.1.4). The Difference command querying the MDate for Phases I and II confirms that both Phases represent statistically different periods (Table 12.1.5).

12.1.3.3 Phase II

One further palisade construction Phase is identified at MA2 (Phase II), supported by the Felling Dates of four posts: MA2P15 (AD 1800–1810, 95% HPD), MA2P152 (AD 1799–1812, 95% HPD), MA2P153 (AD 1800–1810, 95% HPD), and MA2P154 (AD 1800–1810, 95% HPD). The Modelled Date for Phase II reports a date range of AD 1795–1815 (95% HPD), which, in addition to the four Felling Dates (Figure 12.1.4), strongly indicates that this phase of palisade construction occurred in the early 1800s. As all five sampled posts were positioned within the same inner palisade row, this construction activity (Phase II) is interpreted as a palisade repair episode (following its initial construction in Phase I).

12.1.3.4 Occupation Span

The Span query (encompassing both identified Phases) supports that MA2 was occupied as a pā for between 58–168 years (95% HPD). While the raised mound and palisade defences identified at MA2 are less extensive than those identified at MA1, the archaeological evidence recorded at MA2 still suggests a moderate occupation history. As discussed in Section 4.1.1.2, evidence of multiple raised storehouses, cooking and processing areas, and formal structures

were identified during the 1968 excavations. The floors of these identified structures and activity areas were shown to be built up over time, with several floors exhibiting successive (superimposed) sand layers and living debris of up to 80 cm (Bellwood, 1972b, p. 29). Additionally, Trench E contained 14 primary sand lenses, varying in size and shape, interpreted as evidence of four phases of occupation. Year-round occupation of the site was also hypothesised, highlighting three houses built with solid walls and hearths (presumably for heating). Therefore, given the extensive archaeological evidence identified at MA2, and the WMD and Bayesian sequence analysis results presented here, an occupation span of 58–168 years is considered a reasonable representation of how long the site was potentially occupied as a pā.

12.1.4 Lake Mangahia (MGA)

Event scale analysis (WMD) conducted on the post assemblage from MGA yielded five Felling Dates, representing four spatially distinct palisade rows (Figure 12.1.6). These five Felling Dates were incorporated into an OxCal Sequence model (see Appendix E.3) consisting of four sequential Phases (Phases I–IV) (Table 12.1.6, Figure 12.1.7 and Figure 12.1.8), supported by the results of Interval, Difference, and Span commands. One minor outlier, 113_MGAP316 (173–181), was detected and down-weighted during the analysis, with a prior outlier probability of 6% (prior: 5%). This minor outlier was discussed in detail in Section 8.5 and resulted from a ^{14}C age offset over the calibration plateau in the eighteenth century. Again, all the D_Sequence models included in the local scale Sequence model pass the A_{comb} (An) threshold and exhibit universally high (> 95%) convergence.

Table 12.1.6. Results of the site sequence model for MGA.

MGA	Felling Date and MDate Results					
	Parameter	Median Cal. Age	68% HPD	95% HPD	C	A_{comb} (An)
Phase I	**MGAP313**	**AD 1554 ± 23**	**AD 1542–1564**	**AD 1532–1636**	**99**	**82 (31.6)**
	MDate	AD 1563 ± 50	AD 1528–1620	AD 1483–1693	99	-
Interval 1	-	-	76–216 (yrs)	1–220 (yrs)	100	-
Phase II	**MGAP311**	**AD 1774 ± 4**	**AD 1770–1779**	**AD 1765–1783**	**100**	**59 (26.7)**
	MDate	AD 1769 ± 29	AD 1758–1783	AD 1690–1788	**100**	**-**
Interval 2	-	-	1–8 (yrs)	1–15 (yrs)	100	-
Phase III	**MGAP281**	**AD 1788 ± 3**	**AD 1785–1791**	**AD 1783–1794**	**100**	**86 (31.6)**
	MGAP316	**AD 1787 ± 3**	**AD 1785–1791**	**AD 1781–1794**	**100**	**62 (31.6)**
	MDate	AD 1788 ± 4	AD 1784–1792	AD 1780–1797	100	-
Interval 3	-	-	1–12 (yrs)	1–20 (yrs)	100	-
Phase IV	**MGAP320**	**AD 1806 ± 4**	**AD 1802–1811**	**AD 1799–1815**	100	**131 (31.6)**
	MDate	AD 1808 ± 21	AD 1798–1816	AD 1790–1851	100	-
Span	-	-	248–326 (yrs)	175–418 (yrs)	96	-

Note. Felling Dates produced from posts sampled from MGA are presented in bold. Interval and Span results are presented in years (yrs).

Table 12.1.7. Results of the difference queries included in the local scale Sequence model for MA2.

MDate Queried	Difference range (BP)	Different (yes/no)
Phase I – II	-239 to -143 (68%) -279 to -59 (95%)	Yes
Phase II – III	-31 to -4 (68%) -98 to -1 (95%)	Yes
Phase III – IV	-28 to -9 (68%) -61 to -2 (95%)	Yes

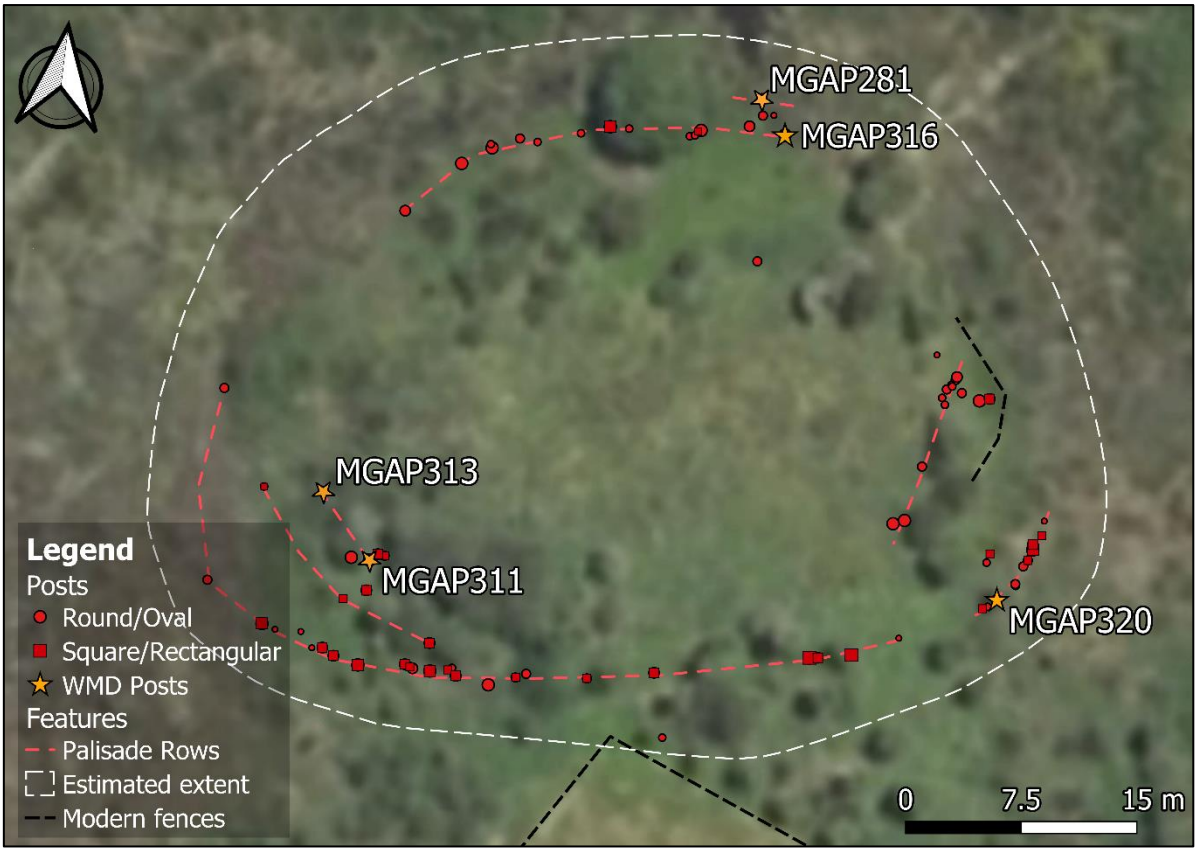

Figure 12.1.6. Site plan of MGA showing the location of posts that produced successful Felling Dates[48].

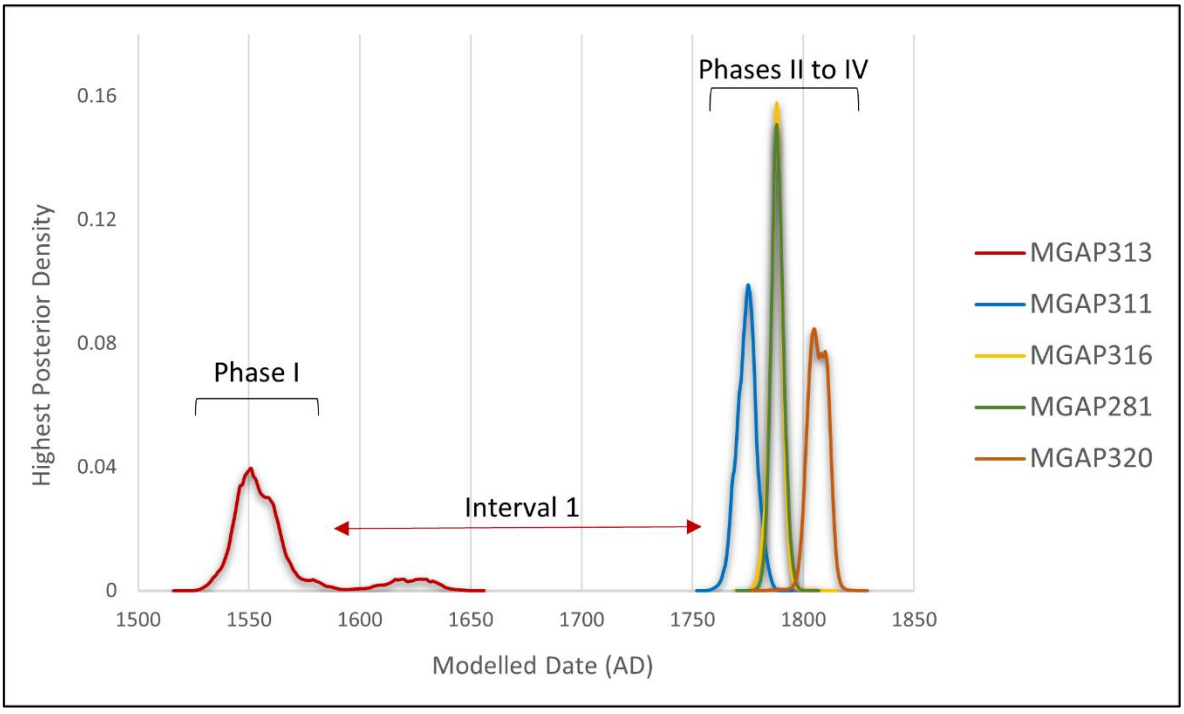

Figure 12.1.7. Felling Dates and phasing identified at MGA.

[48] This figure contains data sourced from the LINZ Data Service, licensed for reuse under the CC BY 4.0.

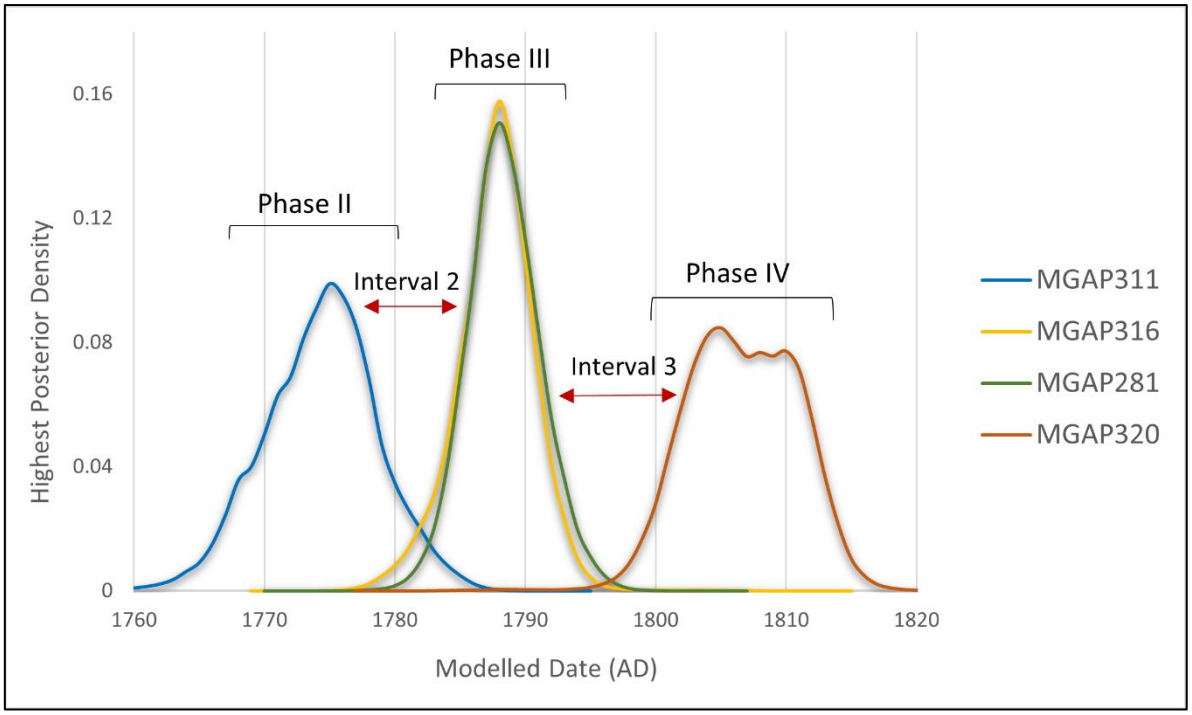

Figure 12.1.8 Felling Dates and phasing identified at MGA (Phase II–IV).

12.1.4.1 Phase I

The earliest evidence of palisade construction at MGA (Phase I) is provided by the Felling Date of MGAP313 (AD 1532–1636, 95% HPD). MGAP313 was positioned within the innermost palisade row identified, located at the base of the raised mound on the southwestern side of the pā. The Modelled Date for Phase I provides a date range of AD 1532–1636 (95% HPD), which, in addition to the Felling Date for MGAP313 (Figure 12.1.7), strongly indicates that this phase of palisade construction occurred in the middle 1500s (see 68% HPD in Table 12.1.6). As the Felling Date for MGAP313 provides the earliest direct evidence of palisade construction at MGA, Phase I is interpreted as the likely date at which the site was first fortified.

12.1.4.2 Interval 1

The interval between Phases I and II is modelled as 1–220 years (95% HPD) (Table 12.1.6). The Difference command querying the MDate for Phases I and II confirms that both Phases represent statistically different periods (Table 12.1.7).

12.1.4.3 Phase II

The second palisade construction phase (Phase II) is supported by the Felling Date of MGAP311 (AD 1765–1783, 95% HPD). MGAP311 was also positioned within the innermost palisade row identified on the southwestern side of the pā (same row as MGAP313). The Modelled Date for Phase II reports a date range of AD 1690–1788 (95% HPD), which, in addition to the Felling Date for MGAP311 (Figure 12.1.8), strongly indicates that this phase of palisade construction occurred in the middle to late 1700s (Table 12.1.6). As this is the second palisade construction event identified within this row, Phase II is interpreted as a palisade repair activity during the mid to late 1700s.

12.1.4.4 Interval 2

The interval between Phases II and III is modelled as 1–15 years (95% HPD) (Table 12.1.6). The Difference command querying the MDate for Phases II and III confirms that both Phases represent statistically different periods (Table 12.1.7).

12.1.4.5 Phase III

The third construction phase (Phase III) identified at MGA is supported by the Felling Dates of MGAP281 (AD 1783–1794, 95% HPD) and MGAP316 (AD 1781–1794, 95% HPD). Both posts were located close to the northern extent of MGA. MGAP281 was located in the second palisade row, while MGAP316 was located in the third palisade row (working from the raised pā mound outwards). The Modelled Date for Phase III reports a date range of AD 1780–1797 (95% HPD), which, in addition to the two Felling Dates (Figure 12.1.8), strongly indicates that this phase of palisade construction occurred during the late 1700s. As this is the third construction phase identified at MGA, representing the addition of two palisade rows at MGA, it is interpreted as a palisade redevelopment activity.

12.1.4.6 Interval 3

The interval between Phases III and IV is modelled as 1–20 years (95% HPD) (Table 12.1.6). The Difference command querying the MDate for Phases II and III confirms that both Phases represent statistically different periods (Table 12.1.7).

12.1.4.7 Phase IV

The fourth and final palisade construction Phase identified at MGA (Phase IV) is supported by the Felling Date of MGAP320 (AD 1799–1815, 95% HPD). MGAP320 was located on the southeastern side of the pā, within the outermost palisade row identified. The Modelled Date for Phase IV reports a date range of AD 1790–1851 (95% HPD), which, in addition to the Felling Date for MGAP320 (Figure 12.1.8), strongly indicates that this phase of palisade construction occurred during the early 1800s. As this is the last (fourth) palisade construction event identified at MGA, representing the addition of the outermost palisade row, Phase IV is interpreted as a palisade redevelopment activity.

12.1.4.8 Occupation Span

The span query (encompassing all four identified Phases) supports that MGA was occupied as a pā for between 175–418 years (95% HPD). As presented in Section 8.1, the pā at Lake Mangahia is heavily stratified, exhibiting multiple terraces and raised living surfaces. Excavations showed that the raised mound was constructed using multiple imported sediments (forming up to 10 layers in some areas), implying that the pā was occupied over a long period. Therefore, given the extensive evidence of long-term occupation at MGA, and the WMD and Bayesian sequence analysis results presented here, an occupation span of 175–418 years is considered a reasonable representation of how long the site was potentially occupied as a pā

12.1.5 Taraheke Pā (TAR)

Event scale analysis (WMD) conducted on the post assemblage from TAR yielded two successful Felling Dates (Section 9.5). Both posts originate from a single post alignment extending out from the tip of the headland into the adjacent stream (Figure 12.1.10). This alignment is interpreted as a defensive structure, canoe (waka) landing or eel ware (pā tuna). As the defensive nature of this alignment cannot be categorically stated, the produced Felling Dates can only be used as a proxy for the occupation of Taraheke pā and not as an interpretation of fortification. Both successful WMDs were incorporated into an OxCal Sequence model (see Appendix E.4) consisting of two sequential phases (Phase I and II) (Figure 12.1.9), supported by the results of Interval, Difference, and Span commands (Table 12.1.8). While the Felling Date of TARP131 does not pass the A_{comb} > An threshold, the accuracy of this result was

discussed in detail in Section 9.5.1. No outliers were detected during the analysis, and convergence values (C) remained universally high (>95%).

Table 12.1.8. TAR local scale Sequence model results.

TAR	Felling Date and MDate Results					
	Parameter	Median Cal. Age	68% HPD	95% HPD	C	A_{comb} (An)
Phase I	**TARP132**	**AD 1515 ± 10**	**AD 1506–1525**	**AD 1500–1538**	**98**	**87 (35)**
	MDate	AD 1516 ± 24	AD 1503–1533	AD 1474–1552	98	
Interval 1	-	-	0–25 (yrs)	0–41 (yrs)	99	-
Phase II	**TARP131**	**AD 1556 ± 4**	**AD 1552–1560**	**AD 1548–1565**	**99**	**24 (25)**
	MDate	AD 1557 ± 25	AD 1545–1567	AD 1526–1600	99	
Span	-	-	30–83 (yrs)	4–177 (yrs)	95	-

Note. Felling Dates produced from posts sampled from TAR are presented in bold. Interval and Span results are presented in years (yrs).

Table 12.1.9. Results of the difference query included in the local scale Sequence model for TAR.

MDate Queried	Difference range (BP)	Different (yes/no)
Phase I – Phase II	-56 to -16 (68%) -107 to -2 (95%)	Yes

Note. The BP age range does not cross zero, indicating a difference.

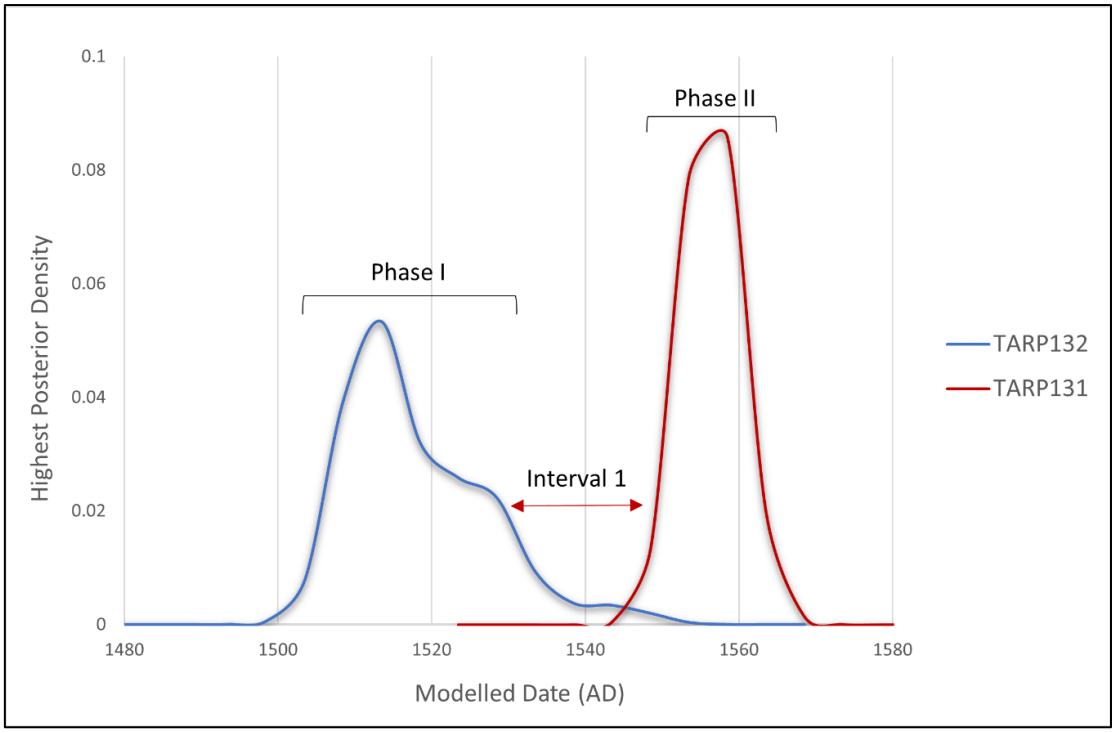

Figure 12.1.9. Felling Dates and phasing identified at TAR.

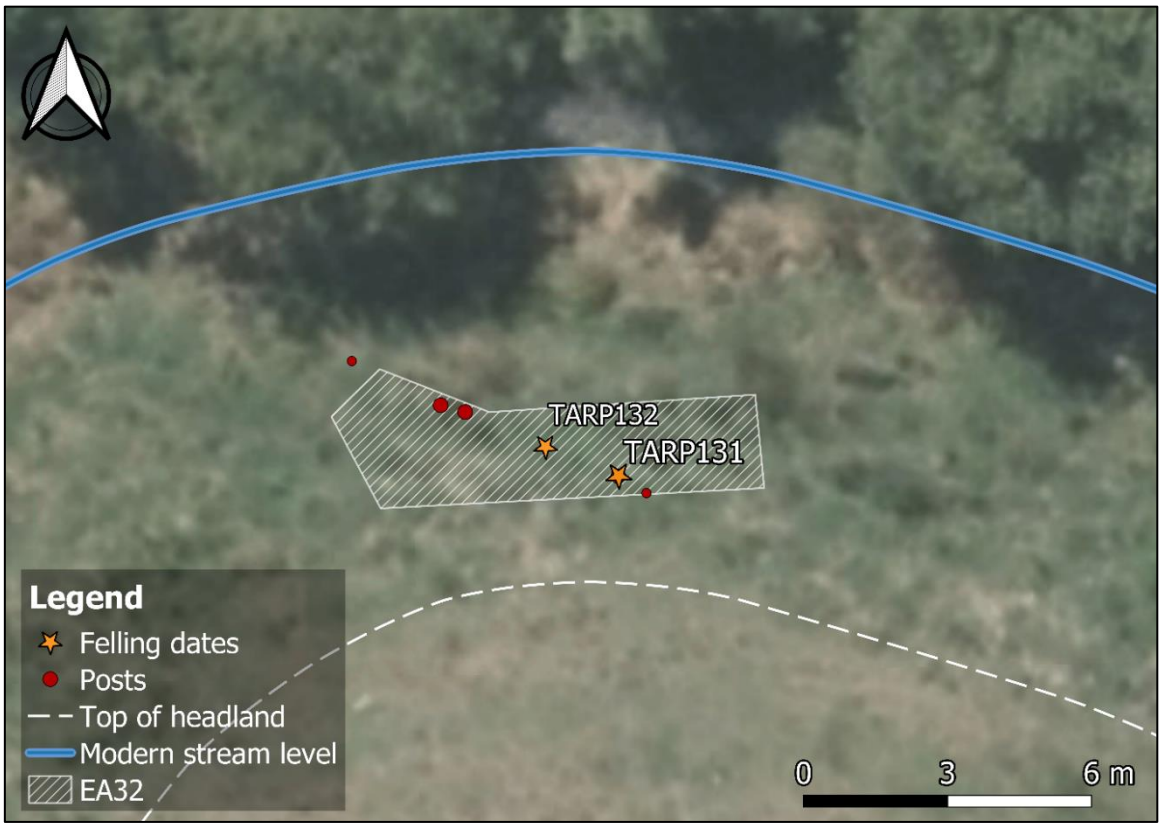

Figure 12.1.10. Plan drawing of EA32 at TAR showing the location of posts that produced successful Felling Dates[49].

[49] This figure contains data sourced from the LINZ Data Service, licensed for reuse under the CC BY 4.0.

12.1.5.1 Phase I

The earliest evidence of occupation at TAR (Phase I) is provided by the Felling Date of TARP132 (AD 1500–1538, 95% HPD). The Modelled Date for Phase I provides a date range of AD 1474–1552 (95% HPD). This evidence strongly suggests that this structure was first constructed in the early 1500s (Figure 12.1.9), providing clear evidence that Taraheke Pā was occupied during this period. While the defensive features identified at Taraheke Pā (multiple defensive ditches) unequivocally identify that the site was occupied as a pā at some point in time, it cannot be certain that these defences were in use during Phase I.

12.1.5.2 Interval 1

The interval between Phases I and II is modelled as 0–41 years (95% HPD) (Table 12.1.8). The Difference command querying the Modelled Dates for Phases I and II confirms that both Phases represent statistically different periods (Table 12.1.9).

12.1.5.3 Phase II

One further construction Phase is identified at TAR (Phase II), supported by the Felling Date of TARP131 (AD 1548–1565, 95% HPD). The Modelled Date for Phase II provides a date range of AD 1526–1600 (95% HPD). Both the Felling Date for TARP131 (Figure 12.1.9) and the Modelled Date for Phase II strongly indicate that this phase of construction activity occurred in the middle of the 1500s (Table 12.1.8). As both posts were sampled from the same alignment, Phase II is interpreted as the repair of this structure (following its initial construction in Phase I).

12.1.5.4 Occupation Span

The Span query supports that Taraheke Pā was occupied for 4–177 years (95% HPD). As this span query only relates to the two phases of structure construction activity identified at the site, it is likely a poor reflection of the occupation history of Taraheke Pā. Further, archaeological and chronological evidence is required to determine the extent of the occupation at this site.

12.1.6 Te Uapata Pā (TEU)

Event scale analysis (WMD) conducted on the post assemblage from TEU yielded three successful Felling Dates (Section 10.5). All three posts originate from a single palisade row on the headland pā's eastern side. This alignment is split into a northern and southern portion by a gap in the defences (Figure 12.1.11). Additionally, as discussed in Section 4.1.4, Te Uapata was the only pā included in this study with complementary ^{14}C dates of suitable provenance from previous mitigation investigations at the pā (see Gainsford and Gumbley (2020) for details). These ^{14}C dates include eight short-lived charcoal samples from three fire features and a linear depression. The Modelled Date ranges for these ^{14}C dates provide evidence to support that Te Uapata was occupied between AD 1650–1850 (95% HPD). Unfortunately, their lack of precision (owing to their relationship with a calibration plateau) limits the use of these results in the local scale analysis, which aims to identify palisade construction phases on a timescale of a single generation. For this reason, these ^{14}C dates are not included in the local scale sequence model. The three successful WMDs (D_Sequence models) were incorporated into an OxCal Sequence model (see Appendix E.5) consisting of two sequential phases (Phase I and II), supported by the results of Interval, Difference, and Span commands (Table 12.1.10, Table 12.1.11 and Figure 12.1.12).

Table 12.1.10. Results of local scale Sequence model for TEU.

TEU	**Felling Date and MDate Results**					
	Parameter	Median Cal. Age	68% HPD	95% HPD	C	A_{comb} (An)
Phase I	**TEUP219**	**AD 1788 ± 6**	**AD 1781–1794**	**AD 1776–1803**	**100**	**109 (32)**
	MDate	AD 1788 ± 15	AD 1779–1797	AD 1759–1810	100	-
Interval 1	-	-	0–16 (yrs)	0–26 (yrs)	100	-
Phase II	**TEUP234**	**AD 1810 ± 3**	**AD 1806–1814**	**AD 1802–1817**	**100**	**51 (29)**
	TEUP244	**AD 1811 ± 3**	**AD 1807–1816**	**AD 1803–1820**	**100**	**82 (32)**
	MDate	AD 1811 ± 7	AD 1805–1816	AD 1796–1828	100	-
Span	-	-	18–49 (yrs)	0–87 (yrs)	99	-

Note. Felling Dates produced from posts sampled from MA2 are presented in bold. Interval and Span results are presented in years (yrs).

Table 12.1.11. Results of the difference queries included in the local scale Sequence model for TEU.

MDate Queried	Difference range (BP)	Different (yes/no)
Phase I – Phase II	-32 to -12 (68%) -54 to -1 (95%)	Yes (68%) Yes (95%)

Note. The BP age range does not cross zero, indicating a difference.

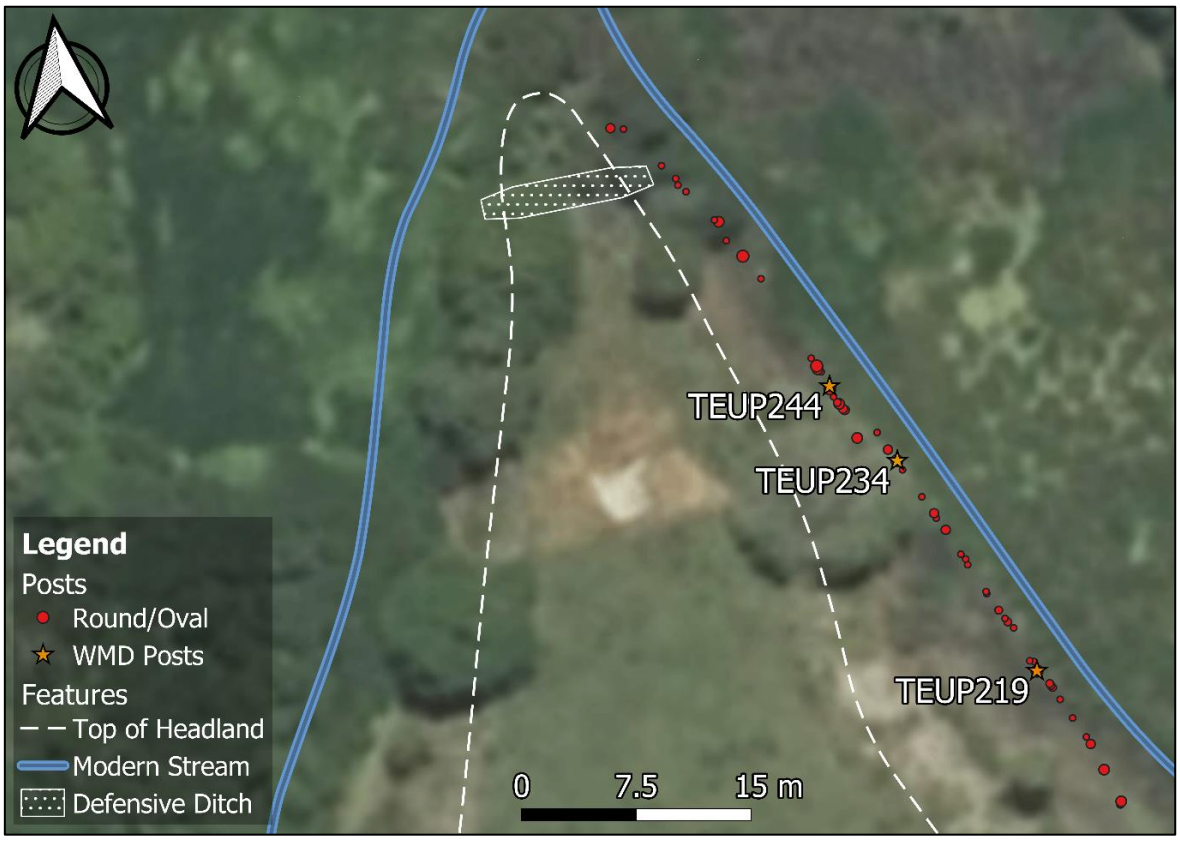

Figure 12.1.11. Site plan of MGA showing the location of posts that produced successful Felling Dates[50].

[50] This figure contains data sourced from the LINZ Data Service, licensed for reuse under the CC BY 4.0.

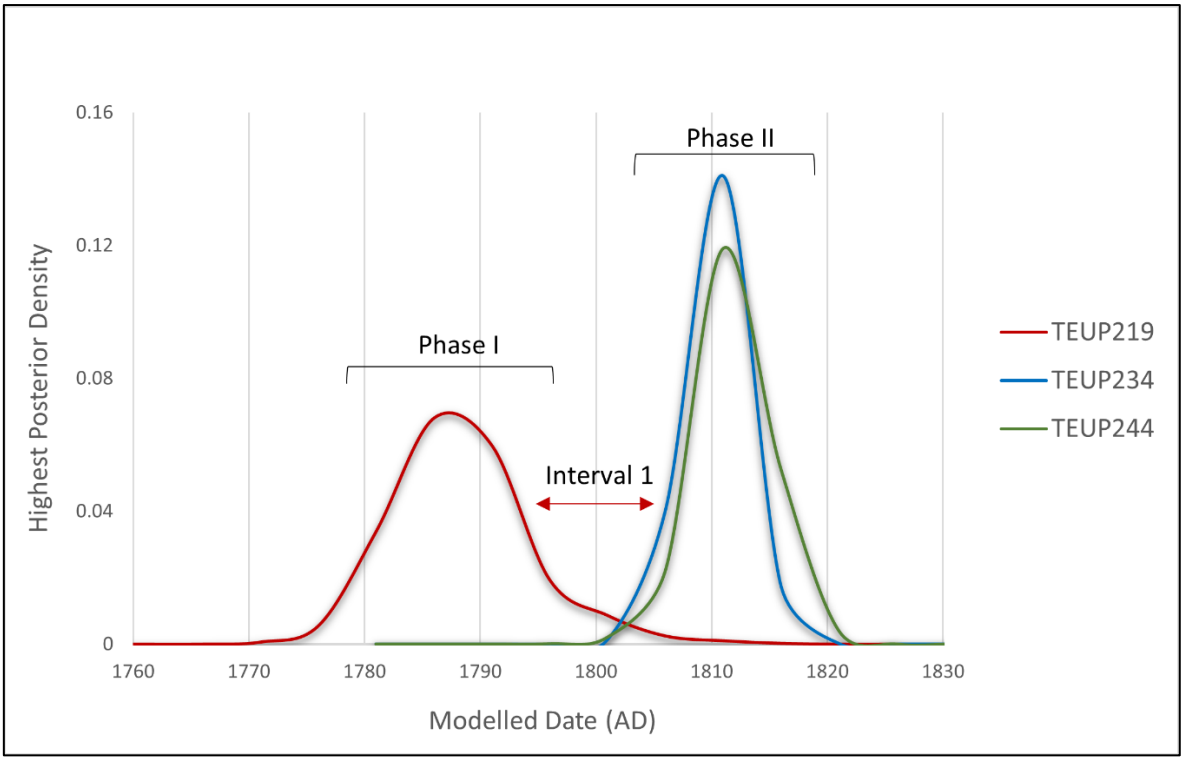

Figure 12.1.12. Felling Dates and phasing identified at TEU.

12.1.6.1 Phase I

The earliest evidence of palisade construction at Te Uapata Pā (Phase I) is provided by the Felling Date of TEUP219 (AD 1776–1803, 95% HPD), which, in addition to the Modelled Date for Phase I (AD 1759–1810, 95% HPD), strongly indicates this phase of palisade construction occurred during the late 1700s (Figure 12.1.12). These results provide the earliest direct evidence of palisade construction at this site, indicating TEU was occupied as a defended place during this period.

12.1.6.2 Interval 1

The interval between Phases I and II at Te Uapata Pā is modelled at 0–26 years (95% HPD) (Table 12.1.4). The Difference command querying the MDate for Phases I and II confirms that both Phases represent statistically different periods (Table 12.1.5).

12.1.6.3 Phase II

One further palisade construction Phase is identified at TEU (Phase II), supported by the Felling Dates of TEUP234 (AD 1802–1817, 95% HPD) and TEUP244 (AD 1803–1820, 95% HPD). The Modelled Date for Phase II provides a date range of AD 1796–1828 (95% HPD), which, in addition to the Felling Dates (Figure 12.1.12), strongly indicates that this phase of palisade construction occurred during the early 1800s. While all three posts from Phase 1 and Phase II are in the same alignment, the two Felling Dates included in Phase II are close to a gap in the palisade defences (possible entranceway). Therefore, this second Phase of palisade construction (Phase II) could represent the repair of this palisade row or the installation of this entranceway.

12.1.6.4 Occupation Span

The Span query supports that Te Uapata Pā was occupied as a defended place for 0–87 years (95% HPD). As the calculated span only relates to the two brief phases of palisade construction activity, it is possibly a poor reflection of the occupation history of the site given the recorded traditional history, the small assemblage size, and the additional radiocarbon evidence produced by Gainsford and Gumbley (2020). However, from the current archaeological and chronological evidence, it appears that Te Uapata Pā may have been occupied as an undefended site (without palisade defences) for some time (from as early as AD 1650), with the palisade defences constructed in the late 1700s.

12.1.7 Lake Rotokauri (ROT)

WMD analysis conducted on the post assemblage from the pā at Lake Rotokauri yielded one successful Felling Date. This Felling Date represents a post (ROTP353) used to construct a palisade defence on the northeastern boundary of the pā (see Section 11.1). As this was the only successful Felling Date resulting from the event scale analysis, local scale analysis was not conducted. Instead, the Felling Date of ROTP353 (AD 1499–1536, 95% HPD) is used as evidence for when this palisade was constructed (see Section 11.5.1), providing evidence for when this site was occupied as a pā.

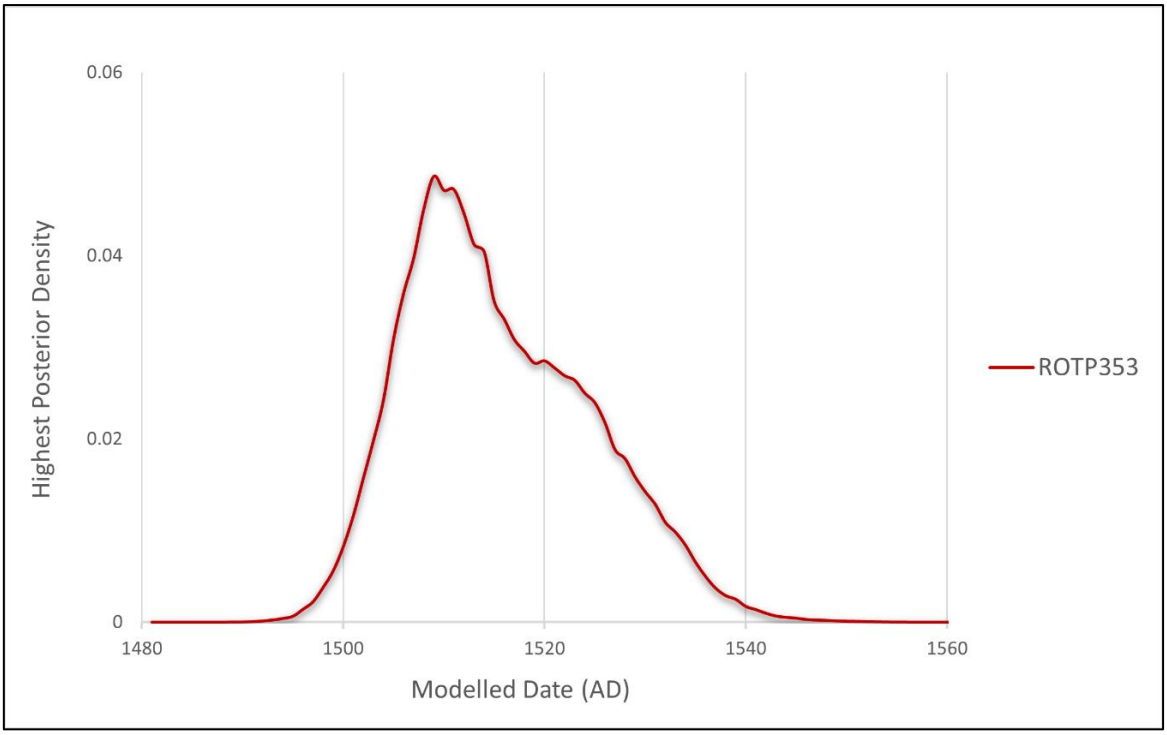

Figure 12.1.13. The Felling Date produced for ROTP353 from ROT.

12.2 Regional Scale Analysis

The third objective of this thesis focuses on the regional scale, exploring the spatio-temporal relationship between seven pā by identifying shared spatio-temporal patterns of palisade construction activity, including initial construction, repair and redevelopment episodes. Here, shared regional episodes of palisade construction activity are interpreted as evidence of overarching (controlling) variables responsible for the emergence, spread, and development of pā over time within the subject area. A regional chronological framework was developed to achieve this objective, using two Bayesian Sequence models incorporating the results of the event and local scale analyses. Three additional WMDs previously produced on posts recovered from Otāhau Pā (OTA) (Hogg et al., 2017) were also included in the regional scale analysis (Figure 12.2.1), providing further evidence of palisade construction activity in the north of the subject area (Taupiri). As with the local scale analysis, both regional scale Sequence models were constructed using the Bayesian Sequence analysis option in OxCal v 4.4. They were implemented using the SHCal20 atmospheric calibration curve, and their internal consistency was tested using the SSimple s-type outlier model. As above, specialised OxCal commands offered by OxCal v 4.4 were used to develop and test each model, providing evidence to support the interpretation of shared episodes of palisade construction across the

region (Table 12.1.1). The structure of both regional scale Sequence models is discussed in detail below (see also Appendix F).

Figure 12.2.1. The location of the pā included in the regional scale analyses (Middle Waikato Basin)[51].

[51] This figure contains data sourced from the LINZ Data Service, licensed for reuse under the CC BY 4.0.

12.2.1 Overlapping Sequence Model

The first Sequence model is used to identify shared Phases of palisade construction activity between each of the seven pā. This Sequence model consisted of a single Phase, including seven overlapping Sequences (See Appendix F.1). Each overlapping Sequence relates to one of the seven pā (MA1, MA2, MGA, TAR, TEU, ROT and OTA). For those pā included in the local scale analysis (MA1, MA2, MGA, TAR and TEU), their Sequence structure is identical to that presented in Section 12.1. For the pā not included in the local scale analysis (ROT and OTA), their Sequence structure consists of a single Phase bound by a start and end Boundary. As with the local scale analysis, each Phase (within each Sequence) contains the D_Sequence models (WMD) corresponding to that particular construction period (as evidenced by the event and local scale analyses). Also, as with the local scale, a Date command (Modelled Date) is included within each specific Phase from each pā, providing a posterior distribution with a modelled date range that integrates all of the available Felling Dates. These Modelled Dates are utilised in 36 Difference queries. In this application, the Difference command is used in two specific ways: (i) to determine that two distinct phases, identified at two different pā, represent a shared episode of palisade construction (i.e., BP age range crosses zero), and (ii) to determine that two distinct phases, identified at two different pā, do not represent a shared episode of palisade construction (i.e., BP age range does not cross zero). By utilising the Difference command in these two ways (in association with the event and local scale results), the multiple phases within each overlapping Sequence can be organised into a regional chronological sequence. The results of each Difference command are summarised in Table 12.2.1.

It is important to note here that when attempting to determine the structure (Phasing) of the regional chronological framework (Section 12.2.2), a distinct effort was made not to overly generalise the patterns of shared palisade construction activity into broad regional Phases (RP#). Therefore, in several cases, the difference commands could not determine a statistical ‘difference’ or ‘similarity’ between two Phases at a 95% probability when anticipated (e.g. Difference 8, 9 and 10). In such cases, further OxCal Sequence modelling was undertaken, examining the results of the difference commands (68% probability) and the Felling Dates within each queried Phase to determine their probable grouping (in association with the results of the event and local scale analyses).

Table 12.2.1. Results of the difference commands included in the overlapping regional scale Sequence model.

Phase Test	Command	Phase Mdates Queried	Difference (Y/N)	
			BP Age Range (68%)	BP Age Range (95%)
RP1	Difference 1	TAR Phase I vs ROT Phase I	-158 to 141 (N)	-479 to 346 (N)
	Difference 2	TAR Phase I vs MGA Phase I	-97 to -7 (Y)	-183 to 31 (N)
	Difference 3	ROT Phase I vs MGA Phase I	-213 to 98 (N)	-413 to 423 (N)
	Difference 4	TAR Phase II vs MGA Phase I	-63 to 30 (N)	-139 to 79 (N)
	Difference 5	TAR Phase II vs ROT Phase I	-112 to 185 (N)	-433 to 392 (N)
RP2	Difference 6	MA1 Phase I vs MA2 Phase I	-45 to -6.2 (Y)	-80 to 26 (N)
RP2-RP3	Difference 7	MA1 Phase I vs OTA Phase I	-65 to -41 (Y)	-88 to -20 (Y)
	Difference 8	MA1 Phase I vs MGA Phase II	-73 to -35 (Y)	-92 top 36 (N)
	Difference 9	MA2 Phase I vs OTA Phase I	-44 to -9 (Y)	-82 to 26 (N)
	Difference 10	MA2 Phase I vs MGA Phase II	-50 to -1 (Y)	-88 to 78 (N)
RP3	Difference 11	OTA Phase I vs MA1 Phase II	1 to 24 (Y)	-22 to 43 (N)
	Difference 12	OTA Phase I vs MGA Phase II	-18 to 16 (N)	-33 to 94 (N)
	Difference 13	MA1 Phase II vs MGA Phase II	-32 to 7 (N)	-49 to 72 (N)
RP3-RP4	Difference 14	OTA Phase I vs TEU Phase I	-32 to -10 (Y)	-51 to 18 (N)
	Difference 15	OTA Phase I vs MGA Phase III	-28 to -14 (Y)	-44 to 1 (N)
	Difference 16	MA1 Phase II vs MGA Phase III	-44 to -23 (Y)	-58 to -6 (Y)
	Difference 17	MA1 Phase II vs TEU Phase I	-47 to -19 (Y)	-63 to 3 (N)
	Difference 18	MGA Phase II vs TEU Phase I	-38 to -1 (Y)	-113 to 20 (N)
RP4	Difference 19	MGA Phase III vs TEU Phase I	-10 to 9 (N)	-22 to 26 (N)
RP4-RP5	Difference 20	MGA Phase III vs MA1 Phase III	-22 to -5 (Y)	28 to 11 (N)
	Difference 21	MGA Phase III vs MA1 Phase IV	-28 to -22 (Y)	-52 to 14 (Y)
	Difference 22	MGA Phase III vs MA2 Phase II	-23 to -12 (Y)	-30 to -4 (Y)
	Difference 23	MGA Phase III vs TEU Phase II	-29 to -17 (Y)	-39 to -8 (Y)
	Difference 24	TEU Phase I vs MA1 Phase III	-24 to -1 (Y)	-41 to 20 (N)
	Difference 25	TEU Phase I vs MA1 Phase IV	-42 to -19 (Y)	-65 to -6 (Y)
	Difference 26	TEU Phase I vs MA2 Phase II	-27 to -7 (Y)	-45 to 6 (N)
	Difference 27	TEU Phase I vs MGA Phase IV	-33 to -6 (Y)	-69 to 7 (N)
RP5	Difference 28	MA1 Phase III vs MA2 Phase II	-13 to 4 (N)	-30 to 12 (N)
	Difference 29	MA1 Phase III vs MGA Phase IV	-20 to 5 (N)	-50 to 15 (N)
	Difference 30	MA1 Phase III vs TEU Phase II	-19 to -1 (Y)	-37 to 7 (N)
	Difference 31	MA1 Phase IV vs MA2 Phase II	5 to 21 (Y)	-4 to 37 (N)
	Difference 32	MA1 Phase IV vs MGA Phase IV	0 to 23 (Y)	-33 to 42 (N)
	Difference 33	MA1 Phase IV vs TEU Phase II	-1 to 16 (N)	-13 to 33 (N)
	Difference 34	MA2 Phase II vs MGA Phase IV	-11 to 8 (N)	-42 to 18 (N)
	Difference 35	MA2 Phase II vs TEU Phase II	-12 to 1 (N)	-24 to 10 (N)
	Difference 36	MGA Phase IV vs TEU Phase II	-14 to 7 (N)	-28 to 39 (N)

Note. Difference is determined if the BP age range crosses zero. (Y) = Different, (N) = Not Different. RP = regional phase.

12.2.2 Sequential Sequence Model

Following the results of the overlapping Sequence model presented in Section 12.2.1, one further Sequence model was constructed (see Appendix F.2). This Sequence model comprises

a single Sequence consisting of five sequential regional Phases (RP1–5). Each regional Phase includes palisade construction activity identified within a defined period shared by more than one pā, as determined by the results of the overlapping sequence model. An Interval command separates each regional Phase, modelling the time (years) between each defined period of palisade construction activity. Again, a 'Date' command is included within each Phase (MDate), providing a posterior distribution with a date range that integrates the results of all the included Felling Dates. In addition to providing a date range for each regional Phase, these Modelled Dates are evaluated using Difference commands, providing further evidence that each regional Phase is distinct in time compared to the Phase that immediately proceeds or follows it. The results of this analysis are presented in Table 12.2.2 and Table 12.2.3, with the results discussed below. For a complete discussion and interpretation of these results, see Section 13.1.7.

As discussed above, a distinct effort was made not to overly generalise the patterns of shared palisade construction activity into broad regional phases. This approach is particularly relevant for the phases RP2–5, which, as a result, are separated by small intervals (see Section 12.2.2). While these short Intervals are likely the result of the small sample number (i.e., these short intervals likely represent a continuation of regional palisade construction activity rather than a distinct pause in activity, and the length of these interval periods would likely change as more data is added to the regional framework), by defining the regional phasing in this way, distinct narrow periods of shared palisade construction activity are identified on a timescale of fewer than 25 years that, in the future, can be used to test hypotheses about these specific pā in relation to the archaeological landscape of the Middle Waikato Basin. For example, these hypotheses could include testing the chronological relationships between these pā and known conflict periods, population migrations, or horticultural activities.

It is also important to note that the Felling Date (D_Sequence model) results stemming from this Sequence model are not used to interpret precisely when a specific palisade row was constructed at a pā (as with the local scale analysis). Instead, this Sequence model provides a broader interpretation of the shared temporal patterns of palisade construction activity identified across the study area. For this reason, the parameter of interest is the Modelled Date for each regional Phase. As each MDate is defined by the modelled start and end Boundary of each specific Phase, the resulting posterior distribution produces a broader date range compared

to the included Felling Dates. As presented in Section 12.1.1, using the Modelled Dates in this way removes the possibility that specific Felling Dates are overly defined (precise) in their calendar position due to (minor) unidentified errors in the D_Sequence model prior information (see Section 13.1.5.1), or inconsistencies associated with their calibration against SHCal20 (see Section 13.1.5.2).

Table 12.2.2. Regional palisade construction phases identified in the Middle Waikato Basin.

Phase	Site ID	Felling Date and Modelled Date Results			
		Parameter	Median cal. Age	68% HPD	95% HPD
RP1	TAR	TARP132	AD 1519 ± 10	AD 1508–1531	AD 1504–1546
	ROT	ROTP353	AD 1520 ± 10	AD 1508–1529	AD 1502–1539
	TAR	TARP131	AD 1555 ± 4	AD 1552–1560	AD 1549–1563
	MGA	MGAP316	AD 1550 ± 9	AD 1542–1558	AD 1533–1567
		MDate RP1	-	**AD 1514–1562**	**AD 1484–1601**
Interval 1				85–155 (yrs)	18–162 (yrs)
RP2	MA1	MA1P204	AD 1713 ± 6	AD 1707–1720	AD 1702–1726
	MA2	MA2P161	AD 1735 ± 4	AD 1732–1739	AD 1728–1744
		MDate RP2	-	**AD 1703–1742**	**AD 1654–1752**
Interval 2				1–14 (yrs)	1–22 (yrs)
RP3	MA1	MA1P53	AD 1757 ± 3	AD 1754–1760	AD 1751–1764
	OTA	OTAP003	AD 1763 ± 5	AD 1758–1769	AD 1756–1775
	OTA	OTAP005	AD 1768 ± 2	AD 1767–1770	AD 1764–1772
	OTA	OTAP007	AD 1766 ± 3	AD 1764–1769	AD 1757–1772
	MGA	MGAP311	AD 1770 ± 4	AD 1767–1775	AD 1763–1779
		MDate RP3	-	**AD 1757–1771**	**AD 1750–1778**
Interval 3				1–8 (yrs)	1–15 (yrs)
RP4	MGA	MGAP281	AD 1787 ± 3	AD 1784–1790	AD 1781–1794
	MGA	MGAP316	AD 1783 ± 4	AD 1779–1787	AD 1776–1791
	TEU	TEUP219	AD 1786 ± 4	AD 1782–1790	AD 1779–1793
		MDate RP4	-	**AD 1781–1791**	**AD 1776–1796**
Interval 4				7–19 (yrs)	1–22 (yrs)
RP5	MA1	MA1P190	AD 1806 ± 2	AD 1805–1809	AD 1801–1811
	MA1	MA1P208	AD 1807 ± 2	AD 1806–1812	AD 1804–1816
	MA2	MA2P15	AD 1808 ± 3	AD 1805–1809	AD 1802–1711
	MA2	MA2P152	AD 1808 ± 2	AD 1806–1811	AD 1802–1813
	MA2	MA2P153	AD 1807 ± 2	AD 1805–1809	AD 1802–1811
	MA2	MA2P154	AD 1807 ± 2	AD 1805–1810	AD 1802–1811
	MGA	MGAP320	AD 1807 ± 3	AD 1805–1810	AD 1802–1813
	TEU	TEUP234	AD 1808 ± 2	AD 1807–1811	AD 1805–1813
	TEU	TEUP244	AD 1809 ± 3	AD 1807–1812	AD 1804–1816
		MDate RP5	-	**AD 1805–1811**	**AD 1801–1815**
Span				289–320 (yrs)	276–354 (yrs)

Table 12.2.3. Results of the difference commands included in the sequential regional scale Sequence model.

MDate Queried	Difference Age Range (BP)	Different (yes/no)
RP1 – RP2	-214 to -145 (68%) -242 to -88(95%)	Yes
RP2 – RP3	-63 to -21 (68%) -112 to -8 (95%)	Yes
RP3 – RP4	-30 to -13 (68%) -38 to -6 (95%)	Yes
RP4 – RP5	-28 to -16 (68%) -34 to -10 (95%)	Yes

Note. The BP age range does not cross zero, indicating a difference.

12.2.2.1 Regional Phase 1 (RP1)

The earliest evidence of shared palisade construction activity across the Middle Waikato Basin is identified during RP1 (MDate: AD 1484–1601, 95% HPD), with the results strongly indicating RP1 took place during the early to middle 1500s (MDate: AD 1514–1562, 68% HPD). RP1 includes four Felling Dates produced on posts recovered from three pā: TAR, ROT and MGA. Three of these Felling Dates represent the first evidence of construction at each of these pā, including the earliest evidence of palisade construction at ROT and MGA and the construction of a structure identified at TAR. The final Felling Date for TARP131 represents the repair of the identified structure at TAR. Collectively, these three pā span the entire spatial extent of the subject area, indicating pā construction had potentially spread throughout the region by this period.

Table 12.2.4. Regional Phase 1.

Phase	Site ID	Felling Date and Modelled Date Results			
		Parameter	Median cal. age	68% HPD	95% HPD
RP1	TAR	TARP132	AD 1519 ± 10	AD 1508–1531	AD 1504–1546
	ROT	ROTP353	AD 1520 ± 10	AD 1508–1529	AD 1502–1539
	TAR	TARP131	AD 1555 ± 4	AD 1552–1560	AD 1549–1563
	MGA	MGAP316	AD 1550 ± 9	AD 1542–1558	AD 1533–1567
		MDate RP1	-	**AD 1514–1562**	**AD 1484–1601**

12.2.2.2 Interval 1

The results of Interval 1 indicate that the end RP1 is separated from the start of RP2 by 18–162 years (95% HPD). Interval 1 represents a considerable break in the regional chronology, with no evidence of palisade construction activity (shared or not) identified throughout the seventeenth century. A pause in palisade construction activity of this length is striking, indicating that once the first identified wave of pā construction was complete (RP1), the influence of the hypothesised overarching (controlling) variable responsible for pā construction during this period is reduced.

12.2.2.3 Regional Phase 2 (RP2)

The second Phase of shared palisade construction activity in the Middle Waikato Basin is identified during RP2 (MDate: AD 1654–1752, 95% HPD), with the results strongly suggesting this activity took place across the early 1700s (MDate: AD 1703–1742, 68% HPD). In contrast to the results of Interval 1, the start of RP2 represents the beginning of a (likely) continuous period of palisade construction activity across the study area, spanning the entirety of the eighteenth century and into the nineteenth century, highlighted by short intervals (Intervals 2–4) between each of these later phases (RP2–5). RP2 is supported by one Felling Date from each of the two pā surrounding Lake Mangakaware (MA1 and MA2), representing the earliest evidence of palisade construction at both these pā.

Table 12.2.5. Regional Phase 2 results.

Phase	Site ID	Felling Date and Modelled Date Results			
		Parameter	Median cal. Age	68% HPD	95% HPD
RP2	MA1	MA1P204	AD 1713 ± 6	AD 1707–1720	AD 1702–1726
	MA2	MA2P161	AD 1735 ± 4	AD 1732–1739	AD 1728–1744
		MDate RP2	-	**AD 1703–1742**	**AD 1654–1752**

12.2.2.4 Interval 2

The results of Interval 2 suggest that the end of RP2 is separated from the start of RP3 by 1–22 years (95% HPD). The short period between RP2 and RP3 indicates that the hypothesised controlling variable responsible for the emergence of pā around Lake Mangakaware is sustained (and potentially magnified). This short interval (and subsequent intervals between

RP4 and RP5) starkly contrasts with Interval 1, suggesting a different motivation for the palisade construction activity identified after RP1.

12.2.2.5 Regional Phase 3 (RP3)

The third Phase of shared palisade construction activity in the Middle Waikato Basin is identified during RP3 (MDate: AD 1750–1778, 95% HPD), with the results strongly suggesting this activity took place between the middle to late 1700s (MDate: AD 1757–1771, 68% HPD). RP3 is supported by five individual Felling Dates, spread across three pā: MA1 and MGA in the south and OTA in the north of the subject area. The Felling Dates included within RP3 represent the earliest evidence of palisade construction at OTA, the construction of a fighting stage at MA1, and a palisade repair episode at MGA. Crucially, RP3 represents the first evidence of palisade repair and redevelopment within the study area. This activity shows the local populations' active management of these defences, responding to perceived or real pressures (stress) present in the regional landscape.

Table 12.2.6. Regional Phase 3.

Phase	Site ID	Felling Date and Modelled Date Results			
		Parameter	Median cal. Age	68% HPD	95% HPD
RP3	MA1	MA1P53	AD 1757 ± 3	AD 1754–1760	AD 1751–1764
	OTA	OTAP003	AD 1763 ± 5	AD 1758–1769	AD 1756–1775
	OTA	OTAP005	AD 1768 ± 2	AD 1767–1770	AD 1764–1772
	OTA	OTAP007	AD 1766 ± 3	AD 1764–1769	AD 1757–1772
	MGA	MGAP311	AD 1770 ± 4	AD 1767–1775	AD 1763–1779
		MDate RP3	-	**AD 1757–1771**	**AD 1750–1778**

12.2.2.6 Interval 3

The results of Interval 3 suggest that the end of RP3 is separated from the start of RP4 by 1–15 years (95% HPD). This short time interval is interesting, as again, it suggests an ongoing period of stress affecting populations across the Middle Waikato Basin that is not diminishing over time.

12.2.2.7 Regional Phase 4 (RP4)

The fourth Phase of shared palisade construction activity in the Middle Waikato Basin is identified during RP4 (MDate: AD 1776–1796, 95% HPD). RP4 is supported by three Felling Dates, two from MGA in the south and one from TEU in the north. Both Felling Dates from MGA represent palisade redevelopment, including the addition of two new palisade rows at the pā. The Felling Date from TEU represents the earliest evidence of palisade construction at the site. Crucially, all seven pā included in this regional chronology show evidence of at least one palisade row during RP4.

Table 12.2.7. Regional Phase 4.

Phase	Site ID	Felling Date and Modelled Date Results			
		Parameter	Median cal. Age	68% HPD	95% HPD
RP4	MGA	MGAP281	AD 1787 ± 3	AD 1784–1790	AD 1781–1794
	MGA	MGAP316	AD 1783 ± 4	AD 1779–1787	AD 1776–1791
	TEU	TEUP219	AD 1786 ± 4	AD 1782–1790	AD 1779–1793
		MDate RP4	-	**AD 1781–1791**	**AD 1776–1796**

12.2.2.8 Interval 4

The results of Interval 4 suggest that the end RP4 is separated from the start of RP5 by 1–22 years (95% HPD). Again, this short time interval shows a continued period of stress affecting populations across the Middle Waikato Basin that is not diminishing over time.

12.2.2.9 Regional Phase 5 (RP5)

The fifth and final Phase of shared palisade construction activity in the Middle Waikato Basin is identified during RP5 (MDate: AD 1801–1815, 95% HPD). Crucially, RP5 represents a region-wide shared episode of palisade repair and redevelopment, with these activities identified across four of the seven pā: MA1, MA2, MGA and TEU (Table 12.2.8). Again, this activity demonstrates the active management of these defences.

Table 12.2.8. Regional Phase 5.

Phase	Site ID	Felling Date and Modelled Date Results			
		Parameter	Median cal. Age	68% HPD	95% HPD
RP5	MA1	MA1P190	AD 1806 ± 2	AD 1805–1809	AD 1801–1811
	MA1	MA1P208	AD 1807 ± 2	AD 1806–1812	AD 1804–1816
	MA2	MA2P15	AD 1808 ± 3	AD 1805–1809	AD 1802–1711
	MA2	MA2P152	AD 1808 ± 2	AD 1806–1811	AD 1802–1813
	MA2	MA2P153	AD 1807 ± 2	AD 1805–1809	AD 1802–1811
	MA2	MA2P154	AD 1807 ± 2	AD 1805–1810	AD 1802–1811
	MGA	MGAP320	AD 1807 ± 3	AD 1805–1810	AD 1802–1813
	TEU	TEUP234	AD 1808 ± 2	AD 1807–1811	AD 1805–1813
	TEU	TEUP244	AD 1809 ± 3	AD 1807–1812	AD 1804–1816
		MDate RP5	-	**AD 1805–1811**	**AD 1801–1815**

The results of the Span command indicate that palisade construction activity (indicating pā occupation and active management of the palisade defences) has occurred across the Middle Waikato Basin for between 276–354 years (95% HPD).

12.3 Chapter Summary

This chapter concentrated on this study's second and third objectives, which applied a local and regional scale of analysis to the post assemblage analysed in this research. First, successful Felling Dates produced from each site were combined into six Sequence models, identifying distinct palisade construction phases at each pā. This analysis successfully identified direct evidence for when palisade defences were potentially first constructed at each pā (apart from at Taraheke Pā). Additionally, sequential phases of palisade construction, relating to palisade repair and redevelopment periods, were identified at four pā: MA1, MA2, MGA, and TEU. Second, a regional chronological framework of shared palisade construction activity was established. This analysis successfully provided potential evidence of the first wave of pā construction regionally, suggesting a sustained fortification period throughout the Middle Waikato Basin during AD 1484–1601. The regional scale analysis also identified a distinct pause in palisade construction activity between RP1 and RP2 (Interval 1), potentially encompassing the seventeenth century. Following this break in the chronology, palisade construction activity is shown to be relatively constant throughout the eighteenth century. Finally, the early nineteenth century is proposed as a period of region-wide palisade repair and redevelopment. These shared episodes of palisade construction activity indicate the influence

of overarching controlling variables responsible for the emergence, occupation and development of pā across the Middle Waikato Basin. The implications of these results are discussed further in Chapter 13.

Chapter 13. Synthesis

13.1 Discussion

This study represents the first attempt at establishing a comprehensive chronological framework of pā construction, proliferation, and development within the Middle Waikato Basin, contextualising pā to the broader archaeological and cultural landscape. Six pā were investigated, with excavations focusing on recording and sampling identified palisade defences for ^{14}C WMD purposes. The WMDs produced in this study were interpreted using the theory of time perspectivism, utilising a multi-scalar research approach focused on three primary objectives. The first objective focused on the event scale, producing accurate and precise calendar dates for the felling of a tree (Felling Date) used in the construction of a palisade row. The second objective focused on the local scale, creating a chronology that tracked the development of the palisade defences through time at each pā. The third objective focused on the regional scale, establishing a comprehensive regional chronological framework that identified shared episodes of palisade construction activity across seven pā within the Middle Waikato Basin. Six key conclusions have resulted from this research:

1. Palisade defences are preserved at pā located in wetlands throughout the Middle Waikato Basin and, in turn, are likely retained in wetland environments elsewhere across the country. Therefore, the analytical approach applied in this study could be applied in other regions across the country where suitable posts can be identified. However, most of the posts identified in this study were moderately decayed. This observation indicates that this preservation state is time-limited as further decay could restrict the availability of posts for use in any further research.
2. A range of tree species was used to construct the identified palisade defences. The broad array of species identified reflects the vegetation growing within the respective catchments of each pā. This finding indicates that populations used whatever species were found locally, targeting timber of suitable size and quality.
3. Tree-ring analysis of New Zealand tree taxa can be challenging, often inhibited by tree-ring growth abnormalities resulting from the poor growing conditions surrounding the

wetland pā. Despite these limitations, accurate ring counts can be produced across various species, with accuracy dependent on the quality of each sample.

4. WMD can be successfully applied to suitable posts within New Zealand archaeological contexts. However, the applicability of this ^{14}C dating method is limited, as it relies on a specific, well-preserved artefact type that does not exhibit characteristics that could affect the accuracy or precision of the results.
5. The ^{14}C dating method applied in this study (WMD and Bayesian Sequence analysis) can successfully track the development of the palisade defences over time. Distinct palisade construction phasing was identified at four pā sites (five including the posts analysed at Taraheke Pā), providing direct evidence for the likely earliest period of palisade construction and successive episodes of palisade repair and redevelopment activities. This identified phasing shows that these defences were actively managed over time, responding to various proposed variables from the cultural landscape.
6. The ^{14}C dating method applied in this study also successfully identified regional phases of shared palisade construction activity across the Middle Waikato Basin. These regional phases are interpreted as evidence for environmental and/or cultural processes that were impacting populations within the subject area, resulting the emergence, occupation, and proliferation of pā within the region.

These research conclusions are discussed below concerning each analysis stage, highlighting the limitations, interpretations and conclusions produced from the evidence identified.

13.1.1 Fieldwork and Post Assemblage

Palisade defences were recorded at five of six pā investigated, with a post alignment (structure) acting as a proxy for palisade defences at TAR. A total of 354 posts were recorded across the entire subject area, with a subset of 73 posts extracted, of which 43 were analysed (Table 13.1.1). As discussed in Section 5.1.1, a specific sampling strategy was applied to determine which posts were extracted and sampled for analysis. While this strategy aimed to ensure robust sampling practices, it also limited the assemblage size. Notably, just over 20% of the posts identified passed the selection criteria for extraction, and only 12% were determined to be suitable for sampling.

Table 13.1.1. Details of posts identified, extracted and sampled from each pā site.

Site	Posts Identified	Posts Extracted	Posts Sampled
MA1	130	22	10
MA2	43	19	13
MGA	87	12	7
TAR	6	6	4
TEU	84	9	7
ROT	4	4	2
Total	**354**	**72**	**43**

Although this study succeeded in producing samples suitable for WMD at each pā, several critical palisade contexts (rows) were represented by only a few posts that met the sampling criteria. In contrast, other rows did not have any (Table 13.1.2). This situation was primarily the result of poor post preservation. While initially not an issue, this limitation became evident during post-excavation analysis, as further samples were removed from the assemblage due to limiting characteristics (e.g. poor sample condition, tree-ring analysis limitations, and poor Felling Date precision following calibration). These limitations most affected the samples from MA1, where multiple rows of palisades were identified, including a minimum of six palisade rows in Area A. Only four posts from three of the palisade rows passed the sampling criteria from Area A, and only one post returned a successful Felling Date. With these results in mind, the applied sampling strategy was occasionally expanded during excavations conducted later in the project (i.e., at MGA, TAR, TEU and ROT), including posts with some of the limiting characteristics discussed above when insufficient appropriate posts could be identified and extracted.

Table 13.1.2. Palisade rows identified and sampled at each pā site.

Site	Area	Rows identified	Rows sampled
MA1	Area A (northern lake edge)	6	3
MA1	Area B (southern side of pā)	3	3
MA2	Area A (eastern lake edge)	1	1
MA2	Area B (southeastern corner)	2	2
MGA	Entire pā circumference is represented	4	4
TEU	Eastern alignment (one row in two parts)	2	2
TAR	EA32 (northern tip of pā)	1	1
ROT	Northeastern corner (outer row)	1	1

Despite these sampling limitations, the posts extracted were still moderately well-preserved below the ground surface (average post depth = 134 cm), with the average length of extracted

posts across all six pā recorded as >1 m (Table 13.1.3). Extrapolating from this finding, palisade defences surrounding other pā in wetland environments throughout the Waikato and New Zealand are likely to be preserved *in situ*, depending on local environmental conditions.

Table 13.1.3. Average dimensional measurements of extracted posts at each site.

Site	Average Length (cm)	Average Diameter (cm)
MA1	180	15.0
MA2	203	12.8
MGA	221	15.0
TAR	107	16.3
TEU	182	12.9
ROT	259	15.6
Total	**189**	**14.2**

Five distinct taper types were identified across the six pā investigated (Table 13.1.4), recorded using a purpose-designed classification system developed to capture the varied taper typologies (see Section 5.1.2). The most common taper type identified across the assemblage was the short taper (44%). The short taper is one of the more expedient tapers to make, which in many cases appears to have been formed as the tree was felled. The long taper was the next most common (33%), characterised by a meticulous pattern of adzing >30 cm in length. Notched and bulbed tapers were far less frequent. The notched taper is characterised by a distinctive notch cut into the side of the taper, while the bulbed taper is characterised by its distinctive bulb-shaped end. Notably, these two taper types were only identified on larger posts, supporting Bellwood's (1978a) earlier observation that bulb taper types (found on Bellwood's Type A posts) were reserved for use on large posts from the inner palisade rows. Finally, the irregular taper was defined as any taper which does not conform to the above categories.

Table 13.1.4. Details of taper types identified across the post assemblage[52].

Taper Type	MA1	MA2	MGA	TAR	TEU	ROT	Total
Long	1	5	1	0	7	0	**14**
Short	2	5	8	2	2	0	**19**
Bulbed	2	0	0	0	0	1	**3**
Notched	1	0	1	0	0	0	**2**
Irregular	0	0	1	1	0	3	**5**
Total	**6**	**10**	**11**	**3**	**9**	**4**	**43**

13.1.2 Sample Condition Assessment

The sample condition assessment reviewed several sample characteristics (see Section 5.5), including preservation quality, the presence of charring, scarring, dark staining (limiting tree-ring visibility), and any tree-ring growth anomalies that could limit ring count accuracy (Table 13.1.5). Growth anomalies were prevalent across the entire assemblage (100%), highlighting the poor growing conditions affecting the trees in the local catchment areas. Dark staining, resulting from the anaerobic environments responsible for the post's preservation, was also prevalent (50%). This staining was often retained following sample bleaching and occasionally adversely affected the visibility of the tree-ring growth sequence in some periods. Finally, 33% of samples failed the condition assessment due to poor preservation. Although the sampling strategy actively selected against poorly preserved posts, the extent of a post's decay was occasionally not recognised in the field, or poorly preserved posts were sampled because well-preserved posts were limited. Following this assessment, samples exhibiting characteristics that would limit the accuracy of tree-ring analysis or would not survive sample preparation (i.e., bleaching and sanding) or ^{14}C pretreatment (physical or chemical) were immediately excluded from further analysis. The condition assessment resulted in another twelve samples being removed from the assemblage.

[52] Posts at MA1 were extracted using an alternate method compared to other sites, owing to the size of the posts identified at the site. This meant posts were not fully extracted from the ground surface, and the taper type could not be recorded for each post.

Table 13.1.5. Condition assessment of post assemblage relating to each pā site.

Site ID	Poor preservation	Charring present	Scarring present	Dark staining	Growth anomalies	Total # of Posts
MA1	2	1	3	6	9	9
MA2	6	0	1	5	13	13
MGA	0	1	1	1	7	7
TAR	2	1	2	3	4	4
TEU	4	0	0	4	7	5
ROT	0	1	0	1	2	2
Total	**14**	**4**	**7**	**20**	**42**	**42**

13.1.3 Species Identification

Ten tree species were identified across the post assemblage (Table 13.1.6). The most common species was pukatea (*L. novae-zelandiae*, 44%), which was prevalent in the assemblage, specifically at the three pā in the south of the study region (MA1, MA2 and MGA). Kahikatea (*D. dacrydioides*) was the second most common species (12%). Interestingly, this result agrees with previous research conducted at Lake Mangakaware (see Wallace, 1985, pp. 121–123), where pukatea was identified as the most common species used for house timbers and palisade construction, followed by kahikatea.

Table 13.1.6. Tree species identified across the post assemblage at each pā.

Species	MA1	MA2	MGA	TAR	TEU	ROT	Total
Pukatea	6	7	5	0	1	0	**19**
Miro	0	0	0	2	2	0	**4**
Matai	0	0	0	2	1	0	**3**
Kahikatea	2	1	1	0	0	2	**6**
Rimu	1	0	0	0	1	1	**3**
Rewarewa	2	0	0	0	0	0	**2**
Titoki	1	2	0	0	0	0	**3**
Tawa	0	2	0	0	0	0	**2**
Tanekaha	0	0	1	0	0	0	**1**
Pigeonwood	0	1	0	0	0	0	**1**
Unknown	0	0	0	0	2	0	**2**
Total	**12**	**13**	**7**	**4**	**7**	**3**	**46**

Note. The table includes three additional samples identified to species level but not included in the post-assemblage.

Before the effects of human settlement, the Waikato region is shown to have been dominated by a range of conifer-broadleaf species (Newnham et al., 1989; Leathwick et al., 1995; Burns & Merrett, 1999; Burns & Smale, 2002; Smale et al., 2005; Wilcox, 2010). Within this

environment, kahikatea (*D. dacrydioides*) forest, including pukatea (*L. novae-zelandiae*) and swamp maire (*Syzygium maire*), was prevalent on the poorly drained alluvial plains of the Waikato (Burns & Merrett, 1999). Across the drier free-draining substrates, matai (*P. taxifolia*), rimu (*D. cupressinum*), rewarewa (*K. excelsa*), rimu (*D. cupressinum*) and tawa (*B. tawa*) become the prevalent canopy species (Leathwick et al., 1995; Whaley et al., 1997; Burns & Merrett, 1999; Burns & Smale, 2002). This differing forest ecology is reflected in the results.

The three pā in the south of the study area are located around two small c. 20,000-year-old peat lakes situated in small alluvium-dammed valleys surrounded by low hills: Lake Mangakaware (a blocked-valley riverine lake) and Lake Mangahia (a blocked-valley riverine-phytogenic lake) (Lowe & Green, 2024). Therefore, it is unsurprising that pukatea and kahikatea represent most of the assemblage, preferring the wetland environment surrounding these lakeside pā. At the two headland pā located in the north of the region, Taraheke and Te Uapata Pā, matai (*P. taxifolia*), miro (*P. ferruginea*) and rimu (*D. cupressinum*) were identified. As expected, the species identified at each pā reflect the varied forest ecology within the local catchments surrounding these pā. Notably, all ten species identified have been previously recorded at archaeological sites in New Zealand (see Section 5.3).

13.1.4 Tree-ring Analysis

Tree-ring analysis was a critical stage in the analysis method, whereby the characteristics of each sample's tree-ring growth sequence were observed and recorded (see Section 5.6). Four key steps were undertaken during this analysis: initial tree-ring observation and track selection, tree-ring count and measurement, ring count reconciliation, and ring-block sampling. As mentioned in Section 5.6, the challenges of conducting tree-ring analysis on many New Zealand tree species in dendrochronological settings are well-documented, because of limiting growth characteristics and ring anomalies that are common in many New Zealand tree species. (Dunwiddie, 1979; Bellingham, 1982; Boswijk & Johns, 2018; Boswijk et al., 2019; Boswijk et al., 2021).

Of the 29 post samples selected for tree-ring count and measurement analysis, 25 produced reconciled ring counts. However, as anticipated, tree-ring growth anomalies were prevalent across the assemblages (see Section 13.1.2). Tree-ring suppression was identified across all species identified, resulting in narrow annual growth periods and locally absent rings (as presented in Chapters 6–11). These characteristics made the production of reconciled ring counts challenging, as these tree-ring growth anomalies reduced the clarity of the growth sequence in particular periods (as the tree-ring boundaries were very close together). These growth anomalies also affected the ring-block sampling accuracy of 19 samples because the width of the tree rings present was so narrow that they could not be accurately sampled without the scalpel blade crossing the ring boundary. Consequently, following additional ring-block sample checks conducted after the samples had been radiocarbon-dated, these ring-block samples were reassessed to contain more than or fewer than five tree rings (see Chapters 6–11 for details). Unfortunately, these samples could not be reanalysed due to cost pressures associated with the project. Despite these challenges, ring-block samples were obtained from six tree species – pukatea, kahikatea, miro, matai, tītoki, tanekaha and rimu. This outcome suggests that WMD can produce successful Felling Dates using these species, but it is dependent on the ring morphology and preservation condition of each sample attempted.

13.1.5 Event Scale Analysis (WMD)

WMD (OxCal D_Sequence model) was attempted on 25 post samples retained following tree-ring analysis, resulting in 20 successful Felling Dates (see Chapters 6–11). These 20 Felling Dates represent the construction date of 11 palisade rows identified across the six pā investigated. This success rate equates to a sample retention rate of 47%, from posts sampled for analysis to a successful Felling Date being produced (Table 13.1.7). As described in Section 5.8.4, a range of factors can influence the accuracy and precision of a WMD. Therefore, the results of each D_Sequence model were closely scrutinised before determining a viable Felling Date. This scrutiny involved reviewing the results of the calibration continuity standards, assessing the posterior outlier values of each ^{14}C date within the D_Sequence model, recalibrating each model using alternative outlier detection methods (i.e., RScaled outlier models and agreement index analysis), comparing the likelihood and posterior distributions of each ^{14}C date within the series, and evaluating the structure (shape) of the WMD in relation to SHCal20. This process highlighted two primary inconsistencies across the results, presenting

as ^{14}C date offsets (minor outliers) from SHCal20 (Section 13.1.5.1 and Section 13.1.5.2). When these offsets were identified, possible causes were explored to determine each Felling Date's likely accuracy and precision.

Table 13.1.7. The sample retention rate of posts sampled to successful Felling Date produced.

Site	Sampled Posts	WMD Attempted	WMD Success	Success Rate
MA1	10	6	4	40%
MA2	13	7	5	38%
MGA	7	5	5	71%
TAR	4	2	2	50%
TEU	7	3	3	43%
ROT	2	2	1	50%
Total	**43**	**25**	**20**	**47% (average)**

13.1.5.1 Ring Count Inconsistencies

Six WMDs are proposed to have been affected by errors within the reconciled ring count used to determine the known calendar periods between each ^{14}C date (see Chapters 6–11), resulting in four non-viable Felling Dates. These proposed ring count errors presented as minor and major outliers within the D_Sequence series, appearing horizontally offset to SHCal20 on the curve plot (Figure 13.1). These outliers were characterised as calendar year offsets, indicating that larger Gaps between specific ^{14}C dates would produce a better 'match' against SHCal20. When a potential (previously unknown) calendar year offset was identified, the tree-ring analysis data were reviewed, paying careful attention to inherent characteristics (scarring or dark staining) or episodes of tree-ring growth anomalies that could cause errors within the reconciled ring count. If observations made during tree-ring analysis correlated with the timing of the suspected calendar year offsets, ring count errors were determined to be the most likely cause of the WMD's poor fit with SHCal20. In all cases, the suspected ring count errors could not be satisfactorily resolved through revised reconciled ring counts (owing to the severity of the growth anomaly causing the error) and affected WMDs were thus removed from further analyses.

Two cases highlight the importance of ring-block sampling strategies for WMD purposes, especially for posts exhibiting poor growth characteristics that could affect the accuracy of the applied reconciled ring count. Two D_Sequence models produced for posts recovered from

TEU (TEUP219 and TEUP234) were suspected to contain ring count errors resulting from tree-ring growth anomalies identified early in the growth sequence. In both cases, these errors caused the WMD to produce a poor match against SHCal20, with several ^{14}C dates within the D_Sequence series presenting as suspected calendar year offsets. However, in both cases, the ^{14}C age order reversals observed within the D_Sequence series indicated their calendar position should be located over the calibration plateau in the late eighteenth century. When reassessing these samples, it was observed that both suffered from significant episodes of tree-ring suppression early in their growth sequence, indicating potential ring count errors resulting from this period of growth. However, in both cases, the later portion of the growth sequence was unaffected, indicating that the 'gap' values between the last five ^{14}C dates in the D_Sequence model were unaffected by possible missing tree rings. Because both D_Sequence models contained more than five ^{14}C dates within the series, the first two ^{14}C dates from each D_Sequence model could be removed (while retaining a good spread of ^{14}C dates across SHCal20), thus negating the effect of the possible ring count errors on the result. In both cases, removing the first two samples improved the results, with the new Felling Dates for both samples passing the threshold for a successful Felling Date.

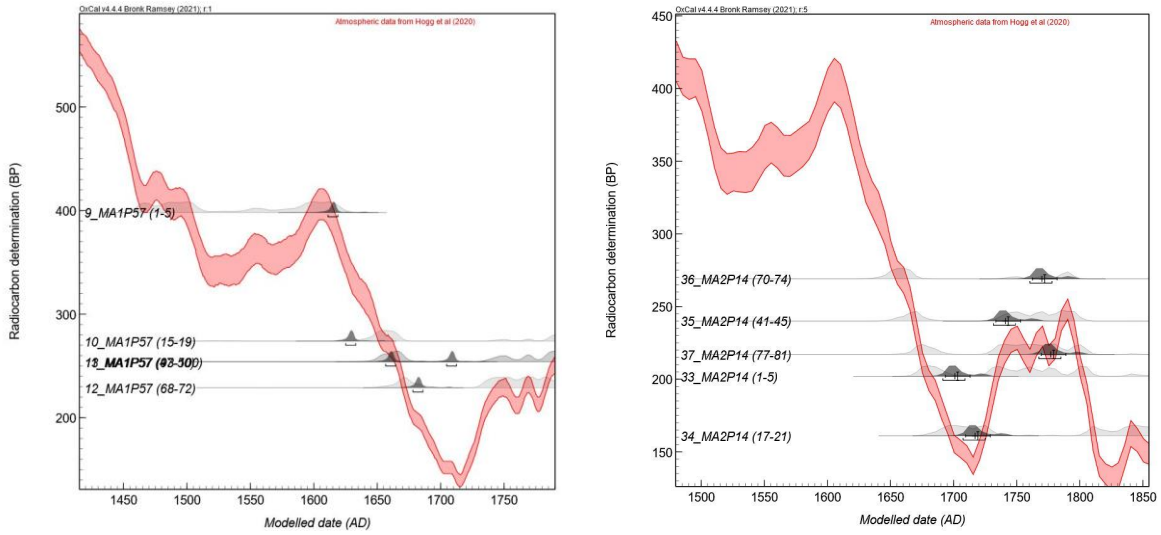

(A) *(B)*

Figure 13.1. Two D_Sequence models suspected to contain calendar year offsets: (A) MA1P57 and (B) MA2P15.

This strategy is essential for future applications of this dating method in New Zealand because such growth characteristics significantly affect the tree species available for analysis. By increasing the number of ring-block samples and sampling through the entire growth sequence, early growth sequence anomalies can be identified and removed, with the later portion of the growth sequence still providing enough ^{14}C dates to produce a successful Felling Date. Maximising the spread of the ^{14}C dates across the growth sequence should be prioritised. However, when dealing with a limited assemblage size exhibiting poor growth characteristics, this strategy can maximise the chances of producing viable results.

13.1.5.2 Calibration Inconsistencies

Potential radiocarbon age offsets, characterised by a ^{14}C date floating above or below SHCal20 on the curve plot, were also commonly identified across the WMD results. These offsets are often presented as minor outliers identified by the SSimple outlier model (Figure 13.2). Offsets of this nature indicate that the ^{14}C age of the sample differs slightly from the atmospheric calibration curve data during a specific period. It is important to note that SHCal20 is a modelled probability band describing a combined ^{14}C calibration dataset (of varying resolution) within a defined calendar period. Therefore, minor offsets (and outliers) observed between a ^{14}C result and the calibration curve that can be identified and down-weighted by the applied outlier models are somewhat anticipated. However, this offset type primarily affected the ^{14}C dates across the calibration plateaux within SHCal20. This plateau positioning was particularly true for samples with ^{14}C ages of 177–301 cal BP (average of 256 cal BP), situated over the calibration plateau in the late eighteenth century (Table 13.1.8). The consistency of the ^{14}C age and calendar position of these ^{14}C dates, coupled with the observation that these offsets were not consistent across all samples from the same D_Sequence model or sample wheel (AMS samples analysed in the same batch), suggests that these results are not related to environmental, laboratory or measurement errors. Additionally, the continuity standards run with the ^{14}C dates within each wheel were not flagged as problematic following measurement. It is, therefore, possible that inconsistencies in the Southern Hemisphere calibration curve datasets may be responsible.

As discussed in Section 3.2.2, the ability of an atmospheric calibration curve to provide accurate calendar date information for radiocarbon dates derived from samples from a specific

locality is influenced by a variety of factors (see Hogg et al., 2013b; Bayliss et al., 2017; Hogg et al., 2017; Hogg et al., 2019a). Despite the improvements made to SHCal20 (compared with previous versions), the possibility of inter-laboratory biases affecting specific datasets and periods within the SHCal20 calibration curve persists (See Section 3.2.5). Specifically, Hogg (2023 personal communication) has potentially identified three periods of concern (AD 1450–1649, AD 1650–1829 and AD 1830–1855), with his interim results suggesting that some specific datasets within SHCal20 may be biased towards young ages. However, the results of these investigations are not yet published, and more work is required to confirm them.

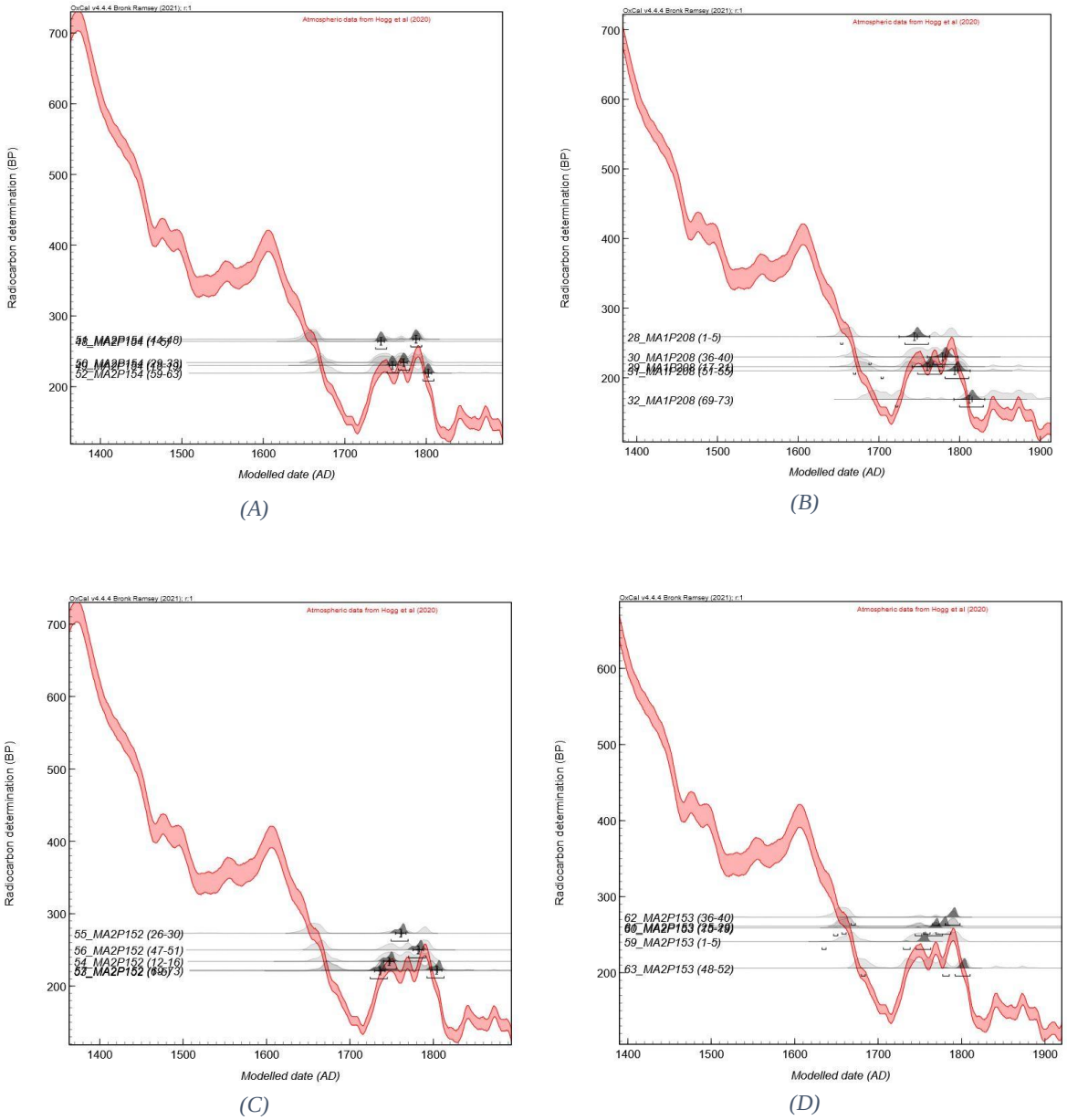

Figure 13.2. Four examples of identified ^{14}C age offsets within a D_Sequence series:(A) MA2P154, (B) MA1P208, (C) MA2P152 and (D) MA2P153.

Another possible cause of these ^{14}C age offsets could be related to the ^{14}C sample types included in the datasets that are combined to construct SHCal20. As discussed, the WMD technique relies heavily on the applied calibration curve accurately reflecting short-term variations in atmospheric ^{14}C. However, SHCal20 is a modelled probability band representing several combined datasets that vary in resolution (i.e., decadal, bi-decadal, five-year, two-year and single-year). Therefore, short-term variations in atmospheric ^{14}C production are potentially not well represented within the calibration curve, as these variations may require a single-year resolution to identify. This problem was noted by Bayliss et al. (2017), who reported the difficulty of accurately WMD short tree-ring sequences (25–35 yrs) in the Northern Hemisphere over a period of IntCal13 that was not of single-year resolution. Therefore, it is possible that these offsets represent periods of unidentified variation in atmospheric ^{14}C levels over the calibration plateaux within SHCal20.

Table 13.1.8. ^{14}C samples that exhibit a minor ^{14}C age offset over the eighteenth-century calibration plateau (SHCal20)

Wk Number	Sample ID	CRA	Tree Species
52737	14_MA1P190 (1–5)	245 ± 22	Pukatea (*L. novae-zelandiae*)
52740	17_MA1P190 (41–45)	264 ± 22	Pukatea (*L. novae-zelandiae*)
52751	28_MA1P208 (1–5)	259 ± 21	Titoki (*A. Excelsus*)
52360	36_MA2P14 (70–74)	269 ± 21	Pukatea (*L. novae-zelandiae*)
52361	39_MA2P15 (12–16)	177 ± 22	Pukatea (*L. novae-zelandiae*)
52229	43_MA2P149 (1–5)	261 ± 21	Kahikatea (*D. dacrydioides*)
52230	44_MA2P149 (13–16)	246 ± 21	Kahikatea (*D. dacrydioides*)
52231	45_MA2P149 (27–29)	267 ± 21	Kahikatea (*D. dacrydioides*)
52232	46_MA2P149 (37–41)	301 ± 22	Kahikatea (*D. dacrydioides*)
52241	55_MA2P152 (26–30)	273 ± 23	Pukatea (*L. novae-zelandiae*)
52244	59_MA2P153 (1–5)	241 ± 24	Pukatea (*L. novae-zelandiae*)
52245	60_MA2P153 (15–19)	259 ± 22	Pukatea (*L. novae-zelandiae*)
52246	61_MA2P153 (25–29)	261 ± 21	Pukatea (*L. novae-zelandiae*)
52247	62_MA2P153 (36–40)	273 ± 22	Pukatea (*L. novae-zelandiae*)
52234	48_MA2P154 (1–5)	264 ± 21	Pukatea (*L. novae-zelandiae*)
52237	51_MA2P154 (44–48)	267 ± 22	Pukatea (*L. novae-zelandiae*)
53342	115_MGAP281 (24–28)	247 ± 20	Pukatea (*L. novae-zelandiae*)
53339	112_MGAP316 (158–162)	266 ± 20	Pukatea (*L. novae-zelandiae*)
53340	113_MGAP316 (173–181)	195 ± 20	Pukatea (*L. novae-zelandiae*)
52881	98_TEUP234 (131–135)	259 ± 21	Miro (*P. ferruginea*)
52883	100_TEUP234 (150–154)	288 ± 20	Miro (*P. ferruginea*)

Note. The CRA of all identified samples relates to a specific ^{14}C age period.

Regardless of the cause of these offsets, these findings have considerable implications when considering the application of radiocarbon dating in New Zealand. These implications arise because the calibration plateaux within SHCal20 cover large portions of New Zealand's occupational and settlement history. Crucially, these offsets were only identified because the affected ^{14}C dates were included within a D_Sequence series, locked into a calendar position across SHCal20 by known calendar (ring count) intervals. If offsets of this type affected ^{14}C dates produced on single samples, as is typical for archaeological dating in New Zealand, they could have produced a calendar result in a different period (depending on the scale of the identified ^{14}C age offset).

Considering this discussion, additional considerations were required to assess the accuracy and precision of Felling Dates resulting from WMDs that include ^{14}C dates exhibiting a minor ^{14}C age offset. Firstly, careful consideration was given to the order of the ^{14}C ages within each D_Sequence series. Specifically, ^{14}C age order reversals were used to support that the WMD should have a calendar position over a calibration plateau. Generally, the observed ^{14}C age order reversals within a WMD would only correspond to calendar positions of SHCal20 that exhibit a plateau instead of a slope on the calibration curve. Once this likely calendar position was confirmed, the results from the D_Sequence model were further scrutinised. As discussed in Section 5.8.3, every D_Sequence model was calibrated three separate times using alternative outlier detection methods (SSimple s-type outlier model, RScaled r-type outlier model and Agreement Index analysis). The results of these three analyses were compared to determine their effect on the results. Specifically, the posterior outlier values produced by each outlier model (SSimple and Rscaled) were compared with the agreement values of the D_Sequence calibrated without an outlier model (agreement index analysis). Generally, this comparison identified an improvement in the results of the D_Sequence model calibrated using the RScaled outlier model (i.e., a reduction in the posterior outlier value of the ^{14}C date suspected to be a ^{14}C offset, and an improvement in the A_{comb} value of the WMD). If this improvement was observed while maintaining a calendar date range similar to the original model (in most cases, the calendar age ranges were identical between the two models), the original Felling Date (SSimple outlier model) was interpreted as accurate and precise (viable). If the results did not maintain similar calendar age ranges or did not improve the posterior outlier values and A_{comb} results, the original Felling Date was interpreted as inaccurate and was dropped from

consideration for further analyses. The discussion presented above is used to justify this approach until this hypothesis can be tested further.

13.1.5.3 WMD Method Applicability

This research concludes that when applied in the appropriate situations (see points below), WMD can produce calendar age ranges for specific events in time (the felling of a tree used in the construction of a palisade defence) with high accuracy and precision in New Zealand archaeological contexts. This conclusion is supported by this study's 20 successful Felling Dates. Specifically, this research shows that to produce a successful WMD, several critical steps must first be satisfied:

1. Identify a specific wooden artefact type (timber used in defences, structures, or canoes) that has retained evidence of the terminal tree ring and is without characteristics that could affect the analysis.
2. Determine that that artefact is well preserved, with limited decay or damage that could affect the analysis.
3. Establish that the tree species used is suitable for tree-ring analysis (i.e., a tree that reliably puts on a new tree ring annually throughout its life span).
4. Determine that the tree-ring growth sequence can produce an accurate ring count and that tree-ring growth anomalies (while present) can be observed and accounted for during tree-ring analysis.
5. Identify and account for minor and major outliers detected during Bayesian modelling. D_Sequence models should be run multiple times, using various outlier detection methods (agreement index and outlier model analysis) to confirm the accuracy of the results. Suspect outliers should be evaluated for possible ring count inconsistencies, contamination, fractionation, and laboratory offsets where possible.
6. Establish a high standard for the success of a Felling Date and exclude WMD from consideration when the accuracy or precision cannot be firmly relied upon.

These six factors ultimately result in a particular set of requirements. As shown in this research, just 12% of the posts identified met the criteria for sampling, and only 6% produced a

successful Felling Date (Table 13.1.7). Therefore, in future applications of this dating method, it is recommended that priority should be given to sampling as many suitable artefacts (posts) as feasible in anticipation of a number of samples being rejected. Given the cost of the WMD method (requiring multiple AMS ^{14}C dates per artefact dated), tree-ring analysis should be used to initially narrow down the number of artefacts dated within the assemblage so that the samples with the best tree-ring characteristics are targeted. While resulting in more work during field sampling and tree-ring analysis, this approach will limit the analytical cost of radiocarbon dating when producing Felling Dates and will avoid unnecessary expenditure on less valuable samples.

13.1.6 Local Scale Analysis

The local scale analysis established chronologies that tracked the development of the palisade defences identified at each pā over time, providing direct evidence for the earliest episode of palisade construction and any successive episodes of palisade construction activity. Crucially, these chronologies highlighted specific periods where the palisade defences were maintained or redeveloped, indicating the active management of these defences in response to postulated environmental and/or cultural processes within the landscape. These variables have previously been interpreted as evidence for resource-driven conflict, resulting in competition between populations for key resource zones and territories.

13.1.6.1 Lake Mangakaware (MA1 and MA2)

Local scale analysis of the post assemblage from MA1, located on the eastern side of Lake Mangakaware, identified four sequential phases of palisade construction activity. The earliest evidence of palisade construction at MA1 (Phase I) was identified in the early 1700s (Felling Date of MA1P204: AD 1702–1725, 95% HPD). Three further phases of palisade construction activity were identified (Phase II–IV), representing the construction of a fighting stage on the northern side of the pā (Felling Date of MA1P53: 1749–1761, 95% HPD) and the addition of the outermost palisade row on the southern side of the pā (Felling Date of MA1P190: AD 1794–1811, 95% HPD), before the repair of this outermost palisade row shortly after its initial construction date (Felling Date of MA1P208: AD 1807–1828, 95% HPD).

This palisade construction activity is mirrored at MA2, located across the lake on the western side, with local scale analysis identifying two sequential phases of palisade construction activity (Phase I–II). The earliest evidence of palisade construction activity at MA2 was also identified in the early 1700s (Felling Date of MA2P161: AD 1730–1747, 95% HPD), confirming the chronological relationship hypothesised by Bellwood (1978a), suggesting MA2 was occupied shortly after the establishment of MA1. The second phase of palisade construction activity at MA2 was identified in the late 1700s to early 1800s (Phase II MDate: AD 1795–1815, 95% HPD), representing the repair of the palisade row initially constructed during the early 1700s.

This local scale analysis identifies the early 1700s as a period of establishment and possible growth at Lake Mangakaware, exemplified by the construction of two pā around the lake. This growth could reflect two possible scenarios: (i) population growth at MA1 resulting in the need for a second pā at the lake (population pressure), and/or (ii) a response to growing socio-political tensions in the area. This second scenario can be interpreted as:

1. Internal competition: with two related populations (each represented by an individual pā) laying claim over Lake Mangakaware and the surrounding area.
2. External competition: with the population at Lake Mangakaware (MA1 and MA2) responding to a perceived or real threat from a competing population from the wider area, strengthening their claim over the lake through the construction of a second pā, providing a physical representation of their strength and control over this critical resource area.

The population growth scenario for Lake Mangakaware is supported by the presence of MA3 (a low mound adjacent to MA1), which is considered an extension of MA1, acting as a possible annexe for cooking and processing activities. However, this extension does not negate the possibility of growing socio-political pressures from the cultural landscape influencing the occupation at Lake Mangakaware, represented by the identified palisade construction activity. Increasing socio-political pressure (stress) affecting the population at Lake Mangakaware is demonstrated by the addition of the fighting stage to the northern palisade defences at MA1 (MA1 Phase II) in the middle 1700s. This evidence suggests that by this time, MA1 was heavily fortified and protected by multiple palisade rows and structures. This level of fortification is

interpreted as evidence of increasing socio-political tensions in the cultural landscape, indicating that the occupation at MA1 was responding to a real or perceived threat from a competing population within the local area.

Secondly, the local scale analysis identifies another period of stress on the population(s) occupying Lake Mangakaware between the late 1700s and early 1800s. At this time, the last palisade construction activity phase identified at MA2 (MA2 Phase II) coincides with the timing of the last two phases of palisade construction activity identified at MA1 (MA1 Phase III and IV). As discussed in Section 4.1.1.2, Bellwood (1978a, p. 19) suggests that a cluster of artefacts close to an entrance within the palisade defences at MA2 could represent the result of a 'battle'. This area (Trench C of original excavations in 1969) is approximately 20 m west of the palisade rows identified in Area B at MA2. Therefore, the evidence of repair to the inner palisade row at MA2 during this period could reflect the anticipation or aftermath of such an event. Further alluding to this hypothesis, one further Felling Date was produced from MA2 that was excluded from this local scale analysis due to imprecision (MA2P149). MA2P149 was the only post analysed from the second (outer) palisade row at MA2. The Felling Date for MA2P149 had a date range between AD 1799–1806 (68% HPD), indicating that the repair of the first (inner) palisade row was possibly undertaken when the second (outer) palisade row was constructed or repaired in this area. Unfortunately, this interpretation cannot be categorically stated due to sampling restrictions and the imprecision of the Felling date for MA2P149.

Following this interpretation, given the short period (MA1 Interval 3: 1–19 years) between the initial construction of the outer palisade row at MA1 (MA1 Phase III) and its repair (MA1 Phase IV), this palisade construction activity is unlikely to be the result of natural decay to the palisade row. Therefore, the repair of the palisade defences at MA1, identified during Phase IV, could also reflect the anticipation or aftermath of an event (attack) at MA1. When examining the results of the local scale analysis further, the results for the Modelled Date of Phase II at MA2 indicate this repair activity likely took place during AD 1802–1809 (68% HPD). This date range suggests that this repair episode coincides with the construction of the outer palisade row (Phase III) at MA1 (Felling Date of MA1P190: AD 1799–1807, 68% HPD)

rather than the subsequent repair episode (Phase IV) at MA1 (Felling Date of MA1P208: AD 1814–1823, 68% HPD). Again, this interpretation suggests two possible scenarios:

1. Local competition between the inhabitants of MA1 and MA2 resulted in an attack on MA2 by the population of MA1 during the early 1800s, evidenced by the palisade repair identified during MA2 Phase II. Just before or after this attack, the population at MA1 strengthened the palisade defences with an additional palisade row (MA1 Phase III). The population of MA2 then attacked MA1 as a reprisal for the attack on MA2, resulting in damage to the outer palisade row at MA1 that was then repaired during Phase IV.
2. External competition between the populations of Lake Mangakaware (MA1 and MA2 together) and another population from the wider landscape resulted in two subsequent attacks at Lake Mangakaware, the first at MA2 (resulting in the repair of the palisade row at MA2 (MA2 Phase II) and a strengthening of the palisade defences at MA1 (MA2 Phase III)), followed by a second attack at MA1 (resulting in the repair of the outer palisade defences in MA1 Phase IV).

Regardless of the accuracy of these scenarios, this evidence strongly suggests the influence of increasing socio-political tensions during the late 1700s and early 1800s at Lake Mangakaware.

13.1.6.2 Lake Mangahia (MGA)

Local scale analysis of the post assemblage from Lake Mangahia (MGA) identified four sequential phases of palisade construction activity. The earliest evidence of palisade construction (Phase I) was identified in the middle 1500s (Felling Date of MGAP313: AD 1532–1636, 95% HPD), with the results strongly indicating the initial construction of palisade defences between AD 1542–1564 (68% HPD). Three successive phases of palisade construction activity were identified (Phase II–IV) during the late 1700s, representing the repair of the palisade row constructed in Phase I (Felling Date of MGAP311: AD 1765–1783, 95% HPD), the addition of two more palisade rows (Phase III MDate: AD 1780–1797, 95% HPD), and the addition of a final palisade row (Felling Date of MGAP320: AD 1799–1815, 95% HPD).

This local scale analysis indicates that the pā was fortified during the period that Schmidt (1996) proposes as the onset of pā construction nationally (AD 1500–1550). Therefore, this palisade construction activity could be associated with the first regional wave of pā construction within the Middle Waikato Basin. This initial phase of palisade construction activity is separated from the second phase by a long absence of identified palisade construction activity (Interval 1: 1–220 years). This is a substantial length of time for a palisade to stand without some evidence of maintenance. Three possible hypotheses could explain a break in palisade construction activity of this length:

1. Additional evidence of palisade construction activity was not captured within the small post assemblage size.
2. The break represents a period of site abandonment and re-occupation/re-purposing.
3. The lack of identified palisade construction activity within this period reflects stability in the cultural landscape.

As discussed in Section 12.1.4, the raised pā mound at Lake Mangahia sits more than 2 m above the modern lake level and exhibits multiple terraces and raised living surfaces. Excavations showed that the raised mound was constructed using multiple imported sediments (forming up to 10 layers in some areas), implying that the pā was occupied over a long period (see Section 4.1.2). Additionally, the pā is located next to a critical resource zone (Lake Mangahia) and is near the horticultural sites close to the Waipa River at the mouth of the Mangahia Stream (<5 km away). Therefore, the complete abandonment of this site during this period is considered unlikely, with at least a seasonal occupation maintained at the pā associated with periods of resource exploitation at the lake.

Secondly, the local scale analysis also identifies the late 1700s and early 1800s as a period of three rapid palisade construction phases (Phase II–IV). This period from AD 1765–1783 to AD 1799–1815 represents an episode of sustained fortification at Lake Mangahia, with the repair of the palisade row constructed in the middle 1500s and three additional palisade rows constructed between these periods. This evidence shows that by the early 1800s, the pā at Lake Mangahia was heavily fortified and protected by multiple palisade rows. This activity is interpreted as a response to rising socio-political stress in the cultural landscape, with the

population at Lake Mangahia responding to a real or perceived threat from a competing population within the area, strengthening the palisade defences and their claim over the lake and surrounding area.

13.1.6.3 Taraheke Pā (TAR)

No evidence of traditional palisade defences were identified at Taraheke Pā. However, an alignment of posts extending from the tip of the headland pā into the adjacent stream was identified. This alignment is possibly that of an eel weir (pā tuna), canoe (waka) landing, or a defensive structure built into the steam to protect access to the pā. Given that the defensive nature of this structure cannot be categorically stated, it is used only as proxy evidence for the occupation of Taraheke Pā. Local scale analysis determined that this structure was initially constructed during the early 1500s (Felling Date of TARP132: AD 1500–1538, 95% HPD), with one successive phase of repair identified during the middle 1500s (Felling Date of TARP131: AD 1548–1565, 95% HPD). Because of the nature of this evidence, we can only interpret that TAR was occupied during this period. This occupation date is no surprise, given the known traditional history of the area, outlining potential conflicts in Taupiri during this period, and the importance of controlling the rich resource zones surrounding Taupiri, as well as the movement of people and resources up and down the rivers, including the junction of the Waikato River and the Mangawara Stream, which is just downstream (north) of junction between the Waipā and Waikato rivers at Ngāruawāhia.

13.1.6.4 Te Uapata Pā (TEU)

Local scale analysis of the post assemblage from Te Uapata Pā identified two sequential phases of palisade construction activity. The earliest evidence of palisade construction (Phase I) was identified in the late 1700s (Felling Date of TEUP219: AD 1776–1803, 95% HPD), with the results strongly indicating the initial construction of palisade defences up to 20 years before AD 1800 (AD 1781–1794, 68% HPD). One successive phase of palisade construction activity was identified (Phase II) from the late 1700s to the early 1800s, representing either the repair of the palisade row constructed in Phase I (repair episode) or the installation of an entranceway (redevelopment activity) through the palisade defences (Phase II MDate: AD 1796–1828, 95% HPD). The results indicate that this second phase of palisade construction activity occurred

after AD 1800 (Phase II MDate: AD 1805–1816, 68% HPD). Given the short interval between these two phases of palisade construction activity (Interval 1: 0–26 years, 95% HPD), and the lack of archaeological evidence for an event (i.e., attack) at Te Uapata Pā during this period, it is considered more likely that Phase II represents the installation of an entranceway rather than the repair of the palisade defences following natural decay or an event (i.e., attack).

As discussed in Section 4.1.4, Te Uapata Pā is associated with the prominent ancestor Mahuta, who is thought to have established the pā following his migration inland from Kawhia (Jones & Biggs, 1995; Phillips, 1995). This history suggests Te Uapata is an early pā associated with the Tainui migration inland from Kawhia, with inland Tainui migration in the Waikato proposed to begin around AD 1520 (Anderson, 2014, pp. 114–119). Therefore, it was a surprise that the Felling Date results did not reflect a calendar date range from this early period. Furthermore, additional radiocarbon dating by Gainsford and Gumbley (2020) provides evidence for the occupation of TEU between AD 1650–1850 (see Section 4.1.4), with no evidence of occupation before this date. While it is possible that earlier phases of palisade construction activity are not captured within the small assemblage size (three posts), the lack of radiocarbon evidence for occupation before AD 1650 suggests that the pā was not occupied during this early period. Despite this consideration, the palisade construction activity identified at Te Uapata Pā is interpreted as evidence for increasing socio-political tensions within the cultural landscape of the late 1700s (mirroring palisade construction activity identified in the south of the study area, described earlier for Lake Mangakaware and Lake Mangahia). This activity indicates that the population at Te Uapata was experiencing some real or perceived threat from competing populations within the area, resulting in the need to fortify and strengthen their claim and control over the pā and the surrounding area.

13.1.7 Regional Scale Analysis

The regional scale analysis incorporates this palisade construction activity, as identified at seven pā, into a regional chronological framework for the Middle Waikato Basin. This chronological framework identified periods of shared palisade construction activity between two or more pā, which could then be interpreted as evidence for postulated overarching (controlling) variables responsible for the emergence, proliferation, and development of pā

within the subject area. This analysis provided direct evidence supporting the possible timing of the initial (early) wave of pā construction regionally (RP1). Additionally, three successive regional phases of palisade construction activity are identified throughout the eighteenth century (RP2–RP4). Finally, a region-wide palisade repair and redevelopment episode is identified in the early nineteenth century (RP5). Each one of these phases is discussed in detail below.

13.1.7.1 Regional Phase 1 (RP1)

The Modelled Date for RP1 represents the first direct evidence of palisade construction activity and pā occupation across the study area (AD 1484–1601, 95% HPD), with RP1 including Felling Dates from three individual pā: TAR, MGA and ROT. As previously stated, the results of RP1 (MDate: AD 1514–1562, 68% HPD) strongly indicate this activity occurred across the period Schmidt (1996) proposes as the national onset of pā construction during the sixteenth century (AD 1500-1550). As no palisade construction activity was identified before RP1, and as these three pā are located across the spatial extent of the Middle Waikato Basin, this phase could reflect the initial regional wave of pā fortification.

RP1 occurs within the Transitional Period (AD 1450–1650). As discussed in Section 2.1, Anderson (2016) proposes that pā construction during this period reflects a period of cultural change in Māori society, influenced by a range of interconnected environmental and cultural processes. These processes include regionally specific climate declines (related to the LIA), the development of horticultural practices, fluctuating population dynamics, population migration episodes, and changes in the socio-political structures of Māori society (i.e., hapū formation and the divergence of kinship relationships) (see Newnham et al., 1998a; Anderson, 2014; Lorrey et al., 2014; Roop, 2015; Anderson, 2016; McCoy & Ladefoged, 2019; Brown & Crema, 2021; Bunbury et al., 2022).

Additionally, the traditional ‘ecological model’ of warfare proposed by Vayda (1956, 1960, 1976) associates the period after AD 1450 with endemic levels of Māori warfare, related to competition over favourable gardening areas in the northern horticultural zone of New Zealand

(and the difficulty of clearing land for gardening). This hypothesis suggests that warfare became a crucial feature of Māori society during this period, as indicated by the construction and proliferation of pā. However, as also discussed in Section 2.2.3, more recent research on pā and Māori warfare implies that this initial period of pā construction and occupation (during the Transitional Period) is not solely related to resource-driven conflict and territoriality between populations. Instead, pā construction during this period is proposed to reflect an episode of expansion, as demographic pressures spurred migration into previously unoccupied or sparsely populated areas (that were undefended) that retained the environmental conditions for viable horticultural production (particularly kūmara), with these populations seeking to establish themselves (vie pā construction) within the changing cultural and physical landscape (see Allen, 2012; Irwin, 2013; Anderson, 2014; McCoy & Carpenter, 2014; McCoy et al., 2014; Allen, 2016; Anderson, 2016; McCoy & Ladefoged, 2019; Irwin, 2020).

Therefore, in the context of the Middle Waikato Basin, RP1 is proposed to reflect the result of this expansion process, with the motivations for this initial fortification period related to the cultural and environmental processes spurring this period of cultural development and change.

13.1.7.2 Interval 1

The regional chronological framework supports this expansion thesis. Specifically, the end of RP1 (MDate: AD 1484–1601, 95% HPD) is separated from the start of RP2 (MDate: AD 1654–1752, 95% HPD) by a defined break in the regional chronology of 18–162 years (Interval 1, 95% HPD). The length of Interval 1 is crucial because endemic (structural) levels of warfare associated with competition over favourable horticultural zones should logically be represented within the archaeological record by ongoing palisade construction activity, as the occupants actively respond to threats by maintaining and strengthening their pā's defences to combat ongoing conflict or increasing tensions. Instead, the regional chronology identifies a long pause in regional palisade construction activity, interpreted here as evidence of socio-political stability. In this scenario, once populations had moved into and established control over key areas in new regions, including through the construction of pā, competition subsides, resulting in a period of socio-political stability (Interval 1) where clear zones of influence and control are set within the physical landscape, and levels of conflict and competition decrease. Crucially,

the juxtaposition between the length of Interval 1 and intervals 2–4 indicates that the longstanding pause identified in Interval 1 is evidence of a region-wide stasis rather than a statistical bias within the dataset.

A critical factor in this scenario is the availability of productive horticultural soils. Importantly, as recently presented by Gumbley (2021), the systematisation of horticultural production in the Waikato (Waikato Horticultural Complex) is demonstrated to have been established at some point in the sixteenth century, with continuous replication until the early or middle nineteenth century. Radiocarbon evidence indicates that the Cambridge/Leamington area was the early focus of these activities, with horticultural sites near the river appearing in the early to middle sixteenth century. Horticultural sites farther from the river are consistently younger, albeit demonstrating a relatively rapid uptake of this technology. From the late sixteenth to early seventeenth centuries, systemised horticultural production had spread ~50 km downstream along the Waikato River, at least as far as Taupiri.

Extrapolating from Gumbley's (2021) findings, it is proposed that RP1 takes place after systemised horticultural production has been established but before it was fully developed and spread to the areas surrounding these pā. Although horticulture would still have played an important role in the subsistence strategy implemented by these populations, competition for horticultural soils would have been comparatively low compared with the competition level exhibited during the eighteenth and early nineteenth centuries. Additionally, the faunal resources (eels, birds, freshwater mussels, etc.) located in the local environment surrounding the pā occupied in RP1 would also have formed an important part of the subsistence strategy used by these populations. This consideration highlights the need to establish (create new) or protect existing (against other populations moving into and around the region) zones of community control and influence, providing a substantial reason to fortify these areas to protect access to local resources. Additionally, by not solely representing a period of resource-driven conflict associated with competition over horticultural zones, this evidence also proposes alternate social motivations for pā construction and conflict during this period (i.e., community identity, prestige (mana), revenge (utu), violations of tapu (something sacred or prohibited), etc.).

Therefore, it is proposed that Interval 1 represents the period when the Waikato Horticultural Complex (systemised horticultural practices) had been developed and was spreading throughout the study region. This period of socio-political stability, resulting from the construction of pā during RP1 and the establishment of these new zones of influence and control within the landscape, provided the time and stability necessary to experiment with various horticultural systems and develop suitable agronomic practices. Only after it had spread widely would the soils suitable for these practices become limited, resulting in renewed competition and territoriality. Therefore, it is suggested that the palisade construction activity identified during RP1 cannot be directly attributed to increased levels of conflict resulting from competition over viable horticultural zones. Instead, as discussed in Section 2.2, pā construction during this period must be contextualised with respect to the varied roles these fortified places provided for communities. Pā were multifunctional spaces, symbolising population identity within a contested landscape and facilitating interests (i.e., economic, religious and domestic) beyond defence alone. However, defence must continue to be considered a primary function of this site type, as the fortifications at these sites likely protected access to and control over other resources within the local environment.

13.1.7.3 Regional Phase 2 (RP2)

Following Interval 1, regional palisade construction activity is shown to be relatively continuous throughout the eighteenth century within the Middle Waikato Basin, with three distinct phases of regional palisade construction activity identified (RP2–4). Interestingly, McCoy and Ladefoged (2019) propose that warfare in the era after sustained European contact (AD 1769) was endemic (see Section2.2.3), supported by several other studies that show evidence of competition and warfare from AD 1650 onwards (e.g., C. Phillips, 2000; Sutton et al., 2003; Allen, 2012; McCoy & Carpenter, 2014; McCoy et al., 2014; Allen, 2016). In the Waikato, traditional history records also describe an increased level of warfare in the eighteenth century, with conflict beginning between Ngāti Raukawa and other Waikato groups, and then further north between Waikato and Ngā Puhi about AD 1750. (Anderson, 2022, p. 51).

Crucially, as discussed above, the development and spread of systemised horticultural production would have occurred throughout the study area by the late sixteenth to early

seventeenth centuries, beginning in the southern Cambridge/Leamington area before spreading north down the Waikato River (Gumbley, 2021). As hypothesised, the regional patterns of palisade construction activity during the eighteenth century suggest that this activity could mirror the spread of the Waikato Horticultural Complex, beginning in the south of the study area. The second regional phase of palisade construction activity is identified between AD 1654–1752 (MDate, 95% HPD), with the results strongly suggesting RP2 took place over the early 1700s (MDate: AD 1703–1742, 68% HPD). The palisade construction activity during RP2 represents the construction of two pā at Lake Mangakaware, interpreted as evidence of increasing population size and/or a response to growing socio-political tensions (stress) in the cultural landscape. This stress is proposed to be the result of internal or external competition affecting the occupation of Lake Mangakaware. Regardless of the internal or external nature of this implied competition, the construction of MA1 and MA2 during this period indicates a response to a real or perceived threat from the cultural landscape through a period of fortification. It is proposed here that this fortification is related to growing tensions throughout the south of the Middle Waikato Basin.

This hypothesis highlights that by the beginning of RP2, competition over available horticultural soils suitable for the adapted agronomy would have increased, particularly in the southern portion of the Middle Waikato Basin, as these sites are closer to the origin of these horticultural practices. Therefore, as tensions and resource-driven territoriality in the study area's south increase, competition and conflict emerge as populations vie for control and access to these horticultural soils. This conflict ultimately results in populations that retain and lose access to these resource zones. While this competition period is related to access and control over horticultural zones, it also creates a situation where access to other environments (lakes and rivers) and control over other resources within the landscape becomes even more critical. As previously discussed, this situation would also inherently lead to alternate motives (e.g., revenge) for competition and conflict during this period (not just resource-driven conflict). This results in a renewed period of increasing socio-political tensions, as reflected by the identified palisade construction activity at Lake Mangakaware.

13.1.7.4 Interval 2

This proposed change in motivation for constructing and occupying pā during this period is further evidenced in the regional chronological framework. Specifically, the end of RP2 (MDate: AD 1654–1752, 95% HPD) is separated from the start of RP3 (MDate: AD 1750–1778, 95% HPD) by a break in the regional chronology of just 1–22 years (Interval 2, 95% HPD). While the long period of absent palisade construction activity during Interval 1 suggests socio-political stability, ongoing evidence of palisade construction activity represented by the short period of Interval 2 indicates a period of growing socio-political tensions. Crucially, the short length of Interval 2 (and Intervals 3–4) is not interpreted as definitive evidence for a short pause in regional palisade construction activity. Obviously, the length of these intervals would likely change as additional WMD evidence was added to the dataset from other pā within the region. However, the short length of the intervals within this period are interpreted as evidence of an ongoing period of socio-political stress, representing a change in the motivations for occupying or variables responsible for the palisade construction activity observed in RP2–5 compared with RP1.

13.1.7.5 Regional Phase 3 (RP3)

Continued evidence of palisade construction activity in the eighteenth century was identified during RP3 (MDate: AD 1750–1778, 95% HPD), with the results strongly suggesting RP3 took place during the middle to late 1700s (MDate: AD 1757–1771, 68% HPD). RP3 includes evidence of adding a fighting stage at MA1, constructing the palisade defences at OTA, and repairing a palisade row at MGA. This palisade construction activity spans the spatial extent of the study region, indicating the hypothesised socio-political tensions beginning in the south of the region during RP2 have spread northward to Taupiri, as represented by the construction of palisade defences at OTA. As Taupiri is within the northern extent of the Waikato Horticultural complex and removed from the proposed origin of these horticultural practices, the palisade construction activity identified at OTA is proposed to reflect this spread, as prime horticultural zones in the north of the region become limited, fuelling rising socio-political tensions via competition and territoriality. Additionally, the palisade repair and redevelopment activities identified at MA1 and MGA during this period indicate the ongoing active management of these palisade defences, representing a physical response to a perceived or real

threat in the cultural landscape, indicating this period of socio-political stress is sustained and potentially becoming entrenched in the south.

13.1.7.6 Interval 3

As with Interval 2, a sustained and increasing period of socio-political stress in the cultural landscape of the study area, potentially related to resource-driven competition and territoriality, is further evidenced in the regional chronological framework by the results of Interval 3. Specifically, the end of RP3 (MDate: AD 1750–1778, 95% HPD) is separated from the start of RP4 (MDate: AD 1776–1796, 95% HPD) by a break in the regional chronology of 1–15 years (Interval 3, 95% HPD). Again, the short time frame between these two phases of palisade construction activity is proposed to reflect a period of sustained and increasing socio-political tensions spreading throughout the subject area.

13.1.7.7 Regional Phase 4 (RP4)

The last period of regional palisade construction activity in the eighteenth century was identified during RP4 (MDate: AD 1776–1796, 95% HPD), with the results strongly suggesting RP4 took place during the late 1700s (MDate: AD 1781–1791, 68% HPD). RP4 includes evidence of palisade redevelopment at MGA and the establishment of palisade defences at Te Uapata. Crucially, by this period, all seven pā included in the regional chronology exhibit evidence of palisade construction or occupation, as well as repair and redevelopment activities identified at MA1 and MGA. As described for RP3, this activity represents the active management of these defences, responding to real or perceived threats in the cultural landscape, indicating sustained socio-political tensions via territoriality and conflict are becoming entrenched across the Middle Waikato Basin.

13.1.7.8 Interval 4

This entrenched period of socio-political stress in the cultural landscape is further evidenced in the regional chronological framework by the results of Interval 4. The end of RP4 (MDate: AD 1776–1796, 95% HPD) is separated from the start of RP5 (MDate: AD 1801–1815, 95% HPD) by a break in the regional chronology of 1–22 years (Interval 4, 95% HPD). Again, the short

time frame between these two phases of palisade construction activity is proposed to reflect a period of sustained competition and conflict across the subject area.

13.1.7.9 Regional Phase 5 (RP5)

Finally, a region-wide episode of palisade construction activity is identified at four pā during the early 1800s in RP5 (MDate: AD 1801–1815, 95% HPD), with the results strongly suggesting this activity took place between AD 1805–1811 (MDate, 68% HPD). The palisade construction activity identified during RP5 represents episodes of repair and redevelopment across the region at four pā: MA1, MA2, MGA and TEU. Crucially, this activity includes evidence of potential events (i.e., attacks) at MA1 and MA2 and the end of a sustained fortification period at MGA. This evidence strongly suggests that the identified activity is a response to an entrenched period of socio-political stress that is affecting the entire subject region resulting from resource-driven competition and conflict, particularly over available horticultural soil, but also probably other resources (e.g., tuna (eels), birds, freshwater mussels, etc.), resulting in the escalation of conflict captured within the archaeological record through palisade construction activity. Again, this activity demonstrates the active management of these defences, suggesting that they are more than a symbolic representation of identity, control, and strength by this period. As noted earlier, Gumbley (2021) identifies the eighteenth to early nineteenth centuries as the period where the Waikato Horticultural Complex spread to even the most remote sites within the region. Therefore, competition for available horticultural zones and the resources they produce would have been at its highest point by this period.

It is important to note that while resource-driven conflict is highlighted during this period, owing to the perceived relationship to the Waikato Horticultural Complex, that does not mean that this is the sole variable proposed to influence conflict and pā construction during this period. While influential, resource-driven conflict does not come at the expense of other possible cultural processes (as discussed previously: community identity, prestige (mana), revenge (utu), violations of tapu, etc.), and indeed, resource-driven conflict could result in many of these other social-driven conflict motivators. Also of note during this period is the battle of Hingakākā at Ngāroto, recorded in Māori traditional history circa AD 1807 (Jones & Biggs, 1995; Ballara, 2003). This battle was fought between Ngāti Toa (Pikauterangi) and

Ngāti Mahuta (Te Rauangaanga) and their allies (Anderson, 2022, p. 51). Hingakākā is considered the largest battle ever fought in New Zealand, with an estimated 13,000 warriors involved, providing clear evidence of the potential scale of conflict undertaken during this period. Therefore, the critical influence identified in the regional chronological framework between RP2–5 is the sustained period of socio-political stress within the cultural landscape that magnifies and becomes entrenched over time. This period of socio-political stress can be related to various processes, encompassing the influence of one or many at any one time.

13.1.7.10 Regional Hypothesis Summary

The established regional chronological framework highlights three key periods within the Middle Waikato Basin between the sixteenth and early nineteenth centuries. These periods not only relate to identified episodes of palisade construction activity, representing the influence (stress/pressure) of environmental and/or cultural processes within the subject area, but also to pauses and continuations of this construction activity, implying a reduction, increase or entrenchment of socio-political stress within the cultural landscape. Interestingly, these three periods correlate with the later two of Anderson's (2022) phases of long-term patterns in warfare and migration (see Section 2.1.3), further implying an inherent cyclical nature of structural socio-political stress and conflict affecting Māori society during these periods.

Period 1, represented by RP1, is proposed to be linked to the environmental and cultural processes occurring within the Transitional Period. During this period, regionally specific climate declines (related to the LIA), coupled with population levels that were reaching a critical threshold, are thought to have spurred migration into more sparsely populated areas where kūmara production remained viable. This migration process is evident in the Waikato, with the Tainui migration out of Kawhia recorded circa AD 1520. These processes resulted in changes to the social structures and cultural landscape of Māori society (i.e., hapū formation and diverging kinship relationships), resulting in a need for these migrating communities to establish and consolidate zones of influence and control as they moved into these newly contested landscapes (such as the Middle Waikato Basin). This need is represented in the archaeological record through an initial fortification period, as populations moving into these areas established physical representations of their community identity within the landscape,

providing a communal space for economic, domestic and religious activities, while also exhibiting their strength to potential threats within the landscape and facilitating (enhancing) their control over critical resource zones.

Period 2, represented by Interval 1, is a period of proposed socio-political stability, represented by a lack of identified evidence of palisade construction activity. Following the fortification period identified during RP1, socio-political stress within the cultural landscape diminishes as clear zones of influence and control are set within the physical landscape (via pā construction), resulting in reduced levels of conflict and competition. It is important to note that while Interval 1 is interpreted as a period of stability, that does not mean a complete absence of conflict during this period. Instead, compared to later periods, Interval 1 is proposed to be largely free from the influence of structural socio-political stress, which would encourage widespread conflict. However, a reduced level of conflict associated with accessory motivations for warfare and competition would still be occurring during this period (i.e., utu (revenge), mana (prestige and status), violations of tapu (e.g., rāhui), etc.). This period of relative stability allowed the time necessary for the spread of newly developed systemised regional horticultural practices (the Waikato Horticultural Complex). Once developed, these horticultural practices were quickly implemented throughout the subject area, spreading rapidly downriver from their origin in Cambridge/Leamington. However, with the continued spread of these horticultural practices in the context of renewed demographic growth, the availability of the soils suitable for these systemised gardens became limited, instigating a renewed period of socio-political stress in the cultural landscape.

Period 3 reflects this renewed episode of socio-political stress within the Middle Waikato Basin, characterised by a sustained period of palisade construction activity across the eighteenth and early nineteenth centuries (RP2–5), accompanied by brief intervals between these phases (Interval 2, 3 and 4). Competition and territoriality are suggested to have begun in the south of the subject area before spreading north towards Taupiri following the proposed spread of the Waikato Horticultural Complex. Resource-driven competition related to available horticultural zones influenced this period of tension, creating an environment where protecting access and control over all available resource zones was paramount. This environment

culminated in what appears to have been endemic levels of warfare (influenced by a range of motivations and processes, both cultural and economic), represented by RP4–5, as competition and territoriality create region-wide socio-political stress, evidenced by the identified episodes of palisade construction, repair and redevelopment. While this spatial pattern of palisade construction activity (spreading from south to north within the subject area) is hypothesised here, it is also acknowledged that this regional pattern is based on a limited sample size of pā, and that further chronological evidence is required to categorically determine the accuracy of this spatio-tempral pattern. Therefore, the critical finding of the regional chronological framework during this period is the evidence of a sustained period of socio-political stress within the Middle Waikato Basin.

13.2 Concluding Remarks

This research sought to contextualise identified palisade construction activity with respect to the wider cultural and archaeological landscape, providing a way to explore the important connections between pā and the environmental and cultural processes affecting Māori communities regionally and nationally. New Zealand's short occupation history (and limited time depth) provides a challenging context for exploring these connections, requiring high-precision ^{14}C dating methods and in-depth analysis. However, by taking a considered chronological approach, focusing on multiple scales of analysis, meaningful conclusions can be drawn about the people and communities that occupied these pā throughout the country. While the link between pā and pre-European horticulture has long been hypothesised, the connection between the spread of the Waikato Horticultural Complex and increased evidence of socio-political stress identified in the Middle Waikato Basin further ties these two archaeological features together. This relationship again highlights how these features played a crucial role in the development of Māori society over time. However, the chronological frameworks developed during this study demonstrate the potential for more research to better understand pā and how they relate to other processes within the archaeological landscape.

13.3 Future Research Potential

This research has established detailed chronological frameworks for pā construction and occupation on both a local and regional scale, from which further archaeological research and interpretations should be considered. The chronology of pā construction and occupation inter-regionally and nationally warrants further study. Therefore, it is hoped that this research will act as a template for future applications in other regions of New Zealand. Two regions of interest should be chiefly considered in the first instance: the Bay of Plenty and Taranaki. Both regions include the necessary wetland pā sites, which are currently under-researched compared to other regions within New Zealand archaeological discourse. Such research would allow for a comprehensive inter-regional comparison and contribute significantly to the national archaeological discourse on pā. Also, it is hoped that this research sparks a renewed interest in pā studies within New Zealand. Recent research focusing on pā has been limited and mainly relies on data from past excavations. Thus, a renewed archaeological interest in pā, incorporating modern techniques, larger-scale excavations, and comprehensive sampling and dating strategies, has the potential to provide a far greater understanding of the role pā played within New Zealand's archaeological landscape.

References

Abram, N. (2014). Evolution of the southern annular mode during the past millennium. *Nature Climate Change, 4*, 564–569.

Adams, R. (1973). Review of radiocarbon variations and absolute chronology by Ingrid U. Olsson. *Journal of Near Eastern Studies, 32*, 253–256.

Aitchison, T., Leese, M., Michezynska, D., Mook, W., Otlet, R., Ottaway, B., . . . Weninger, B. (1989). A comparison of methods used for the calibration of radiocarbon dates. *Radiocarbon, 31*, 846–864.

Aitken, M. (1990). Radiocarbon - I. In M. Aitken (Ed.), *Science-based dating in archaeology* (pp. 56–75). London: Routledge.

Allen, K. (1987). *Ultra high sensitivity mass spectrometry with accelerator*. London: Royal Society Carlton House Terrace.

Allen, M. (1994). *Warfare and economic power in simple chiefdoms: The development of fortified villages and polities in Mid-Hawke's Bay, New Zealand* [Doctoral Thesis, University of California]. ProQuest Dissertations & Theses.

Allen, M. (1996). Pathways to economic power in māori chiefdoms: Ecology and warfare in prehistoric Hawke's Bay. *Research in Economic Anthropology, 17*, 171–225.

Allen, M. (2008a). Hillforts and the cycling of Maori chiefdoms: Do good fences make good neighbors? In J. Railey & R. Reycraft (Eds.), *Global perspectives on the collapse of complex systems* (pp. 65–81). Albuquerque: Maxwell Museum of Anthropology.

Allen, M. (2008b). Transformations in Maori Warfare: Toa, Pa, and Pu. In E. Arkush & M. Allen (Eds.), *The archaeology of warfare: Prehistories of raiding and conquest* (pp. 184–213). Gainesville: University Press of Florida.

Allen, M. (2012). Molluscan foraging efficiency and patterns of mobility amongst foraging agriculturalists: A case study from northern New Zealand. *Journal of Archaeological Science, 39*(2), 395–307.

Allen, M. (2016). Food, fighting and fortifications in pre-European New Zealand: Beyond the ecological model of māori warfare. In A. VanDerwarjer & G. Wilson (Eds.), *The archaeology of food and warfare: Food insecurity in prehistory* (pp. 41–59). New York: Springer International Publishing.

Allentoft, M., Heller, R., Oskam, C., Lorenzen, E., Hale, M., Gilbert, M., . . . Bunce, M. (2014). Extinct New Zealand megafauna were not in decline before human colonization. *Proceedings of the National Academy of Sciences, 111*(13), 4922–4927.

Altizer, W. (2008). Time perspectivism, temporal dynamics, and battlefield archaeology: A case study from the Santiago campaign of 1898. *Nebraska Anthropologist, 36*, 62–79.

Ambrose, W. (1962). Further investigations at Kauri Point, Katikati. *New Zealand Archaeological Association Newsletter, 5*(1), 56–67.

Ambrose, W. (1967). *Kauri Point*. Paper presented at the NZAA Conference, New Plymouth, New Zealand.

Anderson, A. (1991). The chronology of colonization in New Zealand. *Antiquity, 65*(249), 767–795.

Anderson, A. (1995). Current approaches in East Polynesian colonisation research. *Journal of the Polynesian Society, 104*, 110–132.

Anderson, A. (1998). *The welcome of strangers: An ethnohistory of southern Maori A.D. 1650–18*. Dunedin: Otago University Press.

Anderson, A. (2001). No meat of that beautiful shore: The prehistoric abandonment of subtropical Polynesian islands. *International Journal of Osteoarchaeology, 11*(1), 14–23.

Anderson, A. (2002). Faunal collapse, landscape change and settlement history in remote Oceania. *World Archaeology, 33*(3), 375–390.

Anderson, A. (2014). Emerging societies. In A. Anderson, J. Binney, & A. Harris (Eds.), *Tangata whenua: An illustrated history* (pp. 102–129). Wellington, New Zealand: Bridget Williams Books.

Anderson, A. (2016). The making of the māori middle ages. *Journal of New Zealand Studies, 23*, 2–18.

Anderson, A. (2022). War is their principal profession: On the frequency and causes of Maori warfare and migration, 1250–1850 CE. In G. Clarke, & M. Litster (Eds.). *Archaeological perspectives on conflict and warfare in Australia and the Pacific* (pp. 39–61). (Vol. 54). Canberra: ANU Press.

Anderson, A., & McGlone, M. (1992). Living on the edge - prehistoric land and people in New Zealand. In J. Dodson (Ed.), *The naive lands: Prehistory and environmental change in Australia and the south-west Pacific* (pp. 199–241). Melbourne: Longman Cheshire.

Anderson, A., & Petchey, F. (2020). The transfer of kūmara (*Ipomoea batatas*) from the east to south Polynesia and its dispersal in New Zealand. *Journal of the Polynesian Society, 129*(4), 352–381.

Anschuetz, K., Wilshusen, R., & Scheick, C. (2001). An archaeology of landscapes: Perspectives and directions. *Journal of Archaeological Science, 9*(2), 157–211.

Arnold, J., & Libby, W. (1949). Age determinations by radiocarbon content: Checks with samples of known age. *Science, 110*, 289–315.

Arnold, J., & Libby, W. (1950). Radiocarbon dates. *Science, 113*, 111–120.

Ashmore, P. (1999). Single entity dating. *Mémoires de la société préhistorique française, 26,* 65–71.

Bader, H. (2013). Report on S18-investigation of S15/103 Orakau Pā: Authority #2013/476. *New Zealand Historic Places Trust/Pouhere Taonga*.

Bailey, G. (1981). Concepts, time-scales and explanations in economic prehistory. In A. Sheridan & G. Bailey (Eds.), *Economic archaeology* (pp. 97–117). Oxford: British Archaeological Reports International Series.

Bailey, G. (1983). Concepts of time in quaternary prehistory. *Annual Review of Anthropology, 12*, 165–192.

Bailey, G. (1987). Breaking the time barrier. *Archaeological Review from Cambridge, 6,* 5–20.

Bailey, G. (2005). Concepts of time. In C. Renfrew & P. Bahn (Eds.), *Archaeology: The key concepts.* (pp. 268–273). London: Routledge.

Bailey, G. (2007). Time perspectives, palimpsests and the archaeology of time. *Journal of Anthropological Archaeology, 26*, 198–223.

Bailey, G. (2008). Time perspectivism: origins and consquences. In S. Holdaway & L. Wandsnider (Eds.), *Time in archaeology: Time perspectivism revisited* (pp. 13–30). Salt Lake City: The University of Utah Press.

Baillie, M. (1982). *Tree-ring dating and archaeology*. Chicago: The University of Chicago Press.

Baillie, M., & Pilcher, J. R. (1973). A simple cross-dating program for tree ring research. *Tree Ring Bulletin, 33*, 7–14.

Ballara, A. 1976. The role of warfare in Maori society in the early contact period. *Journal of the Polynesian Society, 85*(4), 487–506.

Ballara, A. (1998). *Iwi: The dynamics of Maori tribal organisation from 1769–1945*. Wellington: Victoria University Press.

Ballara, A. (2003). *Taua: 'Musket wars', 'land wars' or tikanga? Warfare in Maori society in the early nineteenth century.* Auckland: Penguin.

Barber, I. (1996). Loss, change, and monumental landscaping: Towards a new interpretation of the "classic" Maaori emergence. *The University of Chicago Press on behalf of Wenner-Gren Foundation for Anthropological Research, 37*, 868–880.

Barber, I. (2004). Crops on the border: The growth of archaeological knowledge of Polynesian cultivation in New Zealand. In L. Furey & S. Holdaway (Eds.), *Change through time: 50 years of New Zealand archaeology* (pp. 169–192). Auckland: New Zealand Archaeological Association.

Barber, I. (2010). Diffusion or innovation? Explaining extensive lithic cultivation fields on the southern Polynesian margins. *World Archaeology, 26*(1), 75–90.

Barber, I. (2012). A fast yam to Polynesia: New thinking on the problem of American sweet potato in Oceania. *Rapa Nui Journal, 26*, 31–42.

Barber, I., & Higham, T. (2021). Archaeological science meets Māori knowledge to model pre-Columbian sweet potato (*Ipomoea batatas)* dispersal to Polynesia's southernmost habitable margins. *PloS one, 16*(4), e0247643.

Bard, E., Arnold, M., Hamelin, B., Tisnerat-Laborde, N., & Cabioch, G. (1998). Radiocarbon calibration by means of mass spectrometric 230th/234u and ^{14}c ages of corals: An updated database including samples from Barbados, Bururoa and Tahiti. *Radiocarbon, 4*, 1085–1092.

Bassett, K., Gordon, H., Nobes, D., & Jacomb, C. (2004). Gardening at the edge: Documenting the limits of tropical Polynesian kumara horticulture in southern New Zealand. *Geoarchaeology, 19*, 185–218.

Bayliss, A. (2009). Rolling out revolution: Using radiocarbon dating in archaeology. *Radiocarbon, 51*(1), 123–147.

Bayliss, A. (2015). Quality in Bayesian chronological models in archaeology. *World Archaeology, 47*(4), 677–700.

Bayliss, A., Bronk Ramsey, C., van Der Plicht, J., & Whittle, A. (2007). Bradshaw and Bayes: Towards a timetable for the neolithic. *Cambridge Journal of Archaeology, 17*, 1–28.

Bayliss, A., Marshall, P., Bronk Ramsey, C., & Cook, C. (2017). Informing conservation: Towards ^{14}C wiggle-matching of short tree-ring sequences from medieval buildings in England. *Radiocarbon, 59*(3), 985–1007.

Bé, M.M., Chisté, V., Dulieu, C., Browne, E., Chechev, V., Kuzmenko, N., Helmer, R., Nichols, A., Schönfeld, E. and Dersch, R., (2004). Monographie BIPM-5—Table of radionuclides, Vol. 4. Internet: http://www. nucleide.org.

Bedford, S. (2013). From Paeroa to Pohue Pa: Remnant landscapes of events that once shook the world. In M. Campbell, S. Holdaway, & Macready, S. (Eds*) Finding our recent past: Historical archaeology in New Zealand* (pp. 59–76). New Zealand Archaeological Association.

Bellingham, P. (1982). *Some ecological aspects of matai (Podocarpus spicatus R. BR. Ex Mirbel) in west Taupo indigenous forests.* [Bachelor of Forestry Science Degree], University of Canterbury, Christchurch.

Bellwood, P. (1969a). *Lake Mangakaware southern end* [excavation photograph]. Department of Anthropology: University of Auckland.

Bellwood, P. (1969b). Pā excavations at Otakanini, South Kaipara and Lake Mangakaware, Waikato. *New Zealand Archaeological Association Newsletter, 12*, 38–49.

Bellwood, P. (1971a). Archaeological research at Lake Mangakaware, Waikato: A summary of results. *New Zealand Archaeological Association Newsletter, 14*, 113–125.

Bellwood, P. (1971b). Fortifications and economy in prehistoric New Zealand. *The Proceedings of the Prehistoric Society, 37*(1), 56–95.

Bellwood, P. (1971c). Otakanini Pā, South Kaipara. *New Zealand Archaeological Association Newsletter, 14*, 74–76.
Bellwood, P. (1972a). Excavations at Otakanini Pa, South Kaipara Habour. *Journal of the Royal Society of New Zealand, 2*, 259–291.
Bellwood, P. (1972b). A prehistoric Maori settlement: Lake Mangakaware, Te Rore. In D. Goodall (Ed.), *The Waikato: Man and his environment* (Vol. 2, pp. 27–29). Waikato: New Zealand Geographical Society.
Bellwood, P. (1978a). *Archaeological research at Lake Mangakaware, Waikato, 1968–1970* (Vol. 12). University of Otago: New Zealand Archaeological Association
Bellwood, P. (1978b). *Man's conquest of the Pacific*. Auckland: Collins.
Best, E. (1925). *Maori agriculture*. Wellington: Board of Maori Ethnological Research.
Best, E. (1927). *The Paa Maori* (Vol. 6). Wellington: Dominion Musem Bulletin
Beverly, R., Beaumont, W., Tauz, D., Ormsby, K., Von Reden, K., Santos, G., & Southon, J. (2010). The Keck Carbon Cycle AMS Laboratory, University of California, Irvine: Status report. *Radiocarbon, 52*(2), 301–309.
Binford, L. (1980). Willow smoke and dogs' tails: Hunter-gatherer settlement systems and archaeological site formation. *American Antiquity, 45*(1), 4–20.
Binford, L. (1981). Behavioural archaeology and the "Pompeii Premise". *Journal of Anthropological Research, 37*, 95–208.
Bintliff, J. (1991). *The Annales School and Archaeology*. Leicester: Leicester University Press.
Blaauw, M., Christen, A., Bennett, K., & Paula, J. (2018). Double the dates and go for Bayes — Impacts of model choice, dating density and quality on chronologies. *Quaternary Science Reviews, 188*, 58–66.
Blaauw, M., Heuvelink, G., Mauquoy, D., van der Plicht, J., & van Geel, B. (2003). A numerical approach to ^{14}C wiggle-match dating of organic deposits: Best fits and confidence intervals. *Quaternary Science Reviews, 22*(14), 1485–1500.
Blackwell, P., & Buck, C. (2008). Estimating radiocarbon calibration curves. *Bayesian Analysis, 3*(2), 225–248.
Boswijk, G., Brassey, R., Bader, H., Adamson, J., & Jones, M. (2016). Dendrochronological dating of kauri timbers from Browne's Spar Station (1832–1836), Mahurangi, Auckland, New Zealand. *Journal of Archaeological Science, 7*, 129–137.
Boswijk, G., & Johns, D. (2018). Assessing the potential to calendar date Māori waka (canoes) using dendrochronology. *Journal of Archaeological Science, 17*, 442–448.
Boswijk, G., Johns, D., & Hogg, A. (2019). Dendroarchaeology in New Zealand: Assessing the potential to extend the suite of useful tree species beyond kauri (*Agathis australis*). *Journal of Pacific Archaeology, 10*(1), 33–44.
Boswijk, G., Loader, N., Young, G., & Hogg, A. (2021). Developing tree-ring chronologies from New Zealand matai (*Prumnopitys taxifolia*) and miro (*Prumnopitys ferruginea*) for archaeological dating: Progress and problems. *Dendrochronologia, 69*, 1–11.
Bradley, R. (1991). Ritual, time and history. *World Archaeology, 23*, 209–2019.
Braudel, F. (1972). *The Mediterranean and the Mediterranean world in the age of Phillip II.* London: Collins.
Braudel, F. (1980). *On history*. London: Weidenfeld & Nicolson.
Bronk Ramsey, C. (1994). Analysis of chronological information and radiocarbon calibration: The program OxCal. *Archaeological Computing Newsletter, 41*, 11–16.
Bronk Ramsey, C. (1995). Radiocarbon calibration and the analysis of stratigraphy: The OxCal program. *Radiocarbon, 37*, 425–430.
Bronk Ramsey, C. (2001). Development of the radiocarbon calibration program Oxcal. *Radiocarbon, 43*, 355–363.

Bronk Ramsey, C. (2008). Radiocarbon dating: Revolutions in understanding. *Archaeometry, 20*(2), 249–275.
Bronk Ramsey, C. (2009a). Bayesian analysis of radiocarbon dates. *Radiocarbon, 51*(1), 337–360.
Bronk Ramsey, C. (2009b). Dealing with outliers and offsets in radiocarbon dating. *Radiocarbon, 51*(3), 1023–1045.
Bronk Ramsey, C., Brenninkmeijer, C., Jockel, P., Kjeldsen, H., & Masarik, J. (2007). Direct measurement of the radiocarbon production at altitude. *Nuclear instruments & methods in physics research. Section B, Beam interactions with materials and atoms, 259*(1), 558–564.
Bronk Ramsey, C., Buck, C., Manning, M., Reimer, P., & Van Der Plicht, H. (2006). Developments in radiocarbon calibration for archaeology. *Quaternary Science Reviews, 25*(5), 783–798.
Bronk Ramsey, C., Dee, M., Lee, S., Nakagawa, T., & Staff, R. (2010a). Developments in the calibration and modelling of radiocarbon dates. *Radiocarbon, 52*(2–3), 953–961.
Bronk Ramsey, C., Dee, M., Rowland, J., Higham, T., Harris, A., Brock, F., . . . Shortland, A. (2010b). Radiocarbon based chronology for dynastic Eygpt. *Science, 328*, 1554–1557.
Bronk Ramsey, C., Van Der Plicht, J., & Weninger, B. (2001). 'Wiggle Matching' radiocarbon dates. *Radiocarbon, 43*, 381–389.
Brown, A., & Crema, E. (2021). Māori population growth in pre-contact New Zealand: Regional population dynamics inferred from summed probability distributions of radiocarbon dates. *The Journal of Island and Coastal Archaeology, 16*(2–4), 572–590.
Buck, C., & Blackwell, P. (2004). Formal statistical models for estimating radiocarbon calibration curves. *Radiocarbon, 46*(3), 1093–1102.
Buck, C., Cavanagh, W., & Litton, C. (1996). *Bayesian approach to interpreting archaeological data*. Chichester: Wiley.
Buck, C., Christen, J., & James, G. (1999). BCal: An on-line bayesian radiocarbon calibration tool. *Internet Archaeology,* (7). https://doi.org/10.11141/ia.7.1
Buck, C., Kenworthy, J., Litton, C., & Smith, A. (1991). Combining archaeological and radiocarbon information: A Bayesian approach to calibration. *Antiquity, 65,* 808–821.
Buck, C., Litton, C., & Scott, E. (1994). Making the most of radiocarbon dating: Some statistical considerations. *Antiquity, 68*(259), 252–263.
Buck, C., Litton, C., & Smith, A. (1992). Calibration of radiocarbon dates pertaining to related archaeological events. *Journal of Archaeological Science, 19*, 497–512.
Buck, C., & Millard, A. (2004). *Tools for constructing chronologies: Crossing disciplinary boundaries.* London: Springer.
Buck, P. (1950). *The coming of the Māori*. Wellington: Whitcombe and Tombs.
Buist, A. (1964). Archaeology in North Taranaki, New Zealand: A study of field monuments in the Pukearuhe-Mimi-Urenui area. *NZ Archaeological Association Monograph*.
Bunbury, M., Petchey, F., & Bickler, S. (2022). A new chronology for the Māori settlement of Aotearoa (NZ) and the potential role of climate change in demographic developments. *Proceedings of the National Academy of Sciences of the United States of America, 119*(46), 1–8.
Burleigh, R., Longworth, I., & Wainwright, G. (1972). Relative and absolute dating of four late Neolithic enclosures: An exercise in the interpretation of radiocarbon determinations. *Proceedings of the Prehistoric Society, 38*, 389–407.
Burns, B., & Merrett, M. (1999). *Dynamics of kahikatea forest remnants in middle North Island: Implications for threatened and local plants* (Vol. 113). Wellington: Science for Conservation 113.

Burns, B., & Smale, M. (2002). Lowland forests. In B. Clarkson, M. Merrett, & T. Downs (Eds.), *Botany of the Waikato* (pp. 73–81). Hamilton: Waikato Botanical Society Inc.

Burr, G., Correge, T., Donahue, D., & O'Malley, J. (1998). A high-resolution radiocarbon calibration between 11,700 and 12,400 calendar years BP derived from 230Th ages of corals from Espiritu Santo Island, Vanuatu. *Radiocarbon, 40*, 1093–1105.

Burtenshaw, M., & Harris, A. (2007). Experimental archaeology gardens: Assessing the productivity of ancient Māori cultivars of sweet potato, *Ipomoea batatas* [L.] Lam. *Economic Botany, 13*, 235.

Burtenshaw, M., Harris, G., Davidson, J., & Leach, F. (2003). Experimental growing of pre-European cultivars of kumara (sweet potato, *Ipomoea batatus* [L.] lam) at the southern margins of Māori horticulture. *New Zealand Journal of Archaeology, 23*(161–188).

Campbell, M. (2008). *Paeroa Pā, Moturua, Bay of Islands: Archaeological assessment*. Unpublished report to Explore NZ Ltd.

Carr, C. (1987). Dissecting intrasite artifact palimpsests using Fourier methods. In S. Kent (Ed.), *Method and theory for activity area research* (pp. 236–291). New York: Columbia Univesity Press.

Cassels, R. (1972a). Human ecology in the prehistoric Waikato. *The Journal of the Polynesian Society, 81*(2), 196–247.

Cassels, R. (1972b). Locational analysis of prehistoric settlement in New Zealand. *The Australian Journal of Anthropology, 8*(3), 212–222.

Channell, J., Stoner, J., & Hodell, D. (2000). Geomagnetic paleointensity for the last 100 kyr from the sub-Antarctic South Atlantic: A tool for inter-hemispheric correlation. *Earth and Planetary Science Letters, 175*, 145–160.

Childe, V. (1957). *The dawn of European civilisation* (6th ed.). London: Routledge.

Christen, J. (1994). Summarizing a set of radiocarbon determinations: A robust approach. *Journal of Royal Statistical Society: Series C, 43*(3), 489–503.

Christen, J., & Litton, C. (1995). A Bayesian approach to wiggle-matching. *22*, 119–725.

Clark, G. (1970). *Aspects of prehistory*. Berkeley, California: University of California Press.

Clarke, G., & Litster, M. (Eds.). (2022). *Archaeological perspectives on conflict and warfare in Australia and the Pacific*. (Vol. 54). Canberra: ANU Press.

Clark, R. (1975). A calibration curve for radiocarbon dates. *Antiquity, 49*(251–266).

Clarke, A. (1977). Māori modified soils of the Upper Waikato. *New Zealand Archaeological Association Newsletter, 20*, 204–222.

Clarke, A. (1980). *The early century settlement patterns of the Lower Waikato Basin*. Hamilton.

Cleal, R., Walker, K., & Montague, R. (1995). *Stonehenge in its landscape: Twentieth-century excavations*. London: English Heritage.

Cooper, Z. (1993). Perceptions of time in the Andaman Islands. *World Archaeology, 25*, 261–267.

Damon, P., Donahue, D., Gore, B., Hatheway, A., Jull, A., Linick, T., . . . Tite, M. (1989). Radiocarbon dating of the Shroud of Turin. *Nature, 337*, 611–615.

Damon, P., Ferguson, C., Long, A., & Wallick, E. (1974). Dendrochronologic calibration of the radiocarbon time scale. *American Antiquity, 39*(2), 350–366.

Damon, P., Kaimei, D., Kocharov, G., Mikheeva, I., & Peristykh, A. (1995). Radiocarbon production by the gamma-ray component of supernova explosions. *Radiocarbon, 37*(2), 599–604.

Damon, P., Lerman, J., & Long, A. (1978). Temporal fluctuations of atmospheric ^{14}C: Causal factors and implications. *Annual Review of Earth Planetary Science, 6*, 457–494.

Daugherty, J. (1979). *Polynesian warfare and fortifications.* [Doctoral Thesis, University of Auckland]. Research Hub, The University of Auckland.

Davidson, J. (1984). *The prehistory of New Zealand*. Auckland: Longman Paul.
Davidson, J. (1985). New Zealand prehistory. In F. Wendorf (Ed.), *Advances in world archaeology* (Vol. 4, pp. 239–291). New York: Academic Press.
Davidson, J. (1987). The Paa Maori revisited. *Journal of the Polynesian Society, 96*, 7–26.
Davidson, J. (2011). Archaeological investigations at Maungarei: A large Māori settlement on a volcanic cone in Auckland, New Zealand. *Tuhinga, 22*, 19–100.
Dawson, J., & Lucas, R. (2016). *Field guide to New Zealand's native trees* (Vol. 2). Nelson, New Zealand: Craig Potton Publishing.
de Jong, A., Mook, W., & Becker, B. (1979). Confirmation of the Suess wiggles: 3200–3700 BC. *Nature, 280*, 48–49.
de Vries, H. (1958). Variation in concentration of radiocarbon with time and location on earth. *Proc. Koninkl. Nederl. Akad. Wetenschappen, B*(61), 1–9.
de Vries, H. (1959). Measurement and use of natural radiocarbon. In P. Abelson (Ed.), *Researches in geochemistry* (pp. 169–189). New York: John and Wiley & sons.
Deitler, M., & Herbich, I. (1993). Living on Luo time: Recloning sequence, duration, history and biography in rural African society. *American Antiquity, 25*, 13–22.
Dennell, R. (1987). Accelerator dating: The first years reviewed. *Antiquity, 61*(231), 137–138.
Duff, R. (1956). *The moa-hunter period of Māori culture*. Wellington: Government Printer.
Dunwiddie, P. (1979). Dendrochronological studies of indigenous New Zealand trees. *New Zealand Journal of Botany, 17*, 251–266.
Ebert, J. (1992). *Distributional archaeology*. Salt Lake City: University of Utah Press.
Engelkemeir, A., Hamil, W., Ingham, M., & Libby, W. (1949). The half-life of radiocarbon. *The Physical Review, 75*(12), 1825–1833.
Epp, T. (2010). Time perspectivism as applied to three Mennonite cemeteries in York County, Nebraska. *Nebraska Anthropologist, 53*, 51–72.
Ferguson, R. (2008). Ten points on war. *Social Analysis, 52*, 32–49.
Ferguson, C., Huber, B., & Suess, H. (1966). Determination of the age of Swiss lake dwellings as an example of dendrochronologically-calibrated radiocarbon dating. *Zeitschrift für Naturforschung, 21*(7), 1173–1177.
Field, J., & Lape, P. (2010). Paleoclimate and the emergency of fortifications in the tropical Pacific islands. *Journal of Anthropological Archaeology, 29*(1), 113–124.
Fish, S. (1999). Conclusions: The settlement patterns concept from an Americanist perspective. In B.R Billman & G.M. Feinman (Eds), *Settlement Pattern Studies in the Americas: Fifty Years Since Virú* (pp. 203–208). Washington: Smithsonian Institute Press.
Foley, R. (1981). A model of regional archaeological structure. *Proceedings of the Prehistoric Society, 47*, 1–17.
Fomison, T. (1959). Site survey of Kaikoura peninsula. *NZ Archaeological Association Newsletter, 3*, 4–15.
Fowler, A., Boswijk, G., Lorrey, A., Gergis, J., Pyrie, M., McCloskey, S., & Wunder, J. (2012). Multi-centennial ENSO insights from New Zealand forest giants. *Nature Climate Change, 2*, 172–176.
Fox, A. (1976). *Prehistoric Maori fortifications in the North Island of New Zealand*. Auckland: Longman Paul.
Furey, L. (1996). *Oruarangi: The archaeology and material culture of a Hauraki pa* (Vol. 17). Auckland: Bulletin of the Auckland Institute and Museum.
Furey, L. (2006). *Māori gardening: An archaeological perspective*. Wellington: Science and Technical Publishing, Department of Conservation.
Furey, L., Emmitt, J., & Wallace, R. (2017). Matakawau Stingray Point Pa excavation, Ahuahu Great Mercury Island 1955–56. *Records of the Auckland Museum, 52*, 39–57.

Gainsford, M., & Gumbley, W. (2020). *Archaeological investigation and management report: Te Uapata Pā (S14/20), Otaahau Pā (S14/21) & Rua's House (S14/178)*. Unpublished report to Heritage New Zealand Pouhere Taonga.
Galimberti, M., Bronk Ramsey, C., & Manning, M. (2004). Wiggle-match dating of tree-ring sequences. *Radiocarbon, 46*(2), 917–924.
Gardner, A. (2001). The times of archaeology and archaeologies of time. *Papers from the Institute of Archaeology, 12*, 35–47.
Gardner, A. (2012). Time and empire in the Roman world. *Journal of Social Archaeology, 12*(2), 145–166.
Gillespie, R., & Brook, B. (2006). Is there a Pleistocene archaeological site at Cuddie Springs? *Archaeology in Oceania, 41*(1), 1–11.
Godwin, H. (1962). Half-life of radiocarbon *Nature, 195*, 984.
Golson, J. (1957). Field archaeology in New Zealand. *Journal of the Polynesian Society, 66*, 64–109.
Golson, J. (1959). Culture change in prehistoric New Zealand. In J. Freeman & W. Geddes (Eds.), *Anthropology in the south seas: Essays presented to H.D. Skinner* (pp. 29–74). New Plymouth: Thomas Avery and Sons.
Golson, J. (1960a). Excavations at Mt. Wellington. *NZ Archaeological Association Newsletter, 3*, 31–34.
Golson, J. (1960b). Excavations at Pakotore, Paengaroa, Bay of Plenty. *NZ Archaeological Association Newsletter, 3*, 11–14.
Golson, J. (1961a). Investigations at Kauri Point Katikati. *New Zealand Archaeological Association Newsletter, 4*(2), 13–41.
Golson, J. (1961b). Investigations at Kauri Point, Katikati, Western Bay of Plenty – 3 The excavations. *New Zealand Archaeological Association Newsletter, 4*, 61–62.
Golson, J., & Green, R. (1958). A handbook to field recording in New Zealand. *NZ Archaeological Association Monograph*.
Goodwin, I., Browning, S., & Anderson, A. (2014). Climate windows for Polynesian voyaging to New Zealand and Easter Island. *Proceedings of the National Academy of Sciences, 111*(41), 14716–14721.
Goosse, H., Brovkin, V., Meissner, K. J., Menviel, L., Mouchet, A., Muscheler, R., & Nilsson, A. (2024). Atmospheric $\Delta^{14}C$ in the Northern and Southern Hemispheres over the past two millennia: Role of production rate, Southern Hemisphere westerly winds and ocean circulation changes. *Quaternary Science Reviews*, 326, 108502.
Gorbey, K. (1970). *Pā distribution in New Zealand.* [Doctoral Thesis, University of Auckland]. Research Hub, The University of Auckland.
Gosden, C. (1994). *Social being and time*. Oxford: Basil Blackwell.
Goslar, T., & Madry, W. (1998). Using the Bayesian method to study the precision of dating by wiggle-matching. *Radiocarbon, 40*(1), 551–560.
Grange, L., Taylor, N., Sutherland, C., Dixon, J., Hodgson, L., Seelye, F., . . . Smallfield, P. (1939). Soils and agriculture of part of Waipa County. *New Zealand Department of Scientific and Industrial Research Bulletin, 76*.
Graves, M., & Sweeney. (1993). Ritual behaviour and ceremonial structures in Eastern Polynesia: changing perspectives on archaeological variability. In M. Graves & R. Green (Eds.), *The evolution and organization of prehistoric society in Polynesia* (pp. 106–125). Auckland: New Zealand Archaeological Association Monograph 19.
Green, R. (1967). Settlement patterns: Four case studies from Polynesia. In W. Solheim (Ed.), *Archaeology at the eleventh Pacific Science Congress* (pp. 101–132). Honolulu: University of Hawaii.

Green, R. (1970). *A review of the prehistoric sequence in the Auckland province* (2nd Ed.). Dunedin: University Bookshop.
Green, R. (1972). Moa-hunters, agriculture and changing analogies in New Zealand prehistory. *New Zealand Archaeological Association Newsletter, 15*(1), 16–39.
Green, R. (1975). Adaptation and change in Maori culture. In G. Kuschel (Ed.), *Biogeography and ecology in New Zealand*. Springer Science & Business Media.
Green, R. (1978). Dating the Kauri Point sequence. *History Review, 26*(1), 32–45.
Green, R., & Shawcross, W. (1962). Cultural sequence in the Auckland province. *New Zealand Archaeological Association Newsletter, 5*, 210–222.
Gregory, D., & Jensen, P. (2006). The importance of analysing waterlogged wooden artefacts and environmental conditions when considering their *in situ* preservation. *Journal of Wetland Archaeology, 6*(1), 65–81.
Groube, L. (1964a). *Settlement patterns in prehistoric New Zealand.* [Doctoral Thesis, University of Auckland]. Research Hub, The University of Auckland.
Groube, L. (1964b) *Archaeology in the Bay of Islands*. [Unpublished report], Anthropology Department, University of Otago, Dunedin
Groube, L. (1965). Excavations on Paeroa Village, Bay of Islands. *New Zealand Historic Places Trust Newsletter, 9*, 5–7.
Groube, L. (1966). Rescue excavations in the Bay of Islands. N.Z. *Archaeological Association Newsletter 9(3)*, 108–114.
Groube, L. (1967). Models in prehistory: A consideration of the New Zealand evidence. *Archaeology and Physical Anthropology in Oceania, 2*, 1–27.
Groube, L. (1970). The origin and development of earthwork fortifications in the Pacific. In R. Green & M. Kelly (Eds.), *Studies in oceanic culture history* (pp. 133–164). Honolulu: Bishop Museum.
Gumbley, W. (2014a). *The Cabana Site (T12/3), Whangamata: Results of the 2007 investigation*. Unpublished report to Thames-Coromandel District Council.
Gumbley, W. (2014b). *Orakau Pā: A review of historical information and a consideration of its location.* Unpublished report to New Zealand Historic Places Trust/Pouhere Taonga, 1–48.
Gumbley, W. (2021). *The Waikato horticultural complex: An archaeological reconstruction of a Polynesian horticultural system.* [Doctoral Thesis, The Australian National University]. University of Canberra Research Portal.
Gumbley, W., Higham, T., & Lowe, D.J. (2004). Prehistoric horticultural adaptation of soils in the Middle Waikato Basin: Review and evidence from S14/201 and S14/185, Hamilton. *New Zealand Journal of Archaeology, 25*, 5–30.
Gumbley, W., & Hutchinson, M. (2013). *Pre-European Maori garden sites in Waipa District: An assessment of the state of the resource*. Report to the New Zealand Historic Places Trust.
Gumbley, W., & Laumea, M. (2019). *T12/3 – The Cabana Site, Whangamata, New Zealand. Results of the 2016 investigation.* Unpublished report to Thames-Coromandel District Council.
Gurevuch, A. (1995). The French historical revolution. The Annales School. In I. Hodder, M. Shanks, A. Alexandri, V. Buchli, J. Carmen, J. Last, & G. Lucas (Eds.), *Interpreting archaeology: Finding meaning in the past*. London: Routledge.
Hafner, A., Reich, J., Ballmer, A., Bolliger, M., Antolín, F., Charles, M., . . . Tinner, W. (2021). First absolute chronologies of Neolithic and Bronze Age settlements at Lake Ohrid based on dendrochronology and radiocarbon dating. *Journal of Archaeological Science: Reports, 38*, 103–107.

Hajdas, I. (2009). Applications of radiocarbon dating method. *Radiocarbon, 51*, 79–90.
Hajdas, I., Ascough, P., Garnett, M., Fallon, S., Pearson, C., Quarta, C., . . . Yoneda, M. (2021). Radiocarbon dating. *Nature Reviews Methods Primers, 1*(62), 1–65.
Hamilton, W., Bayliss, A., Menuge, A., Bronk Ramsey, C., & Cook, G. (2007). `Rev Thomas Bayes: Get ready to 'wiggle', Bayesian modelling, radiocarbon wiggle-matching, and the North Wing of Baguley Hall. *Vernacular Architecture, 38*(1), 87–97.
Harding, J. (2005). Rethinking the great divide: Long-term structural history and the temporality of event. *Norwegian Archaeological Review, 38*(2), 88–101.
Harris, D., Gove, H., & Damon, P. (1987). The impact on archaeology of radiocarbon dating by accelerator mass spectrometry. *Philosophical Transactions of the Royal Society of London A, 323*(1569), 23–43.
Harris, O. (2017). Assemblages and scale in archaeology. *Cambridge Archaeological Journal, 27*(1), 127–137.
Hather, J. (2000). *The identification of northern European woods: A guide for archaeologists and conservators.* London: Routledge.
Heaton, T., Bard, E., Bronk Ramsey, C., Butzin, M., Köhler, P., Muscheler, R., . . . Wacker, L. (2021). Radiocarbon: a key tracer for studying earth's dynamo, climate system, carbon cycle, and sun. *Science, 374*, 65–68.
Heaton, T., Blaauw, M., Blackwell, P., Bronk Ramsey, C., Reimer, J., & Scott, E. (2020a). The IntCal20 approach to radiocarbon calibration curve construction: a new methodology using Bayesian splines and errors-in-variables. *Radiocarbon, 62*(4), 821–863.
Heaton, T., Blackwell, P., & Buck, C. (2009). A Bayesian approach to the estimation of radiocarbon calibration curves: the IntCal09 methodology. *Radiocarbon, 51*(4), 1151–1164.
Heaton, T., Köhler, P., Butzin, M., Bard, E., Reimer, R., Austin, W., . . . Skinner, L. (2020b). Marine20 — The marine radiocarbon age calibration curve (0–55,000 cal BP). *Radiocarbon, 62*(4), 779–820. doi:10.1017/RDC.2020.68
Henry, D. (2012). The palimpsest problem, hearth pattern analysis, and middle Paleolithic site structure. *Quaternary International, 247*, 246–266.
Herdrich, D., & Clark, J. (1993). Samoan tia 'ave and social structure: Methodological and theoretical considerations. In M. Graves & R. Green (Eds.), *The evolution and organization of pre-historic society in Polynesia* (pp. 52–63). Auckland: New Zealand Archaeological Association Monograph 19.
Herzfeld, M. (2009). Rhythm, tempo, and historical time: Experiencing temporality in the neoliberal age. *Public Archaeology, 8*(2), 108–123.
Hewitt, A., Balks, M., & Lowe, D. (2021a). Anthropic soils. In A. Hewitt, M. Balks, & D.J. Lowe, *The soils of Aotearoa New Zealand* (pp. 41–55). Springer International Publishing.
Hewitt, A., Balks, M., & Lowe, D.J. (2021b). *The soils of Aotearoa New Zealand*. Cham, Switzerland: Springer International Publishing, pp. xx – 332.
Higham, T., Douka, K., Wood, R., Bronk Ramsey, C., Brock, F., Basell, L., . . . Jacobi, R. (2014). The timing and spatiotemporal patterning of Neanderthal disappearance. *Nature, 512*(7514), 306–309. doi:10.1038/nature13621
Higham, T., & Gumbley, W. (2001). Early preserved Polynesian kumara cultivations in New Zealand. *Antiquity, 75*, 511–512.
Higham, T., & Hogg, A. (1997). Evidence for late Polynesian colonisation of New Zealand: University of Waikato Radiocarbon measurements. *Radiocarbon, 39*, 149–192.
Higham, T., Jacobi, R., Julien, M., David, F., Basell, L., Wood, R., . . . Bronk Ramsey, C. (2010). Chronology of the Grotte du Renne (France) and implications for the context

of ornaments and human remains within the Chatelperronian. *National Academy of Sciences, 107*(47), 20234–20239.
Higham, T., & Jones, M. (2004). Chronology and settlement. In L. Furey & R. Holdaway (Eds.), *Change through time: 50 years of New Zealand archaeology* (Vol. 1, pp. 215–234). Auckland: New Zealand Archaeological Association.
Hillam, J., & Tylers, I. (1995). Reliability and repeatability in dendrochronological analysis: Tests using the Fletcher Archive of panel-painting data. *Archaeometry, 37*, 395–405.
Hitiri te, P., & Mair, G. (1888). *Description of the Battle of Orakau, As given by the native chief Hitiri te Paerata of the Ngatiraukawa Tribe, at the parliamentary buildings, 4th August, 1888*. Wellington: G. Didsbury, Government Printer.
Hodder, I. (1987). *Archaeology as long-term history*. Cambridge: Cambridge University Press.
Hogg, A. (2023). [Interim results of laboratory bias testing in SHCal20].
Hogg, A., Gumbley, W., Boswijk, G., Petchey, F., Southon, J., Anderson, A., . . . Donaldson, L. (2017). The first accurate and precise calendar dating of New Zealand Māori Pā, using Otāhau Pā as a case study. *Journal of Archaeological Science: Reports, 12*, 124–133.
Hogg, A., Heaton, T., Bronk Ramsey, C., Boswijk, G., Palmer, J., Turney, C., . . . Gumbley, W. (2019a). The influence of calibration curve construction and composition on the accuracy and precision of radiocarbon wiggle-matching of tree rings, illustrated by Southern Hemisphere atmospheric data sets from AD 1500–1950. *Radiocarbon, 61*(5), 1265–1291.
Hogg, A., Heaton, T., Hua, Q., Palmer, J., Turney, C., Southon, J., . . . Wacker, L. (2020). SHCal20 Southern Hemisphere calibration, 0–55,000 years cal BP. *Radiocarbon, 62*(4), 759–778.
Hogg, A., Higham, T., Lowe, D., Palmer, J., Reimer, P., & Newnham, R. (2003). A wiggle-match date for the Polynesian settlement of New Zealand. *Antiquity, 77*, 116–125.
Hogg, A., Hua, Q., Blackwell, P., Niu, M., Buck, C., Guilderson, T., . . . Zimmerman, S. (2013a). SHCal13 Southern Hemisphere calibration, 0–50,000 yrs cal BP. *Radiocarbon, 55*(4), 1889–1903.
Hogg, A., Lorrey, A., Turney, C., Palmer, J., Boswijk, G., & Fenwick, P. (2022). Advances and limitations in establishing a contiguous high-resolution atmospheric radiocarbon record derived from subfossil kauri tree tings for the interval 60–27 cal kyr BP *Quaternary Geochronology, 68*, 1–13.
Hogg, A., Lowe, D., Palmer, J., Boswijk, G., & Bronk Ramsey, C. (2012). Revised calendar date for the Taupo eruption derived by ^{14}C wiggle-match dating using a New Zealand kauri ^{14}C calibration data set. *The Holocene, 22*(4), 439–449.
Hogg, A., McCormac, F., Higham, T., Reimer, P., Bailey, M., & Palmer, J. (2002). High-precision radiocarbon measurements of contemporaneous tree-ring dated wood from the British Isles and New Zealand. *Radiocarbon, 44*, 633–640.
Hogg, A., Turney, C., Palmer, J., & Buckley, B. (2013b). Is there any evidence for regional ^{14}C offsets in the Southern Hemisphere? *Radiocarbon, 55*(4), 2029–2034.
Hogg, A., Wilson, C., Lowe, D., Turney, C., White, P., Lorrey, A., . . . Petchey, F. (2019b). wiggle-match radiocarbon dating of the Taupo eruption. *Nature Communications, 10,* 46–69.
Holdaway, R., & Wandsnider, L. (2006). Temporal scales and archaeological landscapes from the eastern desert of Australia and intermontane North America. In G. Lock & B. Molyneaux (Eds.), *Confronting scale in archaeology: Issues of theory & practice.* (pp. 183–202). New York: Springer Science and Business Media.

Holdaway, S., & Wandsnider, L. (2008). Time in archaeology: An introduction. In S. Holdaway & L. Wandsnider (Eds.), *Time in archaeology: Time perspectivism revisited* (pp. 1–12). Salt Lake City: University of Utah Press.

Hua, Q., Ulm, S., Yu, K., Clark, T., Nothdurft, L., Leonard, N., . . . Zhao, J. (2020). Temporal variability in the Holocene marine radiocarbon reservoir effect for the tropical and south Pacific. *Quaternary Science Reviews, 249*, 106613.

Hughen, K., Baillie, M., Bard, E., Beck, J., Bertrand, C., Blackwell, P., . . . Edwards, R. (2004a). Marine04 marine radiocarbon age calibration 0–26 cal kyr BP. *Radiocarbon, 46*(3), 1059–1086.

Hughen, K., Lehman, S., Southon, J., Overpeck, J., Herring, C., & Turnbull, J. (2004b). C-14 activity and global carbon cycle changes over the past 50,000 years. *Science, 303*, 202–207.

Hughen, K., Overpeck, J., Lehman, S., Kashgarian, M., & Southon, J. (1998). A new ^{14}C calibration dataset for the last deglaciation based on marine varves. *Radiocarbon, 40*, 483–494.

Hull, K. (2005). Process, perception, and practice: Time perspectivism in Yosemite native demography. *Journal of Anthropological Archaeology, 24*, 354–377.

Irwin, G. (1982). Creation myths and the origin of pa. *New Zealand Archaeological Association Newsletter, 25*, 258–267.

Irwin, G. (1985). *Land, pa and polity: A study based on the Maori fortifications of Pouto*. Auckland: New Zealand Archaeological Association Monograph 15.

Irwin, G. (2004a). Excavations and site history at Kohika. In G. Irwin (Ed.), *Kohika: The archaeology of a late māori lake village in the Ngāti Awa rohe, Bay of Plenty, New Zealand*. Auckland: Auckland University Press.

Irwin, G. (2004b). *Kohika: The archaeology of a late Māori lake village in the Ngāti Awa rohe, Bay of Plenty, New Zealand*. Auckland: Auckland University Press.

Irwin, G. (2013). Wetland archaeology and the study of late māori settlement patterns and social organisation in northern New Zealand. *The Journal of the Polynesian Society, 122*(4), 311–332.

Irwin, G. (2020). The archaeology of māori settlement and pā on Pōnui Island, Inner Hauraki Gulf, AD 1400–1800. *Journal of Pacific Archaeology, 129*(1), 29–58.

Irwin, G., Johns, D., Flay, R., Munaro, F., Sung, Y., & Mackrell, T. (2017). A review of archaeological Maori canoes (waka) reveals changes in sailing technology and maritime communications in Aotearoa/New Zealand, AD 1300–1800. *Journal of Pacific Archaeology, 8*(2), 31–43.

Irwin, G., & Jones, M. (2004). Site chronology. In G. Irwin (Ed.), *Kohika: The archaeology of a late Maori village in the Ngati Awa Rohe, Bay of Plenty, New Zealand* (Vol. 1, pp. 76–82). Auckland: Auckland University Press.

Jacomb, C., Holdaway, R., Allentoft, M., Bunce, M., Oskam, C., Walter, R., & Brooks, E. (2014). High-precision dating and ancient DNA profiling of moa (*Aves: Dinornithiformes*) eggshell documents a complex feature at Wairau Bar and refines the chronology of New Zealand Settlement by Polynesians. *Journal of Archaeological Science, 50*, 24–30.

Jennings, J. (1979). *The prehistory of Polynesia*. Canberra: Australian National University Press.

Johns, D., Irwin, G., & Sung, Y. (2014). An early sophisticated East Polynesian voyaging canoe discovered on New Zealand's coast. *Proceedings of the National Academy of Sciences, 111*(41), 14728–14733.

Jones, K. (1983). Pā in two western segments of the Waiotahi and Whakatane Valleys, Bay of Plenty. *NZ Archaeological Association Newsletter, 26*, 165–173.

Jones, K. (1994). *Nga tohuwhenua mai te rangi: A New Zealand archaeology in aerial photographs*. Wellington: Victoria University Press.

Jones, M., & Nicholls, G. (2002). New radiocarbon calibration software. *Radiocarbon, 44*(3), 663–674.

Jones, P., & Biggs, B. (1995). *Ngā Iwi O Tainui. The traditional history of the Tainui people.* Auckland: Auckland University Press.

Jull, A., Panyushkina, I., Lange, T., Kukarskih, V., Myglan, V., Clark, K., . . . Leavitt, S. (2014). Excursions in the ^{14}C record at A.D. 774–775 in tree rings from Russia and America. *Geophysical Research Letters, 41*(8), 3004–3010.

Kaennel, J., & Schweingruber, F. (1995). Multilingual glossary of dendrochronology. *WSL FNP, Haupt, 133*, 162–184.

Keith, S. (2019). *Taupiri subdivision: S14/489 final report*. Unpublished report to New Zealand Historic Places Trust/Pouhere Taonga.

Kelly, L. (2002). *Tainui: The story of Hoturoa and his descendants* (Second ed.). Christchurch: Cadsonbury Publications.

Kennet, D., Anderson, A., & Winterhalder, B. (2006). The ideal free distribution, food production, and the colonization of Oceania. In D. Kennet & B. Winterhalder (Eds.), *Behavioural ecology and the transition to agriculture* (pp. 265–288). Berkeley: University of California Press.

Kennet, D. & McClure, S. (2012). The archaeology of Rapan fortifications. In Anderson, A. & Kennett, D. (Eds), *Taking the high ground: The archaeology of Rapa, a fortified island in remote East Polynesia* (Terra Australis 37). Canberra, Australia: Australian National University Press.

Kidson, J. (2000). An analysis of New Zealand synoptic types and their use in defining weather regimes. *International Journal of Climatology, 20*, 299–316.

Kirch, P. (1984a). Archaeological investigation in Waiotahi Valley, Bay of Plenty, November 1981. *New Zealand Archaeological Association Newsletter, 27*, 109–118.

Kirch, P. (1984b). *The evolution of the Polynesian chiefdom*. Cambridge: University of Cambridge Press.

Kirch, P. (1986). Rethinking East Polynesian prehistory. *Journal of the Polynesian Society, 95*, 9–40.

Kirch, P. (1990). Monumental architecture and power in Polynesian chiefdoms: A comparison of Tonga and Hawaii. *World Archaeology, 22*, 206–222.

Kirch, P. (2000). The Polynesian cheiftoms. In. P. Kirch (Ed.), *On the road of the winds, An archaeological history of the Pacific Islands before European contact* (pp. 246–301). California: University of California Press.

Kirch, P. (2004). Environment, agriculture, and settlement patterns in a marginal Polynesian landscape. *Proceedings of the National Academy of Sciences, 101*(26), 9936–9941.

Kirch, P. (2007). Like shoals of fish: Archaeology and population in pre-contact Hawaii. In P. Kirch & J. Rallu (Eds.), *The growth and collapse of Pacific Island societies: Archaeological and demographic perspectives* (pp. 52–69). Honolulu: University of Hawaii Press.

Kirch, P., & Green, R. (2001). *Hawaiki, ancestral Polynesia*. Cambridge University Press: Cambridge.

Kirch, P., & Rallu, J. (2007). *The growth and collapse of Pacific Island societies: Archaeological and demographic perspectives.* Honolulu: University of Hawaii Press.

Knapp, B. (1992). *Archaeology, annales and ethnohistory*. Cambridge: Cambridge University Press.
Kolb, M. (1994). Monumentality and the rise of religious authority in pre-contact Hawaii. *Current Anthropology, 34*, 521–547.
Kruschke, J., & Liddell, T. (2018). Bayesian data analysis for newcomers. *Psychonomic Bulletin & Review, 25*(1), 155–177.
Kuzmin, Y. (2009). Radiocarbon and the old world archaeology: Shaping a chronological framework. *Radiocarbon, 43*, 149–172.
Ladefoged, T., & Graves, M. (2007). Modelling agricultural development and demography in Kohala, Hawaii. In P. Kirch & J. Rallu (Eds.), *The growth and collapse of Pacific Island societies: Archaeological and demographic perspectives* (pp. 70–89). Honolulu: University of Hawaii Press.
Laj, C., Kissel, C., Mazaud, A., Channell, J., & Beer, J. (2000). North Atlantic palaeointensity stack since 75 ka (NAPIS-75) and the duration of the Laschamp event. *Philosophical Transactions of the Royal Society of London Series, a-Mathematical Physical and Engineering Sciences, 358*, 1009–1025.
Laj, C., Kissel, C., Scao, V., Beer, J., Thomas, D., Guillou, H., . . . Wagner, G. (2002). Geomagnetic intensity and inclination variations at Hawaii for the past 98 kyr from Core SOH-4 (Big Island): A new study and a comparison with existing contemporary data. *Physics of the Earth and Planetary Interiors, 129*, 205–243.
Lange, M. (1998). Wadi Shaw 82/52: ^{14}C dates from a Peridynastic site in Northwest Sudan, supporting the Egyptian historical chronology. *Radiocarbon, 40*(2), 687–699.
Last, J. (1995). The nature of history. In I. Hodder, M. Shanks, A. Alexandri, V. Buchli, J. Carmen, J. Last, & G. Lucas (Eds.), *Interpreting archaeology: Finding meaning in the past* (pp. 141–157). London: Routledge.
Law, G. (1968). Māori soils in the Lower Waikato. *New Zealand Archaeological Association Newsletter, 11*(2), 67–75.
Law, G. (2008). *Archaeology of the Bay of Plenty*. Department of Conservation: Science and Technical Publishing.
Law, G., & Green, R. (1972). An economic interpretation of Taniwha Pa, Lower Waikato, New Zealand. *Mankind, 8*, 255–269.
Leach, B., & Leach, H. (1979). The Wairarapa Archaeological Research Project. In b. Leach & H. Leach (Eds.), *Prehistoric Man in Palliser Bay* (pp. 1–10). Wellington: National Museum of NZ.
Leach, F. (1981). The prehistory of the Southern Wairarapa. *Journal of the Royal Society of New Zealand, 11*, 11–33.
Leach, H. (1979a). Evidence of prehistoric gardening in Eastern Palliser Bay. In B. Leach & H. Leach (Eds.), *Prehistoric man in Palliser Bay*. Wellington: National Museum of New Zealand Bulletin 21.
Leach, H. (1979b). The significance of early horticulture in Palliser Bay for New Zealand prehistory. In B. Leach & H. Leach (Eds.), *Prehistoric man in Palliser Bay*. Wellington: National Museum of New Zealand Bulletin 21.
Leach, H. (2005). *Ufi kumara, the sweet potato as yam*. Sydney: Oceania Monographs.
Leathwick, J., Clarkson, B., & Whaley, P. (1995). *Vegetation of the Waikato region: Current and historical perspective*. Hamilton, New Zealand: Landcare Research.
Lee, C., & Tuljapurkar, S. (2008). Population and prehistory I: Food-dependant population growth in constant environments. *Theoretical Population Biology, 73*(4), 473–482.

Lerman, J., Mook, W., & Vogel, J. (1970). ^{14}C in tree rings from different localities. In I. Olson (Ed.), *Radiocarbon variations and absolute chronology* (pp. 275–301). New York: Wiley.

Libby, W. (1951). Radiocarbon dates II. *Science, 114*, 291–296.

Lilburn, K. (1985). *Maori pa: A method for analysing settlement.* [Doctoral Thesis, University of Auckland]. Research Hub, The University of Auckland.

Litherland, A. (1980). Ultrasensitive mass spectrometry with accelerators. *Annual Review of Nuclear and Particle Science, 30*, 437–473.

Lock, G., & Molyneaux, B. (2006). *Confronting scale in archaeology*. New York: Springer Verlag.

Lorrey, A. (2008). Speleothem stable isotope records interpreted within a multi-proxy framework and implications for New Zealand palaeoclimate reconstruction. *Quaternary International, 187*, 52–75.

Lorrey, A., Fauchereau, N., Stanton, C., Chappell, P., Phipps, S., Mackintosh, A., . . . Fowler, A. (2014). The Little Ice Age climate of New Zealand reconstructed from Southern Alps cirque glaciers: A synoptic type approach. *Climate Dynamics, 42*, 11–12.

Lowe, D.J. (2010). *Introduction to the landscapes and soils of the Hamilton Basin*. In D.J. Lowe, V. Neall, M. Hedley, B. Clothier, & A. Mackay (Eds.), Guidebook for pre-conference North Island, New Zealand "volcanoes to oceans" field tour (27–30 July). 19th World Soils Congress, International Union of Soil Sciences, Brisbane. *Soil and Earth Sciences Occasional Publication No. 3*, Massey University, Palmerston North, pp. 1.24–1.61 (printed), pp. 64–75 (digital).

Lowe, D.J. (2023). Soils and landscapes of the Hamilton Basin and part South Waikato area – a summary. *Earth Sciences group, School of Science-Te Aka Mātuatua, University of Waikato,* Hamilton. 51 pp. [Online resource] https://www.researchgate.net/publication/369998946_Soils_and_landscapes_of_the_Hamilton_Basin_and_part_South_Waikato_area_-_a_summary

Lowe, D.J., & Green, J.D. (2024). Origins and ages. In D. Özkundakci, N. Grainger, & T. Dean-Speirs (Eds.), *The hidden gems of the Waikato – The history, ecology and management of the Waikato lakes – Ō Tātou Roto - He Taonga Tuku Iho (*pp. 15–57). Hamilton: Waikato Regional Council.

Lowe, D.J., McFadgen, B., Higham, T., Hogg, A., Froggatt, P., & Nairn, I. (1998). Radiocarbon age of the Kaharoa Tephra, a key marker for late Holocene stratigraphy and archaeology in New Zealand. *The Holocene, 8*, 401–407.

Lowe, D.J., Newnham, R., & McCraw, J. (2002). Volcanism and early Maori society in New Zealand. In R. Torrence & J. Grattan (Eds.), *Natural disasters and cultural change* (pp. 126–161). London, Routledge.

Lowe, D.J., & Newnham, R. (2004). Role of tephra in dating Polynesian settlement and impact, New Zealand. In V. Hall, B. Alloway, C. Kull, & L. Christen (Eds.), *Tephra. Past Global Changes, 14,* 5–7.

Lowe, D.J., & Pittari, A. (2021). The Taupō eruption sequence of AD 232 ± 10 in Aotearoa New Zealand: a retrospection. *Journal of Geography (Chigaku Zasshi), 130 (1),* 117–141.

Lucas, G. (2005). *The archaeology of time*. London: Routledge.

Lucas, G. (2008). Time and the archaeological event. *Cambridge Archaeological Journal, 18*(1), 59–65.

Lucas, G. (2010). Time and the archaeology archive. *The Journal of Theory and Practice, 14*, 343–359.

Lucas, G. (2012). *Understanding the archaeological record*. Cambridge: Cambridge University Press.
Lucas, G. (2015). Archaeology and contemporaneity. *Archaeological Dialogues, 22*(1), 1–15.
Mann, M. (2009). Global signatures and dynamical origins of the Little Ice Age and Medieval climate anomaly. *Science, 326*, 1256–1260.
Manning, M., Bronk Ramsey, C., Kutschera, W., Higham, T., Kromer, B., Steier, P., & Wild, E. (2006). Chronology for the Aegean late Bronze Age 1700–1400 B.C. *Science, 312*(5773), 565–569.
Manning, M., & Weninger, B. (1992). A light in the dark: Archaeological wiggle-matching and the absolute chronology of the close of the Aegean late Bronze Age. *Antiquity, 66*, 635–663.
Manning, S. (2014). Radiocarbon dating and archaeology: History, progress and present status. In R. Chapman & A. Wylie (Eds.), *Material evidence: Learning from archaeological practice* (pp. 1–20). London: Routledge.
Manning, S., Kromer, B., Kuniholm, P., & Newton, M. (2001). Anatolian tree rings and a new chronology for the east Mediterranean Bronze-Iron Ages. *Science, 294*, 2532–2535.
Manning, S., Wacker, L., Būntgen, U., Bronk Ramsey, C., Dee, M., Kromer, B., . . . Tegal, W. (2020). Radiocarbon offsets and old world chronology as relevant to Mesopotamia, Egypt, Anatolia and Thera (Santorini). *Scientific Reports, 10*(13785).
Marra, M., Alloway, B., & Newnham, R. (2006). Paleoenvironmental reconstruction of a well-preserved stage 7 forest sequence catastrophically buried by basaltic eruptive deposits, Northern New Zealand. *Quaternary Science Reviews, 25*(17–18), 2143–2161.
Marshall, Y. (1987). *Antiquity, form, and function of terracing at Pouerua Pā.* [Doctoral Thesis, University of Auckland]. Research Hub, The University of Auckland.
Marshall, Y. (2004). Social organisation. In *Change through time: 50 years of New Zealand archaeology* (pp. 55–84). Auckland: New Zealand Archaeological Association.
Masarik, J., & Beer, J. (1999). Simulation of particle fluxes and cosmogenic nuclide production in the Earth's atmosphere. *Journal of Geophysical Research, 104*, 12099–12111.
Masarik, J., & Reedy, R. (1995). Terrestrial cosmogenic-nuclide production systematics calculated from numerical simulations. *Earth and Planetary Science Letters, 136*, 381–395.
McCormac, F., Hogg, A., Blackwell, P., Buck, C., Higham, T., & Reimer, J. (2004). SHCAL04 Southern Hemisphere calibration, 0–11 cal KYR BP. *Radiocarbon, 46*(3), 1087–1092.
McCormac, F., Hogg, A., Higham, T., Baillie, M., Palmer, J., Xiong, L., . . . Hoper, S. (1998a). Variations of radiocarbon in tree rings: Southern Hemisphere offset preliminary results. *Radiocarbon, 40*(3), 1153–1159.
McCormac, F., Hogg, A., Higham, T., Lynch Stieglitz, J., Broecker, W., Baillie, M., . . . Hoper, S. (1998b). Temporal variation in the interhemispheric ^{14}C offset. *Geophysical Research Letters, 25*(9), 1321–1324.
McCormac, F., Reimer, P., Hogg, A., Higham, T., Baillie, M., Palmer, J., & Stuiver, M. (2002). Calibration of the radiocarbon timescale for the Southern Hemisphere: AD 1850–950. *Radiocarbon, 44*, 641–651.
McCoy, M. (2009). *A report on intensive archaeological survey and geophysical survey of northern Urupukapuka Island and Waewaetorea Island, Bay of Islands, New Zealand*. Unpublished report to New Zealand Historic Places Trust/Pouhere Taonga.
McCoy, M., & Carpenter, J. (2014). Strategies for obtaining obsidian in pre-European contact era New Zealand. *PloS one, 9*(1).

McCoy, M., & Ladefoged, T. (2012). Northland archaeological project: A summary report of 2012 archaeological field research in Urupukapuka Bay, Urupukapuka Island. *Report on file with the Department of Conservation*.

McCoy, M., & Ladefoged, T. (2019). In pursuit of Māori warfare: New archaeological research on conflict in pre-European contact New Zealand. *Journal of Anthropological Archaeology, 56*, 1–14.

McCoy, M., Ladefoged, T., Codlin, M., & Sutton, D. (2014). Does Carneiro's circumscription theory help us understand Maori history? An analysis of the obsidian assemblage from Pouerua Pā, New Zealand (Aotearoa). *Journal of Archaeological Science, 42*, 467–475.

McCoy, M., & Robles, H. (2016). The geographic range of interaction spheres during the colonization of New Zealand (Aotearoa): New evidence for obsidian circulation in Southern New Zealand. *Journal of Island Coastal Archaeology, 11*(2), 285–293.

McFadgen, B., Higham, T., & Sparks, R. (2000). New Zealand Radiocarbon Database for Archaeology. *Archaeology in New Zealand, 43*(4), 297–300.

McGlade, J. (1995a). Archaeology and the ecodynamics of human-modified landscapes. *Antiquity, 69*, 113–132.

McGlade, J. (1995b). The times of history: Archaeology, narrative, and non-linear causality. In T. Murray (Ed.), *Time and archaeology* (pp. 139–163). London: Routledge.

McGlone, M. (1983). Polynesian deforestation of New Zealand: A preliminary synthesis. *Archaeology in Oceania, 18*, 11–25.

McGlone, M., Anderson, A., & Holdaway, R. (1994). An ecological approach to the Polynesian settlement of New Zealand. In D. Sutton (Ed.), *The origins of the first New Zealanders* (pp. 139–163). Auckland: University of Auckland Press.

McIvor, I., & Ladefoged, T. (2015). A multi-scalar analysis of Maori land use on Ahuahu (Great Mercury Island), New Zealand. *Archaeology in Oceania, 00*, 1–17.

Meadows, J., Barclay, A., & Bayliss, A. (2007). A short passage of time: The dating of Hazelton Long Cairn revisited. *Cambridge Archaeological Journal, 17*, 45–64.

Meadows, J., & Zunde, M. (2014). A lake fortress, a floating chronology and an atmospheric anomaly: The surprising results of a radiocarbon wiggle-match from Araisi, Latvia. *Geochronometria, 41*(3), 223–233.

Mellstrom, A., Muschelar, R., Snowball, I., Ning, W., & Haltia, E. (2013). A numerical approach to ^{14}C wiggle-match dating of organic deposits: Best fits and confidence intervals. *Radiocarbon, 55*(3), 1173–1186.

Meylan, B., & Butterfield, B. (1978). *The structure of New Zealand woods*. Wellington: Department of Scientific and Industrial Research.

Mihaljevic, J. (1973). *The prehistoric polity in New Zealand. An exercise in theoretical palaeosociology.* [Doctoral Thesis, University of Auckland]. Research Hub, The University of Auckland.

Miyake, F., Masuda, K., & Nakamura, T. (2013). Another rapid event in the Carbob-14 content of tree rings. *Nature Communications, 4*(1), 1748–1748.

Miyake, F., Nagaya, K., Masuda, K., & Nakamura, T. (2012). A signature of cosmic-ray increase in AD 774–775 from tree rings in Japan. *Nature, 486*, 7402.

Molle, G. & Marolleau, V. (2022). The 'enata way of war: An ethnoarchaeological perspective on warfare dynamics in the Marquesas Islands. In G. Clarke & M. Litster (Eds.). (2022). *Archaeological perspectives on conflict and warfare in Australia and the Pacific*. (Vol. 54). Canberra: ANU Press.

Morrison, A., & O'Connor, J. (2018). Settlement pattern studies in Polynesia: Past projects, current progress, and future prospects. In E. Cochrane & T. Hunt (Eds.), *The Oxford handbook of prehistoric Oceania*. Oxford University Press.

Murray, T. (1999). *Time and archaeology*. London: Routledge.
Nakamura, T., Miyahara, H., Masuda, K., Menjo, H., Kuwana, K., Kimura, K., . . . Rakowski, A. (2007). High precision ^{14}C measurements and wiggle-match dating of tree rings at Nagoya University. *Nuclear Instruments and Methods in Physics Research Section B: Beam Interactions with Materials and Atoms, 259*(1), 408–413.
Needham, S., Bronk Ramsey, C., Coombs, D., Cartwright, C., & Pettitt, P. (1997). An independent chronology for British Bronze Age metalwork: The results of the Oxford Radiocarbon Accelerator Programme. *Archaeological Journal, 154*(1), 55–107. doi:10.1080/00665983.1997.11078784
Newnham, R., Lowe, D.J., Gehrels, M., & Augustinus, P. (2018). Two-step human-environmental impact history for northern New Zealand linked to late-Holocene climate change. *The Holocene, 28*, 1093–1106.
Newnham, R., Lowe, D.J., & Green, J. (1989). Palynology, vegetation and climate of the Waikato lowlands, North Island, New Zealand, since c. 18,000 years ago. *Journal of the Royal Society of New Zealand, 19*(2), 127–150.
Newnham, R., Lowe, D.J., & Matthews, B. (1998a). A late-Holocene and prehistoric tephropalynological record of environmental change from Lake Waikaremoana, New Zealand. *The Holocene, 8*, 443–454.
Newnham, R., Lowe, D.J., McGlone, M., Wilmshurst, J., & Higham, T. (1998b). The Kaharoa Tephra as a critical datum for earliest human impact in northern New Zealand. *Journal of Archaeological Science, 25*, 533–544.
Nicholls, G., & Jones, M. (2001). Radiocarbon dating with temporal order constraints. *Journal of the Royal Society of New Zealand, 50*, 503–521.
Niu, M., Heaton, T., Blackwell, P., & Buck, C. (2013). The Bayesian approach to radiocarbon calibration curve estimation: the IntCal13, Marine13, and SHCal13 methodologies. *Radiocarbon, 55*(4), 1905–1922.
O'Brian, M., & Lyman, R. (2000). Chronometry and units in early archaeology and paleontology. *American Antiquity, 665*, 691–707.
O'Brien, K. (1979). Secular variations in the production of cosmogenic isotopes in the Earth's atmosphere. *Journal of Geophysical Research, 84*, 423–431.
O'Keeffe, M. (1991). *Prehistoric settlement in the Western Bay of Plenty.* [Doctoral Thesis, Univesity of Auckland]. Research Hub, The University of Auckland.
O'Malley, V. (2013). Choosing peace or war: the 1863 invasion of Waikato. *Journal of History, 47*, 39–58.
O'Malley, V. (2016). *The great war for New Zealand, Waikato 1800–2000*. Wellington: Bridget Williams Books.
Oeschger, H., Siegenthaler, U., Schotter, U., & Gugelmann, A. (1975). A box diffusion model to study the carbon dioxide exchange in nature. *Tellus, 27*, 168–192.
Palmer, J. G. (1982). *A dendrochronological study of kauri (Agathis australis Salisb.).* [Masters Thesis, University of Auckland]. Research Hub, the University of Auckland.
Palmer, J. G. (1989). *A dendroclimatic study of Phyllocladus trichomanoides D. Don (tanekaha).* [Doctoral Thesis, University of Auckland]. Research Hub, the University of Auckland.
Pandow, M., Mackay, C., & Wolfgang, R. (1960). The reaction of atomic carbon with oxygen: Significance for the natural radiocarbon cycle. *Journal of Inorganic Nuclear Chemistry, 14*, 153–158.
Pardoe, C. 2014. Conflict and territoriality in Aboriginal Australia: Evidence from biology and ethnography. In M.W. Allen and T.L. Jones (Eds). *Violence and warfare among hunter-gatherers* (pp. 112–132). California: Left Coast Press.

Parker, R. (1962). Aspect and phase of Skipper's Ridge (Opiuo) and Kumara-Kaiamo (Urenui). *NZ Archaeological Association Newsletter, 5*, 222–232.
Patel, R. (1967a). Wood anatomy of podocarpaceae indigenous to New Zealand 1. *Dacrydium*. *New Zealand Journal of Botany, 5*(2), 171–184.
Patel, R. (1967b). Wood anatomy of podocarpaceae indigenous to New Zealand 2. *Podocarpus*. *New Zealand Journal of Botany, 5*(3), 307–321.
Patel, R. (1968). Wood anatomy of podocarpaceae indigenous to New Zealand 3. *Phyllocladus*. *New Zealand Journal of Botany, 6*(1), 3–8.
Patel, R. (1973). Wood anatomy of the dicotyledons indigenous to New Zealand. *New Zealand Journal of Botany, 11*(1), 3–2273.
Patel, R. (1987). Wood anatomy of the dicotyledons indigenous to New Zealand 16. *Lauraceae*. *New Zealand Journal of Botany, 25*(4), 477–488.
Pearson, G. (1979). Precise ^{14}C measurement by liquid scintillation counting. *Radiocarbon, 21*(1), 1–21.
Pearson, G., Pilcher, J., Baillie, M., & Hillam, J. (1977). Absolute radiocarbon dating using a low altitude European tree-ring calibration. *Nature, 270*, 25–28.
Pearson, G., & Stuiver, M. (1986). High-precision calibration of the radiocarbon time scale, 500–2500 BC. *Radiocarbon, 28*, 839–862.
Perry, G., Wheeler, A., Jamie, R., Wood, J., Janet, M., & Wilmshurst, J. (2014). A high-precision chronology for the rapid extinction of New Zealand moa (*Aves. Dinornithiformes*). *Quaternary Science Reviews, 105*, 126–135.
Petchey, F., Bickler, S., Hughes, L., & Bunbury, M. (2022). The Aotearoa New Zealand Radiocarbon Database Upgrade. *Archaeology in New Zealand, 65*(3), 32–40.
Petchey, F., & Schmid, M. (2020). Vital evidence: Change in the marine ^{14}C reservoir around New Zealand (Aotearoa) and implications for the timing of Polynesian settlement. *Scientific Reports (Nature Publisher Group), 10*(1), 1–9.
Peters, K. (1971). Excavations at Lake Mangakaware 1, N.65/28. *New Zealand Archaeological Association Newsletter, 14*, 126–140.
Phillips, C. (2000). *Waihou journeys the archaeology of 400 years of Maori settlement*. Auckland: Auckland University Press.
Phillips, C., & Campbell, M. (2004). From settlement patterns to interdisciplinary landscapes in New Zealand. In L. Furey & S. Holdaway (Eds.), *Change through time: 50 years of New Zealand Archaeology* (pp. 85–104). Auckland: New Zealand Archaeological Association Monograph 26.
Phillips, F. (1995). *Nga tohu a Tainui: Landmarks of Tainui, a geographical record of Tainui traditional history*. Otorohanga: Tohu Publishers.
Pick, D. (1968). Waikato island and swamp pa. *Newsletter of the New Zealand Archaeological Association, 11*(1), 30–34.
Piggott, S. (1954). *Neolithic cultures of the British Isles: A study of the stone-using agricultural communities of Britain in the second millennium BC*. Cambridge: Cambridge University Press.
Pilcher, J., Baillie, M., Schmidt, B., & Becker, B. (1984). A 7,272-year tree-ring chronology for Western Europe. *Nature, 312*, 150–152.
Prickett, N. (1980). Maori fortifications at Omata and Oakura Districts, Taranaki. *Records of the Auckland Institute and Museum, 17*, 1–48.
Prickett, N. (1982). Maori fortifications of the Tararaimaka District, Taranaki. *Records of the Auckland Institute and Museum, 19*, 1–52.
Prickett, N. (1983). Maori fortifications of the Okato District, Taranaki. *Records of the Auckland Institute and Museum, 20*, 1–39.

Pulestion, C., & Tuljapurkar, S. (2008). Population and prehistory II: Space-limited human populations in constant environments. *Theoretical Population Biology, 74*(2), 147–160.
Quarta, G., Pezzo, M., Marconi, S., Tecchiati, U., D'Elia, M., & Calcagnile, L. (2010). Wiggle-match dating of wooden samples from Iron Age sites in northern Italy. *Radiocarbon, 52*(2), 915–923.
Ralph, E., Michael, H., & Han, M. (1974). Radiocarbon dates and reality. *Archaeology of Eastern North America, 2*(1), 1–20.
Ralph, E., & Struckenrath, R. (1960). Carbon-14 measurements of known age samples. *Nature, 188*(4746), 185–187.
Ramenofsky, A., & Steffen, A. (1998). *Unit issues in archaeology: Measuring time, space and material*. Salt Lake City: University of Utah Press.
Reimer, J. (2022). Evolution of radiocarbon calibration. *Radiocarbon, 64*(3), 523–539.
Reimer, J., Austin, W., Bayliss, A., Blackwell, P., Bronk Ramsey, C., Butzin, M., . . . Talamo, S. (2020). The IntCal20 Northern Hemisphere radiocarbon age calibration curve (0–55 cal kBP). *Radiocarbon, 62*(4), 725–757.
Reimer, J., Bard, E., Bayliss, A., Beck, J., Blackwell, P., Bronk Ramsey, C., . . . Van Der Plicht, J. (2013). IntCal13 and Marine13 radiocarbon age calibration curves 0–50,000 years cal BP. *Radiocarbon, 55*(4), 1869–1887.
Reimer, P. (2004). IntCal04: Terrestrial radiocarbon age calibration, 0–26 cal kyr BP. *Radiocarbon, 46*(3), 1029–1058.
Reimer, P., Hughen, K., Guilderson, T., McCormac, F., Baillie, M., Bard, E., . . . Van Der Plicht, J. (2009). IntCal09 and Marine09 radiocarbon age calibration curves, 0–50,000 years cal BP. *Radiocarbon, 51*(1111–1150).
Renfrew, C. (1973). *Before civilization: The radiocarbon revolution and prehistoric Europe*. Cambridge: Cambridge University Press.
Renfrew, C. (1981). Space, time and man. *Transactions of the Institute of British Geographers, 6*(3), 257–278.
Renfrew, C., & Clark, R. (1974). Problems of the radiocarbon calendar and its calibration. *Archaeometry, 16*, 5–18.
Rinn, F. (2002–2015). TSAPWin Scientific 4.69i, 4.69 ed *RINNTECH, Heidelberg*.
Robb, J., & Pauketat, T. (2013). From moments to millennia: Theorising scale and change in human history. In J. Robb, T. Pauketat, & N. Sante Fe (Eds.), *Big histories, human lives: Tackling the problem of scale in archaeology* (pp. 3–33). Santa Fe: School for Advanced Research (SAR) Press.
Rodgers, K., Mikaloff-Fletcher, S., Bianchi, D., Hogg, A., Iudicone, D., Lintner, B., . . . Reimer, P. (2011). Interhemispheric gradient of atmospheric radiocarbon reveals natural variability of southern ocean winds. *Climate of the Past, 7*, 1123–1138.
Roop, H. (2015). *Late-Holocene climate variability in southern New Zealand: A reconstruction of regional climate from an annually laminated sediment sequence from Lake Ohau.* [Doctoral Thesis, Victoria University of Wellington] Open Access Te Herenga Waka-Victoria University of Wellington.
Rossignol, J., & Wandsnider, L. (1992). *Space, time and archaeological landscapes*. New York: Plenum.
Rzepecki, S. (2014). Palimpsest, time perspectivism and megaliths. *Sprawozdania Archeologiczne, 66*, 9–27.
Santos, G., Southon, J., Druffel-Rodriguez, K., Griffin, S., & Mazon, M. (2004). Magnesium perchlorate as an alternative water trap in AMS graphite sample preparation: A report of sample preparation at KCCAMS at the University of California, Irvine. *Radiocarbon, 46*(1), 165–173.

Santos, G., Southon, J., Griffin, S., Beaupre, S., & Druffel, E. (2007). Ultra small-mass AMS ^{14}C sample preparation and analyses at KCCAMS/UCI facility. *Nuclear Instruments and Methods in Physics Research, 259*(1), 293–302.
Scaglion, M. (2008). *Māori warfare: Prefiguring contemporary directions in ecological science*. London: Altamira Press.
Schacht, R. (1984). The comtemporaneity problem. *American Antiquity, 49*(4), 678–695.
Schiffer, M. (1976). *Behavioural archaeology*. New York: Academic Press.
Schiffer, M. (1985). Is there a "Pompeii premise" in archaeology? *Journal of Anthropological Research, 41*, 18–41.
Schiffer, M. (1987). *Formation processes of the archaeological record*. Albuquerque: University of New Mexico Press.
Schmidt, M. (1996). The commencement of pā construction in New Zealand prehistory. *Journal of the Polynesian Society, 105*, 105: 104.
Schwimmer, E. (1978). Levi-Strauss and Maori social structure. *Anthropologie, 2*, 201–222.
Shanks, M., & Tilley, C. (1987). *Social theory and archaeology*. Albuquerque: University of New Mexico Press.
Sharon, G., Zaidner, Y., & Hovers, E. (2014). Opportunities, problems and future directions in the study of open-air middle Paleolithic sites. *Quaternary International, 331*, 1–5.
Sharon, I., Gilboa, A., Jull, A., & Boaretto, E. (2007). Report on the first stage of the Iron Age dating project in Israel: Supporting a low chronology. *Radiocarbon, 49*(1), 1–46.
Shawcross, W. (1963). Kauri point swamp: An interim report. *NZ Archaeological Association Newsletter, 6*(1), 6–10.
Shawcross, W. (1964). Archaeological investigations at Ongari Point, Katikati, Bay of Plenty. *NZ Archaeological Association Newsletter, 6*(1), 6–10.
Shawcross, W. (1966). Ongari Point - Second season. *NZ Archaeological Association Newsletter, 9*, 53–71.
Shawcross, W. (1968). The Ngaroto site. *NZ Archaeological Association Newsletter, 11*, 2–29.
Singleton, P. (1988). Cultivation and soil modification by the early Maori in the Waikato. *New Zealand Soil News, 36*, 49–57.
Sissons, J. (1988). Rethinking tribal origins. *Journal of the Polynesian Society, 97*(2), 199–204.
Skinner, L., Muschitiello, F., & Scrivner, A. (2019). Marine reservoir age variability over the last deglaciation: Implications for marine carbon cycling and prospects for regional radiocarbon calibrations. *Paleoceanography and Paleoclimatology, 34*(11), 1807–1815.
Smale, M., Ross, C., & Arnold, G. (2005). Vegetation recovery in rural kahikatea (*Dacrycarpus dacrydioides*) forest fragments in the Waikato region, New Zealand, following retirement from grazing. *New Zealand Journal of Ecology, 29*(2), 261–269.
Sparks, R., Melhuish, J., Ogden, J., Palmer, J., & Molloy, B. (1995). ^{14}C calibration in the Southern Hemisphere and the date of the last Taupo eruption: Evidence from tree-ring sequences. *Radiocarbon, 30*(2), 155–163.
Spriggs, M. (1989). The dating of the island Southeast Asian Neolithic: An attempt at chronometric hygiene and linguistic correlation. *Antiquity, 63*, 587–613.
Spriggs, M., & Anderson, A. (1993). Late colonization of East Polynesia. *Antiquity, 63*, 200–217.
Spurk, M., Friedrich, M., Hofmann, J., Remmele, S., Frenzel, B., Leuschner, H., & Kromer, B. (1998). Revisions and extension of the Hohenheim oak and pine chronologies: New evidence about the timing of the Younger Dryas/Preboreal Transition. *Radiocarbon, 40*, 1107–1116.
Stahl, A. (1993). Concepts of time and approaches to analogical reasoning. *American Antiquity, 34*, 235–260.

Steinhof, A. (2016). Accelerator mass spectrometry of radiocarbon. In E. Schuur, E. Druffel, & S. Trumbore (Eds.), *Radiocarbon and climate change*: Springer Cham.
Stern, N. (1994). The implication of time-averaging for reconstructing the land-use patterns of early tool-using hominids. *Journal of Human Evolution, 27*(89–105).
Stern, N., Porch, N., & McDougall, I. (2002). A window into a 1.5-Million-Year-Old palaeolandscape in the Okote Member of the Koobi Fora Formation, Northern Kenya. *Geoarchaeology, 17*, 349–392.
Stuiver, M. (1961). Variations in radiocarbon concentration and sunspot activity. *Journal of Geophysical Research, 66*, 273–274.
Stuiver, M. (1965). Carbon-14 content of 18th and 19th century wood: Variations correlated with sunspot activity. *Science, 149*, 533–534.
Stuiver, M., & Becker, B. (1986). High-precision decadal calibration of the radiocarbon time scale, AD 1950–2500 BC. *Radiocarbon, 28*, 863–910.
Stuiver, M., Brazuiunas, T., Becker, B., & Kromer, B. (1991). Climatic, solar, oceanic, and geomagnetic influences on late-glacial and Holocene atmospheric $^{14}C/^{12}C$ change. *Quaternary Research, 35*, 1–24.
Stuiver, M., & Pearson, G. (1986). High-precision calibration of the radiocarbon time scale, AD 1950–500 BC. *Radiocarbon, 28*(2B), 805–838.
Stuiver, M., Pearson, G., & Brazuiunas, T. (1986). Radiocarbon age calibration of marine samples back to 9000 cal yr BP. *Radiocarbon, 28*, 980–1021.
Stuiver, M., & Quay, P. (1980). Changes in atmospheric ^{14}C attributed to a variable sun. *Science, 207*, 11–19.
Stuiver, M., Reimer, J., Bard, E., Beck, J., Burr, G., Hughen, K., . . . Spurk, M. (1998a). IntCal98 radiocarbon age calibration, 24,000–0 cal BP. *Radiocarbon, 40*(3), 1041–1083.
Stuiver, M., & Reimer, P. (1986). A computer-program for radiocarbon age calibration. *Radiocarbon, 28*, 1022–1030.
Stuiver, M., & Reimer, P. (1993). CALIB rev. 8. *Radiocarbon, 35*, 215–230.
Stuiver, M., Reimer, P., & Brazuiunas, T. (1998b). High-precision radiocarbon age calibration for terrestrial and marine samples. *Radiocarbon, 40*(3), 1127–1151.
Stuiver, M., Robinson, S., & Yang, I. (1979). *^{14}C dating up to 60,000 years BP with high efficiency proportional counters.* Paper presented at the Proceedings of the 9th International Radiocarbon Dating Conference, Berkley.
Stuiver, M., & Suess, H. (1966). On the relationship between radiocarbon dates and true sample ages. *Radiocarbon, 8*, 534–540.
Suess, H. (1955). Radiocarbon concentration in modern wood. *Science, 122*(3166), 415–417.
Suess, H. (1965). Secular variations of the cosmic-ray produced carbon 14 in the atmosphere and their interpretations. *Journal of Geophysical Research, 70*, 5937–5952.
Suess, H. (1967). *Bristlecone pine calibration of the radiocarbon time scale from 4100 BC to 1500 BC.* Paper presented at the Proceedings of the Radioactive Dating and Methods of Low-level Counting, Monaco.
Suess, H. (1970). *Bristlecone pine calibration of the radiocarbon time-scale 5200 B.C. to the present.* Paper presented at the Proceedings of the Twelfth Nobel Symposium, Uppsala, Sweden.
Sullivan, A. (1972). Stone walled complexes of central Auckland. *New Zealand Archaeology, 15*, 148–160.
Sullivan, A. (2008). Time perspectivism and the interpretive potential of palimpsests: Theoretical and methodological considerations of assemblage formation history and

contemporaneity. In R. Holdaway & L. Wandsnider (Eds.), *Time in archaeology: Time perspectivism revisited* (pp. 1–225). Utah: University of Utah Press.
Sutton, D. (1987). A paradigmatic shift in Polynesian prehistory: Implications for New Zealand. *New Zealand Journal of Archaeology, 9*, 135–155.
Sutton, D. (1990). Organization and ontology: The origins and operation of the Northern Maori chiefdom, New Zealand. *Man, 25*, 667–692.
Sutton, D. (1991). The archaeology of belief: Structuralism in stratigraphical context. In A. Pawley (Ed.), *Man and a half: Essays in Pacific anthropology and ethnobiology in honour of Ralph Bulmer* (pp. 540–550). Auckland: Polynesian Society Monograph 48.
Sutton, D. (1993a). *The archaeology of the peripheral Pā at Pouerua, Northland, New Zealand*. Auckland: Auckland University Press.
Sutton, D. (1993b). Conclusion: The archaeology of the peripheral pā at Pouerua, Northland, New Zealand. In D. Sutton (Ed.), *The archaeology of the peripheral Pā at Pouerua, Northland, New Zealand* (pp. 97–103). Auckland: Auckland University Press.
Sutton, D., Furey, L., & Marshall, Y. (2003). *The archaeology of Pouerua*. Auckland: Auckland University Press.
Switsur, V. (1973). The radiocarbon calendar recalibrated. *Antiquity, 47*(186), 131.
Synal, H., & Wacker, L. (2010). AMS measurement technique after 30 years: Possibilities and limitations of low energy systems. *Nuclear instruments & methods in physics research. Section B, Beam interactions with materials and atoms, 268*, 701–707.
Tans, P., & Mook, W. (1978). Design, construction and calibration of a high accuracy carbon-14 counting set up. *Radiocarbon, 21*(1), 22–40.
Taylor, N. (1958). Soil science and New Zealand prehistory. *New Zealand Science Reviews, 16*, 71–79.
Taylor, R. (1995). Radiocarbon dating: The continuing revolution. *Evolutionary Anthropology: Issues, News and Reviews, 4*(5), 169–181.
Taylor, R., & Bar-Yosef, O. (2014a). Basic elements. In R. Taylor & O. Bar-Yosef (Eds.), *Radiocarbon dating: An archaeological perspective* (pp. 19–42). Abingdon: Routledge.
Taylor, R., & Bar-Yosef, O. (2014b). *Radiocarbon dating: An archaeological perspective* (2 Ed.). California: Left Coast Press.
Thomas, H., & Ehrich, R. (1969). Some problems in chronology. *World Archaeology, 1*, 143–156.
Thomas, J. (1996). *Time, culture and identity: An interpretive archaeology*. London: Routledge.
Thomas, T. (2008). The long pause and the last pulse: Mapping east Polynesian colonisation, seafaring and the archaeology of maritime landscapes. In S. O'Connor, G. Clark, & F. Leach (Eds.), *Islands of inquiry: Colonisation, seafaring and the archaeology of maritime landscapes*. Canberra: Australian National University Online Press.
Thorpe, I. (2003). Anthropology, archaeology, and the origin of warfare. *World Archaeology, 35*, 145–165. doi.org/10.1080/0043824032000079198.
Tilley, C. (1981). Economy and society: What relationship? In A. Sheridan & G. Bailey (Eds.), *Economic archaeology* (pp. 131–148). Oxford: British Archaeological Reports.
Trotter, M., & McCulloch, B. (1997). *Digging up the past: New Zealand's archaeological history*. Auckland: Penguin Books.
Trotter, M., & McCulloch, B. (1999). How far south? The southern limits of kumara growing in preEuropean New Zealand. *Archaeology in New Zealand, 42*, 129–133.
Usoskin, I., Kromer, B., Ludlow, F., Beer, J., Friedrich, M., Kovaltsov, G., . . . Wacker, L. (2013). The AD 775 cosmic event revisited: the sun is to blame. *Astronomy and Astrophysics Letters, 552*(3).

van Der Plicht, J. (1993). The Groningen Radiocarbon Calibration Program. *Radiocarbon, 35*(1), 231–237.
Van der Plicht, J., Bronk Ramsey, C., Heaton, T., Scott, E., & Talamo, S. (2020). Recent developments in calibration for archaeological and environmental samples. *Radiocarbon, 62*(4), 1095–1117.
Vayda, A. (1956). Maori conquests in relation to the New Zealand environment. *Journal of Pacific Archaeology, 65*, 204–211.
Vayda, A. (1960). *Maori warfare* (Vol. vol 2.). Auckland: A.H. and A.W. Reed.
Vayda, A. (1976). *War in ecological perspective: Persistence, change and adaptive processes in three Oceanian societies.* New York: Plenum Press.
Voelker, A., Grootes, P., Nadeau, M., & Sarnthein, M. (2000). Radiocarbon levels in the Iceland sea from 25–53 kyr and their link to the Earth's magnetic field intensity. *Radiocarbon, 42*, 437–452.
Vogel, J., Fuls, A., Visser, E., & Becker, B. (1986). Radiocarbon fluctuations during the third Millennium BC. *Radiocarbon, 28*(2B), 935–938.
Vogt, S., Herzog, G., & Reedy, R. (1990). Cosmogenic nuclides in extraterrestrial materials. *Reviews of Geophysics, 28*, 253–275.
Wagner, G., Beer, J., Laj, C., Kissel, C., Masarik, J., Muscheler, R., & Synal, H. (2000). Chlorine-36 evidence for the Mono Lake Event in the Summit GRIP Ice Core. *Earth and Planetary Science Letters, 181*, 1–6.
Waikato Radiocarbon Dating Laboratory. (2017). *AMS Processing Technical Report.* https://www.waikato.ac.nz/assets/Uploads/Research/Services-and-facilities/Radiocarbon-dating/Waikato-Radiocarbon-Dating-Laboratory-AMS-Processing-Technical-Report-2017.pdf
Wallace, R. (1985). *Studies on the conservation of waterlogged wood in New Zealand.* [Doctoral Thesis, University of Waikato].
Wallace, R. (1989). A preliminary study of wood types used in pre-European Maori wooden artefacts. In D. Sutton (Ed.), *Saying so doesn't make it so: Papers in honour of B. Foss Leach*. Dunedin: New Zealand Archaeological Association.
Wallace, R., & Irwin, G. (2004a). Houses, pataka and wood carving at Kohika. In G. Irwin (Ed.), *Kohika: The archaeology of a late Māori lake village in the Ngāti Awa rohe* (pp. 122–148)*, Bay of Plenty, New Zealand*. Auckland: Auckland University Press.
Wallace, R., & Irwin, G. (2004b). The wooden artefacts of Kohika. In G. Irwin (Ed.), *Kohika: The archaeology of a late Māori lake village in the Ngāti Awa rohe, Bay of Plenty, New Zealand* (pp. 83–121). Auckland: Auckland University Press.
Walter, R., Buckley, H., Jacomb, C., & Matisoo-Smith, E. (2017). Mass migration and the Polynesian settlement of New Zealand. *Journal of World Prehistory, 30*, 351–376.
Walter, R., & Jacomb, C. (2007). New Zealand. In D. Pearsal (Ed.), *Encyclopaedia of archaeology* (Vol. 3, pp. 1738–1747). New York: Academic Press.
Walter, R., Jacomb, C., & Bowron-Muth, S. (2010). Colonisation, mobility and exchange in New Zealand Prehistory. *Antiquity, 84*, 497–513.
Wandsnider, L. (1996). Describing and comparing archaeological spatial structures. *Journal of Archaeological Method and Theory, 3*(4), 319.
Wandsnider, L. (2004). Solving the puzzle of the archaeological labyrinth: Time perspectivism in Mediterranean surface archaeology. In S. Alcock & J. Cherry (Eds.), *Side-by-side survey: Comparative regional studies in the Mediterranean world* (pp. 49–62). Oxford: Oxbow Books.
Wandsnider, L. (2008). Time averaged deposits and multitemporal processes in the Wyoming Basin, Intermontane North America: A preliminary consideration of land tenure in

terms of occupation frequency and integration. In R. Holdaway & L. Wandsnider (Eds.), *Time in archaeology: Time perspectivism revisited* (pp. 61–93). Salt Lake City: University of Utah Press.

Wendland, W., & Donley, D. (1971). Radiocarbon calendar age relationship. *Earth and Planetary Science Letters, 11*(135–139).

Weninger, B. (1995). Stratified ^{14}C dates and ceramic chronologies: Case studies for the early Bronze Age at Troy (Turkey) and Ezero (Bulgaria). *Radiocarbon, 37*(2), 443–456.

Weninger, B. (1997). Monte Carlo Wiggle Matching. Zur Statistischen Auswertung der Mittelneolithischen ^{14}C-daten von Hasselsweiler 2, Inden 3, and Inden 1. In E. Biermann (Ed.), *Großgartach und Oberlauterbach*. Archäologische Berichte: Interregionale Beziehungen im süddeutschen Mittelneolithikum.

Whaley, P., Clarkson, B., & Smale, M. (1997). Claudelands Bush: Ecology of an urban kahikatea (*Dacrycarpus dacrydioides*) forest remnant in Hamilton, New Zealand. *Tane, 36*, 131–155.

Whittle, A., & Bayliss, A. (2007). The times of their lives: From chronological precision to kinds of history and change. *Cambridge Archaeological Journal, 17*, 27–28.

Whittle, A., Healy, F., & Bayliss, A. (2011). *Gathering time: Dating the early Neolithic enclosures of southern Britain and Ireland*. Oxford: Oxbow Books.

Wilcox, J. (2010). *Vegetation recovery and management of kahikatea (Dacrycarpus dacrydioides) dominated forest remnants in the Waikato Region.* [Masters Thesis, The University of Waikato].

Wilkes, O. (1995). Site recording, site types, and site distribution on the King Country Coast. *Archaeology in New Zealand, 38*, 236–256.

Willis, E., Tauber, H., & Munnich, K. (1960). Variations in the atmospheric radiocarbon concentration over the past 1300 years. *American Journal of Science Radiocarbon Supplement, 2*(1), 1–4.

Wilmshurst, J., Anderson, A., Higham, T., & Worthy, T. (2008). Dating the late prehistoric dispersal of Polynesians to New Zealand using the commensal Pacific rat. *Proceedings of the National Academy of Sciences of the United States, 14*, 7676–7680.

Wilmshurst, J., Hunt, T., Lipo, C., & Anderson, A. (2011). High-precision radiocarbon dating shows recent and rapid initial human colonization of East Polynesia. *Proceedings of the National Academy of the United States of America, 108*, 1815–1820.

Yen, D. (1961). The adaptation of kumara by the New Zealand Māori. *Journal of the Polynesian Society, 70*(3), 338–348.

Younger, S. (2008). Conditions and mechanisms for peace in precontact Polynesia. *Current Anthropology, 49*(5), 927–934.

Zimmerman S, Guilderson T, Buckley B, Cook E. (2010). Extension of the Southern Hemisphere atmospheric radiocarbon curve, 2120–850 years BP: Results from Tasmanian Huon Pine. *Radiocarbon*. 52(3), 887–894.

Zvelebil, M. (1993). Concepts of time and 'presencing' the Mesolithic. *Archaeological Review from Cambridge, 12*(2), 51–70.